THE UNIVERSITY of ADELAIDE

Sedimentation and geochemistry of the Loxton-Parilla Sands in the Murray Basin, southeastern Australia

Stephanie Margaret McLennan

Submitted in fulfilment of the requirements of the degree of

Doctor of Philosophy

February 2016

Department of Geology & Geophysics

University of Adelaide

Abstract

The Loxton-Parilla Sands are a well-preserved Neogene strandplain sequence in southeastern Australia. They provide an opportunity to understand the interactions of fluvial and shoreline sedimentary systems, groundwater and subaerial weathering, with implications for mineral exploration within the strandplain and its underlying geology. I undertook a detailed paleogeographical and geochemical study of the western Murray Basin from the scale of the basin to individual grains to assess the geochemical processes and depositional environment of Neogene sediments.

The observed distribution of heavy minerals supports previous studies that found that temporal and spatial variations in heavy mineral assemblages and zircon populations is related to access to different source regions and local depositional processes. Detrital zircon ages, from six locations including HMS deposits, range from the Cretaceous to the Mesoproterozoic and are consistent with major sediment sources in the neighbouring Adelaide Fold Belt, Lachlan Fold Belt, Grampians, Coleraine Volcanics, New England Fold Belt and Whitsunday Volcanic Province (WVP). Zircons from the WVP travelled up to 3000 km and are most likely to have been recycled through the Eromanga Basin. Gold is locally present at low concentrations and is distributed near the goldfields of Victoria. Geochemistry of Au that is non-repeatable, unrelated to the Fe-oxide indurated horizons, pathfinder elements, and heavy mineral concentrations is consistent with a detrital origin.

I used geological logs from over 8000 drill holes to model the geometry of the Loxton-Parilla Sands and associated Neogene units in 3 dimensions. Curvilinear depocenters are interpreted to represent the path of ancient channels draining the Murray Basin during the Neogene. The Murray River west of Balranald has migrated north up to 80 km while the outlet of river has moved 300 km to the northwest of its former location near Edenhope to its current location. There was a major confluence of Neogene drainage channels east of Ouyen.

Detailed whole rock geochemistry, mineralogy, and major element mapping indicates the two major controls on geochemistry in the Loxton-Parilla Sands are detrital minerals and post-depositional weathering. The post-depositional geochemistry is characterised by accumulation of secondary goethite and hematite (up to 80 wt. %) and silica, clay minerals, and minor carbonate and sulphate. Incorporation of Al into secondary Fe-oxides, mobilisation of Si in the weathering profile, and precipitation of barite point to strongly acidic weathering conditions as the result of acid sulphate soil development and ferrolysis. The range of morphologies of indurated materials is consistent with progressive induration and formation which began with interaction of groundwater and oxidised sediments in the coastal and near-coastal system. As the ocean further regressed, leaving the dunes 'stranded', the induration was overprinted by disaggregation, transport, and further induration of ferricretes to produce a range of internal textures.

Whole rock geochemistry and element mapping reveal complex patterns of major and trace element distribution within Fe-oxides from indurated horizons in the Loxton-Parilla Sands. These patterns record fluctuating Eh and pH conditions related to wetting and drying of coastal sediments during and immediately following deposition. Concentrations of trace elements that are important pathfinders for a range of mineralisation styles are heterogeneous and reflect these temporally varying groundwater interactions rather than proximity to mineralisation. The Loxton-Parilla Sands and associated weathering profile are a complex system of sedimentary and post-depositional geochemical processes superimposed on eustuatic and neotectonic processes. This study underlines the importance of understanding the whole system in order to identify weathering processes and their application to regional mineral exploration.

Statement of originality

I certify that this work contains no material which has been accepted for the award of any other degree or diploma in any other university or tertiary institution to Stephanie Margaret McLennan and, to the best of my knowledge and belief, contains no material previously published or written by another person, except where due reference has been made in the text. In addition, I certify that no part of this work will, in the future, be used in a submission for any other degree or diploma in any university or other tertiary institution without the prior approval of the University of Adelaide.

I give consent for this copy of my thesis when deposited in the University Library, being made available for loan and photocopying, subject to the provisions of the Copyright Act 1968.

I give permission for the digital version of my thesis to be made available on the web, via the University's digital research repository, the Library catalogue following the end of a 12 month embargo as per the Deep Exploration Technologies Cooperative Research Centre Participants Agreement.

Stephanie Margaret McLennan

Table of Contents

Acknowledgements

This thesis, like the Loxton-Parilla Sands, has undergone years of evolution and modification and there is no single defining control on the resultant thesis/stratigraphy. The sand analogies will stop there. I am indebted to my supervisors Prof. David Giles, Dr Steve Hill, and Prof. Karin Barovich for their insight, guidance, wisdom, and good humour. I am grateful for the expertise of Dr Ben Wade and Aoife McFadden at Adelaide Microscopy (and assurance that, "it's meant to make that sound"). The assistance of Acme Laboratories in Vancouver and Adelaide Petrographic Laboratories as well as the core repositories of the Geological Survey of South Australia (GSSA), Geological Survey of Victoria, and Geoscience Australia is gratefully acknowledged. I would like to thank Simon van der Wielen from the Deep Exploration Technologies Cooperative Research Centre (DET CRC) for his assistance and expertise with GOCAD® and 3D modelling. Further thanks go to Georgina Gordon of the GSSA and Matilda Thomas at Geoscience Australia for their expertise in HyLogger™. I am grateful for the outstanding support and opportunities provided by the DET CRC throughout my PhD and for Geoscience Australia for providing the flexibility and support to complete this thesis while working full-time.

On a personal level, I'd like to thank my family especially my mum (sorry about all the rocks in the shed) and Andrew, Jessica, Patrick, and Georgia. Mum, thank you for instilling in me a passion for learning and supporting me in your own gently inimitable way. Dad, I'm sorry you didn't get to read this; I think you really would have got a kick out of it. To Simon, the love of my life, words fall short of capturing my gratitude for your support, humour, and encouragement during this undertaking. No more late night lab visits. I promise. A huge thank you to the Gunson family, the van der Wielen family, Dr Ashlyn Johnson and Charlotte Mitchell, and the postgraduate cohort at Adelaide. Thank you to my friends and colleagues at Geoscience Australia for keeping me somewhat sane in this last year.

Finally, I'd like to acknowledge the exceptional research that has come before me, the scientists whose shoulders I stand on: Drs Tony Stephenson and the late Campbell Brown, as well as Drs Jim Bowler, Louise-Goldie Divko, Andrew Kotsonis, Phil Macumber, Sandra McLaren, John Miranda, Mark Paine, Peter Roy, and Keith Sircombe.

Chapter 1 Introduction

Strandplains are the result of the interaction between marginal marine and fluvial processes during a marine regression. On a coastline where sediment supply outstrips the accommodation space generated by the regression, the coast progrades by the deposition and subsequent 'stranding' of a series of beach and nearshore facies sediments parallel to the shoreline. Strandplains are important settings to study paleogeography and sedimentology because they record the prolonged interaction of fluvial and marine processes (Dunbar *et al.* 1992) (Figure 1.1). When accurate depositional ages can be established strandplain deposits are sensitive records of isostasy, climate, and sea level fluctuations (Fraser *et al.* 2005, Foyle & Norton 2006, López & Rink 2008, Miranda *et al.* 2009, Hein *et al.* 2013). For example, detailed studies of stacked Pleistocene and Holocene strandplains in Brazil have revealed a rapid sea level fall of 1.5 m over the past 1000 years, during a period when global sea levels were gradually on the rise (Hein *et al.* 2013).

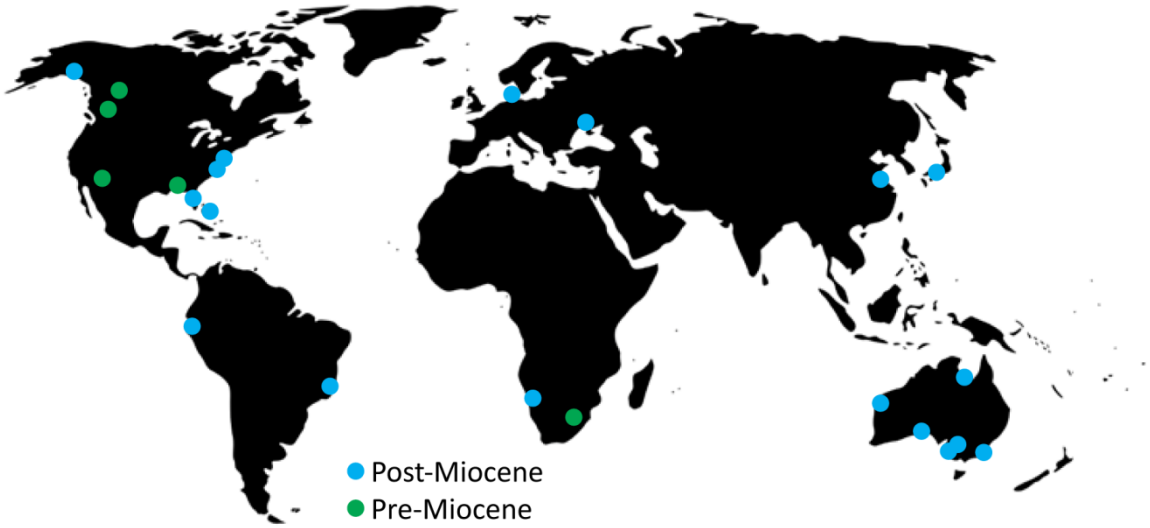

Figure 1.1 Location of young (post-Miocene) (blue) and older (Miocene to Cretaceous) strandplains (green) around the world.

Strandplain systems are important oil and gas reservoirs, characterised by high porosity, permeability, and recovery rates (Tyler & Ambrose 1986). The Jackson-Yegua Sandstone

strandplain in Texas has produced over 625 x 10^6 barrels of oil, with estimated reserves of over 1 x 10^9 barrells (Hamilton 1995). The importance of understanding facies and stratigraphic architecture of these deposits for improved recovery is well recognised (Wallis *et al.* 1991, Dunbar *et al.* 1992). Their permeability means that strandplain sequences are also potentially important aquifers. For example, the Holocene Ocean Bight strandplain in the Bahamas supplies potable water to an isolated island community (Wallis *et al.* 1991) whilst the Late Miocene-Pliocene Loxton-Parilla Sands provides irrigation water for a vast semi-arid area of southeast Australia. Understanding the architecture and hydraulic properties of strandplain facies is important for maximising the value of these groundwater resources.

Strandplains are potentially important to mineral exploration in two ways: Firstly, as hosts to heavy mineral sands (HMS) deposits which are globally significant repositories of zircon, ilmenite, and rutile used in pigments for paint and ceramics. Heavy mineral sands concentrated in strandplain sequences are found throughout Australia – in the Eucla Basin (Hou *et al.* 2003) and the southeast Australian coast (Roy 1999), as well as China (Li *et al.* 2001), and the United States (McCubbin 1982, Dunbar *et al.* 1992). Understanding sedimentary processes, from the potential source region of the heavy minerals and through the fluvial transport pathways to the site of deposition then reworking, concentration, and preservation in the shoreface environment, is vital to exploration for these deposits.

Secondly, strandplain sediments have the potential to capture geochemical signatures of concealed mineralisation due to dispersion and concentration of geochemical signals during weathering processes and via groundwater migration. Groundwater has the potential to transport dissolved geochemical signatures which might be measured directly from hydrogeochemistry (Gray 2001, Caritat *et al.* 2005, Arne *et al.* 2009, Gray *et al.* 2010) or concentrated at particular interfaces due to chemical processes within the aquifer (McQueen & Munro 2003). Such processes could be related to facies variations within the unit, an extreme example of which is roll front U deposits (Fisher *et*

al. 1970), and interaction with overlying or underlying formations. Processes related to groundwater and weathering systems in which large volumes of reduced Fe have been transported represents a particularly interesting case because of the tendency for Fe-oxides to scavenge metals from co-existing fluids, leading to the widespread use of Fe-oxide indurated weathering materials as an exploration sampling media (Smith *et al.* 2000, McQueen & Munro 2003).

THE MURRAY BASIN

The Murray Basin covers 300,000 km^2 of southeast Australia and contains the world's largest near surface strandplain sequence, the Late Miocene-Pliocene Loxton-Parilla Sands, and its laterally equivalent fluvial sequence, the Calivil Formation (Figure 1.2). The Loxton-Parilla Sands is an ideal unit to study the breadth of processes associated with strandplain sequences and their mineral exploration potential because:

- the strandplain sediments are well-preserved at, or near, the surface, providing easy access for sampling and mapping;
- the importance of the Loxton-Parilla Sands as an agricultural aquifer means there are records of thousands of bores with logged stratigraphy;
- low subsidence rates and lack of isostatic rebound means the system is dominated by the influences of eustasy and neotectonics (Miranda *et al.* 2009);
- it is a cyclic, well-dated sedimentary record of a regression over an important period of global climate change in the Neogene (Bowler *et al.* 2006, Miranda *et al.* 2009);
- it is a rare example of a strongly weathered strandplain sequence, providing the opportunity to study the influence of the depositional environment on redox-driven weathering profile development;
- it contains numerous heavy mineral deposits; and
- it is surrounded by geological terrains that host a range of mineralisation types, a number of which are projected to underlie the Murray Basin with largely untested mineral prospectivity.

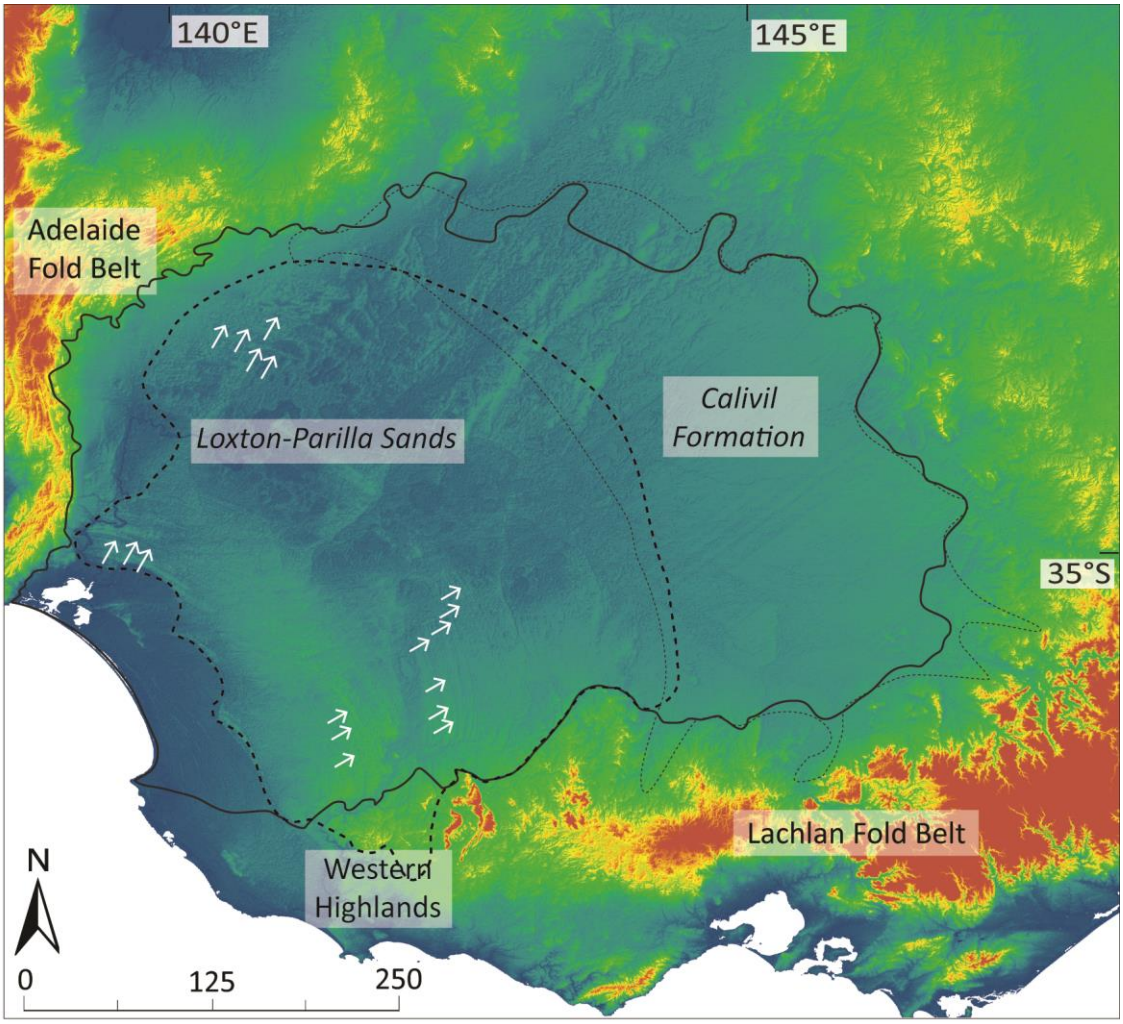

Figure 1.2 Digital elevation model of southeastern Australia (Gallant et al 2011) with key physiographic features labelled. The Murray Basin is outlined in black. Dashed lines show the extent of the Loxton-Parilla Sands (west) and Calivil Formation (east). Some of the (approximately) 600 curvilinear parallel ridges of the Loxton-Parilla Sands are highlighted (white arrows).

The Murray Basin contains some of the most productive agricultural land in Australia. Irrigated agricultural land in the Murray-Darling Basin accounts for 66% of irrigated land in Australia, covering 14,000 km^2 of the region (Australian Bureau of Statistics 2013). Further production includes dryland farming, and sheep and cattle grazing. The basin sediments, including the Loxton-Parilla Sands, are important aquifers that sustain agriculture. Clearance of native vegetation since European settlement, however, has resulted in increased infiltration, thereby raising water tables.

This has led to salt accession in the landscape and decline in native vegetation health and groundwater quality (McLennan *et al.* 2013). Consequently, there has been considerable research effort aimed at understanding the modern groundwater system in the Murray Basin (Brown & Radke 1989, Brown & Stephenson 1991, Macumber 1991, Odins *et al.* 1991, Petrides *et al.* 2006, Cartwright *et al.* 2007, Goldie-Divko 2008), utilising data from thousands of water bores and stratigraphic drill holes. These drill holes provide an invaluable but as yet underutilised repository of geological data with which to reconstruct the evolution and 3D architecture of the basin.

The excellent exposure of the Loxton-Parilla Sands and long-term preservation of physiographic depositional features such as dune ridges (Figure 1.2) has allowed for detailed studies of the depositional environment of the Loxton-Parilla Sands (most recently, Paine 2004, Bowler *et al.* 2006, Miranda 2007, Robson & Webb 2011). Early studies (Blackburn 1962, Colwell 1976, Brown & Stephenson 1991, Roy *et al.* 2000) established that the Loxton-Parilla Sands were deposited in a marginal marine to fluvial environment during a marine regression which remains the prevailing depositional model. Dating of brachiopods using Sr isotopes places constraints on the age of deposition from just prior to 7.2 Ma until about 5.0 Ma (Miranda *et al.* 2009). Strandlines were deposited in approximately 20 ka phases, related to Milankovitch cycles, superimposed on a more gradual marine regression (Roy *et al.* 2000), with relative see level dropping over a period of about 2.2 million years (Bowler *et al.* 2006).

The Loxton-Parilla Sands host economic heavy mineral sands deposits formed in the near-shore environment (coarse grained, low tonnage) and deeper water environments (sheet-like, fine grained) (Roy *et al.* 2000, Olshina & van Kann 2012). Research to increase understanding of formation of heavy mineral deposits has revealed the important association between accumulation of heavy minerals with growth faulting and minor headlands (Roy *et al.* 2000). The differences in heavy mineral assemblages and zircon populations between older and younger components of the strandplain reflect increased input of different source regions (Roy *et al.* 2000). Zircon is an

economically heavy mineral and a useful geochronometer that enables matching of sediments to source terranes.

The Loxton-Parilla Sands differs from many post-Miocene strandplains in that it includes extensive Fe-oxide and silica induration. The geochemistry and mineralogy of secondary Fe-oxides in the near surface environment has long been recognised as a record of the conditions in which the Fe-oxides formed. This work has tended to focus on *in situ* weathering processes (Anand & Gilkes 1987, Firman 1994, Bourman 2010, Bestland & Stainer 2013) although there has been increasing recognition on the lateral migration of geochemical signals within surface and groundwater (Smith *et al.* 2000). The trace element chemistry of Fe-oxides has been widely used for mineral exploration with numerous studies, many of which have focussed on the Yilgarn region of Western Australia, particularly "lateritic" weathering profiles (for example, Anand & Gilkes 1987, Butt 1988, Ollier *et al.* 1988, Butt *et al.* 2000, Anand & Paine 2002). A number of studies in southeastern Australia have addressed the morphology of ferricretes (Milnes *et al.* 1985, Bourman 1993, Firman 1994, Twidale & Bourne 1998) but few have addressed their geochemistry (although see Kotsonis 1995).

Another key finding of a number of studies on Australian ferricretes was that the *in situ* accumulation of Fe-oxide was interpreted to be in response to periods of increased weathering triggered by temporally discrete shifts in climate (Bourman 1993, Firman 1994, Kotsonis 1995). In this context, indurated rocks in the Loxton-Parilla Sands have been attributed to a single, widespread, time-correlative unit, the Karoonda Surface (Firman 1966, Kotsonis 1995, Paine 2004, Miranda *et al.* 2009). However, there is no dating of indurated materials to support this interpretation and alternatives of syn-depositional and ongoing processes have not been strongly considered. Nor are there detailed studies that examine the geochemical signature of those materials as an integrated product of source, transport networks, the depositional environment and weathering and groundwater interactions.

This study aims to understand the geochemistry of the Loxton-Parilla Sands and its application to mineral exploration. The Loxton-Parilla Sands is a complex system that has been developed by numerous sedimentary processes and subsequently overprinted by extensive post-depositional weathering. It is important to establish sediment sources, facies architecture, and 3D geometry and post-depositional weathering and groundwater interactions. I achieve this by establishing the nature of the sedimentary system, its sources and geometry, in the first two chapters of this thesis. These two chapters demonstrate the close relationship between the fluvial and marginal marine environments where sediment is transported and supplied to the gulf before being further transported by longshore drift and deposited in the strandplain. I follow this stratigraphic architecture with analysing geochemistry of the unit from the basin scale to the grain scale. Groundwater flow and vertical migration of elements in pedogenic weathering profiles are important processes to understand in order to establish the use of weathering materials in mineral exploration.

CHAPTER OUTLINE

This thesis consists of four main chapters and a synthesis. Chapters are ordered in terms of scale, from continental to basin to grain scale processes. I have written each chapter as a manuscript for submission to various international journals and there is necessarily some repetition of background and methods details. I have chosen to keep these sections in the thesis so each chapter can be read as a stand-alone document.

Chapter 2: *Diverse provenance of the Loxton-Parilla Sands and implications for heavy mineral sand and gold exploration in the Murray Basin, southeast Australia*

This chapter reassesses published geochronology data and new whole rock geochemistry in the context of geological evolution of eastern Australia. It provides insights to the dominant sedimentary processes active during deposition of sediments in the Neogene in southeastern Australia.

Chapter 3: *Neogene paleodrainage evolution and neotectonism in the western Murray Basin, southeast Australia, from 3D modelling of the Loxton-Parilla Sands.*

Chapter 3 models the 3 dimensional geometry of Neogene stratigraphy in the Murray Basin to infer paleodrainage systems draining the basin in the Late Cenozoic. In this chapter I focus on the relationship between landscape evolution and depositional environment and the major controls on sedimentation. Early isopach representations of the Murray Basin stratigraphy were limited by the spatial constraints of the study area or jurisdiction of the agency undertaking the study. This work strives to overcome spatial limitations of previous studies by incorporating data from disparate and otherwise incompatible datasets to develop a basin-wide 3D framework and demonstrate the importance of neotectonism in controlling sedimentation.

Chapter 4: *Late Miocene-Pliocene coastal acid sulphate system in southeast Australia and implications for genetic mechanisms of Fe-oxide induration*

In chapter 4 I study the relationship between depositional environment and the formation of the weathering profile, which is dominated by the precipitation of secondary Fe-oxides. I describe the geochemical processes from basin to outcrop to grain scale, from observations and detailed data collection in the field complemented by microanalysis.

Chapter 5: *Secondary Fe-oxides as sample media for exploration through deep transported sediments, Murray Basin, southeast Australia*

In this chapter I take the genetic model of the various weathering materials in the Loxton-Parilla Sands and study the trace element deportment in these materials. I assess the geochemical processes and mineralogical controls on the trace element geochemistry to address a key research question, whether these iron indurated sediments can be of use for mineral exploration in southeastern Australia.

Chapter 6: Synthesis

This chapter provides a synthesis of the findings of this research and an overview of the significance of the Loxton-Parilla Sands in the Cenozoic evolution of south eastern Australia. I discuss and summarise the themes investigated in this thesis.

Supplementary datasets associated with this research are presented in the appendices.

Chapter 2 Diverse provenance of the Loxton-Parilla Sands and implications for heavy mineral sand and gold exploration in the Murray Basin, SE Australia

FOREWARD

This chapter is a compilation and reinterpretation of published detrital zircon geochronology from south eastern Australia and new whole rock geochemistry. It aims to provide a provenance and paleogeographical reconstruction of the Murray Basin. I discuss the implications of sediment sources for the evolution of eastern Australia and similar continental settings during the Cenozoic in the context of heavy mineral and gold exploration. In this chapter I attempt to set the wider geological context and articulate the sedimentary processes active in the Murray Basin during deposition of the Loxton-Parilla Sands. This chapter is written as a manuscript that will be submitted for review to *Sedimentary Geology*. The manuscript will be co-authored by Prof. David Giles, Prof. Karin Barovich, and Dr Steven Hill who I have included because they have contributed to conceptualisation of the study and assisted with interpretation of the data. Signed statements from co-authors have been included following the abstract of this thesis. I have used the nomenclature of *Sedimentary Geology* for this chapter and throughout the thesis, for consistency. I would like to acknowledge Geoscience Australia, the Geological Survey of South Australia, and the Geological Survey of Victoria for sample access and Acme Laboratories in Canada for analyses.

Statement of Authorship

Title of Paper	Diverse provenance of the Loxton-Parilla Sands and implications for heavy mineral sand and gold exploration in the Murray Basin, SE Australia
Publication Status	○ Published, ○ Accepted for Publication, ○ Submitted for Publication, ◉ Publication style
Publication Details	

Author Contributions

By signing the Statement of Authorship, each author certifies that their stated contribution to the publication is accurate and that permission is granted for the publication to be included in the candidate's thesis.

Name of Principal Author (Candidate)	Stephanie McLennan
Contribution to the Paper	Project design, fieldwork and sampling, data processing, data interpretation, manuscript design and composition, and design and generation of figures and tables.
Signature	Date: 28.10.2015

Name of Co-Author	Prof. David Giles
Contribution to the Paper	Helped with project conceptualisation, data interpretation, and manuscript revision.
Signature	Date: 29-10-15

Name of Co-Author	Prof. Karin Barovich
Contribution to the Paper	Helped with data interpretation and manuscript revision.
Signature	Date: 29/10/15

Name of Co-Author	Dr Steven Hill
Contribution to the Paper	Manuscript revision
Signature	Date: 29-10-15

ABSTRACT

This multidisciplinary study integrates published detrital zircon geochronology with whole rock geochemistry to constrain the paleogeography and evolution of the Murray Basin during the Late Neogene. Changes in sediment source are reflected in multiple detrital zircon populations that vary across the extent of the unit. Zircon results suggest largely proximal sources of sediment such as the Lachlan and Adelaide Fold Belts, the Grampians Group, and volcanics in southwest Victoria, with minor input from more distal sources such as the New England Fold Belt and northeast Australian coast. Zircons dating from the Jurassic and Cretaceous have been sourced from Queensland as well as input from the Coleraine Volcanics of western Victoria. Carboniferous-Permian zircons are likely from the New England Fold Belt, while earlier Ordovician-Devonian grains are derived from the plutons of the Lachlan Fold Belt. Cambrian zircons have been eroded from syn- and post-tectonic Delamerian Orogen granites as well as reworked via Ordovician turbidites. Neoproterozoic and older grains have a proto-source in the Transgondwanan Supermountains associated with the East African-Antarctic orogeny but have been reworked as part of the Moralana Supergroup, Grampians Group, and Lachlan Fold Belt. Changes in sediment source due to uplift of source regions and drainage migration have been homogenised by longshore drift towards the centre of the basin. Heavy minerals with slight changes in density and entrainment properties have been fractionated by hydraulic processes during deposition in the swash and nearshore facies. At the basin-scale zircon age populations show mixed source regions that have changed relative sediment contributions as the strandplain was deposited. Gold in the Loxton-Parilla Sands is detrital, likely derived from gold-bearing plutons in the Lachlan Fold Belt. A detailed understanding of the processes contributing to sediment deposition will contribute to more targeted heavy mineral exploration approaches.

KEYWORDS

Neogene; Australia; paleogeography; sedimentation; gold; heavy minerals

2.1 INTRODUCTION

The Murray Basin contains a transgressive-regressive sequence of marine, marginal marine, and fluvial sediments deposited on the cratonic margin of Australia during the Cenozoic. The most striking physiographic features of the Murray Basin are the laterally extensive series of arcuate strandlines of the Loxton-Parilla Sands that were deposited during the regressive phase of a Late Miocene to Pliocene marine transgression. The strandlines are interpreted as a proxy for eustatic change over the Miocene-Pliocene (Brown & Stephenson 1991, Kotsonis 1995). Economic and sub-economic heavy mineral deposits, such as Gingko, Douglas, Wemen, Balranald, Nepean, Mindarie, and Euston, occur within the marginal marine facies of the Loxton-Parilla Sands. The Loxton-Parilla Sands present the opportunity to study the interaction of eustatic change and sediment deposition across a diachronous unit. Longshore drift and reworking of sediments by wave action are important hydraulic processes acting on the composition of heavy mineral suites (Morton & Hallsworth 1999).

This paper presents a reinterpretation of published detrital zircon geochronology in combination with whole rock geochemistry, including detrital minerals and Au, and a paleogeographical reconstruction of eastern Australia. The focus of this paper is the wider provenance of the Loxton-Parilla Sands and associated evolution of the Murray Basin. Whole rock analyses for Au geochemistry are combined with published detrital zircon geochronology to determine potential sources of sediment. Determining the regional controls on sedimentation aid in assessing heavy mineral prospectivity while understanding source and depositional controls on heavy mineral accumulation will lead to more targeted heavy mineral exploration strategies in the Murray Basin and similar settings worldwide. The data help to constrain basin evolution and drainage and the consequent geometry of sediments.

2.2 REGIONAL SETTING

2.2.1 Stratigraphy

The Murray Basin is an intracratonic basin up to 600 m deep, covering 300,000 km^2 of south eastern Australia (Figure 2.1). Rifting of southern Australia and Antarctica during the breakup on Gondwana initiated subsidence and the onset of sedimentation in the Murray Basin in the Early Cenozoic. Sediments of the Murray Basin unconformably overlie heterogeneous basement lithologies and Paleozoic-Mesozoic infrabasins (Brown & Stephenson 1991).

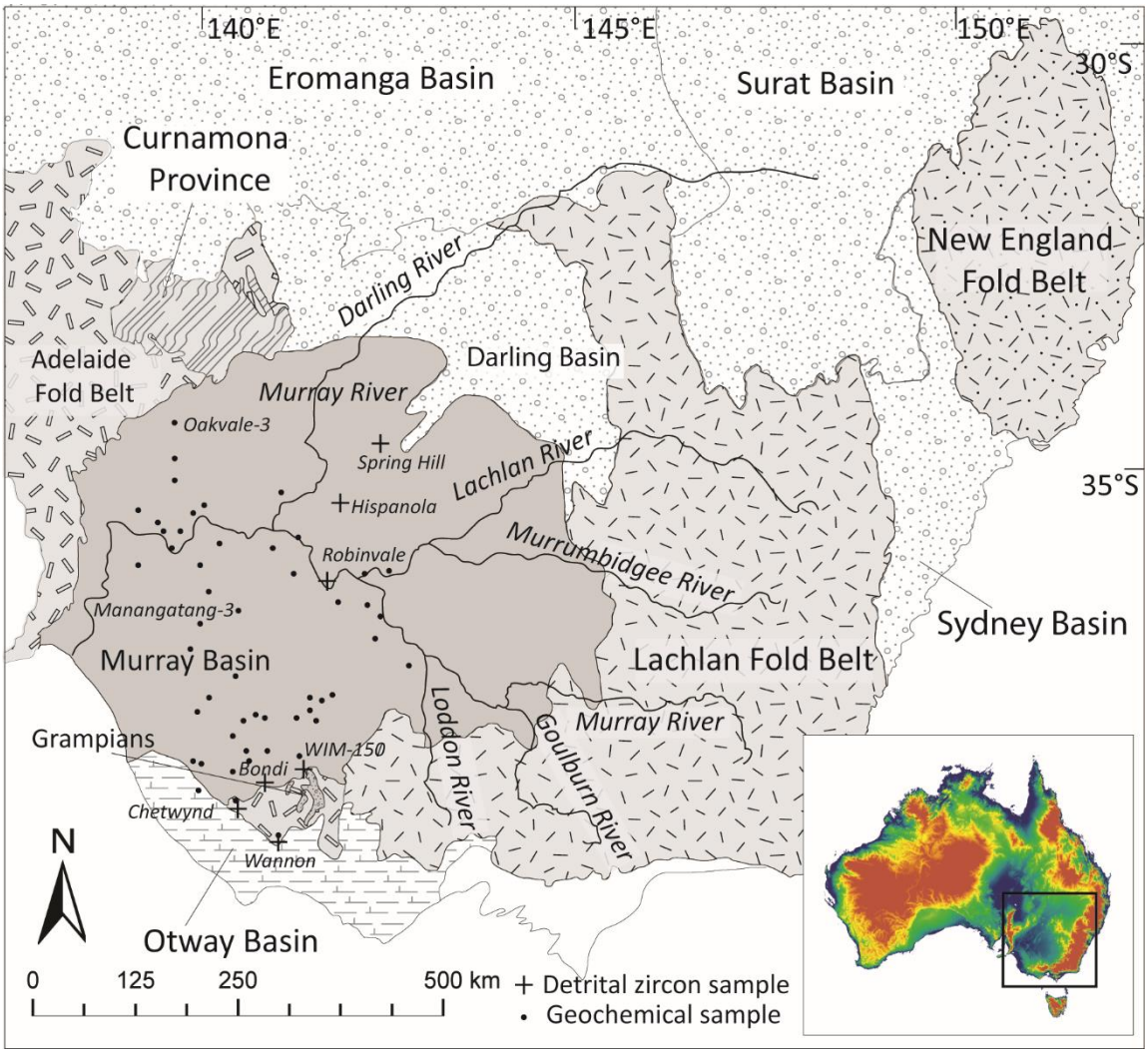

Figure 2.1 Location of the Murray Basin and major geological provinces in southeast Australia. Inset shows digital elevation model of Australia (Gallant et al. 2011) .

The basin contains a package of flat-lying sediments up to 600 m thick deposited across four main depositional cycles in the Cenozoic and Quaternary (Brown & Stephenson 1991) (Figure 2.2):

1) Marginal marine, fluvial, and lacustrine sediments deposited in the Paleocene to Early Oligocene (Renmark Group);

2) Shallow marine carbonates with minor sand and silt deposited in the Oligocene to Mid-Miocene (Murray Group);

3) Shallow marine, marginal marine, minor fluvial and estuarine sediments (including the Loxton-Parilla Sands, Calivil Sands, Bookpurnong Formation, and Norwest Bend Formation) deposited from the Late Miocene to Early Pliocene; and

4) Lacustrine and marginal marine sediments deposited in the Pliocene to present (Blanchetown Clay, Bungunnia Limestone, Shepparton Formation, and later sediments).

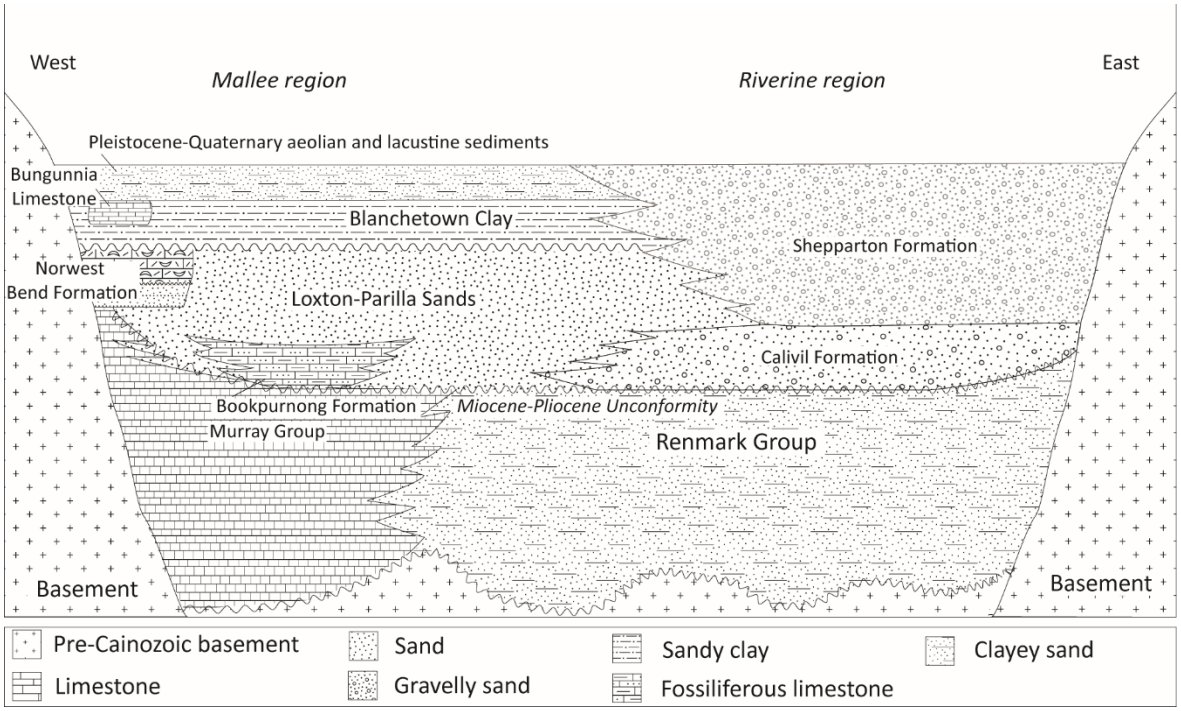

Figure 2.2 Schematic of Murray Basin stratigraphy. Modified from Miranda et al. (2009) and Brown and Stephenson (1991).

The Loxton-Parilla Sands is a composite strandplain generally 15 – 60 m thick but up to 150 m thick in parts. Early interpretations suggested ridges were underlain by extensions of the Grampians sandstone in southern Victoria (Dennant 1886, Hills 1939) or valleys created by streams (Fenner

1918). The elongate ridges were later recognised as paleo-shorelines (Blackburn 1962). The sediment package comprises shallow to marginal marine facies, interpreted to have been formed by long-period swell waves (Roy *et al.* 2000).

The lithology of the Loxton-Parilla Sands is dominated by quartz with minor feldspar and local concentrations of detrital muscovite and heavy minerals. In places, heavy mineral concentrations are of economic grade with accumulations up to 40 m thick that strike over 10-40 km (Whitehouse 2009). The heavy mineral assemblage is typically composed of rutile, ilmenite, zircon with minor spinel, xenotime, tourmaline, monazite, and leucoxene (Dickson 1999, Paine *et al.* 2004). The distribution of heavy minerals in the Loxton-Parilla Sands is strongly connected to growth faulting on basement ridges that were exposed as coastal headlands, for example the Neckarboo and Iona Ridges (Roy *et al.* 2000).

Deposition of the Loxton-Parilla Sands took place during a series of oscillatory regressions and transgressions during the Late Miocene (Roy *et al.* 2000, Miranda *et al.* 2009, McLaren *et al.* 2011). The porosity of the sands and extensive post-depositional weathering has made it difficult to determine the absolute timing of deposition of the unit. Miranda e*t al*. (2009) used Sr isotopes recovered from unaltered molluscs, such as brachiopods, pectens, and bivalves, for the first direct dating of the unit. From these results the period of deposition has been defined as starting in the northeast of the basin at 7.2 Ma to about 5.4 Ma in the southwest (Miranda *et al.* 2009, McLaren *et al.* 2011).

2.2.2 Paleotopography and possible sources

WESTERN MARGIN OF MURRAY BASIN

The western margin of the Murray Basin is bounded by the Adelaide Fold Belt, which includes the Mount Lofty and Flinders Ranges (Figure 2.1). The geology of this region includes late Proterozoic to Cambrian sediments that were deformed and metamorphosed by the Cambrian Delamerian

Orogeny and associated magmatism. Syn- and post-tectonic granites and felsic volcanics were formed from 514-485 Ma (Foden *et al.* 2002) (Figure 2.3a). The Adelaide Fold Belt extends under the sediments of the Murray Basin, eastwards to the Glenelg Zone and Grampians-Stavely Zone in Victoria. Uplift of the Mount Lofty and Flinders Ranges is relatively recent, contemporaneous with deposition of the Loxton-Parilla Sands (Sandiford 2003).

Prior to the Delamerian Orogeny a phase of Cambrian sedimentation (545-515 Ma) is recorded by the Moralana Supergroup, exposed in both the Adelaide Fold Belt and in southwest Victoria (Preiss 1982). The dominant detrital zircon age population in the Kanmantoo Group, part of the Moralana Supergroup in South Australia, is 600-500 Ma and 1200-1000 Ma (Ireland *et al.* 1998) (Figure 2.3a). Zircons in the Moralana Supergroup exposed in southwest Victoria (Steep Bank Greywacke Member) have a peak around 700 – 500 Ma, with a minor cluster around 1100 Ma, 1500 Ma, and 2500 Ma (Ireland *et al.* 2002) (Figure 2.3b).

The northwest margin of the Murray Basin onlaps the Proterozoic Curnamona Province, the oldest basement rocks proximal to the basin. The region is a fragment of Paleo- to Mesoproterozoic crust under a thin cover sequence (Preiss 2006). The Willyama Supergroup is the dominant rock package in the Broken Hill Domain in the southeast region of the Curnamona Province, the result of sedimentation and syn-sedimentary magmatism (Preiss 2006). Within the Willyama Supergroup, the Broken Hill Group hosts the giant Pb-Zn-Ag Broken Hill deposit and other smaller metallic deposits. Expected age ranges for zircons derived from this area range from 2300-1590 Ma (Page *et al.* 2005, Barovich & Hand 2008) (Figure 2.3c).

SOUTHERN AND EASTERN MARGINS OF MURRAY BASIN (WESTERN HIGHLANDS AND LACHLAN FOLD BELT)

Sediments in the southern and eastern Murray Basin onlap deformed and intruded rocks of the Adelaide and Lachlan Fold Belts, and the Grampians Group in Victoria (Figure 2.1). Later volcanics are also exposed in southwest Victoria. In western Victoria, continuation of the Adelaide

Fold Belt is divided into the Glenelg and Grampians-Stavely structural zones, both of which are largely covered by Cenozoic sediments of the Murray Basin. The Western Highlands in southwest Victoria have been recently uplifted and exposes some of these Paleozoic basement rocks (Joyce 1992).

The history of the Lachlan Fold Belt involves a complex, prolonged history of sedimentation, volcanism, and intrusion, largely defined by three tectonic cycles. Sedimentation is recorded by Ordovician turbidite fan sequences associated with the Benambran Cycle (Glen 2005) (Figure 2.3d). Thought to be formed by sediment shedding from Delamerian Orogen, zircon populations in the Ordovician turbidites are dominated by ages from 600-450 Ma with a minor component from 1200-900 Ma (Coney *et al.* 1990, Fergusson & Coney 1992, Fergusson & Fanning 2002, Williams *et al.* 2002). During the Tabberabberan Cycle (380-430 Ma) voluminous granites intruded basement from Victoria to northern Queensland (Glen 2005). S-type granites, derived from buried Ordovician turbidites, were emplaced in the western Lachlan Fold Belt around 430-410 Ma (Keay *et al.* 1999, Maas *et al.* 2001). The final cycle in the Lachlan Orogeny (Kanimblan Cycle – 320-380 Ma) is associated with extensional A-type granites, felsic volcanics, and post-tectonic I-type granites (Glen 2005).

The Glenthompson Sandstone is also exposed along the southern margin of the Murray Basin. It is a late Cambrian turbidite sequence from the late stages of the Delamerian Orogeny and is considered a correlative of the Lachlan Fold Belt turbidites. The Glenthompson Sandstone has a dominant zircon age of 600-550 Ma with minor peaks at 1200-800 Ma, and 2800-2400 Ma (Fanning & Morand 2002) (Figure 2.3e).

Deposition of the fluvial and marginal marine Grampians Group was possibly associated with deposition of the Ordovician turbidite fans. Following deposition, the Grampians Group was deformed and intruded by granites, around 420-400 Ma (VandenBerg *et al.* 2000, Morand *et al.*

2003). Some of these granitic intrusions host weakly mineralised Au veins (Cayley & Taylor 1997). Detrital zircons from the Grampians Group contain a dominant age group around 520-440 Ma, with subordinate populations at 650-600 Ma and 1300-1000 Ma (Fanning & Morand 2002) ((Previous page) Figure 2.3f). The Grampians Ranges were emergent during at least the late Cenozoic in the Murray Basin. Nearby Mount Arapiles shows shore platforms, concordant with the upper surface of the Loxton-Parilla Sands (Cayley & Taylor 1997).

Coeval with the high-level intrusion of the Grampians Group, the Rocklands Volcanics were extruded in southwest Victoria, post-dating orogenic activity in the region (Cayley & Taylor 1997, Morand *et al.* 2003). The volcanism was extensive, covering about 2000 km^2 and has been dated to 410 ± 3 Ma (Fanning 1991). At Wannon the Nigretta Ignimbrite of the Rocklands Volcanics is unconformably overlain by the Loxton-Parilla Sands.

The mafic to intermediate Coleraine Volcanics are exposed in the Western Highlands of southwest Victoria, dated by K/Ar at 191 ± 10 Ma to 153 ± 3 Ma (Morand *et al.* 2003). Total magnetic intensity results suggest the Coleraine Volcanics extend west, under the younger Murray Basin rocks, to the South Australian border (Morand *et al.* 2003).

POSSIBLE DISTAL NORTHEAST SOURCES (NEW SOUTH WALES AND QUEENSLAND)

The New England Fold Belt along the east coast of Australia coast provides a possible distal source of sediment to the basin due to the wide catchment area of the Darling River, extending into southern Queensland (Figure 2.1). Two major periods of intrusion and volcanism in the New England Orogeny occurred in the Late Carboniferous and Late Permian-Triassic (Coney *et al.* 1990, Allen *et al.* 1998, Glen 2005). There are over 100 granitic plutons associated with the southern New England Fold Belt alone (Shaw & Flood 1981).

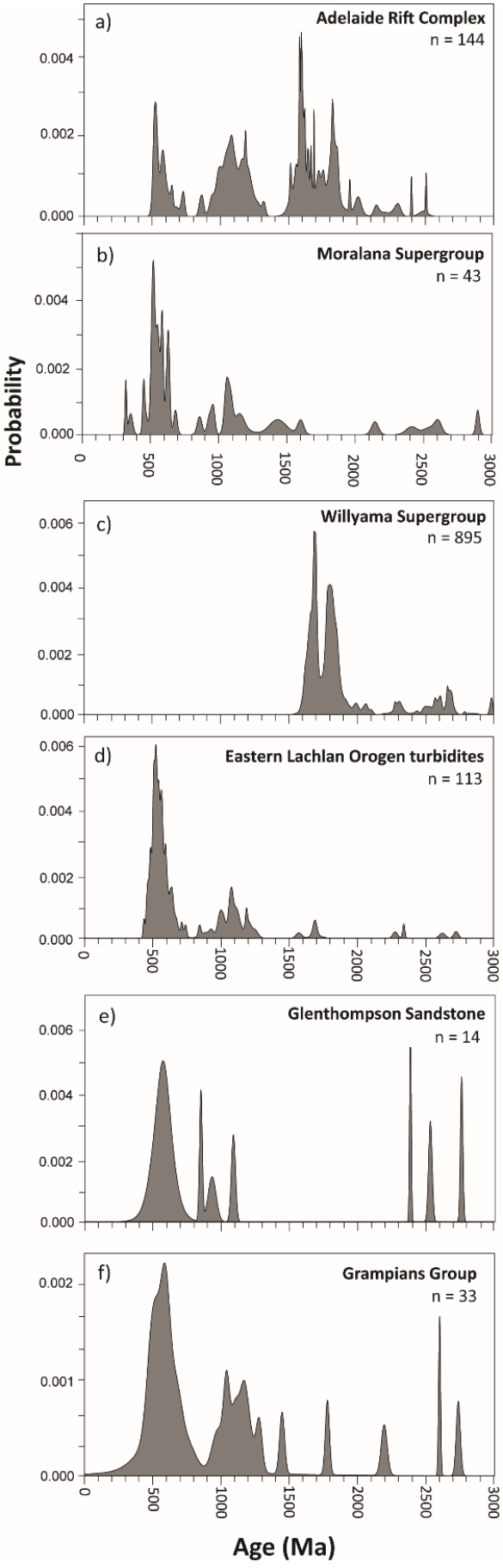
a)
Adelaide Rift Complex
n = 144
b)
Moralana Supergroup
n = 43
c)
Willyama Supergroup
n = 895
d)
Eastern Lachlan Orogen turbidites
n = 113
e)
Glenthompson Sandstone
n = 14
f)
Grampians Group
n = 33
Probability
Age (Ma)

(Previous page) Figure 2.3 Probability density distribution plots of detrital zircon ages from representative lithologies of major source terranes: a) Adelaide Rift Complex (Ireland et al. 1998, Preiss 2000), b) Moralana Supergroup (Steep Bank Greywacke Member, SW Victoria) (Ireland et al. 2002), c) Willyama Supergroup (Page et al. 2005), d) Turbidites from the eastern Lachlan Fold Belt (Bumballa Formation and Adaminaby Group) (Fergusson & Fanning 2002), e) Glenthompson Sandstone (Fanning & Morand 2002), f) Grampians Group (Fanning & Morand 2002)

2.3 METHODS

2.3.1 Whole rock geochemistry

We collected samples for geochemical analysis from vertical profiles exposed in quarries, train and road cuttings, and along the banks of the Murray River. Sample locations were chosen for ease of access and where the greatest vertical exposure was available in the region. Core and drill cutting samples were used to supplement field exposures, where there was no natural exposure or field profiles were shallow. Samples are predominantly from the upper sections of the Loxton-Parilla Sands stratigraphy. Field locations and top-of-profile elevations were recorded from GPS (MGA 94, Zone 54). Approximately 2 kg of sediment was collected at 1 m intervals in vertical profiles sections and narrower intervals if there was a noticeable change in lithology or weathering material morphology. We sampled drill cuttings and core stored in the core repositories of Geoscience Australia, and Geological Surveys of South Australia and Victoria. The sample size for drill cuttings from the Geological Surveys and Geoscience Australia was 15 g. This is the minimum sample size required by Acme Laboratories for geochemical analysis. Samples of core from the core repositories were approximately 100 g each. Drill cutting samples from the core libraries represent a minimum of 1 m because they were largely from reverse circulation or air core drilling (except for 'Horsham' bores which were fully cored). Stratigraphic logs were compiled from field observations with reference to the work of Kotsonis (1995), Miranda (2007), and Paine (2004).

All whole rock analyses were conducted at Acme Laboratories in Vancouver, Canada in seven batches over a three year period. All samples were prepared and analysed by the same methods.

Rocks were crushed and sieved to -200 mesh. Major oxides were analysed via XRF with a lithium borate/lithium metaborate fusion. Rare earth and refractory elements were analysed via ICP-MS with a lithium borate fusion and dilute acid digestion. Precious metals, base metals, and pathfinder elements were analysed via ICP-MS following Aqua Regia digestion. The elements discussed in this chapter (SiO_2, Fe_2O_3, Al_2O_3, TiO_2, Nb, Hf, La, Eu, Zr, Au, and Cu), units of measurement, and their lower limit of detection are presented in Table 1.

Quality control was managed by the use of certified reference materials (CRMs), sample splits, field duplicates, and preparation and analytical blanks. Analytical accuracy was controlled by the use of CRMs including DS8, DS9, DS10, GS311-1, GS910-4, OREAS45CA, OREAS45EA, OREAS72A, OREAS72B, OREAS76A, SY-4(D), SO-18, and CSC. The laboratory also inserts analytical blanks to track reagent contamination and preparation blanks to track contamination of crushing equipment. Systematic error, calculated by comparing the expected concentration of a CRM with the mean values of repeat analyses (Caritat & Cooper 2011), was between 90-110 % for analysed elements. Analytical precision was determined by duplicate splits of prepared samples (inserted at a rate of 1 in 8 samples) and expressed as the coefficient of variation (*CV*) which is

Element	**Units**	**LLD**
Al_2O_3	wt. %	0.01
Au	ppb	0.5
Cu	ppm	0.1
Eu	ppm	0.1
Fe_2O_3	wt. %	0.01
Hf	ppm	0.1
La	ppm	0.1
Nb	ppm	0.1
SiO_2	wt. %	0.1
TiO_2	wt. %	0.01
Zr	ppm	0.1

Table 1 Elements discussed in this chapter, units of measurement, and lower detection limit.

considered an unbiased estimate of relative error for geochemical data (Stanley & Lawie 2007). The *CV* was calculated on duplicate pairs where both analyses were above analytical detection limit. For elements discussed in this chapter, analytical precision was ±10% except for Au (18%). Sampling precision was determined by field duplicates inserted at a rate of 1 in 15 samples at random intervals and is expressed as *CV*. Despite the geochemical heterogeneity of the Loxton-Parilla Sands, particularly the ferricrete, sampling precision was good, less than 10% for most elements, except for Au (21%).

Geochemical data were processed and analysed using ioGAS (REFLEX). The correlation matrix uses the Spearman rank method, which is not influenced by outliers and has no assumptions about the distribution of data, more suited for geochemical datasets. This approach provides a more unbiased picture of element correlations from geochemical data (Grunsky 2010).

2.3.2 Geochronology

Detrital zircon U-Pb geochronology results are used from Sircombe (1999) and Paine (2004). Sircombe (1999) analysed grains from four sites in the Murray Basin by Sensitive High-Resolution Ion Microprobe (SHRIMP). Paine (2004) analysed detrital zircons from three sites by Laser Ablation Inductively Coupled Plasma Mass Spectrometry (LA-ICPMS). For a detailed description of analytical techniques and data analysis used please refer to Sircombe (1999) and Paine (2004). The WIM-150 sample came from a fine-grained, relatively low grade heavy mineral deposit. Robinvale, Hispanola, and Spring Hill are from strandline heavy mineral deposits that tend to be coarser grained. Wannon and Chetwynd samples are from quarries in the Western Highlands that expose the Loxton-Parilla Sands. For this study we interrogated the compiled data and produced probability density distribution diagrams in the AgeDisplay workbook which was developed and described in Sircombe (2004). Data for both groups of samples have been grouped into 25 million year divisions for consistency.

2.4 RESULTS

2.4.1 Major element geochemistry

The dominant elements (by volume) in the Loxton-Parilla Sands are Si (measured as SiO_2), Al (measured as Al_2O_3), and Fe (measured as Fe_2O_3) (Figure 2.4). Quartz sand is the dominant mineral while other sources of silica include zircon, muscovite, clay minerals, and microcrystalline quartz from silcretes. Iron oxide concentration in these samples varies from less than 1 wt. % to almost 80 wt. %. The highest Fe-oxide concentrations are in the weathering profile in goethite and hematite filling pore spaces. Ilmenite and leucoxene in the Loxton-Parilla Sands is also a source of Fe-oxide. Maximum Al_2O_3 values are around 20 wt. %, generally towards the top of the Loxton-Parilla Sands. Detrital muscovite also accounts for Al_2O_3. The major element geochemistry will be described in further detail in Chapter 4 of this thesis.

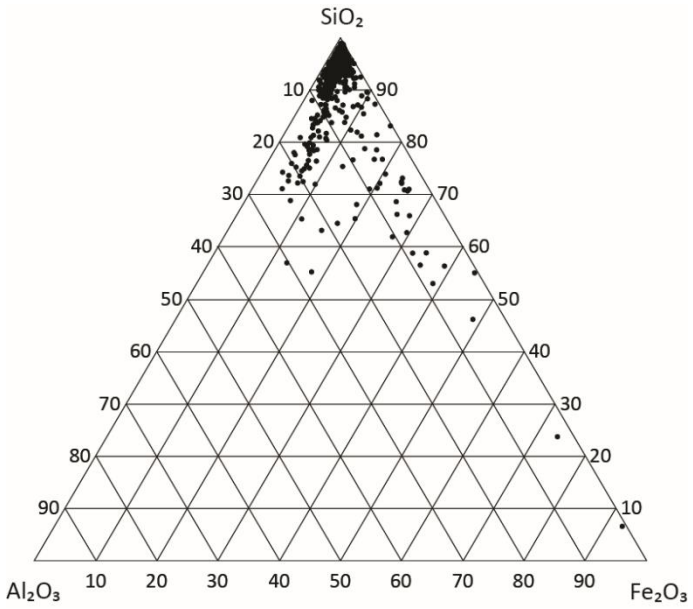

Figure 2.4 Ternary diagram of major elements (SiO_2, Al_2O_3, and Fe_2O_3) in the Loxton-Parilla Sands (603 samples).

2.4.2 Heavy minerals

Titanium is closely associated with Nb (correlation coefficient = 0.96) (Figure 2.5a) while Zr closely correlates with Hf (correlation coefficient = 0.99) (Figure 2.5b) Rare earth elements are associated with TiO_2 (correlation coefficients = 0.66 to 0.79) and Zr (correlation coefficients = 0.65 to 0.84).There are three main groups of samples that form trends in TiO_2 vs Zr, the first group is high Zr, the second group is low Zr, high TiO_2 (these samples are from the Oakvale-3 bore in South Australia), and the third group is high TiO_2 (these samples form a large proportion of the Manangatang-3 bore in Victoria) (Figure 2.5c). Titanium is also broadly associated with Fe_2O_3 (correlation coefficient = 0.53) but the trend is obscured by the presence of strongly indurated samples (high Fe), and high Zr samples (Figure 2.5d).

2.4.3 Gold

Gold concentrations in the Loxton-Parilla Sands range from below detection limit up to 60.7 ppb. The background concentration threshold for Au is 2.4 ppb (Figure 2.6) and was taken as the upper outlier threshold ($Quartile_3$ + 1.5(interquartile range)). There is no relationship between Au concentration and grain size, landscape position, or stratigraphic horizon. The correlation coefficients between Au and other elements range from -0.06 (with Fe_2O_3) up to 0.29 (with Cu).

Field duplicates were analysed to assess the repeatability of Au concentrations. Major elements were in good agreement despite inherent geochemical heterogeneity in the strongly weathered Loxton-Parilla Sands. Gold concentrations are largely non-repeatable.

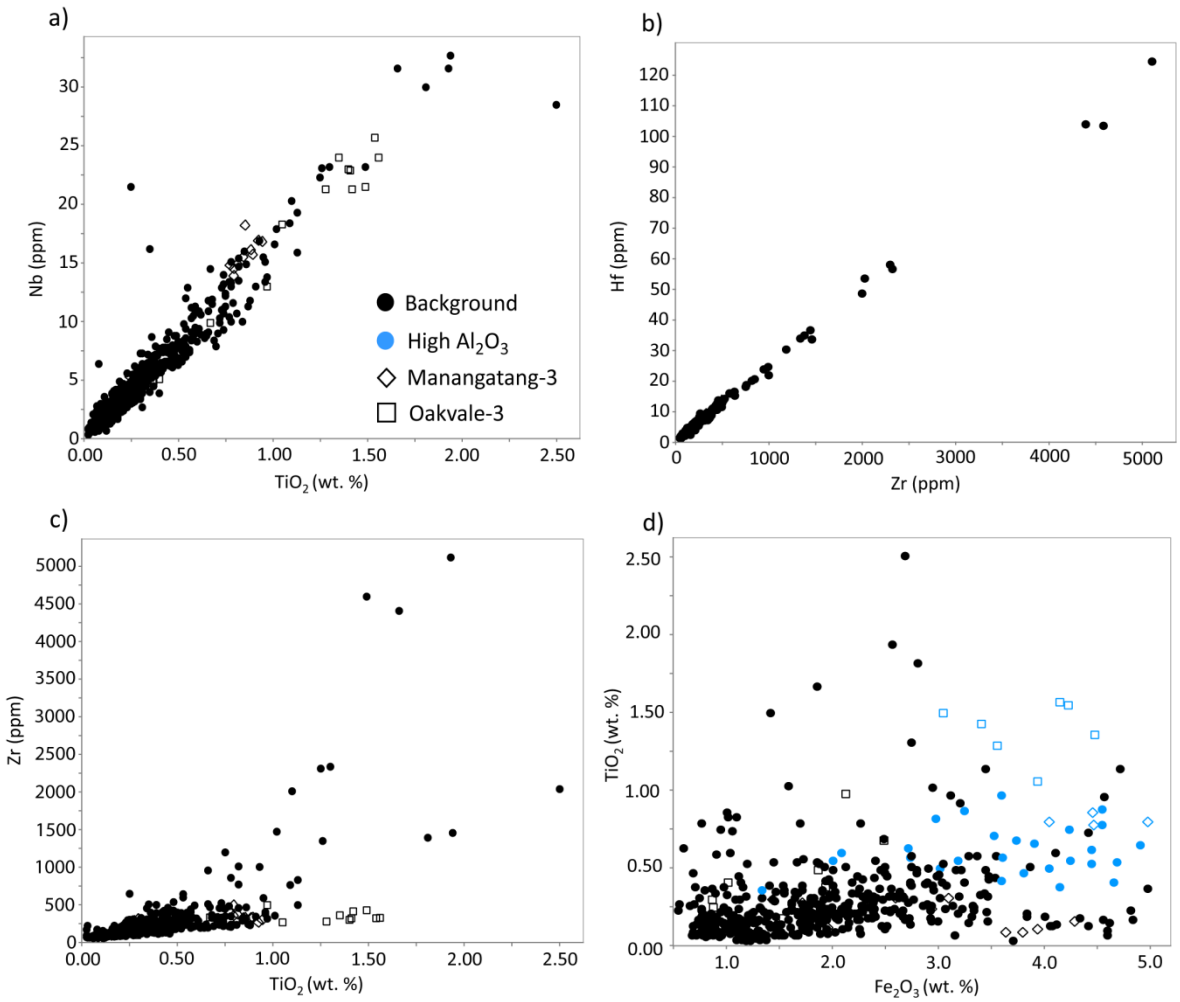

Figure 2.5 Geochemical plots of elements associated with heavy minerals, with key groups of samples highlighted –samples from the Oakvale-3 and Manangatang-3 bores that cluster more noticeably than other profiles, d) TiO_2 vs Fe_2O_3, with high Fe_2O_3 (>5 wt. %) samples removed to show broadly positive relationship with TiO_2 due to ilmenite. Blue samples are high in Al_2O_3 and include Oakvale-3 samples but not Manangatang-3 samples.

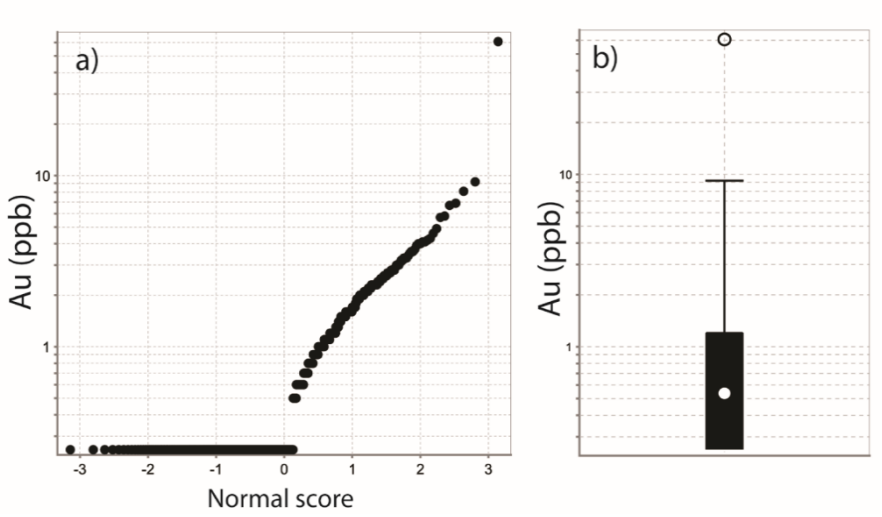

Figure 2.6 a) Probability distribution plot for Au concentration in the Loxton-Parilla Sands (603 samples). Note logarithmic scale for concentration. b) Box plot of Au concentration from the Loxton-Parilla Sands, calculated from 603 samples. The upper outlier threshold is 2.4 ppb. Maximum value = 60.7 ppb, minimum value = 0.5 ppb, 90 percentile = 2.3 ppb.

2.4.4 Geochronology

Most of the detrital zircon U-Pb ages fall into five populations (Figure 2.7):

JURASSIC-CRETACEOUS

The youngest zircon grains are found at Spring Hill, Hispanola, Robinvale, and Chetwynd. This population is completely absent from samples at Bondi, Wannon, and WIM-150. Detrital grains making up the younger population fall between about 100-210 Ma. The narrow peaks in this age population suggest discrete magmatic age populations relating to specific rocks within the source region.

PERMIAN-TRIASSIC

Grains dating to this age period are present at all sample sites but are poorly represented at WIM-150. A peak at around 300 Ma is only present at Wannon, while a cluster of grains around 245 Ma is found at Hispanola, Chetwynd, and Bondi. Zircon grains dating to 260 Ma are at most sites

(Bondi, Chetwynd, Spring Hill, Hispanola, and Robinvale). Narrow age peaks in populations of this age and younger suggest discrete source regions.

LATE ORDOVICIAN-DEVONIAN

The detrital zircon population at WIM-150 is dominated by a population at 380 Ma. It is less prominent at Bondi and Wannon and absent at other sites. Wannon and Chetwynd both have distinct peaks in zircon ages around 420 Ma, as does Bondi.

CAMBRIAN – EARLY ORDOVICIAN

There is a group of zircons with ages around 460 Ma at Bondi, Hispanola, and Chetwynd. Zircon ages ranging from around 520 Ma to 480 Ma are from Chetwynd, Wannon, Bondi, and Spring Hill. This age population at Bondi appears to be made up of more discrete dates than at other sites and could reflect a different source.

NEOPROTEROZOIC AND OLDER GRAINS

Grains with dates ranging from 600 – 520 Ma are at all sites. There is a prominent peak around 590 Ma at Robinvale, Bondi, Wannon, and Chetwynd. There are sparse zircons with low, broad peaks dating between 1200-1000 Ma and 2800-1400 Ma amongst the samples, except for Robinvale where the oldest grains are younger than 700 Ma. Mixed sources are suggested by broad population peaks.

(Next page) Figure 2.7 Detrital zircon populations from Bondi, Chetwynd, and Wannon (Paine, 2004), and Spring Hill, Hispanola, Robinvale, and WIM-150 (Sircombe, 1999). Coloured bars represent major population groupings.

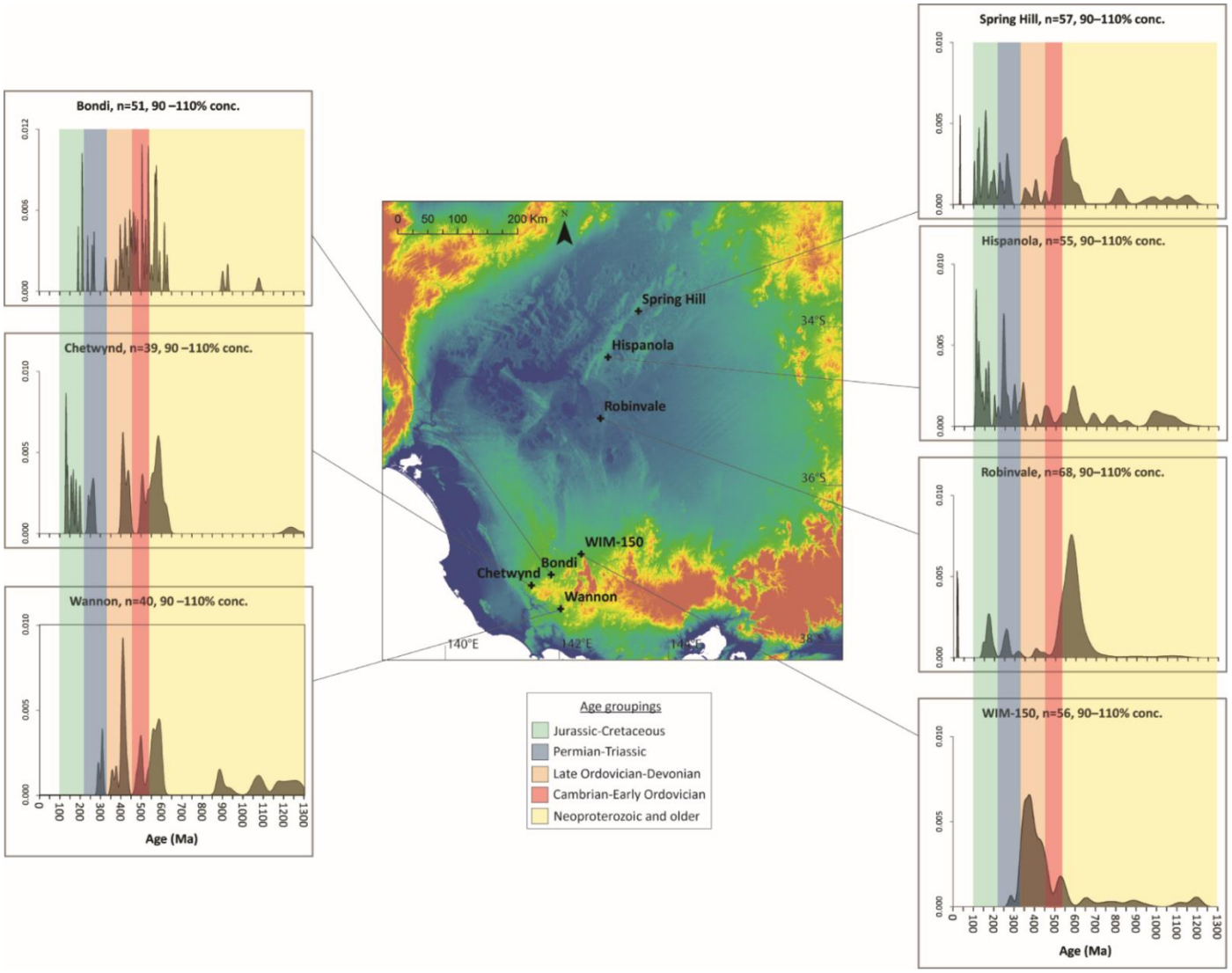
Bondi, n=51, 90 –110% conc.
Chetwynd, n=39, 90 –110% conc.
Wannon, n=40, 90 –110% conc.
Age (Ma)
0 50 100 200 Km
N
Spring Hill
Hispanola
Robinvale
WIM-150
Bondi
Chetwynd
Wannon
34°S
36°S
38°S
140°E
142°E
Age groupings
Jurassic-Cretaceous
Permian-Triassic
Late Ordovician-Devonian
Cambrian-Early Ordovician
Neoproterozoic and older
Spring Hill, n=57, 90–110% conc.
Hispanola, n=55, 90–110% conc.
Robinvale, n=68, 90–110% conc.
WIM-150, n=56, 90–110% conc.
Age (Ma)

2.5 DISCUSSION

The Loxton-Parilla Sands is considered an excellent proxy for assessing diachronous sedimentation from the Late Miocene to Pliocene (Kotsonis 1995, Miranda *et al.* 2009). The geological, particularly the magmatic, history of eastern Australia is well constrained. Consequently we have interpreted the detrital zircon age of events in light of the major orogenic events and probability of relative contribution of sediment. Previous workers have suggested a multi-stage reworking process for the Loxton-Parilla Sands and this is extended here to a basin-hinterland synthesis for the Late Cenozoic.

2.5.1 Sediment sources for the Loxton-Parilla Sands

JURASSIC – CRETACEOUS (COLERAINE VOLCANICS AND WHITSUNDAY VOLCANIC PROVINCE)

Two possible sources of Jurassic-Cretaceous age zircons are suggested to be the Whitsunday Volcanic Province in northern Queensland (Sircombe 1999) and the Coleraine Volcanics of southwest Victoria (Paine 2004). A combination of the two source regions is likely. The northern samples (Hispanola, Spring Hill, and Robinvale) are more likely to contain sediment from volcanics in Queensland while Jurassic zircons further south (Chetwynd and Bondi) are more likely to have received sediment from the Coleraine Volcanics. Volcanism in the Whitsunday Province (132-95 Ma, dominated by an event from 125-105 Ma (Bryan *et al.* 1997)), a good match for Jurassic age populations from Spring Hill, Hispanola, and Robinvale. The Whitsunday Volcanic Province is now east of the drainage divide, however, in the Cretaceous there was transport of sediment to what is now mainland Australia (Smart & Senior 1980) (Figure 2.8a). The Darling River has been active since the Late Cretaceous (Gibson & Chan 1999) and provides a mechanism for transporting volcanogenic sediment southwards from the Eromanga and Surat Basins (Figure 2.8b).

The Coleraine Volcanics are exposed in the Western Highlands near Chetwynd, having formed around 200-150 Ma (Figure 2.8b) (Morand *et al.* 2003). The proximity of the volcanics to the southern Murray Basin makes it a likely source for Jurassic-aged zircons at Chetwynd. In this sample the Jurassic zircons largely date between 200-140 Ma and are slightly too old to have come from the Whitsunday Province. Further, if the Whitsunday Province was the source of these zircons in the southern Murray Basin the population would be expected to be better represented in other southern Murray Basin samples.

PERMIAN-TRIASSIC (NEW ENGLAND FOLD BELT)

Rocks recording Permian-Triassic magmatic events are not adjacent to the Murray Basin, however, zircon age populations dating from about 350 Ma to 225 Ma correspond with the timing of granite emplacement in the New England Fold Belt. The Darling River and tributaries eroding the New England Fold Belt supplied sediment to the Murray Basin as early as the Cretaceous (Gibson & Chan 1999) where it could have been incorporated into earlier units before being reworked into the Loxton-Parilla Sands. Further, the Darling River catchment was actively eroding in the Late Miocene-Pliocene and could have supplied further fluvial sediment directly into the ocean which was reworked and deposited as the Loxton-Parilla Sands.

ORDOVICIAN-DEVONIAN (LACHLAN FOLD BELT)

The Lachlan Fold Belt borders the Murray Basin to the south and east, making it a highly likely contributor of sediment. There are over 350 mappable magmatic units as part of the Lachlan Fold Belt in just the Victorian portion (Ferguson & VandenBerg 2003) so correlation with individual plutons is difficult given the mixing of sediment in the marine depositional setting.

The Rocklands Volcanics crop out in the Western Highlands in southwest Victoria and are a likely proximal source of sediment for the southern Murray Basin. The Western Highlands, however, were only partly emergent during the Miocene and preservation of the Permian Bacchus Marsh Formation suggests there has not been major erosion since the Mesozoic (Joyce *et al.* 2003). There

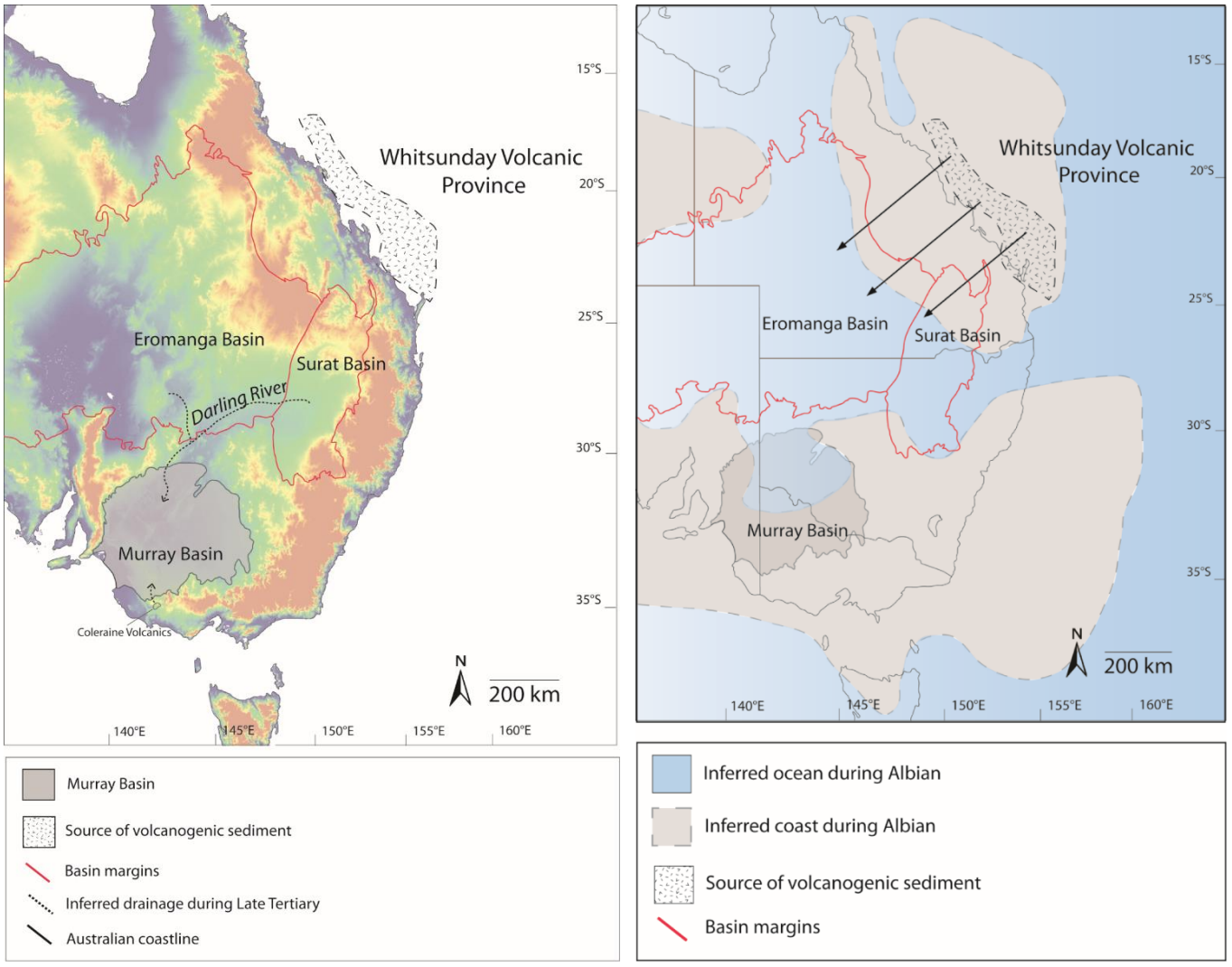
Whitsunday Volcanic Province
Eromanga Basin
Surat Basin
Darling River
Murray Basin
Coleraine Volcanics
15°S
20°S
25°S
30°S
35°S
140°E
145°E
150°E
155°E
160°E
N
200 km
Murray Basin
Source of volcanogenic sediment
Basin margins
Inferred drainage during Late Tertiary
Australian coastline
Inferred ocean during Albian
Inferred coast during Albian
Source of volcanogenic sediment
Basin margins

(Previous page) Figure 2.8 Inferred coastline of Gondwana during the Albian (~112-98 Ma, adapted from Frakes et al. (1987) and the migration of volcanogenic sediment from the Whitsunday Volcanic Province into the Eromanga and Surat Basins (after Bryan et al. (1997), b) Eastern Australia during the late Tertiary as the Darling River brings sediment eroded from the Eromanga and Surat Basins southwards to the Murray Basin. The Whitsunday Volcanic Province is now on the other side of the drainage divide.

is an unconformity between the Loxton-Parilla Sands and underlying Nigretta Ignimbrite (part of the Rocklands Volcanics) exposed at Wannon, however, field observations suggest the volcanics were weathered at the same time as the sands. This explains why the detrital zircon signature of the Rocklands Volcanics makes up a small proportion of Devonian-aged zircons in the southern Murray Basin. During the Miocene this region was relatively low-lying and would not have been a major source of sediment.

A cluster of zircons around 360 Ma (Devonian peak) is most prominent at the WIM-150 site. The WIM-150 deposit is fine grained compared to other heavy mineral accumulations. The hydraulic behaviour of heavy minerals changes with grain size (Rubey 1933) but it is not clear why this would preferentially fractionate a particular zircon population.

CAMBRIAN (DELAMERIAN OROGENY)

Plutons from syn- and post-tectonic magmatism of the Delamerian Orogeny are exposed on the western and south eastern margins of the Murray Basin. Syn-tectonic granites, such as the Wando Tonalite and Loftus Creek Granodiorite, of the Delamerian Orogeny are exposed in the Western Highlands (Ireland *et al.* 2002). The Fleurieu Peninsula south of Adelaide contains Late Cambrian syn-orogenic granites and Early-Mid Ordovician post-orogenic granites associated with the Delamerian Orogeny (Foden *et al.* 2002). Both groups of granites as well as the Kanmantoo Group are likely sources for Cambrian zircon grains with Miocene-Pliocene longshore drift moving sand in a southwest-direction. Data to discriminate sediment input from the Moralana Supergroup in

Victoria and South Australia is needed. Detrital zircon studies from further west in the Murray Basin could show the extent of sediment input from the Adelaide Fold Belt.

NEOPROTEROZOIC AND OLDER POPULATIONS

The 700-500 Ma detrital zircon population is common throughout sediments of eastern Australia, from Ordovician turbidites to Triassic sandstones (Veevers 2015). The Transgondwanan Supermountains associated with the East African-Antarctic orogeny has been identified as the likely source for most of this population, based on Hf-isotope T_{DM} model ages with a subordinate contribution from the Gamburtsev Subglacial Mountains (Veevers *et al.* 2006, Veevers 2015). There are several intermediate repositories of this zircon population including the Moralana Supergroup and Kanmantoo Group, the Grampians Group, and the Ordovician turbidites of the Lachlan Fold Belt. Paine (2004) suggests the Grampians Group or Moralana Supergroup as intermediate repositories for zircons dating to older than 550 Ma. During deposition of the Loxton-Parilla Sands the Grampians were already uplifted and exposed throughout the marine transgression (Cayley & Taylor 1997). Given the exposure of the Adelaide Fold Belt, Moralana Supergroup, Grampians Group, and Lachlan Fold Belt during formation of the Murray Basin all of these lithologies are suggested as contributors of sediment to the Loxton-Parilla Sands. Further detrital zircon studies from the western Loxton-Parilla Sands could help to constrain the sediment contribution from South Australian and Victorian exposures.

There are few grains older than 1300 Ma in these samples from the Murray Basin, suggesting little detrital input from the Curnamona Province. The presence of age populations from the late Paleoproterozoic would indicate sediment contribution from the Broken Hill Domain and Willyama Supergroup (Page *et al.* 2005). Drainage channels draining the Barrier Ranges in the Curnamona Province drain towards the Darling River and Menindee Lakes and are a likely source of sediment in the northwest Murray Basin (Hill *et al.* 2003). It could be that this sediment was deposited only a short distance from the ranges. If drainage along this margin of the basin was

sluggish, sediment would not be transported hundreds of kilometres to where the Spring Hill, Hispanola, and Robinvale samples were taken and probably did not pass the ancient Darling River outlet on the coast.

2.5.2 Heavy minerals and muscovite

Heavy minerals are an important detrital component of the Loxton-Parilla Sands. The mineralogy controls some SiO_2 (zircon) and Al_2O_3 (muscovite, tourmaline) content and most of the TiO_2, Zr, Hf, Nb, and rare earth element concentrations in the unit (ilmenite, rutile, zircon, tourmaline, monazite). Variations in the assemblage through the strandplain result are evident in trace element associations. Multiple trends with elements such as Ti, Zr, and Fe are due to shifting proportions of zircon, rutile, and ilmenite. Titanium (in rutile and ilmenite) is very well correlated with Nb and has strong associations with rare earth elements. Zircon is very strongly linked to Hf (substituting for Zr) as well as rare earth elements. Results of the whole rock geochemistry suggest three dominant heavy mineral and Fe-oxide assemblages: a) rutile and zircon dominated with lesser ilmenite, b) rutile, zircon, and ilmenite dominated and associated with Fe-oxide induration, and c) low heavy mineral content, dominated by Fe-oxide induration.

Some relatively unweathered profiles have geochemical complexity introduced by variable heavy mineral assemblages and clay minerals. Manangatang-3 and Oakvale-3 samples have high clay contents. Titanium and MgO anomalies in these samples suggest tourmaline as well as rutile is part of the heavy mineral assemblage. Tourmaline is a more prominent component of the heavy mineral assemblage in the southern Murray Basin (Roy *et al.* 2000) and is found in a number of fine-grained heavy mineral deposits like WIM150 (Olshina & van Kann 2012). Tourmaline has a lower density than rutile and zircon and tends to be concentrated in lower energy facies, such as the surf and shoaling zones, rather than the breaker zone (Paine *et al.* 2005). The whole rock geochemistry suggests several variations in heavy mineral facies and mineral chemistry between sites, For

example, Oakvale-3 facies have high-Ti tourmaline in addition to rutile, Manangatang-3 samples have low Ti-tourmaline, while the RC86KI-1 samples have high Fe tourmaline.

Detrital zircon ages and the scale of sediment transport in the Murray Basin shows that there is not one single source of heavy minerals and muscovite for the Loxton-Parilla Sands. Studies of ilmenite in heavy mineral deposits in the Murray Basin suggest two stages of alteration; an initial stage of weathering in the source region then further degradation following deposition in the Loxton-Parilla Sands (Pownceby 2005, 2010). Whole rock geochemistry results suggest heavy mineral assemblages tend to vary on a regional scale with minor local variations likely due to fractionation in local depositional environments, a similar outcome to the detailed analysis of Paine *et al.* (2005). The detrital zircon populations show, however, that the first order control on the detrital mineralogy of the Loxton-Parilla Sands is erosion of source regions and the activation of fluvial transport pathways.

2.5.3 Gold exploration

The discrete nature of Au geochemical results suggests that it has been eroded and reworked from Au-bearing basement in the south of the Murray Basin, including Stawell and Bendigo, and also numerous auriferous intrusions in the Lachlan Fold Belt. Figure 2.9 shows the proportion of whole rock analyses from the Loxton-Parilla Sands with Au > 2.4 ppb (above background) compared to the total number of samples in each profile with detectable Au. It suggests that where Au is present in the sediment, higher values tend to occur in the southeast of the Murray Basin, adjacent to the Lachlan Fold Belt and Victorian Western Highlands. Alluvial workings have been a significant source of Au in Victoria since the 19th century and the primary source of some placer deposits has been difficult to determine (Birch 2003). Gold is not associated directly with heavy mineral accumulations in the Loxton-Parilla Sands due to the different hydraulic behaviour of heavy mineral grains and particulate Au (Rittenhouse 1943). Mechanical dispersion of Au shows the potential transport distance for sediments from source regions. Poor association with heavy mineral

concentrations, however, further shows the strongly influence of slight differences in density and entrainment properties (e.g., tourmaline and zircon) to affect fractionation in local depositional environments during reworking and up-grading.

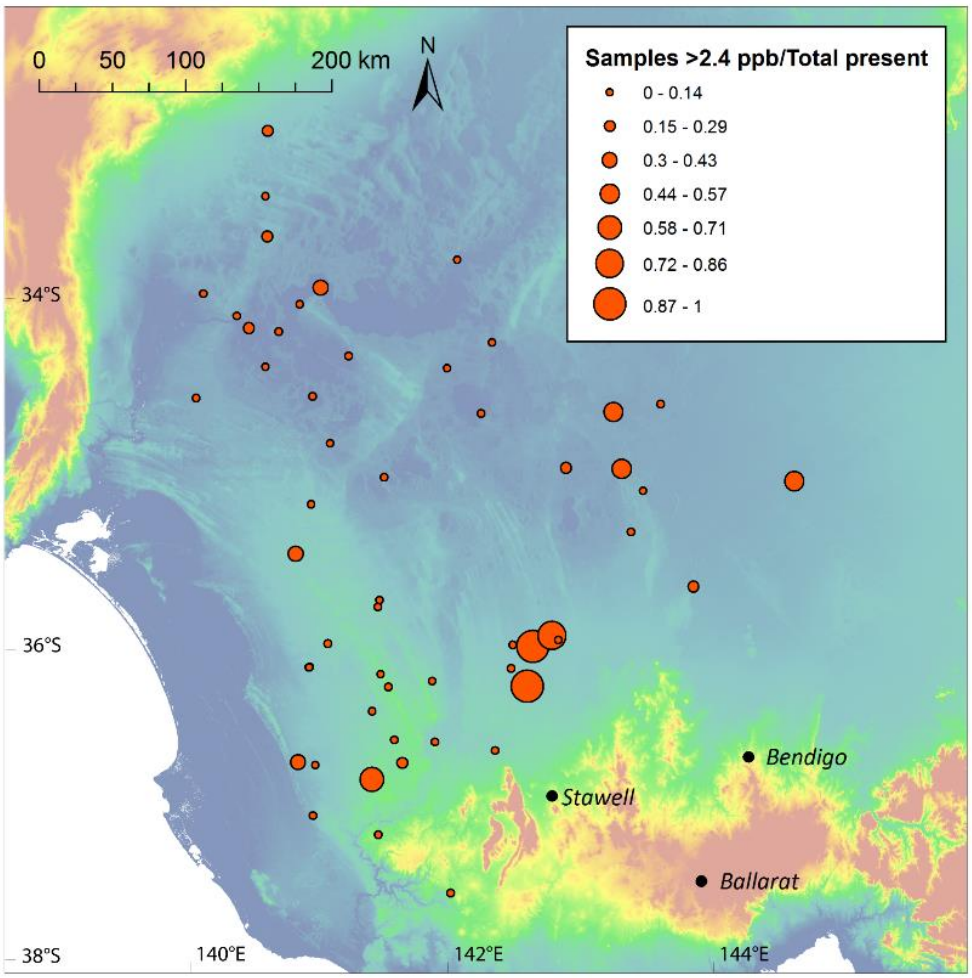

Figure 2.9 Distribution of Au concentrations across the Loxton-Parilla Sands calculated from whole rock analyses of 596 samples of the Loxton-Parilla Sands. Ratio represents the proportion of samples with > 2.4 ppb Au (above background concentration) relative to the number of samples in each profile with detectable Au. It suggests that higher concentrations of Au tend to occur in proximity to the Lachlan Fold Belt.

2.5.4 Provenance and Paleogeography Implications

Multiple sediment sources for the Loxton-Parilla Sands have long been suggested (Besley & Plimer 1999, Roy *et al.* 2000) but it is only now by combining the detrital zircon geochronology of Sircombe (1999) and Paine (2004) that the range of proximal and distal sources of sediment can be recognised. Longshore drift and barrier stacking during deposition might be expected to homogenise the detrital zircon signature of source regions. Instead the diachronous deposition of the Loxton-Parilla Sands has controlled the distribution of detrital zircon.

Roy *et al.* (2000) suggest two ways in which sediment was incorporated into the Loxton-Parilla Sands in the Late Miocene-Pliocene:

1. Sediment was deposited in the Murray Basin in the mid Cenozoic as part of the fluvial Olney Formation (Upper Renmark Group). This unit then formed the base of a gulf during the Late Miocene-Pliocene marine transgression. The Olney Formation was reworked and heavy mineral sands concentrations were upgraded to form beach placer deposits in the Loxton-Parilla Sands. Or,
2. Sediment was introduced to the continental shelf during the Late Miocene-Pliocene marine transgression by various drainage systems and contemporaneously reworked into the Bookpurnong Formation and Loxton-Parilla Sands.

It is likely that reworking of the Olney Formation occurred during the early stages of the marine regression as it formed the base of the gulf during this time. Heavy minerals in the Olney Formation could have been reworked and effectively up-graded into heavy mineral deposits in the northern Murray Basin (Roy *et al.* 2000). Given the uplift of the highlands in eastern Australia occurred by the Cenozoic (Veevers 1984) it is likely that sediment for the Olney Formation was sourced from similar regions to the later Loxton-Parilla Sands, except for the Adelaide Fold Belt which was not yet uplifted. A comparative detrital zircon study of the Loxton-Parilla Sands and Olney Formation could show if reworking of sediment occurred. Systematic sampling of the Loxton-Parilla Sands from the northeast-southwest and also with samples in the western Murray

Basin could resolve the input of sediment from the Adelaide Fold Belt and Curnamona Province and progressive changes in sediment source.

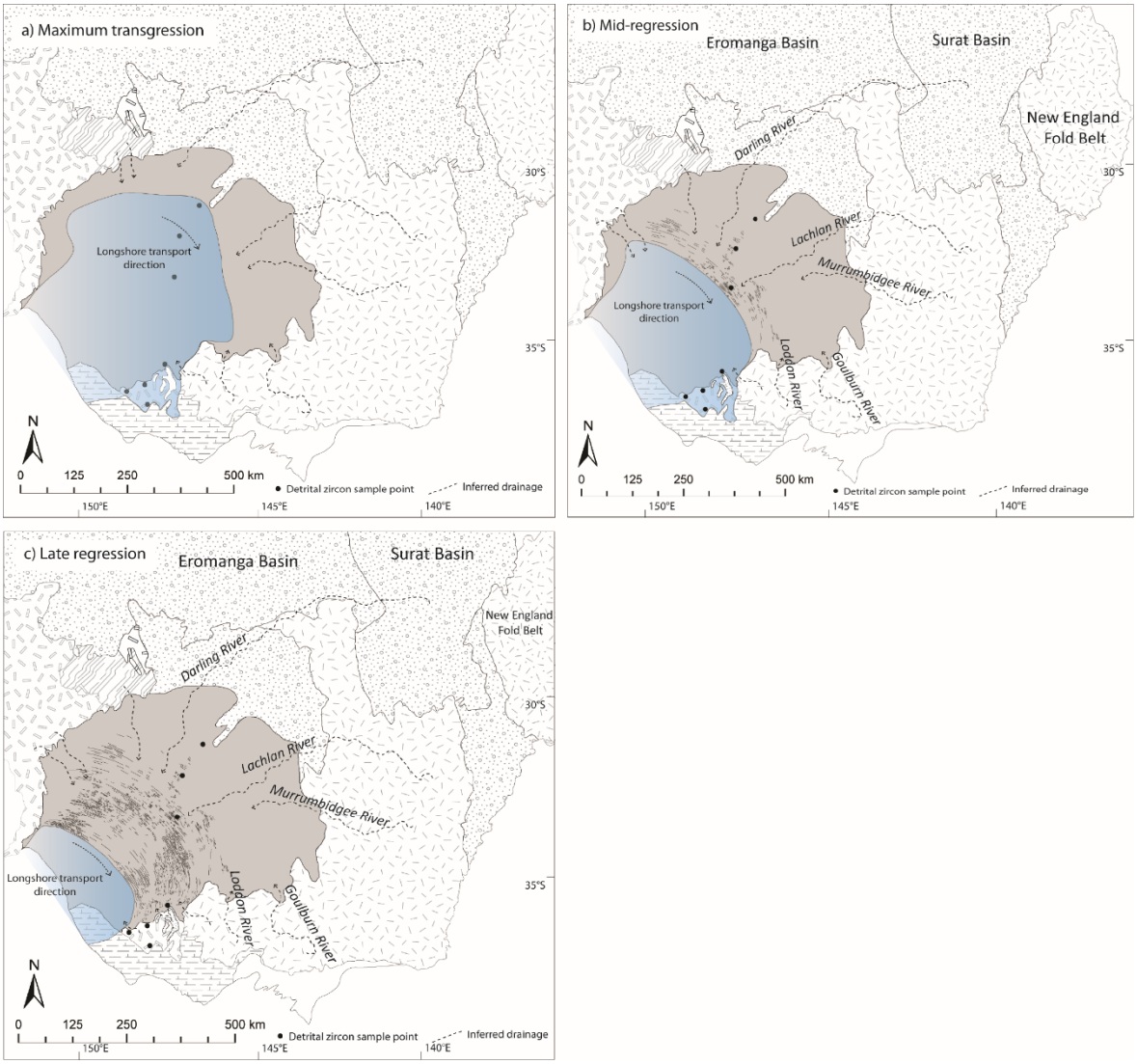

Figure 2.10 Time series showing progressive deposition of the Loxton-Parilla Sands over the Late Miocene-Pliocene and introduction of sediment sources. a) Maximum transgression (mid-Miocene) b) Mid-regression (late Miocene), c) Late regression (Early Pliocene). Strandlines are adapted from Miranda et al. (2009).

The detrital zircon populations in the Loxton-Parilla Sands are controlled by the progressive introduction of drainage channels as the ocean regressed in the Late Miocene to Pliocene. Figure 2.10a shows that at the maximum transgression in the Miocene the only active sediment sources were the New England Fold Belt, the Eromanga and Surat Basins, the northern Lachlan Fold Belt

and the Curnamona Province to the west. At this stage the Western Highlands and southern Lachlan Fold Belt were largely submerged and would not have been supplying sediment to the northern Murray Basin. Further, the Mount Lofty and Flinders Ranges on the western margins were not uplifted. As the ocean regressed and the western margin was uplifted, more sediment sources become viable in the Loxton-Parilla Sands (Figure 2.10b). Towards the end of the marine regression in the late Pliocene (Figure 2.10c) regions including the southern Lachlan Fold Belt, the Grampians Group, lithologies exposed on the Western Highlands, and the Adelaide Fold Belt as well as the New England Fold Belt and Eromanga and Surat Basins were acting as sediment sources.

2.6 CONCLUSIONS

Assessment of a compilation of detrital zircon results for the Loxton-Parilla Sands shows that sediment has been sourced from terranes adjacent to the Murray Basin as well as distally, undergoing multiple phases of reworking. The major proximal sources of sediment are plutons associated with the Delamerian and Lachlan Orogenies with input from intrusions in the distal New England Fold Belt and Whitsunday Volcanic Province. Where sediment is deposited near the highlands the zircon population is controlled by local fluvial and landscape processes. The diachronous deposition of the strandplain means that not all source regions were contributing sediment contemporaneously. The distribution of zircon populations towards the centre of the basin is controlled by longshore drift and reworking of sediment prior to deposition. Distinguishing sediment contributions from the South Australian and Victoria exposures of the Adelaide Fold Belt is difficult given their similar ages but could be resolved with further isotopic data. Detrital zircon studies from the western Loxton-Parilla Sands could help to constrain longshore drift and sediment transport. Gold is part of the detrital component of the sediment, like zircon, but its different entrainment properties compared to heavy minerals mean Au is not strongly associated with heavy mineral accumulations.

Chapter 3 Neogene Paleodrainage evolution and neotectonism in the western Murray Basin, southeast Australia from 3D modelling of the Loxton-Parilla Sands

FOREWARD

Based on the results of the 3D geometry of the Loxton-Parilla Sands and associated Neogene units I have inferred the likely drainage channels that supplied sediment to the coast during the Miocene-Pliocene marine regression. This sediment was reworked into the Loxton-Parilla Sands. The 3D model in this chapter was the result of, in part, digitising an archival stratigraphic database from the Bureau of Mineral Resources (now Geoscience Australia) and generating the first 3D geological model for the entire Murray Basin. The BMR database was created in the 1980s and has not been used since; existing only as poorly quality scans of microform records. In addition to the paleogeographical and sedimentation implications, I think the results of this chapter show the potential that exists for historical datasets to provide new insights to Australian geology. This chapter is written as a manuscript that will be a submission to the *Australian Journal of Earth Sciences.* My co-authors will be Prof. David Giles who assisted in conception of the project and interpretation of isopachs, Simon van der Wielen who helped in the quality control of the compiled stratigraphy and assisted with creating the model in GOCAD® and Dr Steven Hill who assisted with manuscript revision.

Statement of Authorship

Title of Paper	Neogene Paleodrainage evolution and neotectonism in the western Murray Basin, southeast Australia from 3D modelling of the Loxton-Parilla Sands
Publication Status	○ Published, ○ Accepted for Publication, ○ Submitted for Publication, ◉ Publication style
Publication Details	

Author Contributions

By signing the Statement of Authorship, each author certifies that their stated contribution to the publication is accurate and that permission is granted for the publication to be included in the candidate's thesis.

Name of Principal Author (Candidate)	Stephanie McLennan
Contribution to the Paper	Project conceptualisation, data collection and processing, data interpretation, manuscript design and composition, and generation of figures and tables.
Signature	Date: 28·10·2015

Name of Co-Author	Prof. David Giles
Contribution to the Paper	Supervised development of work, helped in data interpretation and manuscript revision.
Signature	Date: 29-10-15

Name of Co-Author	Simon van der Wielen
Contribution to the Paper	Assisted with data QA/QC and modelling workflow and generation.
Signature	Date: 29/10/15

Name of Co-Author	Dr Steven Hill
Contribution to the Paper	Manuscript revision.
Signature	Date: 29-10-15

ABSTRACT

This study presents a 3D geological model of the Neogene units of Murray Basin, in southeastern Australia, to model the stratigraphic geometry and infer paleodrainage courses. We compiled data from over 8000 drill holes to model the geometry of basin stratigraphy, particularly the Late Miocene to Pliocene Loxton-Parilla Sands. The model shows curvilinear depocenters in the Loxton-Parilla Sands, with widths of approximately 50km and a broadly meandering pattern which we interpret as paleodrainage, active during the Neogene. These features are continuous with similar depositional features in the Calivil Formation, the time equivalent fluvial counterpart of the Loxton-Parilla Sands. The inferred drainage patterns in the Murray Basin have interacted with reactivated faults and have undergone significant reorganisation since the Late Miocene. The Murray River, between Balranald and Loxton, has moved north by up to 80km. The Loddon and Goulburn Rivers have remained relatively stable. Model results also suggest a major confluence of a southeastern-draining system west of Ouyen which then drained to the Southern Ocean. The evolving drainage pattern has been strongly influenced by relative displacement on north to north-east trending basement structures along with broad uplift of the Padthaway Ridge and the Western Highlands. The results provide insight into the sensitivity of drainage patterns to tectonics in regions of low topographic relief.

KEYWORDS

Murray Basin, paleodrainage, basin analysis, neotectonism, 3D model

3.1 INTRODUCTION

Sediments in the Murray Basin form a well-preserved record of Cenozoic marginal marine and continental depositional environments, covering some 300,000 km^2 of south eastern Australia (Figure 3.1). The Loxton-Parilla Sands are a regressive strandplain, consisting of predominantly marginal marine and lesser fluvial sediments, deposited during a retreat of sea level between 7.2 Ma and approximately 5.0 Ma (Miranda *et al.* 2009). Similar sequences exist in Brazil (Dominguez & Wanless 2009, Hein *et al.* 2013), Denmark (Tanner 1993), and the Gulf of Mexico (Tanner 1992). Such systems have been studied extensively because of their importance as facies models in hydrocarbon systems (Tyler & Ambrose 1986), as near surface aquifers (Wallis *et al.* 1991, Dunbar *et al.* 1992), for their heavy mineral sands potential (Swift *et al.* 1971, Roy 1999), and as a sensitive record of eustasy, tectonics and isostasy (Fraser *et al.* 2005, Hein *et al.* 2013). Isostatic subsidence due to sediment loading has been minimal in the Murray Basin due to the relatively thin sedimentary sequence and low sedimentation rates (Brown & Stephenson 1991). As a result, neotectonism and eustasy are the dominant controls on the deposition of the Loxton-Parilla Sands and other Late Neogene units within the Murray Basin.

The depositional setting and sedimentary facies of the Loxton-Parilla Sands have been the subject of a number of publications (Brown & Stephenson 1991, Kotsonis 1995, Roy *et al.* 2000, Paine *et al.* 2004, Bowler *et al.* 2006, Miranda *et al.* 2009, Robson & Webb 2011). Such studies have looked at the marginal marine depositional environment of the Loxton-Parilla Sands and the preservation of neotectonism and eustatic change (Bowler *et al.* 2006, Miranda *et al.* 2009) as well as their significance for accumulation of heavy mineral sands (Roy *et al.* 2000, Paine 2005). Questions still arise, however, about the path of the ancient Murray River, the geography of the western Murray Basin and associated coastal and fluvial environments, and the extent of neotectonic influence. In this study we build on the current understanding of the Neogene stratigraphy and create a picture of the fluvial systems and associated sediment transport through time.

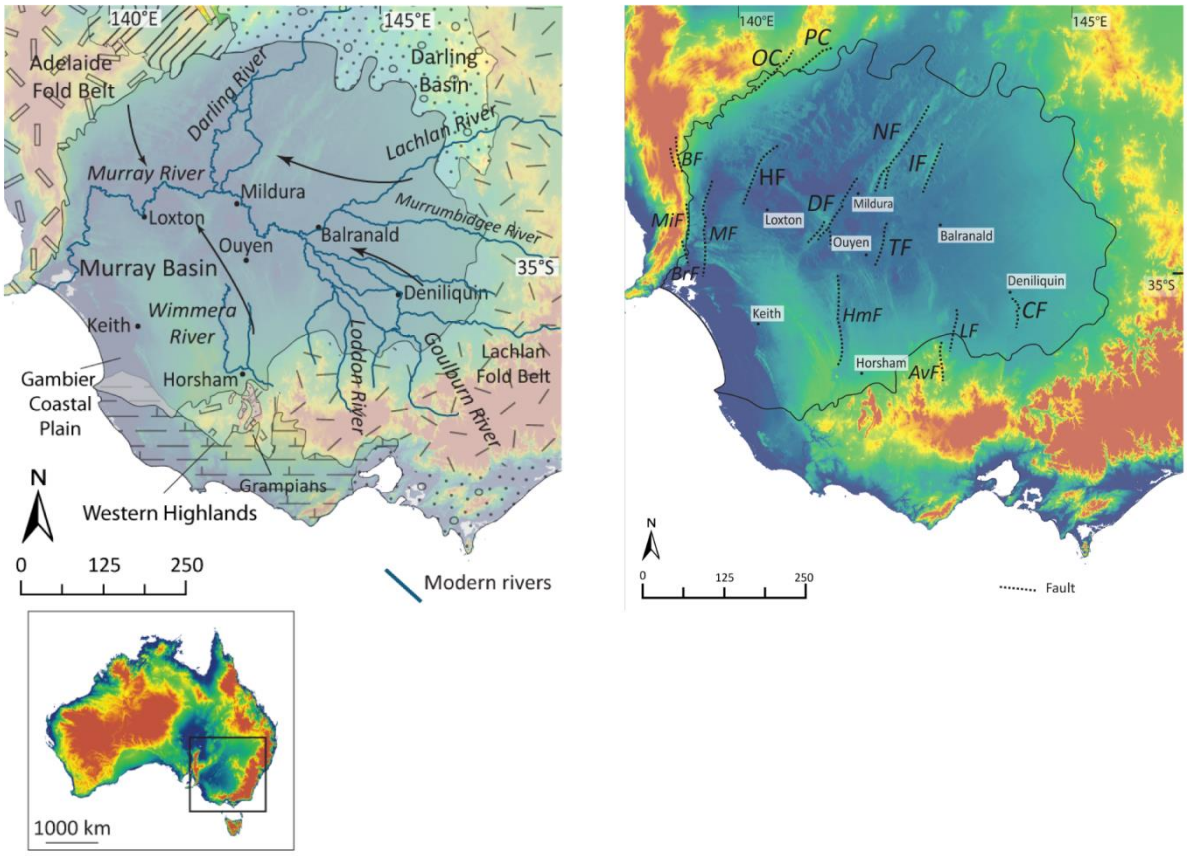

Figure 3.1 Study location in the Murray Basin, SE Australia. Modern groundwater flow lines and major rivers are shown. Background is the 1 second digital elevation model (Geoscience Australia), b)Major faults in the Murray Basin, OC – Olary Creek Fault, PC – Pine Creek fault, MF – Morgan Fault, HF – Hamley Fault, NF – Neckarboo Fault, DF- Danyo Fault, IF – Iona Fault, TF – Tyrrell Fault, AvF – Avoca Fault, LF – Leaghur Fault, CF – Cadell Fault (Neotectonics Database).

We compiled a database of over 8000 stratigraphic drill holes and field observations to produce the first 3D model of the entire Murray Basin. By modelling the large-scale geometry of sedimentary units we are able to infer likely rivers draining the Murray Basin and supplying clastic sediment to the ancient gulf, reworked into the Loxton-Parilla Sands. The results of the model reveal how paleodrainage systems interacted with reactivated faults and the significance of Pre-Cenozoic basement topography and structure in shaping Cenozoic sedimentary deposits. By developing a regional geological model we can better understand the structural and stratigraphic architecture of the Murray Basin, in particular the Neogene marginal marine and fluvial sediments.

3.2 GEOLOGICAL SETTING

3.2.1 Stratigraphy

The Murray Basin is a saucer-shaped intracratonic basin in southeastern Australia (Figure 3.1). The basin contains a sediment package 200-600 m thick that includes fluvial, lacustrine, and marine sands, gravel, and limestone. Sediments were deposited over four major eustatic depositional cycles from the Late Cretaceous to the Pliocene (Brown & Stephenson 1991) (Figure 3.2). The Loxton-Parilla Sands is an informal name referring to the composite strandplain comprising the Loxton Sand and Parilla Sand, covering 140,000 km^2 of the western Murray Basin (Brown & Stephenson 1991). Early interpretations suggested ridges were underlain by extensions of the Grampians sandstone in southern Victoria (Dennant 1886, Hills 1939) or valleys created by streams (Fenner 1918). The elongate ridges were later recognised as paleo-shorelines (Blackburn 1962). The Loxton-Parilla Sands consist predominantly of marginal marine facies with minor fluvial facies, and an upper surface comprised of a series of parallel to sub-parallel arcuate sand ridges that have been interpreted as paleoshorelines (Blackburn 1962, Colwell 1976, Brown & Stephenson 1991, Kotsonis 1995, Rogers *et al.* 1995) and beach ridges (Miranda *et al.* 2009). These sand ridges have been interpreted as the result of transgression-regression cycles over 20 Ka periods, related to Milankovitch cycles (Roy et al 2000). These cycles were superimposed on marine regression between 7.2 Ma and 5.4 Ma (Miranda *et al.* 2009, McLaren *et al.* 2011).

3.2.2 Faulting and neotectonism

The influence of pre-Cenozoic basement structures in shaping drainage systems of the Murray Basin been recognised for some time (Brown *et al.* 1988). Faulting in the Murray Basin is dominated by NE-SW trending basement faults (Lachlan Fold Belt) (Figure 3.1b), reactivated under intraplate compressional stress (Clark *et al.* 2011). The current stress regime was established in the Late Miocene in response to renewed activity along the Australian-Pacific plate boundary (Coblentz *et al.* 1995, Dickinson *et al.* 2001, Sandiford 2003, Hillis *et al.* 2008). Activation of

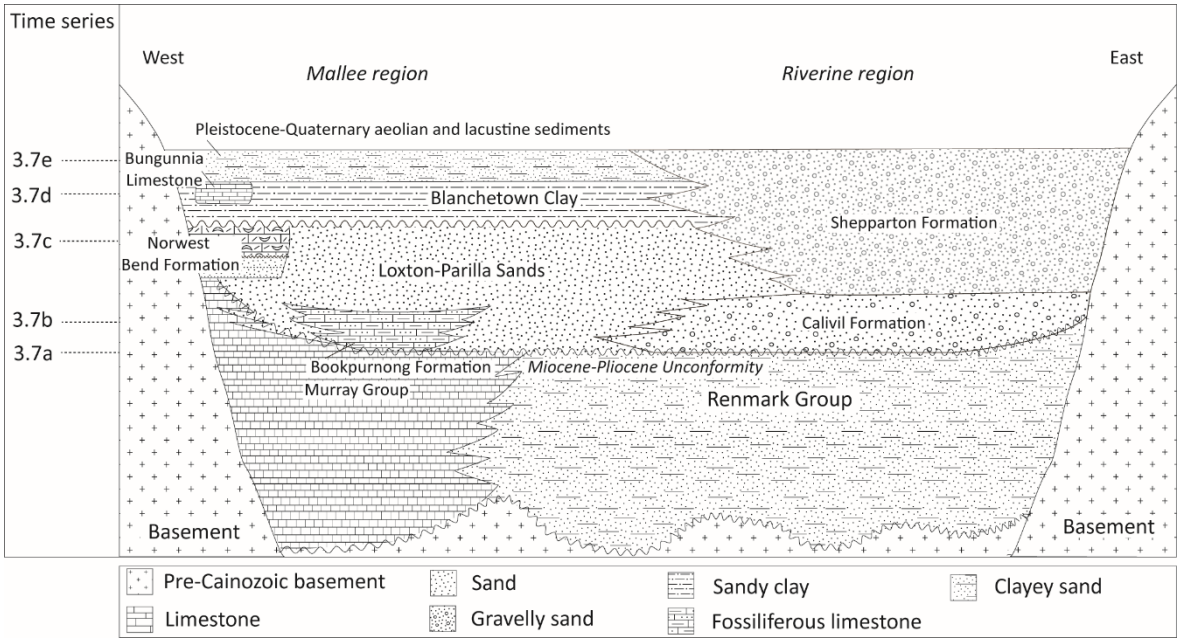

Figure 3.2 Cenozoic stratigraphy of the Murray Basin (after Brown and Stephenson 1991). Numbers on the left indicate position of time-series in Figure 3.7.

structures on the western margin of the Murray Basin associated with uplift of the Mount Lofty Ranges directed the Murray River into its contemporary southerly course (Stephenson & Brown 1989). Avulsion of the Murray River is also evident south of Deniliquin (Figure 3.1a) where recent (from 70 ka) uplift along the Cadell Fault diverted the river north (Edward River) and south (Clark *et al.* 2007).

3.2.3 Modern rivers and paleodrainage

Early interpretations of the course of the lower Murray River suggested a long-lived drainage system, around its present location in eastern South Australia, active for millions of years (Ludbrook 1961, Firman 1972, Twidale *et al.* 1978, Brown & Stephenson 1991, Pufahl *et al.* 2004). More recent research has suggested the Murray River has only been flowing through western South Australia since the Pleistocene (Bowler *et al.* 2006, Miranda *et al.* 2008).

In western Victoria an incised channel known as the Douglas Depression (Figure 3.1b) (Brownbill *et al.* 1995) hosts the north-flowing Wimmera River. Long recognised as a post-Miocene

paleodrainage system (Hills 1939, Blackburn 1962), recent interpretations suggest the Douglas Depression was incised by a south-flowing river in the early to late Pliocene, incising the Loxton-Parilla Sands (McLaren *et al.* 2011). The river then was blocked leading to the formation of the enormous Lake Bungunnia (Miranda *et al.* 2009). Sedimentation in this trough is thought to be controlled by basement topography, the Dimboola High (Brownbill *et al.* 1995, Radke & Howard 2007). McLaren *et al.* (2011), however, suggest movement along the 'Hindmarsh Fault' initiated drainage. This feature is poorly constrained, however, and is probably not a structural feature (Moore 1996, Clark 2012).

Provenance of sediment in the Loxton-Parilla Sands varies across its extent likely due to changes in drainage and uplift of source regions (this thesis – chapter 2). Detrital zircon analysis is consistent with clastic sediments sourced from the Adelaide Fold Belt, Lachlan Fold Belt, New England Fold Belt, Whitsunday Volcanic Province in North Queensland, and southwest Victoria (this thesis - chapter 2, Sircombe 1999, Paine 2004). The heterogeneity of detrital zircon sources is due to changes in fluvial systems transporting sediment from various source regions as well as uplift and erosion of these sources (this thesis, chapter 2).

3.3 METHODS

3.3.1 Data collection

We compiled a stratigraphic database of over 8000 boreholes in the Murray Basin from pre-existing datasets. Data came from five sources – Murray Basin Subsurface Stratigraphic Database from the Bureau of Mineral Resources (now Geoscience Australia) (Brown & Stephenson 1986), South Australian Resource Information Geoserver (SARIG), Geological Survey of Victoria, logging of exposures in the field, and published geological logs (Kotsonis 1995, Paine *et al.* 2004, Miranda *et al.* 2009, McLaren *et al.* 2011). The Murray Basin Subsurface Stratigraphic Database (Brown & Stephenson 1986) is a valuable resource but was preserved as poor quality scanned microform records. We manually entered almost 3000 individual borehole entries (location

coordinates, 250K map sheet, elevation, depth, and stratigraphic intersections) into Microsoft Excel then checked for accuracy and consistency. Quality control practices for all datasets included checking the arithmetic of logged intersections and checking the location of boreholes with their designated 250K map sheet extent in ArcGIS (Esri). The original dataset underwent quality control and quality assurance during compilation. This included assessing suitability of lithologic logs (for example, out of 27,000 available logs in South Australia, only 5000 were considered suitable for the database) (Brown & Stephenson 1986) and clarifying the identification of stratigraphic units in the Murray Basin (Brown & Stephenson 1991).

GOCAD® requires uniform input files including collars, survey (depth, azimuth, and dip), and geology (stratigraphic intersections). Collar locations are in GDA94, MGA Zone 54. Drill hole collars from Brown and Stephenson (1986) were reprojected from AGD66 into GDA94 in ArcGIS. Collar locations from the Brown and Stephenson (1986) database are accurate to approximately 1 km. Locations in the database were pre-GPS and used aerial photographs to locate drill holes. The elevations of boreholes in the new database were calculated from the 1 Second Digital Elevation Model (Gallant *et al.* 2011) for consistency using ArcGIS. Where azimuth and dip are not specified in the input data, we assumed the bores are vertical. This is a reasonable assumption given most boreholes are water bores or targeting heavy mineral sands. Lithological logs recorded in the database are assumed to be accurate, however, where there was an obvious inconsistency (for example, stratigraphy was significantly inconsistent with known local occurrences, logged thicknesses are 50% greater than other known intersections) records were removed from the database. Where the Loxton-Parilla Sands was divided into the Loxton Sand and Parilla Sand these lithologies were combined for continuity between states. Records where unit intersections overlapped by more than five metres or where the stratigraphy did not make sense compared to known geology were removed. In regions of the Murray Basin with sparse drill hole coverage Brown and Stephenson (1986) interpreted poor quality lithologic logs in the context of the local stratigraphy and basin setting.

3.3.2 3D modelling

We used GOCAD® (Paradigm Software) with the Mira Geoscience mining add-in to produce the 3D geological model. The input files from each data source were imported separately into GOCAD® so any errors could be easily traced back to the source data. To create surfaces, the bounding polygon of each unit was defined manually and taken as the extent of each unit from the boreholes (logged occurrences of each formation). The northern limit of the Loxton-Parilla Sands in the model lies further southwest than has been mapped due to few constraints in this area. A point set of markers defining the top and base of each geological unit was generated and set as control nodes and a triangulated mesh between the control nodes delineates the surface. A Discrete Smooth Interpolation (DSI) was run over 1,000,000 times on each surface. The density of data points, and therefore modelled surface constraints, is determined by the number of boreholes intersecting a particular unit. The control node density decreases from the top to the bottom surface of units where boreholes terminate within the unit. Faults used in this study are from the Geoscience Australia Neotectonic Features Database (Clark 2012).

3.4 RESULTS

3.4.1 Miocene-Pliocene Unconformity

The Miocene-Pliocene unconformity is defined by the top surface of the Murray Group, Winnambool Formation, Geera Clay, and Olney Formation (Figure 3.3a) (Macumber 1978, Brown & Stephenson 1991) and forms the unconformity onto which the Bookpurnong Formation and Loxton-Parilla Sands were deposited. The density of boreholes intersecting the unconformity and other units varies considerably across the basin with South Australia having the best coverage of wells with logged stratigraphy (Figure 3.3b, figure 3.4b, and figure 3.5a). Elevation surfaces appear more uneven in the western Murray Basin because of the high borehole density, compared to the longer wavelength features in the eastern part of the basin.

The Miocene-Pliocene unconformity rises to 160 m above sea level along the southern and western margins of the basin (Figure 3.3c). North of the Western Highlands an area of 300 km by 200 km of the unconformity is uplifted over 100 m above sea level (Figure 3.3c). Approximately 90 km NNE of Horsham there is narrow embayment, 30 km wide that has been cut into this uplifted area. The unconformity dips to 120 m below sea level in the centre of the basin. The lowest regions of the unconformity correspond with the thickest parts of the basin sedimentary package. On the south western side of the Padthaway Ridge the unconformity drops in elevation, and underlies what is now the Mount Gambier Coastal Plain. There is a small uplifted area (<40 km wide) corresponding to the southern end of the Neckarboo Ridge, near Mildura. A low area 50 km wide east of the Danyo Fault corresponds with the downthrown side of a steeply W-dipping reverse fault (Clark *et al.* 2011). The most marked changes in elevation occur in two circular features, about 50 km wide, northeast of Ouyen. One region corresponds with the northern end of the Tyrrell Fault. The other feature is west of the Iona Fault but there are few drill holes nearby, restricting the certainty of the absolute depth here. There is a linear feature trending NE-SW, northeast of Balranald (Figure 3.3c). There are few nearby drill holes to constrain this feature and it is likely it is an artefact of the surface interpolation.

3.4.2 Loxton-Parilla Sands

Most features visible within the elevation surface and isopachs are moderate wavelength features, ranging from 20 to 60 km wide (figure 3.4b, c). An area of very dense drilling 100 km NNE of Horsham shows closely-spaced NW-SE trending linear trends in the elevation surface and isopach. These are dune ridges of the Loxton-Parilla Sands strandplain, delineated by heavy mineral exploration drilling.

The thickness of the Loxton-Parilla Sands generally decreases moving from its most landward margin towards the southwest margin of the basin (Figure 3.4c). Thinning of the Loxton-Parilla Sands at the southern margin of the basin corresponds with regions of post-depositional uplift of

the Western Highlands and the Padthaway Ridge. Similarly, the Loxton-Parilla Sands thin along the western margin of the basin where the Mount Lofty Ranges have been uplifted. The thickest tracts of the Loxton-Parilla Sands form a band near Balranald, a region that is depressed in the Miocene-Pliocene unconformity. There are not many drill holes in this area to define this feature, however, and the extent of the sedimentation here may be an artefact. A small feature 30 km wide NE of Horsham with up to 140 m Loxton-Parilla Sands is the thickest part of the formation. A further area of increased thickness lies between Loxton, Mildura, and Ouyen (figure 3.4c), corresponding with the deepest parts of the Miocene-Pliocene unconformity.

3.4.3 Calivil Formation

Fluvial sediments of the Calivil Formation overlie the Olney Formation and intercalate with the easternmost Loxton-Parilla Sands. We have not modelled this relationship because of its complexity and the lack of drill holes in this area. The elevation of the upper surface of the Calivil Formation dips basinward, away from the eastern highlands. The deepest points of the Calivil Formation are 60 m below sea level, between Balranald and Deniliquin but the lack of constraints in the western extent limits the certainty of these depths.

The unit thickens from the south to the centre of the unit, from almost completely absent to over 100 m thick. Thin, narrow, tongues of sediment in highlands fan out into thicker fluvial deposits in the basin (Figure 3.5c). The thickest deposits of the Calivil Formation lie north of Balranald and south of Deniliquin. The thicker deposits near Balranald continue westwards to the Loxton-Parilla Sands.

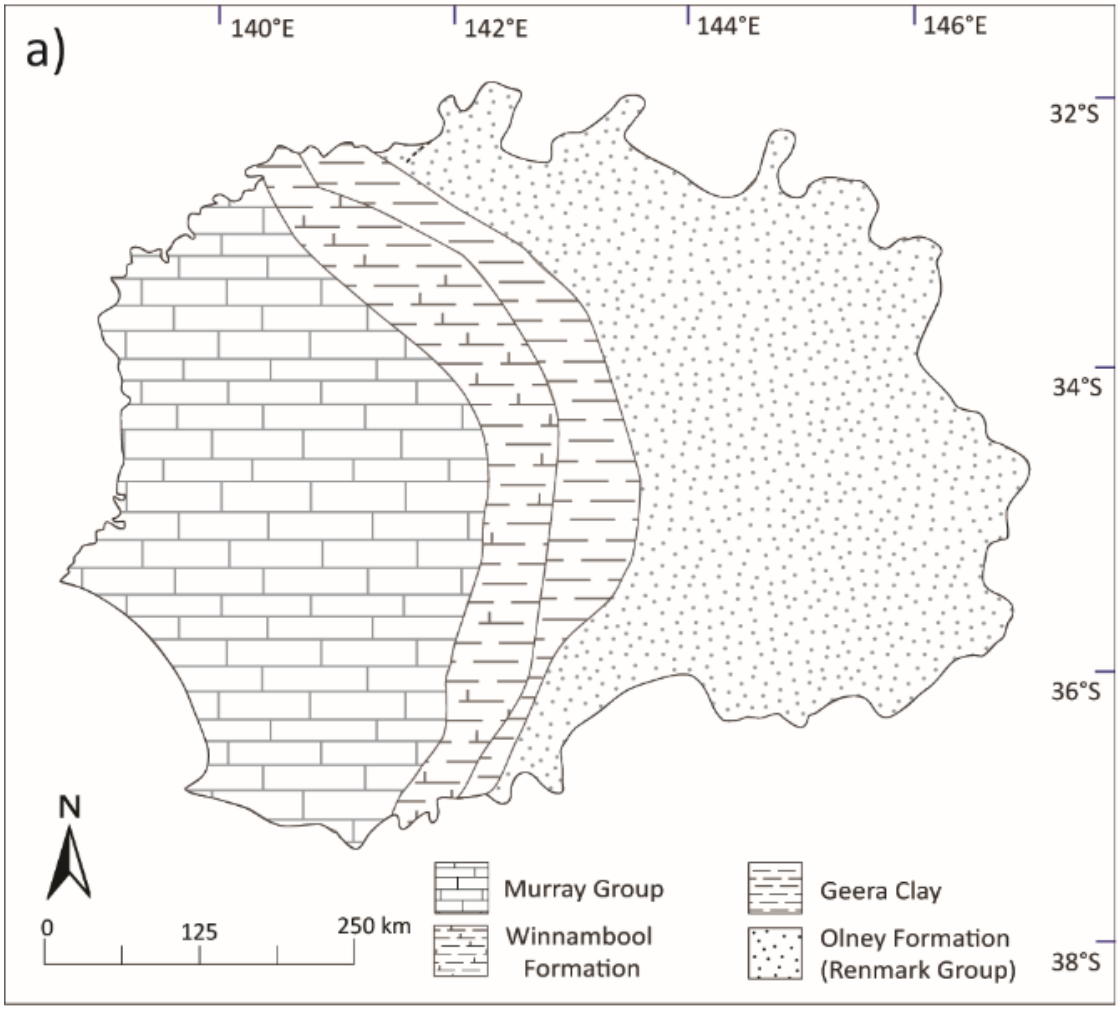

(Continued in following pages) Figure 3.3 a) Units comprising the Miocene-Pliocene unconformity, b) Distance between drill holes constraining the Miocene-Pliocene unconformity, c) Elevation of the Miocene-Pliocene unconformity.

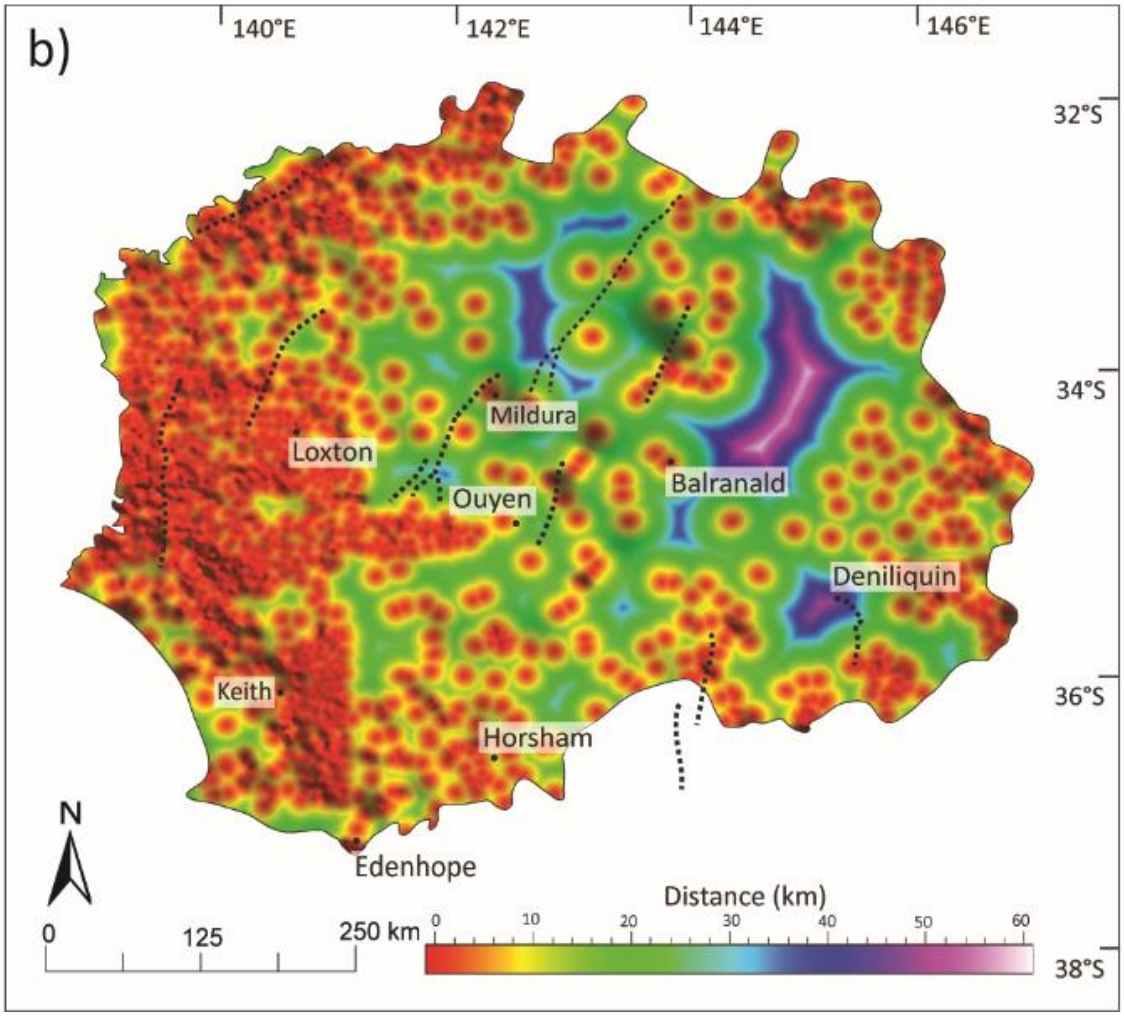
b)
140°E
142°E
144°E
146°E
32°S
34°S
36°S
38°S
Mildura
Loxton
Ouyen
Balranald
Deniliquin
Keith
Horsham
Edenhope
N
0
125
250 km
Distance (km)
0
10
20
30
40
50
60

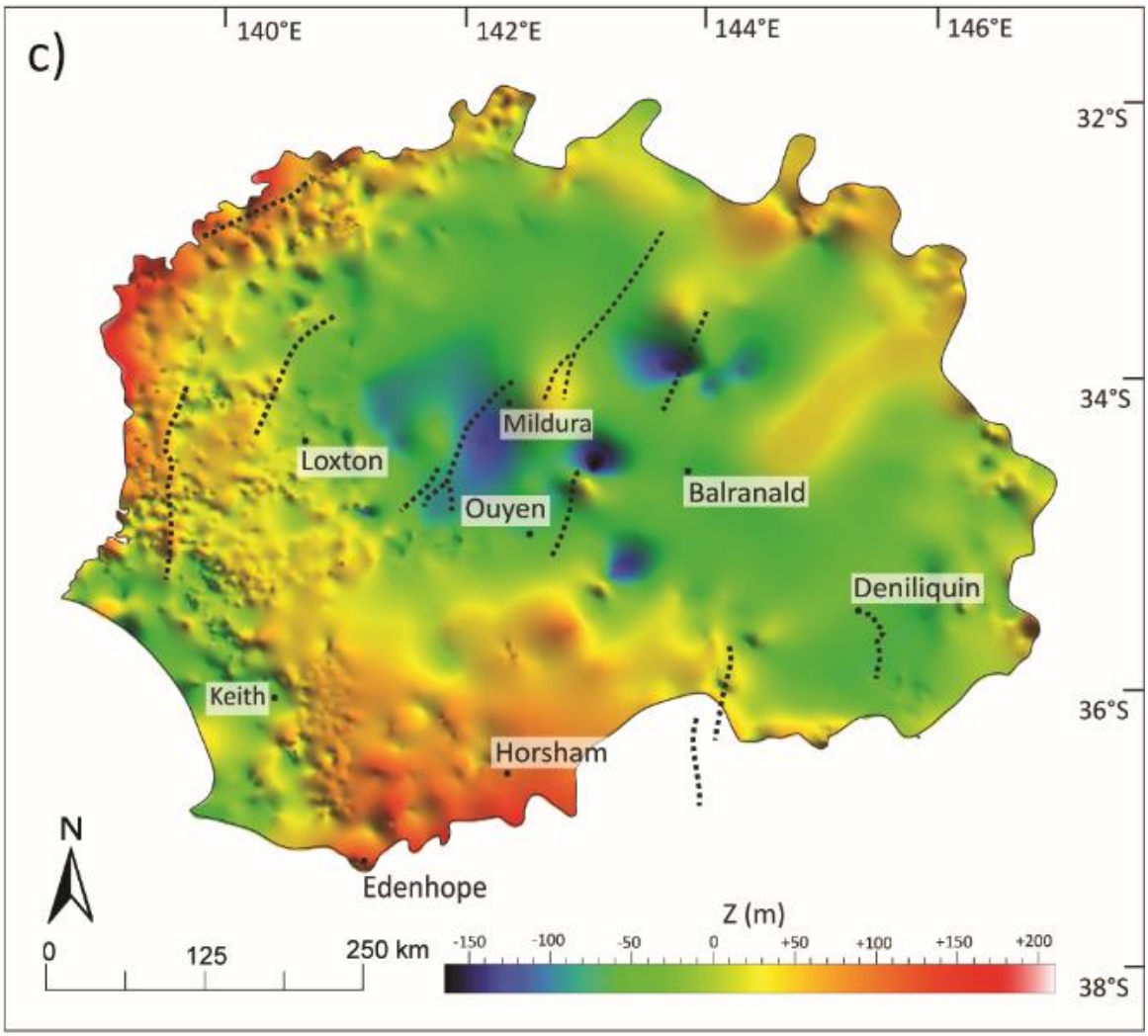
c)
140°E
142°E
144°E
146°E
32°S
34°S
36°S
38°S
Mildura
Loxton
Ouyen
Balranald
Deniliquin
Keith
Horsham
Edenhope
N
0
125
250 km
Z (m)
-150
-100
-50
0
+50
+100
+150
+200

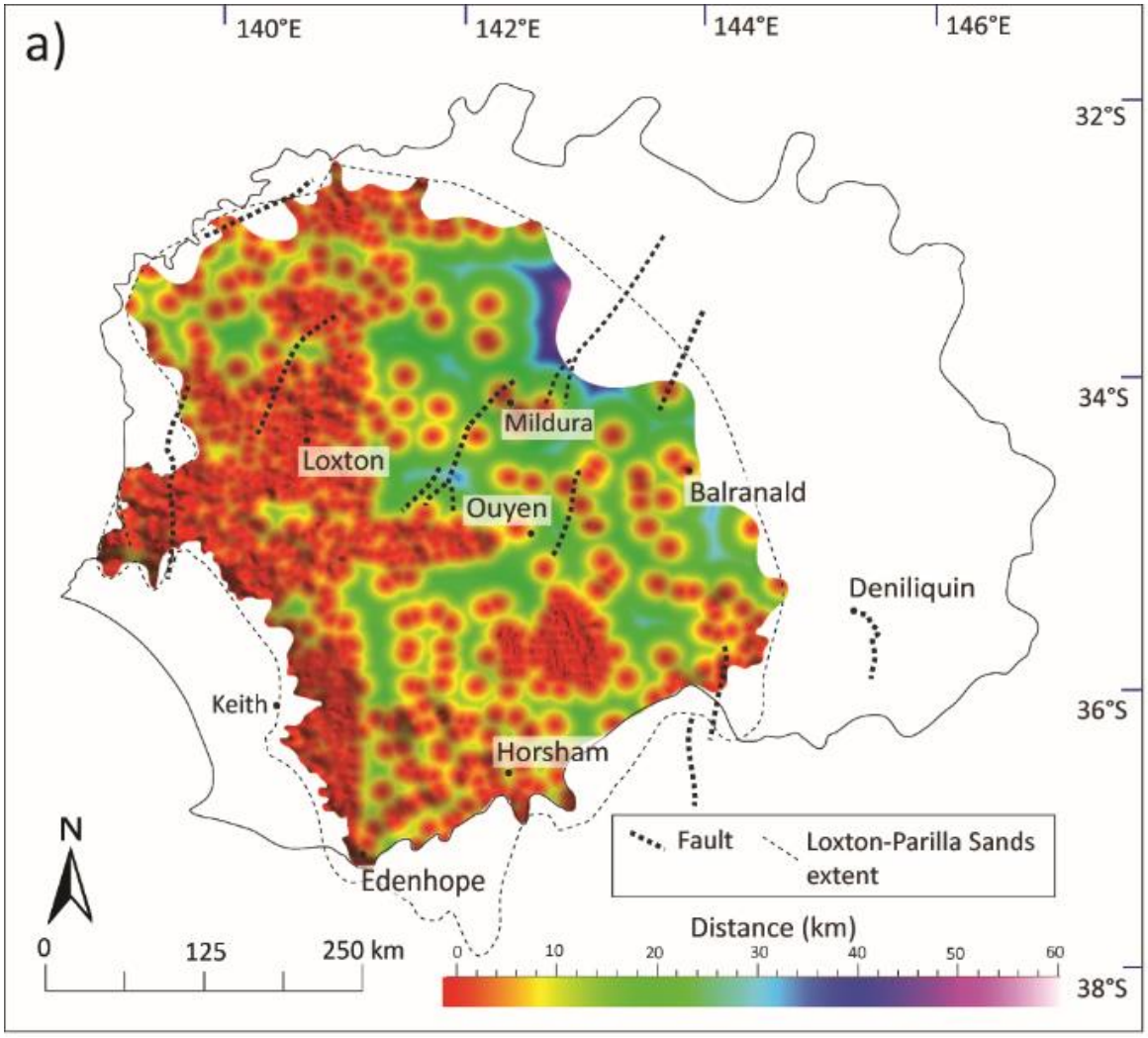

(Continued on following pages) Figure 3.4 a) Distance between drill holes constraining the Loxton-Parilla Sands, b) Elevation of the upper surface of the Loxton-Parilla Sands, c) Isopach of the Loxton-Parilla Sands.

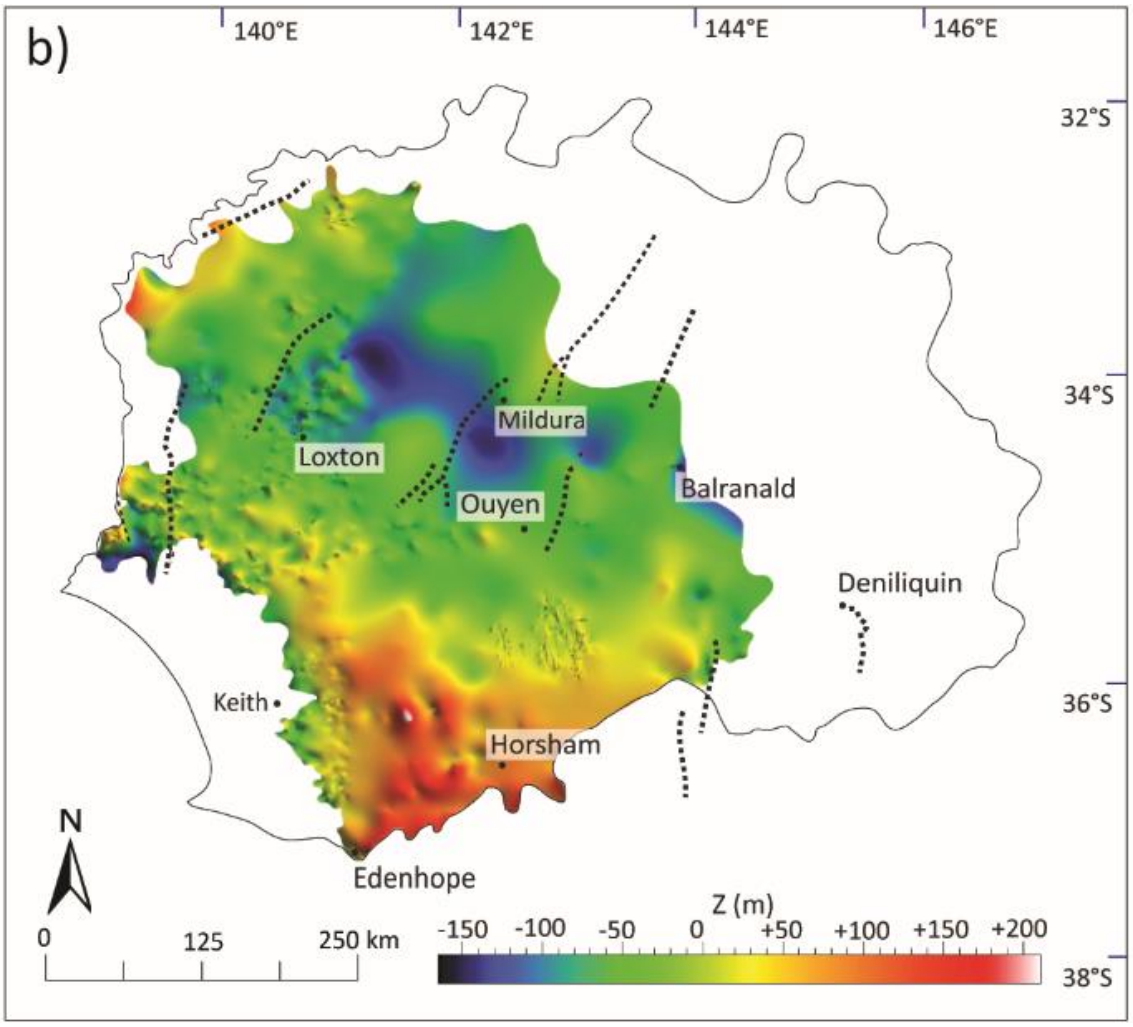
b)
140°E
142°E
144°E
146°E
32°S
34°S
36°S
38°S
Mildura
Loxton
Ouyen
Balranald
Deniliquin
Keith
Horsham
Edenhope
N
0
125
250 km
Z (m)
-150
-100
-50
0
+50
+100
+150
+200

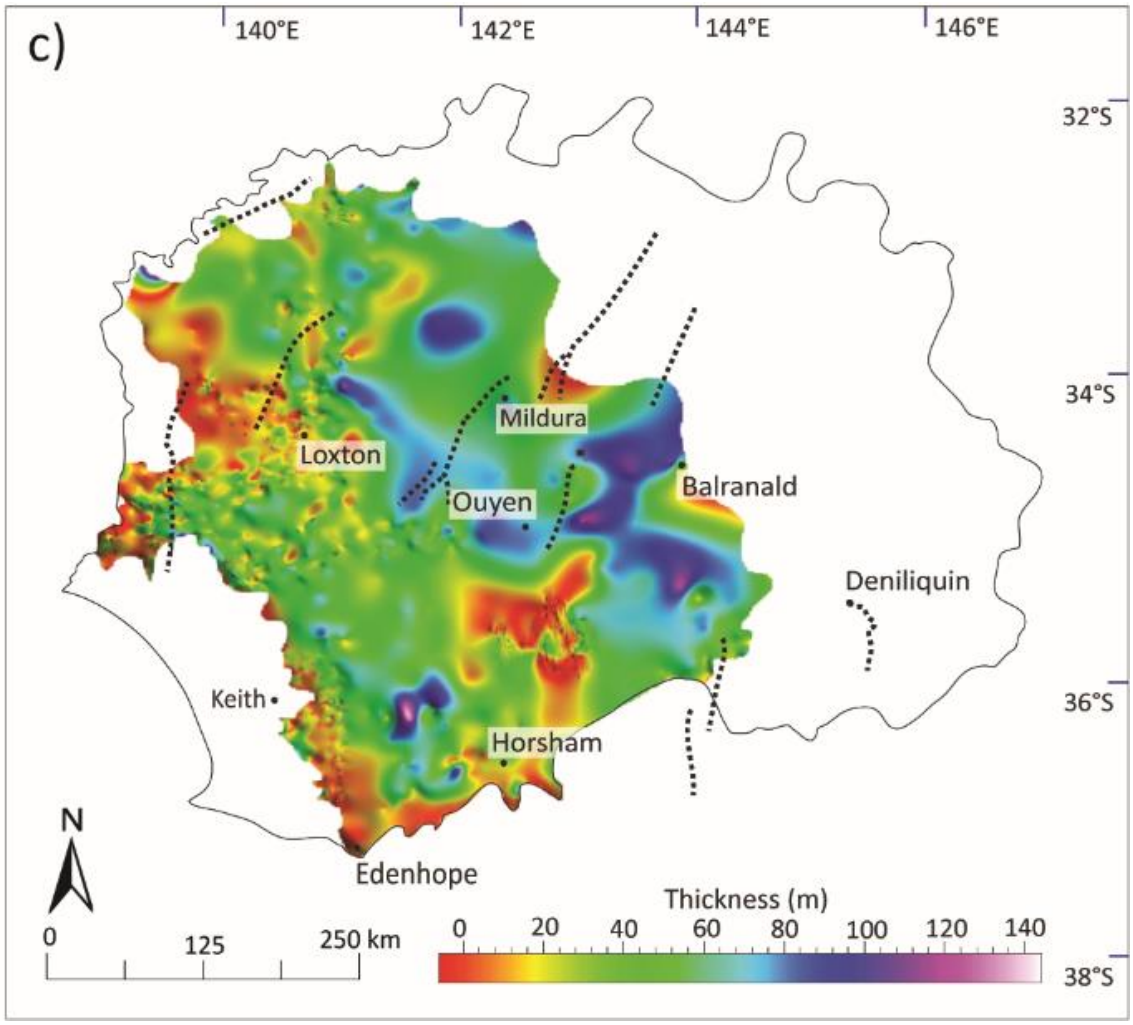
c)
140°E
142°E
144°E
146°E
32°S
34°S
36°S
38°S
Mildura
Loxton
Ouyen
Balranald
Deniliquin
Keith
Horsham
Edenhope
N
0
125
250 km
Thickness (m)
0
20
40
60
80
100
120
140

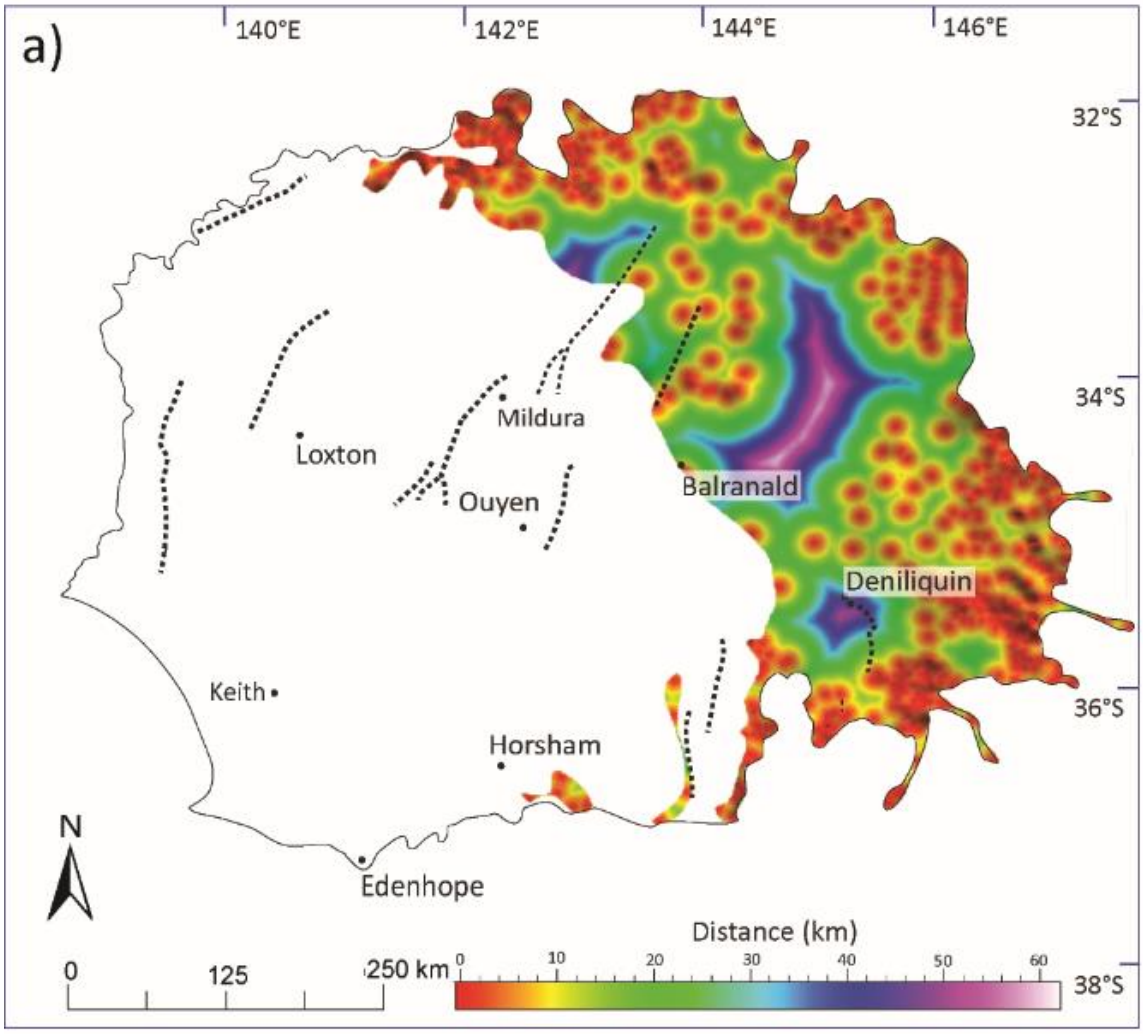

(Continued on following pages) Figure 3.5 a) Distance between drill holes constraining the Calivil Formation, b) Elevation of the upper surface of the Calivil Formation, c) Isopach of the Calivil Formation.

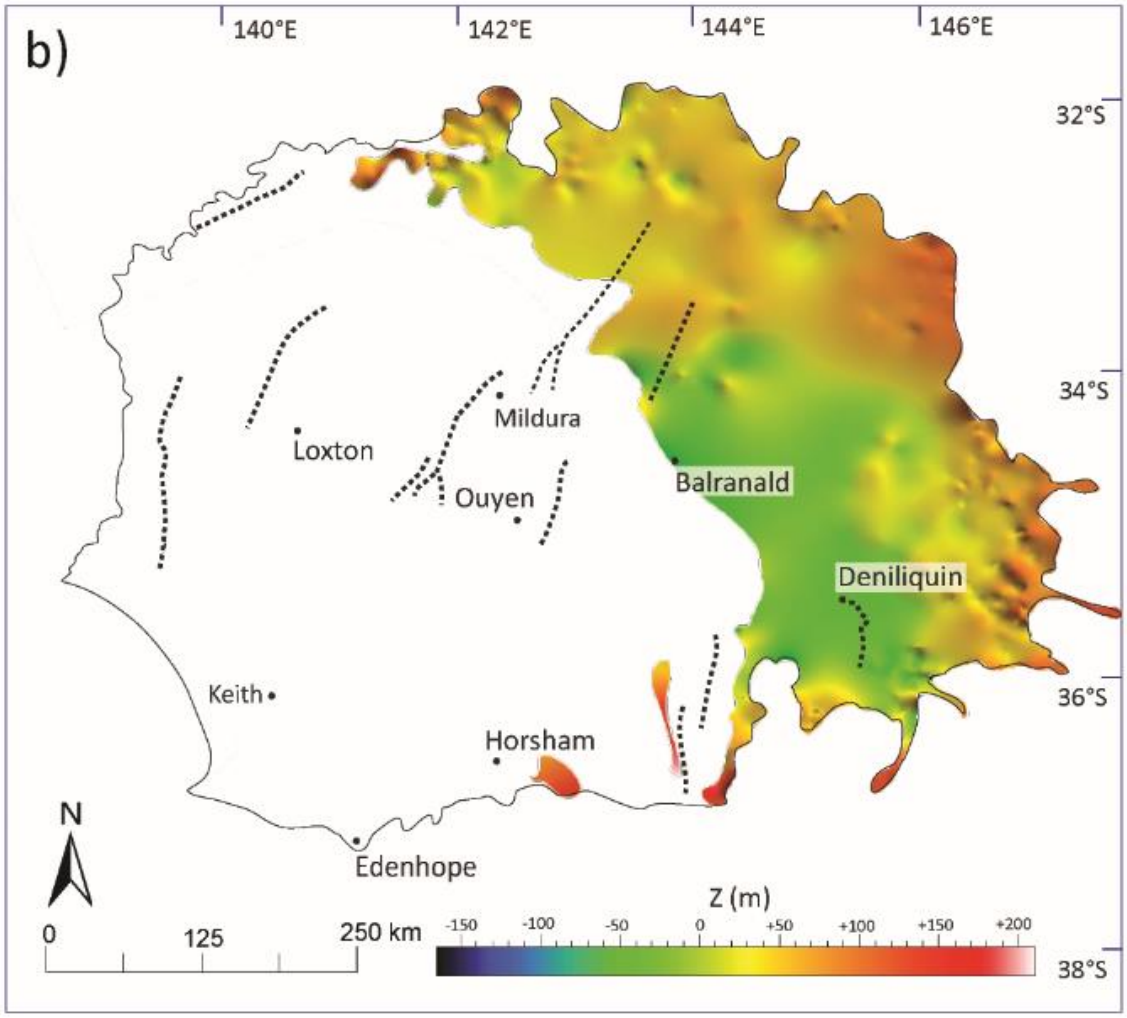
b)
140°E
142°E
144°E
146°E
32°S
34°S
36°S
38°S
Mildura
Loxton
Ouyen
Balranald
Deniliquin
Keith
Horsham
Edenhope
N
0
125
250 km
Z (m)
-150
-100
-50
0
+50
+100
+150
+200

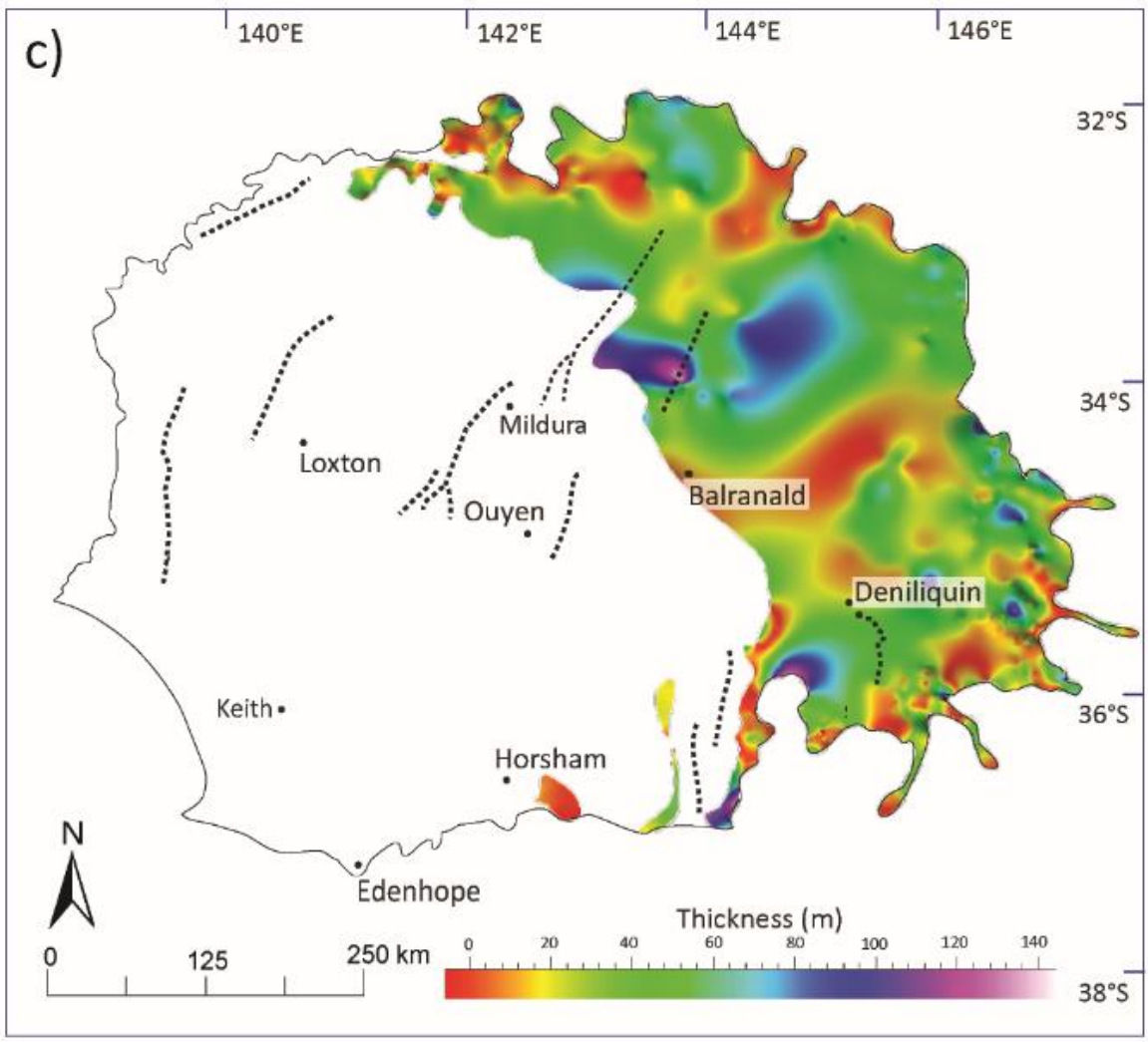
c)
140°E
142°E
144°E
146°E
32°S
34°S
36°S
38°S
Mildura
Loxton
Ouyen
Balranald
Deniliquin
Keith
Horsham
Edenhope
N
0
125
250 km
Thickness (m)
0
20
40
60
80
100
120
140

3.4.4 Sediment thickness and paleodrainage

Fluvial facies are poorly recorded in the Loxton-Parilla Sands because of their similarity to some marginal marine deposits and limited geographical extent. The 3D geological model presented in this study is a regional view of sedimentary depocenters and stratigraphic architecture of the Neogene units of the Murray Basin. Sinuous tracts of increased thickness in the Loxton-Parilla Sands on the order of 30-60 km wide are interpreted as paleodrainage channels. The inferred paths are incised valleys formed during non-deposition and erosion (Miocene-Pliocene unconformity), later reactivated during the marine regression, and having their course altered in response to renewed tectonism. Such incised valleys form during low sea level conditions and can fill with highly variable sediments during rising sea level and regression (Allen & Posamentier 1993). In the Murray Basin scouring of surfaces and increased sediment thickness is a record of paleodrainage systems (Miranda *et al.* 2008, Hill *et al.* 2009). Channels on the continental shelf lead from the Murray Basin and are incised up to 25 m. As many as six transgression-regression cycles in the Quaternary are recorded by stacked channel deposits, now submerged (Hill *et al.* 2009). Drainage channels cut into the Miocene-Pliocene unconformity (during subaerial exposure) were partially infilled by the Bookpurnong Formation and then reactivated as drainage channels as the ocean regressed. Renewed tectonism in southeast Australia in the Late Miocene provided the impetus to alter the course of ancient rivers.

Paleodrainage paths in the eastern Murray Basin (Calivil Formation) are broadly similar to the path of modern rivers while in the west (Loxton-Parilla Sands) channels have migrated tens of kilometres (Figure 3.6). Drill holes around the Lachlan and Murrumbidgee Rivers are sparse so the extent of migration of these systems since the Neogene remains unconstrained by the model. The fluvial channels, referred to as ‘deep leads’, shedding Au-rich sediment from the

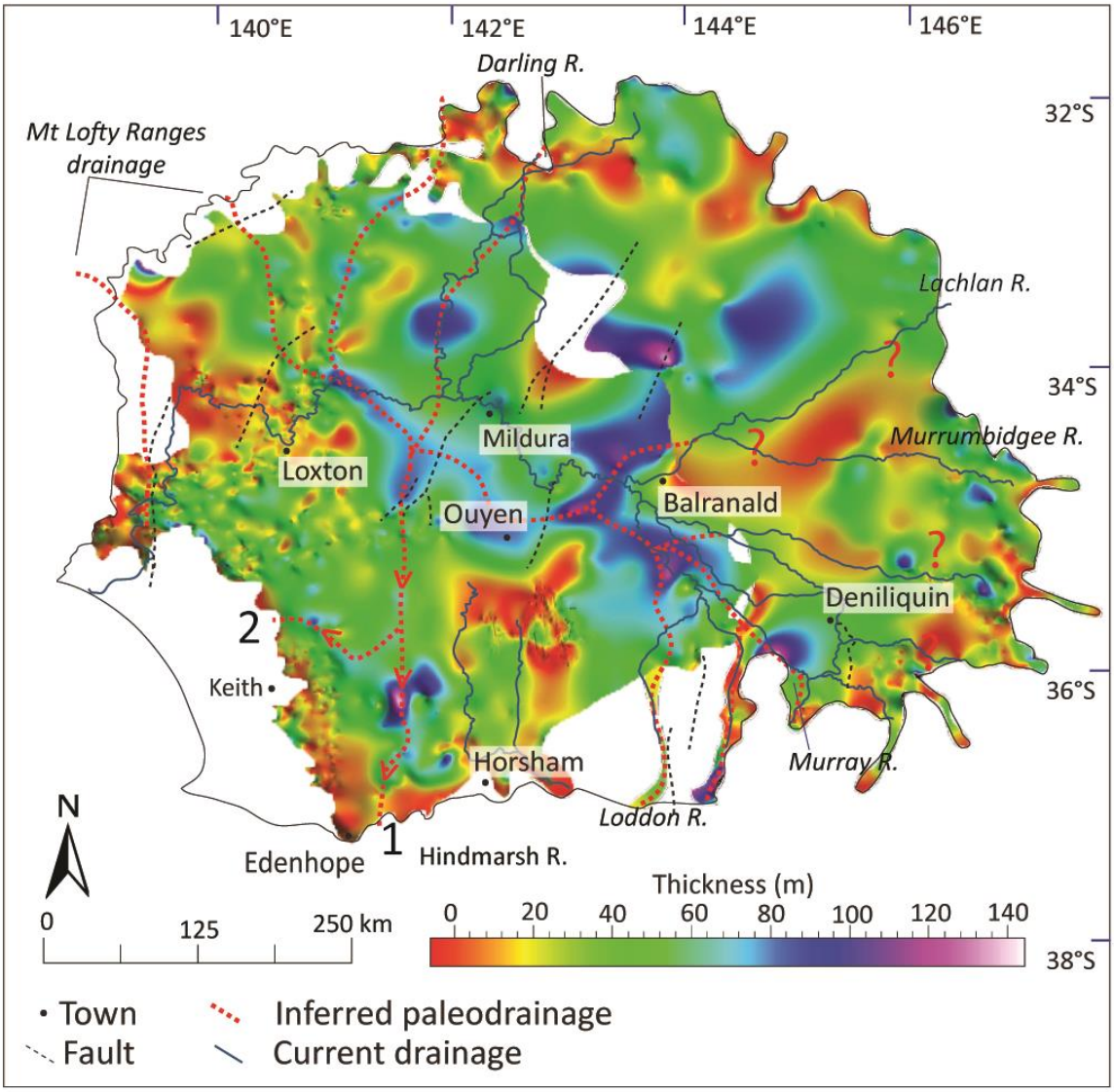

Figure 3.6 Isopachs of the marginal marine Loxton-Parilla Sands (west) and fluvial Calivil Formation (east) with inferred paleodrainage (red), modern rivers (blue), and faults (black dash). Flow direction of the southern channel is indicated by arrows. The two outlets active at different stages are located near Edenhope (1), and a later outlet near Keith (2). The path of the ancient Lachlan and Murrumbidgee Rivers in the eastern Murray Basin is not clear due to the large area with low drill hole control.

highlands in the Lachlan Fold Belt have been active since the Eocene (Cayley & Taylor 2001). Our results support this stability, at least at the regional scale. The Murray River south of Deniliquin has diverted around the Cadell Fault and may have supplied the depocenter nearby. Paleogeographical studies of the eastern highlands have shown most uplift occurred in the Mesozoic in association

with the opening of the Tasman Sea (VandenBerg 2010) and most control on these deep leads has been due to change in base level with eustatic fluctuations.

In contrast to the relatively stable drainage of the eastern drainage courses the western Murray Basin drainage has changed considerably. Broadly linear tracts of thicker Loxton-Parilla Sands north and south of Balranald extend west and converge towards Ouyen. This course then drains northwest where it meets with a northerly channel between Mildura and Loxton, in the central western Murray Basin (Figure 3.4c). Tributaries are broadly continuous from the fluvial Calivil Formation westwards into the Loxton-Parilla Sands. The central drainage system follows regional groundwater flow to the main depocenter in the central west of the Murray Basin. The Danyo Fault west of Ouyen coincides with a southwest shift of the easterly drainage channel. The northerly channel coincides with the modern Darling River which is controlled by basement half-grabens (Brown & Stephenson 1991). A shallow southeast trending valley is visible from the northern Adelaide Fold Belt, south of the Pine Creek and Olary fault scarps. This channel crosses the Hamley Fault and connects with a larger NW-SE channel near Loxton. There is a circular feature in the Loxton-Parilla Sands, about 60 km wide and up to 100 m thick, 75 km northwest of Horsham which we interpret to be a depocenter. Trending north from this depocenter is a faint thickening of the Loxton-Parilla Sands extending towards the Danyo Fault. This is interpreted as the southern passage of the ancient Murray River. The Douglas Depression in central Victoria did not form as a drainage system until after the Loxton-Parilla Sands were deposited.

There are two likely outlets for the ancient Murray River that were active at different times. Initially the outlet for the basin drainage was in southwest Victoria, near the town of Edenhope (Figure 3.6). This interpretation supports the later path of McLaren *et al.* (2011) who suggest outflow occurred southwest of Edenhope due to a channel that has been preserved under basalts. Further, submarine canyons on the continental shelf (Sprigg 1952, Gingele *et al.* 2004) provide further evidence for a major drainage outlet in this part of the basin. In the Early Pliocene, as uplift

of the Western Highlands took place, drainage was diverted and entered the south coast near the town of Keith (Figure 3.6). The low topographic gradient of the Murray Basin and lack of markedly incised channels mean these drainage channels were probably short-lived and migrated as the coast prograded. Lack of major fluvial deposits also suggests these rivers were probably a similar size or smaller to modern systems which have a similar footprint and sediment load.

3.4.5 Controls on basin geometry and paleodrainage

Neotectonism and eustasy have been recognised as important controls on sedimentation in the Quaternary on continental shelf sedimentation during glacial maxima (Hill *et al.* 2009). These are also recognised as important influences on sedimentation on the Mount Gambier Coastal Plain in the Pleistocene (Sprigg 1952, Brown & Stephenson 1991). The results of the 3D model suggest the geometry of sediments in the Murray Basin and ancestral rivers are controlled by faults and underlying basement structures that have been reactivated during the Cenozoic. These features are recognisable in the current landscape but their significance in terms of paleodrainage is only evident with a view of the 3D geometry of units. Our model supports previous interpretations of strong structural control on the regional geometry of the basin and the important role of neotectonism in shaping stratigraphic geometry (Brown & Stephenson 1991, Bowler *et al.* 2006, Miranda *et al.* 2009). Detrital zircon sources also indicate these drainage systems were not static and migrated over time (this thesis, chapter 2, Sircombe 1999, Paine 2004). Reactivation of drainage channels in the Murray Basin and nearby continental shelf is recorded through its geological history. Stacked channels and evidence of re-incision of fluvial channels by the Quaternary Murray River on the Lacepede Shelf show repeated incision of the same channels over multiple depositional (sea level) cycles (Hill *et al.* 2009). Migration of the Quaternary Murray River on the shelf was in response to local neotectonism (Hill *et al.* 2009). Rainfall in catchment regions is potentially also an important driver for the development of a large river system carrying lots of sediment. Thus climate also plays a role in sedimentation, but one that is difficult to determine from the results of stratigraphic modelling alone.

Southeast Australia experience renewed tectonism and uplift in the Late Miocene to Pliocene owing to changes in motion and forces at the Australia-Pacific plate margins (Coblentz *et al.* 1995, Dickinson *et al.* 2001, Sandiford 2003, Sandiford *et al.* 2004, Hillis *et al.* 2008). The increase in siliciclastic sedimentation in basins in southeast Australia during this time is also attributed to this neotectonism (Dickinson *et al.* 2002). A ready supply of clastic sediment for the Loxton-Parilla Sands strandplain was generated as the sheet was being deposited in addition to reworking of the ocean floor. Erosion and reworking of the Olney Formation in the northeast Murray Basin is a potential source of some sediment (Roy *et al.* 2000), however, as the coast moved southeast over calcareous units another source of sediment is required. Further, it is unlikely that the shelf region contained enough sediment to supply and maintain a laterally extensive prograding coastline (Heward 1981). Emergence of faults like the Morgan, Hamley, Danyo, and Tyrrell Faults, during the marine regression is recognised as facilitating development of lakes by diverting drainage into small sub-basins (Bowler *et al.* 2006). Growth faulting is also associated with the development of heavy mineral deposits, particularly in the northern Loxton-Parilla Sands (Roy *et al.* 2000).

Sediment depositional patterns revealed by isopachs suggest the predominant course of drainage of the Murray Basin during the early stages of the Miocene-Pliocene marine regression was a south-draining course west of the Douglas Depression (Figure 3.6). The mechanism for the direction of drainage to this position is unclear. Constraints on the existence of a fault (the Hindmarsh Fault) running parallel to this proposed ancient river are not strong (McLaren *et al.* 2011, Clark 2012). Our results suggest there has been some uplift and incision of the Miocene-Pliocene in this area but there is not enough evidence to suggest a fault in the area. In the Early Pliocene uplift of the Western Highlands reversed the drainage gradient and this channel was diverted to an outlet near Keith (Figure 3.6). Later initiation of drainage of the Western Highlands into the Murray Basin was captured by the Douglas Depression.

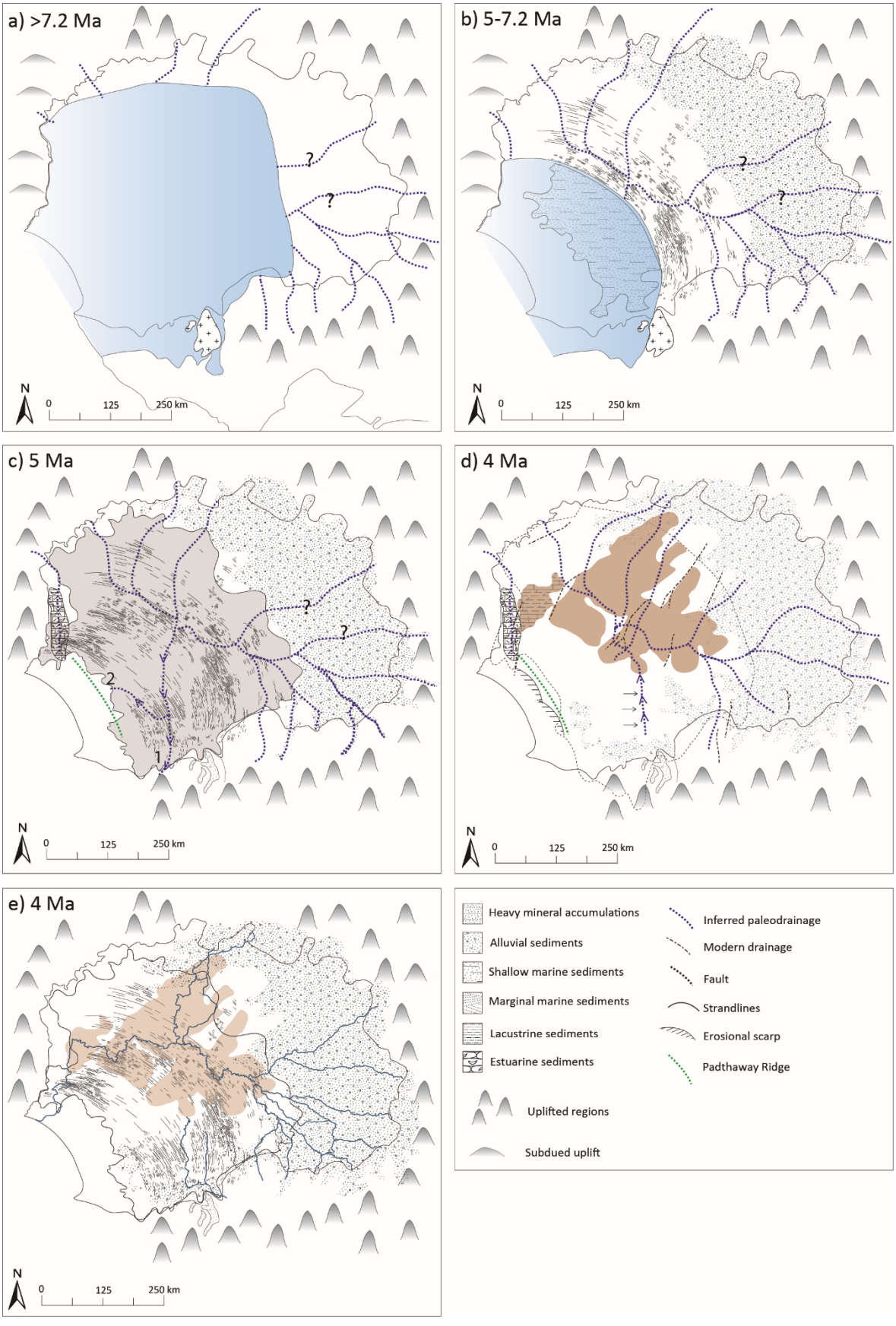
a) >7.2 Ma
b) 5-7.2 Ma
c) 5 Ma
d) 4 Ma
e) 4 Ma
N
0
125
250 km
?
1
2
Heavy mineral accumulations
Alluvial sediments
Shallow marine sediments
Marginal marine sediments
Lacustrine sediments
Estuarine sediments
Uplifted regions
Subdued uplift
Inferred paleodrainage
Modern drainage
Fault
Strandlines
Erosional scarp
Padthaway Ridge

(Previous page) Figure 3.7 Time series landscape reconstruction with location and development of various drainage channels, uplift of faults, a) Maximum transgression – Calivil Formation deposited, Lachlan Fold Belt uplifted, minor topography along the western margin, b) Mid-regression – Calivil Formation continues to be deposited, marginal marine and strandplain sediments of the Loxton-Parilla Sands deposited (strandlines marked), drainage directed towards central depocenter of the basin, shallow marine Bookpurnong Formation deposited in offshore environment, c) Late regression – Loxton-Parilla Sands continue deposition, uplift of the Mount Lofty and Flinders Ranges creating drainage along the western margin of the basin. Later estuarine sedimentation of the Norwest Bend Formation formed. Uplift of the Western Highlands provided volcanogenic sediment to the Loxton-Parilla Sands. Further uplift re-directed the main drainage channel of the basin further west, d) Uplift in the southern Murray Basin block outlet of the ancient Murray River, Lake Bungunnia forms and deposits lacustrine clay (Blanchetown Clay) and limestone (Bungunnia Limestone). Starved of sediment erosion creates the Kanawinka Escarpment along the southern coast, e) Defeat of the Padthaway Ridge and drainage of the basin is renewed, the main drainage channel is now directed towards its current location near the western margin of the basin.

3.4.6 Paleoenvironmental reconstruction

Based on the results of our geological modelling and present day detailed digital elevation models, we present a series of maps of the Murray Basin in Figure 3.7 showing paleogeographical evolution of the region and likely courses of major drainage channels through the Neogene. In the Mid-Late Miocene the sea level was at its maximum (Figure 3.7a). At this stage the Calivil Formation was being deposited on top of the Miocene-Pliocene unconformity in the eastern Murray Basin, and the transgressive facies of the Bookpurnong Formation was deposited in the gulf. The course of eastern drainage channels is broadly similar to present day, draining the Eastern Highlands but the nature of the convergences has likely been rearranged (Figure 3.6). As the Miocene ocean regressed, the Loxton-Parilla Sands was deposited in a predominantly marginal marine environment and minor fluvial facies, reactivating channels incised into the Miocene-Pliocene unconformity (Figure 3.7b). Major drainage channels during this time were directed to the centre of the basin, the location of major depocenters. The limited topography of the Mount Lofty and Flinders Ranges initiated relatively minor channels providing sediment to the far western Murray Basin, which later formed the Norwest Bend Estuary. The Western Highlands were still submerged at this stage. Growth faulting along the Neckarboo and Iona ridges, as the strandplain was deposited, facilitated development of heavy mineral sand deposits (Roy *et al.* 2000).

As the ocean regressed further the Loxton-Parilla Sands was deposited as a series of strandlines that were increasingly influenced by neotectonism. Uplift of the Western Highlands and parts of southwestern Victoria reversed the topographic gradient and re-directed the main drainage channel to the west (Figure 3.7c). Uplift also initiated erosion of the highlands, supplying volcanogenic sediment of the Coleraine Volcanics to the Loxton-Parilla Sands (this thesis, chapter 2). Uplift of the Hamley Fault, associated with the Mount Lofty Ranges, confined estuarine sedimentation of the Norwest Bend Formation from around 5.83 Ma (Miranda *et al.* 2008, McLaren *et al.* 2011) (Figure 3.7c). Pliocene to Pleistocene sediments of the Shepparton Formation were deposited over the Calivil Formation in the eastern Murray Basin and around the margins.

Drainage was defeated in the Pliocene and the ancient megalake Lake Bungunnia was flooded in the central western part of the basin with depocenters strongly influenced by the location of faults (Figure 3.7d). The coastline, starved of sediment, continued to be eroded during this time forming the Kanawinka Escarpment (Miranda *et al.* 2009). Location of dam that formed Lake Bungunnia is not known but recent studies favour uplift of the Padthaway Ridge (Miranda *et al.* 2009). Our interpretations support the uplift of this area as the main control on the formation of Lake Bungunnia. This was preceded by uplift of the southern Murray Basin which redirected the southern drainage channel to a short-lived outlet near Keith. In the Late Pliocene the Murray River was able to drain the basin once again but the reason for renewed drainage of the basin is not clear. Uplift of the Western Highlands continued and contributed to incision of the Douglas Depression by the Wimmera River (Figure 3.7e).

3.5 CONCLUSION

Our presentation and interpretations of the first basin-wide 3D geological model provide new insights and detail on the likely course of ancient Murray Basin paleodrainage and associated depositional environments in the Neogene. Our results also reveal the basin-wide 3D stratigraphic architecture and the major influence of tectonism on sedimentation throughout the Cenozoic. The geometry of the Loxton-Parilla Sands shows that regional structures resulting from neotectonism are superimposed on sedimentary sequences deposited in response to long term sea level change and climatic fluctuations. The primary conclusion supported here is that during the Late Miocene-Pliocene marine regression the lower Murray River flowed up to 80 km south of its current course and entered the Southern Ocean 300 km southeast of its current location. The geological model results show the control that neotectonism has had on river courses throughout the history of the Murray Basin, influence that continues in the current landscape. This control is revealed at the basin-scale and is most apparent when we are able to visualise the geometry of sediments in 3D.

Chapter 4 Late Miocene-Pliocene coastal acid sulphate system in southeastern Australia and implications for genetic mechanisms of iron oxide induration

FOREWARD

This chapter is based on whole rock geochemical results of 603 samples of the Loxton-Parilla Sands and major and trace element maps of petrographic thin sections. With knowledge from the previous chapters about the sedimentary environment and paleogeography of the western Murray Basin I address the gap in current research about the geochemical processes responsible for formation of the weathering profile. I intend to submit this chapter as a manuscript to *Catena*, with co-authors Prof. David Giles who helped with interpretation of geochemical results and Dr Steven Hill who helped with project conceptualisation and interpretation of the whole rock geochemistry. Benjamin Wade and Aoife McFadden from Adelaide Microscopy helped me with setting up the electron microprobe and laser ablation instruments. Acme Laboratories in Vancouver, Canada, performed the sample preparation and whole rock analysis. Prof. Karin Barovich and Dr Steven Hill assisted with collecting samples in the field. Geoscience Australia, the Geological Survey of South Australia, and Geological Survey of Victoria allowed me access to the core repositories where I collected core samples. I also extend my thanks to Georgina Gordon and Matilda Thomas for their help with acquiring and interpreting the HyLogger^{TM} data.

Statement of Authorship

Title of Paper	Late Miocene-Pliocene coastal acid sulphate system in southeastern Australia and implications for genetic mechanisms of iron oxide induration
Publication Status	○ Published, ○ Accepted for Publication, ○ Submitted for Publication, ◉ Publication style
Publication Details	

Author Contributions

By signing the Statement of Authorship, each author certifies that their stated contribution to the publication is accurate and that permission is granted for the publication to be included in the candidate's thesis.

Name of Principal Author (Candidate)	Stephanie McLennan		
Contribution to the Paper	Project conceptualisation, sample collection and preparation, data collection, data interpretation, manuscript design and composition, and generation of figures and tables.		
Signature		Date	28·10·2015

Name of Co-Author	Prof. David Giles		
Contribution to the Paper	Supervised development of work, helped in data interpretation and manuscript revision.		
Signature		Date	29-10-15

Name of Co-Author	Dr Steven Hill		
Contribution to the Paper	Assisted with project conceptualisation, helped in data interpretation and manuscript revision.		
Signature		Date	29-10-15

Name of Co-Author			
Contribution to the Paper			
Signature		Date	

ABSTRACT

The key processes controlling secondary iron oxide geochemistry in a Neogene strandplain are identified and interpreted in the context of a coastal acid sulphate weathering system. Textural and geochemical variations in weathering materials indurated by hematite and goethite – ferricrete – represent a record of *in situ* induration, erosion, and reworking. This development took place within an environment of fluctuating pH and Eh and subaerial wetting and drying cycles. The ferricretes have three morphological types, flat-lying indurations, concentric pisoliths, and rounded nodules with fragmented internal textures. We distinguished depositional and post-depositional processes based on the results of whole rock geochemistry, hyperspectral mineralogy, and major and trace element maps of petrographic thin sections. Successive laminae of Fe-oxides and hydroxides in all morphological types of ferricrete have variable Fe, Al, and Si abundances, reflecting cyclic precipitation and groundwater chemistry changes. Episodic wetting and drying of near coastal sediments was superimposed on a long-term trend of marine regression and local tectonic uplift (from ~7 Ma to present). This resulted in the diachronous exposure of relatively reduced shoreline sediments and concomitant acid production due to ferrolysis and the oxidation of biogenic sulphide. Local landform variations contributed to a wide variety of weathering materials. Acid sulphate weathering recorded by these indurated sediments is similar conditions that are observed now in the shallow water estuary of the Lower Lakes, near the mouth of the Murray River.

KEYWORDS

Ferricrete; Neogene; weathering; ferricrete; silcrete; Australia;

4.1 INTRODUCTION

Iron indurated sediments – ferricretes – are a common feature of weathering systems around the world, particularly in Africa (Beauvais & Roquin 1996) and Australia (Firman 1979, Anand & Gilkes 1984, Bourman 1993, Singh & Gilkes 1996, Löhr *et al.* 2010), in a variety of climates ranging from semi-arid to tropical (Macumber 1991, Bourman *et al.* 2010, Löhr *et al.* 2010), and at a number of stages in the geological record (Milnes *et al.* 1985, Firman 1994, Anand & Verrall 2011). The two fundamental end-members of formation are *in situ* accumulation of goethite and hematite (collectively referred to as Fe-oxides in this study) (for example, Beauvais & Roquin 1996) and disaggregated, transported ferricretes (for example, Bourman 1993). Increasingly, studies are recognising the importance of several stages of formation, including transportation, erosion, and further alteration of indurated sediments (Milnes *et al.* 1985, Lohr *et al.* 2010). Most of the body of work on the formation of ferricretes is based on field observations, some petrographic observations, and more rarely integrating geochemistry data.

The Loxton-Parilla Sands in the western Murray Basin are a laterally extensive strandplain of predominantly marginal marine and minor fluvial sediments covering 140,000 km^2 of southeastern Australia (Figure 4.1). The unit is a semi-confined aquifer and preserves a textural and mineralogical record of protracted syn- and post-depositional weathering processes during the Late Cenozoic. The stratigraphy and depositional setting of the Loxton-Parilla Sands have been the subject of a number of studies (Brown & Stephenson 1991, Roy *et al.* 2000, Paine *et al.* 2004, Bowler *et al.* 2006, Miranda *et al.* 2009, Robson & Webb 2011), as has the modern hydrogeology (Barnett 1980, Brown & Radke 1989, Brown & Stephenson 1991, Macumber 1991, Cartwright *et al.* 2007, Berens *et al.* 2009, Cartwright *et al.* 2010). The significance of depositional and post-depositional geochemical processes in this system has not been addressed. Though the Loxton-Parilla Sands were deposited in marginal marine and fluvial environments and are predominantly quartz sand, there are marked variations in the morphology and geochemistry of weathering materials in the upper parts of the unit.

The indurated weathering profile in the Loxton-Parilla Sands has been treated as a separate stratigraphic unit. Named the Karoonda Surface by Firman (1975) and the Karoonda Regolith by Kotsonis (1995) it has been regarded as a chronostratigraphic marker, implying it was formed in a

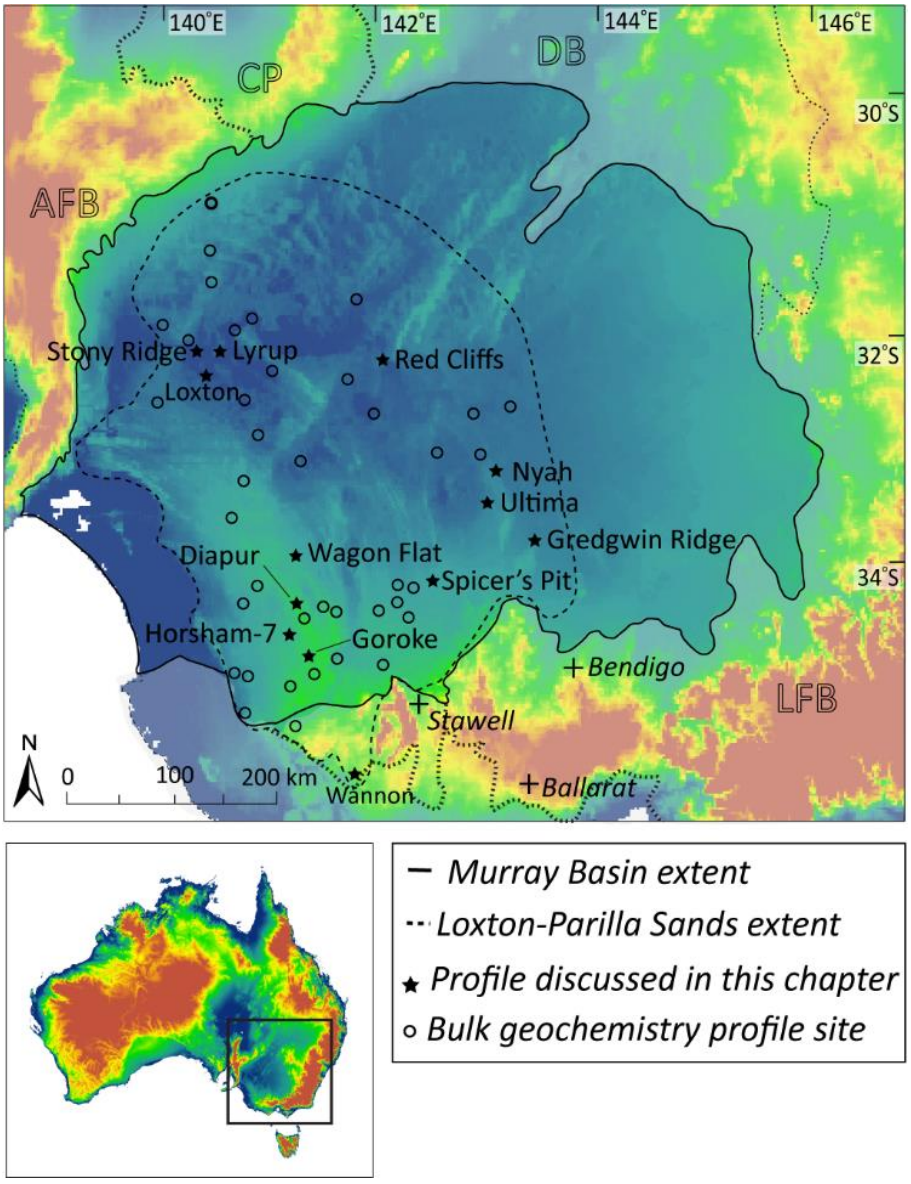

Figure 4.1 Study location and extent of the Loxton-Parilla Sands in the Murray Basin, southeast Australia, and locations of profiles discussed in the text. The basin is bordered by a number of geological terranes: AFB – Adelaide Fold Belt, CP – Curnamona Province,

single continuous event that was initiated well after deposition of the unit. Integration of whole rock geochemistry with microscopic chemical analysis allows us to now address the variety of geochemical processes taking place at different times, the influence of local landforms, and context in the Late Miocene-Pliocene marine regression.

In order to understand the complex genesis of Fe-oxide indurated materials in the Loxton-Parilla Sands, we have utilised electron microprobe analysis. This technique enables visualisation of geochemistry at exceptional spatial resolution in a relatively short amount of time. The Fe-oxide indurated weathering products in the Loxton-Parilla Sands possess a spectrum of morphology and geochemical variations that are not easily recognised in hand specimen or under a petrographic microscope. This work builds on established stratigraphy and chronology of the Loxton-Parilla Sands by presenting new geochemical data and petrographic observations. The result is a novel understanding of how geochemical characteristics and mineralogy of ferricretes vary at different scales. We show the importance of understanding the wider geological context and environment of formation in interpreting the genesis and timing of weathering materials.

4.2 REGIONAL SETTING

4.2.1 Regional geology

The Murray Basin is a shallow, saucer-shaped intracratonic basin blanketing 300,000 km^2 of southeastern Australia (Figure 4.1). Sedimentation began in the Early Cenozoic, following the breakup of Gondwana and rifting of southern Australia and Antarctica. Parts of the basement are faulted, forming ridges up to 300 m high and minor infrabasins (Brown & Stephenson 1991). The Murray Basin is bordered by variable basement blocks and lithologies. In the north, sediments onlap folded Devonian to Early Carboniferous rocks of the Darling Basin (Brown & Stephenson 1991). The eastern and southern margins of the basin are bordered by the Lachlan Fold Belt, containing deformed Ordovician turbidites and Silurian to Carboniferous granites (Glen 2005). To the northwest of the basin it is underlain by the Proterozoic Curnamona Province and

Neoproterozoic Adelaidean rocks. The western margin of the basin is flanked by the Mount Lofty Ranges and southern Flinders Ranges, part of the Proterozoic Adelaide Rift Complex and Cambrian Stansbury Basin.

The Murray Basin contains a package of flat-lying sediments up to 600 m thick deposited over four depositional cycles in the Cenozoic and Quaternary (Brown & Stephenson 1991) (Figure 4.2):

1) Marginal marine, fluvial, and lacustrine sediments deposited in the Paleocene to Early Oligocene (Renmark Group);

2) Shallow marine carbonates with minor sand and silt deposited in the Oligocene to Mid-Miocene (Winnambool Formation, Geera Clay, and Murray Group);

3) Shallow marine, marginal marine, minor fluvial and estuarine sediments (including Loxton-Parilla Sands, Calivil Formation, Bookpurnong Formation, and Norwest Bend Formation) deposited from the Late Miocene to Early Pliocene; and,

4) Lacustrine and marginal marine sediments deposited in the Pliocene to present (Blanchetown Clay, Bungunnia Limestone, Shepparton Formation, and later aeolian and lacustrine sediments).

The Late Miocene to Early Pliocene depositional cycle is most relevant to this study. After a maximum transgression a series of oscillatory regressions and transgressions followed, with an overall trend of falling sea level (Bowler *et al.* 2006). The Bookpurnong Formation is a predominantly calcareous unit deposited in a low energy, marine shelf environment. It is considered to be the lower shore-face equivalent of the overlying Loxton-Parilla Sands (Roy *et al.* 2000) or deposited during the transgression in the Late Miocene (Brown 1985). The Loxton-Parilla Sands strandplain was deposited in the marine regressive phase. The unit is 20-120 m thick but mostly about 60 m thick. The upper surface is a series of arcuate and broadly parallel ridges, or strandlines. Early interpretations suggested ridges were underlain by extensions of the Grampians sandstone in southern Victoria (Dennant 1886, Hills 1939) or valleys created by streams (Fenner

1918). The elongate ridges were later recognised as paleo-shorelines (Blackburn 1962).

The lithology of the Loxton-Parilla Sands varies from silty sands to coarse sand and gravelly clay lenses. It is predominantly quartz sand with minor feldspar and local heavy mineral concentrations. The heavy mineral assemblage in the Loxton-Parilla Sands typically includes zircon, rutile, ilmenite, leucoxene, and monazite (Roy *et al.* 2000). Detrital muscovite is also present, especially in the lower energy depositional facies, formed in the lower shoreface and shelf environments (Paine 2004).

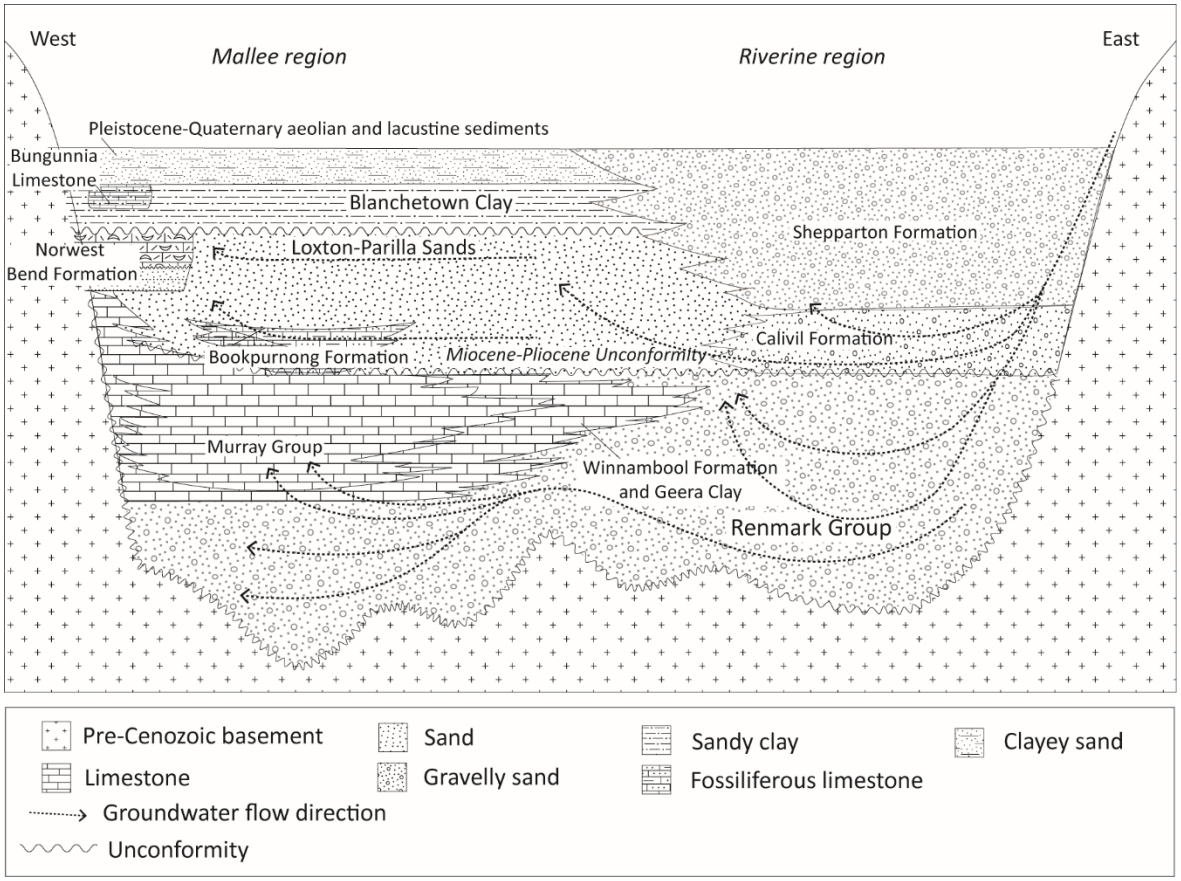

Figure 4.2 Schematic of Murray Basin stratigraphy and groundwater flow lines, after Brown and Stephenson (1991).

High porosity of the Loxton-Parilla Sands and extensive post-depositional weathering has made it difficult to establish the precise timing of deposition of the unit. Miranda *et al.* (2009) and

(McLaren *et al.* 2009), however, compared the $^{87}Sr/^{86}Sr$ ratio of brachiopods, recovered from sites across the Loxton-Parilla Sands, to the Sr calibration curve of McArthur and Howarth (2004) and McArthur *et al.* (2001). These results provide the first direct date of diachronous deposition of the Loxton-Parilla Sands. The approximate onset of deposition has been determined to be prior to 7.2 Ma, continuing into the Latest Miocene, about 5.4 Ma (Miranda 2007).

4.2.2 Geomorphology

The topography of the Murray Basin is generally subdued with surface elevations averaging 40-60 m in the northwest of the basin and up to 120-160 m above sea level in the southwest (Gallant *et al.* 2011). Ridges of the Loxton-Parilla Sands form gently undulating dunes in the western Murray Basin, up to 30 m above the adjoining swales (Gallant *et al.* 2011). Uplift of sediments has occurred along the western margin of the basin, up to 70 m, with uplift of the Mount Lofty Ranges in South Australia. In southwestern Victoria the Western Highlands were uplifted in the Pliocene, elevating the overlying marginal marine sediments of the Loxton-Parilla Sands up to 300 m above sea level (Paine *et al.* 2004, Gallant *et al.* 2011).

4.2.3 Local Geology

The development of the indurated weathering profile of the Loxton-Parilla Sands has been recognised as subaerial weathering of the strandplain as the sea regressed in the Late Miocene-Pliocene (Kotsonis 1995). Ferruginous weathering profiles are also recognised in other Neogene sediments in the Otway Basin of southern Victoria (Gill 1964). The main phase of Fe-oxide induration was thought to have occurred after a change in climate around the mid-Pliocene, interpreted as a shift from silica-dominated to Fe-oxide-dominated weathering (Kotsonis 1995). Strongly indurated parts of the Loxton-Parilla Sands are irregularly distributed across the unit, attributed to differences in rainfall across the western Murray Basin (Miranda 2007). The iron and silica dominated weathering profiles were interpreted as diagnostic of acid sulphate weathering conditions in the Late Miocene-Pliocene (Kotsonis 1995).

Weathering of iron-bearing minerals such as ilmenite (Paine 2004) and remobilisation of iron stones and oxidation of pyrite (Macumber 1991) have been suggested as sources of reduced Fe. Kotsonis (1995) concluded iron was derived locally from lateral or vertical movement of soil water in the vadose zone, not from groundwater. These models, however, do not account for differences in the ancient (marginal marine) and contemporary (inland) landscape settings and differential erosion, as well as the potential for perched groundwater systems within dune ridges and interaction with sea water.

4.3 METHODS

4.3.1 Whole rock geochemistry

We collected samples for geochemical analysis from vertical profiles exposed in quarries, train and road cuttings, and along the banks of the Murray River. Sample locations were chosen for ease of access and where the greatest vertical exposure was available in the region. Core and drill cutting samples were used to supplement field exposures, where there was no natural exposure or field profiles were shallow. Samples are predominantly from the upper sections of the Loxton-Parilla Sands stratigraphy. Field locations and top-of-profile elevations were recorded from GPS (MGA 94, Zone 54). Approximately 2 kg of sediment was collected at 1 m intervals in vertical profiles sections and narrower intervals if there was a noticeable change in lithology or weathering material morphology. We sampled drill cuttings and core stored in the core repositories of Geoscience Australia, and Geological Surveys of South Australia and Victoria. The sample size for drill cuttings from the Geological Surveys and Geoscience Australia was 15 g. This is the minimum sample size required by Acme Laboratories for geochemical analysis. Samples of core from the core repositories were approximately 100 g each. Drill cutting samples from the core libraries represent a minimum of 1 m because they were largely from reverse circulation or air core drilling (except for ‘Horsham’ bores which were fully cored). Stratigraphic logs were compiled from field observations with reference to the work of Kotsonis (1995), Miranda (2007), and Paine (2004).

All whole rock analyses were conducted at Acme Laboratories in Vancouver, Canada in seven batches over a three year period. All samples were prepared and analysed by the same methods. Rocks were crushed and sieved to -200 mesh. Major oxides were analysed via XRF with a lithium borate/lithium metaborate fusion. Rare earth and refractory elements were analysed via ICP-MS with a lithium borate fusion and dilute acid digestion. Precious metals, base metals, and pathfinder elements were analysed via ICP-MS following Aqua Regia digestion. The elements discussed in this chapter (Al_2O_3, Ba, Fe_2O_3, K_2O, Na_2O, SiO_2, TiO_2, Yb, and Zr), units of measurement, and their lower limit of detection are presented in Table 2.

Element	Unit	LLD
Al_2O_3	wt. %	0.01
Ba	ppm	1
Fe_2O_3	wt. %	0.01
K_2O	wt. %	0.01
Na_2O	wt. %	0.01
SiO_2	wt. %	0.01
TiO_2	wt. %	0.01
Yb	ppm	0.05
Zr	ppm	0.1

Table 2 Elements measured and discussed in this chapter, units, and lower detection limits.

Quality control was managed by the use of certified reference materials (CRMs), sample splits, field duplicates, and preparation and analytical blanks. Analytical accuracy was controlled by the use of CRMs including DS8, DS9, DS10, GS311-1, GS910-4, OREAS45CA, OREAS45EA, OREAS72A, OREAS72B, OREAS76A, SY-4(D), SO-18, and CSC. The laboratory also inserted analytical blanks to track reagent contamination and preparation blanks to track contamination of crushing equipment. Systematic error, calculated by comparing the expected concentration of a CRM with the mean values of repeat analyses (Caritat & Cooper 2011), was between 90-110 % for analysed elements in this chapter, except for Sb (88%). Analytical precision was determined by duplicate splits of prepared samples (inserted at a rate of 1 in 8 samples) and expressed as the coefficient of variation (*CV*) which is considered an unbiased estimate of relative error for

geochemical data (Stanley & Lawie 2007). Coefficient of variation was calculated on duplicate pairs where both analyses were above analytical detection limit. Analytical precision was ±10% for elements analysed except for Cr_2O_3 (13%) and Au (18%). Sampling precision was determined by field duplicates inserted at a rate of 1 in 15 samples at random intervals and is expressed as the coefficient of variation. Despite the geochemical heterogeneity of the Loxton-Parilla Sands, particularly the ferricrete, sampling precision was good, less than 10% for most elements, except for Cr_2O_3 (27%), TOT/C (11%), Mo (19%), and Au (21%).

4.3.2 Hyperspectral mineralogy

Reflectance spectra in the very-near infrared (VNIR), shortwave infrared (SWIR), and thermal infrared (TIR) ranges were collected at the Geological Survey of South Australia using the Hylogger™ 3 system developed by CSIRO. The HyLogger™ 3 system consists of a spectrometer with a spectral range of 400 to 14000 nm, high resolution linescan camera, and a laser profilometer. Dried, uncrushed rock samples were portioned into black plastic chip trays before being scanned by the HyLogger™. The spectra in three infrared bands are capable of distinguishing different mineral groups: VNIR (400-1100 nm) – Fe-, Mn-, and Cr- bearing minerals, rare earth element-bearing minerals; SWIR (1100-2500 nm) – Al(OH)-bearing minerals (e.g. kaolinite, montmorillonite, muscovite, phengite, paragonite, and illite), Fe(OH)- and Mn(OH)-bearing minerals, carbonates, sulphates, micas, amphiboles; and TIR (500-14000 nm) – carbonates, silicates (e.g. quartz, albite, microcline, plagioclase, olivine, pyroxene, garnet), sulphates, olivine, garnets, and pyroxenes.

Data were processed by the Geological Survey of South Australia and then further analysed using The Spectral Geologist software developed by CSIRO. The spectra were masked to remove spectral signals from black plastic and other non-geological material in the samples. The TSG program provides an automatic match of the acquired sample spectra compared to known mineral spectra in a reference library (The Spectral Assistant™ feature). We applied scalars to the spectra to calculate the relative abundance of clay minerals (dickite, montmorillonite, and kaolinite), Fe-

oxide minerals (hematite and goethite), as well as a kaolinite disorder index. The degree of kaolin disorder is calculated by measuring the depth of the 2160 nm absorption feature and comparing it to the width of the absorption doublet (Cudahy 1997). Kaolin disorder in weathering profiles has been found to be an important discriminator of transported and *in situ* weathering products (Cudahy 1997). Results are presented here as down-profile plots of clay mineralogy and relative kaolinite disorder.

4.3.3 Microanalysis

SCANNING ELECTRON MICROSCOPY

In order to study microscopic features of the weathering profile, we imaged polished thin sections at Adelaide Microscopy using a Philips XL40 scanning electron microscope fitted with a solid state backscattered electron detector and thin-film energy dispersive x-ray detector. The accelerating voltage was 20 kV and working distance was approximately 10 mm. We acquired images in back-scattered electron mode.

ELECTRON MICROPROBE ANALYSER (EMPA)

Changes in weathering processes would be expected to produce different induration textures and composition. We acquired qualitative element maps using a Cameca SXFive electron microprobe analyser (EMPA) at Adelaide Microscopy. Five wavelength dispersive detectors collected spectra for Si and Al (TAP crystals), Ba and Ti (LPET crystals), and Fe (LLIF crystal). We used an accelerating voltage of 15 kV and beam current of 100 nA. Dwell time per pixel was 50 ms for all maps. Data were collected using ProbeImage software (Probe Software, Inc.) and processed using iTEM (Olympus Soft Imaging Solutions GmbH). The major advantage of electron microprobe elemental analysis over other microanlaytical techniques is the combination of geochemical information and excellent spatial resolution, down to 1 µm.

The element maps we collected by EMPA are qualitative rather than quantitative. Matrix-matching of standards with such geochemically heterogeneous materials is difficult when local Fe_2O_3 concentrations in the indurated weathering horizon can be in excess of 80 wt. %. The aim of the EMPA technique was to image micrometre-scale elemental heterogeneity and as such quantification was a second priority.

4.4 RESULTS

4.4.1 Profile characteristics

The eleven representative profiles from across the Loxton-Parilla Sands described here show sedimentology and stratigraphy as well as weathering and induration features typical of the Loxton-Parilla Sands (Figure 4.3). The unit is typically a mature sediment comprising fine to coarse quartz sand that is white to pale yellow and increasingly orange-red towards the top of the profile (Figure 4.4). Sedimentary features such as cross-bedding (10 cm to 2 m) are preserved in profiles such as Gredgwin Ridge, Loxton, and Ultima. At other locations such features did not form, are not exposed, or have been destroyed or obscured by weathering and erosion.

The sedimentary facies of the Loxton-Parilla Sands are associated with muscovite and heavy mineral abundances, and some clay components of the mineralogy. Muscovite is typically present in the lower shoreface to near-shore facies, generally the basal facies of the Loxton-Parilla Sands. Fine to very fine heavy minerals are concentrated in beds up to 10 m thick in the swash facies. Lenses of gravel and clay in the Loxton-Parilla Sands are relatively rare. Green, clayey coarse sand to gravelly horizons, less than 5 cm thick, occur at Lyrup and Chowilla. The mineralogy of the green clay is unresolved but is possibly vermiculite.

Post-depositional features in profiles of the Loxton-Parilla Sands include mottles, leached zones, solution pipes and hollows, and indurated zones of silcrete and ferricrete with a variety of textures. Mottling of the Loxton-Parilla Sands is very common and increases up-section. The mottles vary in

shape but are mostly laminar (Figure 4.5a) or irregular, with diffuse or sharp boundaries (Figure 4.5b). Irregular, patchy mottles are more common in fine sand with lower permeability, while flat-lying indurations are mostly associated with medium to coarse sand (Figure 4.5). Beneath the weathering zone the sand is white to grey-brown (Figure 4.4), but this transition is rarely exposed in outcrop. Vertical solution pipes at Nyah cross-cut the entire 2 m profile, up to 40 cm wide (Figure 4.6). Pipes are filled with ferric nodules. The outer surface of the nodules has a "candle-wax" appearance from illuviation of silica. Similarly, at Chowilla and Ultima (Figure 4.7a), metre-wide lens-shaped hollows beneath the mottled zone are filled with fragments of sandstone, mud, and iron indurated sand.

The major post-depositional indurated features in the Loxton-Parilla Sands are silcrete and, more commonly, ferricrete. Sequences of the Loxton-Parilla Sands at Ultima and Lyrup (Figure 4.7) are capped by silcretes that are in turn overlain by sandy pisolitic ferricrete. The silcrete at Ultima includes thin (<1 mm) laminae of SiO_2 and TiO_2 that fill voids between very fine sand, stained with goethite (Figure 4.7b). At Lyrup, the massive silcrete is up to 1 m thick and occurs as irregular lenses (Figure 4.7c, d). The upper surface is reworked, with sharp fragments of microcrystalline silica incorporated into the overlying sandstone. Silcrete is also prominent at Nyah where the upper 30 cm of the profile is made up of gently undulating silica-rich bands (Figure 4.7e). This profile is not overlain by pisolitic sandstone but the land surface has been reworked and pisoliths could have been eroded away.

The most strongly Fe-oxide indurated parts of the Loxton-Parilla Sands occur towards the upper few metres of the unit, typically overlie silcrete. Development is patchy across the western Murray Basin. Ferricrete characteristic of the Loxton-Parilla Sands includes indurated laminations, pisolitic sandstone, loosely scattered pisoliths and irregular concretions. In the mottled zone, at a number of profiles, sand is cemented by thin (usually <1 cm), flat-lying or undulating bands of brown-dark brown cement, likely goethite (Figure 4.8a). In the upper sections of profiles at Goroke (Figure

4.8b), Lyrup (Figure 4.8c) and Ultima (Figure 4.7b) is a horizon of densely packed pisoliths and ferruginous concretions. Pisoliths loose above the profile at Goroke have smooth outer surfaces and are generally <1 cm in diameter. Further nodules are incorporated into sandy clay. Pisoliths at Lyrup and Ultima range from 1-3 cm in diameter and are relatively uniform in morphology. They tend to be well-formed, with a red-brown hematite-rich sandy core surrounded by a rim of brown goethite-cemented sand.

Scattered pisoliths at Diapur (Figure 4.8e) are spherical nodules, 1-2 cm in diameter, with either a dark brown hematitic rind or lighter brown goethitic rind. Relatively pale plain bedded fine sand at Spicer's Pit (Figure 4.8d) has occasional vertical red mottles which become more intensely indurated up-section. At this profile the indurated horizon contains large (up to 8 cm) irregular ferruginous concretions with laminated rinds (Figure 4.8d, inset). Small fragments (<2 cm) of ferruginised plant material are also common in the indurated section (Figure 4.9). The internal cellular structure and primary porosity of the plant material is very well preserved and has been completely replaced by hematite.

The Loxton-Parilla Sands rarely directly overlies bedrock. An exposure at Wannon is the only profile on bedrock, where a thin (<8 m) layer of the Loxton-Parilla Sands unconformably overlies the Nigretta Ignimbrite (Figure 4.10a). This outcrop is in the Western Highlands, where the uplifted and dissected landscape is very different to when the Loxton-Parilla Sands was deposited. Very strongly mottled sands in this profile overlie saprolite and ignimbrite (Figure 4.10b). The groundmass of the ignimbrite has been altered to white kaolin while phenocrysts remain intact and *in situ*, preserving the texture of the parent rock (Figure 4.10c). The contact with the overlying Loxton-Parilla Sands is undulating. The mottled zone in the Loxton-Parilla Sands is mantled by a thin layer (<20 cm) of friable clay with small (<0.5 cm) hard, rounded hematitic concretions. The mottled Loxton-Parilla Sands profile is strongly bioturbated by recent ant and termitaria activity.

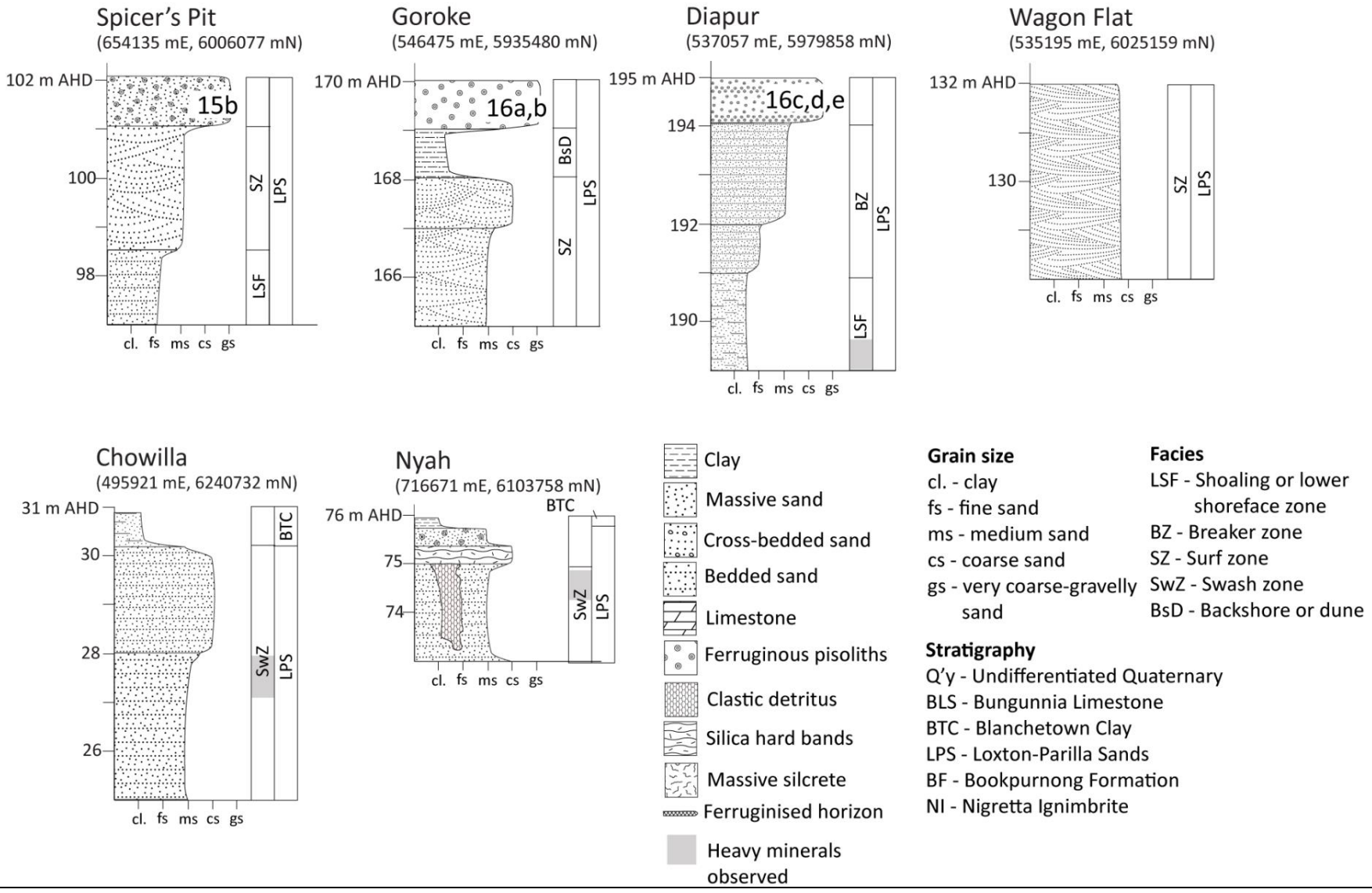
Spicer's Pit
(654135 mE, 6006077 mN)
102 m AHD
100
98
15b
SZ
LSF
LPS
cl. fs ms cs gs
Goroke
(546475 mE, 5935480 mN)
170 m AHD
168
166
16a,b
BsD
SZ
LPS
cl. fs ms cs gs
Diapur
(537057 mE, 5979858 mN)
195 m AHD
194
192
190
16c,d,e
BZ
LSF
LPS
cl. fs ms cs gs
Wagon Flat
(535195 mE, 6025159 mN)
132 m AHD
130
SZ
LPS
cl. fs ms cs gs
Chowilla
(495921 mE, 6240732 mN)
31 m AHD
30
28
26
BTC
SwZ
LPS
cl. fs ms cs gs
Nyah
(716671 mE, 6103758 mN)
76 m AHD
75
74
BTC
SwZ
LPS
cl. fs ms cs gs
Clay
Massive sand
Cross-bedded sand
Bedded sand
Limestone
Ferruginous pisoliths
Clastic detritus
Silica hard bands
Massive silcrete
Ferruginised horizon
Heavy minerals observed
Grain size
cl. - clay
fs - fine sand
ms - medium sand
cs - coarse sand
gs - very coarse-gravelly sand
Facies
LSF - Shoaling or lower shoreface zone
BZ - Breaker zone
SZ - Surf zone
SwZ - Swash zone
BsD - Backshore or dune
Stratigraphy
Q'y - Undifferentiated Quaternary
BLS - Bungunnia Limestone
BTC - Blanchetown Clay
LPS - Loxton-Parilla Sands
BF - Bookpurnong Formation
NI - Nigretta Ignimbrite

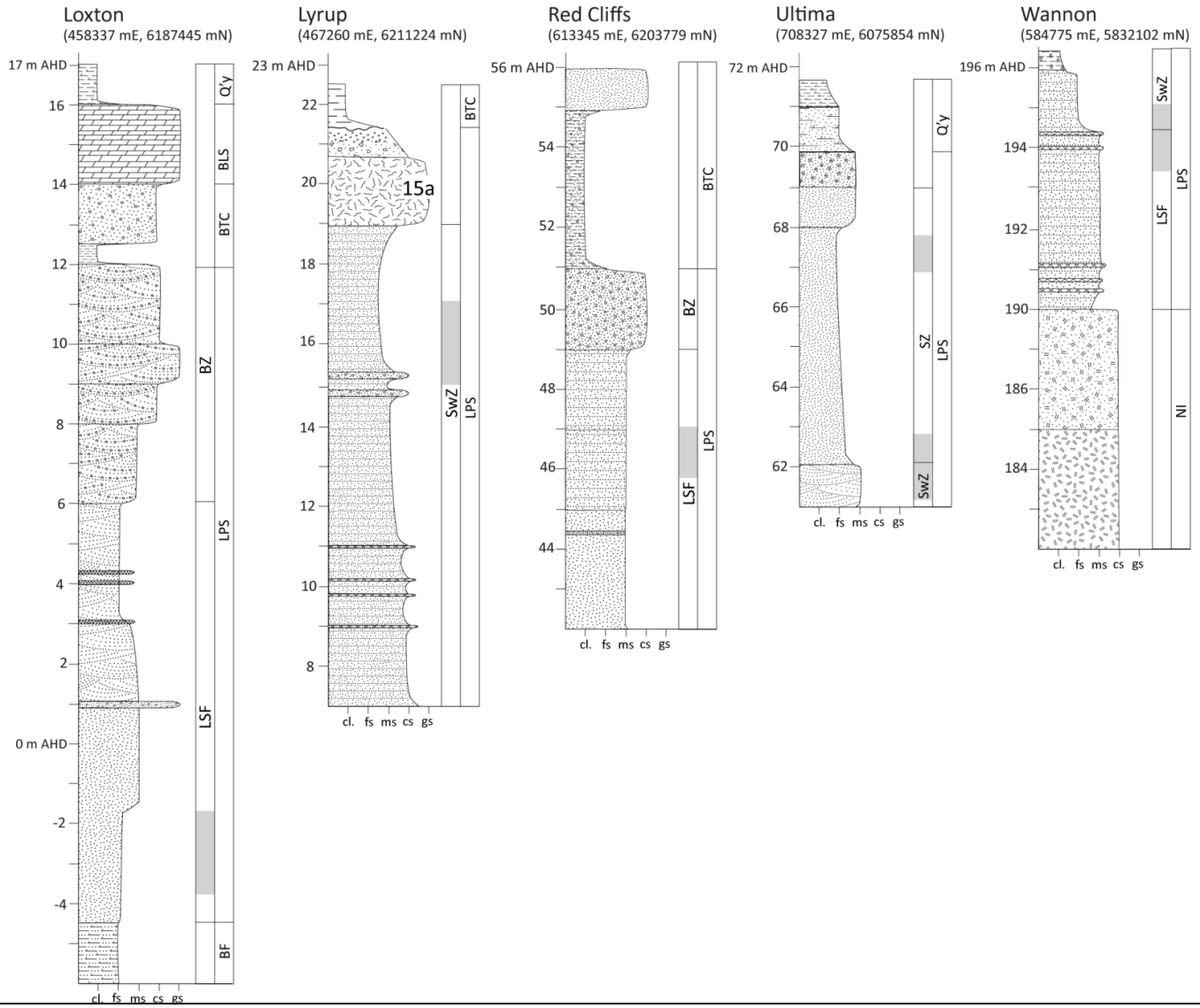
Loxton
(458337 mE, 6187445 mN)
17 m AHD
16
14
12
10
8
6
4
2
0 m AHD
-2
-4
Q'y
BLS
BTC
BZ
LPS
LSF
BF
cl. fs ms cs gs
Lyrup
(467260 mE, 6211224 mN)
23 m AHD
22
20
18
16
14
12
10
8
15a
BTC
SwZ
LPS
cl. fs ms cs gs
Red Cliffs
(613345 mE, 6203779 mN)
56 m AHD
54
52
50
48
46
44
BTC
BZ
LPS
LSF
cl. fs ms cs gs
Ultima
(708327 mE, 6075854 mN)
72 m AHD
70
68
66
64
62
Q'y
SZ
LPS
SwZ
cl. fs ms cs gs
Wannon
(584775 mE, 5832102 mN)
196 m AHD
194
192
190
186
184
SwZ
LSF
LPS
NI
cl. fs ms cs gs

(Previous page) Figure 4.3 Grain size, stratigraphy, and facies logs of the Loxton-Parilla Sands from profiles discussed in this chapter. Also shown are the stratigraphic position of thin sections and the figure number of corresponding major element maps.

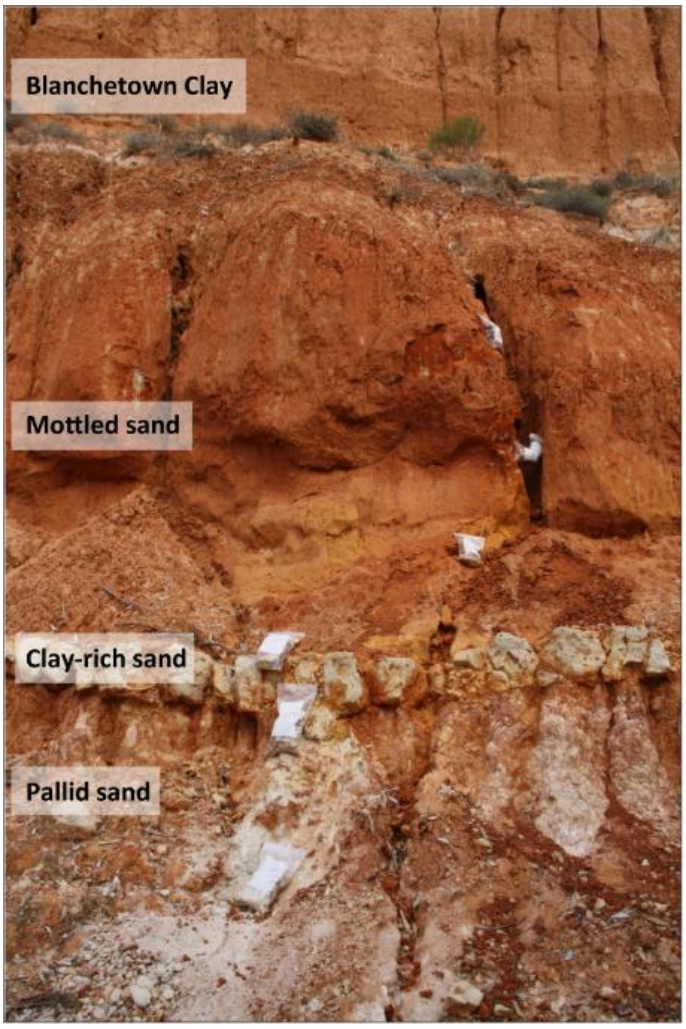

Figure 4.4 Exposed profile of the Loxton-Parilla Sands and Blanchetown Clay at Red Cliffs, typical of exposures of the Loxton-Parilla Sands in the western Murray Basin. Massive, mottled sand with pallid, kaolin-rich zone, overlain by strongly mottled sand (mostly covered by detritus), overlain by the Blanchetown Clay. Bags are 32 cm tall.

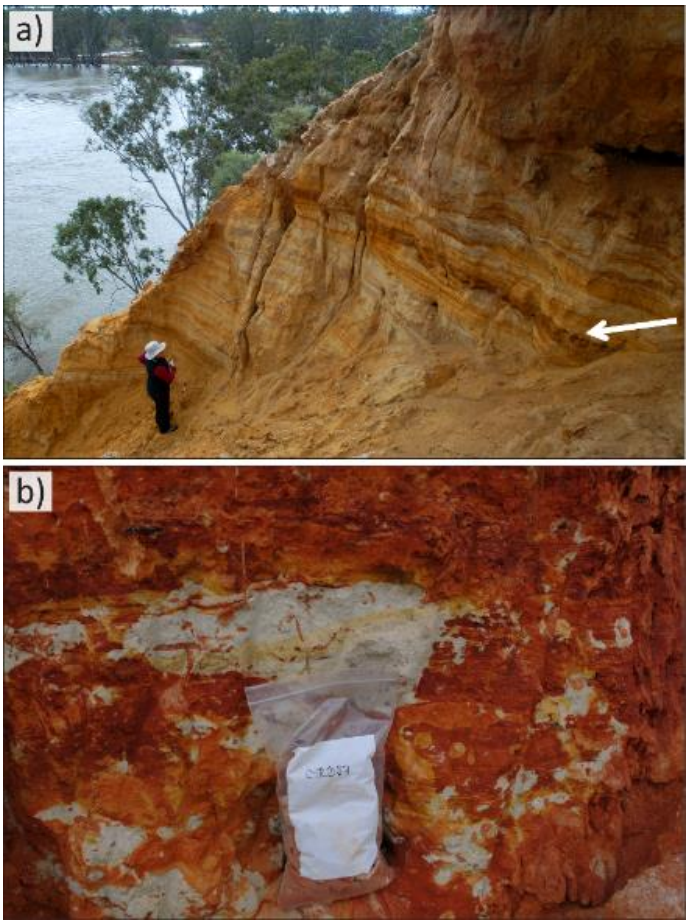

Figure 4.5 a) Loxton-Parilla Sands exposed at Loxton. Plain bedding and trough cross-bedding with laminar mottles and irregular hematitic laminae. Iron-rich laminae (arrow) mark the level of a long-lived paleo-water table. Figure for scale. Photo by S. Hill, b) Irregular mottles in fine sand at Lyrup. Bag is 32 cm tall.

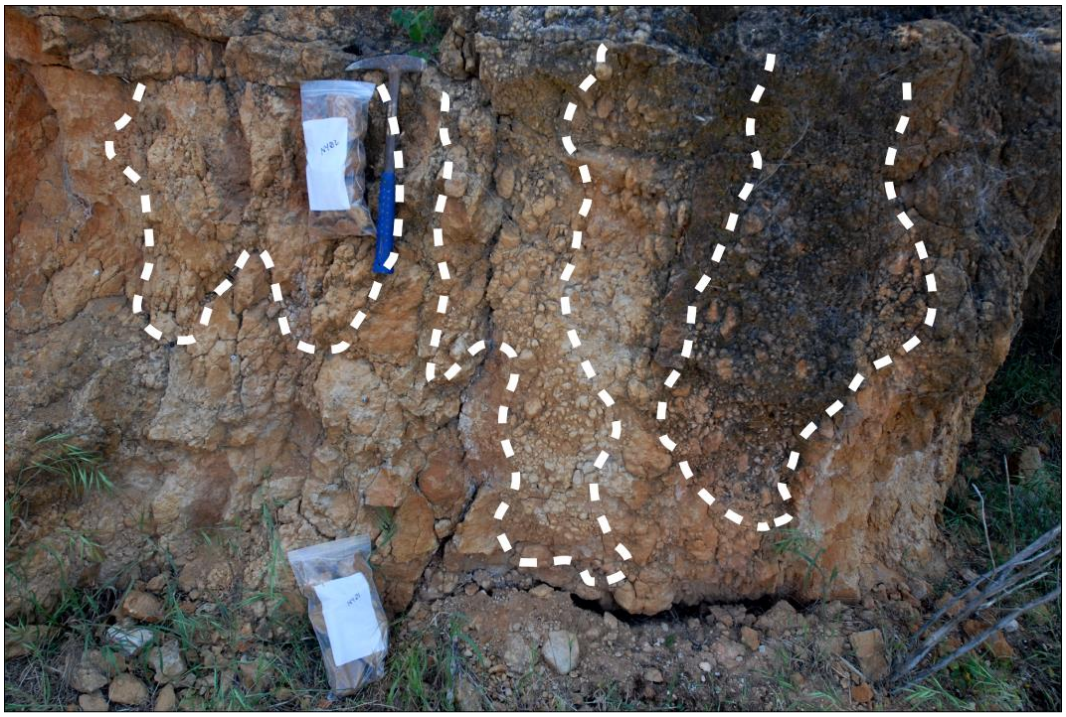

Figure 4.6 Solution pipes in the weathering profile of the Loxton-Parilla Sands at Nyah. The pipes are filled with silicified nodules and iron-mottled clasts of sandstone. Hammer is 45 cm long.

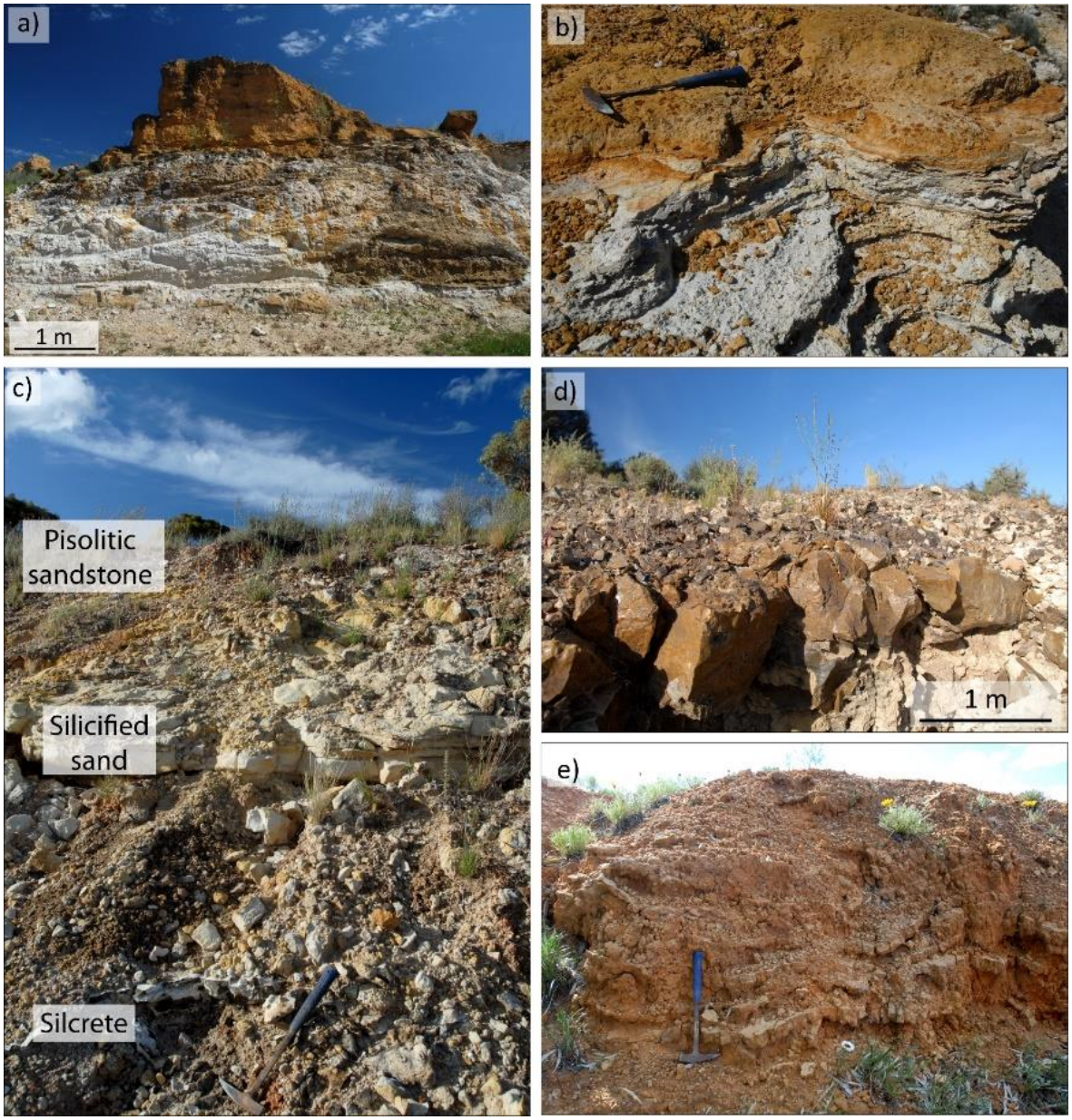

Figure 4.7 a) Profile of the Loxton-Parilla Sands at Ultima. Cross-bedded, muscovitic, fine sand is overlain by laminar silcrete, which is in turn overlain by mottled and pisolitic sandstone. The deep marks in the pale sand are scour marks from quarry machinery which obscure cross-bedding. Note the solution hollow that has been filled with transported material on right hand side of profile, b) which obscure cross-bedding. Note the solution hollow that has been filled with transported material on right hand side of profile, c) Indurated weathering profile of the Loxton-Parilla Sands exposed at Lyrup. Massive silcrete overlain by kaolin-rich sand, which is overlain by mottled and pisolitic sandstone. Hammer is 45 cm long, d) Massive jointed silcrete at Lyrup, e) Undulating silica hard bands at Nyah. Bands are fractured, forming silica-rich nodules. Hammer is 45 cm long.

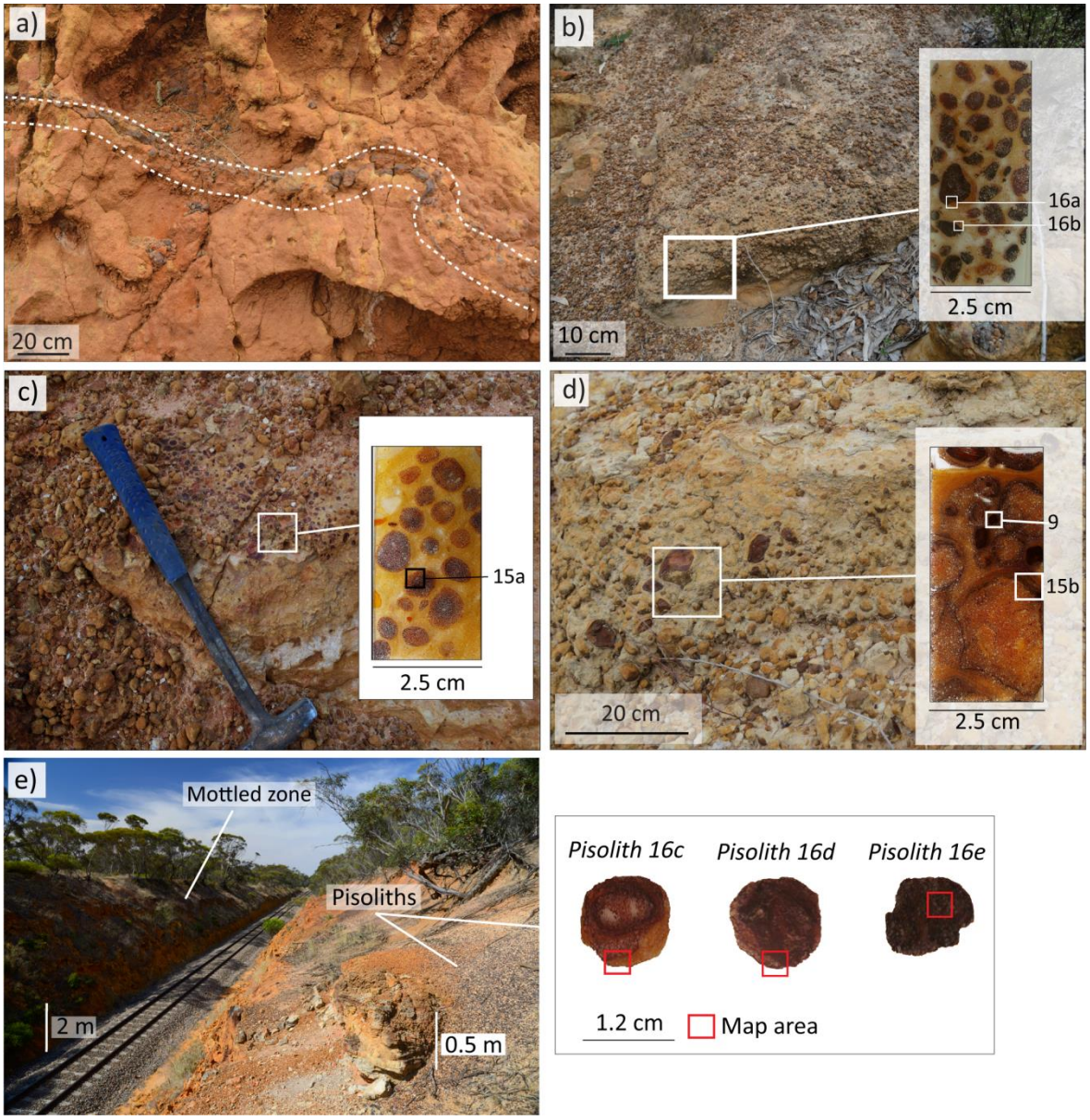

Figure 4.8 a) a. Irregular goethite induration at Goroke. The indurated horizon can be traced for about five metres through the profile, sub-parallel to the land surface. The indurated horizon is fractured and forms nodules from 0.5-10 cm wide, b) Pisoliths in loose sandy clay overlain by loosely scattered pisoliths at Goroke. Inset: thin section showing location of major element maps, c) Well-lithified pisoliths in profile at Lyrup and thin section showing location of major element map. Hammer is 45 cm long, d), irregular-shaped indurated mottles at Spicer's Pit, e) Weathering profile at Diapur, showing loose pisoliths overlying the profile and location of major elements maps in select pisoliths.

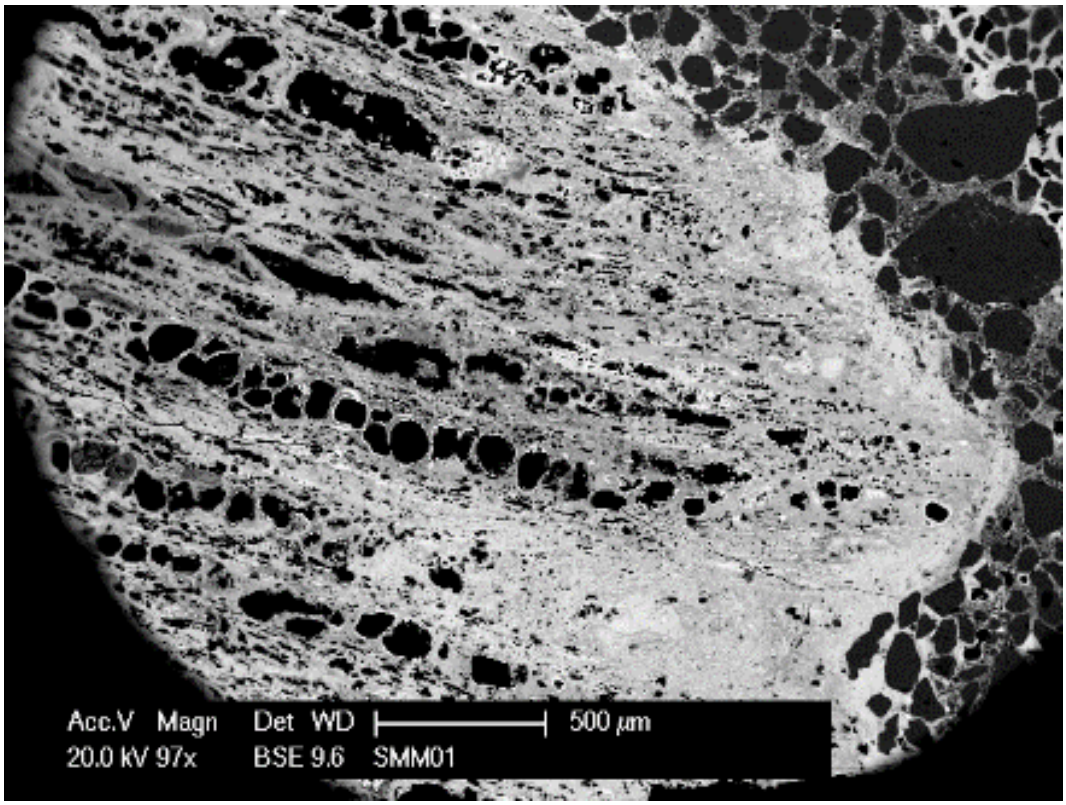

Figure 4.9 Scanning electron micrograph of ferruginised plant material from the indurated zone at Spicer's Pit. Micrograph was taken in back-scattered electron mode.

4.4.2 Profile chemistry and mineralogy

The geochemistry of the Loxton-Parilla Sands is dominated by the major elements Si, Al, and Fe. These elements comprise over 95% of the total whole rock geochemistry in most of the unit. Geochemical results discussed in this chapter are summarised in Figure 4.11 and Figure 4.12. Silicon (measured as SiO_2) is the dominant geochemical component of the Loxton-Parilla Sands (Figure 4.11a). Lower concentrations of SiO_2 are due to dilution by increasing clay contents, concentrations of heavy minerals, carbonates, and Fe-oxide induration (Figure 4.12a). Two-thirds of samples contain more than 85.0 wt. % SiO_2. Geochemical plots and stratigraphic and grain size logs are presented for Horsham-7, a profile characteristic of the Loxton-Parilla Sands (Figure 4.13). Silica is mostly associated with quartz sand which can be almost 100% of the mineralogy particularly in the breaker zone facies. Microcrystalline silica also fills in pore spaces associated with silcrete and some ferricrete horizons.

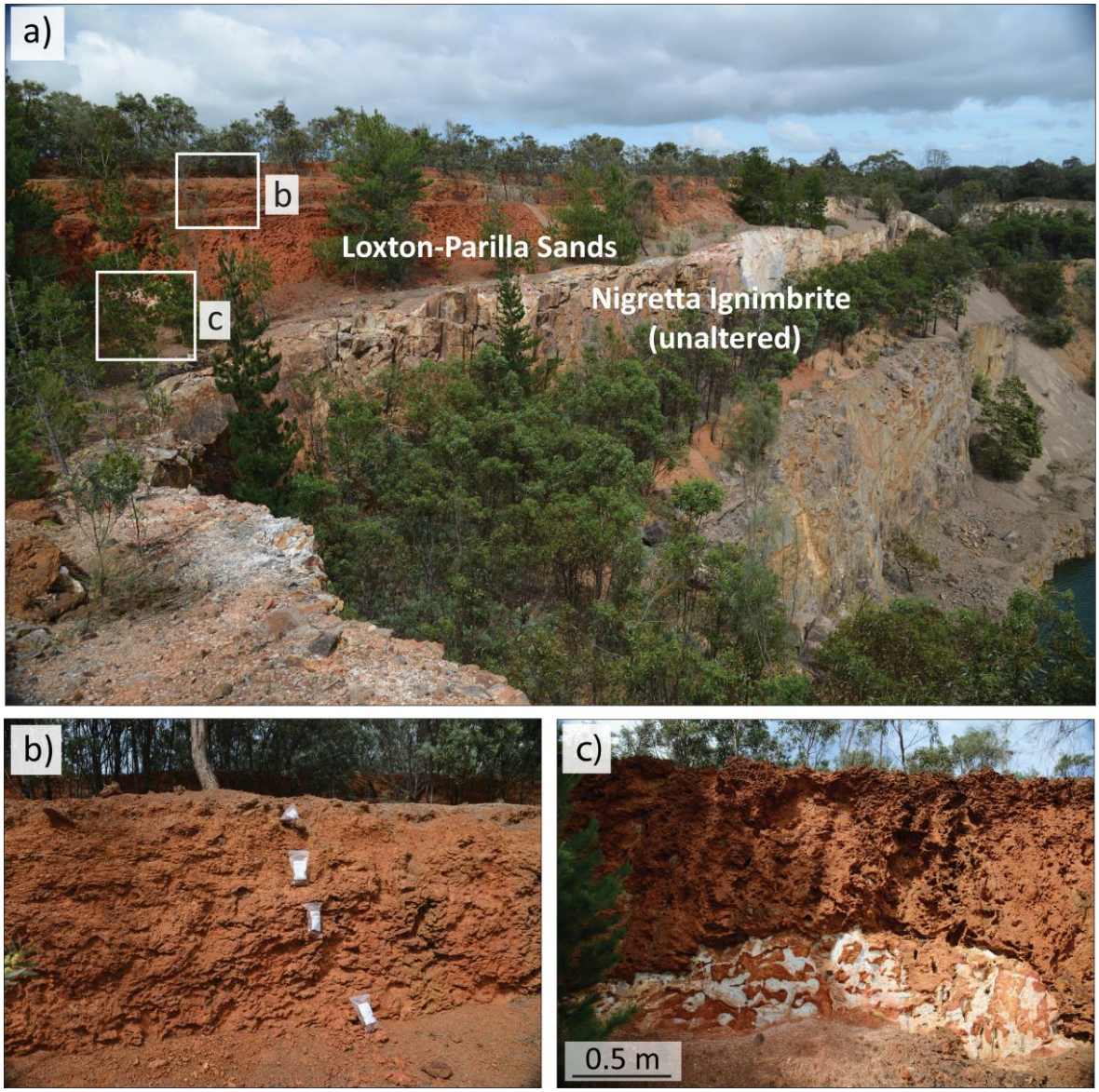

Figure 4.10 a) Strongly mottled Loxton-Parilla Sands at Wannon. Small ferric nodules, less than 1 cm in diameter, lie on top of the profile. Bags are 32 cm high, b) Strongly mottled Loxton-Parilla Sands on top of strongly mottled saprolite at Wannon.

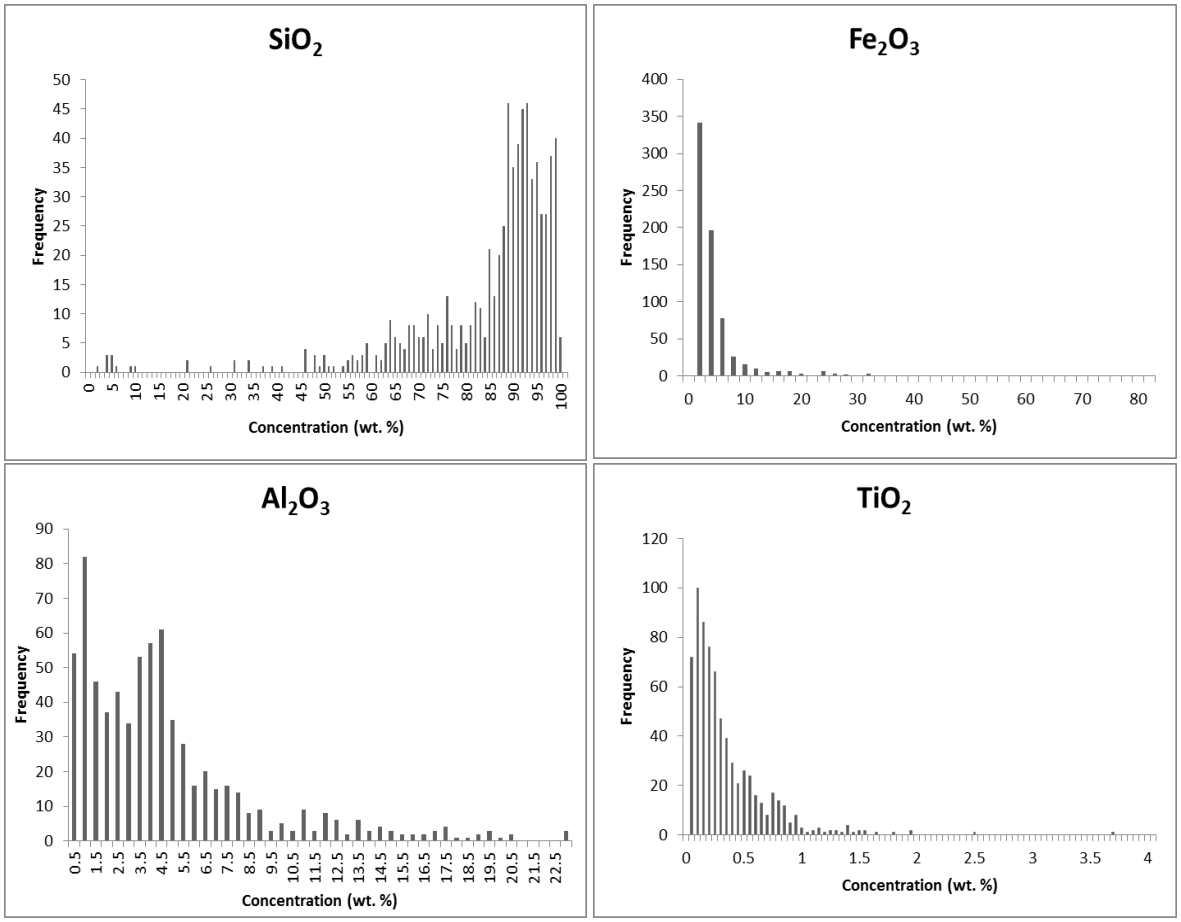

Figure 4.11 Histograms of a) SiO2, b) Al2O3, c) Fe2O3, and d) TiO2 from the Loxton-Parilla Sands (603 samples).

Iron (measured as Fe_2O_3) is the second most abundant major element with a median concentration of 1.97 wt. % and up to 79.66 wt. %. Three-quarters of samples contain less than 5.06 wt. % Fe_2O_3. Samples with Fe_2O_3 concentrations in excess of 5 wt. % correspond to zones with laminated fine grained goethite indurations, pisoliths, strongly Fe-oxide indurated concretions, and massive Fe-oxide precipitation. A ternary plot of Si-Al-Fe (Figure 4.12a) shows there is a continuum of Fe_2O_3 concentrations in the weathering profile, mostly related to the amount of quartz sand and Al_2O_3 incorporated into the matrix of ferricretes (Figure 4.12a). Fe-oxide concentrations tend to increase towards the top of most profiles, with increasing degree of induration. Accumulations of heavy minerals, such as ilmenite and rutile between 60 – 85 m depth in Horsham-7, have resulted in increased Fe_2O_3 and TiO_2 concentrations. This horizon is associated with an increase in Zr, Yb, and other rare earth elements. Infrared spectroscopy shows that the Fe-oxide phase is dominated by

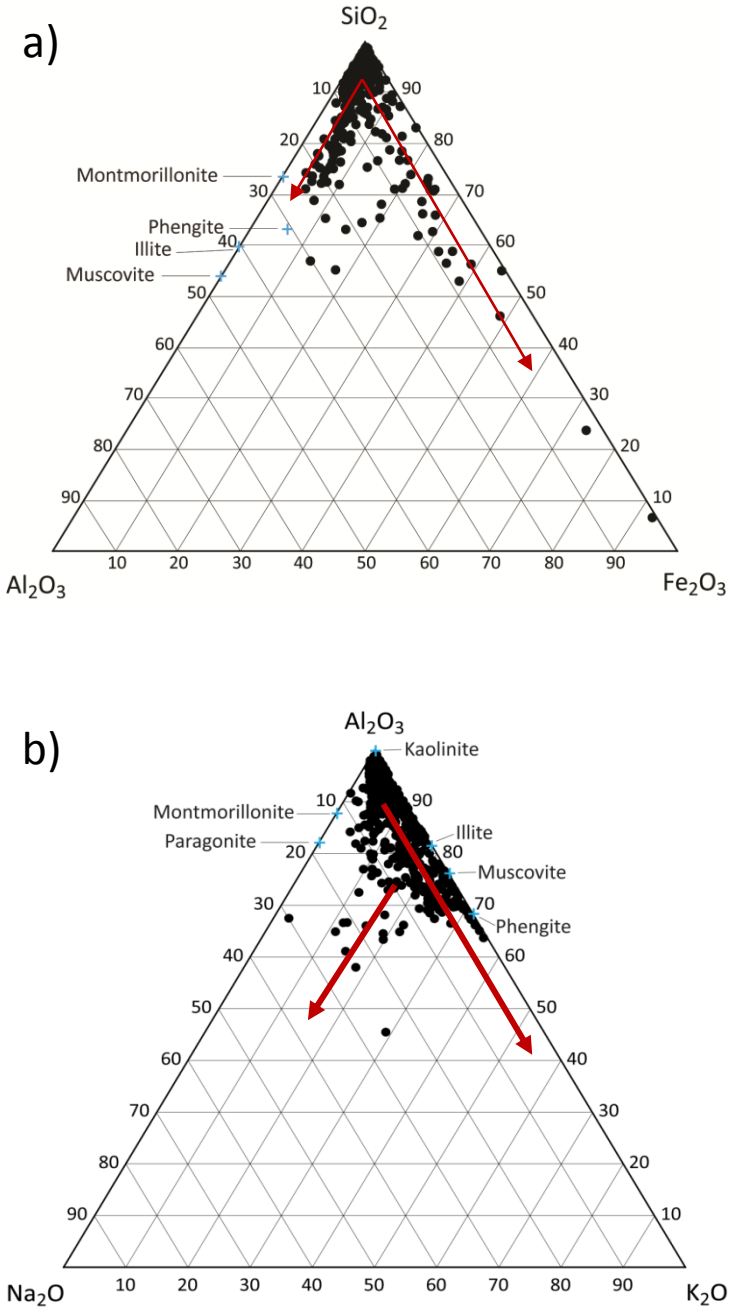

Figure 4.12 a. Si-Al-Fe ternary plot for the Loxton-Parilla Sands (603 samples). Dominant clay and white mica mineral compositions are plotted on the diagram. Red arrows show the general mixing trends for quartz sand with clay minerals (Si-Al) and Fe-oxides (Si-Fe), b) Al-Na-K ternary plot for the Loxton-Parilla Sands (603 samples). Dominant clay and white mica mineral compositions are plotted on the diagram. Red arrows show the mixing trend of kaolinite with K-rich minerals (illite, muscovite, phengite) with Na-rich minerals (montmorillonite, paragonite, and halite).

goethite with hematite only detected in a few samples. Goethite spectra from the Loxton-Parilla Sands (Figure 4.14a) shows the characteristic absorption features near 480nm, 1400nm (OH^- absorption feature), 910 nm, and a broad water absorption feature between 1900-2000 nm, from structural water in goethite crystals (Cudahy & Ramanaidou 1997, Eggleton 2008). Observations of hand samples suggest hematite is more common than the infrared mineralogy results indicate but goethite is so common it appears to dominate the spectra.

Aluminium (measured as Al_2O_3) is also a significant component of the geochemistry and is associated with clay minerals, muscovite, and Fe-oxides. Clay mineralogy is dominated by well- and poorly-crystalline kaolinite, with lesser smectite (montmorillonite) (Figure 4.13). Figure 4.14b shows a kaolinite spectrum from the Gredgwin Ridge profile, characteristic of most of the clay minerals in the Loxton-Parilla Sands. The absorption feature (doublet) near 2160-2210 nm is characteristic of kaolinite (Cudahy 1997). The wide feature between 1900-2000 nm suggests there is significant water in the mineral structure and the mineralogy is probably closer to halloysite ($Al_2Si_2O_5(OH)_4.0\text{-}2H_2O$) or smectite than kaolinite (Cudahy 1997, Eggleton 2008). The montmorillonite spectra (Figure 4.14c), however, also have absorption features near 1400 nm and 1900-2000 nm (related to –OH in the crystal structure) but the single absorption feature near 2200 nm is indicative of montmorillonite (Pontual *et al.* 2010). The Al-Na-K ternary plot (Figure 4.12b) shows most samples plot along the kaolinite -muscovite trend and are pulled out towards the Na_2O apex by montmorillonite and possibly paragonite and halite. Aluminium concentrations tend to increase up-section in Profiles (Figure 4.13) as clay abundance increases. Higher concentrations of Al_2O_3 are also associated with muscovitic horizons in the lower shoreface facies, particularly at the Gredgwin Ridge profile. Many profiles of the Loxton-Parilla Sands contain muscovite in the lower portions of the profile, usually lower shoreface or nearshore facies; however, it was only detected by HyLogger™ in the Gredgwin Ridge and Horsham-7 profiles. The Fe-oxide component of the geochemistry in Figure 4.13a also has a trend of samples with moderate Al_2O_3. The association of Al with Fe-oxides is more apparent at the grain scale and is discussed below.

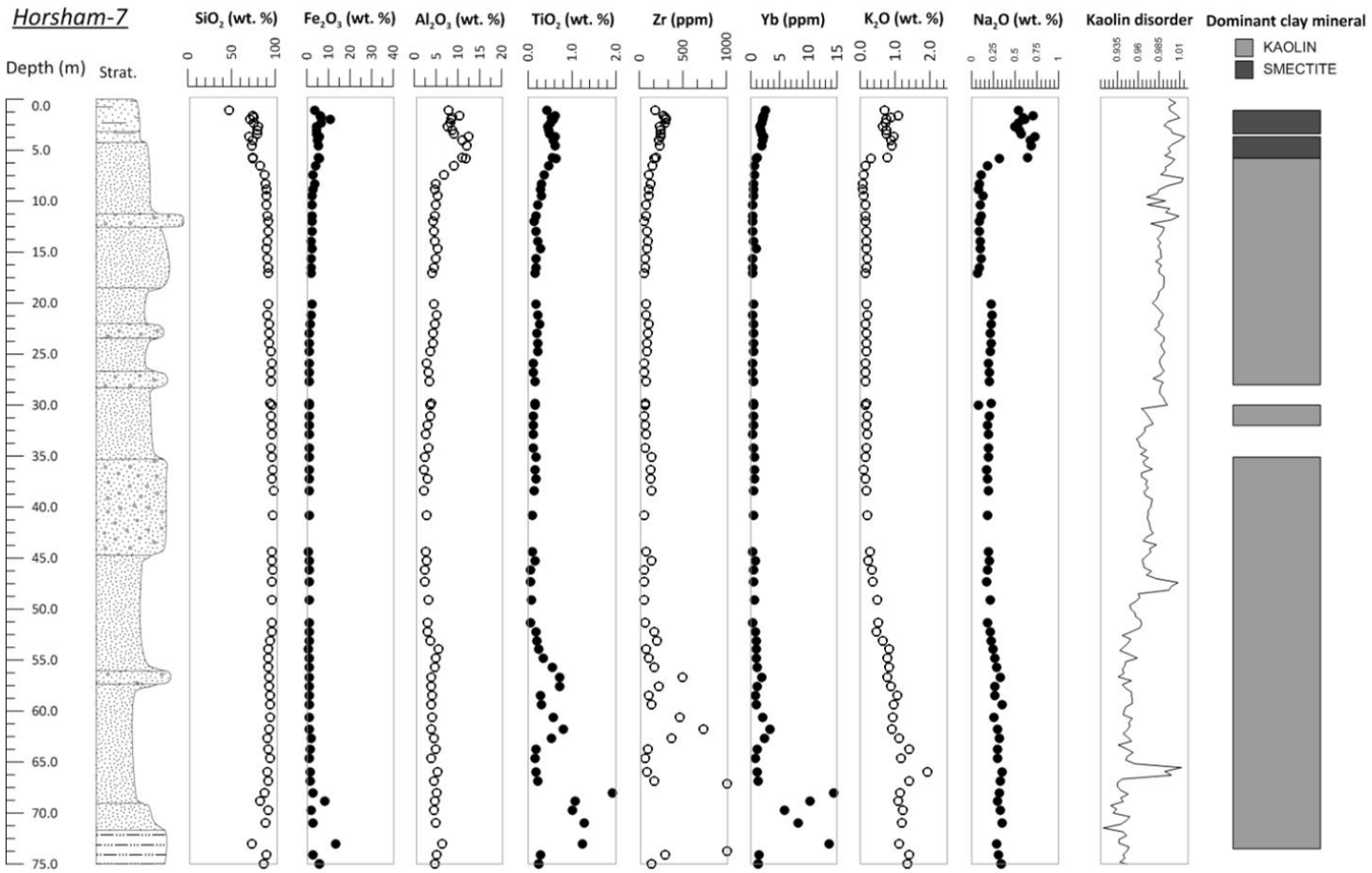

Figure 4.13 Stratigraphy, geochemical plots of SiO2, Fe_2O_3, Al_2O_3, TiO2, Zr, Yb,K2O, Na2O, kaolin disorder index and dominant clay mineral (determined by HyLoggerTM) at Horsham-7 (bore).

a)


Goethite (reference)
Sample goethite (Gredgwin Ridge)
Reflectance
480 nm
910 nm
1415 nm
1900-2000 nm
400 500 600 700 800 900 1000 1100 1200 1300 1400 1500 1600 1700 1800 1900 2000 2100 2200 2300 2400 2500
Wavelength (nm)

b)

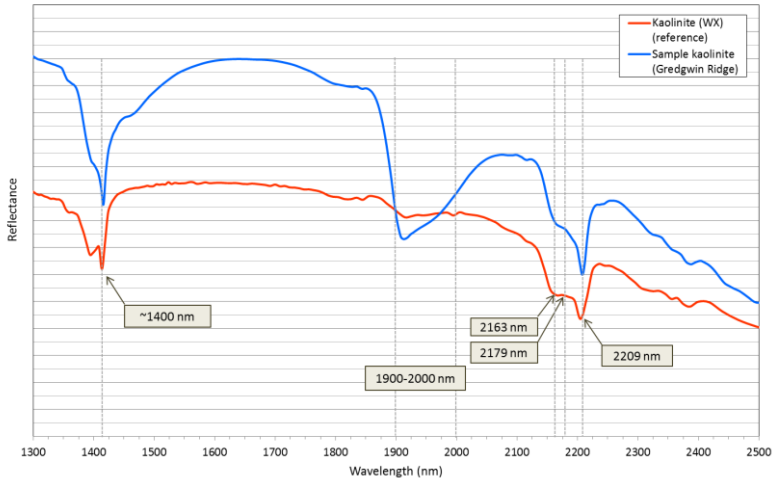
Kaolinite (WX) (reference)
Sample kaolinite (Gredgwin Ridge)
Reflectance
~1400 nm
2163 nm
2179 nm
2209 nm
1900-2000 nm
1300 1400 1500 1600 1700 1800 1900 2000 2100 2200 2300 2400 2500
Wavelength (nm)

c)

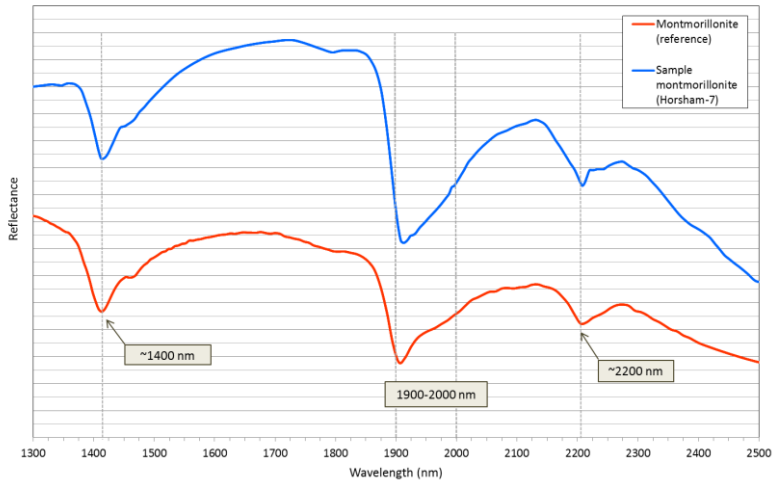
Montmorillonite (reference)
Sample montmorillonite (Horsham-7)
Reflectance
~1400 nm
~2200 nm
1900-2000 nm
1300 1400 1500 1600 1700 1800 1900 2000 2100 2200 2300 2400 2500
Wavelength (nm)

(Previous page) Figure 4.14 HyLogger^{TM} spectra for samples of the Loxton-Parilla Sands (blue) and reference spectra (red) from minerals in the USGS Digital Spectral Library (Clark et al. 2011). Note the wide water absorption features for each sample spectrum between 1900-2000 nm. Reflectance is relative as spectra have been offset for clarity. a) Spectrum for goethite at the Gredgwin Ridge profile (blue) and reference spectrum for goethite (red), b) Spectrum for kaolinite at the Gredgwin Ridge profile (blue) and reference spectrum for kaolinite (red), c) Spectrum for montmorillonite in the Horsham-7profile (blue) and reference spectrum for montmorillonite (red).

4.4.3 Petrography

Pisoliths and concretions in the Loxton-Parilla Sands show a number of variations in grain size, overgrowth and dissolution of quartz grains, chemical composition, and Fe-oxide textures. We used electron microprobe element maps to study textural and compositional changes at the grain scale. These features are closely related. Silicon element maps shows the embayed, sub-angular to angular nature of quartz grains in the indurated Loxton-Parilla Sands. Sand grain size distribution in some ferricretes is relatively uniform (Figure 4.15a) while other ferricretes are very heterogeneous (Figure 4.15b). Ferricretes with heterogeneous sand grain sizes tend to be dominated by the Fe-oxide matrix rather than grain-supported. Some of the pisoliths in these ferricretes have finely laminated (tens of micrometres) bands of hematite and goethite from multiple growth cycles. These laminations can be either concentric around a sand grain (Figure 4.16a) or fragmented (Figure 4.16b). Some sand grains in ferricretes are also fractured (Figure 4.16e). Quartz sand in the Loxton-Parilla Sands tends to be monocrystalline but fractured polycrystalline grains have been observed where Fe has precipitated along grain boundaries.

Well-formed pisoliths in the Loxton-Parilla Sands possess a hematitic core surrounded by a goethite rim (Figure 4.15a). The goethite rim of these pisoliths has relatively high Al, compared to the core. The boundary between the core and rim is sharp, as is the boundary from rim to the surrounding sand. Barite fills some pore spaces, tending to accumulate at the transition between the core and rim. The presence of barite in the indurated weathering profile cannot be resolved in

whole rock geochemistry. Over 90% of samples are below average crustal concentrations (Rudnick & Gao 2014). The pisolitic sandstone at Lyrup, however, has almost four times average crustal abundance of Ba.

Pisoliths loosely scattered on the land surface and incorporated into sandy clay at some profiles have very different internal textures and chemistry to the concentric pisoliths at Lyrup, described above. Pisoliths at Goroke are sub-angular with smooth edges (Figure 4.8b). In thin section these nodules have irregular, fragmented internal textures with alternating bands of moderate and high Fe (Figure 4.16a, b). Pisoliths at Diapur are also smooth, reworked particles approximately 1-2 cm in diameter that are scattered loosely on the land surface (Figure 4.8e). There are two types of pisoliths at Diapur – concentric layers of Fe-oxide between quartz grains surrounded by a goethitic rind reflecting multiple growth phases (Figure 4.8e, Figure 4.16 c) and dark brown throughout with a fragmented internal structure (Figure 4.8e, Figure 4.16b, c). The goethite-rimmed pisoliths have concentric laminations of Fe-oxides (Figure 4.16c), alternating between Al-rich and Al-poor layers. The hematitic pisoliths, however, have a matrix that alternates between Fe-rich and Si-rich, with Al components (Figure 4.16d, e).

Strongly iron-indurated sandstones at some profiles have laminated Fe-oxides and indurated mottles (Figure 4.15b). Thin laminations (<50 μm) alternate between Fe-rich and Fe-poor matrix between sand grains. Relative Al abundance tends to increase towards the outer edge of the concretion (lower left, Figure 4.15b). Similar to the fragmented pisoliths, quartz grain density and packing decreases slightly where there is a greater abundance of Fe-oxide (centre, Figure 4.15b). Plant material has been completely replaced by hematite. Tissue structure and original porosity has been very well preserved. Hematitic plant fragments (<1 cm) are common in the indurated part of this profile.

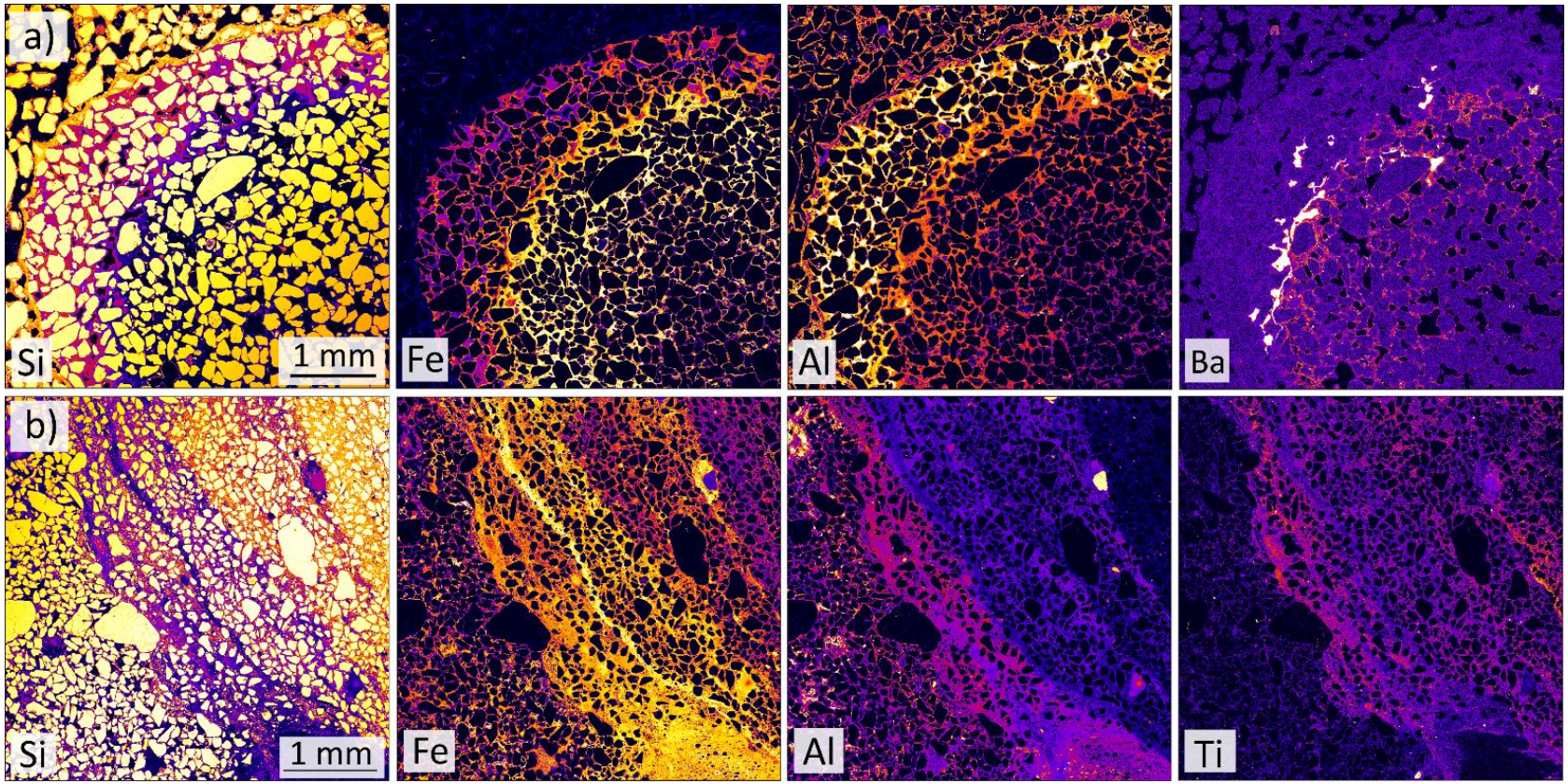

Figure 4.15 Electron microprobe maps of major elements for selected ferricrete samples from the Loxton-Parilla Sands. Relative colour scale, yellow is high abundance, purple-black is low abundance. a) Element maps of Si, Al, Fe, and Ba of the core and rim of a pisolith from Lyrup, b) Element maps of Si, Fe, Al, Ti for fragment of iron indurated sand at Spicer's Pit. Note the small preserved wood fragment in the lower right corner of the micrograph. Also note the relative increase in Al to the left of the micrograph (interior of concretion) and increase in Ti to the right of the micrograph (outside of concretion).

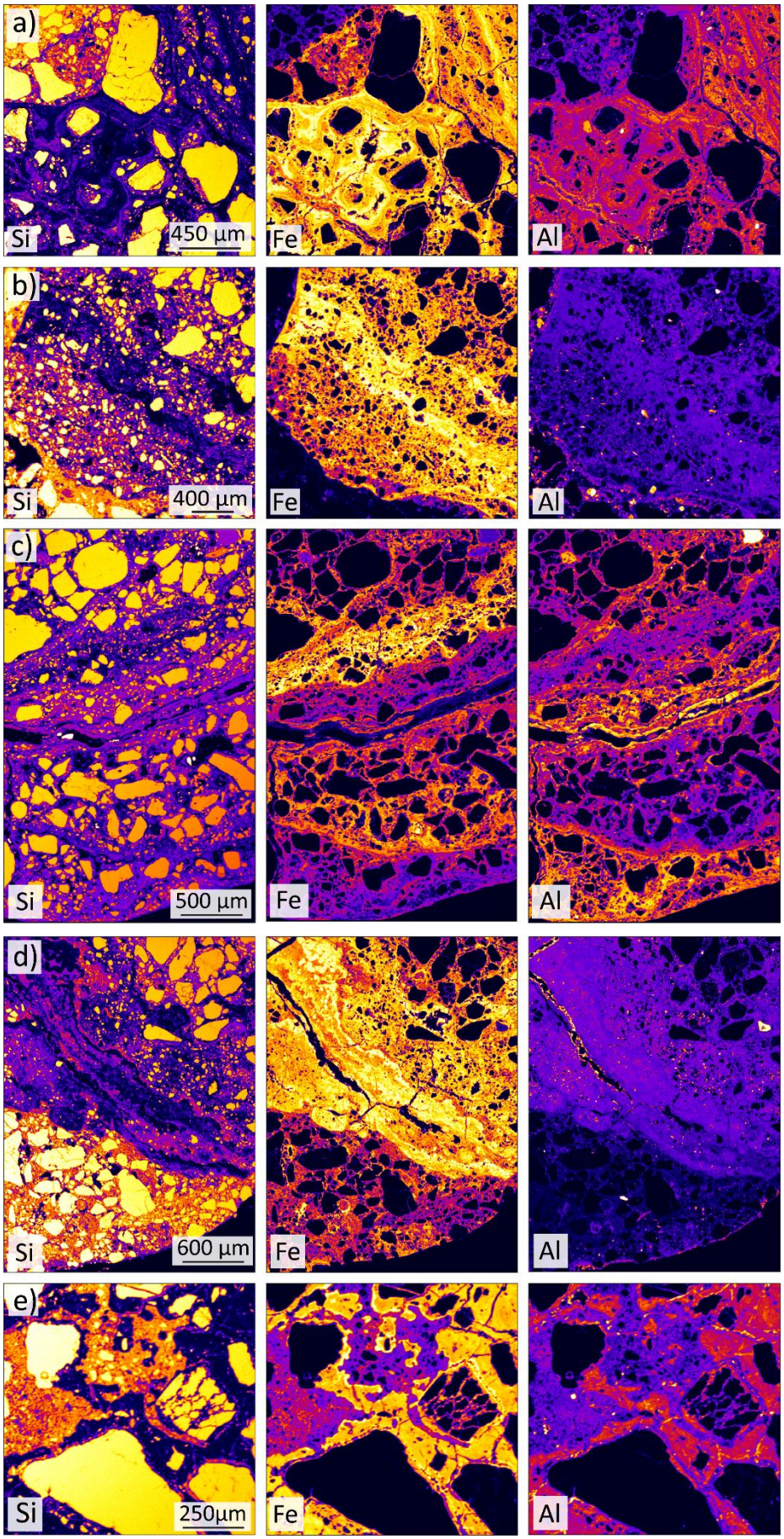
a)
Si
450 µm
Fe
Al
b)
Si
400 µm
Fe
Al
c)
Si
500 µm
Fe
Al
d)
Si
600 µm
Fe
Al
e)
Si
250µm
Fe
Al

(Previous page) Figure 4.16 Electron microprobe element maps for Si, Fe, and Al for pisoliths from the Goroke and Diapur profiles. Relative colour scale, yellow is high abundance; purple-black is low abundance. a) Element maps of the margin of re-worked iron indurated sediment at Goroke. The internal texture is dominated by embayed quartz grains supported by a matrix of laminar Fe-oxide, b) Element maps of the margin of re-worked iron indurated sediment at Goroke. Layers of Fe-oxide indurated fine sand have been broken and are surrounded by a thin layer of clay, c) Element maps for pisoliths of concentric layers of Fe-oxide-indurated sand with a goethite rim from Diapur. Note the alternating layers of Fe and Al abundance, d) Element maps for hematitic pisolith from Diapur. Laminations of Fe-oxide have had further silica and iron indurated sand accreted to the lower half of the pisolith, e) Element maps for hematitic pisoliths from Diapur. Quartz grains are etched and fragmented and the cracks filled with Fe-oxide. Gaps in the Fe-oxide matrix have been filled with iron-stained clay.

4.5 DISCUSSION

4.5.1 Processes controlling induration

The ferricrete component of the Loxton-Parilla Sands has been regarded as a surface or stratigraphic unit (Firman 1973, Kotsonis 1995, Paine 2004, Bowler *et al.* 2006, Miranda *et al.* 2009) as have other iron indurated weathering profiles (Firman 1979, Firman 1994). Our results show, however, that there are close links between the depositional environment and processes controlling the heterogeneous nature of the weathering materials. Micromorphology of Fe-oxide indurations, particularly pisoliths and nodules, is widely overlooked as an important feature in determining and interpreting their origin and formation mechanisms (Schulz *et al.* 2010). The role of ferricrete degradation, transport, and accumulation has been increasingly recognised as an important process during weathering and Fe-oxide induration (Bourman 1993, Eggleton & Taylor 1998, Löhr *et al.* 2010, Anand & Verrall 2011). Ferricrete formation in southeastern Australia has been largely studied in profiles directly overlying bedrock or with a thin layer of transported sediment (Bourman 1993), however, the Loxton-Parilla Sands is different, consisting of entirely transported and reworked quartz sand in the upper stratigraphy of a thin basin.

The variety of morphological types of ferricrete in the Loxton-Parilla Sands reflects two end-member processes – pedogenesis and groundwater induration – as well as more complex combinations of these processes. These processes are a record of conditions during and after the Neogene marine regression that lead to deposition of the Loxton-Parilla Sands. In order to understand the wider implications of these materials it is necessary to understand the profile-scale genetic mechanisms.

Pisoliths with concentric layers, such as those found at Lyrup (Figure 4.15a) are interpreted to be pedogenic in origin. Pisoliths at Lyrup have formed in at least two distinct stages with a hematitic core surrounded by a goethitic rim. The pisoliths are surrounded by a thin (50 μm wide) clay rind on the outer edge. The outermost surface material of these pisoliths is the same at the local matrix suggesting recent addition. There is little change in grain size from the pisolith to the surrounding sand matrix suggesting little to no transport of the nodules during or after formation. Barite precipitated in these pore spaces at late stage in formation. These pisoliths formed as cyclic accumulations of hematite then goethite in the vadose zone of profiles.

Irregular iron indurations, such as those at Spicer's Pit, formed by Fe^{2+} from groundwater nucleating on detrital wood fragments or charcoal. Induration of plant material by Fe-oxides is not well documented. Where it is observed in pisoliths in the channel iron deposits in the Pilbara region of Western Australia (Morris & Ramanaidou 2007), charcoal fragments have been pseudomorphed by ferrihydrite which then transformed to hematite (Schwertmann 1988, Morris & Ramanaidou 2007, Thorne *et al.* 2014). If hematite replacement of charcoal occurred in the Murray Basin, it would suggest there was a distinct drying season during formation of the Spicer's Pit weathering profile in western Victoria. As *Eucalyptus* became more common in southeast Australia from the Late Miocene to Pliocene, regular burning of vegetation became more common (Martin 2006) and would fit with this scenario.

Ferruginous pisoliths and concretions with fragmented internal textures (for example at Diapur and Goroke) are interpreted to have formed via a complex genetic pathway involving multiple phases of precipitation, disaggregation, and transport. Initially there was an indurated horizon formed by a fluctuating water table, similar to that at Goroke (Figure 4.8a), which has been disaggregated by bioturbation from vegetation. Disaggregation could also occur following formation of solution pipes and hollows in the profile. The broken fragments may have been transported a relatively short distance. Where redox conditions were appropriate, the fragments had further Fe-oxide added, resulting in accreted pisoliths and a record of multiple phases of induration. Accreted pisoliths at some profiles have smooth outer edges suggesting further transport and abrading. The lower quartz content in areas of stronger Fe induration is interpreted to have developed as SiO_2 was dissolved and displaced and Fe-oxide precipitated, resulting in matrix-supported nodules (Figure 4.16a). This dissolution-precipitation cycle could also contribute to disaggregation of indurated materials.

Weathering features such as silcrete and solution pipes and hollows have been formed by dissolution and movement of Si by pedogenic and groundwater processes. Silica textures at Nyah have similar features to silcretes formed in near-surface pedogenic environments in the opal fields of South Australia (Thiry & Milnes 1991). In the near-surface environment, rain and floods move soil materials and infiltrate the profile, depositing fine grained material and silica down-profile (Thiry & Milnes 1991). The massive silcrete horizon at Lyrup was probably formed below the water table, where strongly acidic conditions mobilised Al and redistributed silica (Thiry & Milnes 1991).

The physicochemical characteristics of clay minerals in weathering profiles have been useful for interpreting weathering profiles and groundwater processes for transported sediments (Cudahy 1997). The trend of increasing kaolin disorder with height in the Horsham-7 profile is possibly due to infiltration of surface water and weathering of kaolin. Much of the previous work to determine mineralogy from hyperspectral analysis has been undertaken on strongly weathered bedrock with

largely *in situ* weathering profiles (Cudahy 1997, Haest *et al.* 2012). Further interpretations of the results from the HyLogger^{TM} analysis should be undertaken after acquiring spectra from more diverse sediments, particularly clays, in the Murray Basin to characterise distinct mineral phases.

4.5.2 Source of post-depositional induration components

Iron oxide in whole rock geochemistry is predominantly associated with post-depositional precipitation and indurations. The source, or sources, of Fe remains unresolved. Heavy mineral grains have undergone two stages of alteration, prior to and since deposition (Pownceby 2010) pointing to strong chemical weathering in source regions as well as within the Loxton-Parilla Sands. Heavy minerals remain a probable source of some reduced iron. Paine (2004) stated that there is a close spatial relationship between mottles and heavy mineral accumulations in the Loxton-Parilla Sands, however, we have not observed this consistently across the unit. Another possible source of Fe^{2+} is the dissolution of Fe-substituted kaolinite or smectite (Tardy & Nahon 1985) or sedimentary pyrite (Wilkin *et al.* 1996).

Silica that has been precipitated in pore spaces could have come from the partial dissolution and degradation of quartz sand and detrital muscovite. Quartz grains in the indurated weathering profile are no longer grain-supported, instead surrounded by a matrix of Fe-oxide and possibly kaolin and gibbsite. Very fine to silt-sized sand grains are dispersed in the Fe-oxide matrix of ferricretes in areas where this process is more advanced. This is more common in ferricretes with evidence of eroded and transported histories. Ferricretes with densely packed sand grains (for example, at Ultima and Lyrup) do not record evidence of sand grain disintegration.

4.5.3 Development of acidic weathering conditions

Iron oxides precipitating in surface environments are influenced by conditions of pH, temperature, moisture, and Eh, and can indicate the prevailing conditions during formation (Schwertmann and Taylor 1989). Aluminium is known to substitute for Fe^{3+} in the crystal structure of goethite in

considerable quantities, up to 32 mole %, as Al activity increases with decreasing pH (Fitzpatrick & Schwertmann 1982). Most of the ferricretes analysed by EMPA in this study have alternating bands of variable Fe and Al abundance. The relative variation in Al content between subsequent layers of Fe-oxide is likely due to Al-substituted goethite. Analysis of these phases by XRD would characterise the precise mineralogy and degree of substitution which can be used to infer more detailed hydromorphic conditions (Fitzpatrick & Schwertmann 1982).

Embayed and ragged quartz grains observed in some ferricretes as well as development of silcretes show the precipitation of silica in the Loxton-Parilla Sands. A low pH environment in which there is dissolved Al also accounts for the apparent dissolution and re-precipitation of silica in the weathering profile. Dehydration cracks in Fe-oxides further suggest cyclic wetting and dehydration of sediments (Fitzpatrick *et al.* 2009).

Generation of acid in subaerial environments is commonly via oxidation of pyrite (FeS) but can also occur via ferrolysis. Barium (Ba^{2+}) and sulphate (SO_4^{2-}) are both soluble but if present in solution together will form insoluble barite (Hanor 2000). Barite in pore spaces in some ferricretes suggests sulphate was present during weathering in at least some areas of the Loxton-Parilla Sands. Tidal sediments will commonly accumulated large volumes of sulphidic materials due to availability of S in sea water and conditions favourable for biologically mediated sulphide production (Wallace *et al.* 2005). Sulphate minerals, such as barite, jarosite, and alunite, precipitate at low pH (Nordstrom 2011).

In typical tidal sediments with fine-grained pyrite, oxidation forms Fe(II), sulphate, and acidity (H+) by the following reaction (Van Breemen 1982):

$$FeS_2 + \frac{7}{2}\,O_2 + H_2O \rightarrow Fe^{2+} + 2\,SO_4^{2-} + 2H^+ \qquad [1]$$

The complete oxidation of pyrite proceeds as:

$$FeS_2 + \frac{15}{4}\,O_2 + \frac{7}{2}H_2O \rightarrow Fe(OH)_3 + 2\,SO_4^{2-} + 4H^+ \quad [2]$$

Cracks and root channels in coastal sediments can encourage oxidation and acid production by allowing air and oxidised water into the profile (Wallace *et al.* 2005). Further acid can be generated by the hydrolysis of Fe^{2+} (ferrolysis), releasing H^+ and precipitating Fe oxyhydroxide (Schwertmann & Taylor 1989):

$$2\,Fe^{2+} + \frac{1}{2}\,O_2 + 5\,H_2O \rightarrow 2\,Fe(OH)_{3(S)} + 4\,H^+ \quad [3]$$

Jarosite ($KFe_3(SO_4)_2(OH)_6$) is a common product in acid sulphate soils between pH 4 and 2, and forms by incomplete oxidation of pyrite (Van Breemen 1982). It is likely that jarosite was formed in the early stages of weathering in the Loxton-Parilla Sands as reduced sediments were exposed to oxygen. Jarosite is metastable in surface environments, however, and will hydrolyse to goethite (Van Breemen 1982):

$$KFe_3^{3+}(OH)_6(SO_4)_2 \rightarrow 3\,FeOOH + 2\,SO_4^{2-} + K^+ + 3\,H^+ \quad [x]$$

Goethite is the dominant Fe-oxide mineral in the Loxton-Parilla Sands, revealed by both visual identification and HyLogger™ mineralogy. Goethite can form in a number of ways, including via a jarosite intermediate phase, as discussed above. It can also form directly from the oxidation of Fe(II) (Cornell & Schwertmann 2006). Ferrihydrite and schwertmannite are also common oxyhdroxide minerals formed in intermediate pH waters (pH 4.5-6.5) in acid sulphate conditions (Bigham *et al.* 1996). It is likely these minerals formed the metastable precursors to goethite and hematite that now dominate the Fe-oxide mineralogy.

4.5.4 Modern analogues

The development of acid sulphate soils is still an active process in the Murray Basin and around the world. Iron oxidation and precipitation has been observed in coastal sediments in numerous locations include North America and Fraser Island in Queensland (Charette & Sholkovitz 2002,

Lohr *et al.* 2010). Pisolith formation on Fraser Island in northern Queensland is a similar coastal system; similar to what we propose took place during formation of the Loxton-Parilla Sands. Seasonal waterlogging of coastal sediments is an important process for the reduction and oxidation of iron in north Queensland, much like the depositional environment of the Loxton-Parilla Sands (Lohr *et al.* 2010). Smectite has been suggested as an important source of Fe^{2+} in these soils (Murad & Fischer 1988).

In the western Murray Basin, acidic conditions persisted during the Late Miocene-Pliocene marine regression and are still active today in some parts of the basin. Heavy regulation of water flows along the Murray River has allowed sulphidic sediments to build up while rising water tables, due to native vegetation clearance, have introduced saline and sulphate-rich groundwater to the near surface environment (Fitzpatrick *et al.* 2009). When sediments are drained and exposed to oxygen, large amounts of acid can form (Fitzpatrick *et al.* 2009). Downstream, the Coorong lagoons and Murray River mouth in South Australia are dominated by marine influences, as well as the Lower Lakes and adjacent wetlands near Lake Alexandrina. The drained Lower Lakes and the subsequent acidification could be a regional-scale version of estuarine and back-dune components of the Loxton-Parilla Sands during the marine regression. Prior to the drying of the Lower Lakes, marine sediments had not been exposed to oxygen for millennia and sulphidic materials had built up. When the water level dropped below 0 m AHD (Australian Height Datum) sulphides oxidised and developed acidity (Fitzpatrick *et al.* 2009). Complex sulphate minerals identified in the oxidised acidic environments are interpreted as indicating extremes of Eh, pH and Fe and S availability (Fitzpatrick *et al.* 1996, Bigham & Nordstrom 2000). As the water level dropped in the southwest Murray Basin, dehydration of sulphuric materials has formed desiccation features which expose further sulphidic material to oxygen (Fitzpatrick *et al.* 2009).

4.5.5 Summary of weathering profile formation in the western Murray Basin

Key geochemical and physical processes have formed the pedogenic, groundwater-derived, and complex ferricretes in the Loxton-Parilla Sands have been interpreted by observing the close links between geochemistry and micromorphology. The conceptual model in Figure 4.17 summaries these genetic mechanisms active during deposition and weathering of the Loxton-Parilla Sands. Strandlines of the Loxton-Parilla Sands are well-preserved, initially due to colonisation of dune ridges by vegetation (Figure 4.17a). Vegetation stopped loose sand from being blown away after deposition of the strandplain. It could have also acted as a source of organic matter, complexing with Fe, and facilitating Fe accumulation in the profile (Lohr *et al.* 2010). As the climate became cooler and drier in the Late Miocene to Pliocene, *Nothofagus* forest was gradually replaced by *Eucalyptus* (Martin 2006). Geochemical weathering processes, predominantly secondary Fe-oxide precipitation, were initiated with the exposure of ferrous iron in groundwater and sediments to oxygenated seawater and air. Acid was generated through acid sulphate reactions and ferrolysis. Indurated laminar horizons and mottles of Fe-oxides are indicative of long-lived water tables and probably formed at a number of stages shortly following deposition of the dune ridges, and also through the Pliocene, by seasonal wetting and drying of sediments (Figure 4.17a). Pisoliths in some profiles have rounded hematitic cores and goethite rims with little evidence for transport, indicative of pedogenic formation in the vadose zone (Figure 4.17a). Dissolution of clay minerals likely provided Al, and possibly Fe, some of which would have formed hematite and Al-substituted goethite, as well as jarosite and other Fe oxyhydroxides, in the weathering profile.

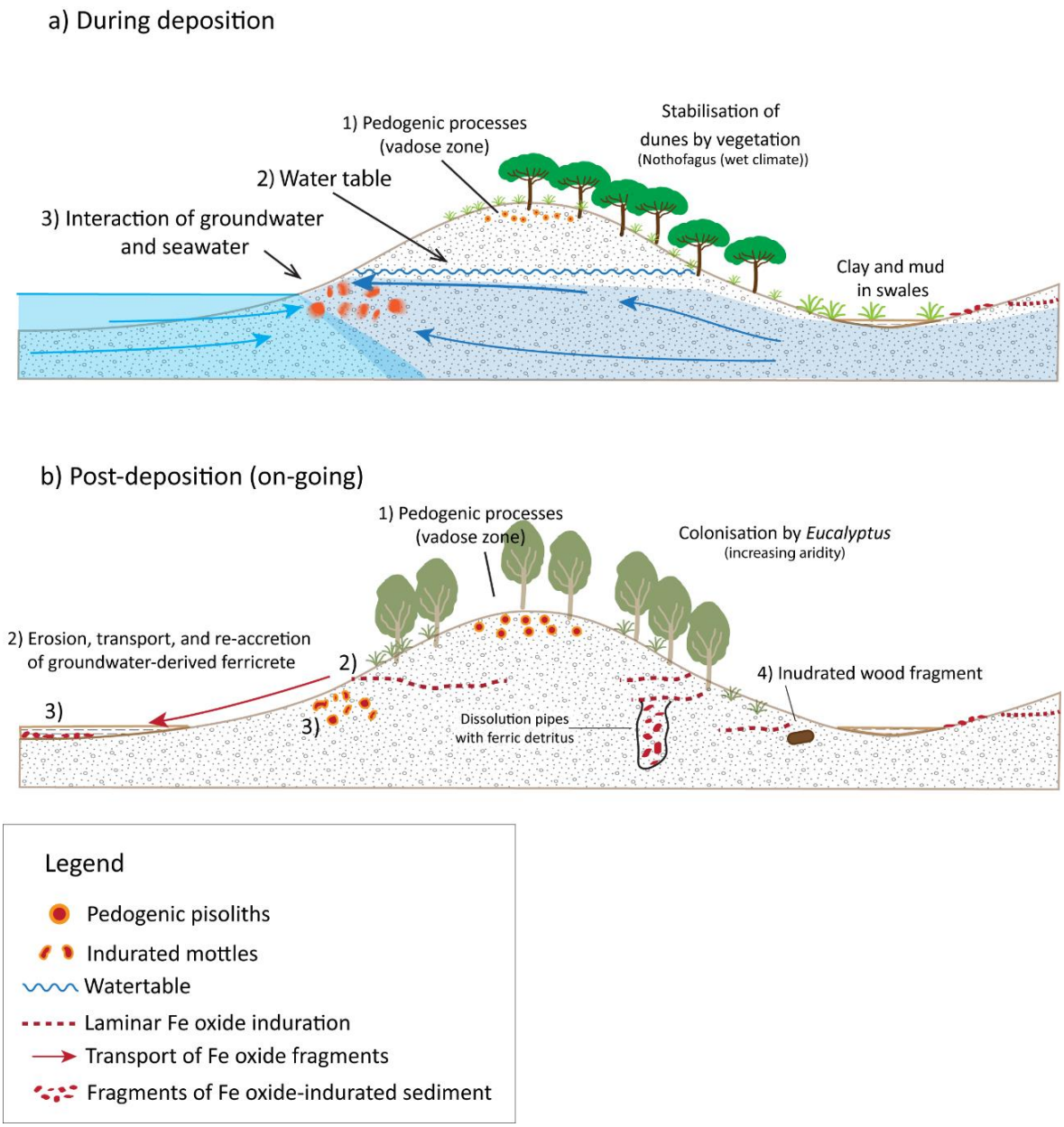

Figure 4.17 Genetic model of formation of ferricrete. a) Dunes deposited during the Late Miocene-Pliocene marine regression were stabilised by vegetation. Percolation of water above the water table formed pedogenic pisoliths while the interaction of oxygenated seawater with reduced groundwater contributed to the formation of Fe-oxide indurations, b) Ferricrete genesis during subaerial weathering, soon after the coast prograded from a given dune. The strandplain was colonised by Sclerophyll vegetation in an increasingly arid climate while seasonal wetting and drying formed acidic groundwater and the progressive precipitation of Fe-oxides in the weathering profile. Acidic conditions also liberated Al and Si from clay minerals and quartz which were re-deposited as silcretes and incorporated into goethite.

Dissolved sulphate combined with Ba to form barite, after formation of pedogenic pisoliths and other ferricretes pisoliths and other ferricretes. Dehydration of precipitated Fe-oxides created cracks in the matrix of these sediments which were later filled with further Fe-oxides or clay.

Ferricretes in some parts of the Loxton-Parilla Sands have fragmented textures and preserve evidence of multiple stages of Fe-oxide induration. Vegetation also plays a role in the disaggregation of ferricretes (Lohr *et al.* 2010), breaking down indurated horizons (for example, at Goroke) (Figure 4.17b). Fragments of Fe-oxide cemented sediment are transported down-slope and, if redox conditions allow and there is a supply of ferrous iron, are re-cemented to form indurated aggregates (Figure 4.17b). Further disaggregation of sediments by vegetation, or dissolution of sand, formed pipes and hollows. These were then filled with ferruginous debris (Figure 4.17b). At Nyah, percolating silica-rich water precipitated on the outer surface of these nodules. At other locations (for example, Ultima and Chowilla) the hollows were filled with sandy clay and mud from the land surface. Charcoal from bushfires, or buried fragments of plant material, are replaced by hematite (Figure 4.17b).

4.6 CONCLUSION

In this study we have utilised electron microprobe element mapping to complement field observations and whole rock geochemistry to identify the mineralogical controls on geochemistry in the weathering profile of the Loxton-Parilla Sands and the implications for formation. Ferricretes in the Loxton-Parilla Sands can be distinguished based on morphological features which reflect different genetic mechanisms. Both pedogenic and groundwater-derived Fe-oxide indurated sediments contain variable degrees of Al-substitution and combinations of goethite and hematite. We have interpreted this to reflecting changing depositional conditions and multiple cycles of precipitation with seasonal wetting and drying of sediments. Local geochemical weathering processes are best interpreted in the context of broader depositional environment. Our results support previous interpretations of an acid sulphate weathering system but our model shows

formation was synchronous with deposition of the Loxton-Parilla Sands and the Miocene-Pliocene marine regression. Acidic and iron-oxide dominated weathering systems persist today as close as the Lower Lakes in South Australia and Fraser Island in Queensland to estuarine sediments in the USA. Acid sulphate systems in the modern Murray Basin are broadly similar to the back-dune environments of the Loxton-Parilla Sands, both driven by the oxidation of reduced sediments.

Chapter 5 Trace element geochemistry of secondary iron oxides and implications for sample media for exploration through transported sediments

FOREWARD

In this chapter I take the understanding developed of the sedimentary and geochemical system from the previous three chapters and address the question that started this project, can the iron indurated sediments of the Loxton-Parilla Sands be utilised in mineral exploration programs through deep sedimentary cover? Are the geochemical processes that have formed the extensive weathering profile such that a signature of mineralised basement can be transported into the cover and trapped? There are geochemical processes active in the sedimentary and weathering system that aid development of geochemical anomalies but there are also components that work against this. Analysis from the basin to the grain scale shows several important processes controlling that geochemistry. In this chapter I attempt to disentangle some of these processes and show that accumulation of secondary Fe-oxides in the environment does not occur in isolation of the geological system that surrounds it.

This chapter will form the basis of manuscript for submission to the *Journal of Geochemical Exploration*. This submission will be co-authored with Prof. David Giles who assisted with interpretation of geochemical data and Dr Steven Hill who assisted with project conceptualisation. I would like to acknowledge Geoscience Australia, the Geological Survey of South Australia, and Geological Survey of Victoria for access to samples as well as Dr Benjamin Wade and Aoife McFadden at Adelaide Microscopy for technical assistance and Acme Laboratories for geochemical analysis.

Statement of Authorship

Title of Paper	Secondary iron oxides as a sample medium for exploration through deep transported sediments, Murray Basin, southeastern Australia
Publication Status	○ Published, ○ Accepted for Publication, ○ Submitted for Publication, ◉ Publication style
Publication Details	

Author Contributions

By signing the Statement of Authorship, each author certifies that their stated contribution to the publication is accurate and that permission is granted for the publication to be included in the candidate's thesis.

Name of Principal Author (Candidate)	Stephanie McLennan		
Contribution to the Paper	Project conceptualisation, sample collection and preparation, data collection, data interpretation, manuscript design and composition, and generation of figures and tables.		
Signature		Date	28·10·2015

Name of Co-Author	Prof. David Giles		
Contribution to the Paper	Supervised development of work, helped with data interpretation and manuscript revision.		
Signature		Date	29-10-15

Name of Co-Author	Dr Steve Hill		
Contribution to the Paper	Assisted with project conceptualisation, helped with data interpretation and manuscript revision.		
Signature		Date	29-10-15

Name of Co-Author			
Contribution to the Paper			
Signature		Date	

ABSTRACT

We have characterised the trace element geochemistry of the Loxton-Parilla Sands in the western Murray Basin, southeast Australia, to assess the viability of this unit as a geochemical sampling medium for mineral exploration. Major and trace element concentrations in the Loxton-Parilla Sands are controlled by six mineralogical associations; quartz; clay and micas; hematite and goethite indurations; heavy minerals; carbonates; and, sulphate minerals. Iron oxide and hydroxide indurated sediments provide the most promising potential sample media because they are widespread and have the capacity to scavenge a range of pathfinder elements thereby increasing their geochemical signature. The indurated weathering profile in the upper sections of the Loxton-Parilla Sands is characterised by accumulations of Fe_2O_3 (up to 80 wt. %). Three morphological types of ferricrete in the Loxton-Parilla Sands record pH and Eh fluctuations and variable degrees of physical transport and disaggregation within the weathering profile. Whole rock V, As, Co, and Pb concentrations have broadly positive correlations with Fe_2O_3. Other pathfinder elements, such as Sb and Mo have poor associations with Fe_2O_3. Microscale element maps show comparable relationships but demonstrate fine-scale partitioning of trace elements into different stages of Fe-oxide precipitation Concentric zones of variable trace element composition on the rinds of pisoliths correspond to variations in the amount of Al_2O_3 incorporated into the Fe-oxide structure. This is consistent with precipitation of trace metals from groundwater at different times, corresponding with fluctuating pH and Eh and episodic drying of the weathering profile. The geochemical results suggest trace element distribution is largely controlled by adsorption to Fe-oxides and hydroxides and clay minerals. Discriminating lateral and vertical geochemical transport of trace elements is difficult in such a complex system. Paleohydrogeology and modern hydrogeology show significant lateral movement of groundwater. There has been minimal vertical migration of groundwater in the Loxton-Parilla Sands, except at the formation margins and where the Geera Clay diverts groundwater upwards. We have identified geochemical signatures consistent with concealed Au and base metal mineralisation in the southern Murray Basin. The predominance of lateral transport of geochemical signatures, however, makes it difficult to define individual targets. The

geochemical signature in ferricretes represents the average geochemistry of the catchment area. The results underline the importance of understanding the whole system, including hydrogeology, stratigraphic architecture, and genetic mechanisms of weathering materials, in order to determine if weathering materials are appropriate sample media for exploration through deep cover.

KEYWORDS

Murray Basin, Neogene, weathering, ferricrete, mineral exploration, cover

5.1 INTRODUCTION

Declining mineral exploration success and increase of costs has necessitated a shift in the way in which we approach regional exploration and the challenge of exploring in areas dominated by barren cover rocks (Hillis *et al.* 2014, Kyser *et al.* 2015). The success of exploration for concealed mineralisation in part relies on the ability to detect secondary accumulation of elements in cover sequences, over and above background geochemistry (Kyser *et al.* 2015). The Loxton-Parilla Sands cover some 140,000 km^2 of southeast Australia, including regions considered highly prospective for Au and base metal mineralisation (Figure 5.1). The unit is a semi-confined aquifer with potential for groundwater interaction with basement rocks (Brown & Stephenson 1991). Following deposition during the Late Miocene-Pliocene marine regression, the Loxton-Parilla Sands strandplain has undergone extensive subaerial weathering, dominated by accumulation of secondary goethite and hematite, collectively referred to as Fe-oxides in this study. Iron indurated sediments – ferricretes – have been of interest for regional mineral exploration for some time, due to their tendency to scavenge elements associated with concealed mineralisation that have been dispersed in overlying sediments (Hawkes & Webb 1962, Chao & Theobald 1976). The usefulness of such materials requires a number of geochemical processes including groundwater capable of transporting a signature from basement rocks, vertical connectivity to basement, and minimal dilution of geochemistry. Detailed studies of the sedimentology and depositional environment of the Loxton-Parilla Sands (this thesis - chapter 2 and 3, Brown & Stephenson 1991, Paine *et al.* 2004, Miranda *et al.* 2009) as well as its post-depositional weathering processes (this thesis - chapter 4, Kotsonis 1995) are a good basis on which to assess the viability of the weathering profile to be of use in regional mineral exploration.

Using indurated materials as sample media assumes that migration of geochemical signatures is predominantly vertical, reflecting the underlying lithology. Further, geochemical data are often normalised to Fe_2O_3 under the assumption pathfinder elements have been scavenged and concentrated by goethite and hematite (Chao & Theobald 1976). Controls on geochemistry in the

regolith, however, are varied, and whole rock geochemistry only provides a snapshot of what is taking place. Determining the genetic mechanisms of weathered materials in the context of the wider geological evolution of a region, such as the Murray Basin, can provide insight to the likelihood of geochemical anomalies being derived from broad catchment-scale signatures, or, from camp-scale concealed mineralisation sources. Microscopic variations in morphology and major element geochemistry of ferricretes record fluctuations in hydromorphic conditions during

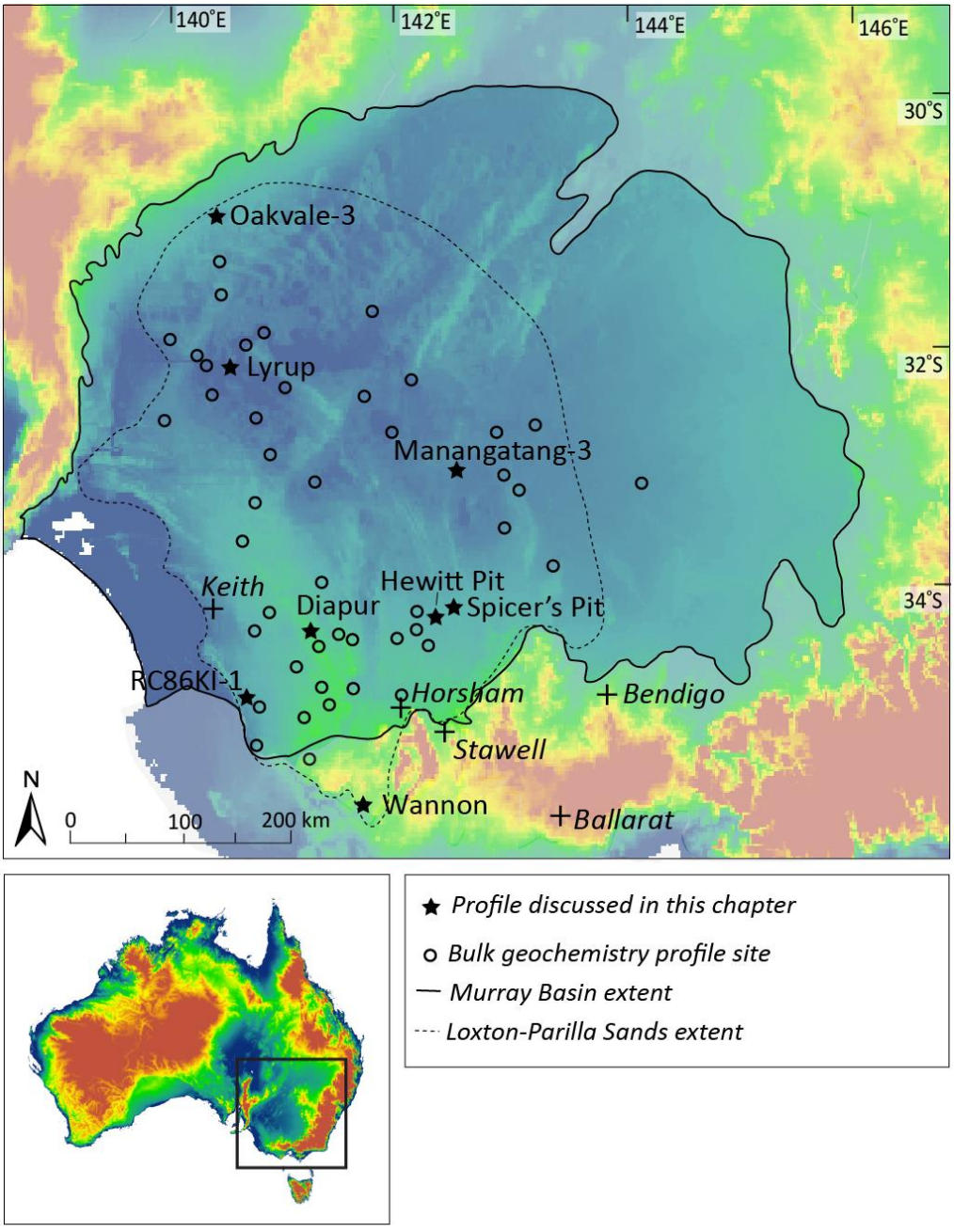

(Previous page) Figure 5.1 Study location and extent of the Loxton-Parilla Sands in the Murray Basin, southeast Australia, and locations of profiles discussed in the text.

formation (this thesis – chapter 4). Advances in cell design of laser ablation systems over the last decade provide the opportunity to spatially map trace elements at low concentrations (Woodhead *et al.* 2007) and analyse the microscopic distribution of trace elements to complement whole rock geochemical data.

In this study we present new major and trace element geochemistry of the Loxton-Parilla Sands and associated ferricrete to assess its usefulness as a sample medium for mineral exploration. Whole rock geochemistry is complemented by field observations and microanalysis, providing the first application of major and trace element mapping of weathered materials in the Murray Basin and Australia. Integrated with a detailed understanding of sedimentary processes and genetic mechanisms of ferricrete formation, the implications for mineral exploration through strongly weathered transported cover are considered.

5.2 REGIONAL SETTING

5.2.1 Regional geology

The Murray Basin forms a thin package of Cenozoic sediments overlying 300,000 km^2 of prospective basement rocks in southeast Australia (Figure 5.1). Sediments are up to 600 m thick but average approximately 200 m. The sedimentary package contains continental and shallow marine sequences that are significant aquifers and contain economic heavy mineral accumulations. Some of these basement terranes are highly prospective for mineralisation, dominated by orogenic Au (Ramsay *et al.* 1998, Lisitsin *et al.* 2010), and potential for base metal magmatic-hydrothermal mineralisation (Seymon 2006, Seymon *et al.* 2009, Schofield *et al.* 2015). The Adelaide Fold Belt includes the Nackara Arc in South Australia and the Glenelg and Grampians-Stavely Zones in the east. The Nackara Arc includes deformed Proterozoic sediments intruded by Cambrian granites (Figure 5.2) and has been explored for gold since the 19th century (Morris & Horn 1990, Preiss

1993). To the east, the Grampians-Stavely Zone contains low-grade volcanics and marine sediments, deposited during the Cambrian Delamerian Orogeny (Morand *et al.* 2003). Igneous intrusions in the Stavely Volcanic Complex are considered prospective for porphyry-epithermal Cu mineralisation and volcanic-hosted massive sulphides (Horvath 1993, Schofield *et al.* 2015). In the Stawell Zone, a tholeiitic volcanic package hosts the large Magdala deposit at the town of Stawell (Phillips *et al.* 2003). Further north, the Wildwood and Kewell Au prospects are under Cenozoic cover of the Murray Basin (Noble 2012). Regional geophysics suggest both the Stawell and Bendigo gold zones extend north under the Murray Basin into New South Wales (Hallett *et al.* 2005).

5.2.2 Local stratigraphy

The Loxton-Parilla Sands in the western Murray Basin comprises marginal marine and lesser fluvial sediments, deposited during a marine regression (Figure 5.3a). It forms a semi-confined aquifer that has undergone extensive post-depositional accumulation of secondary Fe-oxides, silica, and clay. After a transgression a series of oscillatory regressions and transgressions followed, with an overall trend of falling sea level (Roy 2003). The Loxton-Parilla Sands were deposited from at least 7.2 Ma to approximately 5.4 Ma (Miranda *et al.* 2009). Early interpretations suggested ridges were underlain by extensions of the Grampians sandstone in southern Victoria (Dennant 1886, Hills 1939) or valleys created by streams (Fenner 1918). The elongate ridges were later recognised as paleo-shorelines (Blackburn 1962).

The lithology of the Loxton-Parilla Sands varies from silty sands to coarse sand and gravelly clay lenses. The unit is predominantly quartz sand with heavy mineral accumulations and muscovite. The heavy mineral assemblage in the Loxton-Parilla Sands includes zircon, rutile, ilmenite, leucoxene, with lesser monazite and tourmaline (Colwell 1976, Olshina & van Kann 2012). Muscovite is concentrated in the lower shoreface, breaker and swash zone facies (Paine 2004).

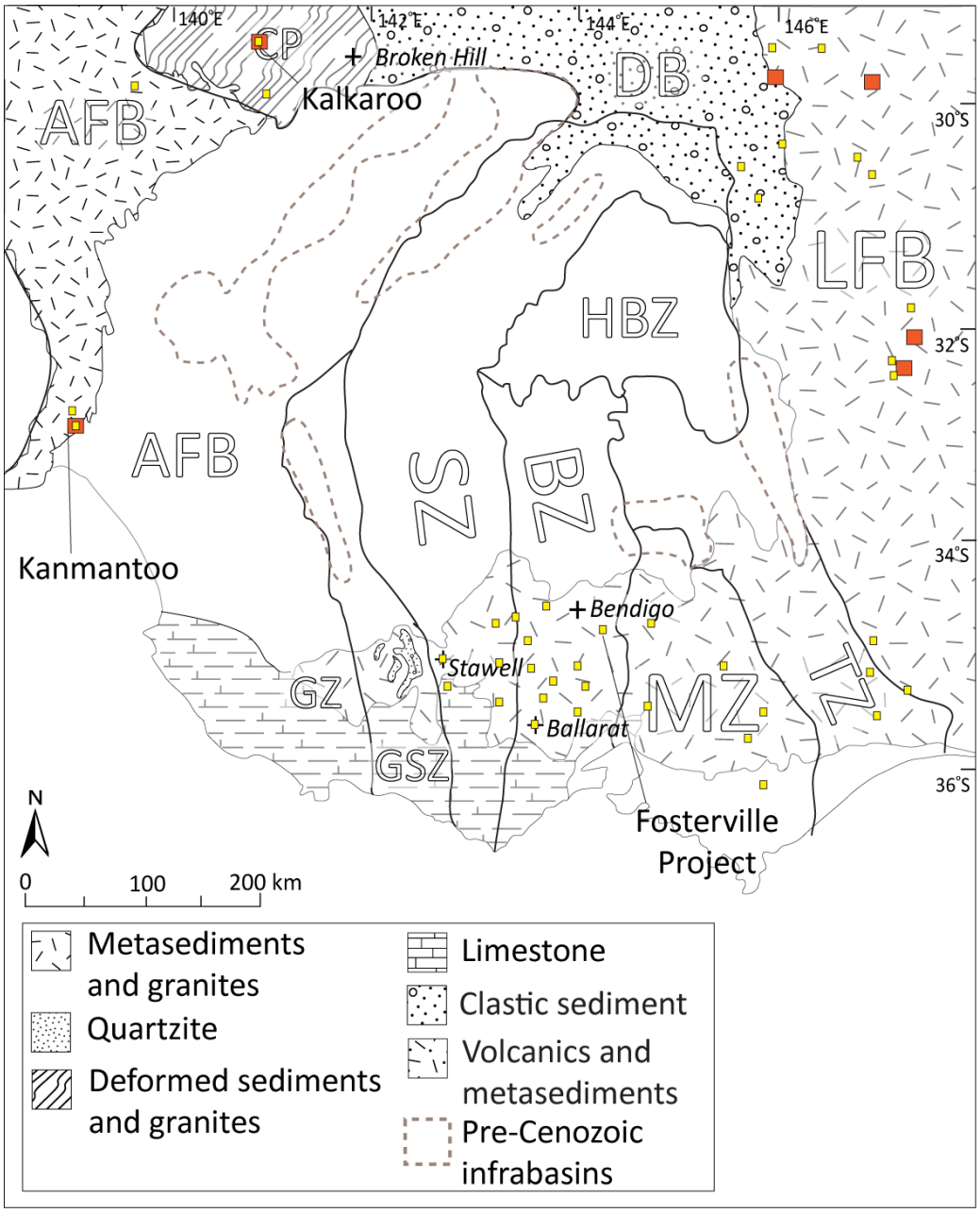

(Previous page) Figure 5.2 Geological provinces surrounding and underlying the Murray Basin. AFB – Adelaide Fold Belt, CP – Curnamona Province, DB – Darling Basin, GZ – Glenelg Zone, GSZ – Grampians Stavely Zone, SZ – Stawell Zone, BZ – Bendigo Zone, HBZ – Hay-Booligal, MZ – Melbourne Zone, TZ – Tabberabbera Zone, and LFB – Lachlan Fold Belt. Yellow squares – Au deposits (JORC compliant resources 2012 – Kalkaroo and Fosterville both have >30 t of contained Au) Orange squares - Cu deposits up to 1m t Cu.

a)

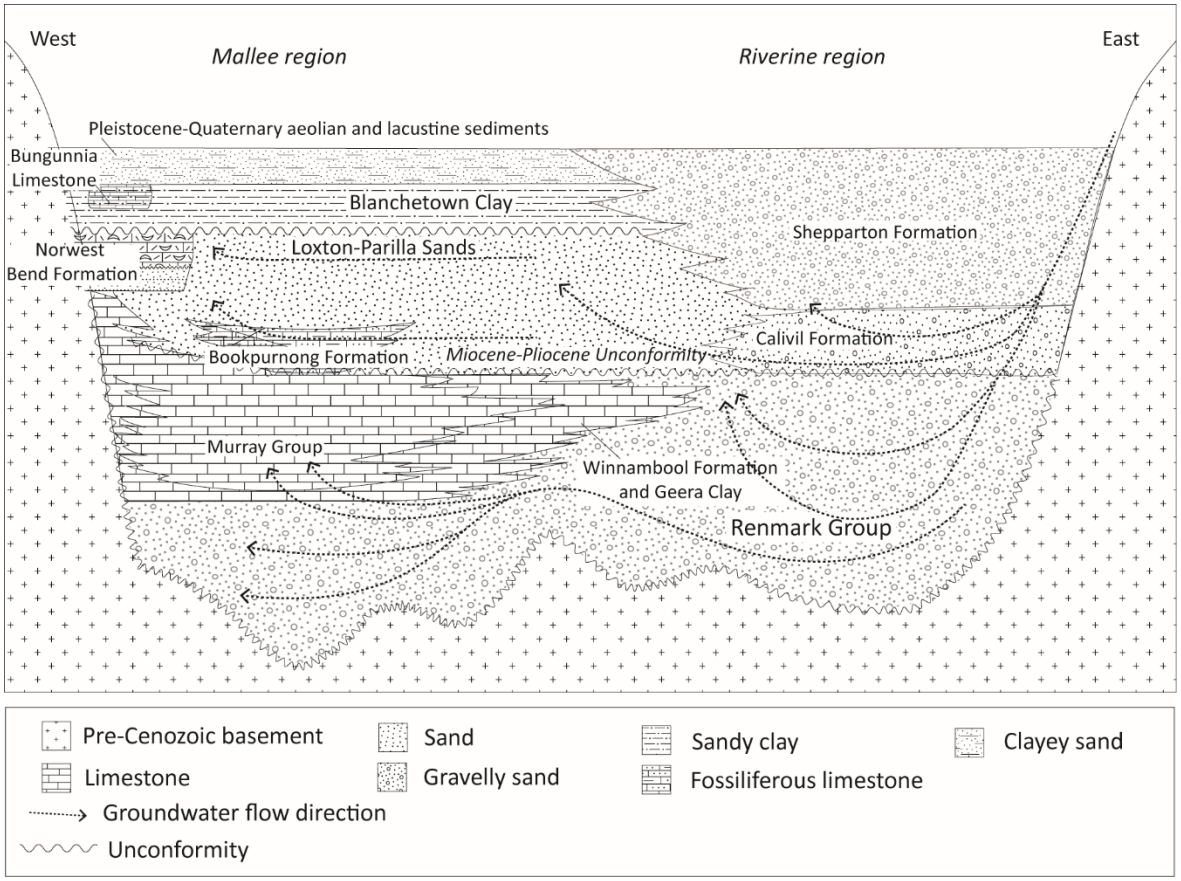
West
Mallee region
Riverine region
East
Pleistocene-Quaternary aeolian and lacustine sediments
Bungunnia Limestone
Blanchetown Clay
Shepparton Formation
Norwest Bend Formation
Loxton-Parilla Sands
Calivil Formation
Bookpurnong Formation
Miocene-Pliocene Unconformity
Murray Group
Winnambool Formation and Geera Clay
Renmark Group
Pre-Cenozoic basement
Sand
Sandy clay
Clayey sand
Limestone
Gravelly sand
Fossiliferous limestone
Groundwater flow direction
Unconformity

b)

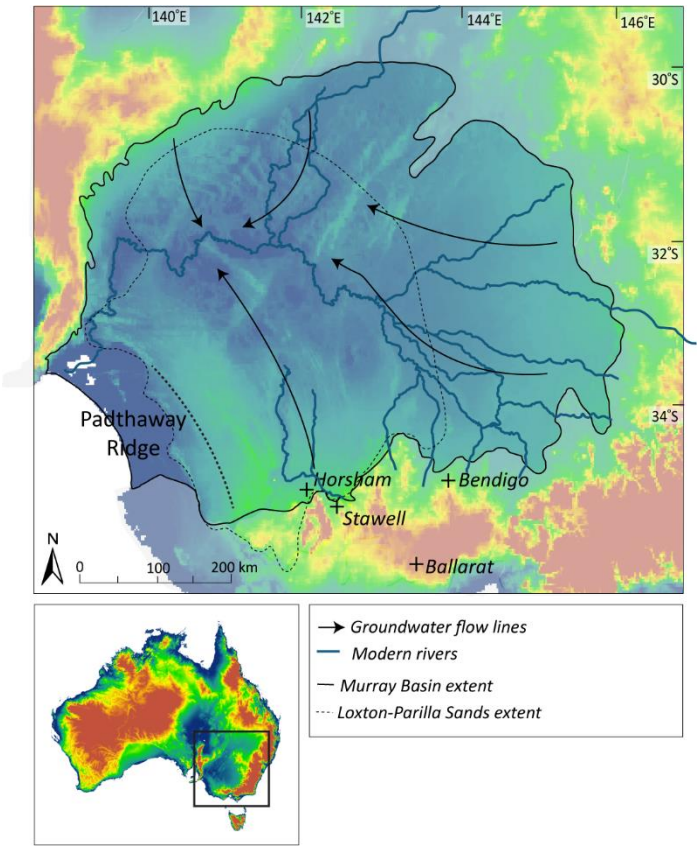

(Previous page and above) Figure 5.3 a) Schematic of Murray Basin stratigraphy and groundwater flow lines, after Brown and Stephenson (1991), b) Groundwater flow lines for the Murray Basin (afterRadke and Howard (2007) and references therein) and the Murray River, the main outlet for groundwater in the Murray Basin.

Ferricretes in the Loxton-Parilla Sands fit into broad three morphological types, flat-lying indurations, concentric pisoliths, and rounded nodules with fragmented internal textures (this thesis – previous chapter). Laminae of Fe-oxides have variable Fe, Al, and Si abundances, reflecting cyclic precipitation and groundwater chemistry changes. Ferruginous weathering profiles are also recognised in other Neogene sediments in the Otway Basin of southern Victoria (Gill 1964). Episodic wetting and drying was superimposed on a long-term trend of marine regression and local tectonic uplift (from ~7 Ma to present). This resulted in the diachronous exposure of relatively reduced shoreline sediments and concomitant acid production due to ferrolysis and the oxidation of biogenic sulphide.

5.2.3 Hydrogeology

Groundwater flow in the Murray Basin is complex. Groundwater flows towards the central western depocenters of the basin where it flows into the Murray River (Brown & Stephenson 1991) (Figure 5.3b). The Murray River is the main path for groundwater and salt to flow into the Southern Ocean, leaving the Murray Basin as an area of internal drainage (Evans & Kellett 1989). Salt lakes form in depressions in the western Murray Basin where the watertable is high and saline groundwater discharges at the surface, evaporates, and concentrates salt and gypsum (Macumber 1991). The Padthaway Ridge forms a barrier to groundwater flowing to the Southern Ocean, except for some minor overflow (Brown & Stephenson 1991). Prior to uplift of the Padthaway Ridge in the Pliocene groundwater flow would have been largely unrestricted to the Southern Ocean.

Recharge of the lower aquifers (Murray Group and Renmark Group) in the east of the basin is largely vertical, via rivers draining the highlands (Brown & Stephenson 1991). Recharge of the Calivil Formation in this region is through infiltration from major alluvial valleys (Woolley 1978). Recharge of the Loxton-Parilla Sands is largely via infiltration of local surface water, with a smaller component of easterly lateral flow from the Calivil and Shepparton Formations (Evans & Kellett 1989).

Weathering of pre-Cenozoic basement rocks has formed a layer of saprolite that confines most groundwater to the overlying basin sediments (Brown & Stephenson 1991). Fractured rock aquifers exist at the basin margins (Brown & Stephenson 1991). In the eastern Murray Basin the major aquifers are interconnected and vertical fluid flow is common. In the west, however, thick confining layers between the major aquifers mean lateral groundwater flow dominates (Cartwright *et al.* 2007) (Figure 5.3a). In the centre of the Murray Basin the calcareous clayey Winnambool Formation and Geera Clay form low-permeability barriers that disrupt groundwater flowing towards the western Murray Basin (Brown & Radke 1989) (Figure 5.3a). The Geera Clay diverts some groundwater flow upwards into the Loxton-Parilla Sands and Calivil Formation aquifers (Brown & Radke 1989).

5.3 METHODS

5.3.1 Whole rock geochemistry

We collected over 600 samples of the Loxton-Parilla Sands – both weathered and unweathered – for geochemical analysis from vertical profiles exposed in quarries, train and road cuttings, and along the banks of the Murray River. We also sampled drill core and cuttings from the core repositories of Geoscience Australia, and Geological Surveys of South Australia and Victoria. Sample locations were chosen for ease of access and where the greatest vertical exposure was available in the region. Core and drill cutting samples were used to supplement field exposures, where there was no natural exposure or field profiles were shallow. Field locations and top-of-profile elevations were recorded from GPS (MGA 94, Zone 54). Approximately 2 kg of sediment was collected at 1 m intervals in vertical profiles sections and narrower intervals if there was a noticeable change in the stratigraphy or weathering morphology. The sample size for drill cuttings from the Geological Surveys and Geoscience Australia was 15 g. This is the minimum sample size required by Acme Laboratories for geochemical analysis. Samples of core from the core repositories were approximately 100 g each. Drill cutting samples from the core libraries represent a minimum of 1 m because they were largely from reverse circulation or air core drilling (except for 'Horsham' bores which were fully cored). Stratigraphic logs were compiled from field observations with reference to the work of Kotsonis (1995), Miranda (2007), and Paine (2004). Stratigraphic logs were also created for all bore holes but features such as sedimentary structures and sub-metre variation in grain size have been destroyed by drilling.

All whole rock analyses were conducted at Acme Laboratories in Vancouver, Canada. We submitted samples for analysis in seven batches over a three-year period. At Acme Laboratories sediments were air dried, crushed, and sieved to -200 mesh. Major oxides were analysed via XRF with a lithium metaborate fusion. Total C and S were determined via Leco CS analyser. Rare earth and refractory elements were analysed via ICP-MS via lithium metaborate fusion and dilute acid digestion. Precious metals, base metals, and pathfinder elements were analysed via ICP-MS

following Aqua Regia digestion. Elements analysed include SiO_2, Al_2O_3, Fe_2O_3, CaO, MgO, Na_2O, K_2O, MnO, TiO_2, P_2O_5, Cr_2O_3, Ba, LOI, C, S, Be, Co, Cs, Ga, Hf, Nb, Rb, Sn, Sr, Ta, Th, U, V, W, Zr, Y, La, Ce, Pr, Nd, Sm, Eu, Gd, Tb, Dy, Ho, Er, Tm, Yb, Lu, Mo, Cu, Pb, Zn, Ni, As, Cd, Sb, Bi, Ag, Au, Hg, Tl, and Se (58 elements). Elements discussed in this chapter, units, and analytical limits of detection are presented in Table 3.

Quality control was managed by the use of certified reference materials (CRMs), sample splits, field duplicates, and preparation and analytical blanks. Analytical accuracy was controlled by the use of CRMs including DS8, DS9, DS10, GS311-1, GS910-4, OREAS45CA, OREAS45EA, OREAS72A, OREAS72B, OREAS76A, SY-4(D), SO-18, and CSC. The laboratory also inserted analytical blanks to track reagent contamination and preparation blanks to track contamination of crushing equipment. Systematic error, calculated by comparing the expected concentration of a CRM with the mean values of repeat analyses (Caritat & Cooper 2011), was between 90-110 % for analysed elements, except for Sb (88%), Hg (81%), Se (119%), and Be (188%). Analytical precision was determined by duplicate splits of prepared samples (inserted at a rate of 1 in 8 samples) and expressed as the coefficient of variation (*CV*) which is an unbiased estimate of relative error for geochemical data (Stanley and Lawrie 2007). Coefficient of variation was calculated on duplicate pairs where both analyses were above analytical detection limit. Analytical precision was ±10% for elements analysed except for Cr_2O_3 (13%), Ta (11%), and Au (18%). Sampling precision was determined by field duplicates inserted at a rate of 1 in 15 samples at random intervals and is expressed as the coefficient of variation. Despite the geochemical heterogeneity of the Loxton-Parilla Sands, particularly the ferricrete, sampling precision was good, less than 10% for most elements, except for Cr_2O_3 (27%), TOT/C (11%), Ta (13%), Mo (19%), Cd (55%), and Au (21%).

Table 3 Element analysed.

Element	Units	LLD
Al_2O_3	wt. %	0.01
As	ppm	0.5
Au	ppb	0.5
Ba	ppm	1
CaO	wt. %	0.01
Co	ppm	0.2
Cr_2O_3	wt. %	0.001
Cu	ppm	0.1
Fe_2O_3	wt. %	0.01
Ga	ppm	0.5
Hf	ppm	0.1
K_2O	wt. %	0.01
La	ppm	0.1
Lu	ppm	0.01
MgO	wt. %	0.01
MnO	wt. %	0.01
Mo	ppm	0.1
Na_2O	wt. %	0.01
Ni	ppm	0.1
P_2O_5	wt. %	0.01
Pb	ppm	0.1
Rb	ppm	0.1
Sb	ppm	0.1
Se	ppm	0.5
SiO_2	wt. %	0.1
Sr	ppm	0.5
Th	ppm	0.2
TiO_2	wt. %	0.01
TOT/C	%	0.02
TOT/S	%	0.02
U	ppm	0.1
V	ppm	8
W	ppm	0.5
Y	ppm	0.1
Yb	ppm	0.05
Zn	ppm	1
Zr	ppm	0.1

Geochemical data were processed and analysed using ioGAS (REFLEX). The correlation matrix uses the Spearman rank method, which is not influenced by outliers and has no assumptions about the distribution of data, more suited for geochemical datasets. This approach provides a more unbiased picture of element correlations from geochemical data (Grunsky 2010).

5.3.2 Microanalysis

SCANNING ELECTRON MICROSCOPY

We imaged polished thin sections at Adelaide Microscopy using a Philips XL40 scanning electron microscope fitted with a solid state backscattered electron detector and thin-film energy dispersive x-ray detector. The accelerating voltage was 20 kV and working distance was approximately 10 mm. We acquired images in back-scattered electron mode.

LASER ABLATION ICP-MS (LA ICP-MS)

We acquired qualitative trace element maps using a Resonetics M-50-LR 193 nm Excimer laser coupled with an Agilent 7700s ICP-MS at Adelaide Microscopy. The spot size was 17 µm and scan rate for the map rasters was 20 µm/s. NIST 612 SRM and BCR-2G SRM (USGS basalt glass) were run before and after map acquisition to monitor instrument drift. The elements analysed were ^{75}As, ^{59}Co, ^{52}Cr, ^{65}Cu, ^{57}Fe, ^{55}Mn, ^{95}Mo, ^{60}Ni, ^{208}Pb, ^{121}Sb, ^{77}Se, ^{49}Ti, ^{51}V, ^{182}W, and ^{66}Zn. Data were processed offline with Iolite (Paton *et al.* 2011) which is an add-in for Igor Pro (Wavemetrics Inc., USA). We used the baseline subtract data reduction scheme and linear fit integration. Detection limits of the LA ICP-MS system are much lower than electron microprobe analysis (Reed 2005) but the resolution of morphological details is coarser.

The element maps we acquired with LA ICP-MS are qualitative. Matrix-matching of standards with such geochemically heterogeneous materials is difficult when local Fe_2O_3 concentrations in the indurated weathering horizon can be in excess of 80 wt. %. The aim of element mapping was to

discover if trace elements were distributed uniformly and as such quantification was a second priority.

5.3.3 Infrared spectroscopy (HyLogger™ analysis)

Reflectance spectra in the very-near infrared (VNIR), shortwave infrared (SWIR), and thermal infrared (TIR) ranges were collected by the Geological Survey of South Australia using the Hylogger™ 3 system developed by CSIRO. Dried, uncrushed rock samples were portioned into black plastic chip trays before being scanned by the HyLogger™. Data were processed by the Geological Survey of South Australia and then further analysed using The Spectral Geologist (CSIRO Australia). The spectra are masked to remove spectral signals from black plastic and other non-geological material in the samples. The software provides an automatic match of the acquired sample spectra compared to known mineral spectra in a reference library (The Spectral Assistant™ feature). Individual sample spectra were also manually compared with the reference library.

5.4 RESULTS

5.4.1 Ferricrete characteristics

Ferricrete development is patchy in the western Murray Basin. Where it occurs, the indurated materials are in the upper few metres of the sediment profile. Ferricretes in the Loxton-Parilla Sands can be discriminated based on major element geochemistry and morphology, which record evidence of their formation. The Loxton-Parilla Sands ferricrete is characterised by accumulation of 5-80 wt. % Fe_2O_3 and 0.5-20 wt. % Al_2O_3. Typical morphologies include pisolitic sandstone (Figure 5.4a), irregular concretions with finely laminated rinds (Figure 5.4b, c), indurated sediments and flat-lying laminations (Figure 5.4d), loosely scattered pisoliths with hematitic or goethitic rinds (Figure 5.4e), and even hematitic plant material.

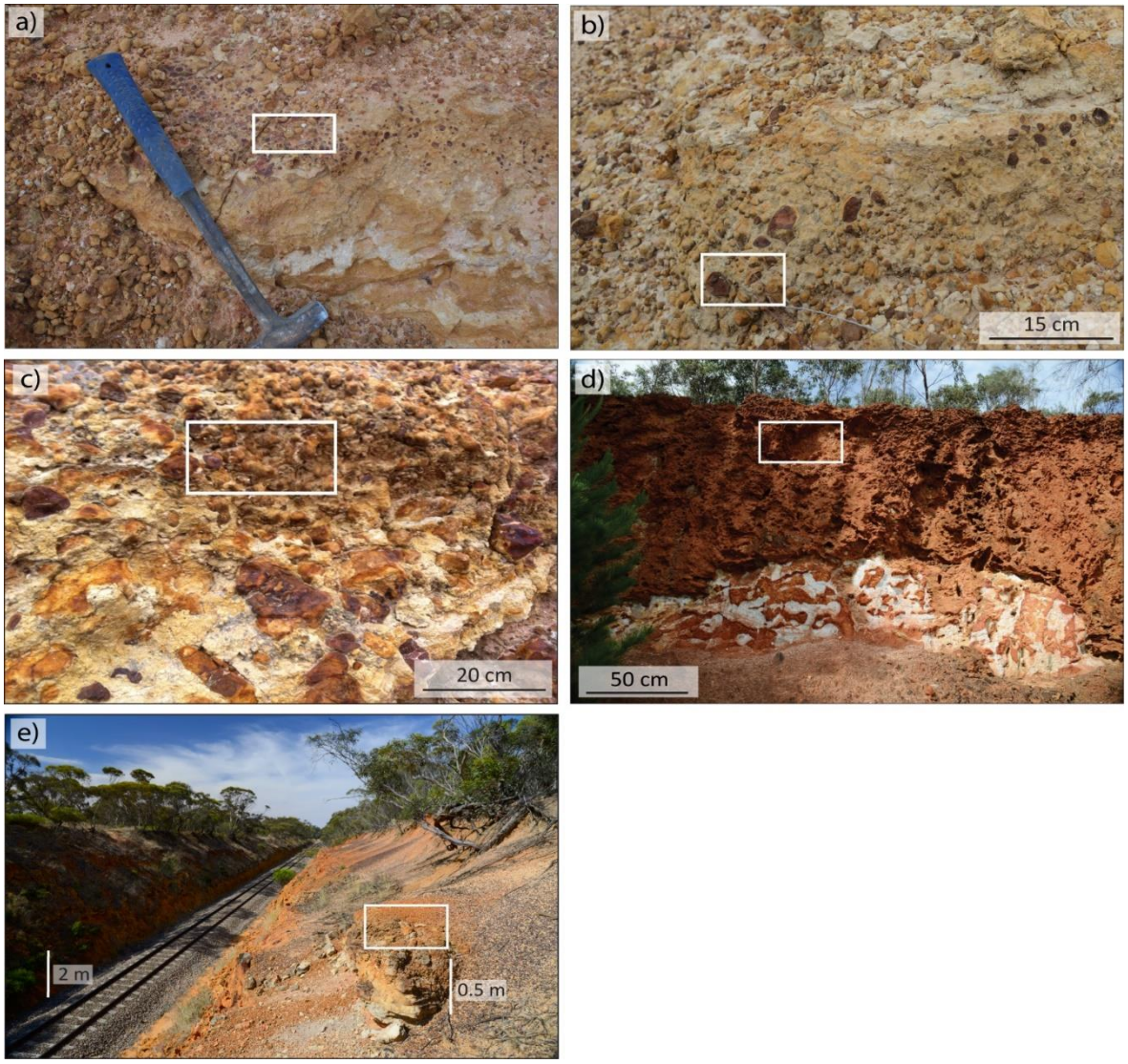

Figure 5.4 Weathering profiles. White boxes show the position of thin sections that have element maps. a) Lyrup, b) Spicer's Pit, c) Hewitt Pit, d) Wannon, e) Diapur.

5.4.2 Mineralogical controls on trace element geochemistry

Whole rock geochemical results show that the geochemistry of the Loxton-Parilla Sands is dominated by Si (measured as SiO_2), Fe (measured as Fe_2O_3), and Al (measured as Al_2O_3). Detailed major element results are described in the previous chapter and will be addressed here in major mineralogical components: silicates, clay minerals, Fe-oxides, heavy minerals, and carbonates and sulphates.

SILICATES

Silica is the dominant mineral in the Loxton-Parilla Sands, mostly as quartz sand, as well as other minor silicate phases. High SiO_2 concentrations tend to dilute other elements (Figure 5.5). Other silicates in the unit are zircon and other heavy minerals, muscovite, and clay minerals. Most samples lie on a negative relationship between SiO_2 and Al_2O_3 (Figure 5.5a), with high CaO and high Fe_2O_3 samples falling below the trend. Samples with very high TiO_2 (Oakvale) and high TiO_2 (Manangatang) are very close to the Al-Si mixing line.

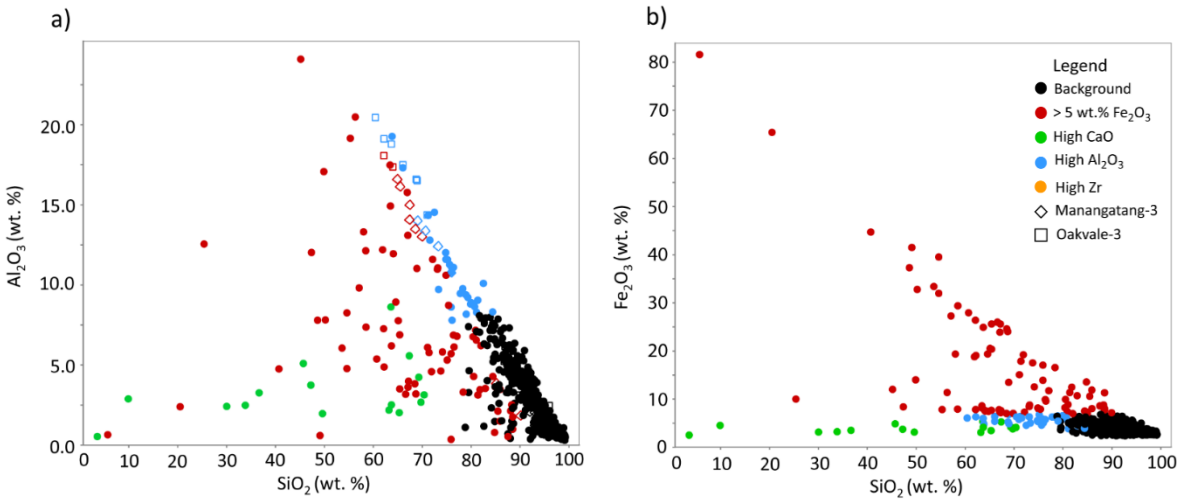

Figure 5.5 Geochemical plots of silicate minerals, with key groups of samples highlighted

CLAYS

Gallium, Th, K_2O, and Rb have the strongest positive relationships with Al_2O_3 (Figure 5.6a). Gallium and Al_2O_3 have the strongest correlation. Potassium and Rb both form two strong positive trends with Al_2O_3 (Figure 5.6b), one with excess K_2O and Rb relative to Al_2O_3, the other a mixing trend. The Manangatang samples cluster above the mixing line. Thorium and Al_2O_3 also have a positive relationship with a group of Fe-rich samples lying above the main trend (Figure 5.6c).

Weaker relationships with Al_2O_3 are evident with TiO_2, Na_2O, and MgO. Sodium and Al_2O_3 form slightly less strong trends. There is also a generally positive relationship between Al_2O_3 and TiO_2 (Figure 5.6d). The Oakvale samples also form a cluster above the TiO_2-Al_2O_3 trend. Samples high in Zr and TiO_2 tend to also fall into the upper trend. Though the trends are present in Na_2O vs

Al_2O_3, they are closer together and more subdued compared to K_2O and Rb. There is a slightly positive relationship between Al_2O_3 and MgO, RC86KI and Manangatang samples lie slightly above the trend, as do samples with high Ca content. HyLogger™ spectra for these samples indicate the presence of phengite.

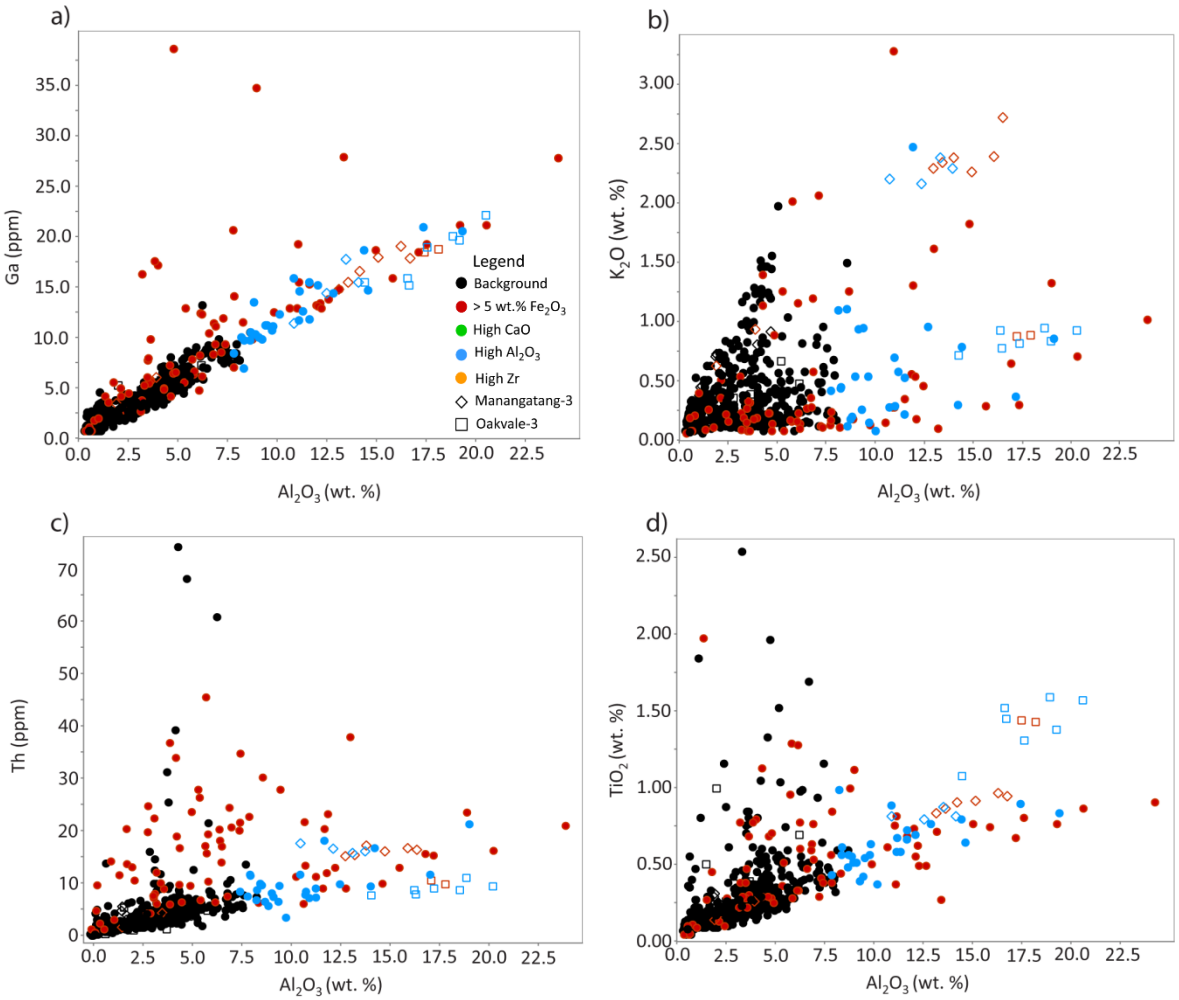

Figure 5.6 Geochemical plots of clay minerals, with key groups of samples highlighted – Fe indurated samples (red), high clay samples (blue), high carbonate samples (green), and samples from the Oakvale-3 and Manangatang-3 bores that cluster more noticeably than other profiles.

IRON OXIDES

There are two key groups of samples in the Fe-oxide geochemistry – low to moderate Fe (as Fe_2O_3), and high Fe_2O_3 (greater than 5 wt. % Fe_2O_3, 50 out of 603 samples). Twelve of these high Fe samples also have high Zr and high TiO_2. Strongly Fe-oxide indurated and weathered samples dominate the high Fe_2O_3 population. The strongest correlations are between Fe_2O_3 and As

(Spearman correlation coefficient 0.69) (Figure 5.7a), and Fe_2O_3 and V (correlation coefficient 0.76) (Figure 5.7b). There are four outliers (OLC02, OLC04, OLC10, HP03) with over 37 wt. % Fe_2O_3 and relatively low As and V and low concentrations of other trace elements. There are weakly positive relationships between Fe_2O_3 and Co (correlation of 0.63), Pb (correlation coefficient = 0.58), Se (correlation coefficient = 0.47), and Th (correlation coefficient = 0.65). Other metal cations that might be expected to correlate with Fe_2O_3 (such as Ni, Cu, Mo, W, Sb) have poor associations in whole rock geochemistry (correlation coefficient < 0.4). The relationship between Fe_2O_3 and Sb and Mo is shown in Figure 5.7c and d. These poor to weakly positive trends are typical of cations in the samples in this study. The relationship between Fe_2O_3 and Sb should be approached with caution because Sb concentrations are close to analytical detection limit. Histograms of geochemical results with high Al_2O_3 and Fe_2O_3 data highlighted show that trace element concentrations are positively skewed towards high Fe_2O_3 (Figure 5.8). Trace element abundance is also slightly positively skewed towards samples with high Al_2O_3 but not as strongly as the Fe-oxides (Figure 5.8).

HEAVY MINERALS

Heavy minerals are contained in the detrital component of the Loxton-Parilla Sands. Elements strongly associated with this mineralogical fraction include TiO_2, Zr, Hf, Nb, and rare earth elements. The results of heavy mineral geochemistry were discussed in detail in Chapter 2 of this thesis.

CARBONATES AND SULPHATES

Carbonate and sulphate minerals comprise a relatively small component of the Loxton-Parilla Sands and are strongly linked with CaO abundance. These mineral phases are also associated with MgO and Ba abundance. Scanning electron microscopy shows thin carbonate laminae growing in the pore spaces of some ferricretes. Calcium distribution is strongly associated with total C (Figure 5.9a) and to a lesser extent with total S (Figure 5.9b). Magnesium is slightly associated with total C but has weak correlations with other elements. Barium has a positive association with total S in a

small group of samples. Scanning electron microscopy shows barite growing in pore spaces in some ferricretes.

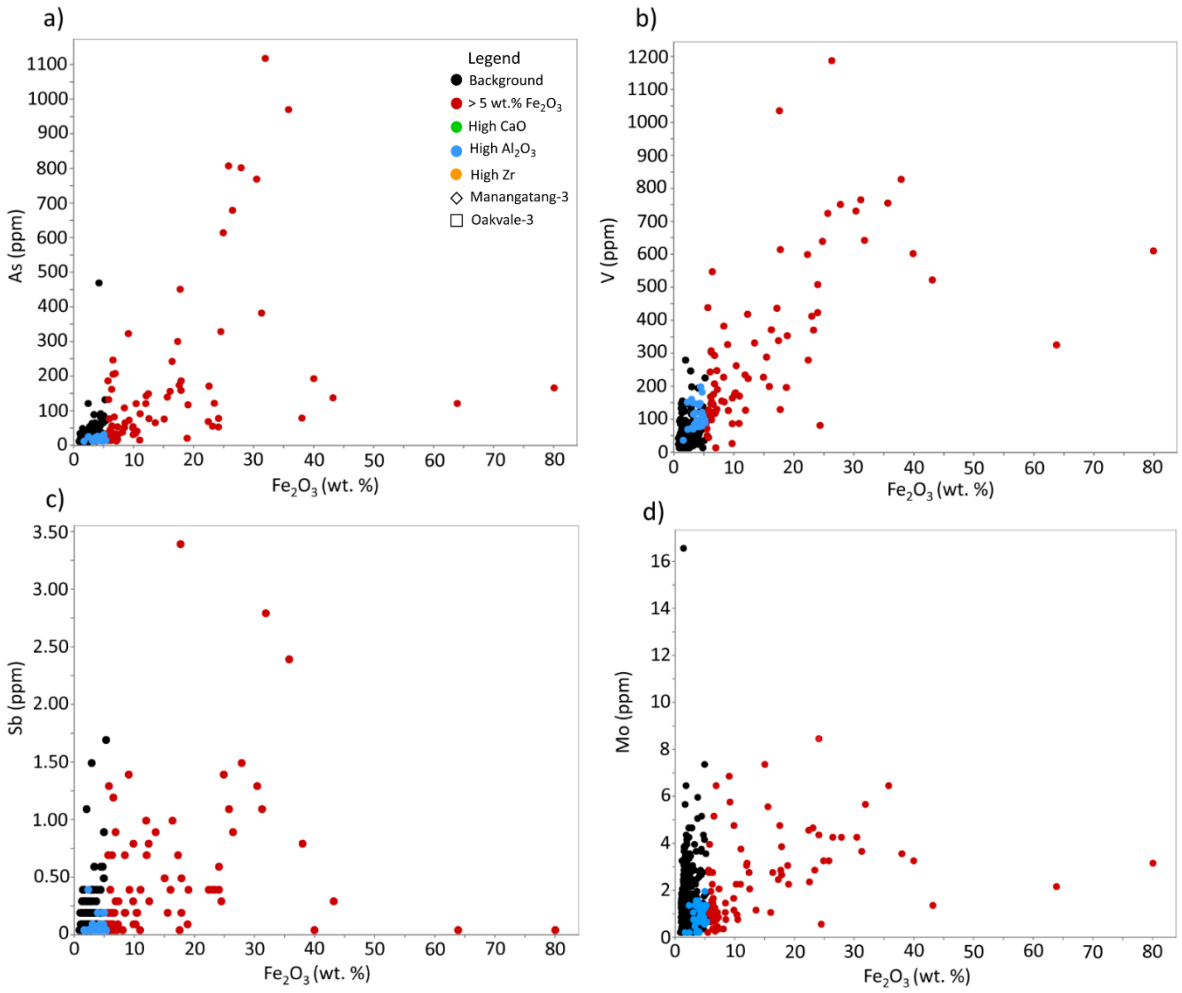

Figure 5.7 Geochemical plots of the main geochemical relationships with Fe_2O3, with key groups of samples highlighted – Fe indurated samples (red) and high clay samples (blue). a) Fe_2O_3 vs As, b) Fe_2O_3 vs V, c) Fe_2O_3 vs Sb, and d) Fe_2O_3 vs M. Note the positive relationships with As and V and weakly positive relationships with Sb and Mo.

5.4.3 Composition and morphology

Laser ablation trace element maps reveal the heterogeneous distribution of trace elements in secondary Fe-oxides. This partitioning is not apparent in the whole rock geochemical results. Arsenic, Co, Cr, and V are most abundant on the edge of the hematitic core of pisoliths (Figure

5.10), the same area barite (identified by EDAX) has accumulated. Lead has a more patchy distribution but occurs in the same part of the pisolith. Titanium and W are associated with the goethitic rim of the pisolith. Spatial partitioning of trace elements in secondary Fe-oxide phases in the indurated weathering surface is most visible in pisoliths and fragments of preserved organic matter at the Spicer's Pit site (Figure 5.11). Cobalt, Cr, Fe, and V are relatively abundant in the centre of the wood fragment (bottom of element map). The edge of the wood fragment, however, has higher As, as well as Mo, Pb, and W. The Fe-concretion has relatively high Cr and V towards the centre (top of element map). Laminae of Fe-oxide parallel to the concretion as well as the outer edge of the wood fragment also have higher concentrations of As, Mo, Pb, and W than the cores.

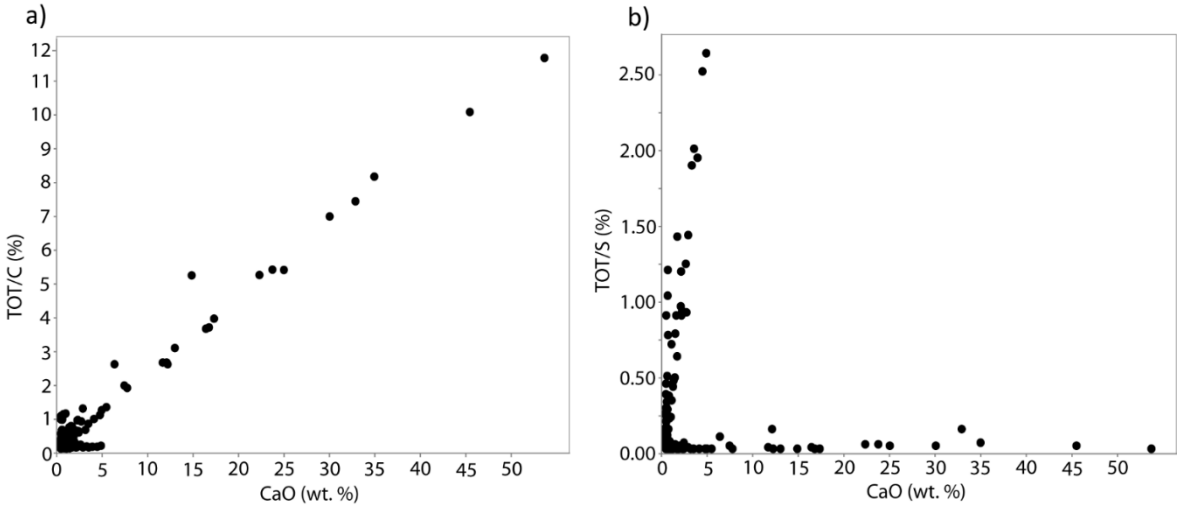

Figure 5.8 Geochemical plots of elements associated with carbonate and sulphate minerals in the Loxton-Parilla Sands. a) CaO vs TOT/C, b) CaO vs TOT/S. Note the split population of samples between Ca and S.

Iron oxide indurations with concentric laminations, for example at Hewitt Pit (Figure 5.12), have slightly different element distribution compared to the pisoliths. Arsenic and V are mostly closely associated with the higher Fe concentrations around the edge whereas Cr and Pb are concentrated in the centre. Titanium and W are spatially associated and form a separate phase to the left of the concretion. Cobalt concentration in this pisolith is not high enough to be detected by LA ICP-MS. Where the Loxton-Parilla Sands overlies bedrock at Wannon trace elements are more homogenously distributed, approximately in proportion to the Fe-oxide distribution (Figure 5.13).

Figure 5.14 shows trace elements analysed by laser ablation in a fragment of dark brown hematitic ferricrete from Diapur. Similar to patterns observed in other samples, As, Cr, Pb, and V as well as Mo are most closely associated with higher concentrations of Fe. Unlike other samples, however, Mn is present and is spatially associated with Co. Manganese concentration is generally low in the Loxton-Parilla Sands (median concentration is equal to analytical detection limit) but this sample shows Mn forms a mineral phase separate to Fe.

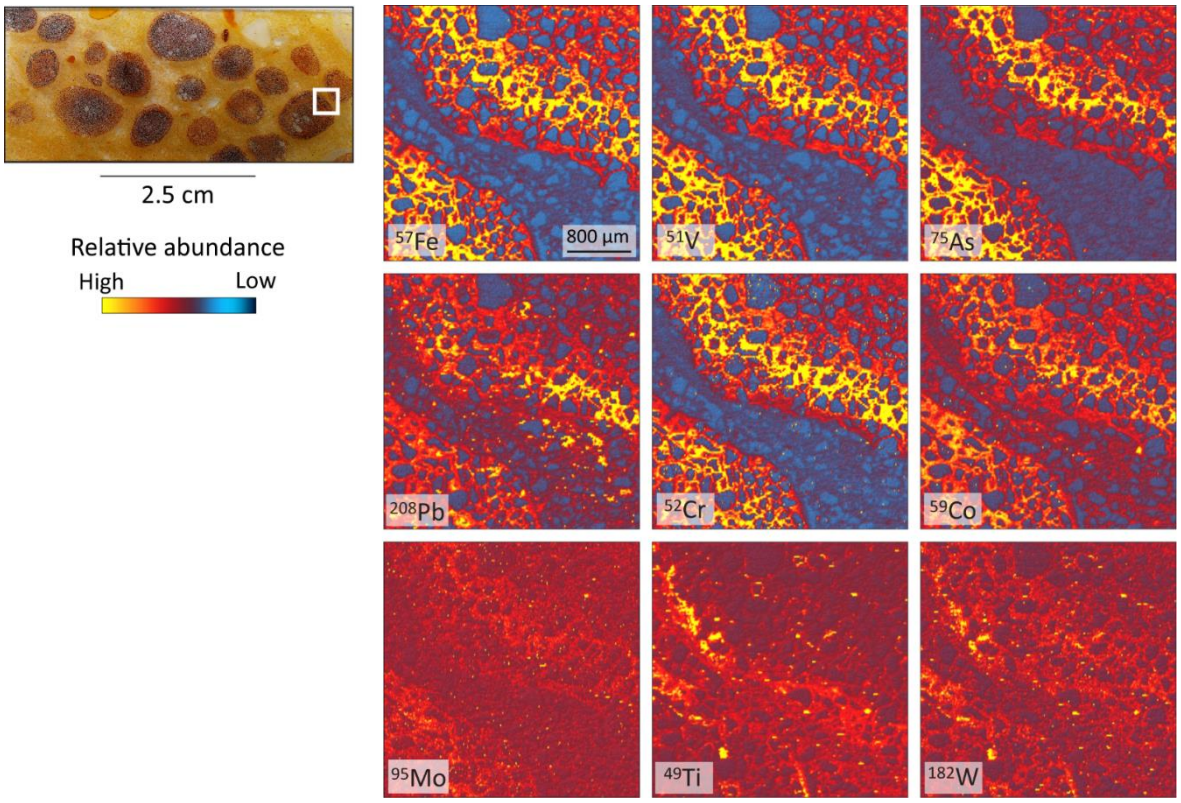

Figure 5.9 Laser ablation trace element map of pisolitic sandstone from Lyrup.

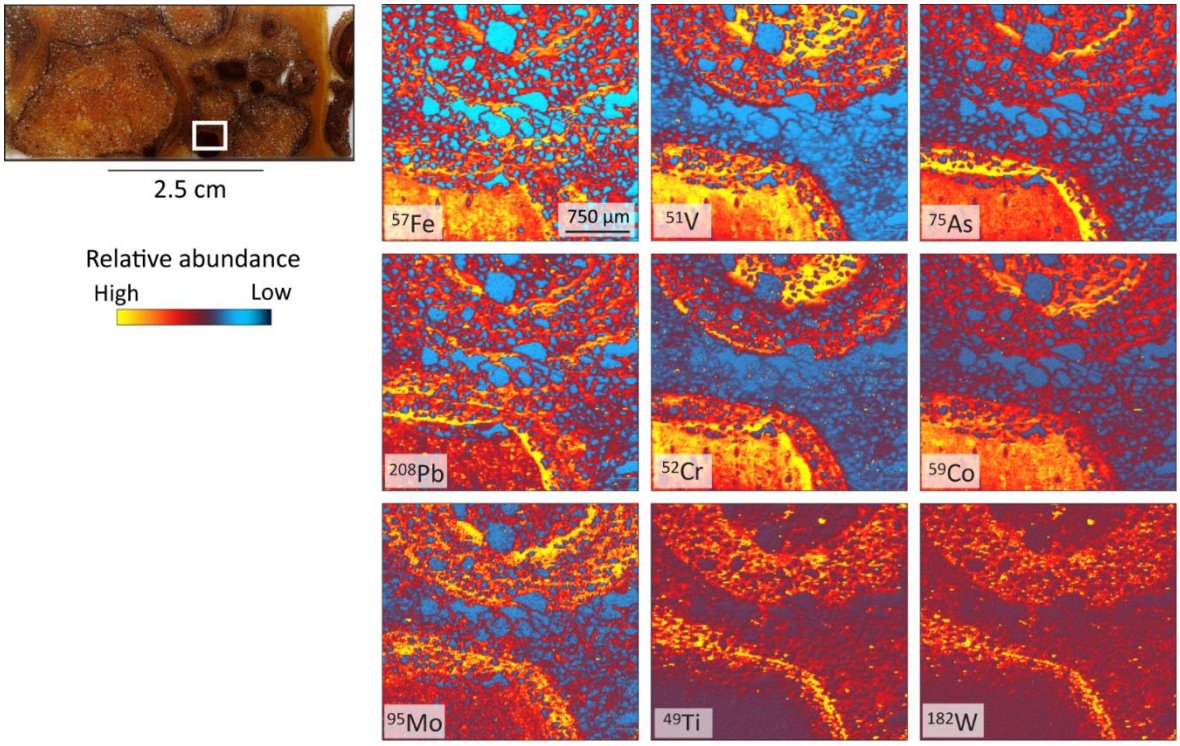

Figure 5.10 Laser ablation trace element maps of ferricrete from Spicer's Pit.

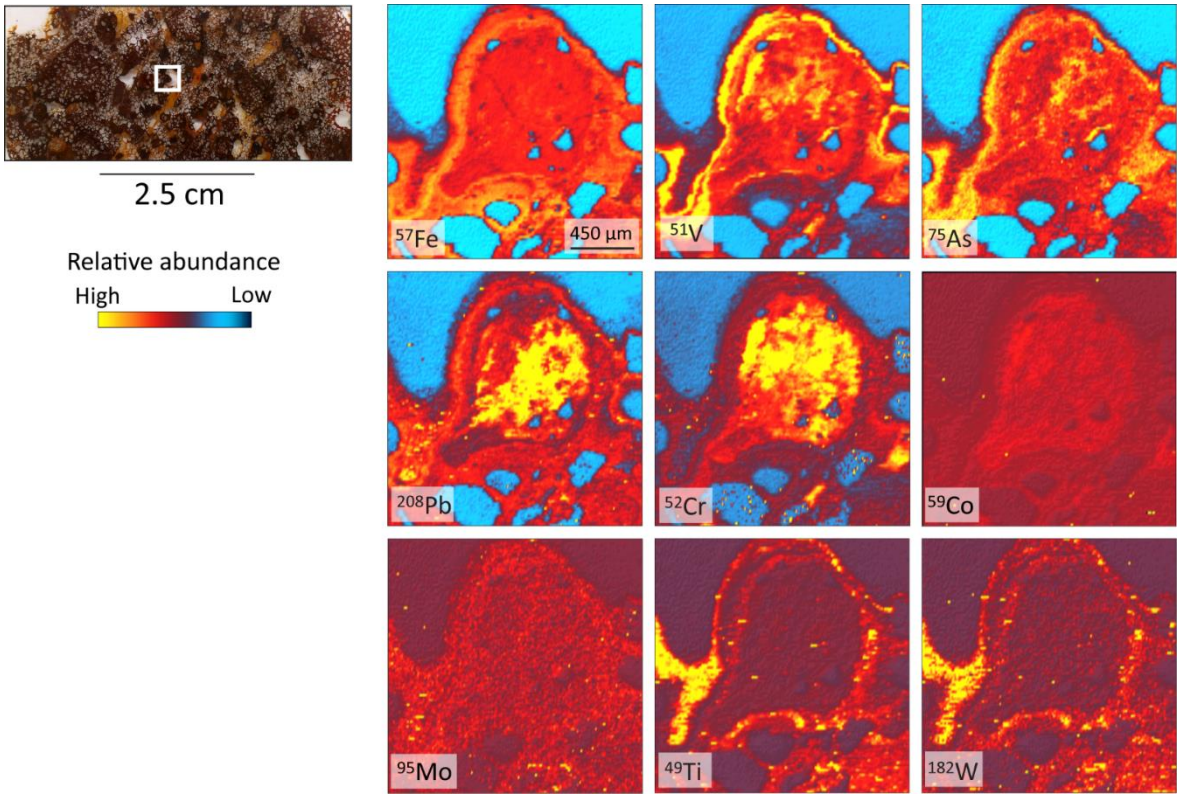

Figure 5.11 Laser ablation trace element map of ferricrete from Hewitt Pit.

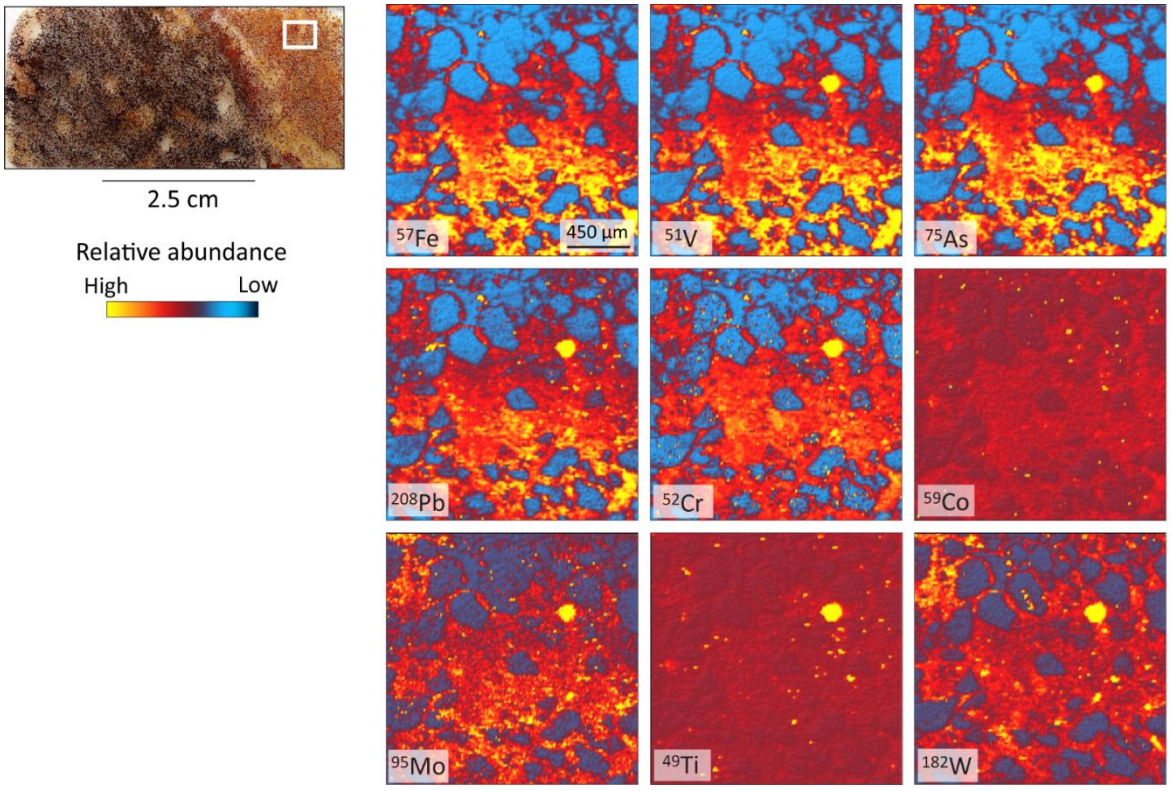

Figure 5.12 Laser ablation trace element maps of ferricrete from Wannon.

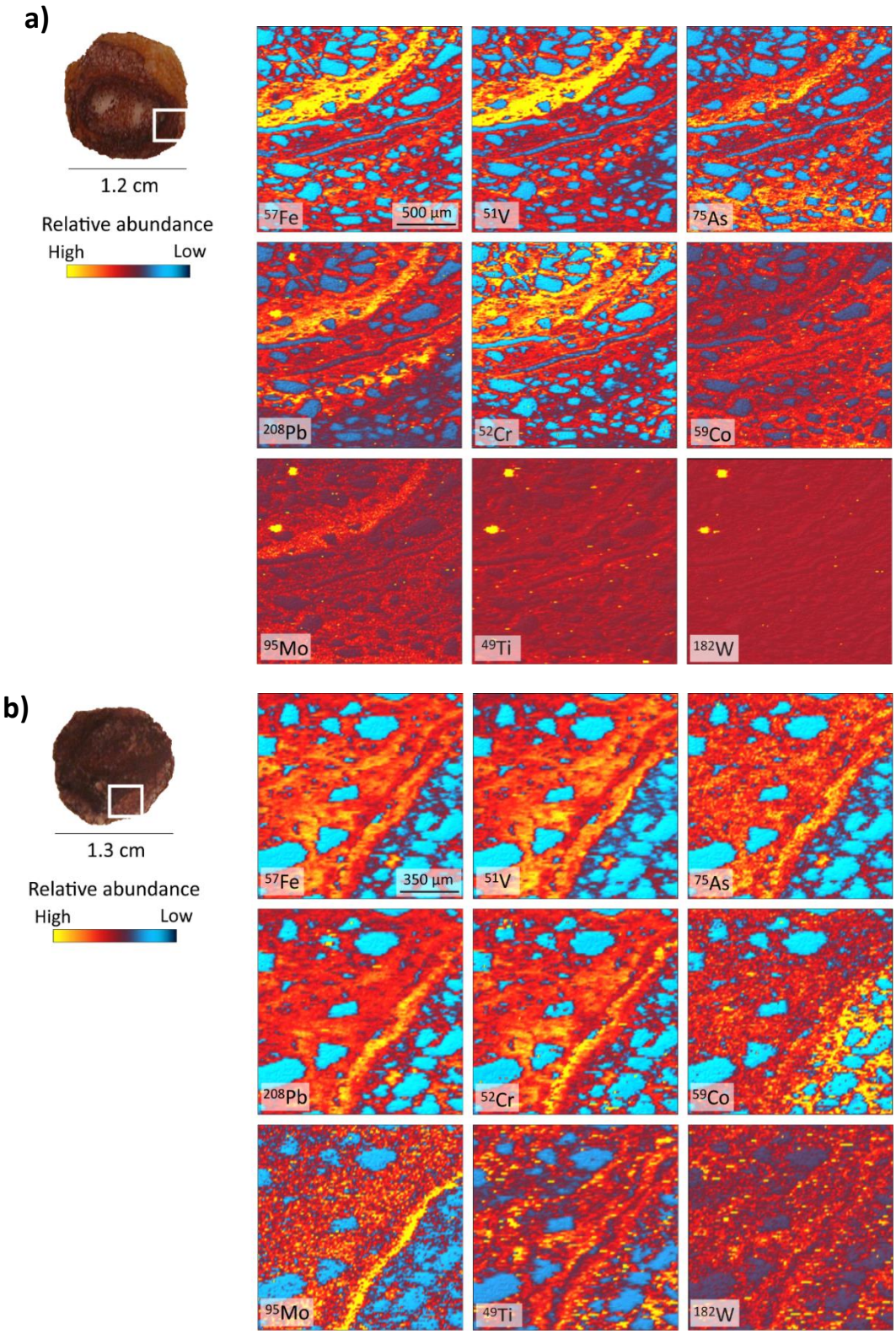

Figure 5.13 Laser ablation trace element maps of pisoliths from Diapur, a) goethitic concentric pisolith, b) hematitic pisolith with fragmented internal texture.

5.5 DISCUSSION

5.5.1 Controls on the trace element geochemistry of the Loxton-Parilla Sands

DEPOSITIONAL AND SEDIMENTARY PROCESSES

Silicates, carbonates, and sulphates

Sedimentary processes control the largest proportion (by volume) of the Loxton-Parilla Sands geochemistry, including most silica, carbonate, and sulphate minerals. Silicate phases including quartz sand, muscovite, and zircon were deposited as part of the Loxton-Parilla Sands during the marine regression and comprise by far the largest component of the geochemistry. The influence of local and regional scale sedimentary processes on the heavy mineral and Au components of the detrital phases were discussed in Chapter 2 of this thesis. Carbonate minerals are predominantly calcite and dolomite and are related to the stratigraphic position of samples in the Loxton-Parilla Sands and are not associated with pathfinder elements. Lower in the stratigraphy the transition zone between the calcareous Bookpurnong Formation and lower shore-face Loxton-Parilla Sands is gradational. In the upper sections of some profiles, particularly in the far western Murray Basin, the lacustrine Bungunnia Limestone has been washed downwards in some profiles, elevating the calcite concentrations in the underlying sand. Calcium and S content is also related to gypsum with large beds of gypsum found in Pliocene lacustrine evaporate deposits (Macumber 1991) that has moved downwards in some profiles.

POST-DEPOSITIONAL GEOCHEMICAL PROCESSES

Clay minerals

Strong associations between Al_2O_3 and Ga and Th shows that the distribution of these elements is largely controlled by the presence of clay minerals. Gallium readily sorbs to clay minerals at a range of pH levels but more readily in acidic conditions (Benedicto *et al.* 2014). Thorium can also be adsorbed by clay minerals or incorporated into new mineral phases in the weathering profile (Sikalidis *et al.* 1989, Braun *et al.* 1993). A positive relationship between Al_2O_3 and TiO_2 in a subgroup of samples suggests adsorption of Ti to clay minerals or even substitution of Ti^{4+} for Al^{3+} into the clay structure (Dolcater *et al.* 1970). Two groups of samples in the Al_2O_3 against K_2O and

Rb suggest a phengite and muscovite dominated group and another cluster characterised by mixing of muscovite and kaolin. Manangatang clusters again, and probably represents a mix of phengite and muscovite (K, Al) with montmorillonite (Na, Ca).

Whole rock geochemistry results show a weakly positive relationship between Al_2O_3 and MgO which is related to montmorillonite and phengite. A cluster of RC86KI samples with low K and weakly elevated Ca were determined to be related to kaolinite by TSG™ software scalars but inspection of the individual spectra suggests montmorillonite. HyLogger™ analysis also shows Rb and Mg anomalies for samples from Manangatang are related to phengite-muscovite solid solution, with AlOH absorption features between 2207-2210 nm (Pontual *et al.* 2010)

Iron oxides

The whole rock geochemistry results show a range of relationships between Fe_2O_3 and trace elements and grain-scale element maps show the complex geochemical processes forming these materials. Strong positive correlations between Fe_2O_3 and As and V suggest incorporation into the structure of hematite and goethite. In subaerial environments As is commonly found as arsenate (As (V)) and is readily absorbed by Fe oxyhydroxides (Boyle & Jonasson 1973). The As content in secondary Fe-oxides is related to the abundance of As in groundwater (Boyle & Jonasson 1973). Vanadium is very redox sensitive and, like a number of cations, has a strong affinity for Fe-oxides (Singh & Gilkes 1992). The large surface area of goethite and hematite and surface reactivity results in ready adsorption of cations while substitution of cations has also been demonstrated (Singh and Gilkes 1992). The weak positive relationship with Fe_2O_3 and cations in the Loxton-Parilla Sands suggests abundance and availability of trace elements in groundwater is a stronger influence on their relationship with Fe-oxides, rather than scavenging and concentration of geochemical signatures. Such processes highlight the risk of normalising geochemical data to Fe_2O_3.

Petrographic and microscopic chemical analysis of ferricretes has provided insight to their formation in the landscape (this thesis – chapter 4) and we have applied this technique to trace element spatial distribution. Ferruginous pisoliths and indurated sediments in the Loxton-Parilla Sands are partly formed by re-working and re-induration of ferruginous duricrust materials (this thesis – chapter 4), much like ferricretes in other parts of Australia (Löhr *et al.* 2013). The results of trace element maps show that the strong correlation between Fe_2O_3 and trace elements like As and V is spatially variable at the grain scale. Even elements that do not have strong positive geochemical associations, such as Pb, Co, W, and Mo, are present in ferricretes but are also zoned. Trace elements in the ferricretes of the Loxton-Parilla Sands are partitioned in successive phases of Fe-oxides. The exception is the ferricrete at Wannon where trace elements are uniformly distributed through the Fe-oxide matrix. In modern systems spatial heterogeneity is observed in trace elements in coastal sediments over the scale of tens of centimetres in northern Australia (Johnston *et al.* 2010, Keene *et al.* 2014). Trace element fractionation in coastal groundwater environments is influenced by local seasonal groundwater fluctuations, tidal hydrology, and topography (Keene *et al.* 2014). At the sub-metre scale microtopography, hydrogeological characteristics of sediments, and local transport of solutes all influence trace element distribution in coastal sediments (Keene *et al.* 2014). Organic matter content is also an important control on the accumulation of Fe in ferruginous weathering profiles (Löhr *et al.* 2010) but we did not identify the degree of organic matter accumulation and its influenced on Fe-oxides in the ancient Loxton-Parilla Sands.

5.5.2 Implications for mineral exploration

A common approach to secondary Fe-oxides in mineral exploration is to normalise geochemical data to Fe_2O_3 to determine geochemical anomalies related to mineralisation. The assumption that goethite and hematite concentrate pathfinder elements in the weathering environment through scavenging can lead to establishing false geochemical anomalies. Reduced Fe can be transported

anywhere from millimetres to kilometres in the landscape, migrating along concentration gradients (Cornell & Schwertmann 2006) which can be lateral or vertical. Redissolved Fe^{2+} can move through the weathering profile until reaching oxidised conditions where Fe^{2+} is re-precipitated as Fe-oxide, producing distinctive redoximorphic patterns in the soil (Cornell & Schwertmann 2006). Given the lateral extent of aquifers in the Murray Basin and the hydraulic conductivity of units such as the Loxton-Parilla Sands, the potential distance for transport of a geochemical signature in the Murray Basin is significant. The Geera Clay acts as a lower confining layer to the Pliocene Sands aquifer, a low-permeability barrier that diverts some lateral groundwater flow upwards (Brown & Radke 1989). In the past this diversion formed groundwater discharge complexes in the Mallee which have since been abandoned (Brown & Radke 1989). This unit was potential a source of some Fe, As, and S in groundwater in the Loxton-Parilla Sands, contributing to formation of the indurated weathering profile.

Studies into the geochemical dispersion of concealed Au mineralisation into modern groundwater and soils in the southern Murray Basin have had mixed results. Arne and House (2009) consider Au, Sb, and As as well as Cu, Mo, W, and Bi the most reliable indicators of Au mineralisation in southern Victoria. Noble (2007) also includes Ni, Ga, Ge, Pb, Zn, Co, Mn, and Se in their geochemical pathfinder suite at an Au prospect near Stawell. Erratic distribution of Au above known mineralisation has been attributed to association with Fe-oxides (Arne *et al.* 2009). Soil sampling over the Lockington East Au prospect (hosted in Ordovician shale and sandstone bedrock) shows a geochemical dispersion halo in cover up to 60 m above the deposit (Arne *et al.* 2009). Hydrogeochemistry has been suggested as a viable sampling technique in the Murray Basin but its usefulness is restricted to areas where the Olney Formation is absent, such as basement highs and where the borehole being sampled has reached the basement (Arne *et al.* 2009). The organic-rich Olney Formation is thought to act as a barrier to the dispersion of metals from basement by creating a reduced zone where metals accumulate rather than migrating further into the cover (Arne *et al.* 2009). Groundwaters in the southern Murray Basin have residence times up

to 30 ka and are subject to inter-aquifer mixing (Cartwright *et al.* 2010). Rather than enhancing the potential for transport of geochemical signatures from basement, this appears to dilute trace element signatures in groundwater flowing through aquifers.

In regions with a relatively small potential catchment area and thin cover, such as at Wannon in southwest Victoria, there is potential for geochemical dispersion of mineralisation signatures. The Wannon site has anomalous As and Sb geochemistry, consistent with Au mineralisation in southern Victoria. The region contains no known Au or other sulphide mineralisation. The sample site is almost 10 km from the nearest major fault. Follow up sampling is warranted, however, to determine the source of signatures of Au mineralisation and to determine the potential hazard such high concentrations of As may pose to groundwater and the nearby Wannon River.

5.6 CONCLUSION

In this study we identified key geochemical processes controlling the trace element distribution in Fe-oxide in the Loxton-Parilla Sands. Whole rock geochemical and microanalysis results suggest Fe-oxides scavenge trace elements when available in the groundwater but do not concentrate geochemical anomalies related to concealed mineralisation. Groundwater that precipitated Fe-oxides during formation of ferricretes likely had a large catchment area in the Murray Basin and thus a geochemical signature sourced from a broad area. Ferricretes in the Murray Basin thus have the potential to provide regional indications of mineralisation but identification of individual targets is difficult. Geochemistry of the Fe-oxides is essentially a record of the average geochemistry of groundwater in the Murray Basin over the last 7 Ma. For geochemical anomalies to form in this environment the dilution and homogenisation effects of regional groundwater must be overcome. This has occurred in the Wannon profile where there is a small catchment of potential geochemical signatures and connectivity with basement.

Chapter 6 Concluding remarks

In this thesis I aimed to identify and characterise the sedimentary and post-depositional processes that contribute to the Loxton-Parilla Sands strandplain system in the western Murray Basin. Three keys aspects of the system, including sediment sources, paleogeography and depositional environments, and geochemistry, have been presented, supported by quantitative geochemical analysis and geochronology and physical observations from the regional tectonic scale to local, outcrop, and grain scales. These studies included an interpretation of major sediment sources of the western Murray Basin in the context of eastern Australia geological evolution; the first 3D model and inferred drainage of the Miocene-Pliocene sediments in the basin; the first geochemical study of the Loxton-Parilla Sands and implications for regional and local weathering processes; and finally an analysis of regional and local geochemical analysis in the western Murray Basin and its implications for mineral exploration in regions covered by deep transported sediment. These studies have been presented as individual manuscripts for journal submission each with separate aims and questions, discussions, conclusions.

A common theme in this thesis is scale – geochemical processes active at the grain scale, responsible for surprising heterogeneity, are superimposed on broader scale processes and influences, from local landscapes to basin-wide sedimentation and neotectonism. This study started by looking at the broad scale sedimentation in the western Murray Basin, in the context of the geological evolution of eastern Australia. Once the regional sedimentation and transport paths had been established, the following chapters shifted to geochemistry from the regional to profile and grain scale. Lateral and vertical groundwater flow over hundreds of metres to hundreds of kilometres is capable of transporting geochemical signatures in the subsurface. These regional signals manifest as fine-scale changes in geochemistry in response to local fluctuations in Eh and pH in the depositional setting. Seasonal fluctuations in redox conditions have influenced post-

depositional geochemistry, which are superimposed on longer time scales of climate and vegetation change, eustasy, and neotectonism.

Another theme of the history and evolution of landforms and stratigraphy in the Murray Basin is persistence. Basement structures have exerted broad controls on the deposition of sedimentary units in the Murray Basin throughout its history, creating depocenters and groundwater diversion, and this study has shown evidence of major river systems being diverted and captured by reactivated faults on multiple occasions. Depositional environments have also been persistent throughout the Cenozoic – the western Murray Basin (Mallee) has been under the influence of marine to marginal marine sedimentation since the early Cenozoic while the eastern Murray Basin (Riverine) records eons of continental fluvial sedimentation. Even in the Anthropocene the stratigraphy continues to shape the landscape and how people live in it, with good land for irrigated crops in the Mallee and good grazing land in the Riverine.

This work has revealed a picture of a large regressive marginal marine depositional environment where the fluvial system evolved at the same time in response to eustatic drop in sea level and regional uplift. Groundwater and weathering systems were not temporally distinct as has been previously interpreted but are dynamic and evolved as ridges were "stranded". Given the range of processes controlling the geochemistry of the Loxton-Parilla Sands it would be unwise to enter into a regional mineral exploration program targeting Fe-oxide indurated sample media without understanding the potential for migration, dilution, and precipitation of geochemical signatures of concealed mineralisation and background geochemistry.

References

ALLEN C., WILLIAMS I., STEPHENS C. & FIELDING C. 1998. Granite genesis and basin formation in an extensional setting: The magmatic history of the Northernmost New England Orogen. *Australian Journal of Earth Sciences* **45**, 875-888.

ALLEN G. P. & POSAMENTIER H. W. 1993. Sequence stratigraphy and facies model of an incised valley fill: the Gironde estuary, France. *Journal of Sedimentary Research* **63**.

ANAND R. & GILKES R. 1984. Weathering of ilmenite in a lateritic pallid zone. *Clays and Clay Minerals* **32**, 363-374.

ANAND R. & GILKES R. 1987. Iron oxides in lateritic soils from Western Australia. *Journal of Soil Science* **38**, 607-622.

ANAND R. & VERRALL M. 2011. Biological origin of minerals in pisoliths in the Darling Range of Western Australia. *Australian Journal of Earth Sciences* **58**, 823-833.

ANAND R. R. & PAINE M. 2002. Regolith geolgy of the Yilgarn Craton, Western Australia: implications for exploration. *Australian Journal of Earth Sciences* **49**, 3-162.

ARNE D. C. & HOUSE E. 2009. Lithogeochemistry haloes surrounding central Victorian gold deposits: Part 2 - Secondary dispersion. *GeoScience Victoria* **16**.

ARNE D. C., HOUSE E., TURNER G., SCOTT K. M. & DRONSEIKA E. 2009. Exploration for deeply buried gold deposits in northern Victoria: soil, regolith and groundwater geochemistry of the Lockington and Lockington East gold deposits. *GeoScience Victoria Gold Undercover Report 10*.

AUSTRALIAN BUREAU OF STATISTICS 2013. *Water Use on Australian Farms*.

BARNETT S. R. 1980. Murray Basin hydrogeological investigation, data assessment - western margin (north). *South Australian Department of Mines and Energy*.

BAROVICH K. & HAND M. 2008. Tectonic setting and provenance of the Paleoproterozoic Willyama Supergroup, Curnamona Province, Australia: Geochemical and Nd isotopic constraints on contrasting source terrain components. *Precambrian Research* **166**, 318-337.

BEAUVAIS A. & ROQUIN C. 1996. Petrological differentiation patterns and geomorphic distribution of ferricretes in Central Africa. *Geoderma* **73**, 63-82.

BENEDICTO A., DEGUELDRE C. & MISSANA T. 2014. Gallium sorption on montmorillonite and illite colloids: Experimental study and modelling by ionic exchange and surface complexation. *Applied Geochemistry* **40**, 43-50.

BERENS V., WHITE M. G. & SOUTER N. J. 2009. Injection of fresh river water into a saline floodplain aquifer in an attempt to improve the condition of river red gum (*Eucalyptus camaldulensis* Dehnh.). *Hydrological Processes* **23**, 3464-3473.

BESLEY R. E. & PLIMER I. R. 1999. The Ivanhoe embayment of the Murray Basin. *Murray Basin Mineral Sands Conference*, Mildura, pp. 10-14. Australian Institute of Geosciences Bulletin.

BESTLAND E. A. & STAINER G. 2013. Down-slope change in soil hydrogeochemistry due to seasonal water table rise: Implications for groundwater weathering. *Catena* **111**, 122-131.

BIGHAM J. & NORDSTROM D. K. 2000. Iron and aluminum hydroxysulfates from acid sulfate waters. *Reviews in mineralogy and geochemistry* **40**, 351-403.

BIGHAM J., SCHWERTMANN U., TRAINA S., WINLAND R. & WOLF M. 1996. Schwertmannite and the chemical modeling of iron in acid sulfate waters. *Geochimica et Cosmochimica Acta* **60**, 2111-2121.

BIRCH W. D. 2003. *Geology of Victoria* (Vol. Special Publication 23). Geological Society of Australia (Victoria Division)

BLACKBURN G. 1962. Stranded coastal dunes in northwestern Victoria. *Australian Journal of Science* **24**, 388-389.

BOURMAN R. P. 1993. Modes of ferricrete genesis: evidence from southeastern Australia. *Zeitschrift für Geomorphologie* **37**, 77-101.

BOURMAN R. P. 2010. Traces from the past: the Cenozoic regolith and intraplate neotectonic history of the Gun Emplacement, a ferricreted bench on the western margin of the Mt Lofty Ranges, South Australia. *Australian Journal of Earth Sciences* **57**, 577-595.

BOURMAN R. P., BUCKMAN S., PILLANS B., WILLIAMS M. & WILLIAMS F. 2010. Traces from the past: the Cenozoic regolith and intraplate neotectonic history of the Gun Emplacement, a ferricreted bench on the western margin of the Mt Lofty Ranges, South Australia. *Australian Journal of Earth Sciences* **57**, 577-595.

BOWLER J. M., KOTSONIS A. & LAWRENCE C. R. 2006. Environmental evolution of the Mallee region, western Murray basin. *Proceedings of the Royal Society of Victoria* **118**, 161-210.

BOYLE R. & JONASSON I. R. 1973. The geochemistry of arsenic and its use as an indicator element in geochemical prospecting. *Journal of Geochemical Exploration* **2**, 251-296.

BRAUN J.-J., PAGEL M., HERBILLN A. & ROSIN C. 1993. Mobilization and redistribution of REEs and thorium in a syenitic lateritic profile: a mass balance study. *Geochimica et Cosmochimica Acta* **57**, 4419-4434.

BROWN C. M. 1985. Murray Basin, Southeastern Australia: Stratigraphy and resource potential - a synopsis: Report 264. *Bureau of Mineral Resources*.

BROWN C. M. & RADKE B. M. 1989. Stratigraphy and sedimentology of mid-Tertiary permeability barriers in the subsurface of the Murray Basin, southeastern Australia. *BMR Journal of Australian Geology and Geophysics* **11**, 367-385.

BROWN C. M. & STEPHENSON A. E. 1986. Murray Basin, southeastern Australia: subsurface stratigraphic database. *Bureau of Mineral Resources Australia Report*.

BROWN C. M. & STEPHENSON A. E. 1991. Geology of the Murray Basin, southeastern Australia. *Bureau of Mineral Resources, Geology and Geophysics Australia Bulletin* **235**.

BROWN C. M., TUCKER D. H. & ANFILOFF V. 1988. An interpretation of the tectonostratigraphic framework of the Murray Basin region of southeastern Australian, based on an examination of airborne magnetic patterns. *Tectonophysics* **154**, 309-333.

BROWNBILL R., LAWRENCE C. & WEAVER T. 1995. Adjoining recharge and discharge systems at the southern margin of the Murray Basin. *Murray Darling 1995 Workshop: Australian Geological Survey Organisation, Canberra*, pp. 61-63.

BRYAN S., CONSTANTINE A., STEPHENS C., EWART A., SCHÖN R. & PARIANOS J. 1997. Early Cretaceous volcano-sedimentary successions along the eastern Australian continental margin: implications for the break-up of eastern Gondwana. *Earth and Planetary Science Letters* **153**, 85-102.

BUTT C. 1988. Genesis of supergene gold deposits in the lateritic regolith of the Yilgarn Block, Western Australia. *The geology of gold deposits: the perspective in*, 460-470.

BUTT C. R. M., LINTER M. J. & ANAND R. R. 2000. Evolution of regoliths and landscapes in deeply weathered terrain - implications for geochemical exploration. *Ore Geology Reviews* **16**, 167-183.

CARITAT P. D. & COOPER M. 2011. National geochemical survey of Australia: data quality assessment. *Geoscience Australia Record* **21**.

CARITAT P. D., KIRSTE D., CARR G. & MCCULLOCH M. 2005. Groundwater in the Broken Hill region, Australia: recognising interaction with bedrock and mineralisation using S, Sr, and Pb isotopes. *Applied Geochemistry* **20**, 767-787.

CARTWRIGHT I., WEAVER T., CENDÓN D. I. & SWANE I. 2010. Environmental isotopes as indicators of inter-aquifer mixing, Wimmera region, Murray Basin, Southeast Australia. *Chemical Geology* **277**, 214-226.

CARTWRIGHT I., WEAVER T. & PETRIDES B. 2007. Controls on $^{87}Sr/^{86}Sr$ ratios of groundwater in silicate-dominated aquifers: SE Murray Basin, Australia. *Chemical Geology* **246**, 107-123.

CAYLEY R. & TAYLOR D. 1997. *Grampians special map area geological report* (Vol. 107). Geological Survey of Victoria

CAYLEY R. & TAYLOR D. 2001. *Ararat: 1: 100 000 Map Area Geological Report*. Department of Natural Resources and Environment.

CHAO T. & THEOBALD P. 1976. The significance of secondary iron and manganese oxides in geochemical exploration. *Economic Geology* **71**, 1560-1569.

CHARETTE M. A. & SHOLKOVITZ E. R. 2002. Oxidative precipitation of groundwater-derived ferrous iron in the subterranean estuary of a coastal bay. *Geophyiscal Research Letters* **29**.

CLARK D. 2012. *Neotectonic Features Database*. Geoscience Australia.

CLARK D., MCPHERSON A. & COLLINS C. 2011. Australia's seismogenic neotectonic record. *Geoscience Australia Record* **11**.

CLARK D., VAN DISSEN R., CUPPER M., COLLINS C. & PRENDERGAST A. 2007. Temporal clustering of surface ruptures on stable continental region faults: a case study from the Cadell Fault scarp, south eastern Australia. *Proceedings of the Australian Earthquake Engineering Society Conference*, pp. 23-25.

COBLENTZ D., SANDIFORD M., RICHARDSON R. M., ZHOU S. & HILLIS R. 1995. The origins of the intraplate stress field in continental Australia. *Earth and Planetary Science Letters* **133**, 299-309.

COLWELL J. 1976. Heavy minerals in the Late Cainozoic sediments of southeastern South Australia. *Bureau of Mineral Resources, Geology and Geophysics*.

CONEY P. J., EDWARDS A., HINE R., MORRISON F. & WINDRIM D. 1990. The regional tectonics of the Tasman orogenic system, eastern Australia. *Journal of Structural Geology* **12**, 519-543.

CORNELL R. M. & SCHWERTMANN U. 2006. *The iron oxides: structure, properties, reactions, occurrences and uses*. John Wiley & Sons.

CUDAHY T. 1997. PIMA-II spectral characteristics of natural kaolins. *Australian Mineral Industries Research Association Limited Exploration and Mining Report*.

CUDAHY T. & RAMANAIDOU E. 1997. Measurement of the hematite: goethite ratio using field visible and near-infrared reflectance spectrometry in channel iron deposits, Western Australia. *Australian Journal of Earth Sciences* **44**, 411-420.

DENNANT J. 1886. Geologic sketch of southwestern Victoria. *Vict. Nat*, 70-74.

DICKINSON J., WALLACE M., HOLDGATE G., DANIELS J., GALLAGHER S. & THOMAS L. 2001. Neogene tectonics in SE Australia: implications for petroleum systems. *APPEA Journal* **41**, 37-52.

DICKINSON J., WALLACE M. W., HOLDGATE G. R., GALLAGHER S. J. & THOMAS L. 2002. Origin and timing of the Miocene-Pliocene unconformity in southeast Australia. *Journal of Sedimentary Research* **72**, 288-303.

DICKSON T. W. 1999. A history of exploration for heavy minerals in the Victorian section of the Murray Basin. Murray Basin Mineral Sands Conference, Mildura, Victoria (unpubl.).

DOLCATER D., SYERS J. & JACKSON M. 1970. Titanium as free oxide and substituted forms in kaolinites and other soil minerals. *Clays Clay Miner* **18**, 71-79.

DOMINGUEZ J. M. L. & WANLESS H. R. 2009. Facies Architecture of a Falling Sea-Level Strandplain, Doce River Coast, Brazil. *In, Shelf Sand and Sandstone Bodies*, pp 257-281, Blackwell Publishing Ltd.

DUNBAR R. W., ZECH R., CRANDALL G. & KATZMAN D. 1992. Strandplain and deltaic depositional models for the Point Lookout Sandstone, San Juan Basin and Four Corners Platform, New Mexico and Colorado. *San Juan Basin IV. New Mexico Geological Society Forty-third Annual Field Conference*, pp. 199-206.

EGGLETON R. & TAYLOR G. 1998. Selected thoughts on 'laterite'. *New Approaches to an Old Continent, 3rd Australian Regolith Conference Proceedings, Regolith '98*, pp. 209-226.

EGGLETON R. A. 2008. Regolith mineralogy. *In:* Scott K. M. & Pain C. F. eds., *Regolith Science*, CSIRO Publishing, Victoria, Australia.

EVANS W. & KELLETT J. 1989. The hydrogeology of the Murray Basin, southeastern Australia. *BMR Journal of Australian Geology and Geophysics* **11**, 147-166.

FANNING C. 1991. Single and multi-grain U-Pb zircon dating of the Rocklands Rhyolite. *Geological Survey of Victoria Unpublished Report*.

FANNING C. & MORAND V. J. 2002. Results of some SHRIMP U-Pb zircon dating of rocks from Victoria. *Geological Survey of Victoria*.

FENNER C. 1918. The physiography of the Glenelg River. *Proceedings of the Royal Society of Victoria* **30**, 99-120.

FERGUSON C. L. & VANDENBERG A. H. M. 2003. Ordovician - the development of craton-derived deep-sea turbidite successions. *In:* Birch W. D. ed., *Geology of Victoria*, Geological Society of Australia (Victoria Division).

FERGUSSON C. & FANNING C. 2002. Late Ordovician stratigraphy, zircon provenance and tectonics, Lachlan Fold Belt, southeastern Australia. *Australian Journal of Earth Sciences* **49**, 423-436.

FERGUSSON C. L. & CONEY P. J. 1992. Implications of a Bengal Fan-type deposit in the Paleozoic Lachlan fold belt of southeastern Australia. *Geology* **20**, 1047-1049.

FIRMAN J. B. 1966. Stratigraphy of the Chowilla area in the Murray Basin. *Quarterly Notes of the Geological Survey of South Australia* **20**, 3-7.

FIRMAN J. B. 1972. Renmark, South Australia - 1:250,000 Geological Series. *Geological Survey of South Australia Explanatory Notes*.

FIRMAN J. B. 1973. Regional stratigraphy of surficial deposits in the Murray Basin and Gambier Embayment. *Department of Mines, Geological Survey of South Australia Report of investigations*.

FIRMAN J. B. 1975. Australia-South Australia. *In:* Fairbridge R. W. ed., *The encyclopedia of world regional geology, part 1: Western Hemisphere (including Antarctica and Australia)*, Vol. 8, pp 61-80, Hutchinson & Ross Inc.

FIRMAN J. B. 1979. Paleopedology applied to land use studies in southern Australia. *Geoderma* **22**, 105-117.

FIRMAN J. B. 1994. Palaeosols in laterite and silcrete profiles: Evidence from the South East Margin of the Australian Precambrian Shield. *Earth-Science Reviews* **36**, 149-179.

FISHER W. L., GALLOWAY W., PROCTOR JR C. V. & NAGLE J. 1970. Depositional Systems in the Jackson Group of Texas their Relationship to Oil Gas, and Uranium.

FITZPATRICK R., FRITSCH E. & SELF P. 1996. Interpretation of soil features produced by ancient and modern processes in degraded landscapes: V. Development of saline sulfidic features in non-tidal seepage areas. *Geoderma* **69**, 1-29.

FITZPATRICK R. & SCHWERTMANN U. 1982. Al-Substituted goethite - An indicator of pedogenic and other weathering environments in South Africa. *Geoderma* **27**, 335-347.

FITZPATRICK R., SHAND P. & MERRY R. H. 2009. Acid Sulfate Soils. *In:* Jennings J. T. ed., *Natual History of the Riverland and Murraylands*, pp 65-111, Royal Society of South Australia (Inc.), Adelaide, South Australia.

FODEN J. D., ELBURG M. A., TURNER S. P., SANDIFORD M., O'CALLAGHAN J. & MITCHELL S. 2002. Granite production in the Delamerian orogen, South Australia. *Journal of the Geological Society* **159**, 557-575.

FOYLE A. M. & NORTON K. P. 2006. Late Holocene nearshore change at a nontidal transgressive systems tract strandplain complex, Presque Isle, Pennsylvania, USA. *Journal of coastal research*, 406-423.

FRAKES L., BURGER D., APTHORPE M., WISEMAN J., DETTMANN M., ALLEY N., FLINT R., GRAVESTOCK D., LUDBROOK N. & BACKHOUSE J. 1987. Australian Cretaceous shorelines, stage by stage. *Palaeogeography, Palaeoclimatology, Palaeoecology* **59**, 31-48.

FRASER C., HILL P. R. & ALLARD M. 2005. Morphology and facies architecture of a falling sea level strandplain, Umiujaq, Hudson Bay, Canada. *Sedimentology* **52**, 141-160.

GALLANT J., WILSON N., DOWLING T., READ A. & INSKEEP C. 2011. *SRTM-derived 1 Second Digital Elevation Models Version 1.0*, Geoscience Australia.

GIBSON D. & CHAN R. A. 1999. Aspects of paleodrainage of the northern Lachlan Fold Belt region. *Regolith '98 Conference, Australian Regolith & Mineral Exploration*, Kalgoorlie, Western Australia, pp. 38-54. CRC LEME.

GILL E. 1964. Rocks contiguous with the basaltic cuirass of western Victoria. *Proceedings of the Royal Society of Victoria* **77**, 331-355.

GINGELE F. X., DE DECKKER P. & HILLENBRAND C.-D. 2004. Late Quaternary terrigenous sediments from the Murray Canyons area, offshore South Australia and their implications for sea level change, palaeoclimate and palaeodrainage of the Murray–Darling Basin. *Marine Geology* **212**, 183-197.

GLEN R. 2005. The Tasmanides of eastern Australia. *Geological Society, London, Special Publications* **246**, 23-96.

GOLDIE-DIVKO L. 2008. Sub-surface Geology of the Kerang District, Murray Basin, Southeast Australia. Doctor of Philosophy thesis, School of Life and Environmental Sciences, Deakin University, Melbourne, Australia (unpubl.).

GRAY D. J. 2001. Hydrogeochemistry in the Yilgarn Craton. *Geochemistry: Exploration, Environment, Analysis* **1**, 253-264.

GRAY D. J., NOBLE R. R. P. & REID N. 2010. Hydrogeochemical mapping of the northeast Yilgarn groundwaters. First Australian Regolith Geoscientists Conference, Arkaroola, South Australia (unpubl.).

GRUNSKY E. C. 2010. The interpretation of geochemical survey data. *Geochemistry: Exploration, Environment, Analysis* **10**, 27-74.

HAEST M., CUDAHY T., LAUKAMP C. & GREGORY S. 2012. Quantitative Mineralogy from Infrared Spectroscopic Data. I. Validation of Mineral Abundance and Composition Scripts at the Rocklea Channel Iron Deposit in Western Australia. *Economic Geology* **107**, 209-228.

HALLETT M., VASSALLO J., GLEN R. & WEBSTER S. 2005. *Murray-Riverine region: an interpretation of bedrock Palaeozoic geology based on geophysical data*. Industries N. D. o. P. **118**, Maitland.

HAMILTON D. S. 1995. Approaches to identifying reservoir heterogeneity in barrier/strandplain reservoirs and the opportunities for increased oil recovery: an example from the prolific oil-producing Jackson-Yegua trend, south Texas. *Marine and Petroleum Geology* **12**, 273-290.

HANOR J. S. 2000. Barite–celestine geochemistry and environments of formation. *Reviews in Mineralogy and Geochemistry* **40**, 193-275.

HAWKES H. E. & WEBB J. S. 1962. Geochemistry in mineral exploration.

HEIN C. J., FITZGERALD D. M., CLEARY W. J., ALBERNAZ M. B., DE MENEZES J. T. & KLEIN A. H. D. F. 2013. Evidence for a transgressive barrier within a regressive strandplain system: Implications for complex coastal response to environmental change. *Sedimentology* **60**, 469-502.

HEWARD A. P. 1981. A review of wave-dominated clastic shoreline deposits. *Earth-Science Reviews* **17**, 223-276.

HILL P., DE DECKKER† P., VON DER BORCH C. & MURRAY-WALLACE C. 2009. Ancestral Murray River on the Lacepede Shelf, southern Australia: Late Quaternary migrations of a major river outlet and strandline development. *Australian Journal of Earth Sciences* **56**, 135-157.

HILL S. M., EGGLETON R. A. & TAYLOR G. 2003. Neotectonic disruption of silicified palaeovalley systems in an intraplate, cratonic landscape: regolith and landscape evolution of the Mulculca range-front, Broken Hill Domain, New South Wales. *Australian Journal of Earth Sciences* **50**, 691-707.

HILLIS R. R., GILES D., VAN DER WIELEN S. E., BAENCH A., CLEVERLEY J. S., FABRIS A., HALLEY S. W., HARRIS B. D., HILL S. M., KANCK P., KEPIC A., SOE S. P., STEWART G. & UVAROVA Y. 2014. Coiled Tubing Drilling and Real-Time Sensing - Enabling Prospecting Drilling in the 21st Century? *Society of Economic Geologists Special Publication* **18**, 243-259.

HILLIS R. R., SANDIFORD M., REYNOLDS S. D. & QUIGLEY M. C. 2008. Present-day stresses, seismicity and Neogene-to-Recent tectonics of Australia's 'passive'margins: intraplate deformation controlled by plate boundary forces. *Geological Society, London, Special Publications* **306**, 71-90.

HILLS E. S. 1939. The physiography of north-western Victoria. *Proceedings of the Royal Society of Victoria* **51**, 297-323.

HORVATH H. S. 1993. *Exploration Licences 2685, 3167, 3337 and 3381, Stavely Project, Victoria: annual report for period ending 6th February, 1993. Expired mineral exploration reports licence file*. Department of Natural Resources and Environment, Victoria.

HOU B., FRAKES L., ALLEY N. & HEITHERSAY P. 2003. Evolution of beach placer shorelines and heavy-mineral deposition in the eastern Eucla Basin, South Australia. *Australian Journal of Earth Sciences* **50**, 955-965.

IRELAND T., FLÖTTMANN T., FANNING C., GIBSON G. & PREISS W. V. 1998. Development of the early Paleozoic Pacific margin of Gondwana from detrital-zircon ages across the Delamerian orogen. *Geology* **26**, 243-246.

IRELAND T., MORAND V. J. & GIBSON G. M. 2002. Results of some recent SHRIMP U-Pb zircon dating of rocks from the Glenelg Zone of western Victoria. *Geological Survey of Victoria*.

JOHNSTON S., BURTON E. D., BUSH R. T., KEENE A. F., SULLVIAN L. A., SMITH D., MCELNEA A. E., AHERN C. R. & POWELL B. 2010. Abundance and fractionation of Al, Fe and trace metals following tidal inundation of a tropical acid sulfate soil. *Applied Geochemistry* **25**, 323-335.

JOYCE E. 1992. The West Victorian Uplands of southeastern Australia: origin and history. *Earth Surface Processes and Landforms* **17**, 407-418.

JOYCE E. B., WEBB J. A., DAHLHAUS P. G., GRIMES K. G., HILL S. M., KOTSONIS A., MARTIN J., MITCHELL M., NEILSON J., ORR M., PETERSON J., ROSENGREN N., ROWAN J., ROWE R., SARGEANT I., STONE T., SMITH B., WHITE S. & JENKIN J. J. 2003. Geomorphology: the evolution of Victorian landscapes. *In:* Birch W. D. ed., *Geology of Victoria*, Geological Society of Australia, Melbourne.

KEAY S., STEELE D. & COMPSTON W. 1999. Identifying granite sources by SHRIMP U-Pb zircon geochronology: An application to the Lachlan foldbelt. *Contributions to Mineralogy and Petrology* **137**, 323-341.

KEENE A. F., JOHNSTON S., BUSH R. T., BURTON E. D., SULLVIAN L. A., DUNDON M., MCELNEA A. E., DOUG SMITH C., AHERN C. R. & POWELL B. 2014. Enrichment and heterogeneity of trace elements at the redox-interface of Fe-rich intertidal sediments. *Chemical Geology* **383**, 1-12.

KOTSONIS A. 1995. Late Cainozoic Climatic and Eustatic Record from the Loxton-Parilla Sands, Murray Basin, Southeastern Australia. Master of Science thesis, School of Earth Sciences, University of Melbourne, Melbourne (unpubl.).

KYSER K., BARR J. & IHLENFELD C. 2015. Applied Geochemistry in Mineral Exploration and Mining. *Elements* **11**, 241-246.

LI C. X., ZHANG J. Q. & DENG B. 2001. Holocene regression and the tidal radial sand ridge system formation in the Jiangsu coastal zone, east China. *Marine Geology* **173**, 97-120.

LISITSIN V., MOORE D., OLSHINA A. & WILLMAN C. 2010. Undiscovered orogenic gold endowment in Northern Victoria, Australia. *Ore Geology Reviews* **38**, 251-269.

LÖHR S., GRIGORESCU M. & COX M. 2013. Iron nodules in ferric soils of the Fraser Coast, Australia: relicts of laterisation or features of contemporary weathering and pedogenesis? *Soil Research* **51**, 77-93.

LOHR S., GRIGORESCU M., HODGKINSON J., COX M. & FRASER S. 2010. Iron occurrence in soils and sediments of a coastal catchment: A multivariate approach using self organising maps. *Geoderma* **156**, 253-266.

LÖHR S., GRIGORESCU M., HODGKINSON J., COX M. & FRASER S. 2010. Iron occurrence in soils and sediments of a coastal catchment: a multivariate approach using self organising maps. *Geoderma* **156**, 253-266.

LÓPEZ G. I. & RINK W. J. 2008. New quartz optical stimulated luminescence ages for beach ridges on the St. Vincent Island Holocene strandplain, Florida, United States. *Journal of coastal research* **24**, 49-62.

LUDBROOK N. H. 1961. Stratigraphy of the Murray Basin in South Australia. *Geological Survey of South Australia Bulletin 36*.

MAAS R., NICHOLLS I., GREIG A. & NEMCHIN A. 2001. U–Pb zircon studies of mid-crustal metasedimentary enclaves from the S-type Deddick Granodiorite, Lachlan Fold Belt, SE Australia. *Journal of Petrology* **42**, 1429-1448.

MACUMBER P. 1978. Evolution of the Murray River during the Tertiary period: evidence from northern Victoria. *Proceedings of the Royal Society of Victoria* **90**, 43-52.

MACUMBER P. G. 1991. *Interaction between groundwater and surface systems in northern Victoria*. Victorian Department of Conservation and Environment.

MARTIN H. 2006. Cenozoic climatic change and the development of the arid vegetation in Australia. *Journal of Arid Environments* **66**, 533-563.

MCARTHUR J., HOWARTH R. & BAILEY T. 2001. Strontium isotope stratigraphy: LOWESS version 3: Best fit to the marine Sr-isotope curve for 0–509 Ma and accompanying look-up table for deriving numerical age. *The Journal of Geology* **109**, 155-170.

MCARTHUR J. & HOWARTH R. J. 2004. Strontium isotope stratigraphy. *In:* Gradstein F. M., Ogg J. G. & Smith A. G. eds., *A Geologic Time Scale 2004*, pp 96-105, Cambridge University Press.

MCCUBBIN D. G. 1982. Barrier-island and strand-plain facies. *In, Sandstone Depositional Environments*.

MCLAREN S., WALLACE M. W., GALLAGHER S. J., MIRANDA J. A., HOLDGATE G. R., GOW L. J., SNOWBALL I. & SANDGREN P. 2011. Palaeogeographic, climatic and tectonic change in southeastern Australia: the Late Neogene evolution of the Murray Basin. *Quaternary Science Reviews* **30**, 1086-1111.

MCLAREN S., WALLACE M. W., PILLANS B. J., GALLAGHER S. J., MIRANDA J. A. & WARNE M. T. 2009. Revised stratigraphy of the Blanchetown Clay, Murray Basin: age constraints on the evolution of paleo Lake Bungunnia. *Australian Journal of Earth Sciences* **56**, 259-270.

MCLENNAN S. M., HILL S. M., HATCH M., BAROVICH K. & BERENS V. 2013. Riparian eucalypt biogeochemical expression of groundwater salinity, Murray River, South Australia. *Geochemistry: Exploration, Environment, Analysis* **13**, 159-168.

MCQUEEN K. G. & MUNRO D. C. 2003. Weathering-controlled fractionation of ore and pathfinder elements at Cobar, NSW. Advances in Regolith 2003(unpubl.).

MILNES A., BOURMAN R. & NORTHCOTE K. 1985. Field relationships of ferricretes and weathered zones in southern South Australia: a contribution to'laterite'studies in Australia. *Soil Research* **23**, 441-465.

MIRANDA J. A. 2007. Late Neogene stratigraphy and sedimentation across the Murray Basin, southeastern Australia. PhD thesis, Science - Earth Sciences, University of Melbourne, Melbourne (unpubl.).

MIRANDA J. A., WALLACE M. W. & MCLAREN S. 2008. The Norwest Bend Formation: Implications for the evolution of Neogene drainage in southeastern Australia. *Sedimentary Geology* **205**, 53-66.

MIRANDA J. A., WALLACE M. W. & MCLAREN S. 2009. Tectonism and eustacy across a Late Miocene strandplain: The Loxton-Parilla Sands, Murray Basin, southeastern Australia. *Sedimentary Geology* **219**, 24-43.

MOORE D. 1996. *Horsham 1:250 000 geophysical interpretation of basement geology*. Geological Survey of Victoria. Department of Natural Resources and Environment.

MORAND V. J., WOHLT K. E., CAYLEY R. A., TAYLOR D. H., KEMP A. I. S., SIMONS B. A. & MAGART A. P. M. 2003. Glenelg Special Map Area Geological Report. *Geological Survey of Victoria Geological Survey of Victoria Report*.

MORRIS B. J. & HORN C. M. 1990. Review of Gold Mineralisation in the Nackara Arc. *Mines and Energy Review* **157**, 51-58.

MORRIS R. C. & RAMANAIDOU E. R. 2007. Genesis of the channel iron deposits (CID) of the Pilbara region, Western Australia. *Australian Journal of Earth Sciences* **54**, 733-756.

MORTON A. C. & HALLSWORTH C. R. 1999. Processes controlling the composition of heavy mineral assemblages in sandstones. *Sedimentary Geology* **124**, 3-29.

MURAD E. & FISCHER W. R. 1988. The geobiochemical cycle of iron. *In:* Stucki J. W., Goodman B. A. & Schwertmann U. eds., *Iron in Soils and Clay Minerals*, pp 1-18, D. Reidel Publishing Company, Dordrecht.

NOBLE R. 2012. Transported cover in northwestern Victoria, Australia—An impediment to geochemical exploration for gold. *Journal of Geochemical Exploration* **112**, 139-151.

NOBLE R. R. P. 2007. Distribution of arsenic in regolith above buried mineralisation: implications for exploratin and environmental management. PhD thesis, Curtin University of Technology (unpubl.).

NORDSTROM D. K. 2011. Hydrogeochemical processes governing the origin, transport and fate of major and trace elements from mine wastes and mineralized rock to surface waters. *Applied Geochemistry* **26**, 1777-1791.

ODINS J., WILLIAMS R., O'NEILL D. & LAWSON S. 1991. Pre-tertiary basement structure of the central Murray Basin, and its effect on groundwater flow patterns. *Exploration Geophysics* **22**, 285-290.

OLLIER C., CHAN R., CRAIG M. & GIBSON D. 1988. Aspects of landscape history and regolith in the Kalgoorlie region, Western Australia. *BMR Journal of Australian Geology and Geophysics* **10**, 309-321.

OLSHINA A. & VAN KANN M. 2012. Heavy mineral sands in the Murray Basin of Victoria. *Geological Survery of Victoria Geological Survey of Victoria Technical Record*.

PAGE R., CONOR C., STEVENS B., GIBSON G., PREISS W. & SOUTHGATE P. 2005. Correlation of Olary and Broken Hill Domains, Curnamona Province: Possible Relationship to Mount Isa and Other North Australian Pb-Zn-Ag-Bearing Successions. *Economic Geology* **100**, 663-676.

PAINE M. 2005. Sedimentology of the Bondi Main heavy mineral beach placer deposit, Murray Basin, southeastern Australia. *Sedimentary Geology* **174**, 177-195.

PAINE M. D. 2004. Distribution, Character, and Provenance of Late Miocene to Pliocene Stranded Coastal Sediments in Southwestern Victoria. PhD thesis, Department of Applied Geology, Curtin University of Technology, Perth, Australia (unpubl.).

PAINE M. D., ANAND R. R., ASPANDIAR M., FITZPATRICK R. R. & VERRALL M. R. 2005. Quantitative heavy-mineral analysis of a Pliocene beach placer deposit in southeastern Australia using the AutoGeoSEM. *Journal of Sedimentary Research* **75**, 742-759.

PAINE M. D., BENNETTS D. A., WEBB J. A. & MORAND V. J. 2004. Nature and extent of Pliocene strandlines in southwestern Victoria and their application to Late Neogene tectonics. *Australian Journal of Earth Sciences* **51**, 407-422.

PATON C., HELLSTROM J., PAUL B., WOODHEAD J. & HERGT J. 2011. Iolite: Freeware for the visualisation and processing of mass spectrometric data. *Journal of Analytical Atomic Spectrometry* **26**, 2508-2518.

PETRIDES B., CARTWRIGHT I. & WEAVER T. 2006. The evolution of groundwater in the Tyrrell catchment, south-central Murray Basin, Victoria, Australia. *Hydrogeology Journal* **14**, 1522-1543.

PHILLIPS D., HUGHES M. J., ARNE D. C., BIERLEIN F. P., CAREY S., JACKSON P. & WILLMAN C. E. 2003. Gold - Historic weatlh, future potential. *In:* Birch W. D. ed., *Geology of Victoria*, Vol. Special Publication 23, pp 377-434, Geological Society of Australia.

PONTUAL S., MERRY N. & GAMSON P. 2010. *GMEX Guides for Mineral Exploration: Spectral Interpretation Field Manual* (Vol. 1). AusSpec International.

POWNCEBY M. 2005. Compositional and textural variation in detrital chrome-spinels from the Murray Basin, southeastern Australia. *Mineralogical Magazine* **69**, 191-204.

POWNCEBY M. 2010. Alteration and associated impurity element enrichment in detrital ilmenites from the Murray Basin, southeast Australia: a product of multistage alteration. *Australian Journal of Earth Sciences* **57**, 243-258.

PREISS W. 2000. The Adelaide Geosyncline of South Australia and its significance in Neoproterozoic continental reconstruction. *Precambrian Research* **100**, 21-63.

PREISS W. V. 1982. Supergroup classification in the Adelaide Geosyncline. *Trans. R. Soc. South Aust* **106**, 81-83.

PREISS W. V. 1993. Neoproterozoic. *In:* Drexel J., Preiss W. V. & Parker A. eds., *The Geology of South Australia 1*, Vol. 54, pp 170-204, Bulletin of the Geological Survey of South Australia, Adelaide.

PREISS W. V. 2006. Tectonic Overview of the Curnamona Province BHEI Conference, Broken Hill (unpubl.).

PUFAHL P. K., JAMES N. P., BONE Y. & LUKASIK J. J. 2004. Pliocene sedimentation in a shallow, cool-water, estuarine gulf, Murray Basin, South Australia. *Sedimentology* **51**, 997-1027.

RADKE L. & HOWARD K. 2007. Influence of groundwater on the evaporative evolution of saline lakes in the Wimmera of south-eastern Australia. *Hydrobiologia* **591**, 185-205.

RAMSAY W. R. H., BIERLEIN F. P., ARNE D. C. & VANDENBERG A. H. M. 1998. Turbidite-hosted gold deposits of Central Victoria, Australia: their regional setting, mineralising styles, and some genetic constraints. *Ore Geology Reviews* **13**, 131-151.

REED S. J. B. 2005. *Electron microprobe analysis and scanning electron microscopy in geology* (Vol. 158). Cambridge University Press Cambridge.

RITTENHOUSE G. 1943. Transportation and deposition of heavy mineral. *Geological Society of America Bulletin* **54**, 1725-1780.

ROBSON T. C. & WEBB J. A. 2011. Late Neogene tectonics in northwestern Victoria: Evidence from the Late Miocene-Pliocene Loxton Sand. *Australian Journal of Earth Sciences* **58**, 579-586.

ROGERS P., LINDSAY J., ALLEY N., BARNETT S., LABLACK K. & KWITKO G. 1995. Murray Basin. *The Geology of South Australia, The Phanerozoic* **2**, 157-163.

ROY P. S. 1999. Heavy Mineral Beach Placers in Southeastern Australia: Their Nature and Genesis. *Economic Geology* **94**, 567-588.

ROY P. S. 2003. Changing Pliocene Sea Levels and the Formation of Heavy Minerals Beach Placers in the Murray Basin, Southeastern Australia. *Economic Geology* **98**, 975-983.

ROY P. S., WHITEHOUSE J., COWELL P. J. & OAKES G. 2000. Mineral Sands Occurrences in the Murray Basin, Southeastern Australia. *Economic Geology* **95**, 1107-1128.

RUBEY W. W. 1933. Settling velocity of gravel, sand, and silt particles. *American Journal of Science*, 325-338.

RUDNICK R. L. & GAO S. 2014. Composition of the Continental Crust. *In:* Holland H. & Turekian K. eds., *Treatise on Geochemistry* (Second edition), Elsevier, Netherlands.

SANDIFORD M. 2003. Neotectonics of southeastern Australia: linking the Quaternary faulting record with seismicity and in situ stress. *Geological Society of America Special Papers* **372**, 107-119.

SANDIFORD M., WALLACE M. & COBLENTZ D. 2004. Origin of the in situ stress field in south-eastern Australia. *Basin Research* **16**, 325-338.

SCHOFIELD A., CAYLEY R., BARTON T., TAYLOR D., NICOLL M. & CAIRNS C. 2015. Regional geology and mineral systems of the Stavely region, western Victoria: Data release 1 - Stratigraphic drilling field data. *Geoscience Australia.*

SCHULZ M. S., VIVIT D., SCHULZ C., FITZPATRICK J. & WHITE A. 2010. Biologic origin of iron nodules in a marine terrace chronosequence, Santa Cruz, California. *Soil Science Society of America Journal* **74**, 550-564.

SCHWERTMANN U. 1988. Occurrence and formation of iron oxides in various pedoenvironments. *In, Iron in soils and clay minerals*, pp 267-308, Springer.

SCHWERTMANN U. & TAYLOR R. 1989. Iron oxides *In:* Dixon J. B. & Weed S. B. eds., *Minerals in Soil Environments*, pp 379-438, Soil Science Society of America, Madison, Wisconsin, USA.

SEYMON A. 2006. Nickel prospectivity in Victoria. *GeoScience Victoria Technical Record* **2006/3**, 76 pp.

SEYMON A., RAETZ M. & LYNCH H. 2009. Copper, gold and nickel discovery opportunities in and around the Dimboola Arc Domain. *GeoScience Victoria Technical Record* **2009/1**, 36 pp.

SHAW S. & FLOOD R. 1981. The New England Batholith, eastern Australia: geochemical variations in time and space. *Journal of Geophysical Research: Solid Earth (1978–2012)* **86**, 10530-10544.

SIKALIDIS C., ALEXIADES C. & MISAELIDES P. 1989. Adsorption of uranium and thorium from aqueous solutions by the clay minerals montmorillonite and vermiculite. *Toxicological & Environmental Chemistry* **20**, 175-180.

SINGH B. & GILKES R. 1992. Properties and distribution of iron oxides and their association with minor elements in the soils of south-western Australia. *Journal of Soil Science* **43**, 77-98.

SINGH B. & GILKES R. 1996. Nature and properties of iron rich glaebules and mottles from some south-west Australian soils. *Geoderma* **71**, 95-120.

SIRCOMBE K. 1999. Tracing provenance through isotope ages of littoral and sedimentary detrital zircon, eastern Australia. *Sedimentary Geology* **124**, 47-67.

SIRCOMBE K. N. 2004. AgeDisplay: an EXCEL workbook to evaluate and display univariate geochronological data using binned frequency histograms and probability density distributions. *Computers & Geosciences* **30**, 21-31.

SMART J. & SENIOR B. R. 1980. The Jurassic-Cretaceous basins of northeastern Australia. *In:* Henderson R. A. & Stephenson P. J. eds., *The Geology and Geophysics of Northeastern Australia*, pp 315-328, Geological Society of Australia, Queensland Division, Brisbane.

SMITH R. E., ANAND R. R. & ALLEY N. F. 2000. Use and implications of palaeoweathering surfaces in mineral exploration in Australia. *Ore Geology Reviews* **16**, 185-204.

SPRIGG R. C. 1952. *The geology of the south-east province, South Australia, with special reference to Quaternary coast-line migrations and modern beach developments*. Department of Mines, Adelaide.

STANLEY C. R. & LAWIE D. 2007. Average relative error in geochemical determinations: Clarification, calculation, and a plea for consistency. *Exploration and Mining Geology* **16**, 267-275.

STEPHENSON A. & BROWN C. 1989. The ancient Murray river system. *BMR Journal of Australian Geology and Geophysics* **11**, 387-395.

SWIFT D. J., DILL JR C. E. & MCHONE J. 1971. Hydraulic fractionation of heavy mineral suites on an unconsolidated retreating coast. *Journal of Sedimentary Research* **41**.

TANNER W. F. 1992. Late Holocene sea-level changes from grain-size data: evidence from the Gulf of Mexico. *The Holocene* **2**, 249-254.

TANNER W. F. 1993. An 8000-year record of sea-level change from grain-size parameters: data from beach ridges in Denmark. *The Holocene* **3**, 220-231.

TARDY Y. & NAHON D. 1985. Geochemistry of laterites, stability of Al-goethite, Al-hematite, and Fe^{3+}-kaolinite in bauxites and ferricretes: an approach to the mechanism of concretion formation. *American Journal of Science* **285**, 865-903.

THIRY M. & MILNES A. R. 1991. Pedogenic and groundwater silcretes at Stuart Creek opal field, South Australia. *Journal of Sedimentary Petrology* **61**, 111-127.

THORNE R., ANAND R. & SUVOROVA A. 2014. The formation of fluvio-lacustrine ferruginous pisoliths in the extensive palaeochannels of the Yilgarn Craton, Western Australia. *Sedimentary Geology* **313**, 32-44.

TWIDALE C. & BOURNE J. 1998. The use of duricrusts and topographic relationships in geomorphological correlation: conclusions based in Australian experience. *Catena* **33**, 105-122.

TWIDALE C. R., LINDSAY J. M. & BOURNE J. A. 1978. Murray Valley Gorge in South Australia: age and origin. *Royal Society of Victoria, Proceedings* **90**, 27-42.

TYLER N. & AMBROSE W. A. 1986. Facies architecture and production characteristics of strand-plain reservoirs in North Markham-North Bay City field, Frio Formation, Texas. *AAPG Bulletin* **70**, 809-829.

VAN BREEMEN N. V. 1982. Genesis, morphology, and classification of acid sulfate soils in coastal plains. *Acid Sulfate Weathering*, 95-108.

VANDENBERG A. H. M. 2010. Paleogene basalts prove early uplift of Victoria's Eastern Uplands. *Australian Journal of Earth Sciences* **57**, 291-315.

VANDENBERG A. H. M., WILLMAN C. E., MAHER S., SIMONS B. A., CAYLEY R. A., TAYLOR D. H., MORAND V. J., MOORE D. H. & RADOJKOVIC A. 2000. The Tasman Fold Belt System in Victoria. *Geological Survey of Victoria Special Publication*.

VEEVERS J. 2015. Beach sand of SE Australia traced by zircon ages through Ordovician turbidites and S-type granites of the Lachlan Orogen to Africa/Antarctica: a review. *Australian Journal of Earth Sciences* **62**, 385-408.

VEEVERS J., BELOUSOVA E., SAEED A., SIRCOMBE K., COOPER A. & READ S. 2006. Pan-Gondwanaland detrital zircons from Australia analysed for Hf-isotopes and trace elements

reflect an ice-covered Antarctic provenance of 700–500 Ma age, T_{DM} of 2.0–1.0 Ga, and alkaline affinity. *Earth-Science Reviews* **76**, 135-174.

VEEVERS J. J. 1984. *Phanerozoic earth history of Australia*. Oxford University Press, USA.

WALLACE L., WELCH S., KIRSTE D., BEAVIS S. & MCPHAIL D. 2005. Characteristics of inland acid sulfate soils of the Lower Murray floodplains, South Australia. *Regolith*, pp. 326-328.

WALLIS T., VACHER H. L. & STEWART M. T. 1991. Hydrogeology of freshwater lens beneath a Holocene strandplain, Great Exuma, Bahamas. *Journal of hydrology* **125**, 93-109.

WHITEHOUSE J. 2009. Mineral Systems of the Murray Basin, New South Wales. *Geological Survey of New South Wales Department of Primary Industries*.

WILKIN R., BARNES H. & BRANTLEY S. 1996. The size distribution of framboidal pyrite in modern sediments: an indicator of redox conditions. *Geochimica et Cosmochimica Acta* **60**, 3897-3912.

WILLIAMS I., GOODGE J. W., MYROW P., BURKE K. & KRAUS J. 2002. Large-scale sediment dispersal associated with the late Neoproterozoic assembly of Gondwana. *Geological Society of Australia Abstracts*, pp. 238-238. Geological Society of Australia; 1999.

WOODHEAD J. D., HELLSTROM J., HERGT J. M., GREIG A. & MAAS R. 2007. Isotopic and elemental imaging of geological materials by laser ablation inductively coupled plasma-mass spectrometry. *Geostandards and Geoanalytical Research* **31**, 331-343.

WOOLLEY D. 1978. Cainozoic sedimentation in the Murray drainage basin. *New South Wales section. Proceedings of the Royal Society of Victoria* **90**, 61-65.

Appendices

Appendix A – Stratigraphic logs and sample locations

Location of geochemical profiles and regional samples:

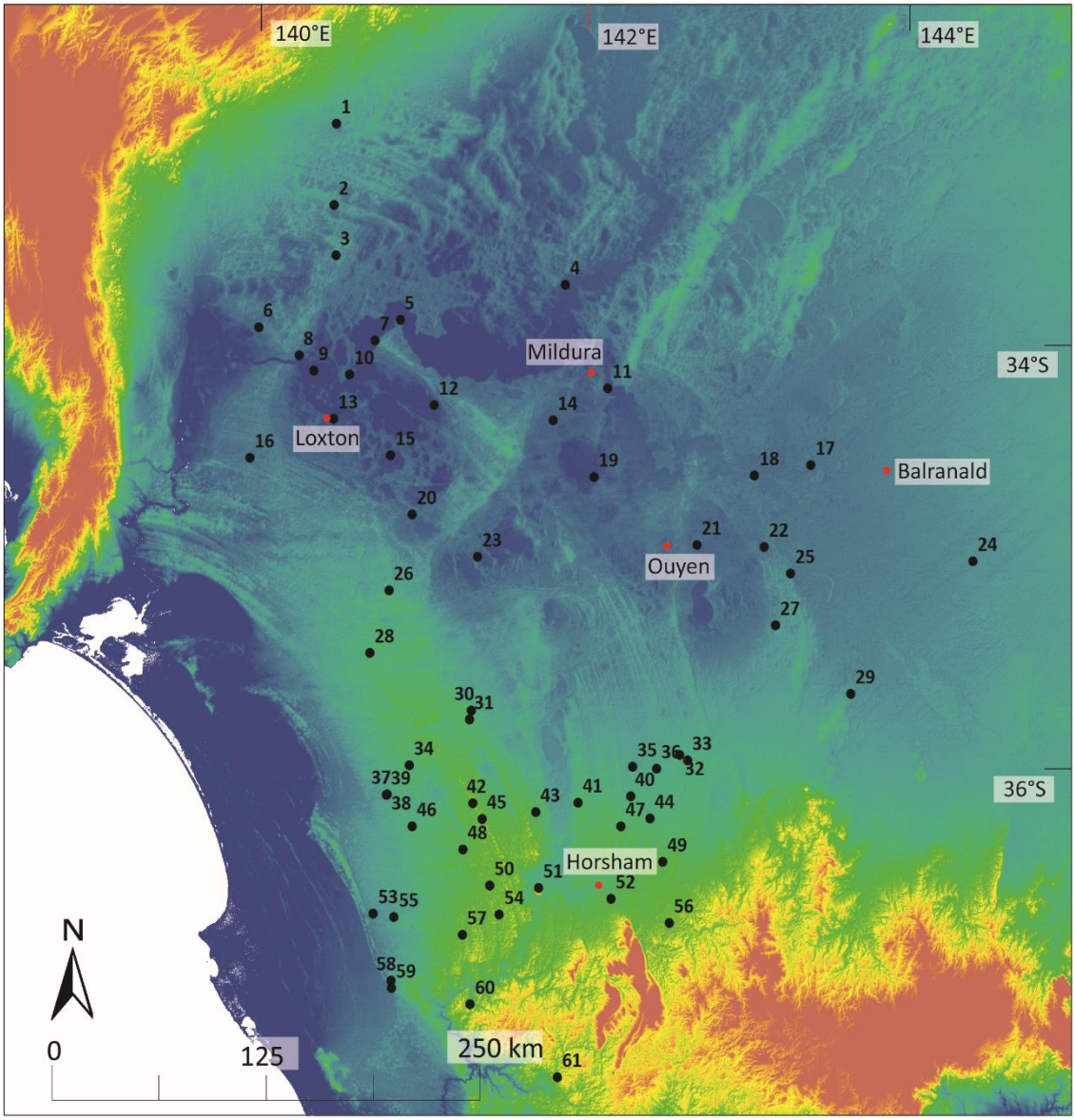

Table 1: Location of geochemical and stratigraphic profiles

Location ID	Profile name	Sample prefix	Samples analysed	Easting (mE)	Northing (mN)
1	Oakvale 3	OAK	19	459922	6346778
2	PV-11	PV	8	458522	6302678
3	M-155	TEM	13	459558	6275618
4	Wentworth-1	WEN	19	589482	6259599
5	Chowilla	CCH	8	495921	6240732
6	M-12	FT	12	415884	6236859
7	Headings Cliff	HC	5	481747	6229730
8	Overland Corner	OLC	12	438788	6221631
9	Stony Ridge	SRQ	9	447078	6213558
10	Lyrup	LYR	15	467260	6211224
11	Red Cliffs	RC	14	613345	6203779
12	Morkalla-3	MOR	19	515120	6194777
13	Loxton	LCP	21	458337	6187445
14	Willah-1	WIL	24	582471	6186577
15	Nadda 1	NDA	4	490574	6167623
16	81MBR31	MBR	11	411013	6166318
17	Balranald-1	BAL	6	728323	6162405
18	Boundary Bend	BB	2	696431	6156869
19	Walpamunda-4	WAL	8	605621	6155927
20	Berrook-1	BER	9	502750	6135800
21	Manangatang-3	MAN	27	663921	6119377
22	Piangil West-2	PIA	12	701821	6118327
23	Koonda-3	KND	13	539521	6112977
24	Bundy-1	BUN	30	819906	6110400
25	Nyah	NY	9	716671	6103758
26	Pinnaroo-1	PIN	7	489513	6094769
27	Ultima	UQ	12	708327	6075854
28	M-138	NGA	39	478839	6061133

Table 1 (cont'd): Location of geochemical and stratigraphic profiles

Location ID	Profile name	Sample prefix	Samples analysed	Easting (mE)	Northing (mN)
29	Gredgwin Ridge	GRQ	10	750903	6039031
30	Wagon Flat North	WFN	4	536229	6029849
31	Wagon Flat	WF	4	535195	6025159
32	Spicers Pit	SP	10	654135	6006077
33	Watchem Pit	MP	2	658556	6002993
34	Telopea Downs	TDQ	5	501004	6000456
35	Henty Highway	HHQ	1	627324	5999664
36	Hewitt Pit	HP	3	641063	5998612
37	2/160	BT	12	488681	5984657
38	2/640	BT	21	488251	5984407
39	2/800	BT	11	488022	5984298
40	Warracknabeal	WRC	1	626367	5983706
41	VIMP-6	SWV	0	596621	5980177
42	Diapur	DIA	8	537057	5979858
43	Nhill Highway	NHW	3	572527	5975160
44	Sheep Hills	SH	3	637346	5971677
45	Kaniva	CW	1	542197	5971471
46	VIMP16	SWV	0	502571	5967452
47	VIMP-14	SWV	0	620661	5967317
48	Horsham-7	HOR7	81	531324	5954988
49	VIMP-5	SWV	0	644361	5948127
50	Goroke	GOR	8	546475	5935480
51	Mitre Rock	MR	2	574311	5934049
52	Green Lake	GL	1	615146	5928243

Table 1 (cont'd): Location of geochemical and stratigraphic profiles

Location ID	Profile name	Sample prefix	Samples analysed	Easting (mE)	Northing (mN)
53	RB-3	RB	4	480710	5920384
54	Horsham-5	HOR5	54	551993	5919759
55	RC86KI1	KI1	13	492425	5918403
56	VIMP-4	SWV	0	648141	5915137
57	Horsham-1	HOR1	20	531155	5908768
58	RC86KI10	KI10	5	490735	5884229
59	RC86KI11	KI11	0	490886	5880023
60	Chetwynd	CW	10	535523	5871387
61	Wannon	WA	11	584775	5832102
		Total samples:	**695 (inc. field duplicates and lithologies other than the Loxton-Parilla Sands)**		

1. Oakvale 3

Location: South Australia
Grid reference: 459922 mE, 6346778 mN

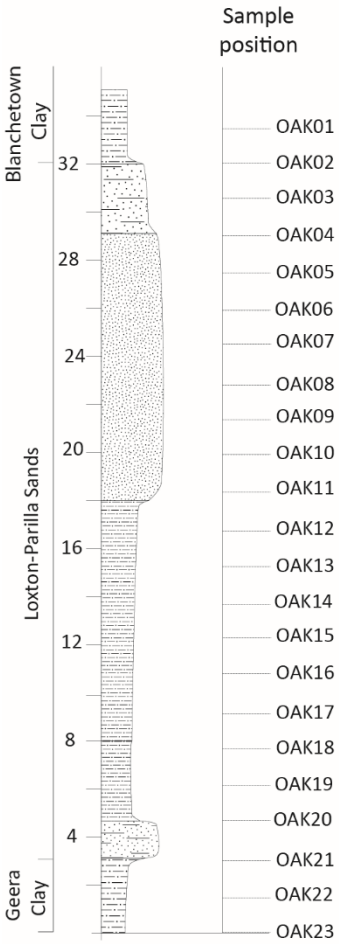

2. PV 11 (bore)

Location: South Australia
Grid reference: 458522 mE 6302678 mN

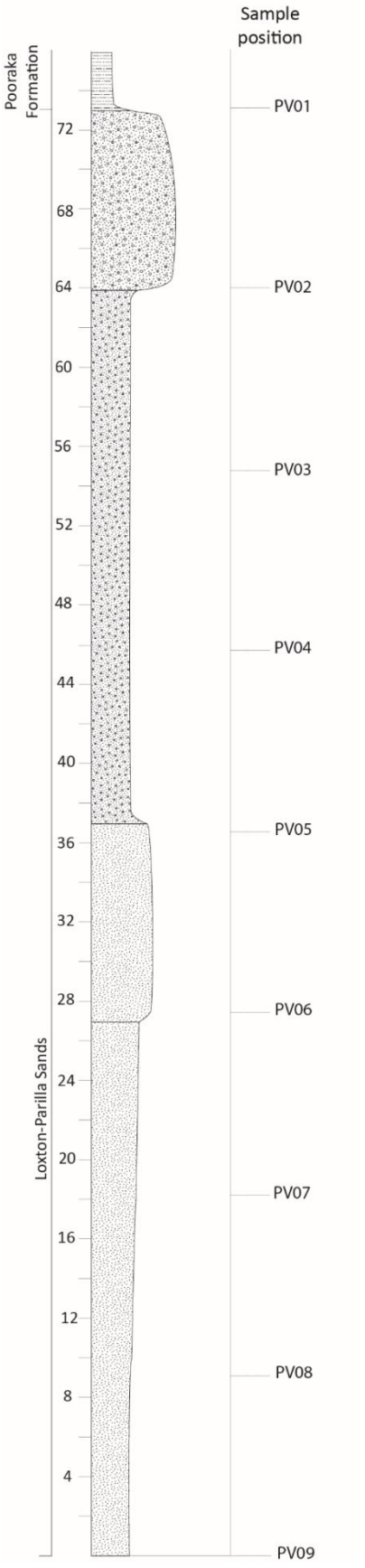

3. M155 (bore)

Location: South Australia
Grid reference: 459558 mE, 6275618 mN

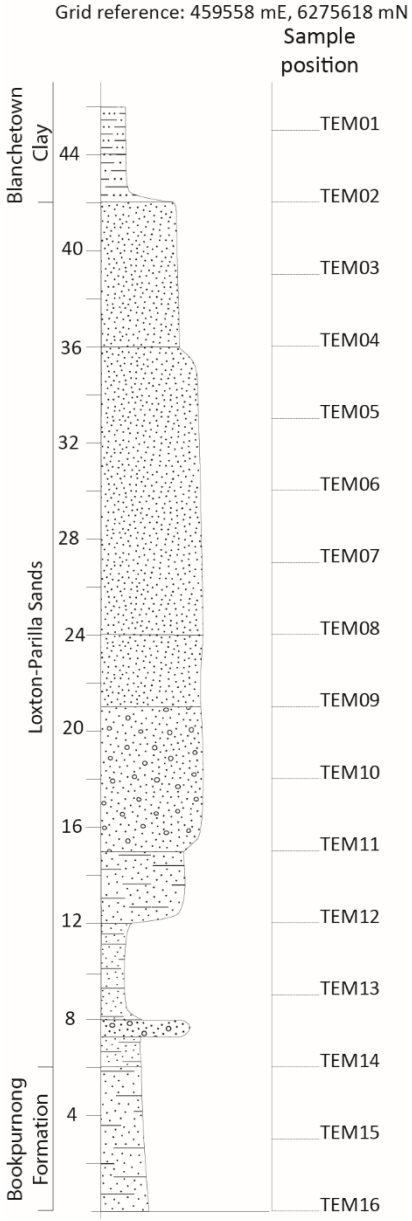

4. Wentworth-1

Location: Western Victoria
Grid reference: 589428 mE 6259599 mN

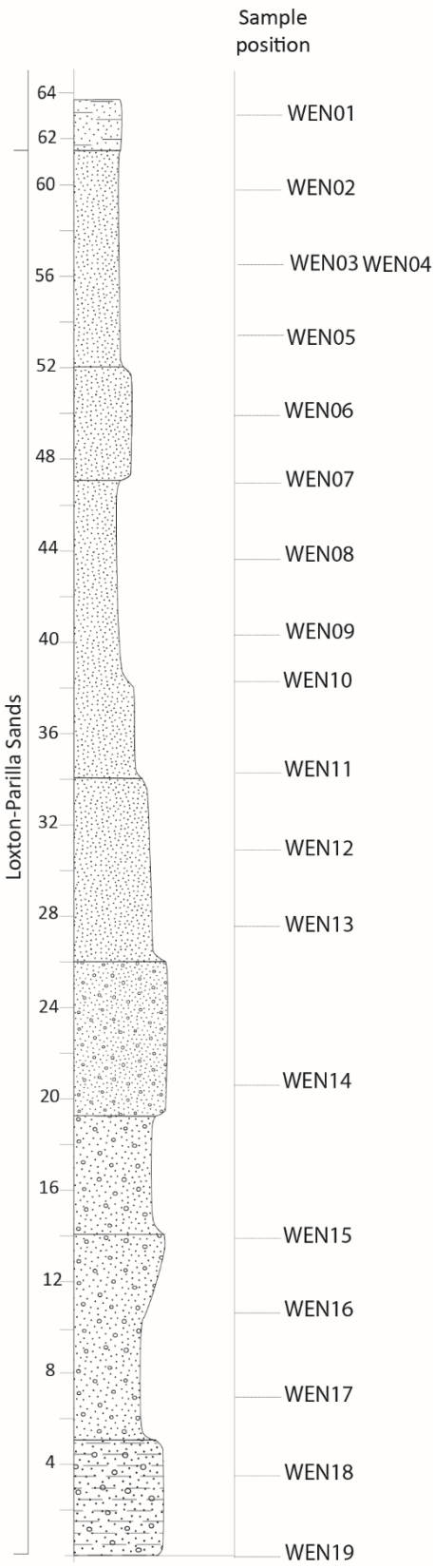

5. Chowilla

Location: Riverland (Chowilla Customs House), South Australia
Grid reference: 495921 E 6240732 N

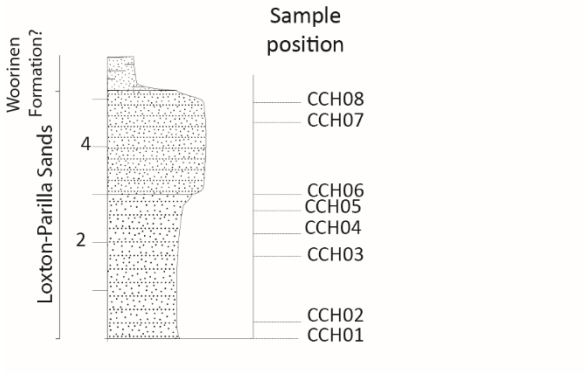

6. M12 (bore)

Location: South Australia
Grid reference: 415884 mE, 6236859 mN

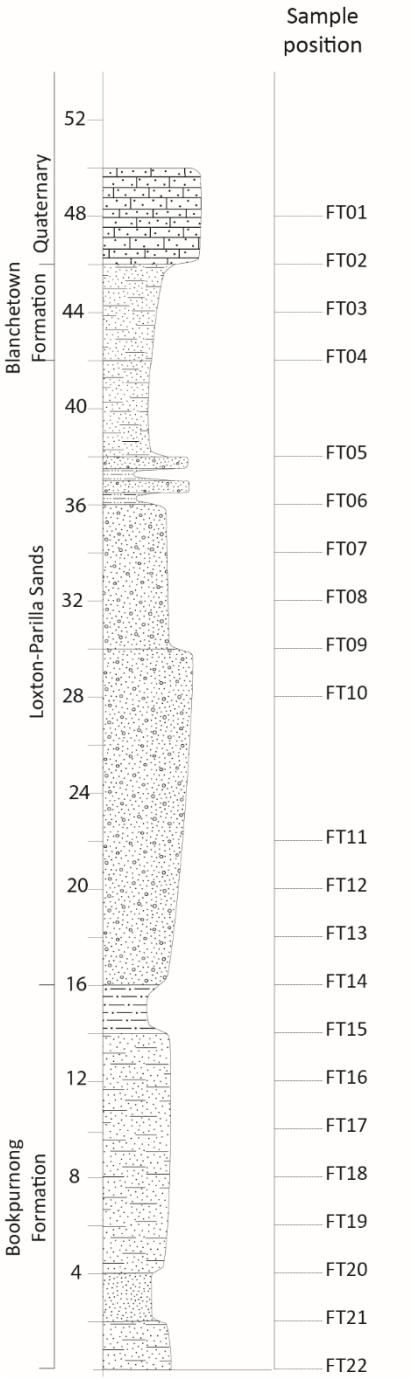

7. Heading's Cliff

Location: southeastern South Australia
Grid reference: 481747 mE 6229730 mN

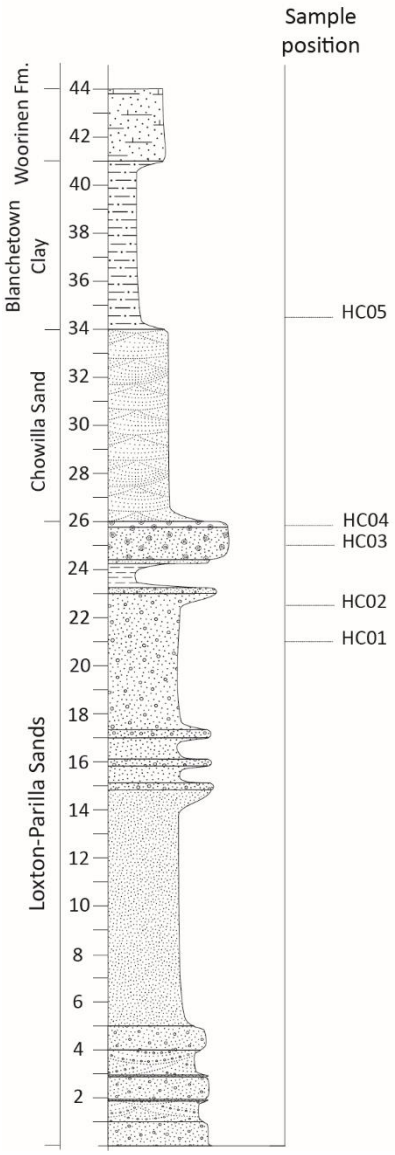

8. Overland Corner

Location: Riverland, South Australia
Grid reference: 439009 mE 6221087 mN

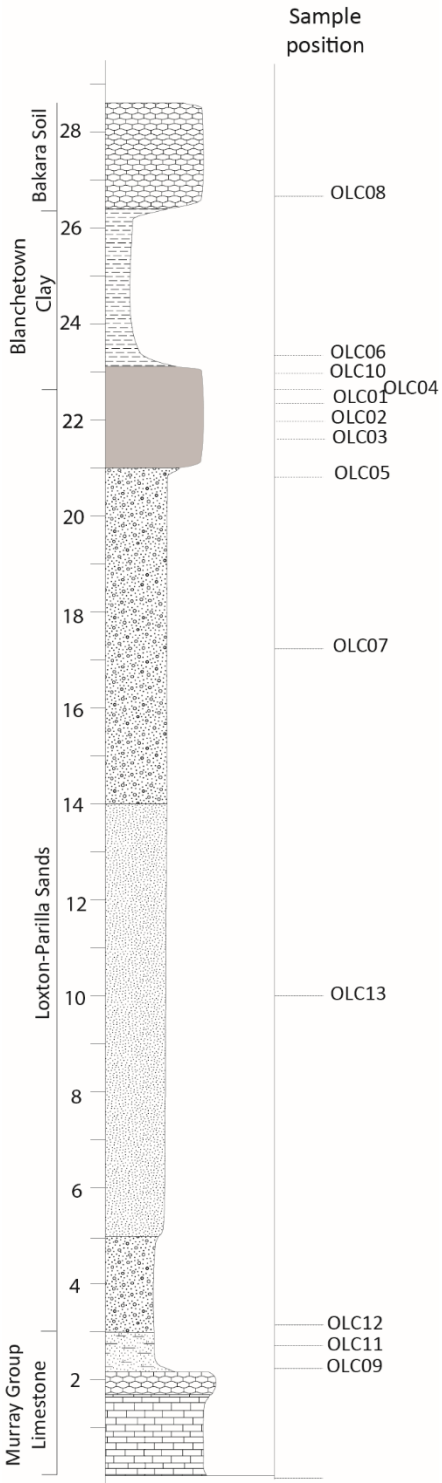

9. Stony Ridge Quarry

Location: Riverland, South Australia
Grid reference: 447078 E 6213558 N

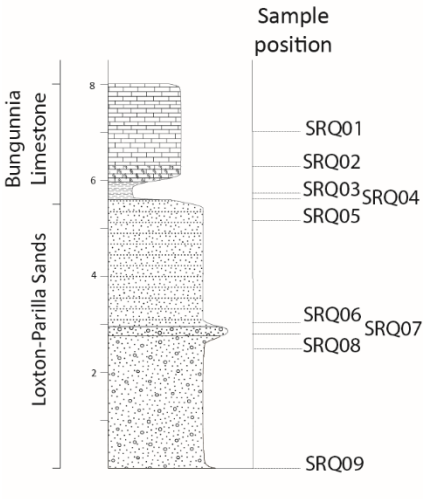

10. Lyrup

Location: Riverland, South Australia
Grid reference: 467260 E, 6211224 E

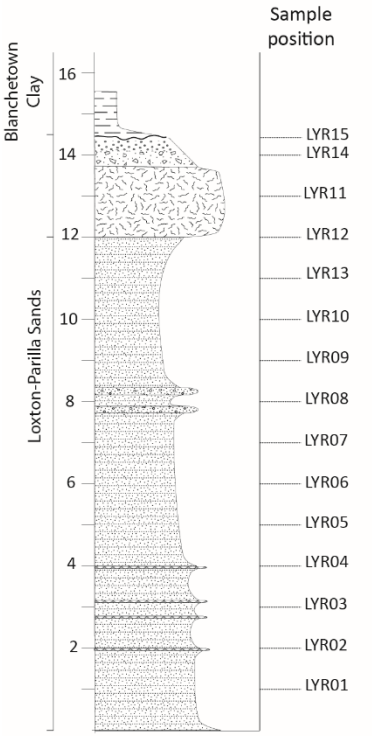

11. Red Cliffs

Location: Northwestern Victoria
Grid reference: 613345 E, 6203779 N

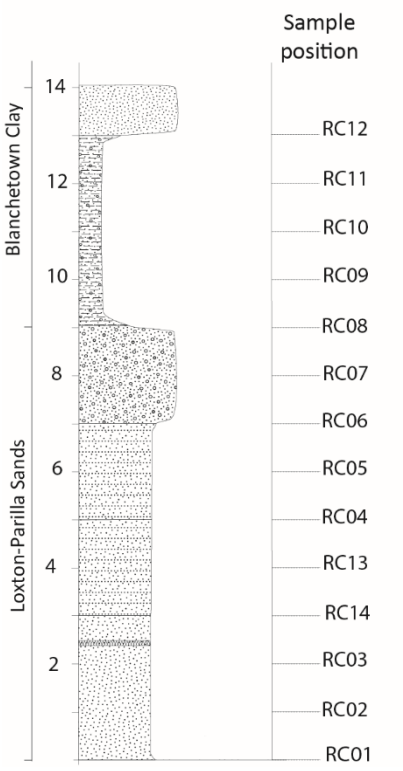

12. Morkalla-3 (bore)

Location: Western Victoria
Grid reference: 515120 mE 6194777 mN

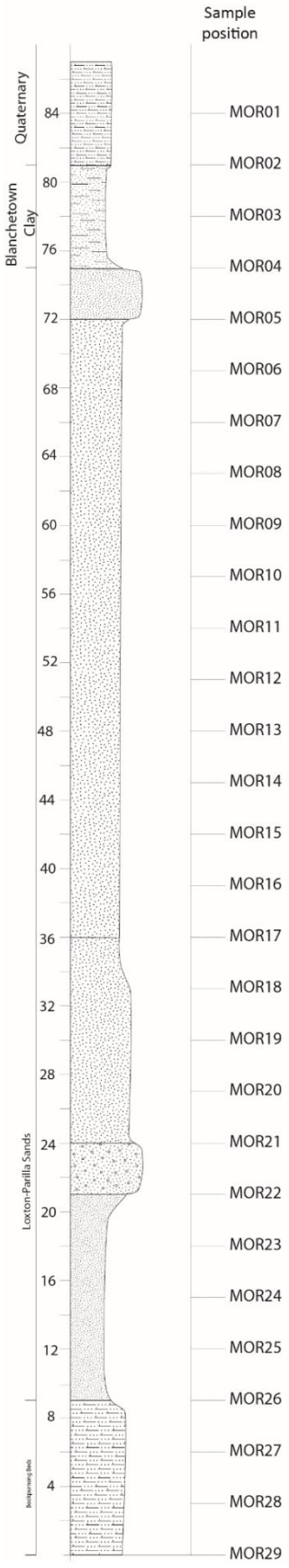

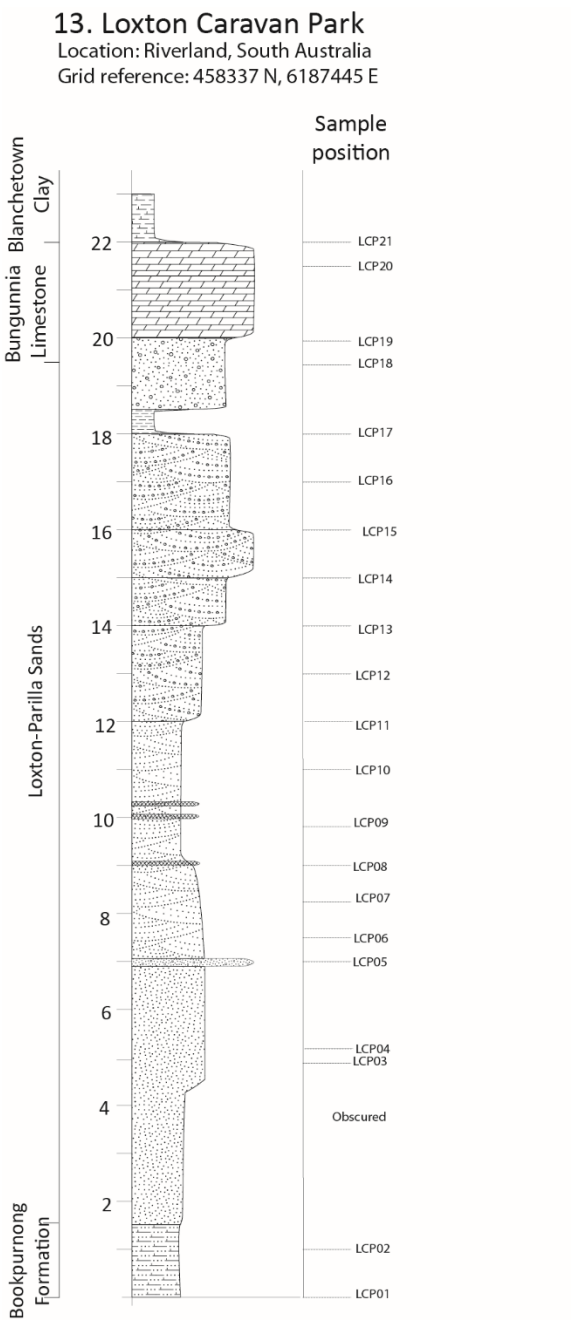
13. Loxton Caravan Park
Location: Riverland, South Australia
Grid reference: 458337 N, 6187445 E
Sample position
Blanchetown Clay
Bungunnia Limestone
Loxton-Parilla Sands
Bookpurnong Formation
22
20
18
16
14
12
10
8
6
4
2
LCP21
LCP20
LCP19
LCP18
LCP17
LCP16
LCP15
LCP14
LCP13
LCP12
LCP11
LCP10
LCP09
LCP08
LCP07
LCP06
LCP05
LCP04
LCP03
Obscured
LCP02
LCP01

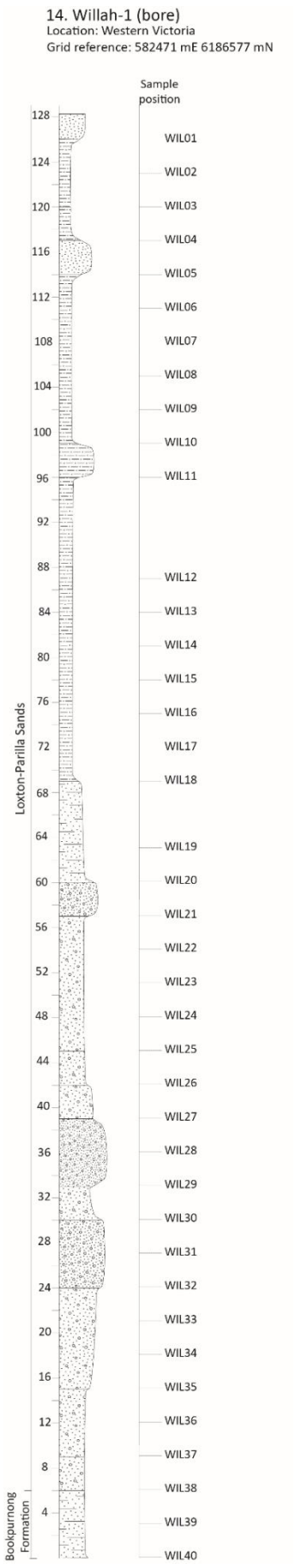
14. Willah-1 (bore)
Location: Western Victoria
Grid reference: 582471 mE 6186577 mN
Sample position
Loxton-Parilla Sands
Bookpurnong Formation
128
124
120
116
112
108
104
100
96
92
88
84
80
76
72
68
64
60
56
52
48
44
40
36
32
28
24
20
16
12
8
4
WIL01
WIL02
WIL03
WIL04
WIL05
WIL06
WIL07
WIL08
WIL09
WIL10
WIL11
WIL12
WIL13
WIL14
WIL15
WIL16
WIL17
WIL18
WIL19
WIL20
WIL21
WIL22
WIL23
WIL24
WIL25
WIL26
WIL27
WIL28
WIL29
WIL30
WIL31
WIL32
WIL33
WIL34
WIL35
WIL36
WIL37
WIL38
WIL39
WIL40

16. 81MBR31 (bore)

Location: South Australia
Grid reference: 411013 mE, 5984298 mN

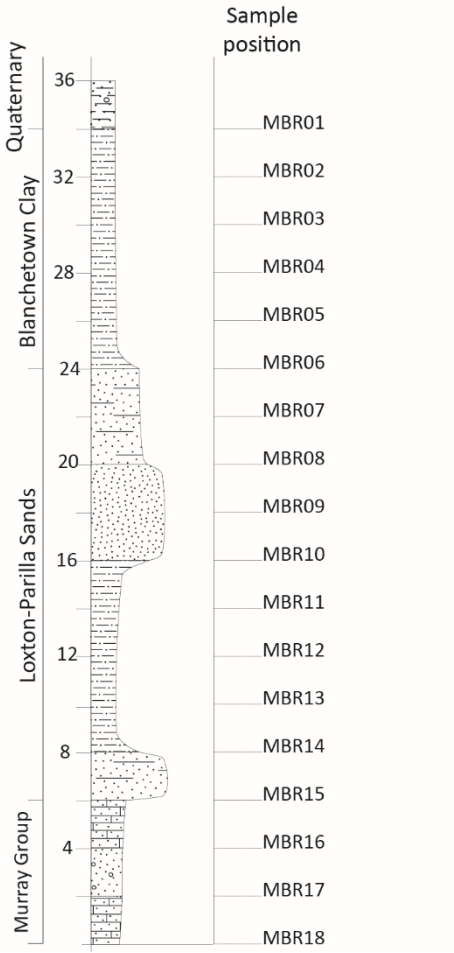

19. Walpamunda-4

Location: Western Victoria
Grid reference: 605621mE 6155927 mN

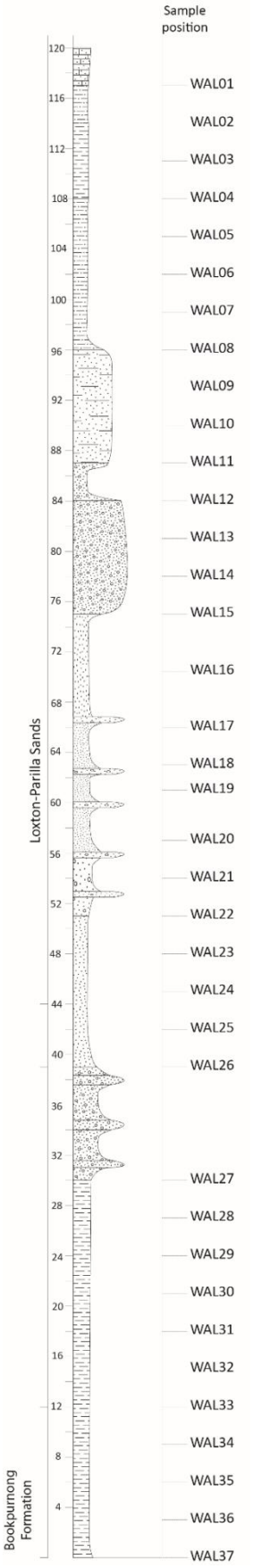

20. Berrook-1 (bore)

Location: Northern Victoria
Grid reference: 502750 mE 6135800 mN

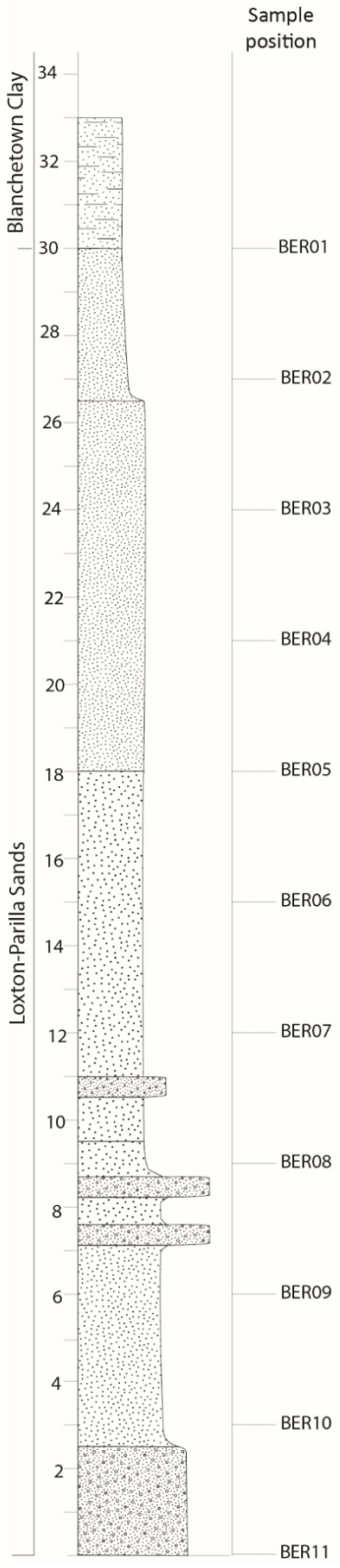

21. Manangatang-1 (bore)

Location: Riverland, South Australia
Grid reference: 480394 E 6229886 N

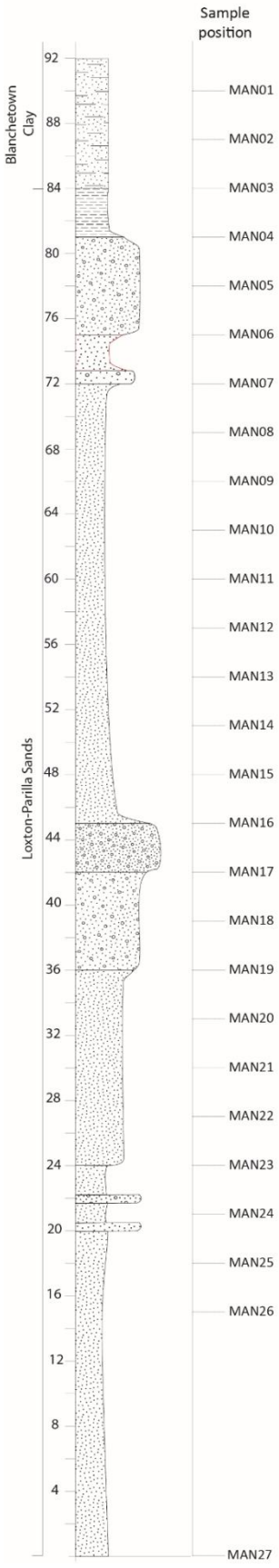

22. Piangil West-2 (bore)

Location: Western Victoria
Grid reference: 701821 mE 6118327 mN

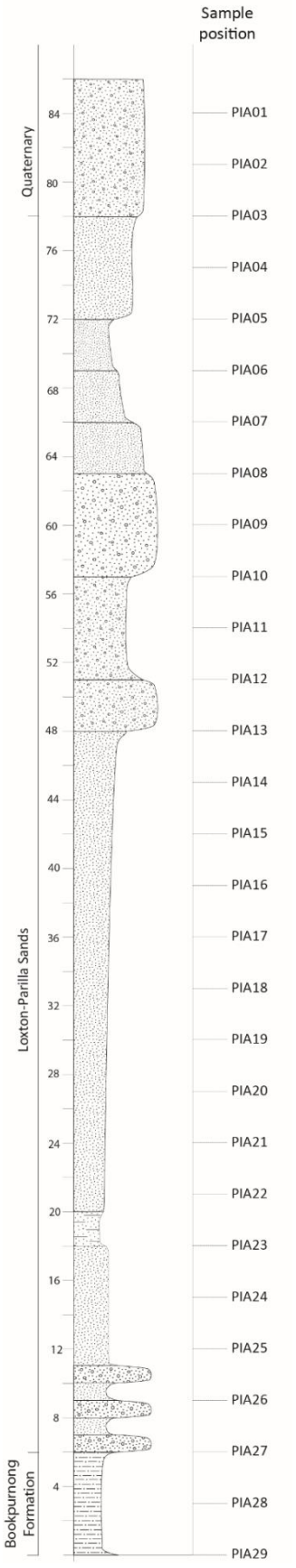

23. Koonda-1 (bore)

Location: Northern Victoria
Grid reference: 539521 mE 6112977 mN

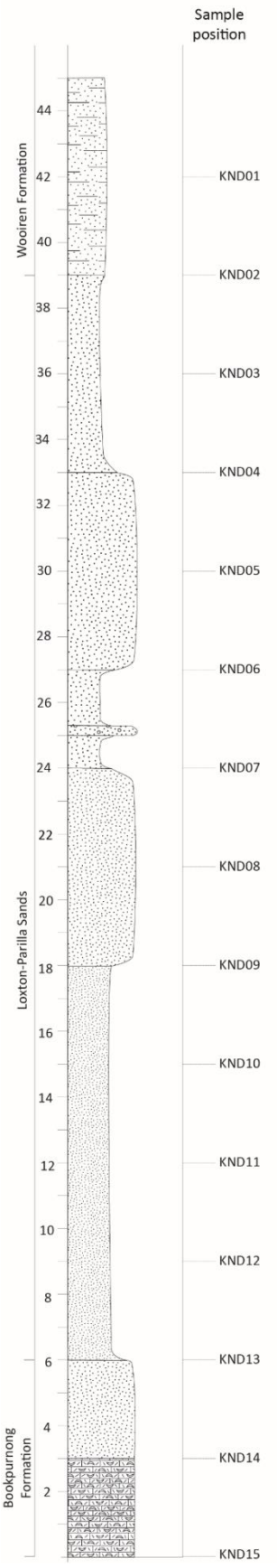

25. Nyah

Location: Victoria
Grid reference: 716671N, 6103758E

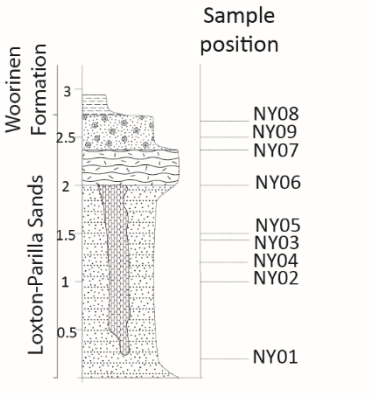

26. Pinnaroo-1 (bore)

Location: South Australia
Grid reference: 489513 mE, 6094769 mN

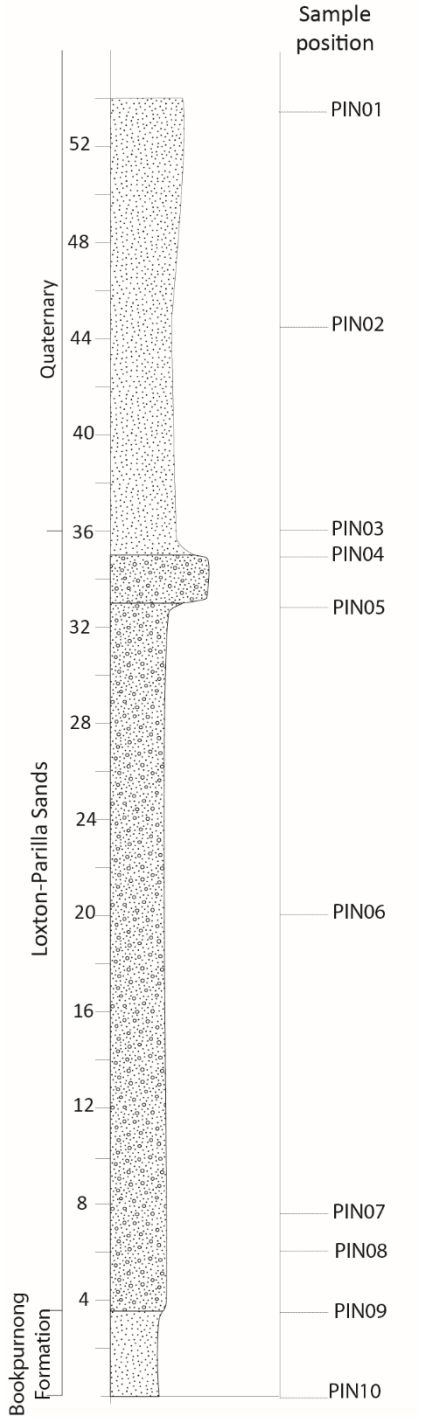

27. Ultima

Location: Western Victoria
Grid reference: 708327 E, 6075854 N

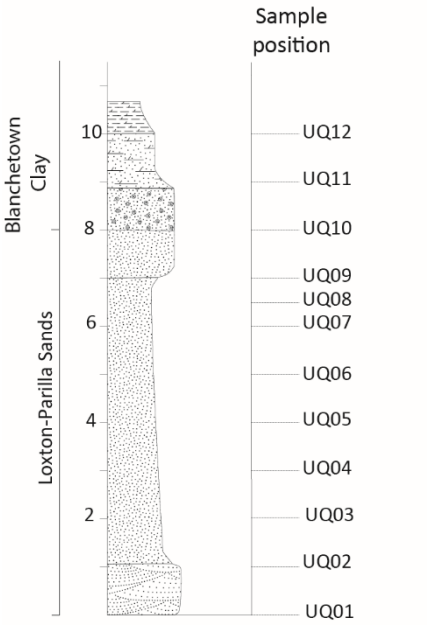

28. M138 (bore)

Location: South Australia
Grid reference: 478839 mE 6061133 mN

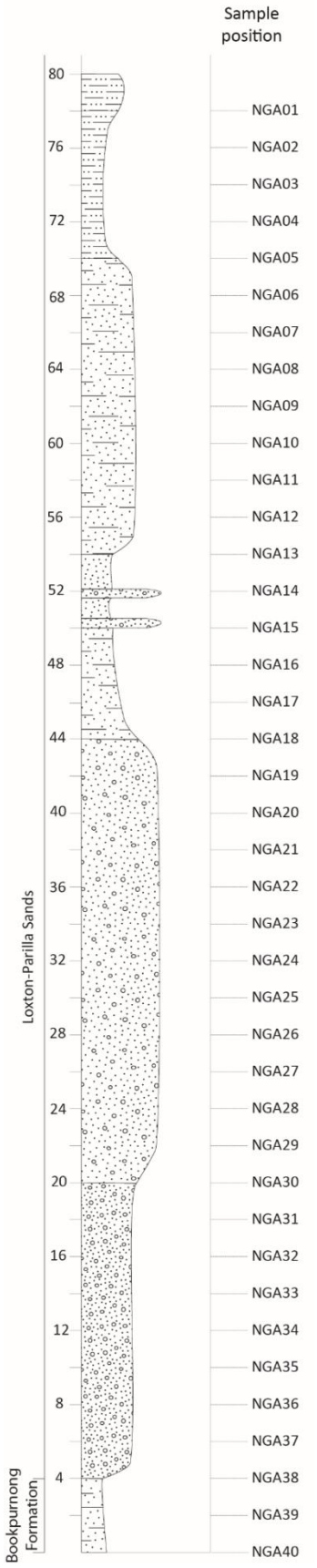

29. Gredgwin Ridge

Location: Central northern Victoria (Gredgwin Ridge Quarry)
Grid reference: 750903 E 603031 N

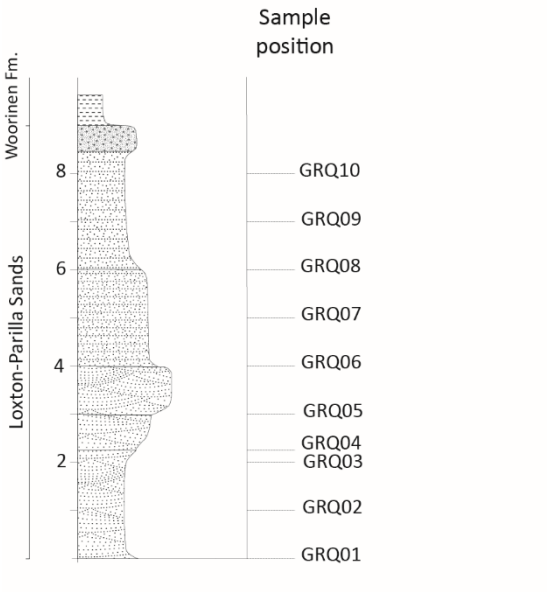

30. Wagon Flat North

Location: Western Victoria
Grid reference: 536229 E, 6029849 N

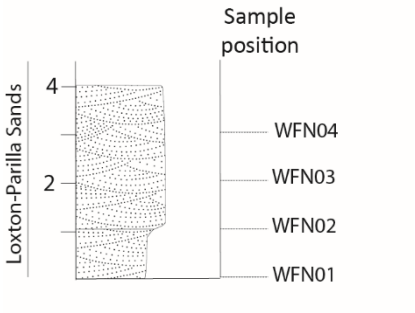

31. Wagon Flat

Location: Western Victoria

Grid reference: 535195 E, 6025159 N

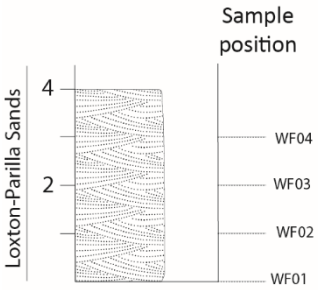

34. Telopea Downs

Location: Western Victoria

Grid reference: 501004 E, 6000456 N

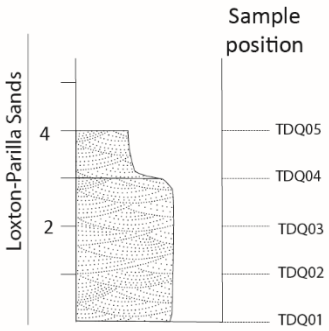

37. 2/160 (bore)

Location: southeastern South Australia
Grid reference: 488681 mE 5984657 mN

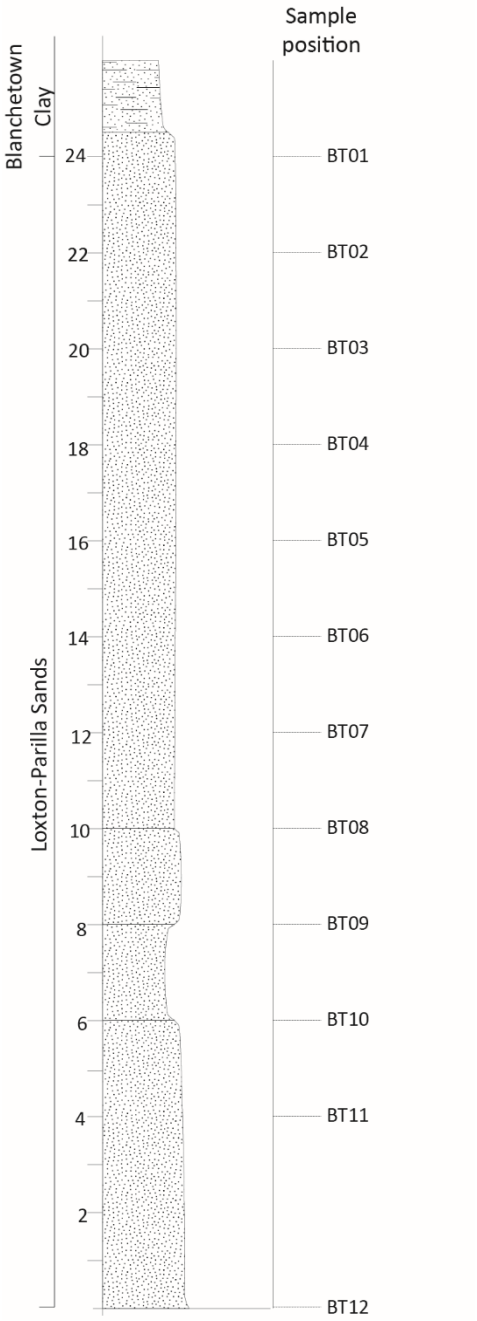

38. 2/640 (bore)

Location: Southeastern South Australia
Grid reference: 488251 mE, 5984407 mN

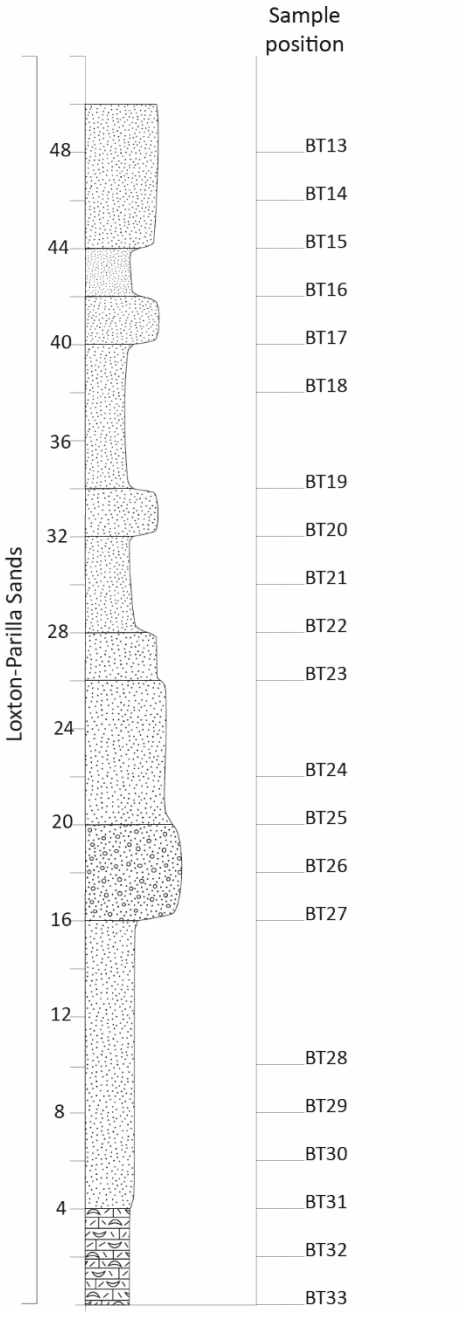

39. 2/880 (bore)

Location: southeastern South Australia
Grid reference: 488022 mE 59847298 mN

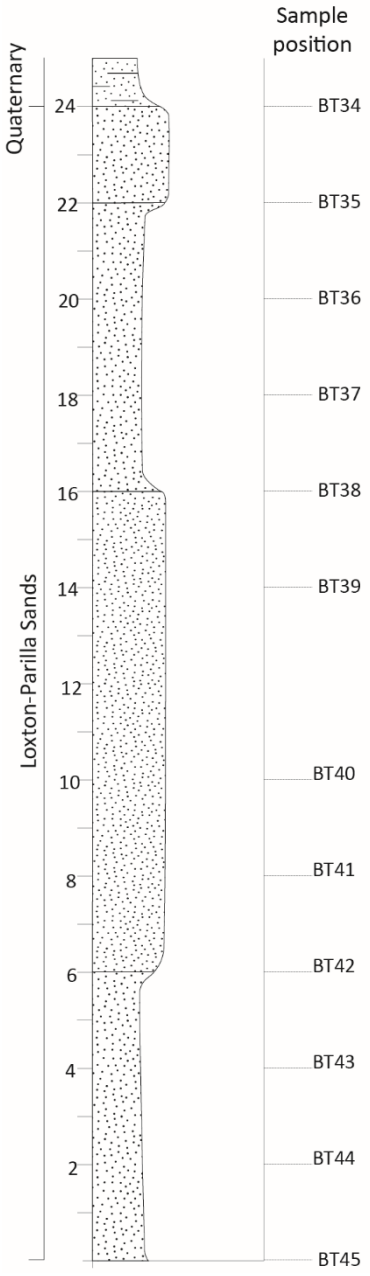

42. Diapur

Location: Southwestern Victoria
Grid reference: 537057 E, 5979858 N

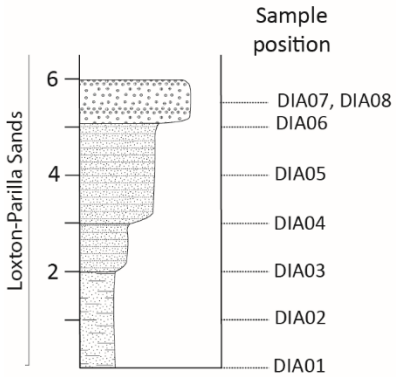

48. Horsham-7 (bore)

Location: Southwestern Victoria
Grid reference: 531391 mE, 5954988 mN

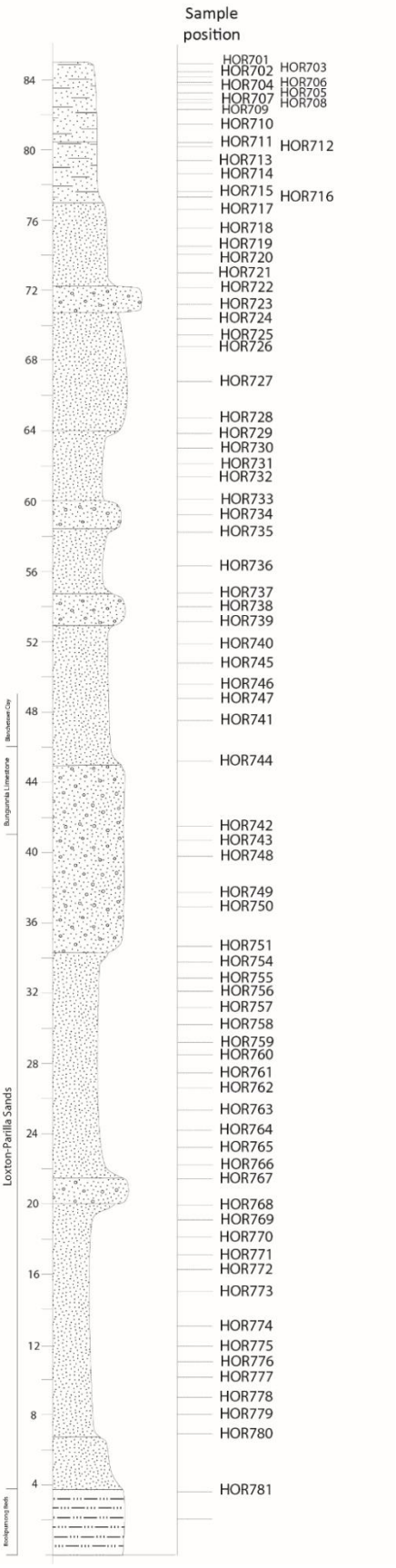

50. Goroke

Location: Western Victoria
Grid reference: 546475 E, 5935480 N

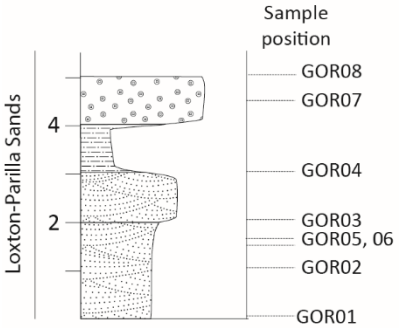

53. RB 3 (bore)

Location: southeastern South Australia
Grid reference: 480710 mE 5920384 mN

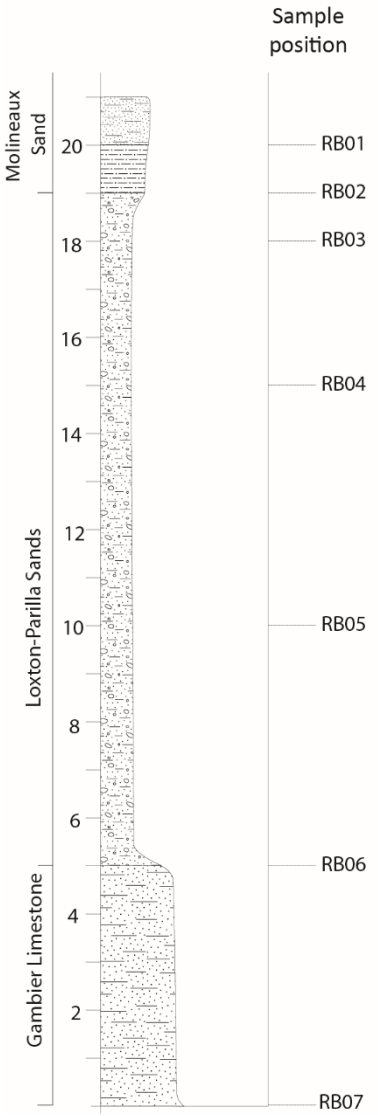

54. Horsham-5 (bore)

Location: Southwestern Victoria
Grid reference: 551993 mE, 5919759 mN

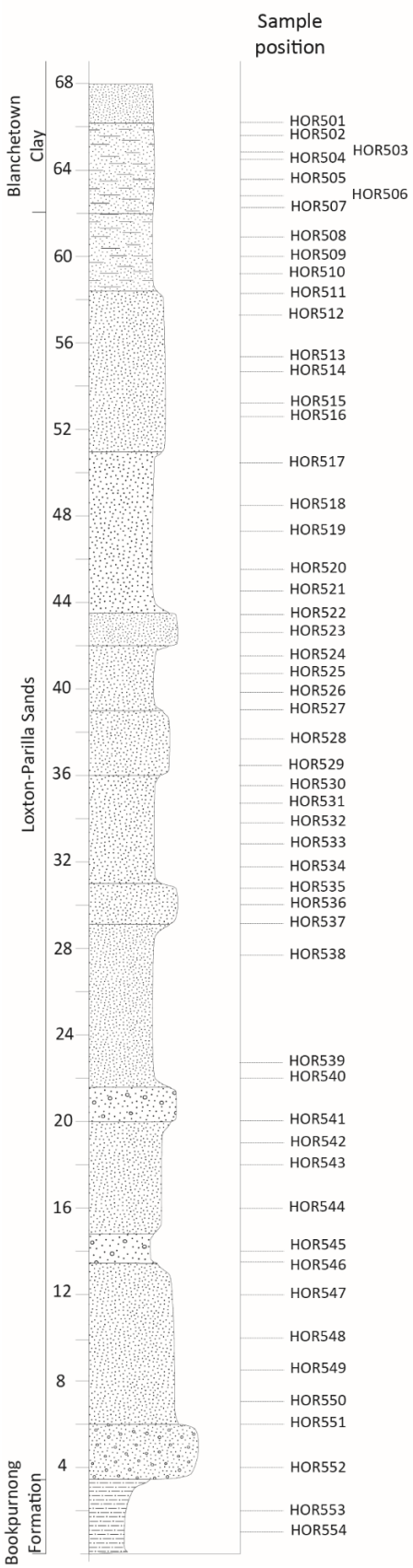

55. RC86KI_1 (bore)

Location: southeastern South Australia
Grid reference: 492425 mE 5918403 mN

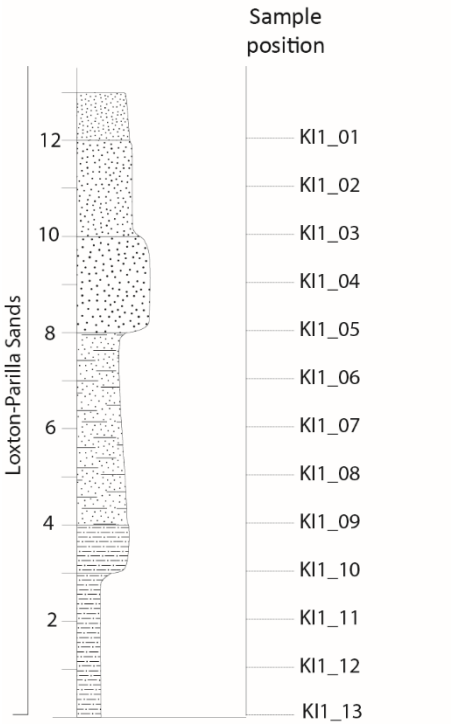

57. Horsham-1 (bore)

Location: Southwestern Victoria
Grid reference: 531352 mE, 5908768 mN

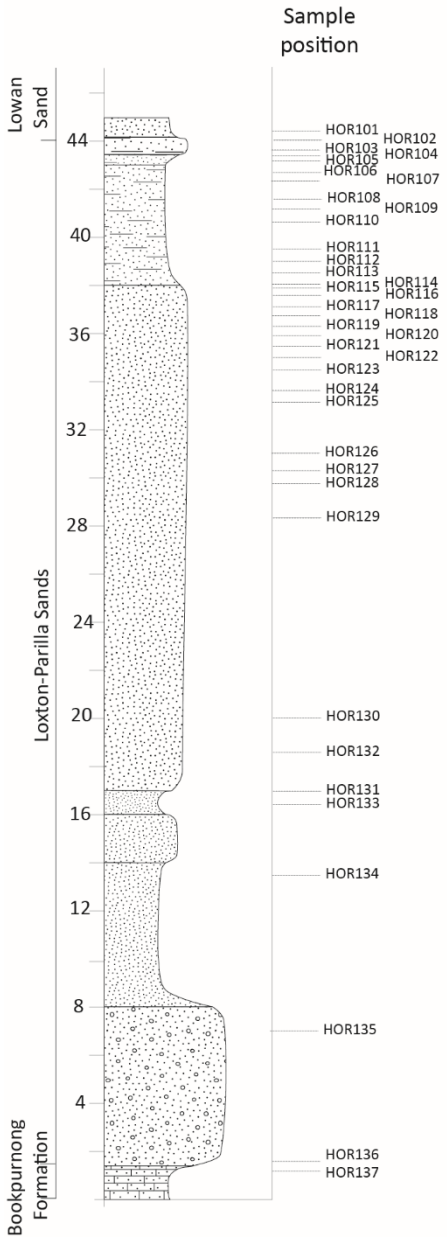

60. Chetwynd

Location: Southwest Victoria
Grid reference: 535523 mE 5871387 mN

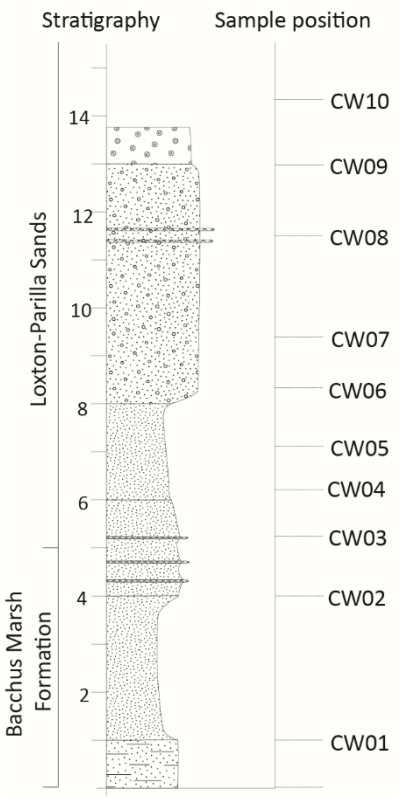

61. Wannon

Location: Southwestern Victoria (near Hamilton)
Grid reference: 584775 mE, 5832102 mN

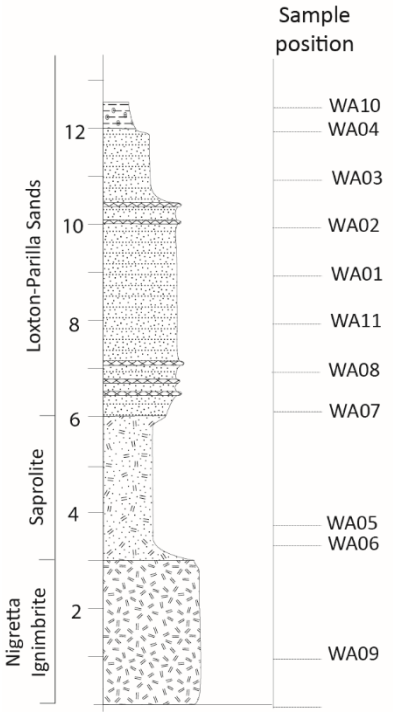

Appendix B – Whole rock geochemistry results

Sample ID	Profile	Ag (ppm)	Al_2O_3 (%)	As (ppm)	Au (ppb)	Ba (%)	Ba (ppm)	Be (ppm)	Bi (ppm)	CaO (%)	Cd (ppm)	Ce (ppm)	Co (ppm)
LYR01	Lyrup	<0.1	0.92	10.7	<0.5	<0.01	220	<1	<0.1	0.03	<0.1	14.2	2.9
LYR02	Lyrup	<0.1	0.94	5.8	0.6	<0.01	56	1	<0.1	0.03	<0.1	4.6	2.0
LYR03	Lyrup	<0.1	0.91	39.4	<0.5	<0.01	39	<1	<0.1	0.07	<0.1	6.0	0.5
LYR04	Lyrup	<0.1	0.72	10.6	0.6	<0.01	71	<1	<0.1	0.02	<0.1	4.9	1.2
LYR05	Lyrup	<0.1	1.69	26.6	<0.5	<0.01	65	<1	<0.1	0.04	<0.1	4.6	0.6
LYR06	Lyrup	<0.1	1.44	9.5	<0.5	<0.01	93	<1	<0.1	0.03	<0.1	7.1	1.3
LYR07	Lyrup	<0.1	1.59	10.8	0.6	<0.01	100	<1	<0.1	0.03	<0.1	6.8	1.3
LYR08	Lyrup	<0.1	1.33	14.5	0.8	<0.01	100	1	<0.1	0.03	<0.1	5.6	2.1
LYR09	Lyrup	<0.1	1.41	109.8	<0.5	<0.01	116	1	<0.1	0.05	<0.1	6.1	1.4
LYR10	Lyrup	<0.1	1.55	31.4	<0.5	<0.01	100	<1	<0.1	0.05	<0.1	6.8	1.5
LYR11	Lyrup	<0.1	1.01	14.3	<0.5	<0.01	58	6	<0.1	0.12	<0.1	138.6	7.5
LYR12	Lyrup	<0.1	2.45	1.0	0.6	0.01	191	1	<0.1	0.06	<0.1	8.7	3.1
LYR13	Lyrup	<0.1	3.02	13.1	0.7	0.02	217	<1	<0.1	0.07	<0.1	13.2	2.8
LYR14	Lyrup	<0.1	3.20	0.7	<0.5	0.05	584	3	<0.1	0.15	<0.1	24.0	13.5
LYR15	Lyrup	0.1	6.04	27.3	<0.5	0.24	2423	3	0.2	0.14	<0.1	13.8	16.6
LCP01	Loxton	<0.1	4.09	16.6	<0.5	0.02	187	1	<0.1	13.31	<0.1	28.3	9.0
LCP02	Loxton	<0.1	2.10	16.9	<0.5	<0.01	146	1	<0.1	16.88	<0.1	12.5	6.4
LCP03	Loxton	<0.1	1.94	7.7	0.7	0.01	141	1	<0.1	16.33	<0.1	14.5	5.6
LCP04	Loxton	<0.1	2.52	13.3	0.9	0.01	166	3	<0.1	2.73	<0.1	20.7	8.1
LCP05	Loxton	<0.1	2.28	14.2	<0.5	0.01	149	1	<0.1	0.05	<0.1	22.3	9.4
LCP06	Loxton	<0.1	1.22	12.0	<0.5	0.01	110	<1	<0.1	0.02	<0.1	22.8	2.7
LCP07	Loxton	<0.1	2.28	6.2	<0.5	0.01	187	<1	<0.1	0.05	<0.1	17.7	3.7
LCP08	Loxton	<0.1	1.96	19.9	<0.5	0.02	164	1	<0.1	0.04	<0.1	15.0	4.5
LCP09	Loxton	<0.1	3.14	16.2	<0.5	0.02	235	<1	<0.1	0.04	<0.1	12.1	4.8
LCP10	Loxton	<0.1	1.95	16.9	<0.5	0.05	539	<1	<0.1	0.03	<0.1	8.2	3.3
LCP11	Loxton	<0.1	1.33	6.7	<0.5	0.01	136	<1	<0.1	0.02	<0.1	5.5	1.3
LCP12	Loxton	<0.1	1.23	7.1	<0.5	0.01	147	1	<0.1	0.03	<0.1	5.4	2.0

Sample ID	Profile	Ag (ppm)	Al_2O_3 (%)	As (ppm)	Au (ppb)	Ba (%)	Ba (ppm)	Be (ppm)	Bi (ppm)	CaO (%)	Cd (ppm)	Ce (ppm)	Co (ppm)
LCP13	Loxton	<0.1	0.50	54.5	0.6	<0.01	46	<1	<0.1	<0.01	<0.1	6.3	3.0
LCP14	Loxton	<0.1	0.44	11.1	<0.5	<0.01	45	<1	<0.1	0.01	<0.1	5.5	1.5
LCP15	Loxton	<0.1	0.70	132.4	4.3	0.01	83	2	<0.1	0.06	<0.1	12.1	14.2
LCP16	Loxton	<0.1	1.29	11.9	1.0	<0.01	51	<1	<0.1	0.02	<0.1	5.5	1.5
LCP17	Loxton	<0.1	0.96	7.9	0.9	<0.01	57	<1	<0.1	0.02	<0.1	4.9	0.8
LCP18	Loxton	<0.1	1.04	10.6	1.7	0.02	220	<1	<0.1	0.02	<0.1	4.7	1.5
LCP19	Loxton	<0.1	0.35	27.9	<0.5	0.01	174	1	<0.1	16.11	<0.1	17.9	11.4
LCP20	Loxton	<0.1	0.28	1.4	<0.5	<0.01	113	<1	<0.1	28.69	<0.1	3.7	4.0
LCP21	Loxton	<0.1	7.29	10.0	0.6	0.02	215	<1	0.1	0.19	<0.1	15.8	3.1
RC01	Red Cliffs	<0.1	5.82	<0.5	<0.5	<0.01	73	<1	<0.1	0.02	<0.1	3.0	1.5
RC02	Red Cliffs	<0.1	10.01	1.3	<0.5	<0.01	64	<1	0.1	0.05	<0.1	2.6	2.2
RC03	Red Cliffs	<0.1	1.10	0.7	<0.5	<0.01	21	<1	<0.1	0.03	<0.1	3.4	1.2
RC04	Red Cliffs	<0.1	4.43	1.8	<0.5	<0.01	48	<1	<0.1	0.07	<0.1	6.7	3.2
RC05	Red Cliffs	<0.1	5.17	3.7	<0.5	0.01	88	1	<0.1	0.07	<0.1	11.3	3.6
RC06	Red Cliffs	<0.1	5.06	3.7	<0.5	0.01	113	1	<0.1	0.02	<0.1	12.9	4.1
RC07	Red Cliffs	<0.1	9.63	9.3	<0.5	0.02	157	<1	0.2	0.03	<0.1	22.3	6.9
RC08	Red Cliffs	<0.1	8.44	6.9	1.7	<0.01	128	2	0.1	0.03	<0.1	23.1	6.2
RC09	Red Cliffs	<0.1	12.01	8.4	0.6	0.07	701	2	0.2	0.06	<0.1	32.6	8.8
RC10	Red Cliffs	<0.1	13.15	5.8	<0.5	0.02	165	<1	<0.1	0.08	<0.1	35.0	8.2
RC11	Red Cliffs	<0.1	12.13	17.6	<0.5	0.03	185	<1	0.2	0.11	<0.1	80.4	9.1
RC12	Red Cliffs	<0.1	2.15	1.3	<0.5	<0.01	23	<1	<0.1	0.06	<0.1	5.2	2.0
RC13	Red Cliffs	<0.1	6.80	9.9	<0.5	0.11	1074	1	0.2	0.03	<0.1	23.0	6.4
RC14	Red Cliffs	<0.1	3.37	4.6	<0.5	0.04	392	<1	0.1	0.02	<0.1	7.1	2.8
NY01	Nyah	<0.1	4.50	2.1	<0.5	<0.01	92	<1	<0.1	0.06	<0.1	12.6	2.8
NY02	Nyah	<0.1	5.43	1.9	<0.5	<0.01	65	<1	<0.1	0.13	<0.1	13.0	4.0

Sample ID	Profile	Ag (ppm)	Al_2O_3 (%)	As (ppm)	Au (ppb)	Ba (%)	Ba (ppm)	Be (ppm)	Bi (ppm)	CaO (%)	Cd (ppm)	Ce (ppm)	Co (ppm)
NY03	Nyah	<0.1	6.19	2.8	0.5	<0.01	80	<1	<0.1	0.10	<0.1	14.8	4.3
NY04	Nyah	<0.1	4.42	2.7	0.5	<0.01	115	<1	<0.1	0.09	<0.1	14.0	3.4
NY05	Nyah	<0.1	5.49	2.5	<0.5	0.01	110	<1	<0.1	0.09	<0.1	17.0	3.7
NY06	Nyah	<0.1	6.55	2.0	<0.5	<0.01	109	1	<0.1	0.06	<0.1	13.5	4.7
NY07	Nyah	<0.1	4.19	3.8	<0.5	<0.01	58	<1	0.1	0.07	<0.1	9.1	2.2
NY08	Nyah	<0.1	7.47	3.4	<0.5	0.02	279	1	0.2	0.23	<0.1	16.8	3.2
NY09	Nyah	<0.1	3.20	2.3	<0.5	<0.01	56	<1	<0.1	0.04	<0.1	8.9	2.1
GRQ01	Gredgwin Ridge	<0.1	8.21	13.4	<0.5	0.01	120	<1	<0.1	0.09	<0.1	30.8	1.5
GRQ02	Gredgwin Ridge	<0.1	7.90	12.9	2.3	0.01	127	4	<0.1	0.03	<0.1	18.0	1.2
GRQ03	Gredgwin Ridge	<0.1	7.22	3.0	<0.5	<0.01	115	1	<0.1	0.03	<0.1	20.9	1.6
GRQ04	Gredgwin Ridge	<0.1	6.17	5.5	3.3	<0.01	90	<1	<0.1	0.03	<0.1	32.3	1.3
GRQ05	Gredgwin Ridge	<0.1	4.42	1.7	1.3	<0.01	79	1	<0.1	0.08	<0.1	27.8	0.7
GRQ06	Gredgwin Ridge	<0.1	4.05	1.2	<0.5	<0.01	68	2	<0.1	0.09	<0.1	18.1	0.7
GRQ07	Gredgwin Ridge	<0.1	5.05	1.2	<0.5	0.03	60	<1	<0.1	0.09	<0.1	297.5	1.7
GRQ08	Gredgwin Ridge	<0.1	5.84	1.3	1.4	0.01	133	<1	<0.1	0.09	<0.1	18.3	1.5
GRQ09	Gredgwin Ridge	<0.1	6.56	1.1	2.0	0.03	155	2	<0.1	0.13	<0.1	245.3	2.7
GRQ11	Gredgwin Ridge	<0.1	8.30	12.7	<0.5	0.01	123	2	<0.1	0.03	<0.1	16.3	1.3
SRQ01	Stony Ridge	<0.1	0.16	40.3	<0.5	<0.01	97	<1	<0.1	30.27	<0.1	2.2	1.8
SRQ02	Stony Ridge	<0.1	0.28	7.2	<0.5	0.01	114	2	<0.1	29.21	<0.1	4.2	3.3
SRQ03	Stony Ridge	<0.1	0.46	10.4	1.6	<0.01	46	4	<0.1	26.79	<0.1	16.4	2.7
SRQ04	Stony Ridge	<0.1	5.68	6.9	<0.5	<0.01	91	3	<0.1	0.19	<0.1	20.5	3.4
SRQ05	Stony Ridge	<0.1	0.75	5.9	1.5	<0.01	56	<1	<0.1	0.07	<0.1	6.2	0.3
SRQ06	Stony Ridge	<0.1	0.57	7.8	<0.5	<0.01	31	1	<0.1	0.05	<0.1	5.7	3.4
SRQ07	Stony Ridge	<0.1	0.84	78.1	2.1	<0.01	58	<1	<0.1	0.07	<0.1	9.8	1.2
SRQ08	Stony Ridge	<0.1	0.62	31.8	<0.5	<0.01	43	<1	<0.1	0.01	<0.1	5.5	0.4
SRQ09	Stony Ridge	<0.1	1.07	37.8	4.2	<0.01	100	1	<0.1	0.04	<0.1	14.5	1.4

Sample ID	Profile	Ag (ppm)	Al_2O_3 (%)	As (ppm)	Au (ppb)	Ba (%)	Ba (ppm)	Be (ppm)	Bi (ppm)	CaO (%)	Cd (ppm)	Ce (ppm)	Co (ppm)
UQ01	Ultima	<0.1	3.09	458.5	<0.5	<0.01	17	<1	<0.1	0.04	<0.1	10.6	2.2
UQ02	Ultima	<0.1	3.05	110.2	<0.5	<0.01	18	1	<0.1	0.04	<0.1	7.5	1.2
UQ03	Ultima	<0.1	7.23	0.6	<0.5	<0.01	108	<1	<0.1	0.04	<0.1	23.4	2.4
UQ04	Ultima	<0.1	8.23	14.8	<0.5	<0.01	103	2	<0.1	0.07	<0.1	25.7	2.9
UQ05	Ultima	<0.1	6.68	71.6	<0.5	0.01	140	2	<0.1	0.08	<0.1	39.3	7.8
UQ06	Ultima	<0.1	6.27	<0.5	<0.5	<0.01	97	2	<0.1	0.02	<0.1	17.7	3.1
UQ07	Ultima	<0.1	6.03	4.7	<0.5	<0.01	98	1	<0.1	0.08	<0.1	11.9	4.8
UQ08	Ultima	<0.1	3.97	1.0	<0.5	0.06	655	2	<0.1	0.08	<0.1	13.8	2.5
UQ09	Ultima	<0.1	5.38	15.9	<0.5	0.03	304	1	<0.1	0.15	<0.1	19.5	6.2
UQ10	Ultima	<0.1	4.72	7.5	0.7	0.01	134	1	<0.1	0.14	<0.1	19.1	3.5
UQ11	Ultima	<0.1	6.52	1.5	<0.5	<0.01	96	1	<0.1	0.18	<0.1	11.7	3.9
UQ12	Ultima	<0.1	13.74	2.5	0.9	0.04	319	3	0.2	2.59	<0.1	41.5	10.6
CCH01	Chowilla	<0.1	2.06	0.8	<0.5	<0.01	47	<1	<0.1	0.03	<0.1	12.7	2.8
CCH02	Chowilla	<0.1	2.26	2.2	0.9	<0.01	135	1	<0.1	0.06	<0.1	9.5	3.4
CCH03	Chowilla	<0.1	5.59	<0.5	3.2	0.02	297	1	<0.1	0.20	<0.1	14.7	4.1
CCH04	Chowilla	<0.1	3.28	<0.5	1.5	0.01	175	<1	<0.1	0.14	<0.1	8.9	3.1
CCH05	Chowilla	<0.1	4.29	<0.5	<0.5	<0.01	181	2	<0.1	0.20	<0.1	13.9	4.8
CCH06	Chowilla	<0.1	5.16	<0.5	<0.5	<0.01	102	1	<0.1	0.17	<0.1	14.6	5.5
CCH07	Chowilla	<0.1	3.99	1.3	<0.5	0.03	302	1	<0.1	0.19	<0.1	16.5	3.5
CCH08	Chowilla	<0.1	3.67	0.6	<0.5	<0.01	153	<1	<0.1	0.12	<0.1	9.5	2.2
FE01	Lake Tyrrell	<0.1	0.82	5.6	<0.5	0.02	142	<1	<0.1	0.05	<0.1	8.9	0.6
NHW01	Nhill	<0.1	4.12	7.6	<0.5	<0.01	42	<1	<0.1	0.02	<0.1	27.3	3.1
NHW02	Nhill	<0.1	4.91	7.2	<0.5	<0.01	68	1	<0.1	0.07	<0.1	14.5	3.0
NHW03	Nhill	<0.1	3.97	6.0	0.6	<0.01	66	<1	<0.1	0.06	<0.1	15.9	2.3
BB01	Boundary Bend	<0.1	7.08	65.9	1.5	0.04	333	<1	0.1	0.21	<0.1	40.1	9.9

Sample ID	Profile	Ag (ppm)	Al_2O_3 (%)	As (ppm)	Au (ppb)	Ba (%)	Ba (ppm)	Be (ppm)	Bi (ppm)	CaO (%)	Cd (ppm)	Ce (ppm)	Co (ppm)
BB02	Boundary Bend	<0.1	11.93	5.4	2.4	0.05	473	2	0.3	0.39	<0.1	89.1	9.9
HC01	Headings Cliff	<0.1	4.15	2.3	0.6	0.02	183	<1	<0.1	0.06	<0.1	6.8	3.0
HC02	Headings Cliff	<0.1	4.43	1.9	<0.5	<0.01	69	<1	<0.1	0.09	<0.1	8.2	2.8
HC03	Headings Cliff	<0.1	4.54	2.3	<0.5	<0.01	85	<1	<0.1	0.05	<0.1	10.7	4.4
HC04	Headings Cliff	<0.1	6.71	23.6	<0.5	0.02	189	<1	0.2	0.13	<0.1	18.2	7.6
HC05	Headings Cliff	<0.1	6.45	3.3	0.8	0.02	189	<1	<0.1	0.15	<0.1	24.5	3.0
GOR01	Goroke	<0.1	3.82	10.2	<0.5	<0.01	38	1	<0.1	0.04	<0.1	7.5	1.6
GOR02	Goroke	<0.1	4.16	13.0	<0.5	0.02	172	<1	<0.1	0.04	<0.1	8.5	2.0
GOR03	Goroke	<0.1	5.77	10.1	<0.5	<0.01	44	<1	0.1	0.08	<0.1	11.1	2.7
GOR04	Goroke	<0.1	23.53	13.2	2.1	<0.01	75	<1	0.3	0.10	<0.1	22.5	7.4
DIA01	Diapur	<0.1	7.52	11.5	<0.5	0.07	735	<1	<0.1	0.15	<0.1	10.0	3.0
DIA02	Diapur	<0.1	4.18	8.8	<0.5	<0.01	47	<1	<0.1	0.02	<0.1	8.4	1.4
DIA03	Diapur	<0.1	5.04	19.9	<0.5	<0.01	37	<1	<0.1	0.02	<0.1	11.6	2.5
DIA04	Diapur	<0.1	4.28	16.5	<0.5	<0.01	41	<1	<0.1	0.01	<0.1	6.6	1.9
DIA05	Diapur	<0.1	4.18	12.4	<0.5	<0.01	38	<1	<0.1	0.02	<0.1	6.1	2.0
DIA06	Diapur	<0.1	4.25	15.5	<0.5	<0.01	33	<1	<0.1	0.02	<0.1	5.9	1.4
WF01	Wagon Flat	<0.1	3.96	17.8	<0.5	<0.01	41	<1	<0.1	0.03	<0.1	10.0	2.2
WF02	Wagon Flat	<0.1	3.86	16.5	<0.5	<0.01	37	<1	<0.1	0.02	<0.1	8.4	2.4
WF03	Wagon Flat	<0.1	4.32	13.5	<0.5	<0.01	43	<1	<0.1	0.02	<0.1	8.3	2.4
WF04	Wagon Flat	<0.1	5.51	19.1	<0.5	<0.01	51	<1	<0.1	0.03	<0.1	10.8	2.3
TDQ01	Telopea Downs	<0.1	3.59	34.9	<0.5	<0.01	58	<1	<0.1	<0.01	<0.1	6.4	2.1
TDQ02	Telopea Downs	<0.1	3.75	25.9	<0.5	<0.01	57	<1	<0.1	0.01	<0.1	6.4	2.0
TDQ03	Telopea Downs	<0.1	3.76	32.3	<0.5	0.01	127	<1	<0.1	<0.01	<0.1	5.5	1.9
TDQ04	Telopea Downs	<0.1	4.00	28.4	<0.5	<0.01	54	<1	<0.1	<0.01	<0.1	6.1	2.4
TDQ05	Telopea Downs	<0.1	4.58	46.2	<0.5	0.01	126	<1	<0.1	0.02	<0.1	6.5	1.9
WFN01	Wagon Flat North	<0.1	4.42	21.2	<0.5	<0.01	48	<1	<0.1	0.08	<0.1	10.3	1.3

Sample ID	Profile	Ag (ppm)	Al_2O_3 (%)	As (ppm)	Au (ppb)	Ba (%)	Ba (ppm)	Be (ppm)	Bi (ppm)	CaO (%)	Cd (ppm)	Ce (ppm)	Co (ppm)
WFN02	Wagon Flat North	<0.1	4.23	15.8	<0.5	<0.01	57	<1	<0.1	0.59	<0.1	10.8	1.5
WFN03	Wagon Flat North	<0.1	4.43	14.5	<0.5	<0.01	112	<1	<0.1	0.07	<0.1	11.4	1.9
GRQ04	Gredgwin Ridge	<0.1	8.43	6.8	<0.5	0.01	111	3	<0.1	0.07	<0.1	41.9	2.1
CCH03	Chowilla	<0.1	6.06	0.7	<0.5	0.03	290	<1	<0.1	0.19	<0.1	16.9	5.3
SRQ09	Stony Ridge	<0.1	1.18	34.9	<0.5	<0.01	93	<1	<0.1	0.04	<0.1	14.8	2.0
SP01	Spicers Pit	<0.1	3.45	61.1	60.7	<0.01	120	1	0.1	0.07	<0.1	11.4	1.6
SP02	Spicers Pit	<0.1	6.99	1.2	5.7	0.01	134	1	<0.1	0.13	<0.1	10.1	2.4
SP03	Spicers Pit	<0.1	4.50	440.2	9.2	0.02	143	2	0.3	0.13	<0.1	16.8	4.1
SP04	Spicers Pit	<0.1	5.78	1.8	3.3	0.01	137	<1	<0.1	0.11	<0.1	10.3	3.2
SP05	Spicers Pit	<0.1	7.58	1.3	2.8	0.04	452	<1	<0.1	0.15	<0.1	12.5	4.0
SP06	Spicers Pit	<0.1	7.83	2.5	2.3	0.03	231	<1	<0.1	0.10	<0.1	21.2	4.4
SP07	Spicers Pit	<0.1	8.00	20.1	2.5	0.02	170	<1	<0.1	0.10	<0.1	30.6	5.9
SP08	Spicers Pit	<0.1	6.12	22.8	<0.5	0.07	676	1	<0.1	0.10	<0.1	24.7	3.9
SP09	Spicers Pit	<0.1	5.29	668.4	<0.5	0.02	172	1	0.2	0.06	<0.1	57.0	13.7
SP10	Spicers Pit	<0.1	6.11	111.0	0.5	0.03	272	2	0.2	0.08	<0.1	25.3	14.3
CW01	Chetwynd	<0.1	23.90	1.3	<0.5	0.29	2559	<1	<0.1	0.44	<0.1	319.4	7.8
CW02	Chetwynd	<0.1	6.53	85.8	<0.5	0.03	183	<1	<0.1	0.06	<0.1	141.1	7.7
CW03	Chetwynd	<0.1	3.09	318.0	<0.5	0.01	68	1	<0.1	0.04	<0.1	77.5	5.6
CW04	Chetwynd	<0.1	4.54	145.3	1.2	<0.01	60	<1	<0.1	0.03	<0.1	48.8	15.7
CW05	Chetwynd	<0.1	5.69	231.8	<0.5	<0.01	32	2	0.2	0.04	<0.1	53.6	6.9
CW06	Chetwynd	<0.1	5.62	138.4	<0.5	<0.01	32	<1	0.2	0.03	<0.1	44.8	4.3
CW07	Chetwynd	<0.1	1.00	16.2	<0.5	<0.01	28	<1	<0.1	0.02	<0.1	42.3	0.5
CW08	Chetwynd	<0.1	1.25	235.9	<0.5	<0.01	34	<1	<0.1	0.02	<0.1	43.4	0.8
CW09	Chetwynd	<0.1	3.75	121.0	0.5	<0.01	23	<1	<0.1	0.03	<0.1	5.4	0.7
CW10	Chetwynd	<0.1	8.85	175.8	<0.5	<0.01	31	<1	0.3	0.04	<0.1	28.4	2.7
WA01	Wannon	<0.1	12.11	289.5	<0.5	<0.01	27	<1	0.2	0.08	<0.1	69.6	7.1

Sample ID	Profile	Ag (ppm)	Al_2O_3 (%)	As (ppm)	Au (ppb)	Ba (%)	Ba (ppm)	Be (ppm)	Bi (ppm)	CaO (%)	Cd (ppm)	Ce (ppm)	Co (ppm)
WA02	Wannon	<0.1	7.18	603.6	<0.5	<0.01	14	<1	0.3	0.04	<0.1	17.5	4.6
WA03	Wannon	<0.1	9.73	796.8	<0.5	<0.01	18	<1	0.3	0.05	<0.1	20.4	4.3
WA04	Wannon	<0.1	8.17	758.4	<0.5	<0.01	15	<1	0.3	0.03	<0.1	13.3	4.7
WA05	Wannon	<0.1	13.23	148.2	1.4	<0.01	4	<1	0.7	0.01	<0.1	9.6	1.9
WA06	Wannon	<0.1	18.23	3.1	<0.5	<0.01	7	<1	0.1	0.01	<0.1	8.2	1.0
WA07	Wannon	<0.1	5.97	1107.4	<0.5	<0.01	21	2	0.2	0.02	<0.1	26.5	11.1
WA08	Wannon	<0.1	7.71	959.4	<0.5	<0.01	22	<1	0.3	0.02	<0.1	28.0	13.7
WA09	Wannon	<0.1	11.94	5.4	<0.5	0.02	131	3	0.3	0.11	0.2	129.4	<0.2
WA10	Wannon	<0.1	10.94	110.0	<0.5	0.02	130	<1	1.1	0.17	0.2	103.5	2.0
WA11	Wannon	<0.1	7.28	791.3	<0.5	<0.01	12	<1	0.2	0.02	<0.1	16.6	3.4
HP01	Hewitt Pit	<0.1	7.78	1.1	2.6	<0.01	108	<1	<0.1	0.05	<0.1	8.3	1.4
HP02	Hewitt Pit	<0.1	2.43	43.0	0.9	0.01	130	<1	0.2	0.04	<0.1	14.2	1.3
HP03	Hewitt Pit	<0.1	4.67	126.7	3.7	0.04	362	<1	0.3	1.02	<0.1	18.0	14.1
GOR05	Goroke	<0.1	3.11	160.6	<0.5	0.03	263	<1	0.2	0.06	<0.1	13.0	1.2
GOR06	Goroke	<0.1	3.90	42.4	1.2	<0.01	56	<1	0.4	0.04	<0.1	21.2	2.3
GOR07	Goroke	<0.1	3.74	44.7	1.1	<0.01	46	<1	0.4	0.02	<0.1	21.9	2.3
GOR08	Goroke	<0.1	10.89	8.4	<0.5	0.01	58	<1	0.2	0.07	<0.1	16.4	3.6
SH01	Sheep Hills	<0.1	3.42	67.2	0.6	0.05	454	<1	0.2	0.19	<0.1	8.6	3.8
SH02	Sheep Hills	<0.1	3.53	58.1	2.4	0.03	270	<1	0.2	0.16	<0.1	12.9	3.9
SH03	Sheep Hills	<0.1	1.67	18.5	1.3	0.01	94	<1	<0.1	0.16	<0.1	10.5	1.3
MP01	Watchem Pit	<0.1	4.23	96.6	<0.5	<0.01	93	<1	0.1	0.06	<0.1	11.9	5.9
MP02	Watchem Pit	<0.1	3.19	26.3	<0.5	0.01	83	<1	0.2	0.10	<0.1	9.3	3.8
GL01	Green Lake	<0.1	7.07	16.5	<0.5	0.02	149	<1	<0.1	0.08	<0.1	24.3	2.1
CW11	Chetwynd	<0.1	5.33	59.7	<0.5	0.18	1820	<1	0.3	0.04	<0.1	21.4	3.7
HHQ01	Henty Highway	<0.1	1.92	12.4	<0.5	<0.01	74	<1	<0.1	0.12	<0.1	5.1	1.7
MR01	Mitre Rock	<0.1	7.73	371.6	<0.5	0.04	300	2	0.2	0.18	<0.1	135.3	5.2

Sample ID	Profile	Ag (ppm)	Al_2O_3 (%)	As (ppm)	Au (ppb)	Ba (%)	Ba (ppm)	Be (ppm)	Bi (ppm)	CaO (%)	Cd (ppm)	Ce (ppm)	Co (ppm)
MR02	Mitre Rock	<0.1	10.72	12.9	0.6	0.02	127	<1	0.2	0.20	<0.1	64.3	2.2
WRC01	Warracknabeal	<0.1	2.31	2.1	1.1	0.02	219	<1	<0.1	20.17	<0.1	12.2	2.5
DIA10	Diapur	<0.1	7.68	106.6	<0.5	0.02	195	2	0.3	0.20	<0.1	17.5	3.6
DIA11	Diapur	<0.1	4.69	68.0	<0.5	0.02	103	<1	0.6	0.16	<0.1	29.8	4.3
BAL01	Balranald-1	<0.1	8.54	23.3	0.8	0.04	434	<1	0.1	7.00	<0.1	44.2	8.8
WEN01	Wentworth-1	<0.1	7.26	3.9	0.9	0.02	234	<1	<0.1	2.42	<0.1	34.7	7.3
WEN02	Wentworth-1	<0.1	7.31	2.5	<0.5	0.02	222	<1	<0.1	0.43	<0.1	40.2	9.6
WEN03	Wentworth-1	<0.1	7.00	2.9	1.1	0.04	352	<1	<0.1	0.33	<0.1	41.2	9.1
WEN04	Wentworth-1	<0.1	8.09	2.7	1.6	0.04	482	<1	<0.1	0.32	<0.1	37.3	10.0
WEN05	Wentworth-1	<0.1	5.12	2.6	1.7	0.02	174	<1	<0.1	0.27	<0.1	38.8	6.9
WEN06	Wentworth-1	0.6	6.23	3.2	0.9	0.03	259	<1	<0.1	0.34	0.2	36.3	8.3
WEN07	Wentworth-1	<0.1	3.97	5.6	1.1	0.02	116	<1	<0.1	0.10	<0.1	15.1	3.3
WEN08	Wentworth-1	0.3	5.57	3.8	1.6	0.02	195	2	<0.1	0.19	0.1	22.4	4.7
WEN09	Wentworth-1	<0.1	4.99	5.4	<0.5	0.02	206	<1	<0.1	0.13	<0.1	19.8	6.8
WEN10	Wentworth-1	<0.1	4.38	5.5	<0.5	0.02	164	<1	<0.1	0.13	<0.1	33.7	9.9
WEN11	Wentworth-1	<0.1	0.87	2.5	<0.5	0.02	96	<1	<0.1	1.53	<0.1	8.1	1.0
WEN12	Wentworth-1	<0.1	0.45	1.9	0.8	<0.01	129	<1	<0.1	0.56	<0.1	4.3	0.3
WEN13	Wentworth-1	<0.1	0.29	5.2	2.9	<0.01	89	<1	<0.1	0.23	<0.1	3.2	2.2
WEN14	Wentworth-1	<0.1	0.38	5.2	1.2	<0.01	65	1	<0.1	0.13	<0.1	7.6	2.2
WEN15	Wentworth-1	<0.1	0.84	15.5	1.2	0.02	126	<1	<0.1	0.21	<0.1	14.8	9.2
WEN16	Wentworth-1	<0.1	0.58	5.3	0.8	<0.01	111	<1	<0.1	0.25	<0.1	10.5	5.5
WEN17	Wentworth-1	<0.1	0.87	8.0	1.0	0.01	126	<1	<0.1	0.23	<0.1	12.1	6.5
WEN18	Wentworth-1	<0.1	3.94	23.5	1.6	0.06	611	2	<0.1	1.27	<0.1	27.3	9.1
WEN19	Wentworth-1	<0.1	3.40	18.3	1.1	0.05	450	<1	<0.1	1.15	<0.1	26.0	9.7
BUN01	Bundy-1	<0.1	2.97	3.3	1.2	0.03	241	<1	<0.1	0.35	<0.1	12.9	2.2
BUN02	Bundy-1	<0.1	3.28	2.3	0.8	0.03	230	<1	<0.1	0.11	<0.1	15.9	1.7

Sample ID	Profile	Ag (ppm)	Al_2O_3 (%)	As (ppm)	Au (ppb)	Ba (%)	Ba (ppm)	Be (ppm)	Bi (ppm)	CaO (%)	Cd (ppm)	Ce (ppm)	Co (ppm)
BUN03	Bundy-1	<0.1	3.28	4.6	1.4	0.03	249	<1	<0.1	0.20	<0.1	15.8	3.1
BUN04	Bundy-1	<0.1	3.54	5.8	0.5	0.04	322	<1	0.1	0.27	<0.1	14.4	3.3
BUN05	Bundy-1	<0.1	6.09	4.4	0.8	0.07	571	<1	0.1	0.28	<0.1	76.2	4.9
BUN06	Bundy-1	<0.1	5.78	7.2	2.6	0.02	235	2	0.2	0.34	<0.1	26.7	2.4
BUN07	Bundy-1	<0.1	3.96	6.5	3.0	0.03	238	<1	0.1	0.27	<0.1	13.5	3.1
BUN08	Bundy-1	<0.1	6.92	6.1	2.2	0.05	484	<1	0.2	0.25	<0.1	37.8	4.7
BUN09	Bundy-1	<0.1	4.95	15.4	<0.5	0.05	496	<1	0.5	0.22	<0.1	18.9	4.4
BUN10	Bundy-1	<0.1	4.56	6.4	9.2	0.03	313	3	0.3	0.16	0.1	48.3	4.5
BUN11	Bundy-1	<0.1	3.59	3.9	6.9	0.02	259	<1	0.2	0.11	<0.1	37.1	4.1
BUN12	Bundy-1	<0.1	3.28	3.7	4.3	0.03	251	<1	0.2	0.12	0.1	28.9	2.5
BUN13	Bundy-1	<0.1	3.01	4.1	2.4	0.02	257	3	0.1	0.08	<0.1	25.7	2.9
BUN14	Bundy-1	<0.1	1.89	1.3	0.8	0.02	143	1	<0.1	0.06	<0.1	17.3	1.7
BUN15	Bundy-1	<0.1	1.64	1.7	4.3	0.02	157	<1	<0.1	0.04	<0.1	13.6	1.2
BUN16	Bundy-1	<0.1	1.38	1.2	6.2	0.02	117	<1	<0.1	0.03	<0.1	12.8	3.3
BUN17	Bundy-1	<0.1	1.43	1.0	2.1	0.01	131	<1	<0.1	0.03	<0.1	14.7	1.1
BUN18	Bundy-1	<0.1	1.39	3.2	2.6	0.02	120	1	0.1	0.05	<0.1	14.3	1.2
BUN19	Bundy-1	<0.1	1.36	2.2	2.0	0.02	148	<1	<0.1	0.04	<0.1	11.8	1.3
BUN20	Bundy-1	<0.1	1.66	1.8	5.1	0.02	156	1	<0.1	0.05	<0.1	11.9	1.2
BUN21	Bundy-1	<0.1	1.06	2.1	2.3	0.01	114	<1	<0.1	7.28	0.1	10.9	3.1
BUN22	Bundy-1	<0.1	1.43	3.9	<0.5	0.02	296	1	<0.1	4.97	0.2	11.2	3.7
BUN23	Bundy-1	<0.1	0.55	2.2	2.1	<0.01	71	<1	<0.1	0.22	<0.1	6.3	11.3
BUN24	Bundy-1	<0.1	0.53	4.6	<0.5	0.01	63	<1	<0.1	0.11	<0.1	4.5	20.2
BUN25	Bundy-1	<0.1	0.81	3.7	0.5	0.01	101	<1	<0.1	0.12	<0.1	8.7	12.2
BUN26	Bundy-1	<0.1	0.86	4.5	1.1	0.01	93	<1	<0.1	0.14	<0.1	7.7	14.0
BUN27	Bundy-1	<0.1	1.14	5.4	2.4	0.01	101	4	<0.1	0.42	<0.1	10.3	10.8
BUN28	Bundy-1	<0.1	0.81	6.6	2.6	<0.01	88	<1	<0.1	0.60	<0.1	7.5	18.1

Sample ID	Profile	Ag (ppm)	Al_2O_3 (%)	As (ppm)	Au (ppb)	Ba (%)	Ba (ppm)	Be (ppm)	Bi (ppm)	CaO (%)	Cd (ppm)	Ce (ppm)	Co (ppm)
BUN29	Bundy-1	<0.1	0.69	33.2	<0.5	<0.01	80	2	<0.1	0.16	<0.1	8.0	41.1
BUN30	Bundy-1	<0.1	0.91	35.8	<0.5	<0.01	138	2	<0.1	0.18	<0.1	11.2	41.3
HOR101	Horsham-1	<0.1	14.88	6.2	2.8	<0.01	49	<1	0.2	0.02	<0.1	17.7	4.3
HOR102	Horsham-1	<0.1	10.98	6.2	3.9	<0.01	48	<1	0.2	0.02	<0.1	16.0	2.8
HOR107	Horsham-1	<0.1	8.72	3.3	1.2	<0.01	28	1	0.1	0.02	<0.1	12.5	2.2
HOR108	Horsham-1	<0.1	6.44	3.1	<0.5	<0.01	26	1	<0.1	0.02	<0.1	9.4	2.5
HOR109	Horsham-1	<0.1	5.21	3.6	<0.5	<0.01	25	<1	<0.1	0.02	<0.1	7.5	1.9
HOR110	Horsham-1	<0.1	4.56	1.5	<0.5	<0.01	21	<1	<0.1	0.02	<0.1	8.6	1.4
HOR111	Horsham-1	<0.1	6.59	5.4	<0.5	<0.01	25	<1	<0.1	0.02	<0.1	8.3	1.6
HOR112	Horsham-1	<0.1	5.00	2.8	<0.5	0.01	100	2	<0.1	0.02	<0.1	6.5	1.6
HOR113	Horsham-1	<0.1	3.54	2.0	<0.5	<0.01	31	2	<0.1	0.02	<0.1	11.1	1.6
HOR114	Horsham-1	<0.1	3.96	2.5	<0.5	<0.01	22	<1	<0.1	0.02	<0.1	6.6	1.5
HOR115	Horsham-1	<0.1	4.78	<0.5	<0.5	0.01	39	<1	<0.1	0.02	<0.1	6.5	1.7
HOR116	Horsham-1	<0.1	3.44	3.8	2.6	<0.01	55	<1	<0.1	<0.01	<0.1	5.8	1.5
HOR117	Horsham-1	<0.1	2.94	2.0	<0.5	<0.01	26	<1	<0.1	<0.01	<0.1	5.9	1.1
HOR118	Horsham-1	<0.1	2.58	4.2	<0.5	<0.01	24	<1	<0.1	<0.01	<0.1	5.8	1.5
HOR119	Horsham-1	<0.1	2.51	10.2	<0.5	<0.01	28	<1	<0.1	<0.01	<0.1	7.5	1.5
HOR120	Horsham-1	<0.1	2.86	25.7	<0.5	<0.01	27	<1	<0.1	<0.01	<0.1	8.6	1.7
HOR121	Horsham-1	<0.1	3.21	10.3	<0.5	<0.01	25	<1	<0.1	<0.01	<0.1	10.1	2.0
HOR122	Horsham-1	<0.1	3.76	2.7	<0.5	<0.01	36	<1	<0.1	<0.01	<0.1	8.5	1.5
HOR123	Horsham-1	<0.1	5.18	<0.5	<0.5	<0.01	34	<1	<0.1	<0.01	<0.1	7.4	1.8
HOR124	Horsham-1	<0.1	3.44	1.7	<0.5	<0.01	40	<1	<0.1	<0.01	<0.1	7.4	1.3
HOR125	Horsham-1	<0.1	3.76	0.9	<0.5	<0.01	40	<1	<0.1	<0.01	<0.1	6.2	1.4
HOR126	Horsham-1	<0.1	3.97	1.3	<0.5	<0.01	37	<1	0.1	<0.01	<0.1	7.0	0.9
HOR127	Horsham-1	<0.1	4.47	0.9	<0.5	<0.01	41	<1	<0.1	<0.01	<0.1	6.6	1.6
HOR128	Horsham-1	<0.1	3.96	1.6	<0.5	<0.01	42	<1	<0.1	<0.01	<0.1	6.6	1.6

Sample ID	Profile	Ag (ppm)	Al_2O_3 (%)	As (ppm)	Au (ppb)	Ba (%)	Ba (ppm)	Be (ppm)	Bi (ppm)	CaO (%)	Cd (ppm)	Ce (ppm)	Co (ppm)
HOR129	Horsham-1	<0.1	5.42	<0.5	<0.5	<0.01	43	<1	<0.1	<0.01	<0.1	8.1	1.5
HOR130	Horsham-1	<0.1	1.84	1.0	4.9	0.12	1136	1	<0.1	0.02	<0.1	12.5	1.0
HOR133	Horsham-1	<0.1	1.79	1.1	<0.5	0.15	1484	<1	<0.1	0.04	<0.1	12.8	0.9
HOR134	Horsham-1	<0.1	1.67	1.6	<0.5	0.26	2459	<1	<0.1	0.03	<0.1	13.0	1.1
HOR135	Horsham-1	<0.1	1.51	<0.5	<0.5	0.09	865	<1	<0.1	0.02	<0.1	10.5	0.7
HOR136	Horsham-1	<0.1	4.75	105.0	<0.5	0.03	239	2	0.1	21.11	<0.1	90.0	28.2
HOR137	Horsham-1	<0.1	5.60	56.8	<0.5	0.03	184	2	0.1	2.21	<0.1	118.4	15.1
HOR501	Horsham-5	<0.1	2.67	1.2	<0.5	<0.01	48	<1	<0.1	0.04	<0.1	9.3	2.1
HOR503	Horsham-5	<0.1	3.94	7.9	<0.5	<0.01	45	<1	<0.1	0.02	<0.1	16.2	2.6
HOR504	Horsham-5	<0.1	13.14	21.7	<0.5	<0.01	50	<1	0.4	0.03	<0.1	18.0	3.5
HOR507	Horsham-5	<0.1	15.69	3.6	<0.5	0.03	267	<1	0.2	0.02	<0.1	17.1	4.7
HOR508	Horsham-5	<0.1	17.40	4.5	<0.5	<0.01	103	<1	0.2	0.03	<0.1	17.4	4.8
HOR509	Horsham-5	<0.1	9.68	3.4	<0.5	<0.01	45	<1	<0.1	0.01	<0.1	11.4	2.7
HOR510	Horsham-5	<0.1	10.52	7.0	<0.5	<0.01	24	1	0.2	0.01	<0.1	10.6	2.5
HOR511	Horsham-5	<0.1	8.56	3.2	<0.5	<0.01	27	<1	<0.1	0.01	<0.1	8.5	2.2
HOR512	Horsham-5	<0.1	7.08	4.8	<0.5	0.01	40	<1	<0.1	<0.01	<0.1	9.4	2.1
HOR513	Horsham-5	<0.1	4.24	6.1	<0.5	<0.01	27	<1	<0.1	0.01	<0.1	8.1	1.5
HOR514	Horsham-5	0.1	5.21	6.1	<0.5	<0.01	34	<1	<0.1	0.01	<0.1	9.7	1.5
HOR515	Horsham-5	<0.1	4.34	12.8	2.2	<0.01	44	2	0.1	0.02	<0.1	9.0	1.6
HOR516	Horsham-5	<0.1	3.31	10.8	<0.5	<0.01	35	2	<0.1	0.01	<0.1	7.0	1.4
HOR517	Horsham-5	<0.1	3.04	7.4	0.9	<0.01	37	<1	<0.1	0.02	<0.1	5.9	1.7
HOR518	Horsham-5	<0.1	2.32	10.1	2.0	<0.01	76	<1	<0.1	0.02	<0.1	7.4	1.9
HOR519	Horsham-5	<0.1	2.28	7.0	<0.5	<0.01	100	<1	<0.1	0.02	<0.1	6.5	1.7
HOR520	Horsham-5	<0.1	2.02	8.4	<0.5	<0.01	86	<1	<0.1	0.02	<0.1	8.6	1.7
HOR521	Horsham-5	<0.1	2.74	7.4	<0.5	0.01	117	<1	<0.1	0.02	<0.1	9.6	2.4
HOR522	Horsham-5	<0.1	2.87	10.8	<0.5	<0.01	83	3	<0.1	0.02	<0.1	14.5	2.9

Sample ID	Profile	Ag (ppm)	Al_2O_3 (%)	As (ppm)	Au (ppb)	Ba (%)	Ba (ppm)	Be (ppm)	Bi (ppm)	CaO (%)	Cd (ppm)	Ce (ppm)	Co (ppm)
HOR523	Horsham-5	<0.1	2.56	7.7	<0.5	<0.01	45	2	<0.1	0.01	<0.1	7.7	1.4
HOR524	Horsham-5	<0.1	2.83	6.9	<0.5	<0.01	62	<1	<0.1	0.02	<0.1	7.9	1.7
HOR528	Horsham-5	<0.1	3.05	8.3	<0.5	<0.01	62	<1	<0.1	0.01	<0.1	11.4	2.2
HOR529	Horsham-5	<0.1	2.91	10.5	<0.5	<0.01	84	3	<0.1	0.02	<0.1	12.2	2.5
HOR530	Horsham-5	<0.1	2.84	8.7	<0.5	<0.01	34	<1	<0.1	0.02	<0.1	10.2	3.1
HOR531	Horsham-5	<0.1	3.36	9.4	<0.5	<0.01	76	<1	<0.1	0.02	<0.1	16.0	2.7
HOR532	Horsham-5	<0.1	3.26	6.5	<0.5	<0.01	63	<1	<0.1	0.02	<0.1	13.0	2.2
HOR533	Horsham-5	<0.1	3.35	6.3	<0.5	<0.01	47	<1	<0.1	0.02	<0.1	9.5	2.3
HOR534	Horsham-5	<0.1	3.40	6.7	<0.5	<0.01	45	<1	<0.1	0.01	<0.1	14.2	2.9
HOR535	Horsham-5	<0.1	3.69	<0.5	<0.5	<0.01	44	<1	<0.1	0.01	<0.1	12.4	1.0
HOR536	Horsham-5	<0.1	3.52	<0.5	<0.5	<0.01	43	<1	<0.1	0.02	<0.1	33.1	1.6
HOR537	Horsham-5	<0.1	3.52	5.2	2.5	<0.01	34	<1	<0.1	0.01	<0.1	15.8	2.6
HOR538	Horsham-5	<0.1	3.64	4.7	<0.5	<0.01	49	<1	<0.1	0.02	<0.1	12.6	2.0
HOR539	Horsham-5	0.1	2.38	<0.5	<0.5	0.01	97	<1	<0.1	0.03	0.1	26.1	1.5
HOR540	Horsham-5	<0.1	1.06	6.5	0.5	<0.01	56	<1	<0.1	0.03	<0.1	9.7	1.1
HOR541	Horsham-5	<0.1	1.15	11.8	<0.5	<0.01	49	<1	<0.1	0.04	<0.1	11.7	1.6
HOR542	Horsham-5	<0.1	1.55	9.3	<0.5	<0.01	61	<1	<0.1	0.03	<0.1	12.8	2.1
HOR543	Horsham-5	<0.1	1.30	5.6	<0.5	0.01	101	<1	<0.1	0.05	<0.1	10.3	1.4
HOR544	Horsham-5	<0.1	1.11	4.3	<0.5	0.01	101	<1	<0.1	0.04	<0.1	9.7	1.0
HOR545	Horsham-5	<0.1	1.14	4.2	<0.5	0.01	123	<1	<0.1	0.05	<0.1	11.2	1.3
HOR546	Horsham-5	<0.1	1.14	4.2	<0.5	0.01	156	<1	<0.1	0.05	<0.1	13.2	1.3
HOR547	Horsham-5	<0.1	0.87	4.0	1.3	0.02	146	<1	<0.1	0.04	<0.1	9.5	1.0
HOR548	Horsham-5	<0.1	0.74	4.6	1.0	0.01	136	<1	<0.1	0.04	<0.1	8.7	0.8
HOR549	Horsham-5	<0.1	0.70	3.5	0.5	0.01	98	<1	<0.1	0.02	<0.1	8.6	0.9
HOR550	Horsham-5	<0.1	0.76	3.8	<0.5	0.02	159	<1	<0.1	0.04	<0.1	7.8	1.1
HOR551	Horsham-5	<0.1	0.56	2.8	0.8	<0.01	68	<1	<0.1	0.02	<0.1	7.5	0.7

Sample ID	Profile	Ag (ppm)	Al_2O_3 (%)	As (ppm)	Au (ppb)	Ba (%)	Ba (ppm)	Be (ppm)	Bi (ppm)	CaO (%)	Cd (ppm)	Ce (ppm)	Co (ppm)
HOR552	Horsham-5	<0.1	0.98	5.9	3.2	<0.01	110	<1	<0.1	0.03	<0.1	12.2	1.3
HOR553	Horsham-5	<0.1	2.34	24.8	2.0	0.02	143	2	0.2	0.05	<0.1	165.4	9.2
HOR554	Horsham-5	<0.1	3.19	101.0	2.6	0.03	125	5	0.2	0.07	<0.1	229.2	38.9
HOR505	Horsham-5	<0.1	19.81	6.9	1.3	0.02	206	<1	0.2	0.04	<0.1	22.6	6.0
HOR506	Horsham-5	<0.1	18.56	12.7	0.9	0.01	91	<1	0.3	0.03	<0.1	26.1	4.9
HOR526	Horsham-5	<0.1	2.79	9.6	<0.5	<0.01	62	<1	<0.1	0.02	<0.1	12.4	2.9
HOR701	Horsham-7	<0.1	7.53	2.3	<0.5	0.03	309	<1	0.1	18.00	<0.1	40.7	6.7
HOR702	Horsham-7	<0.1	10.04	4.2	1.5	0.03	185	2	0.2	0.25	<0.1	57.4	8.4
HOR703	Horsham-7	<0.1	8.26	5.8	<0.5	0.02	189	2	0.2	0.64	<0.1	54.0	8.4
HOR704	Horsham-7	<0.1	7.94	6.9	1.8	0.03	292	<1	0.2	0.94	<0.1	43.9	7.6
HOR705	Horsham-7	<0.1	7.32	3.7	1.3	0.03	208	2	0.1	0.65	<0.1	35.0	6.4
HOR706	Horsham-7	<0.1	8.33	3.9	<0.5	0.03	208	<1	0.1	0.20	<0.1	41.4	6.8
HOR707	Horsham-7	<0.1	8.69	3.4	1.6	0.02	215	<1	<0.1	0.14	<0.1	44.5	7.7
HOR708	Horsham-7	<0.1	12.00	3.8	<0.5	0.03	208	<1	0.1	0.17	<0.1	59.3	9.4
HOR709	Horsham-7	<0.1	10.66	2.9	<0.5	0.03	222	2	0.1	0.15	<0.1	55.6	13.4
HOR710	Horsham-7	<0.1	11.60	4.2	<0.5	0.03	227	<1	0.1	0.14	<0.1	49.5	8.6
HOR711	Horsham-7	<0.1	10.66	3.9	<0.5	0.02	180	<1	0.1	0.12	<0.1	20.2	5.5
HOR712	Horsham-7	<0.1	11.51	5.5	<0.5	0.02	166	<1	0.1	0.05	<0.1	12.5	4.2
HOR713	Horsham-7	<0.1	8.80	5.6	<0.5	<0.01	34	<1	<0.1	0.03	<0.1	7.9	2.8
HOR714	Horsham-7	<0.1	6.32	4.1	<0.5	<0.01	22	<1	<0.1	0.03	<0.1	6.6	2.2
HOR715	Horsham-7	<0.1	4.54	10.3	<0.5	<0.01	22	<1	<0.1	0.02	<0.1	5.0	1.7
HOR716	Horsham-7	<0.1	4.30	4.2	<0.5	<0.01	23	<1	<0.1	0.02	<0.1	5.0	1.6
HOR717	Horsham-7	<0.1	4.90	4.9	<0.5	0.01	80	<1	<0.1	0.02	<0.1	5.5	1.9
HOR718	Horsham-7	<0.1	4.58	9.4	<0.5	<0.01	42	<1	<0.1	0.02	<0.1	6.9	2.1
HOR719	Horsham-7	<0.1	4.38	11.9	<0.5	<0.01	44	<1	<0.1	0.02	<0.1	5.5	2.1
HOR720	Horsham-7	<0.1	3.78	10.8	0.7	<0.01	38	<1	<0.1	0.02	<0.1	5.2	1.8

Sample ID	Profile	Ag (ppm)	Al_2O_3 (%)	As (ppm)	Au (ppb)	Ba (%)	Ba (ppm)	Be (ppm)	Bi (ppm)	CaO (%)	Cd (ppm)	Ce (ppm)	Co (ppm)
HOR721	Horsham-7	0.3	4.10	10.7	<0.5	<0.01	55	<1	<0.1	0.04	0.1	6.3	1.9
HOR722	Horsham-7	<0.1	4.38	7.7	<0.5	<0.01	45	<1	<0.1	0.03	<0.1	7.6	1.8
HOR723	Horsham-7	<0.1	4.82	8.4	<0.5	<0.01	45	<1	<0.1	0.03	<0.1	8.3	1.7
HOR724	Horsham-7	<0.1	4.59	7.9	0.6	<0.01	42	2	<0.1	0.02	<0.1	6.2	1.9
HOR725	Horsham-7	<0.1	4.16	7.8	2.3	<0.01	44	<1	<0.1	0.03	<0.1	6.8	1.9
HOR726	Horsham-7	<0.1	3.57	7.3	<0.5	<0.01	40	<1	<0.1	0.02	<0.1	6.3	1.7
HOR727	Horsham-7	<0.1	4.07	6.3	6.9	<0.01	62	2	<0.1	0.04	0.1	7.3	2.1
HOR728	Horsham-7	<0.1	4.63	3.9	5.8	<0.01	50	<1	<0.1	0.04	<0.1	7.3	1.4
HOR729	Horsham-7	<0.1	4.37	1.1	1.3	<0.01	61	<1	<0.1	0.04	<0.1	8.7	1.7
HOR730	Horsham-7	<0.1	3.93	0.7	1.6	0.01	65	2	<0.1	0.04	<0.1	10.3	1.5
HOR731	Horsham-7	<0.1	3.79	0.5	3.4	<0.01	67	<1	<0.1	0.04	<0.1	8.9	1.7
HOR732	Horsham-7	<0.1	3.21	<0.5	<0.5	<0.01	72	<1	<0.1	0.03	<0.1	10.3	1.1
HOR733	Horsham-7	<0.1	2.31	<0.5	1.6	<0.01	60	2	<0.1	0.03	<0.1	7.6	1.1
HOR734	Horsham-7	<0.1	2.90	0.7	2.0	<0.01	57	<1	<0.1	0.04	<0.1	10.1	1.3
HOR735	Horsham-7	<0.1	2.99	<0.5	4.1	<0.01	65	<1	<0.1	0.04	<0.1	13.5	1.4
HOR736	Horsham-7	<0.1	3.40	0.5	1.6	<0.01	67	3	<0.1	0.04	<0.1	16.9	1.6
HOR737	Horsham-7	<0.1	3.32	<0.5	1.4	<0.01	62	<1	<0.1	0.04	<0.1	16.4	1.5
HOR738	Horsham-7	<0.1	2.50	<0.5	0.9	<0.01	80	<1	<0.1	0.04	<0.1	17.9	1.0
HOR739	Horsham-7	<0.1	2.09	1.0	<0.5	0.01	79	2	<0.1	0.03	<0.1	11.8	1.6
HOR740	Horsham-7	<0.1	2.73	<0.5	<0.5	<0.01	68	<1	<0.1	0.03	<0.1	20.6	1.1
HOR741	Horsham-7	<0.1	1.73	0.8	0.7	<0.01	69	<1	<0.1	0.04	<0.1	15.9	1.1
HOR742	Horsham-7	<0.1	2.18	1.5	<0.5	<0.01	76	<1	<0.1	0.03	<0.1	26.3	1.4
HOR743	Horsham-7	<0.1	2.44	1.5	<0.5	<0.01	77	<1	<0.1	0.04	<0.1	30.5	1.5
HOR744	Horsham-7	<0.1	2.36	1.9	<0.5	0.01	77	<1	<0.1	0.05	<0.1	17.7	1.6
HOR745	Horsham-7	<0.1	1.95	0.6	1.7	<0.01	57	<1	<0.1	0.03	<0.1	51.2	1.6
HOR746	Horsham-7	<0.1	1.66	0.8	0.8	<0.01	56	<1	<0.1	0.04	<0.1	15.7	0.9

Sample ID	Profile	Ag (ppm)	Al_2O_3 (%)	As (ppm)	Au (ppb)	Ba (%)	Ba (ppm)	Be (ppm)	Bi (ppm)	CaO (%)	Cd (ppm)	Ce (ppm)	Co (ppm)
HOR747	Horsham-7	<0.1	2.55	1.3	1.0	<0.01	56	<1	<0.1	0.03	<0.1	20.3	1.3
HOR748	Horsham-7	<0.1	1.96	2.0	<0.5	<0.01	74	<1	<0.1	0.05	<0.1	17.1	1.2
HOR749	Horsham-7	<0.1	2.02	2.2	1.0	<0.01	71	<1	<0.1	0.04	<0.1	17.8	1.4
HOR750	Horsham-7	<0.1	2.71	4.5	<0.5	0.01	94	<1	<0.1	0.04	<0.1	16.7	1.1
HOR751	Horsham-7	<0.1	2.49	14.5	1.0	0.01	103	2	<0.1	0.04	<0.1	14.6	1.9
HOR752	Horsham-7	<0.1	8.04	13.1	0.9	0.04	381	<1	0.3	1.25	<0.1	57.1	9.4
HOR753	Horsham-7	<0.1	3.17	0.5	<0.5	<0.01	65	<1	<0.1	0.02	<0.1	14.7	1.8
HOR754	Horsham-7	<0.1	2.57	12.1	<0.5	0.01	102	<1	<0.1	0.05	<0.1	25.9	1.7
HOR755	Horsham-7	<0.1	3.25	3.1	<0.5	0.02	148	<1	<0.1	0.04	<0.1	28.6	1.7
HOR756	Horsham-7	<0.1	5.19	2.1	<0.5	0.02	196	<1	<0.1	0.05	<0.1	37.9	2.0
HOR757	Horsham-7	<0.1	4.40	1.9	2.1	0.02	194	1	<0.1	0.05	<0.1	41.8	2.1
HOR758	Horsham-7	<0.1	4.19	1.9	<0.5	0.02	195	<1	<0.1	0.04	<0.1	37.5	2.2
HOR759	Horsham-7	<0.1	3.40	2.1	1.0	0.02	198	<1	<0.1	0.05	<0.1	50.8	2.4
HOR760	Horsham-7	<0.1	3.53	2.1	<0.5	0.02	216	1	<0.1	0.04	<0.1	42.0	1.9
HOR761	Horsham-7	<0.1	3.73	1.7	1.6	0.03	239	1	<0.1	0.04	<0.1	40.6	1.6
HOR762	Horsham-7	<0.1	3.36	2.0	0.7	0.02	231	1	<0.1	0.05	<0.1	34.2	1.7
HOR763	Horsham-7	<0.1	3.73	3.0	1.1	0.03	224	<1	<0.1	0.05	<0.1	55.7	2.3
HOR764	Horsham-7	<0.1	3.44	1.9	<0.5	0.02	222	<1	<0.1	0.04	<0.1	65.6	2.3
HOR765	Horsham-7	<0.1	4.06	29.5	0.7	0.03	247	<1	0.2	0.05	<0.1	65.1	3.9
HOR766	Horsham-7	<0.1	4.41	8.1	<0.5	0.03	273	<1	<0.1	0.05	<0.1	35.9	4.7
HOR767	Horsham-7	<0.1	3.35	3.5	2.5	0.03	251	<1	<0.1	0.04	<0.1	30.0	2.5
HOR768	Horsham-7	<0.1	4.99	1.8	0.6	0.03	332	<1	0.1	0.05	<0.1	32.0	2.5
HOR769	Horsham-7	<0.1	4.11	4.0	2.3	0.03	275	<1	0.1	0.05	<0.1	30.5	3.7
HOR770	Horsham-7	<0.1	4.61	3.5	3.0	0.03	245	3	0.2	0.06	<0.1	289.0	6.1
HOR771	Horsham-7	<0.1	4.20	41.3	0.9	0.02	237	7	0.1	0.06	<0.1	421.0	99.4
HOR772	Horsham-7	<0.1	4.13	4.2	<0.5	0.03	251	4	<0.1	0.07	<0.1	111.7	5.1

Sample ID	Profile	Ag (ppm)	Al_2O_3 (%)	As (ppm)	Au (ppb)	Ba (%)	Ba (ppm)	Be (ppm)	Bi (ppm)	CaO (%)	Cd (ppm)	Ce (ppm)	Co (ppm)
HOR773	Horsham-7	<0.1	4.48	8.3	1.1	0.02	253	3	0.1	0.09	<0.1	160.5	7.3
HOR774	Horsham-7	<0.1	6.01	54.7	0.6	0.01	219	5	0.2	0.08	0.1	331.5	54.4
HOR775	Horsham-7	<0.1	4.65	10.8	0.7	0.03	264	<1	0.1	0.07	<0.1	32.2	5.6
HOR776	Horsham-7	<0.1	4.20	33.8	0.6	0.02	268	<1	<0.1	0.07	<0.1	21.0	19.8
HOR777	Horsham-7	<0.1	4.29	23.1	0.8	0.03	288	<1	<0.1	0.08	<0.1	26.2	5.9
HOR778	Horsham-7	<0.1	4.09	13.2	<0.5	0.03	286	<1	<0.1	0.08	<0.1	17.3	13.7
HOR779	Horsham-7	<0.1	6.78	97.4	<0.5	0.02	230	<1	0.1	0.12	<0.1	51.5	9.5
HOR780	Horsham-7	<0.1	6.79	83.5	0.8	0.01	196	2	0.2	0.18	<0.1	178.5	11.5
HOR781	Horsham-7	<0.1	7.38	185.9	<0.5	<0.01	115	2	0.3	9.95	<0.1	161.4	64.9
WIL15	Willah-1	<0.1	13.58	3.9	<0.5	0.02	285	1	0.1	2.82	<0.1	42.6	12.4
WIL16	Willah-1	<0.1	15.55	3.6	<0.5	0.03	279	2	0.2	2.55	<0.1	46.6	13.7
WIL17	Willah-1	<0.1	9.57	2.2	<0.5	0.02	264	<1	0.1	1.13	<0.1	33.6	9.2
WIL18	Willah-1	<0.1	15.08	3.9	<0.5	0.06	589	1	0.2	3.19	<0.1	48.0	15.5
WIL19	Willah-1	<0.1	6.96	1.8	<0.5	0.03	347	1	<0.1	0.69	<0.1	21.7	6.5
WIL20	Willah-1	<0.1	4.13	1.2	<0.5	<0.01	127	1	<0.1	0.73	<0.1	14.8	4.2
WIL21	Willah-1	<0.1	0.35	0.9	<0.5	<0.01	93	<1	<0.1	0.04	<0.1	4.9	1.2
WIL22	Willah-1	<0.1	0.56	0.9	<0.5	<0.01	62	<1	<0.1	0.04	<0.1	4.6	1.1
WIL23	Willah-1	<0.1	0.35	1.3	1.5	<0.01	63	<1	<0.1	0.02	<0.1	4.8	1.9
WIL24	Willah-1	<0.1	0.41	2.8	1.2	<0.01	76	<1	<0.1	0.02	<0.1	5.1	11.9
WIL25	Willah-1	<0.1	0.35	2.7	<0.5	<0.01	68	<1	<0.1	0.01	<0.1	5.1	13.9
WIL26	Willah-1	<0.1	0.63	1.7	<0.5	<0.01	91	<1	<0.1	0.07	<0.1	6.0	5.7
WIL27	Willah-1	<0.1	1.07	10.7	<0.5	<0.01	81	<1	<0.1	0.07	<0.1	7.3	6.2
WIL28	Willah-1	<0.1	0.32	1.2	<0.5	<0.01	56	<1	<0.1	0.01	<0.1	4.8	3.7
WIL29	Willah-1	<0.1	0.87	1.0	<0.5	<0.01	73	<1	<0.1	0.05	<0.1	6.6	4.9
WIL30	Willah-1	<0.1	0.45	0.6	<0.5	<0.01	80	<1	<0.1	0.03	<0.1	4.9	2.4
WIL31	Willah-1	<0.1	0.40	1.0	<0.5	<0.01	66	<1	<0.1	0.03	<0.1	4.7	3.2

Sample ID	Profile	Ag (ppm)	Al_2O_3 (%)	As (ppm)	Au (ppb)	Ba (%)	Ba (ppm)	Be (ppm)	Bi (ppm)	CaO (%)	Cd (ppm)	Ce (ppm)	Co (ppm)
WIL32	Willah-1	<0.1	0.41	1.4	<0.5	<0.01	113	<1	<0.1	0.03	<0.1	5.7	2.6
WIL33	Willah-1	<0.1	0.36	1.1	<0.5	<0.01	70	<1	<0.1	0.02	<0.1	4.1	2.4
WIL34	Willah-1	<0.1	0.40	1.8	<0.5	<0.01	65	<1	<0.1	0.02	<0.1	4.5	2.4
WIL35	Willah-1	<0.1	0.52	2.8	<0.5	0.01	280	2	<0.1	0.03	<0.1	5.0	2.9
WIL36	Willah-1	<0.1	0.83	1.9	<0.5	<0.01	117	<1	<0.1	0.11	<0.1	8.4	4.1
WIL37	Willah-1	<0.1	1.01	2.7	<0.5	<0.01	147	<1	<0.1	0.11	<0.1	9.7	4.9
WIL38	Willah-1	<0.1	2.21	5.2	<0.5	<0.01	140	<1	<0.1	0.18	<0.1	11.3	11.7
PIA04	Pinagil West-2	<0.1	1.77	2.8	<0.5	<0.01	61	<1	<0.1	1.73	<0.1	8.1	1.0
PIA05	Pinagil West-2	<0.1	1.23	1.8	<0.5	<0.01	44	<1	<0.1	0.87	<0.1	9.1	1.4
PIA06	Pinagil West-2	<0.1	1.33	1.4	<0.5	<0.01	55	<1	<0.1	1.25	<0.1	9.8	0.8
PIA07	Pinagil West-2	<0.1	1.04	1.5	<0.5	<0.01	41	<1	<0.1	1.00	<0.1	13.8	1.0
PIA08	Pinagil West-2	<0.1	0.63	3.1	<0.5	<0.01	61	<1	<0.1	0.65	<0.1	8.2	0.6
PIA09	Pinagil West-2	<0.1	0.59	11.7	<0.5	<0.01	39	<1	<0.1	0.80	<0.1	9.6	0.9
PIA10	Pinagil West-2	<0.1	0.84	40.5	<0.5	<0.01	48	<1	<0.1	0.39	<0.1	12.8	1.2
PIA11	Pinagil West-2	<0.1	1.26	53.1	<0.5	<0.01	69	<1	<0.1	1.79	<0.1	13.8	2.6
PIA12	Pinagil West-2	<0.1	1.42	25.8	<0.5	<0.01	77	<1	<0.1	2.46	<0.1	14.0	1.3
PIA13	Pinagil West-2	<0.1	1.09	53.6	<0.5	<0.01	59	<1	<0.1	3.49	<0.1	13.7	3.6
PIA14	Pinagil West-2	<0.1	1.02	68.3	3.6	<0.01	60	1	<0.1	4.44	<0.1	14.0	5.9
PIA15	Pinagil West-2	<0.1	1.43	45.2	1.6	<0.01	83	<1	<0.1	2.20	<0.1	17.3	7.7
KND01	Koonda-3	<0.1	1.22	2.3	2.1	<0.01	56	<1	<0.1	12.19	<0.1	16.0	0.8
KND02	Koonda-3	<0.1	1.64	2.6	2.1	<0.01	63	<1	<0.1	11.73	<0.1	18.5	1.0
KND03	Koonda-3	<0.1	2.24	4.3	<0.5	<0.01	81	<1	<0.1	2.86	<0.1	15.8	1.4
KND04	Koonda-3	<0.1	0.79	3.2	<0.5	<0.01	71	<1	<0.1	1.05	<0.1	11.9	4.1
KND05	Koonda-3	<0.1	0.77	3.1	0.9	<0.01	61	1	<0.1	0.21	<0.1	9.0	2.5
KND06	Koonda-3	<0.1	0.49	2.5	1.1	<0.01	53	<1	<0.1	0.07	<0.1	6.5	2.5
KND07	Koonda-3	<0.1	0.47	3.2	<0.5	<0.01	47	<1	<0.1	0.36	<0.1	7.2	3.2

Sample ID	Profile	Ag (ppm)	Al_2O_3 (%)	As (ppm)	Au (ppb)	Ba (%)	Ba (ppm)	Be (ppm)	Bi (ppm)	CaO (%)	Cd (ppm)	Ce (ppm)	Co (ppm)
KND08	Koonda-3	<0.1	0.50	3.1	0.5	<0.01	39	<1	<0.1	1.69	<0.1	6.9	2.1
KND09	Koonda-3	<0.1	0.62	3.2	<0.5	<0.01	48	<1	<0.1	3.10	<0.1	9.0	2.6
KND10	Koonda-3	<0.1	1.39	4.0	<0.5	<0.01	86	<1	<0.1	4.03	<0.1	19.2	3.1
KND11	Koonda-3	<0.1	1.17	11.1	<0.5	<0.01	84	<1	<0.1	0.63	<0.1	10.3	5.1
KND12	Koonda-3	<0.1	3.11	24.9	<0.5	<0.01	140	<1	<0.1	2.27	<0.1	20.0	6.1
KND13	Koonda-3	<0.1	2.21	21.0	<0.5	<0.01	113	<1	<0.1	1.65	<0.1	18.0	6.3
BER02	Berrook-1	<0.1	1.53	2.9	<0.5	<0.01	64	<1	<0.1	0.13	<0.1	5.3	1.6
BER03	Berrook-1	<0.1	4.56	6.9	<0.5	<0.01	175	<1	<0.1	2.44	<0.1	20.2	4.7
BER04	Berrook-1	<0.1	3.36	5.3	<0.5	<0.01	163	<1	<0.1	1.84	<0.1	14.2	3.2
BER05	Berrook-1	<0.1	3.56	5.7	<0.5	<0.01	149	2	<0.1	1.89	<0.1	14.8	3.6
BER06	Berrook-1	<0.1	1.21	11.6	<0.5	<0.01	93	<1	<0.1	0.17	<0.1	6.7	1.8
BER07	Berrook-1	<0.1	0.61	2.9	<0.5	<0.01	62	<1	<0.1	0.04	<0.1	4.2	0.8
BER08	Berrook-1	<0.1	0.40	2.3	<0.5	<0.01	44	1	<0.1	<0.01	<0.1	4.9	1.4
BER09	Berrook-1	<0.1	0.37	2.1	<0.5	<0.01	47	<1	<0.1	<0.01	<0.1	3.7	0.9
BER10	Berrook-1	<0.1	0.55	2.2	<0.5	<0.01	67	1	<0.1	0.01	<0.1	6.8	1.6
MAN04	Manangatang-3	<0.1	15.05	9.1	<0.5	0.04	466	<1	0.4	0.13	<0.1	46.4	7.8
MAN05	Manangatang-3	<0.1	1.17	3.8	<0.5	<0.01	83	<1	<0.1	0.02	<0.1	7.5	2.0
MAN06	Manangatang-3	<0.1	4.61	4.2	1.9	0.01	227	<1	0.1	0.19	<0.1	20.1	3.9
MAN07	Manangatang-3	<0.1	13.97	4.1	<0.5	0.05	527	2	0.2	0.10	<0.1	61.3	9.0
MAN08	Manangatang-3	<0.1	10.73	8.9	<0.5	0.05	527	<1	0.2	0.11	<0.1	76.4	7.2
MAN09	Manangatang-3	<0.1	12.98	13.6	2.2	0.04	391	1	0.3	0.13	<0.1	94.4	20.9
MAN10	Manangatang-3	<0.1	12.37	3.4	<0.5	0.03	398	1	0.3	0.10	<0.1	70.7	9.5
MAN11	Manangatang-3	<0.1	16.56	4.1	2.7	0.09	898	2	0.4	0.09	<0.1	89.6	7.6
MAN12	Manangatang-3	<0.1	16.10	3.7	1.1	0.07	691	2	0.4	0.10	<0.1	71.0	7.8
MAN13	Manangatang-3	<0.1	14.96	4.8	2.3	0.04	433	3	0.4	0.10	<0.1	77.7	8.9
MAN14	Manangatang-3	<0.1	14.03	3.5	0.5	0.05	515	2	0.4	0.19	0.1	88.6	18.4

Sample ID	Profile	Ag (ppm)	Al_2O_3 (%)	As (ppm)	Au (ppb)	Ba (%)	Ba (ppm)	Be (ppm)	Bi (ppm)	CaO (%)	Cd (ppm)	Ce (ppm)	Co (ppm)
MAN15	Manangatang-3	<0.1	13.45	7.3	0.9	0.04	393	3	0.4	0.18	<0.1	86.1	11.8
MAN16	Manangatang-3	<0.1	13.34	1.7	4.6	0.04	416	3	0.4	0.16	0.2	83.3	10.5
MAN17	Manangatang-3	<0.1	3.81	6.6	1.5	0.02	173	<1	0.1	0.93	<0.1	30.5	9.9
MAN18	Manangatang-3	<0.1	1.80	175.7	<0.5	0.03	342	<1	<0.1	0.16	<0.1	14.9	20.7
MAN19	Manangatang-3	<0.1	2.04	9.5	1.2	<0.01	104	2	<0.1	0.05	<0.1	21.6	8.7
MAN20	Manangatang-3	<0.1	1.07	10.2	<0.5	<0.01	91	1	<0.1	0.03	<0.1	11.1	7.4
MAN21	Manangatang-3	<0.1	1.21	11.3	1.1	<0.01	95	1	<0.1	0.04	<0.1	12.8	11.4
MAN22	Manangatang-3	<0.1	0.99	11.8	1.0	<0.01	89	2	<0.1	0.03	<0.1	11.6	8.3
MAN23	Manangatang-3	<0.1	2.01	9.4	<0.5	<0.01	135	<1	<0.1	0.05	<0.1	19.2	6.7
MAN24	Manangatang-3	<0.1	3.91	18.5	1.1	<0.01	164	2	<0.1	0.56	<0.1	30.6	8.3
MAN25	Manangatang-3	<0.1	0.92	5.6	<0.5	<0.01	87	1	<0.1	0.02	<0.1	11.7	3.1
MAN26	Manangatang-3	<0.1	1.77	3.7	<0.5	<0.01	151	<1	<0.1	0.05	<0.1	23.3	3.2
MAN27	Manangatang-3	<0.1	1.81	4.0	<0.5	0.01	148	1	<0.1	0.03	<0.1	26.8	2.5
WAL11	Walpamunda-4	<0.1	10.33	3.0	0.9	0.08	795	1	0.1	0.20	<0.1	49.4	19.6
WAL12	Walpamunda-4	<0.1	8.64	4.8	0.7	0.07	719	<1	0.1	0.19	<0.1	45.1	23.7
WAL13	Walpamunda-4	<0.1	0.72	3.5	0.8	0.01	225	<1	<0.1	0.04	<0.1	14.9	9.1
WAL14	Walpamunda-4	<0.1	0.53	2.4	0.8	<0.01	79	<1	<0.1	0.01	<0.1	8.7	3.4
WAL15	Walpamunda-4	<0.1	0.55	5.5	<0.5	0.02	272	<1	<0.1	0.02	<0.1	8.3	7.7
WAL16	Walpamunda-4	<0.1	3.19	6.4	1.0	<0.01	192	<1	<0.1	0.02	<0.1	67.5	5.6
WAL17	Walpamunda-4	<0.1	2.49	5.0	<0.5	0.03	389	1	<0.1	0.04	<0.1	18.0	7.4
WAL18	Walpamunda-4	<0.1	2.76	8.5	<0.5	0.05	518	<1	<0.1	0.05	<0.1	18.7	8.5
MOR04	Morkalla	<0.1	5.49	11.4	<0.5	0.03	290	<1	0.1	5.93	<0.1	28.6	7.2
MOR05	Morkalla	<0.1	0.49	1.0	<0.5	<0.01	52	<1	<0.1	0.53	<0.1	3.5	1.8
MOR06	Morkalla	<0.1	0.21	0.7	0.8	<0.01	54	<1	<0.1	0.07	<0.1	3.7	0.8
MOR07	Morkalla	<0.1	0.28	0.6	0.7	<0.01	58	<1	<0.1	0.05	<0.1	3.6	1.0
MOR08	Morkalla	<0.1	0.57	3.8	0.8	<0.01	57	<1	<0.1	0.58	<0.1	4.9	1.5

Sample ID	Profile	Ag (ppm)	Al_2O_3 (%)	As (ppm)	Au (ppb)	Ba (%)	Ba (ppm)	Be (ppm)	Bi (ppm)	CaO (%)	Cd (ppm)	Ce (ppm)	Co (ppm)
MOR09	Morkalla	<0.1	0.27	1.6	<0.5	<0.01	42	<1	<0.1	0.06	<0.1	3.8	1.2
MOR10	Morkalla	<0.1	0.37	3.4	0.9	<0.01	34	<1	<0.1	0.04	<0.1	5.1	1.2
MOR11	Morkalla	<0.1	0.42	3.3	<0.5	<0.01	45	<1	<0.1	0.06	<0.1	4.4	1.1
MOR12	Morkalla	<0.1	0.39	3.0	<0.5	<0.01	47	<1	<0.1	0.06	<0.1	4.4	1.3
MOR13	Morkalla	<0.1	0.38	3.6	<0.5	<0.01	48	<1	<0.1	0.06	<0.1	3.9	1.8
MOR14	Morkalla	<0.1	0.36	5.0	<0.5	<0.01	39	<1	<0.1	0.13	<0.1	4.4	0.9
MOR15	Morkalla	<0.1	0.29	2.1	<0.5	<0.01	24	<1	<0.1	0.04	<0.1	4.3	1.2
MOR16	Morkalla	<0.1	0.48	2.9	<0.5	<0.01	48	<1	<0.1	0.04	<0.1	4.2	0.8
MOR17	Morkalla	<0.1	0.44	2.4	<0.5	<0.01	45	<1	<0.1	0.03	<0.1	4.9	1.2
MOR18	Morkalla	<0.1	0.44	2.4	0.6	<0.01	43	<1	<0.1	0.04	<0.1	4.3	0.9
MOR19	Morkalla	<0.1	0.43	2.4	<0.5	<0.01	43	<1	<0.1	0.05	<0.1	4.8	1.5
MOR20	Morkalla	<0.1	0.50	6.9	3.0	<0.01	49	<1	<0.1	0.03	<0.1	6.0	1.5
MOR21	Morkalla	<0.1	0.52	6.6	1.0	<0.01	42	<1	<0.1	0.05	<0.1	6.4	1.8
MOR22	Morkalla	<0.1	0.42	6.0	0.6	<0.01	36	<1	<0.1	0.03	<0.1	5.6	1.1
BT01	2/160	<0.1	5.43	13.8	<0.5	<0.01	112	<1	<0.1	0.02	<0.1	9.8	2.2
BT02	2/160	<0.1	5.41	20.0	<0.5	<0.01	66	<1	<0.1	0.02	<0.1	7.3	2.4
BT03	2/160	<0.1	4.87	18.9	<0.5	<0.01	67	<1	<0.1	<0.01	<0.1	8.4	2.7
BT04	2/160	<0.1	4.93	29.8	<0.5	<0.01	68	<1	<0.1	<0.01	<0.1	7.7	3.1
BT05	2/160	<0.1	5.21	16.4	<0.5	<0.01	78	<1	<0.1	<0.01	<0.1	8.5	2.5
BT06	2/160	<0.1	4.83	20.2	<0.5	<0.01	66	<1	<0.1	<0.01	<0.1	8.9	3.1
BT07	2/160	<0.1	4.41	7.5	<0.5	<0.01	109	<1	<0.1	<0.01	<0.1	9.5	2.1
BT08	2/160	<0.1	3.76	54.6	<0.5	<0.01	106	<1	<0.1	<0.01	<0.1	16.0	4.7
BT09	2/160	<0.1	3.67	14.2	<0.5	<0.01	98	<1	<0.1	<0.01	<0.1	14.5	2.6
BT10	2/160	<0.1	3.58	4.2	<0.5	<0.01	111	<1	<0.1	0.01	<0.1	14.6	2.0
BT11	2/160	<0.1	3.36	2.8	<0.5	<0.01	111	<1	<0.1	<0.01	<0.1	12.5	1.7
BT12	2/640	<0.1	3.24	18.4	0.7	<0.01	110	<1	<0.1	<0.01	<0.1	13.4	1.8

Sample ID	Profile	Ag (ppm)	Al_2O_3 (%)	As (ppm)	Au (ppb)	Ba (%)	Ba (ppm)	Be (ppm)	Bi (ppm)	CaO (%)	Cd (ppm)	Ce (ppm)	Co (ppm)
BT13	2/640	<0.1	2.73	11.2	0.6	<0.01	109	<1	<0.1	0.01	<0.1	7.5	1.5
BT14	2/640	<0.1	4.36	19.8	<0.5	<0.01	88	<1	<0.1	0.01	<0.1	9.2	2.1
BT15	2/640	<0.1	4.17	18.7	<0.5	<0.01	70	<1	<0.1	<0.01	<0.1	7.4	2.1
BT16	2/640	<0.1	4.46	21.2	<0.5	<0.01	75	<1	<0.1	0.01	<0.1	7.8	2.4
BT17	2/640	<0.1	4.26	15.3	<0.5	<0.01	82	<1	<0.1	0.02	<0.1	9.3	2.0
BT18	2/640	<0.1	4.58	17.0	<0.5	<0.01	78	<1	<0.1	0.01	<0.1	9.1	1.9
BT19	2/640	<0.1	3.92	33.8	<0.5	<0.01	95	<1	<0.1	0.01	<0.1	11.7	3.5
BT20	2/640	<0.1	4.29	48.4	<0.5	<0.01	104	<1	<0.1	0.01	<0.1	13.6	4.3
BT21	2/640	<0.1	4.13	27.6	<0.5	<0.01	106	1	<0.1	<0.01	<0.1	12.1	3.6
BT22	2/640	<0.1	3.79	15.1	0.6	<0.01	111	<1	<0.1	<0.01	<0.1	11.1	3.2
BT23	2/640	<0.1	4.09	9.1	<0.5	<0.01	133	<1	<0.1	<0.01	<0.1	22.8	3.3
BT24	2/640	<0.1	2.95	5.5	<0.5	<0.01	126	1	<0.1	0.01	<0.1	36.3	2.5
BT25	2/640	<0.1	2.65	7.3	<0.5	<0.01	121	1	<0.1	0.01	<0.1	51.5	2.3
BT26	2/640	<0.1	2.24	71.6	<0.5	<0.01	91	<1	<0.1	0.01	<0.1	42.3	6.9
BT27	2/640	<0.1	2.84	22.0	<0.5	0.01	142	1	<0.1	0.02	<0.1	133.6	6.9
BT28	2/640	<0.1	3.81	32.3	<0.5	0.01	226	<1	<0.1	0.07	<0.1	35.3	9.9
BT29	2/640	<0.1	4.67	22.4	1.5	0.01	254	2	<0.1	0.08	<0.1	48.2	6.1
BT30	2/640	<0.1	3.76	16.9	<0.5	0.02	232	<1	<0.1	0.09	<0.1	31.6	5.6
BT31	2/640	<0.1	4.13	20.3	<0.5	0.02	234	<1	<0.1	0.11	<0.1	34.3	6.9
BT32	2/640	<0.1	5.22	151.3	<0.5	0.01	213	<1	0.1	4.33	0.1	55.7	27.9
BT33	2/880	<0.1	0.45	23.5	1.2	<0.01	13	<1	<0.1	53.23	0.3	4.3	0.6
BT35	2/880	<0.1	1.62	6.0	<0.5	<0.01	61	<1	<0.1	0.04	<0.1	8.9	2.9
BT36	2/880	<0.1	6.47	20.8	2.2	0.01	165	<1	0.3	0.05	<0.1	12.4	2.5
BT37	2/880	<0.1	9.30	21.0	1.2	<0.01	56	1	0.2	0.02	<0.1	8.8	3.4
BT38	2/880	<0.1	5.52	23.2	6.7	<0.01	50	<1	0.2	0.01	<0.1	7.2	2.1
BT39	2/880	<0.1	5.19	20.2	1.3	<0.01	58	1	0.1	0.01	<0.1	7.8	2.5

Sample ID	Profile	Ag (ppm)	Al_2O_3 (%)	As (ppm)	Au (ppb)	Ba (%)	Ba (ppm)	Be (ppm)	Bi (ppm)	CaO (%)	Cd (ppm)	Ce (ppm)	Co (ppm)
BT40	2/880	<0.1	4.05	16.5	1.5	<0.01	67	<1	<0.1	0.01	<0.1	7.3	2.7
BT41	2/880	<0.1	4.26	13.9	<0.5	<0.01	60	<1	<0.1	0.01	<0.1	9.0	2.3
BT42	2/880	<0.1	4.45	18.1	0.8	<0.01	69	<1	<0.1	0.02	<0.1	21.8	2.9
BT43	2/880	<0.1	4.44	32.6	<0.5	<0.01	96	<1	<0.1	0.02	<0.1	44.7	5.3
BT44	2/880	<0.1	3.81	13.2	1.2	<0.01	106	<1	<0.1	0.03	<0.1	48.2	4.2
BT45	2/880	<0.1	3.90	14.9	2.2	<0.01	121	2	<0.1	0.03	<0.1	83.4	4.8
MBR06	83MBR31	0.2	7.00	30.2	0.7	0.01	206	<1	0.1	3.45	<0.1	14.4	3.8
MBR07	83MBR31	<0.1	2.43	43.8	1.0	<0.01	78	<1	<0.1	15.98	<0.1	16.6	2.2
MBR08	83MBR31	<0.1	4.15	19.8	<0.5	<0.01	133	<1	<0.1	11.66	<0.1	15.0	2.9
MBR09	83MBR31	<0.1	3.05	29.7	0.9	<0.01	108	1	<0.1	11.23	<0.1	15.6	3.0
MBR10	83MBR31	<0.1	2.59	29.0	<0.5	<0.01	108	<1	<0.1	12.57	<0.1	14.0	2.7
MBR11	83MBR31	<0.1	3.66	14.5	0.8	0.01	188	2	<0.1	23.30	<0.1	18.0	8.4
MBR12	83MBR31	<0.1	3.18	15.8	1.5	0.01	139	1	<0.1	29.60	<0.1	16.1	3.9
MBR13	83MBR31	<0.1	2.33	11.7	0.9	0.07	726	2	<0.1	34.51	<0.1	13.3	4.1
MBR14	83MBR31	<0.1	5.01	17.5	1.4	0.02	249	1	0.1	21.87	<0.1	16.8	4.2
MBR15	83MBR31	<0.1	2.40	9.3	1.8	0.01	137	<1	<0.1	32.44	<0.1	14.4	3.4
MBR16	83MBR31	<0.1	0.72	19.8	1.2	<0.01	42	<1	<0.1	50.73	<0.1	8.1	1.3
FT04	M-12	<0.1	5.71	17.1	1.4	0.02	317	2	<0.1	0.93	<0.1	15.9	4.3
FT05	M-12	<0.1	2.37	13.5	<0.5	<0.01	82	<1	<0.1	0.31	<0.1	6.5	2.5
FT06	M-12	<0.1	3.45	62.0	0.6	0.07	713	<1	0.1	0.23	<0.1	9.2	4.2
FT07	M-12	<0.1	2.54	19.0	0.7	<0.01	143	<1	<0.1	0.07	<0.1	6.9	3.0
FT08	M-12	<0.1	2.23	34.3	<0.5	<0.01	102	<1	<0.1	0.09	<0.1	6.3	2.9
FT09	M-12	<0.1	1.71	26.5	0.6	<0.01	74	<1	<0.1	0.36	<0.1	5.8	2.3
FT10	M-12	<0.1	2.03	312.2	1.2	<0.01	78	<1	0.2	0.10	<0.1	10.0	5.2
FT11	M-12	<0.1	2.72	80.7	1.0	<0.01	105	<1	0.1	0.20	<0.1	12.1	3.5
FT12	M-12	<0.1	2.11	75.2	0.5	<0.01	88	<1	<0.1	0.05	<0.1	8.7	3.8

Sample ID	Profile	Ag (ppm)	Al_2O_3 (%)	As (ppm)	Au (ppb)	Ba (%)	Ba (ppm)	Be (ppm)	Bi (ppm)	CaO (%)	Cd (ppm)	Ce (ppm)	Co (ppm)
FT13	M-12	<0.1	2.05	196.9	1.0	<0.01	101	1	0.1	0.03	<0.1	11.7	4.4
FT14	M-12	<0.1	5.73	80.6	<0.5	0.02	122	2	<0.1	0.06	<0.1	129.1	10.4
FT15	M-12	<0.1	5.28	69.4	1.2	0.02	98	3	<0.1	3.20	<0.1	242.0	21.4
NGA01	M-138	<0.1	9.13	5.4	2.0	<0.01	93	<1	<0.1	0.11	<0.1	33.2	7.3
NGA02	M-138	<0.1	8.53	5.7	1.1	0.07	750	3	0.1	1.28	<0.1	40.3	8.1
NGA03	M-138	<0.1	13.01	6.2	1.7	0.02	247	2	0.2	0.28	<0.1	55.6	8.8
NGA04	M-138	<0.1	14.84	5.2	2.7	0.04	486	2	0.2	0.27	<0.1	30.7	8.7
NGA05	M-138	<0.1	9.38	5.5	2.8	<0.01	131	<1	0.1	0.14	<0.1	21.2	6.9
NGA06	M-138	<0.1	7.10	5.5	2.1	<0.01	75	<1	<0.1	0.11	<0.1	12.3	2.6
NGA07	M-138	<0.1	7.85	4.4	3.0	<0.01	116	2	0.1	0.14	<0.1	14.5	4.0
NGA08	M-138	<0.1	7.37	2.6	1.2	<0.01	88	<1	0.1	0.15	<0.1	13.7	3.4
NGA09	M-138	<0.1	7.32	2.6	2.7	<0.01	92	<1	<0.1	0.14	<0.1	13.0	3.0
NGA10	M-138	<0.1	6.36	3.0	1.0	<0.01	106	1	<0.1	0.11	<0.1	16.8	2.8
NGA11	M-138	<0.1	7.51	4.0	0.5	<0.01	124	<1	0.1	0.24	<0.1	21.1	4.4
NGA12	M-138	<0.1	5.04	3.0	1.6	<0.01	138	<1	<0.1	0.17	<0.1	11.9	1.6
NGA13	M-138	<0.1	5.49	2.3	1.4	<0.01	102	<1	<0.1	0.16	<0.1	11.9	2.2
NGA14	M-138	<0.1	3.82	2.8	4.1	<0.01	69	<1	<0.1	0.09	<0.1	9.0	1.8
NGA15	M-138	<0.1	4.83	1.7	2.3	<0.01	110	<1	<0.1	0.08	<0.1	10.1	2.4
NGA16	M-138	<0.1	2.38	2.0	1.7	<0.01	51	<1	<0.1	0.07	<0.1	7.9	1.1
NGA17	M-138	<0.1	2.06	1.0	2.8	<0.01	50	<1	<0.1	0.06	<0.1	8.1	1.2
NGA18	M-138	<0.1	1.65	1.3	2.7	<0.01	41	<1	<0.1	0.06	<0.1	7.5	1.1
NGA19	M-138	<0.1	0.99	1.1	0.9	<0.01	37	<1	<0.1	0.06	<0.1	7.0	1.0
NGA20	M-138	<0.1	1.04	1.0	2.2	<0.01	38	<1	<0.1	0.04	<0.1	6.2	0.9
NGA21	M-138	<0.1	0.41	0.7	2.0	<0.01	36	<1	<0.1	<0.01	<0.1	6.4	0.7
NGA22	M-138	<0.1	0.88	1.4	1.9	<0.01	36	<1	<0.1	0.05	<0.1	6.4	1.0
NGA23	M-138	<0.1	0.72	1.1	<0.5	<0.01	32	<1	<0.1	0.03	<0.1	4.8	0.8

Sample ID	Profile	Ag (ppm)	Al_2O_3 (%)	As (ppm)	Au (ppb)	Ba (%)	Ba (ppm)	Be (ppm)	Bi (ppm)	CaO (%)	Cd (ppm)	Ce (ppm)	Co (ppm)
NGA24	M-138	<0.1	0.66	0.7	3.3	<0.01	33	<1	<0.1	0.04	<0.1	5.4	0.7
NGA25	M-138	<0.1	0.74	0.8	3.5	<0.01	42	<1	<0.1	0.03	<0.1	6.3	0.8
NGA26	M-138	<0.1	0.49	1.0	2.5	<0.01	33	<1	<0.1	0.02	<0.1	4.9	0.5
NGA27	M-138	<0.1	0.69	0.7	1.2	<0.01	39	<1	<0.1	0.06	<0.1	5.1	0.6
NGA28	M-138	<0.1	0.78	0.6	2.6	<0.01	34	<1	<0.1	0.06	<0.1	6.5	0.8
NGA29	M-138	<0.1	0.44	0.9	2.1	<0.01	37	<1	<0.1	0.02	<0.1	4.8	0.7
NGA30	M-138	<0.1	0.41	1.3	4.0	<0.01	34	<1	<0.1	0.01	<0.1	5.8	0.6
NGA31	M-138	<0.1	0.47	1.1	2.1	<0.01	30	<1	0.2	0.03	<0.1	5.0	0.5
NGA32	M-138	<0.1	0.66	0.7	1.7	<0.01	34	<1	<0.1	0.06	<0.1	6.7	0.9
NGA33	M-138	<0.1	0.63	1.0	4.0	<0.01	40	<1	<0.1	0.04	<0.1	5.4	0.8
NGA34	M-138	<0.1	0.50	13.7	1.7	<0.01	29	<1	<0.1	0.03	<0.1	7.1	3.3
NGA35	M-138	<0.1	0.93	20.0	1.5	<0.01	44	<1	<0.1	0.04	<0.1	8.2	2.1
NGA36	M-138	<0.1	0.70	3.0	2.1	<0.01	39	<1	<0.1	0.05	<0.1	6.3	0.9
NGA37	M-138	<0.1	1.00	5.6	3.1	<0.01	54	<1	<0.1	0.06	<0.1	7.6	1.2
NGA38	M-138	<0.1	3.04	43.4	2.3	<0.01	101	<1	<0.1	0.30	<0.1	41.7	38.9
NGA39	M-138	<0.1	1.65	156.0	2.1	<0.01	72	1	<0.1	0.48	<0.1	25.8	37.9
TEM03	M-155	<0.1	3.63	2.2	<0.5	<0.01	83	<1	0.1	0.03	<0.1	6.9	2.4
TEM04	M-155	<0.1	3.99	2.6	1.8	<0.01	168	<1	<0.1	0.03	<0.1	8.6	2.0
TEM05	M-155	<0.1	3.34	4.9	1.3	<0.01	92	<1	<0.1	0.02	<0.1	6.5	2.1
TEM06	M-155	<0.1	1.06	8.9	2.4	<0.01	103	<1	<0.1	0.03	<0.1	4.4	1.5
TEM07	M-155	<0.1	0.62	4.2	1.1	<0.01	45	<1	<0.1	0.03	<0.1	4.8	1.3
TEM08	M-155	<0.1	0.66	4.4	<0.5	<0.01	51	<1	<0.1	0.02	<0.1	4.4	1.0
TEM09	M-155	<0.1	0.58	2.8	1.6	<0.01	43	<1	<0.1	0.02	<0.1	4.9	1.4
TEM10	M-155	<0.1	0.73	4.3	<0.5	<0.01	47	<1	<0.1	0.02	<0.1	4.8	1.2
TEM11	M-155	<0.1	0.75	4.4	<0.5	<0.01	52	<1	<0.1	0.02	<0.1	4.7	1.4
TEM12	M-155	<0.1	2.29	7.8	<0.5	0.01	230	<1	0.1	0.21	<0.1	10.4	1.7

Sample ID	Profile	Ag (ppm)	Al_2O_3 (%)	As (ppm)	Au (ppb)	Ba (%)	Ba (ppm)	Be (ppm)	Bi (ppm)	CaO (%)	Cd (ppm)	Ce (ppm)	Co (ppm)
TEM13	M-155	<0.1	1.73	4.5	<0.5	<0.01	96	<1	<0.1	0.16	<0.1	8.5	1.9
TEM14	M-155	<0.1	3.30	14.1	1.2	<0.01	99	<1	<0.1	0.04	<0.1	10.7	4.6
TEM15	M-155	<0.1	6.41	27.2	<0.5	<0.01	85	<1	<0.1	0.06	<0.1	44.5	11.1
NDA01	Nadda-1	<0.1	0.74	4.8	1.0	<0.01	60	<1	<0.1	1.13	<0.1	5.5	1.7
NDA02	Nadda-1	<0.1	0.55	3.9	1.0	<0.01	63	<1	<0.1	1.26	<0.1	4.4	1.4
NDA03	Nadda-1	1.0	0.66	7.2	1.0	<0.01	47	2	<0.1	3.80	0.1	8.0	2.6
NDA04	Nadda-1	<0.1	0.50	5.2	0.6	<0.01	61	<1	<0.1	0.17	<0.1	5.4	1.4
OAK03	Oakvale-3	<0.1	1.38	1.2	<0.5	<0.01	106	<1	<0.1	0.11	<0.1	9.4	2.3
OAK04	Oakvale-3	<0.1	1.90	3.1	1.6	<0.01	147	<1	<0.1	0.05	<0.1	19.3	3.0
OAK05	Oakvale-3	<0.1	3.04	1.5	1.6	<0.01	122	<1	<0.1	1.97	<0.1	10.2	1.5
OAK06	Oakvale-3	<0.1	4.04	1.0	1.1	<0.01	140	2	<0.1	0.06	<0.1	19.8	1.4
OAK07	Oakvale-3	<0.1	2.38	1.0	2.0	0.01	176	<1	<0.1	0.04	<0.1	16.4	1.5
OAK08	Oakvale-3	<0.1	5.14	2.4	<0.5	<0.01	132	<1	<0.1	0.65	<0.1	16.9	2.5
OAK09	Oakvale-3	<0.1	2.69	2.1	1.9	<0.01	104	<1	<0.1	0.16	<0.1	14.3	3.4
OAK10	Oakvale-3	<0.1	0.97	1.6	<0.5	<0.01	85	<1	<0.1	0.07	<0.1	8.2	2.3
OAK11	Oakvale-3	<0.1	3.57	7.3	0.9	<0.01	173	2	<0.1	0.12	<0.1	19.5	11.5
OAK12	Oakvale-3	<0.1	16.43	6.5	1.5	0.02	246	<1	<0.1	0.11	<0.1	41.0	7.0
OAK13	Oakvale-3	<0.1	16.51	10.4	<0.5	0.02	214	<1	0.1	0.12	<0.1	39.6	8.1
OAK14	Oakvale-3	<0.1	18.71	9.7	1.2	0.02	228	<1	0.2	0.14	<0.1	77.0	8.7
OAK15	Oakvale-3	<0.1	20.37	15.7	2.3	0.02	214	<1	0.1	0.16	<0.1	68.7	6.9
OAK16	Oakvale-3	<0.1	19.04	14.1	8.1	0.02	183	<1	0.2	0.18	<0.1	70.8	6.9
OAK17	Oakvale-3	<0.1	17.28	36.3	2.0	0.02	214	<1	0.2	0.15	<0.1	66.7	7.9
OAK18	Oakvale-3	<0.1	17.99	45.7	2.6	0.02	201	<1	0.2	0.16	<0.1	56.6	7.8
OAK19	Oakvale-3	<0.1	14.28	14.8	1.3	0.02	172	<1	0.1	0.14	<0.1	57.4	5.8
OAK20	Oakvale-3	<0.1	17.42	6.4	1.9	0.01	193	<1	0.1	0.15	<0.1	58.0	5.5
OAK21	Oakvale-3	<0.1	6.08	2.5	3.6	<0.01	162	<1	<0.1	0.08	<0.1	22.2	2.7

Sample ID	Profile	Ag (ppm)	Al_2O_3 (%)	As (ppm)	Au (ppb)	Ba (%)	Ba (ppm)	Be (ppm)	Bi (ppm)	CaO (%)	Cd (ppm)	Ce (ppm)	Co (ppm)
PIN04	Pinnaroo-1	<0.1	0.67	1.6	2.8	<0.01	58	<1	<0.1	0.09	<0.1	5.5	1.7
PIN05	Pinnaroo-1	<0.1	1.36	2.6	2.3	<0.01	73	<1	<0.1	0.06	<0.1	7.8	2.0
PIN06	Pinnaroo-1	<0.1	0.55	12.1	1.1	<0.01	49	<1	<0.1	0.03	<0.1	14.2	1.7
PIN07	Pinnaroo-1	<0.1	0.47	2.0	1.4	<0.01	47	<1	<0.1	0.02	<0.1	18.2	1.8
PIN08	Pinnaroo-1	<0.1	0.55	2.5	1.5	<0.01	58	<1	<0.1	0.04	<0.1	22.7	2.0
PIN09	Pinnaroo-1	<0.1	0.66	5.9	1.0	<0.01	64	<1	<0.1	0.06	<0.1	14.6	2.5
PIN10	Pinnaroo-1	<0.1	4.12	3.7	1.5	<0.01	149	<1	<0.1	0.12	<0.1	31.8	3.5
PV02	PV-11	<0.1	1.56	2.4	0.6	<0.01	66	<1	0.1	0.07	<0.1	5.8	2.2
PV03	PV-11	<0.1	1.67	2.1	1.6	<0.01	126	<1	<0.1	0.05	<0.1	8.6	2.2
PV04	PV-11	<0.1	2.10	2.7	0.6	<0.01	66	<1	<0.1	0.07	<0.1	8.8	2.0
PV05	PV-11	<0.1	0.60	1.9	1.9	<0.01	47	<1	<0.1	0.04	<0.1	5.2	1.8
PV06	PV-11	<0.1	0.39	2.6	0.8	<0.01	53	<1	<0.1	0.02	<0.1	5.0	2.0
PV07	PV-11	<0.1	0.59	5.4	1.1	<0.01	72	<1	<0.1	0.03	<0.1	7.0	2.6
PV08	PV-11	<0.1	0.42	2.7	<0.5	<0.01	58	<1	<0.1	0.05	<0.1	5.4	2.4
PV09	PV-11	<0.1	0.55	2.8	1.2	<0.01	89	<1	<0.1	0.03	<0.1	6.3	2.3
RB02	PV-11	<0.1	3.22	65.4	0.7	<0.01	46	<1	0.1	0.04	<0.1	12.0	3.0
RB03	PV-11	<0.1	20.40	20.4	2.4	<0.01	81	2	0.2	0.20	<0.1	48.8	12.4
RB04	PV-11	<0.1	16.99	66.4	0.9	<0.01	95	2	0.2	4.51	<0.1	37.0	16.3
RB05	PV-11	<0.1	12.47	54.4	<0.5	0.02	116	1	0.2	24.56	<0.1	71.6	15.6
KI1_01	RC86KI-1	0.4	12.71	4.1	<0.5	0.03	317	<1	0.1	0.25	0.1	76.7	18.2
KI1_02	RC86KI-1	0.2	8.96	3.8	0.5	<0.01	103	<1	0.1	0.08	0.2	26.8	6.8
KI1_03	RC86KI-1	0.3	10.98	3.8	0.7	0.01	136	2	0.1	0.13	0.1	47.6	10.3
KI1_04	RC86KI-1	0.2	11.18	2.4	<0.5	<0.01	136	<1	0.1	1.21	<0.1	26.0	6.7
KI1_05	RC86KI-1	0.2	9.63	3.7	1.1	0.02	163	<1	<0.1	3.67	0.2	39.8	6.7
KI1_06	RC86KI-1	0.4	11.86	8.0	<0.5	0.02	209	2	0.1	5.03	0.3	49.3	8.0
KI1_07	RC86KI-1	0.2	11.51	3.3	0.7	<0.01	97	<1	0.1	1.21	0.2	37.7	6.0

Sample ID	Profile	Ag (ppm)	Al_2O_3 (%)	As (ppm)	Au (ppb)	Ba (%)	Ba (ppm)	Be (ppm)	Bi (ppm)	CaO (%)	Cd (ppm)	Ce (ppm)	Co (ppm)
KI1_08	RC86KI-1	0.2	5.33	2.2	<0.5	<0.01	61	<1	<0.1	1.43	0.1	22.8	3.2
KI1_09	RC86KI-1	0.2	4.91	1.1	<0.5	<0.01	73	<1	<0.1	0.30	0.1	21.4	3.0
KI1_12	RC86KI-1	<0.1	19.19	2.8	<0.5	0.01	108	<1	0.2	0.33	<0.1	119.8	8.6
KI1_13	RC86KI-1	<0.1	24.01	30.4	<0.5	0.03	94	2	0.3	1.31	0.2	219.0	22.6
KI10_01	RC86KI-10	<0.1	12.05	19.3	<0.5	0.01	110	3	0.1	7.32	0.1	75.9	19.2
KI10_02	RC86KI-10	<0.1	7.71	16.0	<0.5	0.02	225	<1	0.1	3.05	<0.1	102.2	24.1
KI10_03	RC86KI-10	<0.1	19.07	9.7	0.6	0.10	441	7	0.4	0.79	<0.1	682.3	15.1
KI10_04	RC86KI-10	<0.1	11.94	22.7	<0.5	0.02	127	2	0.2	11.78	0.3	189.6	41.4
KI10_05	RC86KI-10	<0.1	6.09	14.6	1.5	<0.01	69	<1	<0.1	29.75	0.2	58.3	15.1
OLC01	Overland Corner	<0.1	0.33	24.9	<0.5	0.06	689	<1	<0.1	0.13	<0.1	1.6	1.1
OLC02	Overland Corner	<0.1	0.51	182.1	<0.5	<0.01	93	5	<0.1	0.74	<0.1	7.6	6.4
OLC03	Overland Corner	<0.1	0.27	128.7	<0.5	<0.01	48	<1	<0.1	0.17	<0.1	2.1	6.2
OLC04	Overland Corner	<0.1	2.31	110.2	<0.5	0.02	183	3	<0.1	0.27	<0.1	16.5	5.3
OLC05	Overland Corner	<0.1	3.68	1.7	<0.5	0.01	178	<1	<0.1	0.07	<0.1	8.2	1.9
OLC06	Overland Corner	<0.1	4.79	163.1	<0.5	0.06	577	<1	<0.1	0.08	<0.1	10	3.9
OLC07	Overland Corner	<0.1	1.88	6.4	0.8	0.04	427	<1	<0.1	14.42	<0.1	13.2	2.1
OLC08	Overland Corner	<0.1	1.8	8.4	<0.5	0.03	256	1	<0.1	38.49	<0.1	24.9	6.8
OLC09	Overland Corner	<0.1	0.69	5.3	<0.5	<0.01	14	<1	<0.1	48.6	0.2	6.9	0.8
OLC10	Overland Corner	<0.1	0.56	155.3	<0.5	0.01	97	13	<0.1	0.25	<0.1	29.5	2
OLC11	Overland Corner	<0.1	0.98	18.7	0.7	<0.01	32	<1	<0.1	50.76	<0.1	24.8	6.7
OLC12	Overland Corner	<0.1	2.8	52.6	<0.5	<0.01	42	5	<0.1	45.02	0.3	40.3	18.8

Sample ID	Cr_2O_3 (%)	Cs (ppm)	Cu (ppm)	Dy (ppm)	Er (ppm)	Eu (ppm)	Fe_2O_3 (%)	Ga (ppm)	Gd (ppm)	Hf (ppm)	Hg (ppm)	Ho (ppm)	K_2O (%)
LYR01	0.004	1.5	1.7	1.05	0.70	0.23	1.74	2.9	1.01	3.6	<0.01	0.23	0.30
LYR02	<0.001	0.5	0.9	0.46	0.30	0.05	1.06	1.5	0.41	0.9	<0.01	0.09	0.16
LYR03	0.003	0.6	1.0	0.49	0.38	0.04	9.44	1.5	0.50	0.9	<0.01	0.11	0.35
LYR04	0.004	0.4	1.0	0.43	0.26	0.10	1.15	1.6	0.41	1.1	<0.01	0.12	0.24
LYR05	0.003	0.5	1.7	0.49	0.38	0.05	2.69	1.2	0.31	1.0	<0.01	0.10	0.37
LYR06	0.004	0.9	1.5	0.39	0.26	0.09	1.58	2.3	0.33	1.4	<0.01	0.08	0.34
LYR07	<0.001	0.6	2.5	0.50	0.37	0.09	1.69	2.2	0.45	1.9	<0.01	0.11	0.30
LYR08	0.003	0.7	1.3	0.34	0.24	0.08	1.47	2.6	0.34	0.8	<0.01	0.08	0.25
LYR09	0.003	0.7	1.9	0.54	0.36	0.12	10.00	3.1	0.52	1.7	<0.01	0.11	0.21
LYR10	0.003	0.8	1.7	0.52	0.35	0.11	3.42	2.3	0.46	2.3	<0.01	0.11	0.23
LYR11	<0.001	1.0	2.7	6.93	4.31	1.30	3.25	1.2	6.34	0.9	<0.01	1.51	0.17
LYR12	0.001	0.9	2.2	0.75	0.52	0.16	0.94	2.0	0.65	2.0	<0.01	0.15	0.58
LYR13	0.004	1.4	2.3	1.13	0.80	0.21	1.40	2.9	0.98	4.0	<0.01	0.22	0.65
LYR14	0.002	1.3	6.5	1.42	0.76	0.25	1.76	3.5	1.00	1.8	<0.01	0.28	0.29
LYR15	0.009	1.4	7.0	1.62	0.94	0.24	7.71	12.0	1.25	3.9	<0.01	0.31	0.18
LYR16	0.007	1.3	2.1	0.94	0.65	0.22	1.41	3.0	0.94	3.0	<0.01	0.21	0.66
LCP01	0.007	1.8	2.1	1.70	0.80	0.58	1.97	5.0	1.93	1.5	<0.01	0.31	0.87
LCP02	<0.001	1.0	1.2	0.87	0.50	0.27	1.20	2.6	0.91	0.8	<0.01	0.18	0.50
LCP03	0.006	0.8	0.8	1.71	1.00	0.43	1.58	2.4	1.78	1.0	0.02	0.35	0.52
LCP04	0.007	1.1	1.3	2.03	1.25	0.46	4.07	3.4	2.00	4.9	0.01	0.45	0.77
LCP05	0.016	0.9	1.8	3.53	2.63	0.36	4.68	3.5	2.26	19.0	<0.01	0.77	0.63
LCP06	0.001	0.6	1.4	1.27	0.70	0.20	1.15	1.5	0.91	2.2	<0.01	0.24	0.40
LCP07	0.004	0.9	1.6	1.08	0.61	0.37	1.32	2.7	1.36	2.8	<0.01	0.17	0.79
LCP08	0.004	0.9	1.9	0.84	0.41	0.30	2.22	2.2	1.06	1.3	<0.01	0.12	0.69
LCP09	0.004	1.4	2.1	0.56	0.39	0.20	1.84	3.7	0.60	1.2	<0.01	0.12	1.12
LCP10	0.003	0.8	1.7	0.54	0.32	0.11	1.64	2.4	0.48	1.0	<0.01	0.11	0.64

Sample ID	Cr_2O_3 (%)	Cs (ppm)	Cu (ppm)	Dy (ppm)	Er (ppm)	Eu (ppm)	Fe_2O_3 (%)	Ga (ppm)	Gd (ppm)	Hf (ppm)	Hg (ppm)	Ho (ppm)	K_2O (%)
LCP11	0.001	0.5	1.0	0.31	0.21	0.09	0.70	1.2	0.38	0.5	<0.01	0.08	0.58
LCP12	0.002	0.4	1.4	0.43	0.29	0.08	0.81	1.4	0.34	0.7	<0.01	0.09	0.46
LCP13	<0.001	0.4	1.6	0.99	0.71	0.13	3.12	0.9	0.89	0.7	<0.01	0.24	0.13
LCP14	0.002	0.4	1.2	0.75	0.48	0.03	0.77	0.7	0.52	0.8	<0.01	0.15	0.12
LCP15	0.003	0.4	2.2	2.57	1.61	0.39	11.68	1.3	2.21	1.1	<0.01	0.56	0.16
LCP16	0.004	0.7	1.4	0.71	0.45	0.05	1.45	1.8	0.47	1.2	<0.01	0.16	0.26
LCP17	<0.001	0.7	1.0	0.63	0.34	0.04	1.02	1.4	0.41	1.0	<0.01	0.13	0.33
LCP18	<0.001	0.7	1.9	0.58	0.37	0.05	1.05	2.0	0.44	1.1	<0.01	0.12	0.15
LCP19	0.003	0.1	7.0	9.00	5.54	2.08	1.35	0.8	10.19	0.6	<0.01	2.01	0.04
LCP20	<0.001	<0.1	2.0	2.01	1.31	0.36	0.39	<0.5	2.18	0.2	0.02	0.43	<0.01
LCP21	0.016	2.3	4.7	1.33	0.92	0.25	3.24	8.8	1.17	3.0	<0.01	0.28	0.85
LCP22	0.003	1.3	1.6	0.68	0.35	0.19	1.78	3.0	0.59	0.7	<0.01	0.14	0.99
LCP23	0.005	0.5	1.3	0.45	0.26	0.06	0.92	4.6	0.44	0.7	<0.01	0.08	0.58
RC01	0.003	0.3	1.2	0.45	0.28	0.02	0.52	8.6	0.35	1.7	<0.01	0.11	0.03
RC02	0.005	0.4	1.3	0.39	0.35	0.04	1.30	11.9	0.38	2.6	<0.01	0.13	0.03
RC03	0.005	<0.1	0.9	0.86	0.79	0.08	0.73	3.1	0.50	4.2	<0.01	0.23	0.01
RC04	0.002	0.7	1.3	0.68	0.57	0.08	1.93	5.7	0.52	3.1	<0.01	0.17	0.11
RC05	0.006	1.3	2.9	0.95	0.70	0.16	2.48	6.7	0.82	3.4	<0.01	0.23	0.31
RC06	0.006	1.4	4.4	1.06	0.73	0.19	2.65	6.9	0.89	4.1	<0.01	0.23	0.40
RC07	0.008	2.6	9.4	1.63	1.17	0.33	4.40	12.2	1.34	4.7	<0.01	0.35	0.79
RC08	0.006	2.4	10.5	1.64	1.12	0.33	3.84	10.8	1.40	4.9	<0.01	0.32	0.75
RC09	0.007	3.3	13.6	1.82	1.30	0.44	5.19	14.7	1.78	5.0	<0.01	0.41	1.04
RC10	0.010	3.6	13.1	1.96	1.35	0.49	4.69	16.2	1.95	5.2	<0.01	0.45	1.16
RC11	0.007	3.6	13.9	2.96	1.42	1.53	5.15	14.3	4.80	5.3	<0.01	0.53	1.10
RC12	0.003	0.6	4.1	0.53	0.33	0.06	1.22	2.7	0.40	1.0	<0.01	0.11	0.17
RC13	0.008	1.8	15.3	2.35	1.65	0.49	18.49	10.7	2.15	4.4	<0.01	0.55	0.53

Sample ID	Cr_2O_3 (%)	Cs (ppm)	Cu (ppm)	Dy (ppm)	Er (ppm)	Eu (ppm)	Fe_2O_3 (%)	Ga (ppm)	Gd (ppm)	Hf (ppm)	Hg (ppm)	Ho (ppm)	K_2O (%)
RC14	0.004	0.5	8.1	1.09	0.83	0.13	10.59	5.6	0.75	3.2	<0.01	0.24	0.10
RC15	0.010	2.6	8.6	1.42	1.05	0.31	4.37	11.7	1.29	4.8	<0.01	0.34	0.78
NY01	0.004	1.1	2.2	1.50	1.22	0.17	2.46	5.8	1.06	6.2	<0.01	0.36	0.13
NY02	0.008	1.3	1.9	1.46	1.13	0.18	2.46	6.7	1.07	6.0	<0.01	0.32	0.15
NY07	0.004	1.0	1.9	1.57	1.24	0.12	3.01	6.7	0.83	7.9	<0.01	0.35	0.14
NY08	0.003	2.7	5.3	1.45	1.05	0.22	3.47	10.5	1.14	5.9	<0.01	0.31	0.80
NY09	0.006	0.8	1.6	1.21	1.04	0.12	2.20	5.1	0.80	6.5	<0.01	0.31	0.13
NY10	0.005	3.1	4.8	1.54	1.21	0.23	3.56	10.6	1.27	6.0	<0.01	0.37	0.84
GRQ01	0.009	1.2	1.5	1.84	1.20	0.35	1.97	6.5	1.78	4.7	<0.01	0.38	0.39
GRQ02	0.004	1.4	1.5	1.11	0.69	0.26	1.61	7.4	1.30	2.4	<0.01	0.23	0.50
GRQ03	0.002	1.9	0.9	1.27	0.80	0.22	1.10	7.0	1.23	2.8	<0.01	0.24	0.44
GRQ04	0.006	1.2	0.9	1.71	1.20	0.25	1.12	5.4	1.87	6.2	<0.01	0.36	0.31
GRQ05	0.003	0.7	0.9	1.45	1.12	0.20	0.62	3.6	1.67	6.3	<0.01	0.31	0.17
GRQ06	0.032	0.6	0.9	1.04	0.65	0.14	0.51	3.5	1.16	3.9	<0.01	0.21	0.14
GRQ07	0.029	0.8	2.0	19.61	12.65	1.22	1.38	4.7	20.48	102.3	<0.01	3.86	0.16
GRQ08	0.004	1.2	1.5	1.25	0.86	0.21	0.97	5.5	1.30	3.1	<0.01	0.24	0.37
GRQ09	0.046	1.5	2.0	20.33	15.56	1.08	1.82	8.0	18.08	102.8	<0.01	4.36	0.35
GRQ10	0.013	1.2	2.4	2.96	2.04	0.29	4.53	12.8	2.11	14.9	<0.01	0.59	0.28
GRQ11	0.005	1.4	1.5	1.25	0.63	0.23	1.71	7.5	1.21	1.9	<0.01	0.21	0.49
SRQ01	<0.001	<0.1	0.8	0.54	0.40	0.10	3.46	0.6	0.45	0.3	<0.01	0.13	<0.01
SRQ02	0.003	0.1	1.1	1.11	0.97	0.16	3.22	0.7	0.89	0.3	<0.01	0.27	<0.01
SRQ03	0.006	0.2	1.4	5.34	4.48	0.77	4.23	1.0	4.58	1.0	<0.01	1.25	0.02
SRQ04	0.028	2.5	8.8	2.92	1.47	0.83	9.49	6.4	3.38	8.1	0.04	0.52	3.17
SRQ05	0.008	0.4	1.3	0.73	0.40	0.11	1.86	1.1	0.63	1.4	<0.01	0.14	0.48
SRQ06	0.003	0.4	1.5	1.05	0.70	0.13	2.70	0.9	0.93	1.1	<0.01	0.23	0.18
SRQ07	0.006	0.3	2.5	1.32	1.09	0.14	2.97	1.3	1.05	8.4	0.02	0.32	0.21

Sample ID	Cr_2O_3 (%)	Cs (ppm)	Cu (ppm)	Dy (ppm)	Er (ppm)	Eu (ppm)	Fe_2O_3 (%)	Ga (ppm)	Gd (ppm)	Hf (ppm)	Hg (ppm)	Ho (ppm)	K_2O (%)
SRQ08	0.002	0.3	1.2	0.92	0.56	0.07	1.38	1.0	0.61	1.3	<0.01	0.17	0.16
SRQ09	0.004	0.4	1.0	1.09	0.57	0.33	1.07	1.1	1.15	0.8	<0.01	0.18	0.35
UQ02	0.003	0.3	0.7	0.77	0.43	0.21	2.00	4.0	0.91	1.4	<0.01	0.15	0.06
UQ03	0.008	1.3	0.4	1.67	1.15	0.27	0.56	8.2	1.53	4.1	<0.01	0.34	0.36
UQ04	0.007	1.2	0.4	2.55	1.48	0.32	2.05	9.3	1.94	5.0	<0.01	0.45	0.40
UQ05	0.006	1.3	0.6	3.92	2.29	0.65	6.34	7.9	3.51	3.6	0.02	0.69	0.31
UQ06	0.005	1.6	0.6	1.27	0.75	0.24	0.65	8.2	1.19	2.1	<0.01	0.23	0.28
UQ07	0.003	1.1	0.9	1.10	0.82	0.19	1.87	7.7	1.05	2.0	0.02	0.23	0.21
UQ08	0.011	1.4	1.2	3.40	2.76	0.23	1.66	5.2	2.07	8.5	0.02	0.78	0.22
UQ09	0.010	1.2	3.1	3.56	2.75	0.29	4.38	8.2	2.36	10.6	0.02	0.78	0.12
UQ10	0.012	1.0	1.3	2.10	1.68	0.19	3.33	6.8	1.36	9.7	<0.01	0.49	0.13
UQ11	0.005	1.4	1.4	2.06	1.77	0.19	2.36	7.8	1.28	10.5	<0.01	0.49	0.15
UQ12	0.020	3.8	8.6	3.31	2.16	0.71	5.26	15.1	3.34	7.7	0.01	0.64	0.78
UQ13	0.007	0.2	1.2	0.97	0.54	0.23	3.67	4.0	1.04	1.0	<0.01	0.17	0.05
CCH01	0.002	0.6	1.0	0.58	0.37	0.18	0.98	2.4	0.66	1.2	<0.01	0.13	0.12
CCH02	<0.001	0.6	2.1	0.55	0.35	0.16	1.43	2.4	0.63	1.1	<0.01	0.11	0.14
CCH03	0.003	1.7	3.6	0.97	0.60	0.25	2.15	6.4	0.91	1.9	0.01	0.19	0.46
CCH04	0.004	1.2	3.0	0.84	0.49	0.16	1.30	3.8	0.77	2.1	<0.01	0.17	0.24
CCH05	0.004	1.4	3.7	1.01	0.58	0.29	1.76	5.0	1.08	1.7	<0.01	0.18	0.30
CCH06	0.004	1.6	2.7	1.16	0.82	0.22	1.16	6.3	1.05	3.8	<0.01	0.26	0.44
CCH07	<0.001	1.4	2.8	1.06	0.66	0.33	1.87	4.6	1.29	2.6	<0.01	0.21	0.35
CCH08	<0.001	1.2	2.0	0.47	0.32	0.10	1.15	4.2	0.46	2.2	<0.01	0.11	0.17
CCH09	0.002	1.6	3.4	0.82	0.55	0.19	1.77	5.8	0.78	1.8	<0.01	0.17	0.39
FE01	0.004	0.3	1.9	1.14	0.90	0.16	23.81	1.3	1.01	3.8	<0.01	0.29	0.28
NHW01	0.006	0.8	2.1	2.16	1.29	0.21	2.42	5.1	1.78	10.2	<0.01	0.46	0.12
NHW02	0.004	1.2	2.0	1.39	0.75	0.20	2.30	6.4	1.15	5.3	<0.01	0.31	0.12

Sample ID	Cr_2O_3 (%)	Cs (ppm)	Cu (ppm)	Dy (ppm)	Er (ppm)	Eu (ppm)	Fe_2O_3 (%)	Ga (ppm)	Gd (ppm)	Hf (ppm)	Hg (ppm)	Ho (ppm)	K_2O (%)
NHW03	0.006	0.7	1.5	1.20	0.96	0.16	1.99	5.2	1.00	6.5	<0.01	0.31	0.12
BB01	0.004	4.1	9.0	2.91	1.76	0.58	5.51	8.1	2.89	3.8	<0.01	0.58	2.02
BB02	0.006	7.4	13.0	6.33	3.55	1.04	3.70	14.8	6.56	12.6	<0.01	1.36	2.43
HC01	0.002	1.0	1.7	0.74	0.47	0.10	1.28	5.1	0.48	2.6	<0.01	0.15	0.12
HC02	0.002	1.3	2.0	1.11	0.64	0.13	1.79	5.9	0.72	3.6	<0.01	0.13	0.14
HC03	<0.001	1.5	1.8	1.31	0.84	0.18	1.90	6.2	0.99	2.7	<0.01	0.31	0.14
HC04	0.009	2.5	4.6	2.27	1.59	0.35	9.86	11.0	1.52	5.9	<0.01	0.47	0.23
HC05	0.007	2.1	4.6	1.67	1.10	0.42	2.47	7.8	1.59	4.3	<0.01	0.34	0.77
GOR01	0.002	0.7	1.2	0.74	0.54	0.11	2.25	5.1	0.66	4.4	<0.01	0.16	0.11
GOR02	0.013	0.7	1.3	0.60	0.53	0.10	2.44	5.0	0.54	4.8	<0.01	0.15	0.13
GOR03	<0.001	0.8	1.3	0.77	0.75	0.16	2.73	8.2	0.91	2.7	<0.01	0.26	0.14
GOR04	0.015	4.6	1.3	2.11	1.48	0.40	10.20	27.2	1.71	6.3	0.06	0.52	0.49
DIA01	0.003	1.7	2.1	1.30	1.06	0.17	2.76	8.0	0.97	3.8	<0.01	0.33	0.17
DIA02	0.005	1.4	1.4	0.75	0.63	0.13	1.50	4.3	0.61	2.6	<0.01	0.18	0.12
DIA03	0.016	1.6	1.8	1.27	1.17	0.12	2.37	5.6	1.01	8.2	0.01	0.31	0.14
DIA04	0.001	1.1	1.4	0.56	0.54	0.06	1.73	4.6	0.46	2.3	<0.01	0.15	0.13
DIA05	0.004	1.5	1.6	0.40	0.46	0.10	1.85	4.8	0.51	2.1	0.01	0.13	0.14
DIA06	0.002	1.1	1.5	0.28	0.54	0.07	1.69	4.3	0.53	1.7	<0.01	0.12	0.14
WF01	0.005	1.0	1.9	0.65	0.73	0.10	2.33	4.9	0.78	2.6	<0.01	0.20	0.13
WF02	0.005	1.1	1.5	0.48	0.54	0.10	2.00	4.1	0.56	2.4	<0.01	0.11	0.15
WF03	0.030	1.1	1.8	0.66	0.69	0.12	2.36	4.4	0.79	2.7	<0.01	0.13	0.13
WF04	0.009	1.6	1.3	0.84	0.56	0.19	3.43	8.0	0.77	2.6	<0.01	0.16	0.16
TDQ01	0.005	1.2	1.8	0.47	0.50	0.08	2.34	4.0	0.58	1.5	<0.01	0.11	0.23
TDQ02	<0.001	0.9	1.5	0.30	0.46	0.08	1.86	4.0	0.55	1.7	<0.01	0.09	0.20
TDQ03	0.002	1.1	1.6	0.43	0.46	0.08	2.20	3.5	0.41	1.7	<0.01	0.13	0.19
TDQ04	0.002	0.9	1.9	0.52	0.49	0.06	2.19	4.8	0.49	1.1	<0.01	0.13	0.19

Sample ID	Cr_2O_3 (%)	Cs (ppm)	Cu (ppm)	Dy (ppm)	Er (ppm)	Eu (ppm)	Fe_2O_3 (%)	Ga (ppm)	Gd (ppm)	Hf (ppm)	Hg (ppm)	Ho (ppm)	K_2O (%)
TDQ05	0.006	1.0	1.8	0.39	0.38	0.10	3.03	5.1	0.50	2.7	<0.01	0.09	0.13
WFN01	0.004	0.9	1.6	1.01	0.82	0.10	2.63	6.1	0.93	8.3	<0.01	0.25	0.09
WFN02	0.001	1.0	1.6	1.06	0.96	0.15	2.60	5.9	1.07	6.3	<0.01	0.26	0.09
WFN03	0.002	1.0	1.5	0.65	0.63	0.17	2.59	6.3	0.78	2.5	<0.01	0.20	0.13
WFN04	0.003	1.3	1.9	0.73	0.65	0.13	2.50	5.6	0.66	3.5	<0.01	0.20	0.13
GRQ04	0.009	1.3	1.9	2.78	1.71	0.23	1.51	5.5	2.27	9.2	<0.01	0.58	0.35
CCH03	0.007	1.8	5.4	0.92	0.69	0.32	2.35	7.5	1.33	1.8	0.02	0.17	0.47
SRQ09	0.033	0.5	3.1	1.02	0.61	0.36	1.15	0.9	1.33	1.1	<0.01	0.22	0.33
SP01	0.007	0.6	1.5	0.96	0.67	0.15	4.94	4.5	0.93	3.3	<0.01	0.21	0.13
SP02	0.007	1.1	1.0	0.84	0.69	0.16	0.67	7.9	0.78	2.3	0.01	0.20	0.20
SP03	0.015	0.6	1.2	2.51	1.58	0.86	17.33	6.8	3.21	1.9	<0.01	0.54	0.18
SP04	0.004	1.4	1.0	1.18	0.88	0.17	0.94	5.8	0.92	2.3	0.01	0.21	0.17
SP05	0.007	1.9	0.8	1.17	0.86	0.32	1.08	7.0	1.16	2.5	0.09	0.31	0.20
SP06	0.004	1.7	0.8	1.82	1.24	0.43	1.37	8.0	1.59	2.8	0.03	0.38	0.17
SP07	0.007	1.5	1.2	2.18	1.58	0.29	2.71	7.3	2.32	10.4	0.06	0.53	0.12
SP08	0.007	1.4	0.8	2.30	1.61	0.40	5.12	5.7	2.20	7.8	0.01	0.59	0.09
SP09	0.011	0.6	0.8	5.98	3.48	1.61	26.05	12.5	6.63	6.5	<0.01	1.13	0.03
SP10	0.016	1.0	1.4	4.16	2.74	0.68	23.02	11.9	3.37	7.7	<0.01	0.83	0.05
CW01	0.015	0.7	17.2	11.19	3.97	7.85	5.14	26.3	19.51	9.6	<0.01	1.78	2.47
CW02	0.013	1.1	2.0	10.96	8.16	1.09	6.01	6.6	10.20	66.0	<0.01	2.45	0.34
CW03	0.011	0.8	2.2	7.36	4.88	1.06	24.11	3.3	7.15	29.2	<0.01	1.53	0.18
CW04	0.023	0.7	4.0	4.88	4.13	0.77	15.65	3.7	4.76	22.7	<0.01	1.22	0.18
CW05	0.029	1.1	1.1	4.54	3.25	0.52	15.98	5.9	4.29	32.8	<0.01	0.95	0.11
CW06	0.027	0.9	0.7	4.42	3.59	0.45	12.02	7.4	4.05	23.5	<0.01	1.05	0.12
CW07	0.009	0.2	0.6	5.68	4.68	0.32	2.77	3.0	3.99	33.8	<0.01	1.38	0.03
CW08	0.008	<0.1	0.9	5.98	4.98	0.52	6.13	3.7	4.43	35.5	0.04	1.49	0.04

Sample ID	Cr_2O_3 (%)	Cs (ppm)	Cu (ppm)	Dy (ppm)	Er (ppm)	Eu (ppm)	Fe_2O_3 (%)	Ga (ppm)	Gd (ppm)	Hf (ppm)	Hg (ppm)	Ho (ppm)	K_2O (%)
CW09	0.009	0.6	0.9	0.51	0.37	0.08	4.80	3.5	0.37	1.8	<0.01	0.12	0.07
CW10	0.024	0.8	0.6	3.62	2.66	0.34	17.48	34.5	2.26	17.0	<0.01	0.76	0.13
WA01	0.017	1.2	0.7	2.11	1.25	0.36	16.91	12.5	1.87	9.5	<0.01	0.42	0.13
WA02	0.021	0.9	0.5	1.39	1.11	0.29	24.51	11.5	1.24	11.8	<0.01	0.33	0.07
WA03	0.035	1.1	0.4	1.59	1.43	0.26	25.39	12.1	1.60	13.1	0.01	0.41	0.08
WA04	0.019	0.6	0.4	1.49	0.94	0.24	30.08	11.1	1.10	9.0	<0.01	0.26	0.06
WA11	0.023	0.7	0.6	1.49	0.92	0.25	27.49	8.9	1.43	9.0	0.01	0.32	0.06
HP01	0.007	0.8	1.4	0.81	0.57	0.09	1.43	7.8	0.62	3.7	<0.01	0.20	0.13
HP02	0.007	0.4	0.9	1.34	0.91	0.11	6.90	4.0	1.05	4.7	<0.01	0.27	0.11
HP03	0.009	0.5	3.6	2.37	1.45	0.47	42.81	6.0	2.32	3.2	0.01	0.43	0.03
GOR05	0.017	0.3	0.7	1.03	0.77	0.30	22.14	15.9	1.22	7.2	0.02	0.22	0.04
GOR06	0.020	0.6	1.0	2.17	1.32	0.32	23.71	16.8	1.65	11.0	0.01	0.43	0.14
GOR07	0.018	0.9	1.0	1.75	1.25	0.30	22.73	17.2	1.71	10.1	0.03	0.46	0.13
GOR08	0.009	1.9	0.7	1.72	1.17	0.23	6.58	12.5	1.25	6.9	<0.01	0.34	0.23
SH01	0.017	0.1	2.7	1.62	1.42	0.34	23.72	7.5	1.38	11.5	<0.01	0.38	0.03
SH02	0.014	0.3	4.6	2.76	2.09	0.57	22.01	9.4	2.83	11.6	<0.01	0.71	0.03
SH03	0.013	0.4	1.2	1.84	1.62	0.09	5.87	5.1	1.43	9.5	<0.01	0.59	0.06
MP01	0.014	1.1	2.4	1.52	1.30	0.21	9.16	9.1	1.07	8.6	<0.01	0.37	0.06
MP02	0.008	0.5	0.8	1.36	0.98	0.18	9.47	5.5	0.98	5.7	<0.01	0.26	0.05
GL01	0.007	1.7	1.6	2.21	1.53	0.23	2.95	8.1	1.76	7.0	<0.01	0.47	0.44
CW11	0.015	1.2	1.0	1.77	1.36	0.24	15.77	16.7	1.36	9.6	0.05	0.38	0.18
HHQ01	0.003	0.3	1.1	1.13	1.00	0.10	5.54	2.2	0.68	7.3	<0.01	0.26	0.07
MR01	0.032	1.7	2.4	9.30	4.84	2.80	30.89	13.7	10.78	11.6	<0.01	1.64	0.19
MR02	0.010	2.7	3.1	3.42	2.11	0.60	3.21	15.5	2.94	11.0	<0.01	0.72	0.23
WRC01	0.005	0.9	4.0	1.73	0.99	0.38	1.04	1.5	1.66	2.3	0.02	0.28	0.21
DIA10	0.017	0.9	2.3	1.56	0.95	0.25	18.64	20.3	1.30	8.0	<0.01	0.30	0.08

Sample ID	Cr_2O_3 (%)	Cs (ppm)	Cu (ppm)	Dy (ppm)	Er (ppm)	Eu (ppm)	Fe_2O_3 (%)	Ga (ppm)	Gd (ppm)	Hf (ppm)	Hg (ppm)	Ho (ppm)	K_2O (%)
DIA11	0.037	0.8	2.2	2.87	1.70	0.55	37.62	38.4	2.41	8.0	<0.01	0.59	0.09
BAL01	0.014	4.4	11.4	4.29	2.44	0.70	3.51	10.1	4.11	7.7	0.01	0.87	1.45
BAL02	0.016	0.5	4.4	0.70	0.27	0.03	0.81	2.1	0.84	1.8	0.02	0.13	0.39
BAL03	0.022	0.8	9.2	2.33	0.85	0.49	1.55	3.0	2.61	2.2	0.02	0.34	0.33
BAL04	0.036	1.2	27.6	1.84	1.30	0.31	1.68	3.6	2.36	6.7	0.08	0.46	0.33
BAL05	0.035	0.9	25.3	1.24	1.00	0.18	5.41	5.3	1.67	3.3	0.24	0.24	0.27
BAL06	0.032	1.3	15.0	1.05	0.68	0.18	6.14	7.3	1.24	2.9	0.03	0.26	0.22
WEN01	0.020	1.5	17.1	3.02	1.66	0.78	2.82	7.8	3.25	6.0	0.01	0.71	1.03
WEN02	0.011	2.1	12.1	3.45	2.36	0.79	3.41	8.7	3.68	11.4	0.01	0.60	0.91
WEN03	0.010	1.7	11.6	3.84	2.17	0.73	3.17	8.6	3.41	7.0	0.01	0.69	0.82
WEN04	0.010	2.4	16.5	3.93	2.25	0.72	3.56	9.6	3.88	7.0	0.02	0.91	1.05
WEN05	0.009	1.1	14.4	2.59	2.02	0.54	2.91	7.3	2.94	6.1	<0.01	0.64	0.45
WEN06	0.012	2.0	22.1	3.34	2.16	0.76	3.08	8.0	3.36	8.7	0.01	0.45	0.77
WEN07	0.007	0.7	12.2	0.98	0.59	0.16	1.08	3.4	1.61	3.0	<0.01	0.27	0.23
WEN08	0.009	1.3	20.7	1.63	1.23	0.19	1.93	5.2	2.01	3.2	0.02	0.30	0.53
WEN09	0.009	1.0	14.7	1.20	1.15	0.19	1.89	4.9	1.55	4.3	<0.01	0.28	0.37
WEN10	0.010	1.0	12.5	1.14	1.12	0.22	1.41	4.4	2.01	14.8	0.02	0.19	0.32
WEN11	0.006	<0.1	11.0	0.97	0.38	<0.02	1.04	1.0	0.89	3.9	<0.01	0.25	0.11
WEN12	0.003	0.3	6.1	0.75	0.36	<0.02	6.72	0.6	0.75	1.7	0.01	0.16	0.14
WEN13	0.020	0.1	6.7	0.24	0.30	0.05	4.56	0.7	0.45	1.2	0.05	0.07	0.09
WEN14	0.006	0.3	6.6	0.61	0.28	<0.02	1.82	<0.5	0.71	3.3	0.02	0.14	0.07
WEN15	0.008	0.3	5.7	1.28	0.53	<0.02	3.29	1.0	0.80	7.4	0.06	0.11	0.13
WEN16	0.006	<0.1	8.1	0.94	1.10	0.06	2.34	0.9	1.30	5.6	0.03	0.18	0.09
WEN17	0.007	0.6	6.1	0.90	0.56	0.06	2.90	1.1	1.25	5.0	0.06	0.19	0.14
WEN18	0.009	1.1	7.7	1.63	1.16	0.22	3.83	3.7	1.94	8.3	0.11	0.32	0.31
WEN19	0.009	0.9	16.4	1.52	1.04	0.23	3.44	3.8	1.67	7.2	0.07	0.39	0.29

Sample ID	Cr_2O_3 (%)	Cs (ppm)	Cu (ppm)	Dy (ppm)	Er (ppm)	Eu (ppm)	Fe_2O_3 (%)	Ga (ppm)	Gd (ppm)	Hf (ppm)	Hg (ppm)	Ho (ppm)	K_2O (%)
BUN01	0.006	1.5	4.9	0.62	0.25	0.18	1.15	2.4	1.32	0.6	0.01	0.15	1.53
BUN02	0.006	1.4	4.9	1.43	0.66	0.34	1.37	2.9	1.52	2.1	<0.01	0.25	1.43
BUN03	0.007	1.8	9.7	1.11	0.29	0.21	2.41	3.3	1.39	0.9	0.01	0.34	1.30
BUN04	0.007	3.0	9.8	0.83	1.12	0.27	2.93	3.5	1.12	1.3	0.03	0.20	1.35
BUN05	0.011	3.2	9.1	7.15	4.66	0.68	3.16	6.0	6.02	12.0	0.82	1.31	2.00
BUN06	0.007	1.8	19.7	1.99	0.99	0.30	3.39	6.5	2.67	2.6	0.03	0.33	1.31
BUN07	0.009	1.9	20.7	1.41	0.98	0.21	2.81	3.7	1.31	0.9	0.03	0.27	1.67
BUN08	0.015	4.2	16.4	3.72	2.70	0.40	3.59	7.3	3.56	5.8	0.05	0.68	2.11
BUN09	0.012	2.3	13.1	2.91	2.19	0.27	6.92	5.3	2.06	2.6	<0.01	0.36	1.36
BUN10	0.009	1.7	13.7	3.09	1.79	0.72	4.17	6.0	3.47	4.0	<0.01	0.58	1.25
BUN11	0.007	1.4	16.6	2.54	1.67	0.56	3.45	4.6	2.76	3.0	<0.01	0.48	1.22
BUN12	0.008	1.0	38.9	1.78	1.41	0.43	2.66	3.9	2.20	2.4	0.01	0.39	0.98
BUN13	0.006	0.9	17.3	2.03	1.23	0.39	3.06	3.3	1.79	2.1	<0.01	0.43	1.09
BUN14	0.007	0.6	12.7	1.06	0.65	0.27	1.83	2.3	1.06	1.2	<0.01	0.19	0.76
BUN15	0.005	0.7	10.1	1.03	0.63	0.21	1.82	1.8	1.03	0.9	<0.01	0.23	0.67
BUN16	0.007	0.4	9.1	1.04	0.65	0.18	1.45	1.6	0.99	1.3	0.01	0.19	0.54
BUN17	0.006	0.7	6.8	1.08	0.55	0.20	1.51	1.9	0.96	0.9	<0.01	0.18	0.60
BUN18	0.006	0.6	9.1	0.85	0.50	0.18	2.21	1.6	1.03	0.8	<0.01	0.21	0.53
BUN19	0.007	0.6	7.4	0.90	0.57	0.16	2.10	1.7	0.95	0.9	0.01	0.18	0.54
BUN20	0.005	0.7	5.0	1.08	0.64	0.15	1.74	1.5	0.93	0.7	<0.01	0.23	0.84
BUN21	0.006	0.3	6.1	1.08	0.68	0.15	1.80	1.1	1.03	1.1	<0.01	0.19	0.14
BUN22	0.007	0.9	18.0	1.13	0.79	0.20	5.70	2.3	1.25	2.7	<0.01	0.28	0.26
BUN23	0.005	0.2	8.7	0.36	0.28	0.06	1.10	0.6	0.42	1.1	<0.01	0.08	0.21
BUN24	0.006	0.2	5.4	0.41	0.35	0.05	1.18	0.9	0.32	0.8	0.02	0.08	0.22
BUN25	0.006	0.3	6.5	0.57	0.32	0.08	1.70	1.3	0.55	1.0	0.02	0.10	0.35
BUN26	0.006	0.3	6.3	0.55	0.45	0.09	1.87	1.1	0.56	1.1	0.02	0.15	0.35

Sample ID	Cr_2O_3 (%)	Cs (ppm)	Cu (ppm)	Dy (ppm)	Er (ppm)	Eu (ppm)	Fe_2O_3 (%)	Ga (ppm)	Gd (ppm)	Hf (ppm)	Hg (ppm)	Ho (ppm)	K_2O (%)
BUN27	0.012	0.6	5.7	1.20	0.81	0.22	1.56	1.6	1.28	1.6	0.04	0.22	0.38
BUN28	0.006	0.5	6.2	0.73	0.40	0.11	1.79	0.9	0.79	0.8	0.02	0.14	0.29
BUN29	0.006	0.4	20.9	0.76	0.45	0.11	7.98	0.9	0.66	1.5	0.06	0.15	0.23
BUN30	0.004	0.5	6.9	0.99	0.62	0.15	12.37	1.2	0.95	2.5	0.15	0.16	0.29
HOR101	0.014	2.8	1.3	1.64	1.17	0.31	6.58	19.2	1.55	5.8	0.01	0.36	0.28
HOR102	0.014	2.0	1.7	1.57	1.04	0.31	6.89	15.1	1.49	5.7	<0.01	0.39	0.23
HOR109	0.019	0.9	3.5	1.03	0.67	0.11	2.86	7.5	0.72	3.9	<0.01	0.26	0.10
HOR110	0.006	1.0	1.6	0.85	0.66	0.11	1.68	5.9	0.67	3.8	<0.01	0.18	0.10
HOR111	0.022	0.9	2.9	1.02	0.70	0.14	2.84	7.6	0.70	4.5	<0.01	0.19	0.10
HOR112	0.005	1.3	1.7	0.81	0.55	0.12	1.93	5.5	0.59	3.6	<0.01	0.17	0.10
HOR113	0.023	1.0	3.3	0.98	0.85	0.14	1.97	4.8	0.92	3.6	<0.01	0.27	0.10
HOR114	0.005	0.7	1.9	0.65	0.57	0.08	1.76	5.2	0.60	4.1	<0.01	0.15	0.07
HOR115	0.006	1.1	1.9	0.81	0.58	0.07	1.05	6.2	0.55	3.6	<0.01	0.17	0.11
HOR116	0.025	0.8	3.7	0.57	0.46	0.07	1.88	4.8	0.44	3.2	0.01	0.13	0.07
HOR117	0.008	0.6	2.2	0.59	0.45	0.06	1.79	3.7	0.48	2.6	<0.01	0.12	0.07
HOR118	0.026	0.5	4.1	0.59	0.47	0.09	3.15	3.6	0.57	2.8	0.01	0.15	0.06
HOR119	0.004	0.4	1.9	0.66	0.41	0.12	3.80	3.0	0.56	3.5	<0.01	0.13	0.06
HOR120	0.022	0.6	3.0	0.80	0.41	0.18	4.30	2.5	0.81	2.2	<0.01	0.17	0.06
HOR121	0.006	0.6	2.7	0.95	0.75	0.23	4.78	3.1	0.99	3.5	<0.01	0.23	0.07
HOR122	0.027	1.0	3.7	0.68	0.50	0.11	1.53	3.5	0.63	4.5	0.01	0.18	0.09
HOR123	0.007	1.3	1.8	0.70	0.53	0.09	0.91	4.9	0.56	2.6	0.03	0.13	0.11
HOR124	0.026	0.8	3.2	0.66	0.53	0.10	1.92	3.3	0.61	2.5	0.01	0.15	0.09
HOR125	0.003	0.8	1.7	0.52	0.40	0.07	0.75	3.4	0.40	1.5	<0.01	0.11	0.09
HOR126	0.023	1.1	3.2	0.38	0.37	0.08	1.01	3.7	0.47	1.5	<0.01	0.11	0.09
HOR127	0.006	1.0	1.7	0.53	0.42	0.08	1.13	4.3	0.46	1.7	0.02	0.13	0.10
HOR128	0.026	0.7	3.5	0.57	0.34	0.09	0.88	3.6	0.42	1.3	<0.01	0.10	0.09

Sample ID	Cr_2O_3 (%)	Cs (ppm)	Cu (ppm)	Dy (ppm)	Er (ppm)	Eu (ppm)	Fe_2O_3 (%)	Ga (ppm)	Gd (ppm)	Hf (ppm)	Hg (ppm)	Ho (ppm)	K_2O (%)
HOR129	0.007	1.0	1.7	0.60	0.38	0.12	0.76	4.9	0.54	1.5	0.02	0.12	0.11
HOR130	0.028	0.3	9.2	0.49	0.41	0.12	0.77	1.5	0.58	1.5	0.01	0.12	0.08
HOR131	0.005	1.7	3.1	1.03	0.71	0.26	0.76	4.2	1.08	2.2	0.01	0.22	1.17
HOR132	0.029	0.6	13.9	1.60	1.00	0.41	1.22	3.0	1.86	4.1	0.03	0.34	0.25
HOR133	0.004	0.3	11.9	0.78	0.42	0.13	0.94	2.0	0.72	2.3	<0.01	0.14	0.16
HOR134	0.032	0.5	20.0	0.83	0.55	0.20	1.03	1.5	0.89	2.0	0.01	0.18	0.29
HOR135	0.002	0.8	5.9	0.73	0.51	0.15	0.65	1.6	0.77	1.5	<0.01	0.17	0.58
HOR136	0.017	2.7	4.5	6.62	3.56	1.80	13.62	5.2	8.02	4.0	0.01	1.35	0.81
HOR137	0.012	1.8	6.4	9.02	5.65	1.37	8.33	5.2	8.91	30.3	0.01	1.95	0.87
HOR501	0.002	0.9	2.4	0.87	0.63	0.11	1.35	2.7	0.61	4.0	<0.01	0.21	0.24
HOR503	0.018	1.2	3.7	1.09	0.84	0.24	3.50	5.0	1.17	5.5	<0.01	0.26	0.19
HOR504	0.018	2.9	2.5	1.69	1.28	0.47	15.64	23.1	1.78	6.6	<0.01	0.38	0.30
HOR507	0.026	2.2	3.0	1.69	1.25	0.33	5.91	15.5	1.41	5.3	<0.01	0.37	0.24
HOR508	0.020	2.8	2.4	1.40	1.09	0.36	6.72	18.9	1.59	5.1	<0.01	0.34	0.25
HOR509	0.026	1.0	3.5	1.35	0.92	0.20	4.41	10.7	1.10	6.6	<0.01	0.35	0.10
HOR510	0.021	1.1	1.7	1.35	1.07	0.21	6.28	12.5	1.01	4.2	<0.01	0.36	0.10
HOR511	0.022	1.3	1.4	1.06	0.85	0.15	4.21	10.1	0.83	6.0	<0.01	0.25	0.07
HOR512	0.009	1.3	1.2	1.06	0.77	0.13	3.41	7.3	0.83	5.2	<0.01	0.28	0.07
HOR513	0.022	0.7	2.9	0.98	0.60	0.11	3.00	5.0	0.76	5.2	<0.01	0.20	0.03
HOR514	0.010	1.2	0.7	1.18	0.79	0.17	3.18	6.2	0.95	6.8	<0.01	0.23	0.05
HOR515	0.019	1.1	2.6	1.26	0.83	0.13	2.91	5.8	0.83	6.4	<0.01	0.22	0.06
HOR516	0.005	1.1	1.7	0.71	0.53	0.09	1.88	4.7	0.67	3.6	<0.01	0.17	0.07
HOR517	0.024	0.9	3.7	0.69	0.46	0.06	1.76	4.0	0.60	2.0	<0.01	0.13	0.07
HOR518	0.003	0.7	2.1	0.58	0.45	0.08	2.00	3.9	0.59	2.7	<0.01	0.12	0.08
HOR519	0.026	0.5	5.0	0.70	0.38	0.07	1.70	2.7	0.49	1.5	<0.01	0.13	0.07
HOR520	0.007	0.4	3.2	0.53	0.37	0.10	1.69	2.4	0.64	3.0	<0.01	0.14	0.06

Sample ID	Cr_2O_3 (%)	Cs (ppm)	Cu (ppm)	Dy (ppm)	Er (ppm)	Eu (ppm)	Fe_2O_3 (%)	Ga (ppm)	Gd (ppm)	Hf (ppm)	Hg (ppm)	Ho (ppm)	K_2O (%)
HOR521	0.034	0.8	8.8	0.70	0.38	0.11	2.05	3.7	0.69	4.4	<0.01	0.13	0.10
HOR522	0.005	0.7	2.8	0.98	0.65	0.15	2.36	3.7	1.11	8.3	<0.01	0.23	0.09
HOR523	0.018	0.7	4.8	0.70	0.30	0.10	1.74	2.9	0.58	2.5	<0.01	0.13	0.08
HOR524	0.002	0.9	3.3	0.67	0.42	0.10	1.76	3.1	0.58	2.2	<0.01	0.11	0.09
HOR525	0.026	0.6	5.9	0.62	0.36	0.10	1.74	3.0	0.64	1.1	<0.01	0.09	0.07
HOR527	0.006	0.8	2.7	0.77	0.49	0.12	2.08	3.2	0.76	3.8	<0.01	0.14	0.09
HOR528	0.024	0.7	4.2	0.73	0.52	0.14	2.11	3.7	0.87	3.7	<0.01	0.18	0.08
HOR529	0.009	0.7	2.7	0.96	0.54	0.15	2.20	3.4	0.89	5.5	<0.01	0.21	0.09
HOR530	0.021	0.6	3.9	0.92	0.44	0.12	1.88	3.2	0.79	6.1	<0.01	0.15	0.08
HOR531	0.006	0.7	8.0	1.17	0.76	0.16	2.25	4.9	1.21	6.5	<0.01	0.22	0.09
HOR532	0.024	0.5	4.3	0.87	0.49	0.13	1.94	4.5	0.78	4.1	<0.01	0.17	0.09
HOR533	0.001	0.5	2.7	0.67	0.48	0.10	1.92	4.5	0.69	2.9	<0.01	0.15	0.09
HOR534	0.025	0.6	4.4	1.50	0.89	0.14	2.45	4.1	1.09	8.4	<0.01	0.35	0.09
HOR535	0.004	0.9	2.1	0.82	0.58	0.10	0.76	3.7	0.90	3.5	<0.01	0.19	0.09
HOR536	0.031	0.9	3.2	2.29	1.67	0.19	1.06	4.1	2.30	20.8	<0.01	0.54	0.09
HOR537	0.010	0.8	2.9	1.76	1.42	0.28	2.23	3.9	1.43	19.5	<0.01	0.45	0.09
HOR538	0.018	0.9	3.6	0.95	0.50	0.18	1.58	4.0	0.89	1.7	<0.01	0.17	0.10
HOR539	0.004	0.3	2.2	1.19	0.65	0.18	0.97	2.5	1.03	7.4	<0.01	0.26	0.07
HOR540	0.024	0.2	6.2	0.93	0.62	0.11	1.44	1.4	0.80	1.8	<0.01	0.16	0.04
HOR541	0.003	0.3	3.3	0.94	0.42	0.18	1.68	1.1	0.90	1.5	<0.01	0.14	0.04
HOR542	0.025	0.3	6.7	0.87	0.62	0.19	1.91	2.0	0.92	1.5	<0.01	0.16	0.05
HOR543	0.005	0.3	3.5	0.84	0.44	0.14	1.37	1.3	0.92	2.3	<0.01	0.19	0.05
HOR544	0.018	0.2	5.0	0.87	0.41	0.12	1.06	1.1	0.77	1.6	<0.01	0.15	0.04
HOR545	0.008	0.3	3.8	0.82	0.40	0.12	1.24	1.3	0.76	2.1	<0.01	0.15	0.04
HOR546	0.030	0.2	6.6	0.72	0.46	0.11	1.21	1.4	0.78	4.3	<0.01	0.14	0.04
HOR547	<0.001	0.3	4.3	0.67	0.49	0.07	0.98	1.0	0.65	2.3	<0.01	0.16	0.04

Sample ID	Cr_2O_3 (%)	Cs (ppm)	Cu (ppm)	Dy (ppm)	Er (ppm)	Eu (ppm)	Fe_2O_3 (%)	Ga (ppm)	Gd (ppm)	Hf (ppm)	Hg (ppm)	Ho (ppm)	K_2O (%)
HOR548	0.027	0.2	6.5	0.55	0.44	0.07	1.00	1.0	0.67	1.7	<0.01	0.13	0.04
HOR549	<0.001	<0.1	3.2	0.57	0.36	0.06	0.76	1.3	0.56	1.7	<0.01	0.12	0.04
HOR550	0.028	0.2	7.3	0.69	0.41	0.07	1.00	1.0	0.60	1.2	<0.01	0.13	0.05
HOR551	0.003	0.2	3.4	0.62	0.30	0.06	0.78	0.8	0.67	0.7	<0.01	0.13	0.03
HOR552	0.029	0.2	6.9	0.95	0.56	0.12	1.01	4.1	0.95	2.9	<0.01	0.20	0.08
HOR553	0.010	1.0	4.4	11.23	7.16	1.61	2.47	4.0	12.47	50.8	<0.01	2.40	0.21
HOR554	0.039	0.9	5.4	18.97	11.66	2.85	11.83	4.6	19.69	73.0	<0.01	3.77	0.30
HOR505	0.021	4.7	3.8	2.31	1.30	0.42	8.49	24.2	2.04	4.4	<0.01	0.46	0.53
HOR506	0.017	3.9	2.2	2.57	1.50	0.58	11.37	22.8	2.34	6.8	<0.01	0.40	0.35
HOR526	0.020	0.8	4.3	0.89	0.49	0.13	2.30	3.7	0.97	4.6	0.01	0.16	0.09
HOR701	0.006	2.0	7.0	5.18	2.98	1.41	3.42	9.3	6.22	3.9	<0.01	0.99	0.71
HOR702	0.013	3.1	10.1	4.50	2.14	1.03	5.76	12.7	4.56	6.9	<0.01	0.77	1.10
HOR703	0.008	2.4	10.3	3.32	1.83	0.96	6.26	10.5	4.01	6.9	0.01	0.64	0.88
HOR704	0.013	2.0	7.1	3.24	1.88	0.87	6.32	10.4	3.85	6.5	<0.01	0.59	0.74
HOR705	0.006	1.8	5.9	2.96	1.47	0.73	4.17	8.8	3.00	5.8	<0.01	0.49	0.65
HOR706	0.019	2.5	6.5	3.22	1.92	0.91	4.21	10.8	3.42	6.4	<0.01	0.64	0.75
HOR707	0.007	2.4	5.9	2.96	1.90	0.93	4.12	9.9	3.46	5.5	<0.01	0.65	0.75
HOR708	0.018	4.1	8.1	4.75	2.44	1.32	5.46	14.7	6.27	5.9	<0.01	0.96	0.96
HOR709	0.007	3.6	6.3	4.97	2.81	1.46	4.77	13.3	5.30	6.0	<0.01	0.91	0.88
HOR710	0.012	3.3	11.7	3.24	1.67	0.74	5.29	13.7	3.23	5.4	<0.01	0.54	0.90
HOR711	0.015	3.3	7.3	1.91	1.14	0.39	5.01	13.5	1.80	5.0	<0.01	0.40	0.78
HOR712	0.012	2.1	4.6	1.36	0.81	0.25	5.42	14.9	1.06	4.9	<0.01	0.33	0.30
HOR713	0.018	1.0	3.0	0.80	0.64	0.13	4.01	9.9	0.70	3.3	<0.01	0.17	0.15
HOR714	0.005	0.9	2.0	0.70	0.49	0.07	2.71	8.4	0.38	2.6	<0.01	0.17	0.10
HOR715	0.027	0.4	3.7	0.76	0.54	0.09	3.36	7.6	0.42	3.7	<0.01	0.18	0.07
HOR716	0.002	0.7	2.5	0.62	0.52	0.08	2.38	5.9	0.36	2.3	<0.01	0.14	0.08

Sample ID	Cr_2O_3 (%)	Cs (ppm)	Cu (ppm)	Dy (ppm)	Er (ppm)	Eu (ppm)	Fe_2O_3 (%)	Ga (ppm)	Gd (ppm)	Hf (ppm)	Hg (ppm)	Ho (ppm)	K_2O (%)
HOR717	0.022	0.8	3.1	0.58	0.40	0.07	2.20	6.0	0.46	2.0	<0.01	0.11	0.10
HOR718	0.001	1.1	2.1	0.68	0.35	0.10	1.96	5.1	0.45	1.9	<0.01	0.12	0.14
HOR719	0.026	0.8	4.1	0.51	0.32	0.08	2.02	4.4	0.46	1.7	<0.01	0.10	0.14
HOR720	0.005	0.8	2.6	0.67	0.34	0.06	2.02	4.6	0.39	1.2	<0.01	0.09	0.14
HOR721	0.022	1.1	4.3	0.68	0.36	0.09	2.06	4.7	0.36	1.7	<0.01	0.10	0.17
HOR722	0.002	1.3	3.4	0.58	0.40	0.07	1.85	4.8	0.45	2.3	<0.01	0.12	0.17
HOR723	0.019	1.4	3.8	1.47	0.98	0.08	2.00	5.0	0.77	1.8	<0.01	0.30	0.19
HOR724	0.005	1.6	4.2	0.47	0.31	0.08	1.86	3.9	0.43	1.2	<0.01	0.09	0.20
HOR725	0.025	1.1	4.4	0.63	0.33	0.08	1.90	4.3	0.46	1.7	<0.01	0.11	0.17
HOR726	0.006	1.0	2.7	0.60	0.33	0.08	1.79	4.0	0.40	1.1	<0.01	0.12	0.16
HOR727	0.028	1.4	8.7	0.56	0.34	0.07	1.98	5.1	0.49	1.7	<0.01	0.14	0.18
HOR728	0.004	1.7	2.5	0.52	0.41	0.08	1.69	6.5	0.47	1.2	0.01	0.12	0.20
HOR729	0.021	1.5	3.6	0.59	0.50	0.13	1.09	5.6	0.64	2.5	<0.01	0.12	0.16
HOR730	0.005	1.3	2.6	0.79	0.45	0.09	0.98	5.0	0.60	2.4	<0.01	0.15	0.18
HOR731	0.026	1.3	5.1	0.62	0.42	0.10	0.95	5.1	0.57	2.2	<0.01	0.12	0.19
HOR732	0.004	0.7	2.3	0.53	0.41	0.11	0.73	4.2	0.59	2.2	<0.01	0.15	0.18
HOR733	0.032	0.7	3.7	0.29	0.32	0.07	0.76	2.5	0.40	1.0	<0.01	0.09	0.14
HOR734	0.006	0.9	2.6	0.53	0.37	0.07	0.75	3.1	0.47	1.4	<0.01	0.09	0.16
HOR735	0.030	0.7	4.5	0.74	0.48	0.09	0.87	3.2	0.62	1.7	<0.01	0.11	0.16
HOR736	0.004	0.6	2.9	0.67	0.43	0.12	0.73	3.0	0.57	1.7	<0.01	0.13	0.17
HOR737	0.029	0.8	5.6	0.67	0.35	0.12	0.86	3.0	0.54	1.1	<0.01	0.07	0.20
HOR738	0.003	0.7	2.5	0.67	0.44	0.11	0.68	2.4	0.58	0.9	<0.01	0.13	0.19
HOR739	0.028	0.5	5.1	0.55	0.31	0.08	0.94	2.4	0.45	1.2	<0.01	0.10	0.20
HOR740	0.004	0.5	5.0	0.76	0.41	0.14	0.76	2.8	0.67	1.5	<0.01	0.15	0.17
HOR741	0.023	0.5	5.4	0.82	0.48	0.11	0.70	1.6	0.76	3.3	<0.01	0.14	0.18
HOR742	0.003	0.6	4.8	0.73	0.38	0.13	0.65	1.9	0.75	1.6	<0.01	0.14	0.28

Sample ID	Cr_2O_3 (%)	Cs (ppm)	Cu (ppm)	Dy (ppm)	Er (ppm)	Eu (ppm)	Fe_2O_3 (%)	Ga (ppm)	Gd (ppm)	Hf (ppm)	Hg (ppm)	Ho (ppm)	K_2O (%)
HOR743	0.030	0.5	5.6	1.30	0.89	0.19	0.86	2.3	1.21	2.4	<0.01	0.26	0.24
HOR744	0.006	0.6	5.0	0.59	0.34	0.13	1.04	2.2	0.67	1.3	<0.01	0.11	0.21
HOR745	0.041	0.7	9.2	1.09	0.51	0.10	1.03	1.9	0.82	3.7	<0.01	0.19	0.15
HOR746	0.003	0.6	5.2	1.02	0.70	0.10	0.77	1.9	0.80	2.9	<0.01	0.19	0.11
HOR747	0.029	0.7	6.7	0.78	0.66	0.13	0.82	3.8	0.79	3.0	<0.01	0.20	0.15
HOR748	0.004	0.7	3.3	0.76	0.42	0.15	0.78	1.3	0.67	1.1	0.02	0.15	0.34
HOR749	0.024	0.9	6.0	0.74	0.46	0.13	0.76	2.3	0.82	1.0	<0.01	0.13	0.35
HOR750	0.003	0.9	3.5	0.76	0.51	0.16	0.76	2.4	0.88	0.9	<0.01	0.16	0.49
HOR751	0.023	0.8	4.1	0.76	0.42	0.16	0.83	1.9	0.88	1.1	<0.01	0.12	0.52
HOR752	0.009	2.0	9.0	4.36	2.04	1.17	10.53	11.8	5.17	7.5	0.01	0.67	0.76
HOR753	0.030	0.8	5.6	0.57	0.45	0.11	0.92	3.0	0.67	1.5	<0.01	0.10	0.15
HOR754	0.006	0.7	6.2	1.34	0.67	0.21	0.74	2.0	1.46	3.9	<0.01	0.20	0.46
HOR755	0.020	1.0	4.4	1.67	0.91	0.44	0.73	2.8	1.77	4.4	0.02	0.29	0.64
HOR756	0.007	1.2	5.3	2.14	0.87	0.67	0.66	4.0	2.40	2.0	0.02	0.32	0.83
HOR757	0.026	1.2	5.9	1.99	0.95	0.70	0.83	3.6	2.37	2.6	0.02	0.28	0.77
HOR758	0.008	1.4	3.9	2.01	1.15	0.50	0.87	5.1	2.27	4.6	0.03	0.35	0.82
HOR759	0.033	1.4	5.6	3.03	1.72	0.60	1.02	3.3	3.04	12.5	0.02	0.54	0.78
HOR760	0.008	1.3	2.8	2.40	1.26	0.64	0.91	3.7	2.53	5.1	0.02	0.38	0.88
HOR761	0.020	1.3	4.1	2.24	0.94	0.81	0.71	3.3	2.83	2.7	<0.01	0.36	1.07
HOR762	0.006	1.2	8.2	1.96	0.92	0.59	0.86	3.1	2.24	2.9	<0.01	0.33	0.96
HOR763	0.029	1.4	5.8	3.71	1.90	0.85	1.00	5.0	3.90	10.8	0.01	0.64	0.95
HOR764	0.010	1.6	4.8	5.69	2.89	0.97	0.98	4.3	5.43	17.6	<0.01	1.01	0.91
HOR765	0.038	1.9	8.6	5.13	2.31	1.62	1.69	6.6	6.04	7.7	<0.01	0.86	1.12
HOR766	0.007	1.8	4.3	2.38	1.20	0.79	1.36	4.9	3.06	2.0	<0.01	0.45	1.42
HOR767	0.029	1.7	6.5	2.04	0.93	0.67	1.08	3.7	2.18	1.3	0.01	0.40	1.17
HOR768	0.007	3.0	6.1	2.62	1.18	0.79	1.17	5.7	2.98	2.2	<0.01	0.44	1.93

Sample ID	Cr_2O_3 (%)	Cs (ppm)	Cu (ppm)	Dy (ppm)	Er (ppm)	Eu (ppm)	Fe_2O_3 (%)	Ga (ppm)	Gd (ppm)	Hf (ppm)	Hg (ppm)	Ho (ppm)	K_2O (%)
HOR769	0.039	2.1	7.8	2.63	1.43	0.68	1.29	4.6	2.80	3.8	<0.01	0.52	1.41
HOR770	0.031	1.7	8.3	21.16	14.00	1.99	2.53	5.3	21.63	123.3	0.01	4.52	1.15
HOR771	0.036	1.3	4.2	23.53	10.50	7.76	8.06	4.5	30.50	47.5	<0.01	3.85	1.09
HOR772	0.016	1.4	2.7	8.32	5.01	1.25	1.55	4.7	8.65	32.5	<0.01	1.65	1.23
HOR773	0.052	1.5	6.6	12.73	7.20	1.77	2.71	4.6	13.34	55.5	0.02	2.62	1.20
HOR774	0.024	2.7	5.5	27.30	14.24	5.09	13.18	7.8	29.89	56.9	0.02	5.01	1.11
HOR775	0.030	1.9	5.3	2.32	1.40	0.48	2.61	5.6	2.50	6.0	0.01	0.48	1.40
HOR776	0.005	1.7	3.3	2.26	1.43	0.49	5.64	4.4	2.14	3.1	0.01	0.41	1.35
HOR777	0.026	1.9	5.2	1.93	1.02	0.51	2.23	4.6	2.05	1.9	0.02	0.39	1.42
HOR778	0.006	1.6	3.7	1.60	0.88	0.46	2.63	4.9	1.78	1.9	0.01	0.34	1.47
HOR779	0.022	2.6	5.6	3.20	1.71	0.67	8.03	8.9	3.43	9.5	0.04	0.64	1.15
HOR780	0.024	2.3	6.2	13.36	8.08	2.02	10.72	9.5	13.63	56.4	0.05	2.73	1.02
HOR781	0.021	2.4	7.3	8.82	3.83	2.87	18.43	9.0	11.56	5.6	0.03	1.43	0.75
WIL15	0.006	3.5	23.6	3.49	1.78	0.99	5.95	17.0	4.02	3.6	<0.01	0.70	1.31
WIL16	0.009	4.3	29.8	4.01	2.32	1.06	6.87	19.6	4.65	4.4	<0.01	0.81	1.51
WIL17	0.002	2.4	13.4	3.32	1.82	0.84	4.19	12.2	3.57	4.0	<0.01	0.66	1.01
WIL18	0.010	3.7	20.3	4.37	2.31	1.19	6.66	18.0	4.66	4.1	0.01	0.84	1.49
WIL19	<0.001	1.5	11.8	2.24	1.23	0.55	3.44	9.4	2.29	2.5	<0.01	0.41	0.76
WIL20	0.006	1.0	7.3	1.32	0.81	0.34	2.12	6.1	1.51	1.9	<0.01	0.28	0.47
WIL21	<0.001	<0.1	3.0	0.48	0.36	0.06	1.27	1.9	0.43	0.7	<0.01	0.10	0.10
WIL22	0.017	0.1	5.3	0.42	0.22	0.08	1.26	2.2	0.39	0.7	<0.01	0.07	0.17
WIL23	<0.001	0.1	4.7	0.33	0.23	0.06	0.90	2.1	0.37	0.9	0.01	0.07	0.15
WIL24	0.019	0.1	4.5	0.36	0.27	0.09	0.88	1.8	0.38	1.0	<0.01	0.08	0.17
WIL25	<0.001	<0.1	3.7	0.39	0.28	0.08	0.80	1.7	0.45	1.0	<0.01	0.07	0.15
WIL26	0.019	0.2	4.2	0.57	0.42	0.10	1.22	2.1	0.52	1.8	<0.01	0.10	0.22
WIL27	<0.001	0.2	4.3	0.61	0.32	0.13	1.33	2.4	0.60	1.4	<0.01	0.12	0.23

Sample ID	Cr_2O_3 (%)	Cs (ppm)	Cu (ppm)	Dy (ppm)	Er (ppm)	Eu (ppm)	Fe_2O_3 (%)	Ga (ppm)	Gd (ppm)	Hf (ppm)	Hg (ppm)	Ho (ppm)	K_2O (%)
WIL28	0.015	<0.1	3.4	0.43	0.27	0.06	0.82	1.7	0.36	1.1	<0.01	0.09	0.13
WIL29	<0.001	0.2	4.1	0.58	0.35	0.12	1.11	2.3	0.60	1.2	<0.01	0.12	0.20
WIL30	0.016	0.1	9.9	0.41	0.26	0.09	1.03	1.9	0.44	1.3	<0.01	0.10	0.19
WIL31	<0.001	0.2	13.8	0.48	0.29	0.08	1.06	1.9	0.43	1.1	<0.01	0.09	0.14
WIL32	0.015	<0.1	2.7	0.45	0.25	0.07	1.01	1.6	0.46	0.9	<0.01	0.08	0.15
WIL33	<0.001	<0.1	6.7	0.36	0.28	0.07	1.26	1.7	0.35	1.0	<0.01	0.08	0.15
WIL34	0.027	0.1	4.2	0.32	0.21	0.07	1.34	1.7	0.40	1.2	<0.01	0.06	0.14
WIL35	<0.001	0.2	5.1	0.53	0.33	0.06	1.48	2.0	0.44	1.1	0.02	0.09	0.15
WIL36	0.029	0.3	5.2	0.68	0.38	0.13	2.11	2.1	0.68	1.9	0.02	0.12	0.26
WIL37	<0.001	0.4	5.5	0.71	0.44	0.17	2.17	2.4	0.72	2.7	0.02	0.14	0.29
WIL38	0.026	0.6	5.5	1.01	0.76	0.21	4.55	3.9	0.97	2.6	0.07	0.21	0.41
PIA04	<0.001	0.5	5.0	0.79	0.61	0.10	1.48	3.3	0.71	1.5	<0.01	0.18	0.22
PIA05	0.026	0.4	3.3	0.77	0.49	0.08	1.08	2.9	0.67	1.5	0.02	0.15	0.10
PIA06	<0.001	0.2	4.4	0.84	0.65	0.11	1.09	2.7	0.77	1.7	<0.01	0.20	0.12
PIA07	0.028	0.3	3.8	1.32	0.98	0.11	1.01	2.7	1.15	3.4	0.02	0.30	0.09
PIA08	<0.001	0.2	3.7	0.77	0.41	0.08	0.96	2.0	0.75	1.4	<0.01	0.13	0.07
PIA09	0.032	0.2	3.1	0.98	0.54	0.13	1.18	2.1	0.98	1.3	0.02	0.18	0.08
PIA10	<0.001	0.4	3.9	1.38	0.83	0.22	2.23	2.6	1.28	1.1	0.02	0.26	0.25
PIA11	0.023	0.5	3.8	1.63	1.19	0.26	4.04	2.9	1.69	1.9	0.01	0.35	0.24
PIA12	<0.001	0.5	4.2	1.48	0.89	0.24	2.11	3.0	1.35	2.1	0.02	0.29	0.28
PIA13	<0.001	0.4	4.7	1.83	1.27	0.28	4.38	2.6	1.78	2.5	0.02	0.41	0.19
PIA14	0.025	0.4	3.8	2.01	1.15	0.25	4.56	1.4	1.65	1.9	0.01	0.42	0.15
PIA15	<0.001	0.6	4.2	2.05	1.25	0.22	3.97	1.8	1.64	3.7	0.02	0.40	0.26
KND01	0.018	0.3	2.9	0.63	0.31	0.25	0.87	0.7	0.95	0.7	<0.01	0.11	0.26
KND02	<0.001	0.3	3.6	0.70	0.27	0.25	1.07	0.9	1.03	1.0	<0.01	0.11	0.32
KND03	0.027	0.5	4.4	0.69	0.42	0.15	1.37	1.9	0.59	1.7	<0.01	0.11	0.44

Sample ID	Cr_2O_3 (%)	Cs (ppm)	Cu (ppm)	Dy (ppm)	Er (ppm)	Eu (ppm)	Fe_2O_3 (%)	Ga (ppm)	Gd (ppm)	Hf (ppm)	Hg (ppm)	Ho (ppm)	K_2O (%)
KND04	<0.001	0.2	4.4	0.84	0.50	0.11	1.20	<0.5	0.73	3.5	<0.01	0.17	0.25
KND05	0.027	0.3	3.8	0.61	0.32	0.13	1.17	<0.5	0.61	1.2	<0.01	0.09	0.25
KND06	<0.001	0.1	4.4	0.46	0.26	0.08	1.15	<0.5	0.51	0.8	<0.01	0.10	0.19
KND07	0.032	0.1	3.5	0.55	0.39	0.09	1.18	<0.5	0.56	1.5	<0.01	0.11	0.17
KND08	<0.001	<0.1	3.9	0.58	0.35	0.06	1.06	<0.5	0.49	0.6	<0.01	0.11	0.15
KND09	0.031	0.2	9.8	0.53	0.39	0.11	1.15	<0.5	0.58	0.7	<0.01	0.12	0.19
KND10	<0.001	0.6	7.4	1.50	0.88	0.27	1.10	2.7	1.53	3.7	<0.01	0.35	0.46
KND11	0.030	0.6	5.3	0.88	0.53	0.14	1.71	2.1	0.89	2.0	0.02	0.17	0.46
KND12	<0.001	1.5	6.1	1.49	0.86	0.33	2.90	3.7	1.58	2.3	<0.01	0.32	0.93
KND13	0.026	1.2	8.4	1.34	0.79	0.24	2.48	2.4	1.40	2.1	<0.01	0.27	0.67
BER02	<0.001	0.5	3.7	0.43	0.32	0.08	1.26	1.7	0.39	1.7	<0.01	0.10	0.18
BER03	0.017	1.3	19.0	1.53	0.94	0.36	2.28	4.9	1.61	2.6	<0.01	0.30	0.60
BER04	<0.001	0.8	11.5	1.03	0.68	0.21	1.76	2.8	1.14	2.2	<0.01	0.23	0.44
BER05	0.024	1.2	12.5	1.21	0.65	0.24	1.92	3.5	1.15	2.2	<0.01	0.25	0.47
BER06	<0.001	0.4	6.1	0.46	0.33	0.12	1.85	0.6	0.51	1.0	<0.01	0.10	0.40
BER07	<0.001	0.2	3.5	0.47	0.36	0.05	1.11	<0.5	0.40	0.7	<0.01	0.10	0.26
BER08	0.043	0.2	4.0	0.72	0.49	0.04	1.34	<0.5	0.56	0.9	<0.01	0.16	0.17
BER09	<0.001	0.1	3.0	0.49	0.37	0.03	0.84	<0.5	0.40	0.8	<0.01	0.09	0.17
BER10	0.036	0.4	3.8	0.68	0.45	0.09	1.59	<0.5	0.65	0.7	<0.01	0.15	0.29
MAN04	0.013	7.3	16.5	3.20	1.96	0.57	6.69	18.7	2.92	6.1	<0.01	0.64	2.21
MAN05	<0.001	0.6	4.5	0.79	0.51	0.09	1.75	0.8	0.57	1.1	<0.01	0.16	0.22
MAN06	0.017	2.3	6.6	1.56	1.04	0.27	2.56	4.4	1.60	2.8	<0.01	0.36	0.87
MAN07	0.006	7.8	13.1	4.51	2.83	0.76	4.94	15.1	4.20	9.1	<0.01	0.95	2.25
MAN08	0.015	6.4	10.3	5.49	3.42	0.94	4.01	11.0	5.37	13.2	<0.01	1.19	2.16
MAN09	0.005	7.1	17.1	7.22	3.93	1.60	5.16	14.4	7.98	9.8	0.07	1.41	2.25
MAN10	0.018	6.3	13.5	5.23	3.11	0.98	4.43	14.0	5.46	10.6	0.02	1.07	2.12

Sample ID	Cr_2O_3 (%)	Cs (ppm)	Cu (ppm)	Dy (ppm)	Er (ppm)	Eu (ppm)	Fe_2O_3 (%)	Ga (ppm)	Gd (ppm)	Hf (ppm)	Hg (ppm)	Ho (ppm)	K_2O (%)
MAN11	0.009	7.6	12.4	5.60	3.33	1.43	5.58	17.5	6.49	6.7	0.01	1.09	2.68
MAN12	0.013	7.5	23.9	5.13	3.01	1.17	5.78	18.7	5.86	7.4	<0.01	1.02	2.35
MAN13	0.009	7.6	22.0	5.52	3.18	1.17	5.74	17.6	5.69	8.0	0.02	1.10	2.22
MAN14	0.019	7.7	16.5	6.18	3.69	1.39	5.30	16.2	6.57	8.0	0.02	1.33	2.34
MAN15	0.007	7.1	19.0	5.84	3.45	1.34	5.15	15.1	6.59	8.1	<0.01	1.15	2.30
MAN16	0.020	7.0	12.0	8.35	5.81	1.36	4.42	17.4	7.79	8.8	0.01	1.99	2.34
MAN17	<0.001	2.1	7.9	2.41	1.55	0.42	5.24	5.6	2.28	3.1	<0.01	0.49	0.89
MAN18	0.032	0.9	4.5	1.21	0.80	0.24	5.30	3.0	1.14	1.5	0.01	0.24	0.58
MAN19	<0.001	1.0	4.9	1.79	1.16	0.36	4.25	2.6	1.74	1.8	0.01	0.41	0.51
MAN20	0.025	0.4	3.4	1.11	0.68	0.17	3.60	1.2	0.99	1.0	<0.01	0.22	0.41
MAN21	0.033	0.6	3.7	1.18	0.67	0.19	3.90	1.6	1.04	1.3	<0.01	0.25	0.43
MAN22	<0.001	0.7	4.2	1.04	0.73	0.15	3.76	0.7	0.97	1.3	<0.01	0.23	0.40
MAN23	0.029	0.9	4.1	1.81	1.18	0.24	2.90	2.1	1.55	4.4	<0.01	0.37	0.65
MAN24	<0.001	1.7	81.1	2.55	1.71	0.52	3.06	3.6	2.61	5.6	0.02	0.58	0.76
MAN25	0.031	0.4	30.8	1.15	0.75	0.12	1.92	0.6	0.93	1.8	<0.01	0.24	0.33
MAN26	<0.001	0.5	20.4	2.32	1.55	0.25	1.68	1.6	2.01	7.1	0.01	0.50	0.66
MAN27	0.025	0.9	18.1	2.96	2.08	0.23	1.40	1.5	2.33	8.0	<0.01	0.63	0.68
WAL11	0.009	3.0	28.8	4.36	2.65	1.17	7.85	11.8	4.44	8.6	0.01	0.90	1.36
WAL12	0.025	2.5	26.2	3.74	2.32	0.93	6.02	9.4	3.81	7.2	<0.01	0.77	1.21
WAL13	<0.001	0.3	7.8	1.02	0.66	0.25	1.74	<0.5	1.13	1.4	0.01	0.23	0.14
WAL14	0.034	0.4	4.0	0.64	0.36	0.12	1.48	<0.5	0.64	1.2	<0.01	0.13	0.11
WAL15	<0.001	0.3	5.4	0.63	0.46	0.11	1.99	<0.5	0.71	1.2	<0.01	0.13	0.08
WAL16	0.054	1.1	6.2	6.28	4.77	0.81	2.65	3.7	5.26	52.4	0.04	1.44	0.52
WAL17	<0.001	1.2	18.6	1.37	0.92	0.26	2.41	2.3	1.48	4.2	0.03	0.27	0.54
WAL18	0.034	1.2	13.2	1.43	1.11	0.32	3.21	2.6	1.48	4.9	0.02	0.33	0.56
MOR04	<0.001	1.6	63.3	2.12	1.19	0.50	3.40	5.7	2.33	2.4	0.02	0.38	0.99

Sample ID	Cr_2O_3 (%)	Cs (ppm)	Cu (ppm)	Dy (ppm)	Er (ppm)	Eu (ppm)	Fe_2O_3 (%)	Ga (ppm)	Gd (ppm)	Hf (ppm)	Hg (ppm)	Ho (ppm)	K_2O (%)
MOR05	0.034	0.4	4.2	0.37	0.28	0.04	1.46	<0.5	0.31	1.0	0.01	0.11	0.07
MOR06	<0.001	0.3	4.3	0.30	0.20	0.02	1.14	<0.5	0.34	0.8	<0.01	0.06	0.03
MOR07	0.035	0.2	3.9	0.32	0.20	0.03	1.15	<0.5	0.35	0.7	<0.01	0.06	0.09
MOR08	<0.001	0.3	5.8	0.46	0.23	0.04	1.76	<0.5	0.41	1.0	<0.01	0.10	0.11
MOR09	0.036	0.3	5.7	0.40	0.24	0.03	1.21	<0.5	0.34	0.7	<0.01	0.08	0.11
MOR10	<0.001	0.2	3.8	0.39	0.31	0.05	1.19	<0.5	0.39	1.0	<0.01	0.10	0.12
MOR11	0.035	0.3	9.5	0.47	0.27	0.05	1.33	<0.5	0.40	0.8	<0.01	0.09	0.14
MOR12	<0.001	0.3	18.3	0.43	0.29	0.04	1.24	<0.5	0.38	0.6	<0.01	0.08	0.17
MOR13	0.044	0.3	7.7	0.41	0.26	0.04	1.33	<0.5	0.41	0.7	0.01	0.11	0.18
MOR14	<0.001	0.4	9.4	0.44	0.29	0.04	1.28	<0.5	0.44	0.7	0.01	0.09	0.13
MOR15	0.032	0.4	29.0	0.56	0.36	0.05	1.15	<0.5	0.44	0.8	0.01	0.10	0.09
MOR16	<0.001	0.4	9.8	0.53	0.37	0.06	1.22	<0.5	0.47	0.9	<0.01	0.12	0.23
MOR17	0.033	0.3	8.3	0.58	0.38	0.07	1.17	<0.5	0.46	0.6	<0.01	0.12	0.22
MOR18	<0.001	0.3	9.2	0.45	0.32	0.07	1.09	<0.5	0.41	0.7	<0.01	0.08	0.22
MOR19	0.026	0.3	3.2	0.50	0.36	0.05	1.15	<0.5	0.44	0.9	0.01	0.13	0.19
MOR20	<0.001	0.2	5.3	0.66	0.41	0.08	1.62	0.8	0.63	0.8	<0.01	0.13	0.22
MOR21	0.034	0.2	5.7	0.89	0.52	0.09	1.61	0.9	0.68	0.8	<0.01	0.20	0.20
MOR22	0.001	0.3	4.4	0.61	0.39	0.08	1.42	0.6	0.50	0.8	0.01	0.13	0.15
BT01	<0.001	1.1	3.0	0.88	0.57	0.16	3.09	5.4	0.71	2.3	<0.01	0.18	0.25
BT02	0.017	1.0	3.0	0.67	0.41	0.13	2.89	5.2	0.61	1.5	<0.01	0.13	0.34
BT03	<0.001	1.2	3.1	0.62	0.43	0.14	2.68	4.3	0.66	1.8	<0.01	0.15	0.34
BT04	0.014	1.2	2.7	0.68	0.43	0.12	3.19	4.6	0.71	2.0	<0.01	0.16	0.37
BT05	<0.001	1.4	2.4	0.71	0.49	0.14	2.55	5.0	0.66	1.6	<0.01	0.14	0.37
BT06	0.017	1.3	2.9	0.75	0.43	0.16	3.28	4.3	0.69	1.5	<0.01	0.15	0.38
BT07	<0.001	1.3	2.9	0.75	0.52	0.17	1.64	4.8	0.78	1.6	0.01	0.16	0.63
BT08	0.015	1.3	3.5	1.91	1.02	0.49	4.52	3.6	1.71	1.4	0.01	0.35	0.64

Sample ID	Cr_2O_3 (%)	Cs (ppm)	Cu (ppm)	Dy (ppm)	Er (ppm)	Eu (ppm)	Fe_2O_3 (%)	Ga (ppm)	Gd (ppm)	Hf (ppm)	Hg (ppm)	Ho (ppm)	K_2O (%)
BT09	<0.001	1.1	3.5	1.03	0.68	0.28	2.63	4.0	1.11	1.3	0.01	0.22	0.61
BT10	0.019	1.1	3.6	0.90	0.53	0.23	1.42	3.3	0.93	1.9	<0.01	0.20	0.54
BT11	<0.001	0.9	3.3	0.64	0.36	0.17	1.16	2.9	0.76	1.8	0.02	0.13	0.65
BT12	0.018	1.0	2.4	1.17	0.63	0.25	2.06	2.5	0.97	1.3	0.01	0.19	0.70
BT13	<0.001	0.9	3.7	0.62	0.40	0.11	1.91	2.0	0.52	2.7	<0.01	0.11	0.22
BT14	0.013	1.1	2.8	0.71	0.44	0.15	2.51	3.4	0.66	1.6	<0.01	0.14	0.29
BT15	<0.001	1.1	4.0	0.63	0.36	0.13	2.51	2.9	0.64	1.4	<0.01	0.11	0.30
BT16	0.009	2.0	2.8	0.61	0.41	0.11	2.46	3.7	0.60	1.9	<0.01	0.13	0.30
BT17	<0.001	1.2	3.3	0.80	0.55	0.16	2.31	3.4	0.74	2.3	<0.01	0.15	0.32
BT18	0.016	1.1	2.5	1.08	0.84	0.17	2.64	3.9	0.85	2.3	<0.01	0.26	0.36
BT19	<0.001	1.2	4.2	1.04	0.61	0.22	2.86	3.1	0.92	2.1	<0.01	0.16	0.40
BT20	0.013	1.2	2.9	1.23	0.71	0.30	3.30	3.6	1.12	1.7	<0.01	0.22	0.46
BT21	<0.001	1.2	3.3	1.00	0.65	0.27	2.60	3.3	1.10	1.9	<0.01	0.20	0.49
BT22	0.017	1.1	2.9	0.94	0.53	0.24	2.30	3.2	0.94	1.7	<0.01	0.19	0.56
BT23	<0.001	1.1	4.1	1.57	0.69	0.58	2.37	3.1	1.92	1.9	<0.01	0.25	0.70
BT24	0.027	0.9	3.8	1.90	0.98	0.71	1.91	2.1	2.75	1.8	<0.01	0.38	0.75
BT25	<0.001	0.9	4.0	1.88	0.83	0.68	1.68	1.5	2.55	1.3	<0.01	0.32	0.72
BT26	0.023	0.7	4.5	3.27	1.77	0.87	4.02	1.3	3.49	1.1	<0.01	0.64	0.60
BT27	<0.001	0.9	4.4	6.00	3.14	2.12	2.96	2.0	8.12	2.3	<0.01	1.16	0.80
BT28	0.022	1.6	4.0	3.55	1.94	0.81	2.92	3.3	3.70	4.4	0.01	0.74	1.19
BT29	0.003	2.2	4.1	3.70	2.25	0.66	2.70	4.7	3.94	8.7	0.01	0.77	1.51
BT30	0.019	1.6	3.8	2.23	1.33	0.56	2.31	2.7	2.47	4.4	<0.01	0.43	1.24
BT31	<0.001	1.2	5.2	2.39	1.30	0.72	2.54	3.8	2.87	3.4	0.05	0.45	1.18
BT32	0.023	1.9	5.0	4.15	2.39	1.11	5.92	5.1	4.74	6.0	0.10	0.80	1.21
BT33	0.003	0.2	1.1	0.48	0.29	0.11	0.64	<0.5	0.50	0.3	<0.01	0.09	0.02
BT35	0.077	0.4	6.5	0.71	0.53	0.13	3.16	1.9	0.71	2.8	<0.01	0.17	0.17

Sample ID	Cr_2O_3 (%)	Cs (ppm)	Cu (ppm)	Dy (ppm)	Er (ppm)	Eu (ppm)	Fe_2O_3 (%)	Ga (ppm)	Gd (ppm)	Hf (ppm)	Hg (ppm)	Ho (ppm)	K_2O (%)
BT36	0.003	1.4	2.9	0.97	0.66	0.15	6.99	10.0	0.81	3.0	<0.01	0.22	0.22
BT37	0.030	1.9	4.2	0.79	0.57	0.13	4.62	10.8	0.58	2.8	<0.01	0.17	0.21
BT38	0.002	1.2	3.1	0.72	0.40	0.10	3.10	5.8	0.49	2.1	<0.01	0.14	0.21
BT39	0.015	1.4	2.2	0.54	0.46	0.10	2.82	4.4	0.54	2.0	<0.01	0.12	0.26
BT40	<0.001	0.8	5.3	0.74	0.45	0.12	2.35	3.8	0.56	1.4	<0.01	0.15	0.28
BT41	<0.001	0.9	4.5	0.83	0.48	0.14	2.12	4.2	0.58	1.7	<0.01	0.13	0.27
BT42	<0.001	1.1	4.4	1.49	0.66	0.39	2.36	4.3	1.35	2.2	<0.01	0.21	0.30
BT43	<0.001	1.1	5.6	3.23	2.06	0.88	3.30	3.6	3.71	4.4	0.01	0.63	0.44
BT44	<0.001	1.1	5.2	3.12	1.67	0.80	2.25	3.3	3.31	4.3	<0.01	0.60	0.47
BT45	<0.001	1.3	6.3	3.36	1.68	1.05	2.43	3.0	3.91	1.3	0.01	0.63	0.69
MBR06	0.004	1.8	9.1	1.31	0.77	0.23	3.85	7.8	1.13	4.9	<0.01	0.28	0.54
MBR07	0.004	0.7	4.7	1.71	1.04	0.35	2.26	1.6	1.74	6.6	<0.01	0.37	0.34
MBR08	0.002	1.1	4.7	1.47	0.96	0.32	2.35	3.5	1.42	5.3	<0.01	0.29	0.47
MBR09	0.003	0.8	7.5	1.51	0.88	0.31	2.24	2.7	1.54	6.1	<0.01	0.31	0.43
MBR10	0.005	0.7	4.5	1.63	1.07	0.33	1.92	2.0	1.56	5.4	<0.01	0.32	0.40
MBR11	<0.001	1.2	6.7	1.61	0.97	0.39	1.86	3.3	1.82	3.7	0.01	0.34	0.42
MBR12	0.009	1.0	6.7	1.37	0.75	0.29	1.63	3.0	1.52	3.4	0.02	0.28	0.33
MBR13	<0.001	0.8	6.7	1.24	0.70	0.25	1.27	1.6	1.24	2.8	0.03	0.24	0.28
MBR14	0.013	1.7	5.1	1.37	0.92	0.34	2.98	4.6	1.51	3.4	0.02	0.32	0.52
MBR15	0.002	0.9	7.8	1.26	0.71	0.28	1.35	2.2	1.33	3.2	0.01	0.24	0.31
MBR16	0.002	0.1	8.9	0.59	0.36	0.15	0.75	<0.5	0.75	0.5	<0.01	0.12	0.02
FT04	0.003	1.9	11.0	1.12	0.80	0.24	4.44	6.1	1.15	2.7	<0.01	0.22	0.67
FT05	0.042	0.7	25.0	0.68	0.40	0.09	2.22	2.5	0.55	1.8	<0.01	0.16	0.25
FT06	0.003	0.9	23.2	0.76	0.51	0.14	8.82	5.0	0.74	2.1	<0.01	0.18	0.28
FT07	0.053	1.0	26.5	0.69	0.51	0.10	2.89	2.9	0.43	1.7	<0.01	0.13	0.39
FT08	<0.001	0.9	37.9	0.59	0.43	0.08	3.43	2.2	0.46	1.8	<0.01	0.09	0.35

Sample ID	Cr_2O_3 (%)	Cs (ppm)	Cu (ppm)	Dy (ppm)	Er (ppm)	Eu (ppm)	Fe_2O_3 (%)	Ga (ppm)	Gd (ppm)	Hf (ppm)	Hg (ppm)	Ho (ppm)	K_2O (%)
FT09	0.041	0.8	6.8	0.54	0.32	0.08	2.46	1.4	0.44	1.4	<0.01	0.12	0.29
FT10	0.033	0.5	10.9	0.54	0.35	0.18	8.70	4.5	0.69	1.3	<0.01	0.11	0.31
FT11	0.033	1.2	7.6	0.65	0.39	0.15	4.08	3.8	0.68	1.7	<0.01	0.11	0.39
FT12	<0.001	0.8	16.2	0.67	0.36	0.15	4.58	3.1	0.59	1.6	<0.01	0.09	0.36
FT13	0.043	0.7	8.6	0.65	0.38	0.20	6.51	3.7	0.67	1.5	<0.01	0.12	0.46
FT14	0.013	2.3	5.4	3.61	1.18	1.99	10.66	6.2	6.95	3.1	0.02	0.53	1.97
FT15	0.026	2.1	2.5	9.12	3.59	4.37	8.67	4.7	15.82	2.6	0.03	1.44	1.72
NGA01	<0.001	2.5	6.3	2.87	1.64	0.74	4.11	9.4	2.98	4.3	0.02	0.56	0.89
NGA02	0.014	2.6	8.1	2.60	1.53	0.68	3.77	9.3	3.18	4.7	<0.01	0.55	1.06
NGA03	0.004	3.9	10.5	3.43	1.92	0.79	5.51	14.4	3.65	4.8	<0.01	0.67	1.57
NGA04	0.010	4.6	8.5	2.92	1.64	0.69	6.26	18.3	3.07	5.2	<0.01	0.60	1.78
NGA05	0.004	2.8	8.4	2.14	1.24	0.47	4.41	10.8	2.17	4.6	<0.01	0.42	0.90
NGA06	0.020	1.9	3.7	0.98	0.58	0.18	2.15	7.8	0.76	2.6	<0.01	0.18	0.43
NGA07	0.002	1.9	8.1	1.17	0.80	0.25	2.70	8.9	1.21	3.0	<0.01	0.27	0.63
NGA08	0.013	2.2	3.5	1.00	0.58	0.19	2.22	7.9	1.00	2.8	<0.01	0.21	0.52
NGA09	<0.001	1.9	6.7	1.11	0.66	0.21	2.52	7.5	0.95	2.9	<0.01	0.23	0.57
NGA10	0.015	1.8	4.5	1.09	0.63	0.23	2.35	6.5	1.02	2.9	<0.01	0.23	0.53
NGA11	<0.001	1.9	8.2	1.49	0.91	0.37	3.04	7.8	1.51	3.2	<0.01	0.31	0.73
NGA12	<0.001	1.4	7.0	0.78	0.48	0.13	1.82	5.2	0.84	2.3	<0.01	0.18	0.36
NGA13	<0.001	1.3	5.2	0.84	0.55	0.17	1.68	5.3	0.76	2.1	<0.01	0.17	0.37
NGA14	<0.001	1.2	6.7	0.72	0.48	0.10	1.37	3.2	0.56	2.0	<0.01	0.16	0.26
NGA15	<0.001	1.3	4.0	0.81	0.55	0.15	1.58	4.4	0.73	2.1	<0.01	0.18	0.39
NGA16	<0.001	0.6	4.5	0.60	0.38	0.07	0.91	1.6	0.50	1.4	<0.01	0.12	0.16
NGA17	<0.001	0.6	9.1	0.74	0.51	0.09	0.96	1.6	0.58	1.3	<0.01	0.14	0.14
NGA18	<0.001	0.4	5.2	0.43	0.36	0.08	0.71	0.7	0.50	1.0	<0.01	0.10	0.10
NGA19	<0.001	0.2	11.0	0.77	0.44	0.07	0.88	<0.5	0.63	1.3	<0.01	0.14	0.07

Sample ID	Cr_2O_3 (%)	Cs (ppm)	Cu (ppm)	Dy (ppm)	Er (ppm)	Eu (ppm)	Fe_2O_3 (%)	Ga (ppm)	Gd (ppm)	Hf (ppm)	Hg (ppm)	Ho (ppm)	K_2O (%)
NGA20	<0.001	0.4	7.2	0.77	0.43	0.06	0.76	<0.5	0.61	1.3	<0.01	0.14	0.07
NGA21	<0.001	0.2	12.6	0.79	0.50	0.05	0.82	<0.5	0.60	1.1	<0.01	0.18	0.04
NGA22	<0.001	0.2	7.3	0.62	0.38	0.07	0.86	<0.5	0.56	1.0	<0.01	0.13	0.07
NGA23	<0.001	0.3	9.5	0.70	0.44	0.03	0.79	<0.5	0.51	1.1	<0.01	0.14	0.06
NGA24	<0.001	0.3	6.0	0.79	0.50	0.04	0.72	<0.5	0.57	1.1	<0.01	0.15	0.07
NGA25	<0.001	0.3	6.7	1.00	0.71	0.06	0.77	<0.5	0.64	1.3	<0.01	0.23	0.07
NGA26	<0.001	0.3	5.0	0.77	0.44	0.03	0.73	<0.5	0.57	0.9	<0.01	0.14	0.06
NGA27	<0.001	0.3	9.4	0.64	0.41	0.06	0.78	<0.5	0.45	1.1	<0.01	0.11	0.08
NGA28	<0.001	0.3	7.6	0.77	0.52	0.08	0.82	<0.5	0.64	1.1	<0.01	0.16	0.09
NGA29	<0.001	0.2	6.5	0.57	0.35	0.03	0.80	<0.5	0.45	0.9	<0.01	0.13	0.05
NGA30	<0.001	0.3	5.8	0.66	0.37	0.03	0.78	<0.5	0.53	1.0	<0.01	0.12	0.06
NGA31	<0.001	0.2	6.4	0.61	0.35	0.05	0.68	<0.5	0.51	0.9	<0.01	0.12	0.06
NGA32	<0.001	0.3	5.8	0.72	0.53	0.07	0.80	<0.5	0.67	1.0	<0.01	0.15	0.09
NGA33	<0.001	0.2	4.9	0.62	0.40	0.04	0.74	<0.5	0.50	1.0	<0.01	0.12	0.09
NGA34	<0.001	0.3	10.2	0.69	0.45	0.08	1.25	<0.5	0.71	1.2	<0.01	0.16	0.06
NGA35	<0.001	0.4	6.0	0.92	0.50	0.14	0.93	<0.5	0.75	1.3	<0.01	0.15	0.15
NGA36	<0.001	0.3	5.3	0.62	0.36	0.05	0.72	<0.5	0.54	1.0	<0.01	0.13	0.10
NGA37	<0.001	0.3	5.9	0.76	0.42	0.11	0.89	<0.5	0.69	1.1	<0.01	0.18	0.14
NGA38	0.001	1.2	5.3	3.50	1.83	0.89	9.48	2.2	4.14	3.1	<0.01	0.69	0.49
NGA39	<0.001	0.8	6.3	3.12	1.66	0.71	16.97	1.2	3.22	2.4	<0.01	0.62	0.28
TEM03	<0.001	1.3	5.6	0.51	0.32	0.07	1.82	4.6	0.36	1.5	<0.01	0.11	0.14
TEM04	<0.001	1.2	6.0	0.60	0.38	0.06	1.66	5.2	0.42	1.5	<0.01	0.11	0.17
TEM05	<0.001	1.3	5.9	0.67	0.41	0.07	1.75	4.0	0.53	1.5	<0.01	0.13	0.15
TEM06	<0.001	0.3	11.8	0.42	0.24	0.03	1.27	1.4	0.41	0.9	<0.01	0.08	0.05
TEM07	<0.001	0.3	6.8	0.43	0.34	0.03	1.00	0.8	0.40	1.0	0.01	0.10	0.03
TEM08	<0.001	0.2	5.5	0.46	0.35	0.03	1.05	0.9	0.40	1.2	0.01	0.10	0.03

Sample ID	Cr_2O_3 (%)	Cs (ppm)	Cu (ppm)	Dy (ppm)	Er (ppm)	Eu (ppm)	Fe_2O_3 (%)	Ga (ppm)	Gd (ppm)	Hf (ppm)	Hg (ppm)	Ho (ppm)	K_2O (%)
TEM09	<0.001	0.2	12.3	0.50	0.33	0.03	1.11	0.7	0.39	1.2	<0.01	0.11	0.03
TEM10	<0.001	0.3	6.1	0.41	0.27	0.04	1.05	0.8	0.38	1.0	<0.01	0.09	0.04
TEM13	<0.001	0.4	6.2	0.89	0.51	0.07	1.31	1.7	0.83	1.1	<0.01	0.19	0.11
TEM14	<0.001	0.5	8.5	0.65	0.38	0.16	1.87	2.4	0.72	1.2	0.01	0.14	0.18
TEM15	<0.001	1.7	8.7	2.60	1.12	0.93	2.20	4.6	3.04	2.0	0.01	0.46	0.30
NDA01	<0.001	0.3	8.3	0.46	0.27	0.07	0.96	0.6	0.46	0.6	0.02	0.10	0.21
NDA02	<0.001	0.2	5.7	0.44	0.24	0.06	0.91	<0.5	0.35	0.7	0.01	0.08	0.22
NDA03	<0.001	0.3	54.7	0.81	0.50	0.13	1.26	<0.5	0.68	0.7	0.04	0.18	0.19
NDA04	<0.001	0.4	11.1	0.55	0.31	0.07	0.92	<0.5	0.46	0.7	0.04	0.11	0.28
OAK03	<0.001	0.5	6.8	0.96	0.67	0.15	1.83	2.2	0.82	7.0	0.01	0.23	0.29
OAK04	0.002	0.6	7.2	1.57	1.24	0.19	2.09	4.8	1.31	11.4	0.01	0.36	0.15
OAK05	<0.001	0.6	5.2	0.74	0.52	0.14	0.98	4.3	0.63	4.2	0.02	0.17	0.17
OAK06	<0.001	0.9	5.4	0.49	0.40	0.14	0.83	5.3	0.53	1.5	0.02	0.12	0.20
OAK07	<0.001	0.6	4.9	0.68	0.39	0.14	0.84	2.6	0.64	2.2	<0.01	0.14	0.27
OAK08	<0.001	1.5	7.5	1.14	0.63	0.25	1.91	5.2	1.17	2.4	0.01	0.20	0.62
OAK09	<0.001	0.7	7.3	0.91	0.51	0.24	1.50	2.9	1.16	1.6	0.01	0.18	0.31
OAK10	<0.001	0.2	6.9	0.53	0.33	0.10	0.97	0.8	0.54	1.3	<0.01	0.11	0.11
OAK11	<0.001	0.8	8.7	1.42	0.87	0.30	1.90	3.4	1.37	5.3	0.01	0.29	0.34
OAK12	0.008	3.1	7.5	2.88	1.93	0.60	3.01	15.5	2.65	9.8	<0.01	0.62	0.88
OAK13	0.009	3.3	8.8	2.77	1.78	0.66	3.37	14.8	2.68	9.5	0.01	0.59	0.73
OAK14	0.014	4.9	11.1	5.07	2.72	1.70	4.11	19.7	6.19	7.5	0.02	0.94	0.90
OAK15	0.011	4.9	15.2	4.51	2.36	1.46	4.19	21.8	5.18	7.3	0.02	0.85	0.88
OAK16	0.008	4.6	14.6	4.10	2.23	1.30	4.44	19.3	4.94	8.3	0.04	0.80	0.79
OAK17	0.013	4.2	13.7	3.87	2.22	1.27	5.78	18.1	4.75	7.3	0.02	0.77	0.83
OAK18	0.013	4.4	14.1	3.74	2.14	1.15	5.95	18.4	4.24	7.1	0.03	0.73	0.84
OAK19	0.005	3.4	9.8	3.41	1.71	1.18	3.90	15.1	4.21	5.7	0.01	0.61	0.67

Sample ID	Cr_2O_3 (%)	Cs (ppm)	Cu (ppm)	Dy (ppm)	Er (ppm)	Eu (ppm)	Fe_2O_3 (%)	Ga (ppm)	Gd (ppm)	Hf (ppm)	Hg (ppm)	Ho (ppm)	K_2O (%)
OAK20	0.020	4.3	15.0	3.55	1.97	1.25	3.52	18.6	4.27	6.3	0.03	0.70	0.77
OAK21	0.003	1.2	8.1	1.64	1.00	0.35	2.45	6.8	1.54	7.5	0.06	0.35	0.43
PIN04	0.040	0.3	5.3	0.43	0.26	0.05	1.33	1.6	0.38	0.9	0.01	0.08	0.11
PIN05	<0.001	0.5	14.9	0.51	0.38	0.08	1.92	2.0	0.54	1.0	<0.01	0.13	0.32
PIN06	0.040	0.3	5.3	1.72	1.26	0.16	1.51	0.7	1.44	5.9	<0.01	0.42	0.19
PIN07	<0.001	0.4	12.8	2.32	1.61	0.13	1.61	<0.5	1.76	10.4	<0.01	0.52	0.17
PIN08	0.050	0.4	5.5	2.82	2.04	0.17	1.63	0.6	2.10	15.4	<0.01	0.64	0.20
PIN09	0.002	0.3	15.3	1.77	1.27	0.15	1.97	0.6	1.35	6.7	<0.01	0.41	0.21
PIN10	0.044	1.8	6.7	2.10	1.08	0.62	1.64	3.7	2.56	3.8	0.04	0.42	0.77
PV02	<0.001	0.6	16.1	0.42	0.31	0.08	2.12	1.7	0.38	1.5	<0.01	0.09	0.14
PV03	0.035	0.4	6.0	0.55	0.30	0.09	1.72	1.7	0.60	1.6	<0.01	0.11	0.16
PV04	<0.001	0.8	12.4	0.69	0.41	0.11	1.99	1.8	0.61	1.7	<0.01	0.14	0.22
PV05	0.045	0.2	8.5	0.41	0.28	0.05	1.49	<0.5	0.39	1.4	<0.01	0.10	0.07
PV06	<0.001	0.1	14.2	0.41	0.26	0.07	1.64	<0.5	0.41	1.0	0.01	0.07	0.04
PV07	0.039	0.2	16.2	0.58	0.34	0.10	1.44	<0.5	0.57	1.3	0.01	0.12	0.08
PV08	<0.001	0.2	13.8	0.45	0.26	0.05	1.51	<0.5	0.38	1.0	<0.01	0.08	0.09
PV09	0.044	0.2	5.8	0.46	0.27	0.10	1.49	<0.5	0.48	0.9	<0.01	0.10	0.15
RB02	0.003	0.4	8.9	1.32	0.80	0.27	14.67	4.8	1.21	6.7	<0.01	0.26	0.14
RB03	0.023	5.6	1.2	2.82	1.83	0.61	9.49	20.8	2.61	6.8	0.23	0.62	0.66
RB04	0.017	5.2	3.9	3.73	2.11	0.93	12.12	18.1	3.76	5.5	0.12	0.74	0.60
RB05	0.013	3.8	1.9	7.84	4.27	2.46	8.13	13.4	9.95	3.3	0.06	1.47	0.41
KI1_01	0.004	3.6	11.2	5.76	3.01	1.46	4.20	14.0	6.40	8.0	<0.01	1.09	0.91
KI1_02	0.019	2.6	5.1	2.12	1.30	0.53	2.98	9.6	2.33	6.5	<0.01	0.47	0.49
KI1_03	0.004	3.4	8.5	3.23	1.87	0.81	3.57	11.3	3.63	6.2	0.01	0.66	0.65
KI1_04	0.011	3.2	4.8	2.16	1.22	0.47	2.70	12.2	2.10	6.4	0.01	0.43	0.53
KI1_05	0.003	2.9	9.4	3.75	2.05	1.08	3.15	10.3	4.68	5.6	0.01	0.73	0.49

Sample ID	Cr_2O_3 (%)	Cs (ppm)	Cu (ppm)	Dy (ppm)	Er (ppm)	Eu (ppm)	Fe_2O_3 (%)	Ga (ppm)	Gd (ppm)	Hf (ppm)	Hg (ppm)	Ho (ppm)	K_2O (%)
KI1_06	0.013	3.1	11.9	4.35	2.25	1.24	5.63	12.8	4.87	7.7	0.06	0.80	0.51
KI1_07	0.004	3.0	10.1	3.05	1.76	0.83	3.49	11.4	3.56	6.9	0.04	0.63	0.48
KI1_08	0.016	1.4	6.0	2.11	1.28	0.49	2.09	5.6	2.30	9.4	0.02	0.46	0.24
KI1_09	<0.001	1.3	8.4	1.80	1.18	0.37	1.84	5.1	1.81	8.7	0.01	0.41	0.24
KI1_10	0.013	2.0	7.6	2.95	1.67	0.76	1.82	6.6	3.43	7.7	0.02	0.62	0.40
KI1_11	0.008	3.8	9.8	2.23	1.28	0.53	2.68	14.3	2.12	4.6	0.04	0.44	0.74
KI1_12	0.020	5.5	6.9	3.12	1.85	0.70	2.94	20.2	3.23	5.6	0.03	0.63	0.81
KI1_13	0.019	7.3	16.3	19.22	7.95	8.32	10.13	27.5	31.99	5.2	0.03	3.24	0.97
KI10_01	0.018	3.7	2.5	7.49	4.42	2.06	6.03	13.0	8.50	7.6	0.05	1.48	0.49
KI10_02	0.007	2.6	3.8	11.05	5.93	2.66	3.56	8.0	11.48	6.3	0.02	2.20	0.37
KI10_03	0.033	6.6	3.9	25.66	12.01	9.37	5.95	20.8	37.36	6.6	0.02	4.89	1.28
KI10_04	0.022	6.5	8.2	23.40	11.38	8.62	6.51	12.7	31.86	5.4	0.03	4.47	1.26
KI10_05	0.016	3.0	4.1	9.11	5.03	2.66	3.47	5.8	11.26	3.8	0.03	1.83	0.37
OLC01	0.005	0.2	2.2	0.25	0.12	0.06	3.67	0.8	0.23	0.8	0.01	0.04	0.08
OLC02	0.008	<0.1	2.5	4.01	3.16	0.66	39.6	<0.5	3.09	1.3	0.01	0.94	0.03
OLC03	0.007	<0.1	1.4	0.51	0.38	0.1	15.18	<0.5	0.41	0.2	<0.01	0.11	0.01
OLC04	0.017	1	1.5	4.86	3.93	1	63.51	2.2	4.5	1	<0.01	1.14	0.17
OLC05	0.006	2.5	2.1	0.72	0.62	0.14	1.51	5.1	0.64	3.6	<0.01	0.18	0.64
OLC06	0.007	3.4	5.5	0.94	0.71	0.2	17.17	6.1	0.92	3	<0.01	0.2	0.84
OLC07	0.002	0.7	1.3	1.51	0.88	0.31	1.26	2.1	1.45	2.5	<0.01	0.32	0.41
OLC08	0.006	0.5	4.2	2.46	1.62	0.61	0.9	1.5	2.86	2.5	0.01	0.57	0.12
OLC09	0.004	0.2	0.2	0.52	0.3	0.14	0.79	<0.5	0.59	0.4	<0.01	0.12	<0.01
OLC10	0.016	<0.1	<0.1	10.74	7.94	2	79.66	<0.5	9.37	2.8	<0.01	2.56	0.03
OLC11	0.006	0.3	1	1.79	1.08	0.6	1.43	0.8	2.57	0.4	0.02	0.38	0.04
OLC12	0.007	1.3	1.5	6.97	4.61	1.37	2.65	3.1	6.8	1.2	0.02	1.67	0.15

Sample ID	La (ppm)	LOI (%)	Lu (ppm)	MgO (%)	MnO (%)	Mo (ppm)	Na_2O (%)	Nb (ppm)	Nd (ppm)	Ni (ppm)	P_2O_5 (%)	Pb (ppm)	Pr (ppm)
LYR01	8.9	0.84	0.13	0.12	<0.01	0.8	0.17	6.1	6.5	1.2	<0.01	1.4	1.93
LYR02	2.8	0.71	0.05	0.09	<0.01	0.7	0.09	2.0	1.8	0.6	<0.01	1.2	0.51
LYR03	3.1	1.27	0.05	0.13	<0.01	1.5	0.09	1.9	2.7	1.0	0.03	4.8	0.67
LYR04	2.8	0.59	0.07	0.06	<0.01	0.4	0.15	2.0	2.2	0.6	<0.01	1.4	0.66
LYR05	2.5	1.46	0.05	0.17	<0.01	0.7	0.24	1.9	2.0	1.4	<0.01	2.7	0.52
LYR06	4.1	1.11	0.04	0.17	<0.01	0.2	0.17	3.0	2.6	1.7	<0.01	2.0	0.79
LYR07	4.0	1.46	0.06	0.17	<0.01	0.2	0.25	4.3	2.2	1.3	<0.01	2.1	0.79
LYR08	3.6	1.04	0.04	0.12	<0.01	0.2	0.08	2.5	2.6	1.4	<0.01	1.6	0.64
LYR09	4.0	2.22	0.06	0.11	<0.01	0.8	0.12	3.6	2.6	1.2	0.03	6.1	0.86
LYR10	4.5	1.65	0.06	0.17	<0.01	0.2	0.13	3.5	3.2	1.3	<0.01	2.4	0.90
LYR11	8.1	5.81	0.52	1.45	0.01	<0.1	0.07	1.8	15.6	10.1	<0.01	2.7	3.57
LYR12	6.7	2.76	0.08	0.41	<0.01	<0.1	0.68	4.4	4.8	2.2	<0.01	1.1	1.39
LYR13	8.2	2.30	0.13	0.27	<0.01	0.3	0.47	5.5	6.4	2.9	<0.01	2.2	1.79
LYR14	2.7	10.38	0.12	3.73	<0.01	<0.1	0.46	2.7	3.0	5.9	<0.01	1.6	0.83
LYR15	5.5	7.57	0.14	1.26	<0.01	0.2	0.32	5.2	5.4	6.9	<0.01	6.0	1.24
LYR16	7.9	2.27	0.10	0.28	<0.01	0.3	0.47	5.8	5.2	3.3	<0.01	2.2	1.74
LCP01	14.5	13.50	0.11	1.18	0.02	0.4	0.24	4.7	13.9	6.5	0.02	4.2	3.46
LCP02	5.8	15.06	0.06	0.95	0.04	0.4	0.15	2.9	5.4	3.6	0.01	2.3	1.53
LCP03	8.5	13.88	0.14	0.44	0.03	0.2	0.18	3.9	8.9	3.5	0.01	2.5	2.17
LCP04	9.6	3.66	0.20	0.33	0.03	0.3	0.18	11.0	8.5	6.5	0.03	4.1	2.23
LCP05	10.9	1.76	0.48	0.19	0.04	1.0	0.21	19.0	9.6	5.3	0.05	4.6	2.70
LCP06	5.3	0.54	0.12	0.04	<0.01	1.8	0.05	2.3	4.2	2.0	0.02	2.3	1.30
LCP07	9.7	0.94	0.09	0.15	0.01	0.3	0.23	3.5	10.4	3.6	0.02	2.6	2.54
LCP08	6.9	1.07	0.06	0.14	<0.01	0.7	0.16	2.0	7.0	4.2	0.02	2.1	1.74
LCP09	6.3	1.19	0.05	0.16	<0.01	0.7	0.21	2.7	4.5	3.4	0.02	2.3	1.24
LCP10	4.4	0.93	0.04	0.11	<0.01	0.7	0.13	2.1	2.8	2.8	0.02	2.0	0.86

Sample ID	La (ppm)	LOI (%)	Lu (ppm)	MgO (%)	MnO (%)	Mo (ppm)	Na_2O (%)	Nb (ppm)	Nd (ppm)	Ni (ppm)	P_2O_5 (%)	Pb (ppm)	Pr (ppm)
LCP11	2.9	0.40	0.04	0.04	<0.01	0.2	0.09	1.4	1.8	1.2	<0.01	1.5	0.57
LCP12	3.2	0.47	0.04	0.08	<0.01	0.3	0.09	1.6	1.7	1.8	<0.01	1.5	0.61
LCP15	5.7	2.29	0.23	0.13	0.02	3.0	0.04	1.6	6.5	9.3	0.14	4.4	1.62
LCP16	3.2	1.41	0.07	0.17	<0.01	0.4	0.18	1.2	2.0	1.2	<0.01	1.2	0.60
LCP17	2.8	0.70	0.06	0.10	<0.01	0.9	0.08	1.1	2.0	0.8	<0.01	0.9	0.56
LCP18	2.7	1.34	0.06	0.23	<0.01	2.5	0.16	1.6	1.9	0.8	<0.01	1.2	0.58
LCP19	26.5	25.65	0.66	11.41	0.11	5.9	0.02	0.8	37.6	2.9	0.01	3.9	8.50
LCP20	9.9	45.36	0.14	21.20	0.04	0.1	<0.01	0.3	9.5	2.2	<0.01	0.9	2.10
LCP21	9.9	7.28	0.14	0.91	0.01	1.2	0.93	5.0	6.9	5.6	0.02	5.1	1.95
LCP22	5.0	1.08	0.06	0.16	0.01	0.7	0.18	2.2	4.2	2.3	0.03	1.2	1.07
LCP23	3.3	0.35	0.05	0.05	<0.01	0.3	0.08	1.7	3.0	1.4	0.01	1.0	0.61
RC01	1.5	2.91	0.07	0.10	<0.01	<0.1	0.04	4.0	1.9	1.8	<0.01	1.0	0.33
RC02	1.2	5.46	0.06	0.21	<0.01	<0.1	0.17	5.6	2.0	2.6	<0.01	1.1	0.34
RC03	1.8	0.76	0.15	0.02	<0.01	0.1	0.03	13.0	1.5	0.8	<0.01	0.8	0.36
RC04	4.1	2.93	0.10	0.12	<0.01	0.2	0.18	5.9	2.5	1.7	0.02	1.2	0.71
RC05	7.1	3.64	0.12	0.27	0.01	0.1	0.25	6.3	3.9	3.0	0.01	2.2	1.26
RC06	7.7	3.95	0.12	0.32	0.01	0.2	0.43	6.0	5.6	4.7	0.01	2.1	1.47
RC07	14.1	7.94	0.19	0.62	0.02	0.2	1.16	9.5	8.8	8.7	0.03	3.9	2.52
RC08	14.3	7.46	0.20	0.56	0.02	0.1	1.26	8.9	8.0	8.1	0.03	3.5	2.56
RC09	20.2	9.92	0.22	0.80	0.02	0.1	1.18	10.5	11.6	11.6	0.04	4.3	3.40
RC10	20.8	10.38	0.23	0.84	0.02	<0.1	1.10	13.1	13.1	11.7	0.04	3.5	3.71
RC11	37.4	8.53	0.22	0.78	0.02	0.2	0.67	10.7	38.6	16.9	0.10	7.0	8.91
RC12	3.2	1.73	0.06	0.14	<0.01	<0.1	0.10	2.1	2.1	3.9	<0.01	0.8	0.56
RC13	14.2	7.81	0.24	0.44	0.08	2.9	0.24	7.6	10.0	6.9	0.18	6.0	2.66
RC14	3.6	3.80	0.13	0.18	0.13	2.1	0.03	5.2	2.8	2.3	0.09	2.8	0.71
RC15	13.6	7.72	0.18	0.61	0.02	0.2	1.05	9.0	7.8	9.1	0.03	4.4	2.45

Sample ID	La (ppm)	LOI (%)	Lu (ppm)	MgO (%)	MnO (%)	Mo (ppm)	Na2O (%)	Nb (ppm)	Nd (ppm)	Ni (ppm)	P_2O_5 (%)	Pb (ppm)	Pr (ppm)
NY01	6.9	3.09	0.18	0.14	0.01	0.2	0.04	7.0	4.7	2.6	0.01	1.9	1.37
NY02	7.0	3.93	0.20	0.17	<0.01	0.2	0.06	6.6	4.8	3.0	<0.01	1.7	1.33
NY05	8.4	4.37	0.29	0.18	<0.01	0.2	0.11	8.2	5.1	3.4	0.01	2.8	1.52
NY06	6.8	4.70	0.28	0.18	<0.01	0.2	0.13	7.5	4.1	3.6	<0.01	2.1	1.22
NY07	5.3	3.07	0.20	0.16	<0.01	0.3	0.06	7.2	3.8	2.9	0.01	1.8	1.00
NY08	10.0	6.14	0.19	0.65	0.01	0.2	0.49	7.7	7.0	5.9	0.02	3.4	1.92
NY09	5.4	6.19	0.17	0.14	<0.01	0.2	0.04	7.1	3.4	1.7	0.01	2.0	1.02
NY10	11.0	6.39	0.21	0.70	0.01	0.2	0.52	8.0	7.3	5.7	0.02	3.3	2.05
GRQ01	18.8	6.73	0.17	0.45	<0.01	1.2	1.15	11.7	12.7	2.6	0.02	4.3	3.62
GRQ02	11.1	4.90	0.11	0.35	<0.01	1.0	0.52	7.0	9.2	3.3	0.01	6.2	2.37
GRQ03	11.4	4.16	0.12	0.31	<0.01	0.2	0.32	7.4	8.1	3.4	0.01	4.0	2.27
GRQ04	17.5	3.54	0.19	0.24	<0.01	0.5	0.28	6.8	12.4	3.6	0.01	5.2	3.60
GRQ05	15.4	2.21	0.15	0.12	<0.01	<0.1	0.02	4.6	11.5	2.3	0.01	3.3	3.00
GRQ06	10.3	2.07	0.11	0.09	<0.01	<0.1	0.02	4.3	8.8	2.7	<0.01	2.6	2.06
GRQ07	128.7	2.99	2.02	0.27	0.02	0.1	0.15	22.9	131.4	3.2	0.06	6.2	33.61
GRQ08	9.8	3.14	0.13	0.26	<0.01	<0.1	0.09	5.2	7.6	2.7	<0.01	3.2	2.02
GRQ09	106.2	4.37	2.31	0.54	0.03	0.1	0.26	31.3	111.2	4.7	0.05	6.5	27.44
GRQ10	12.6	4.34	0.38	0.49	<0.01	0.4	0.10	15.2	12.3	4.5	0.01	6.7	3.08
GRQ11	10.1	5.70	0.12	0.41	<0.01	1.0	0.63	6.0	6.7	4.0	0.01	5.3	2.07
SRQ01	1.1	45.46	0.08	19.42	0.21	0.9	<0.01	0.4	1.5	2.4	0.05	1.8	0.33
SRQ02	2.4	44.41	0.18	19.10	0.26	1.0	<0.01	0.4	3.3	3.0	0.07	1.8	0.59
SRQ03	8.8	42.52	0.76	17.96	0.18	0.9	0.02	1.3	11.3	1.8	0.05	2.2	2.21
SRQ04	10.5	13.38	0.22	6.00	0.02	<0.1	1.03	10.5	15.8	5.9	0.04	1.9	3.50
SRQ05	2.7	2.13	0.06	0.47	0.01	0.3	0.42	1.3	2.7	1.4	<0.01	1.0	0.71
SRQ06	2.5	0.84	0.10	0.14	<0.01	1.0	<0.01	1.0	3.2	4.3	0.02	2.2	0.71
SRQ07	4.2	0.96	0.17	0.17	0.01	2.2	0.08	6.3	4.2	2.3	0.02	4.5	1.14

Sample ID	La (ppm)	LOI (%)	Lu (ppm)	MgO (%)	MnO (%)	Mo (ppm)	Na_2O (%)	Nb (ppm)	Nd (ppm)	Ni (ppm)	P_2O_5 (%)	Pb (ppm)	Pr (ppm)
SRQ08	2.7	0.62	0.08	0.06	<0.01	1.8	0.13	1.1	2.2	1.3	<0.01	2.3	0.66
SRQ09	5.0	0.65	0.07	0.10	<0.01	0.4	0.06	1.1	8.2	2.9	0.02	1.8	1.85
SRQ10	2.5	0.47	0.07	0.04	<0.01	1.6	0.09	0.8	2.3	1.2	<0.01	2.2	0.69
UQ01	5.4	2.20	0.08	0.10	<0.01	0.7	0.08	2.1	7.8	3.5	<0.01	9.9	1.75
UQ02	4.1	1.95	0.06	0.09	<0.01	0.6	0.18	3.5	5.4	2.7	<0.01	4.2	1.26
UQ03	9.2	3.40	0.18	0.22	<0.01	<0.1	0.16	10.3	9.4	3.1	<0.01	4.0	2.30
UQ04	10.2	4.30	0.22	0.22	<0.01	<0.1	0.08	9.2	9.7	4.2	<0.01	5.1	2.46
UQ05	14.2	5.17	0.35	0.28	<0.01	0.1	0.18	10.0	15.8	9.1	<0.01	11.6	4.21
UQ06	7.4	3.14	0.13	0.20	<0.01	<0.1	0.16	6.9	7.0	3.2	<0.01	3.1	1.76
UQ07	7.1	3.94	0.12	0.23	<0.01	0.1	0.15	5.1	5.2	5.0	<0.01	2.7	1.60
UQ08	8.1	3.68	0.38	0.12	0.01	<0.1	0.13	12.7	6.3	2.0	<0.01	2.7	1.79
UQ09	7.8	4.16	0.39	0.17	0.01	0.2	0.06	10.0	7.9	5.3	<0.01	2.6	1.95
UQ10	4.5	3.45	0.27	0.25	<0.01	0.2	0.08	8.1	4.5	4.4	<0.01	3.5	1.17
UQ11	5.0	4.32	0.27	0.33	<0.01	0.1	0.10	9.1	5.0	5.0	<0.01	2.5	1.15
UQ12	14.6	11.43	0.34	1.01	0.02	<0.1	0.42	8.6	17.3	18.1	0.02	10.7	4.13
UQ13	5.2	2.20	0.07	0.11	<0.01	0.6	0.09	2.5	6.5	3.8	<0.01	9.5	1.63
CCH01	4.6	2.00	0.07	0.25	<0.01	<0.1	0.12	2.0	3.8	3.4	<0.01	1.3	1.32
CCH02	5.8	2.23	0.06	0.28	<0.01	0.1	0.09	1.4	5.6	4.2	<0.01	1.5	1.49
CCH03	11.7	5.49	0.10	0.57	<0.01	<0.1	0.19	3.6	7.6	4.5	<0.01	2.8	2.44
CCH04	7.7	3.10	0.08	0.38	<0.01	<0.1	0.07	3.2	5.0	4.5	0.01	1.9	1.54
CCH05	11.9	4.88	0.09	0.62	<0.01	<0.1	0.15	3.1	9.4	5.0	0.01	1.8	2.67
CCH06	10.0	3.74	0.14	0.43	<0.01	<0.1	0.09	6.3	5.9	5.5	<0.01	1.9	1.81
CCH07	12.6	3.75	0.11	0.43	<0.01	<0.1	0.09	3.7	10.2	4.6	<0.01	1.9	3.15
CCH08	4.5	2.99	0.06	0.20	<0.01	<0.1	0.11	2.4	2.6	3.3	<0.01	1.9	0.80
CCH09	8.9	4.57	0.10	0.52	<0.01	<0.1	0.13	3.6	5.3	5.2	0.01	2.5	1.67
FE01	4.3	4.22	0.16	0.20	0.02	0.2	0.75	4.1	4.3	1.3	0.01	2.0	1.10

Sample ID	La (ppm)	LOI (%)	Lu (ppm)	MgO (%)	MnO (%)	Mo (ppm)	Na_2O (%)	Nb (ppm)	Nd (ppm)	Ni (ppm)	P_2O_5 (%)	Pb (ppm)	Pr (ppm)
NHW01	13.4	2.31	0.25	0.11	0.02	0.2	0.07	8.5	13.2	3.6	0.01	3.3	3.10
NHW02	7.6	3.24	0.14	0.19	0.01	0.3	0.07	5.9	5.6	3.3	0.01	3.6	1.60
NHW03	8.0	2.33	0.13	0.13	0.01	0.3	0.02	6.2	6.1	3.0	<0.01	3.3	1.72
BB01	18.5	2.86	0.23	0.38	0.06	0.8	0.56	5.9	17.7	10.6	0.15	13.0	4.54
BB02	44.9	4.36	0.60	1.01	0.04	<0.1	0.75	14.2	37.3	17.1	0.05	13.3	10.29
HC01	3.4	2.54	0.10	0.15	<0.01	0.2	0.08	3.1	1.6	2.4	<0.01	2.6	0.62
HC02	4.2	2.73	0.09	0.22	<0.01	0.2	0.20	4.5	3.0	3.0	<0.01	2.0	0.83
HC03	5.2	2.49	0.13	0.13	<0.01	0.4	0.08	7.1	2.4	2.5	<0.01	2.4	1.13
HC04	8.3	4.86	0.26	0.28	<0.01	2.1	0.08	10.6	7.0	4.8	0.02	10.6	1.84
HC05	11.7	3.41	0.17	0.49	0.01	0.3	0.23	5.5	10.1	5.8	0.02	4.4	2.55
GOR01	4.2	2.22	0.11	0.11	0.01	0.3	0.08	4.2	3.5	2.7	<0.01	2.5	0.86
GOR02	4.5	2.66	0.07	0.13	<0.01	0.5	0.08	4.4	3.4	2.8	<0.01	3.4	0.95
GOR03	6.9	3.51	0.12	0.18	<0.01	0.4	0.07	5.5	4.2	2.8	<0.01	4.9	1.25
GOR04	13.1	12.57	0.26	0.49	0.01	1.0	0.09	12.3	8.7	7.3	0.03	19.4	2.57
DIA01	5.8	4.31	0.16	0.28	0.01	0.2	0.05	6.1	3.6	3.2	<0.01	2.8	1.07
DIA02	4.5	2.29	0.13	0.09	<0.01	0.2	0.07	5.6	3.5	2.0	<0.01	1.8	0.83
DIA03	6.0	3.45	0.22	0.21	0.01	0.3	0.26	9.1	5.7	2.4	<0.01	3.6	1.24
DIA04	3.4	2.40	0.10	0.09	<0.01	0.3	0.08	3.2	2.5	2.3	<0.01	1.9	0.65
DIA05	3.7	2.19	0.09	0.07	<0.01	0.2	0.02	3.6	2.7	2.3	<0.01	2.2	0.64
DIA06	3.4	2.33	0.08	0.10	<0.01	0.2	0.04	2.4	2.1	2.8	<0.01	2.2	0.67
WF01	5.4	2.57	0.15	0.12	<0.01	0.4	0.17	3.1	5.2	2.4	<0.01	2.5	1.06
WF02	4.4	2.15	0.09	0.09	0.01	0.3	0.04	2.8	3.5	2.4	<0.01	2.1	0.87
WF03	5.2	2.63	0.11	0.12	0.01	0.3	0.09	3.6	4.8	2.7	<0.01	2.4	0.90
WF04	6.1	3.27	0.10	0.10	<0.01	0.4	<0.01	3.8	4.0	2.5	<0.01	3.3	1.19
TDQ01	3.7	2.25	0.09	0.11	<0.01	0.4	0.11	2.3	2.1	2.5	0.01	2.9	0.70
TDQ02	3.6	2.25	0.05	0.08	<0.01	0.4	0.06	2.3	2.2	2.5	<0.01	1.9	0.68

Sample ID	La (ppm)	LOI (%)	Lu (ppm)	MgO (%)	MnO (%)	Mo (ppm)	Na_2O (%)	Nb (ppm)	Nd (ppm)	Ni (ppm)	P_2O_5 (%)	Pb (ppm)	Pr (ppm)
TDQ03	3.4	2.24	0.09	0.10	<0.01	0.4	0.13	2.6	3.1	2.5	<0.01	2.7	0.63
TDQ04	3.6	2.23	0.09	0.08	<0.01	0.4	<0.01	2.8	1.6	2.9	<0.01	2.2	0.62
TDQ05	3.7	2.71	0.10	0.09	<0.01	0.4	<0.01	3.1	1.6	3.2	<0.01	2.6	0.64
WFN01	5.7	3.35	0.16	0.25	<0.01	0.4	0.26	5.1	4.4	2.1	<0.01	2.2	1.08
WFN02	5.2	3.16	0.13	0.15	<0.01	0.4	0.06	5.8	2.5	2.1	<0.01	2.2	1.20
WFN03	5.5	2.69	0.11	0.11	<0.01	0.5	<0.01	4.1	4.4	2.3	<0.01	2.6	1.03
WFN04	5.1	2.95	0.11	0.12	<0.01	0.4	<0.01	3.9	3.6	4.1	<0.01	2.5	1.00
GRQ04	25.9	3.86	0.26	0.22	<0.01	0.6	0.13	8.3	13.4	3.6	0.02	5.5	4.41
CCH03	15.8	5.54	0.11	0.61	<0.01	0.1	0.25	3.6	13.1	5.9	<0.01	3.1	3.46
SRQ09	6.0	0.63	0.11	0.09	<0.01	0.7	0.06	1.2	9.0	5.0	0.01	2.4	1.91
SP01	6.8	2.70	0.14	0.11	<0.01	0.7	0.05	6.3	4.6	3.1	<0.01	8.5	1.39
SP02	6.6	5.13	0.12	0.17	<0.01	<0.1	0.36	6.0	3.8	3.0	<0.01	3.6	1.12
SP03	14.4	5.21	0.19	0.11	<0.01	2.7	0.18	4.8	17.4	5.1	<0.01	28.3	4.54
SP04	6.2	4.00	0.14	0.27	<0.01	<0.1	0.16	6.1	5.0	3.3	<0.01	4.9	1.27
SP05	6.3	6.66	0.15	0.34	<0.01	<0.1	0.64	6.1	6.1	2.7	<0.01	4.6	1.51
SP06	7.1	6.84	0.19	0.41	<0.01	<0.1	0.68	6.2	8.5	3.1	<0.01	3.9	1.95
SP07	17.1	6.18	0.30	0.35	<0.01	<0.1	0.24	8.8	16.8	3.3	0.01	3.7	3.81
SP08	13.2	5.42	0.28	0.20	<0.01	<0.1	0.20	8.5	13.1	2.5	<0.01	5.0	3.37
SP09	19.8	6.94	0.44	0.10	<0.01	4.1	0.11	8.5	33.7	6.0	0.01	35.9	7.70
SP10	10.8	6.52	0.36	0.09	<0.01	2.7	0.03	12.1	14.0	5.5	0.01	19.3	3.53
CW01	159.2	13.88	0.22	0.73	<0.01	<0.1	1.42	97.4	139.3	20.2	0.76	4.2	35.38
CW02	72.1	4.24	1.38	0.20	0.03	0.5	0.10	22.2	60.8	6.5	0.10	8.5	15.95
CW03	35.7	5.31	0.80	0.09	0.02	0.4	0.02	11.0	35.7	4.0	0.07	14.4	9.13
CW04	23.7	4.96	0.65	0.14	0.04	0.9	0.02	10.6	19.1	11.8	0.10	11.6	5.60
CW05	29.0	5.10	0.53	0.12	0.03	2.6	0.02	22.8	24.2	6.4	0.04	16.9	6.50
CW06	22.8	5.09	0.56	0.11	0.02	2.6	0.03	16.6	18.8	4.9	0.03	12.7	5.32

Sample ID	La (ppm)	LOI (%)	Lu (ppm)	MgO (%)	MnO (%)	Mo (ppm)	Na_2O (%)	Nb (ppm)	Nd (ppm)	Ni (ppm)	P_2O_5 (%)	Pb (ppm)	Pr (ppm)
CW07	21.2	1.04	0.82	0.03	0.01	0.2	0.02	29.7	17.9	1.0	0.02	5.5	4.86
CW08	20.4	1.96	0.86	0.03	<0.01	0.5	0.01	32.4	17.6	0.9	0.02	6.1	4.92
CW09	3.1	3.00	0.06	0.04	<0.01	3.4	<0.01	2.1	2.3	2.0	<0.01	3.9	0.62
CW10	13.6	7.96	0.42	0.10	0.01	2.5	0.02	18.1	10.1	4.3	0.02	13.2	3.11
WA01	7.2	8.18	0.28	0.16	0.01	2.3	0.05	7.7	8.4	6.9	0.03	16.5	2.14
WA02	7.3	5.76	0.19	0.11	0.01	3.1	0.03	6.8	7.4	4.7	0.03	26.2	1.76
WA03	9.3	7.26	0.23	0.12	0.01	3.1	0.02	8.5	8.1	6.0	0.03	29.1	2.21
WA04	7.0	6.96	0.17	0.09	<0.01	4.1	0.02	7.5	7.4	5.3	0.04	32.2	1.84
WA05	2.6	10.43	0.78	0.11	0.01	3.7	1.15	21.2	4.5	1.5	<0.01	29.3	0.99
WA06	2.7	9.63	1.00	0.08	<0.01	<0.1	0.73	25.1	3.9	1.0	<0.01	2.4	0.80
WA07	13.2	8.28	0.26	0.17	0.04	5.5	0.02	7.0	17.6	10.1	0.12	29.5	4.19
WA08	12.1	8.37	0.30	0.22	0.04	6.3	0.05	8.4	20.6	11.1	0.10	34.8	4.64
WA09	63.7	0.45	0.73	0.03	0.02	1.1	4.02	17.8	54.6	0.8	<0.01	12.6	14.70
WA10	46.6	2.05	0.61	0.09	0.03	2.9	2.77	15.9	43.2	4.9	0.03	25.4	11.16
WA11	8.5	6.19	0.18	0.08	0.01	4.1	<0.01	6.3	8.1	4.7	0.03	32.7	2.03
HP01	5.3	5.17	0.12	0.25	<0.01	<0.1	0.20	4.6	2.9	1.2	<0.01	1.7	0.92
HP02	6.9	2.49	0.14	0.08	<0.01	0.2	0.09	3.2	5.7	0.9	<0.01	8.7	1.43
HP03	7.7	10.07	0.19	0.21	0.01	1.2	0.02	4.7	10.1	7.6	0.02	14.8	2.43
GOR05	6.0	5.39	0.13	0.07	<0.01	2.2	0.08	6.5	6.4	1.6	<0.01	18.3	1.63
GOR06	10.7	3.63	0.26	0.05	<0.01	4.2	0.02	13.1	10.2	3.3	0.04	23.1	2.24
GOR07	9.9	3.55	0.24	0.06	0.01	4.5	0.02	11.9	9.3	3.6	0.04	24.7	2.35
GOR08	8.4	7.10	0.22	0.21	<0.01	0.6	0.02	10.7	6.0	5.3	0.01	11.2	1.71
SH01	4.8	6.51	0.21	0.20	<0.01	8.3	0.05	8.8	5.3	4.2	0.04	8.3	1.36
SH02	14.7	6.06	0.32	0.16	<0.01	4.4	0.01	11.5	15.0	4.7	0.03	9.0	3.39
SH03	6.2	2.66	0.29	0.14	<0.01	2.1	0.05	7.5	4.5	1.8	0.01	3.3	1.23
MP01	6.1	3.81	0.23	0.15	0.01	2.2	0.10	8.3	5.9	4.5	0.02	9.1	1.40

Sample ID	La (ppm)	LOI (%)	Lu (ppm)	MgO (%)	MnO (%)	Mo (ppm)	Na_2O (%)	Nb (ppm)	Nd (ppm)	Ni (ppm)	P_2O_5 (%)	Pb (ppm)	Pr (ppm)
MP02	4.6	3.88	0.18	0.10	<0.01	2.0	0.17	7.4	4.2	2.5	0.02	5.8	1.05
GL01	13.6	3.74	0.24	0.25	<0.01	0.4	0.10	8.2	9.4	1.7	0.02	4.1	2.74
CW11	10.7	4.87	0.23	0.14	0.01	2.6	0.02	10.9	7.6	4.7	0.02	23.1	2.35
HHQ01	3.2	2.82	0.19	0.11	<0.01	0.8	0.05	6.1	2.6	1.7	<0.01	7.0	0.73
MR01	68.5	8.73	0.56	0.17	0.01	3.5	0.03	15.1	61.7	8.7	0.47	27.8	15.46
MR02	34.4	7.88	0.32	0.23	<0.01	<0.1	0.10	14.6	19.8	2.7	0.15	19.4	6.04
WRC01	9.7	18.53	0.15	0.99	<0.01	0.2	0.16	2.1	9.3	7.9	<0.01	3.5	2.08
DIA10	7.1	6.81	0.16	0.12	<0.01	2.1	0.05	8.3	7.6	5.0	0.02	12.3	1.62
DIA11	14.2	1.85	0.26	0.07	0.02	3.4	0.01	11.2	12.7	15.0	0.04	47.9	3.61
BAL01	24.8	11.84	0.38	1.82	0.01	0.3	0.96	10.9	20.4	8.8	0.03	8.9	5.20
BAL02	4.8	1.06	0.08	0.13	<0.01	0.6	0.24	2.7	4.7	2.4	<0.01	2.6	0.97
BAL03	18.8	3.29	0.13	0.39	0.01	1.9	0.23	3.0	11.6	5.3	0.02	73.7	4.38
BAL04	11.0	2.27	0.19	0.19	<0.01	2.4	0.25	6.9	9.6	10.1	0.01	26.7	2.99
BAL05	8.6	3.17	0.10	0.19	<0.01	3.8	0.20	5.7	8.0	6.0	0.03	75.5	2.27
BAL06	9.0	2.59	0.09	0.15	<0.01	5.0	0.17	5.1	3.5	4.0	0.03	37.4	1.67
WEN01	16.8	7.43	0.26	0.84	0.04	0.7	0.74	7.4	16.8	14.8	0.08	7.4	4.07
WEN02	21.6	5.25	0.34	0.61	0.04	0.8	1.00	15.6	19.5	10.5	0.10	9.4	5.06
WEN03	19.0	4.60	0.33	0.55	0.03	0.1	0.93	12.7	15.3	9.0	0.09	7.2	4.41
WEN04	20.2	4.94	0.41	0.61	0.04	0.1	1.11	13.1	21.4	10.6	0.08	7.8	5.12
WEN05	16.4	3.94	0.32	0.42	0.02	0.1	0.64	16.3	15.4	6.9	0.12	6.2	4.15
WEN06	14.4	4.11	0.34	0.50	0.03	0.3	0.80	14.8	14.0	10.0	0.09	7.7	3.80
WEN07	7.7	2.30	0.10	0.20	<0.01	0.3	0.32	3.2	7.8	3.4	0.02	3.4	1.64
WEN08	11.0	3.44	0.20	0.36	0.02	0.3	0.55	6.2	11.9	5.8	0.03	4.7	2.52
WEN09	11.2	2.93	0.20	0.27	0.02	0.4	0.44	7.9	8.6	6.9	0.03	4.7	2.08
WEN10	16.1	2.43	0.22	0.23	0.03	0.5	0.33	8.1	14.0	4.8	0.03	4.9	3.36
WEN11	4.4	1.21	0.07	0.08	0.02	0.4	0.15	1.9	2.0	2.1	0.01	2.1	0.92

Sample ID	La (ppm)	LOI (%)	Lu (ppm)	MgO (%)	MnO (%)	Mo (ppm)	Na_2O (%)	Nb (ppm)	Nd (ppm)	Ni (ppm)	P_2O_5 (%)	Pb (ppm)	Pr (ppm)
WEN12	3.7	3.49	0.05	0.08	0.14	0.3	0.12	1.0	2.7	1.0	0.05	1.2	0.56
WEN13	2.9	1.78	0.02	0.05	0.07	0.4	0.12	0.4	1.6	2.4	0.04	1.2	0.39
WEN14	3.8	0.77	0.05	0.03	0.02	0.3	0.12	1.2	4.2	2.8	0.01	1.7	0.95
WEN15	8.2	2.54	0.09	0.05	0.03	1.1	0.14	2.7	6.3	9.2	0.02	5.3	1.64
WEN16	4.9	1.30	0.13	0.05	0.02	0.5	0.13	1.7	4.3	5.6	0.01	3.9	1.20
WEN17	6.2	2.12	0.12	0.06	0.02	0.5	0.13	2.9	3.4	7.9	0.01	4.9	1.45
WEN18	13.6	4.74	0.20	0.27	0.03	0.8	0.21	8.0	17.0	10.5	0.03	8.1	3.03
WEN19	12.1	4.18	0.18	0.24	0.05	0.8	0.19	6.0	7.8	10.1	0.03	6.7	2.59
BUN01	6.6	0.67	0.09	0.07	0.02	0.4	0.40	1.4	6.0	3.6	0.02	6.5	1.33
BUN02	8.8	0.62	0.13	0.09	<0.01	0.2	0.36	2.1	7.9	2.2	0.02	4.4	1.82
BUN03	7.8	0.77	0.11	0.11	0.02	0.5	0.34	1.8	7.3	5.0	0.03	15.3	1.64
BUN04	7.4	0.92	0.15	0.13	0.02	0.5	0.35	1.9	6.3	5.6	0.04	7.7	1.83
BUN05	40.3	1.50	0.66	0.26	0.04	0.8	0.63	7.5	27.6	6.8	0.04	9.2	9.39
BUN06	14.1	2.92	0.16	0.40	0.02	0.9	0.60	5.7	10.4	5.4	0.04	19.8	3.23
BUN07	8.6	1.11	0.15	0.12	0.02	0.6	0.43	2.0	7.0	4.3	0.04	10.5	1.61
BUN08	19.1	1.94	0.39	0.25	0.03	0.9	0.70	7.5	14.0	6.4	0.05	14.3	4.53
BUN09	9.5	2.64	0.15	0.19	0.02	1.4	0.37	3.9	10.6	6.7	0.07	40.0	2.16
BUN10	19.1	2.17	0.27	0.18	0.02	0.7	0.37	5.6	19.0	6.8	0.04	15.7	5.01
BUN11	15.7	1.50	0.24	0.13	0.02	0.6	0.33	4.0	15.0	6.8	0.03	16.2	3.90
BUN12	13.5	2.59	0.17	0.14	0.01	1.1	0.29	3.4	11.8	5.4	0.03	338.5	3.09
BUN13	11.1	1.34	0.19	0.10	0.01	2.1	0.26	2.8	9.7	5.1	0.03	33.8	2.71
BUN14	7.9	0.43	0.09	0.06	0.01	0.4	0.21	2.8	6.0	2.7	0.02	7.5	1.73
BUN15	6.6	0.27	0.08	0.04	0.01	0.5	0.19	1.8	5.5	2.5	0.01	5.4	1.49
BUN16	5.9	0.21	0.09	0.05	0.01	0.5	0.17	1.4	5.1	2.7	0.01	4.1	1.39
BUN17	7.0	0.22	0.08	0.04	0.01	0.3	0.18	1.2	5.3	3.1	0.01	3.4	1.60
BUN18	6.6	0.33	0.08	0.04	0.01	0.8	0.17	1.3	4.7	2.3	0.02	6.7	1.56

Sample ID	La (ppm)	LOI (%)	Lu (ppm)	MgO (%)	MnO (%)	Mo (ppm)	Na_2O (%)	Nb (ppm)	Nd (ppm)	Ni (ppm)	P_2O_5 (%)	Pb (ppm)	Pr (ppm)
BUN19	5.6	0.21	0.06	0.03	0.01	0.7	0.17	1.1	5.9	2.7	0.02	5.4	1.33
BUN20	6.3	0.19	0.10	0.03	0.01	0.3	0.21	1.3	4.1	2.0	0.01	4.1	1.35
BUN21	5.8	5.60	0.11	0.16	0.02	0.3	0.13	1.6	3.8	3.9	0.04	9.0	1.17
BUN22	6.1	4.59	0.12	0.16	0.03	0.5	0.14	3.6	5.2	4.7	0.04	81.4	1.29
BUN23	4.0	0.37	0.05	0.02	<0.01	0.2	0.14	0.9	1.9	9.1	<0.01	4.7	0.62
BUN24	2.8	0.53	0.04	<0.01	<0.01	0.1	0.12	1.1	1.7	16.5	<0.01	4.3	0.47
BUN25	4.3	0.31	0.06	0.02	0.01	0.2	0.16	1.5	3.7	14.7	<0.01	3.6	0.94
BUN26	4.0	0.84	0.05	0.02	0.01	0.3	0.16	1.1	2.6	17.3	<0.01	7.7	0.84
BUN27	5.6	3.70	0.11	0.07	<0.01	0.3	0.16	2.0	5.3	11.5	0.01	9.7	1.30
BUN28	3.9	2.02	0.07	0.04	<0.01	0.3	0.14	1.6	3.6	19.0	0.01	7.0	0.84
BUN29	4.5	7.18	0.07	0.02	0.01	0.6	0.11	1.6	3.5	46.9	<0.01	37.8	0.91
BUN30	5.9	9.75	0.11	0.03	<0.01	0.6	0.11	3.1	3.8	73.3	<0.01	17.6	1.29
HOR101	11.1	8.88	0.19	0.20	<0.01	0.8	0.13	11.4	7.3	3.0	0.02	11.5	2.12
HOR102	9.8	6.87	0.21	0.16	<0.01	0.7	0.13	11.3	7.4	2.6	0.02	9.1	1.97
HOR103	8.4	6.97	0.15	0.21	<0.01	0.8	0.14	8.7	5.5	3.2	0.01	6.3	1.64
HOR104	11.7	9.94	0.21	0.28	<0.01	0.4	0.14	11.0	7.7	2.3	0.02	6.3	2.21
HOR105	10.7	7.93	0.22	0.21	<0.01	0.6	0.14	10.1	6.3	1.3	0.02	5.8	1.87
HOR106	8.3	6.80	0.18	0.17	<0.01	1.2	0.14	8.3	5.4	2.7	0.01	4.8	1.45
HOR107	6.3	5.41	0.17	0.12	<0.01	1.1	0.14	7.9	4.2	2.9	0.01	3.6	1.17
HOR108	5.0	3.89	0.16	0.11	<0.01	1.0	0.16	6.8	3.5	2.5	0.01	3.2	1.00
HOR109	4.5	3.22	0.12	0.10	<0.01	1.1	0.16	5.6	3.6	2.4	0.01	2.5	0.88
HOR110	5.3	2.67	0.10	0.09	<0.01	0.8	0.16	5.3	4.2	1.7	<0.01	2.1	1.06
HOR111	4.6	3.77	0.12	0.10	<0.01	1.1	0.17	5.3	3.6	2.7	<0.01	2.7	0.94
HOR112	4.1	2.90	0.12	0.10	<0.01	1.0	0.16	4.5	3.0	2.0	<0.01	2.4	0.72
HOR113	6.7	2.16	0.13	0.08	<0.01	1.2	0.15	6.6	4.9	2.6	0.01	3.2	1.29
HOR114	4.0	2.22	0.09	0.06	<0.01	1.0	0.14	4.2	3.2	1.2	<0.01	2.5	0.75

Sample ID	La (ppm)	LOI (%)	Lu (ppm)	MgO (%)	MnO (%)	Mo (ppm)	Na_2O (%)	Nb (ppm)	Nd (ppm)	Ni (ppm)	P_2O_5 (%)	Pb (ppm)	Pr (ppm)
HOR115	4.2	2.64	0.12	0.11	<0.01	0.5	0.18	4.3	2.6	1.4	<0.01	2.2	0.71
HOR116	3.2	2.33	0.10	0.08	<0.01	1.4	0.04	3.3	2.4	3.4	<0.01	3.0	0.58
HOR117	3.2	1.90	0.07	0.05	<0.01	1.2	0.04	3.0	2.2	1.8	<0.01	2.5	0.58
HOR118	2.9	1.91	0.08	0.05	<0.01	1.6	0.03	2.8	2.5	3.8	<0.01	3.3	0.68
HOR119	3.9	1.98	0.08	0.05	<0.01	1.1	0.03	2.7	3.4	1.7	<0.01	3.6	0.76
HOR120	4.0	2.28	0.09	0.03	<0.01	1.3	0.02	2.7	4.1	3.6	<0.01	3.1	1.01
HOR121	4.5	2.66	0.12	0.05	<0.01	1.7	0.04	3.0	5.9	2.6	0.01	4.7	1.22
HOR122	4.6	2.22	0.10	0.07	<0.01	1.2	0.05	3.3	3.3	3.4	<0.01	3.0	0.89
HOR123	4.2	2.88	0.09	0.09	<0.01	0.7	0.05	3.0	3.0	1.6	<0.01	2.7	0.75
HOR124	4.0	2.11	0.07	0.06	<0.01	1.1	0.04	3.0	2.5	2.9	<0.01	3.2	0.74
HOR125	4.1	1.96	0.05	0.05	<0.01	1.0	0.04	2.5	2.3	1.4	<0.01	2.1	0.61
HOR126	4.1	2.17	0.07	0.06	<0.01	0.8	0.03	2.7	2.5	3.0	<0.01	2.6	0.60
HOR127	4.4	2.45	0.06	0.07	<0.01	0.7	0.04	2.3	1.9	1.8	<0.01	2.9	0.63
HOR128	4.2	2.11	0.06	0.05	<0.01	1.1	0.04	2.4	1.7	3.1	<0.01	2.5	0.63
HOR129	5.2	2.81	0.07	0.08	<0.01	0.7	0.03	2.9	2.9	2.0	<0.01	2.9	0.83
HOR130	7.5	0.97	0.06	0.03	<0.01	1.2	0.03	1.5	3.5	3.2	<0.01	2.3	1.23
HOR131	9.3	1.33	0.09	0.07	<0.01	1.4	0.08	3.5	5.9	1.6	<0.01	3.6	1.82
HOR132	13.7	1.60	0.15	0.05	<0.01	1.7	0.05	3.6	11.2	3.7	0.01	4.8	3.02
HOR133	7.0	1.13	0.06	0.03	<0.01	1.3	0.04	2.1	3.9	1.4	<0.01	3.7	1.30
HOR134	6.5	0.93	0.09	0.04	<0.01	1.6	0.05	2.7	4.3	3.8	<0.01	5.1	1.35
HOR135	5.2	0.47	0.08	0.01	<0.01	1.3	0.05	1.8	4.3	1.1	<0.01	2.5	1.16
HOR136	34.2	23.56	0.48	1.11	0.24	1.7	0.34	6.8	38.1	15.4	0.20	13.1	9.22
HOR137	53.8	6.77	0.94	0.46	0.13	1.1	0.24	13.1	47.8	9.1	0.13	8.6	12.81
HOR501	4.7	2.72	0.10	0.19	<0.01	0.4	0.06	3.6	3.3	2.6	<0.01	2.0	0.99
HOR503	8.2	3.18	0.11	0.13	<0.01	1.3	0.06	6.1	7.6	4.3	0.01	3.7	1.80
HOR504	9.2	9.17	0.19	0.30	<0.01	1.8	0.16	9.8	8.3	3.8	0.02	20.3	2.26

Sample ID	La (ppm)	LOI (%)	Lu (ppm)	MgO (%)	MnO (%)	Mo (ppm)	Na_2O (%)	Nb (ppm)	Nd (ppm)	Ni (ppm)	P_2O_5 (%)	Pb (ppm)	Pr (ppm)
HOR507	9.4	9.34	0.19	0.23	<0.01	0.7	0.15	9.6	6.3	4.1	0.01	7.4	2.03
HOR508	10.2	10.18	0.19	0.25	<0.01	0.9	0.16	9.7	8.1	2.9	0.01	8.4	2.07
HOR509	5.8	5.87	0.17	0.12	<0.01	1.2	0.10	9.1	3.7	3.2	<0.01	3.2	1.32
HOR510	5.7	6.49	0.20	0.13	<0.01	1.1	0.10	8.7	4.4	2.2	<0.01	5.1	1.22
HOR511	5.0	4.96	0.15	0.09	<0.01	0.8	0.08	7.6	4.3	1.6	<0.01	2.9	1.01
HOR512	4.9	4.16	0.13	0.09	<0.01	0.8	0.08	6.9	4.1	1.4	<0.01	2.8	1.06
HOR513	4.4	2.69	0.13	0.05	<0.01	1.2	0.07	6.0	3.5	3.1	<0.01	2.4	0.86
HOR514	5.0	3.29	0.14	0.07	<0.01	0.9	0.09	7.2	4.5	0.8	<0.01	2.8	1.07
HOR515	4.8	2.70	0.12	0.06	<0.01	1.3	0.05	5.6	3.6	2.3	<0.01	3.6	0.99
HOR516	3.8	2.12	0.07	0.06	<0.01	1.2	0.05	3.2	3.2	1.9	<0.01	2.4	0.84
HOR517	3.3	1.86	0.07	0.06	<0.01	1.6	0.05	2.7	2.3	3.6	<0.01	2.8	0.72
HOR518	4.3	1.55	0.06	0.06	<0.01	1.2	0.06	2.4	2.9	2.2	<0.01	3.6	0.87
HOR519	3.8	1.42	0.06	0.04	<0.01	1.6	0.04	2.3	2.3	4.3	0.01	3.2	0.70
HOR520	4.3	1.19	0.07	0.05	0.01	1.4	0.03	3.4	3.8	2.7	<0.01	3.8	0.91
HOR521	4.8	1.70	0.08	0.09	0.01	1.7	0.05	4.1	3.7	4.3	<0.01	4.6	1.04
HOR522	7.4	1.78	0.13	0.07	0.02	1.3	0.04	6.3	6.0	3.0	0.03	4.8	1.65
HOR523	4.4	1.62	0.05	0.06	0.01	1.1	0.04	3.3	3.2	3.3	0.01	3.5	0.87
HOR524	4.5	1.71	0.06	0.07	<0.01	1.5	0.04	2.6	2.8	2.6	0.02	3.8	0.87
HOR525	3.9	1.70	0.07	0.06	0.01	1.6	0.03	2.0	3.6	4.3	0.02	3.7	0.85
HOR527	5.5	1.84	0.09	0.07	0.01	1.3	0.03	3.3	4.3	2.8	0.02	4.1	1.15
HOR528	5.9	1.92	0.09	0.07	0.01	1.4	0.04	4.0	4.5	4.5	0.03	4.0	1.32
HOR529	6.8	1.85	0.11	0.09	0.01	1.3	0.05	4.5	5.0	3.2	0.02	4.1	1.44
HOR530	5.6	1.71	0.10	0.06	<0.01	1.3	0.04	4.9	3.4	3.6	0.02	3.3	0.93
HOR531	8.5	2.14	0.15	0.07	0.01	1.3	0.06	7.1	6.5	3.3	0.02	4.1	1.52
HOR532	6.8	1.98	0.10	0.07	0.01	1.6	0.04	5.5	4.7	4.6	0.02	3.5	1.28
HOR533	4.4	2.07	0.08	0.07	<0.01	1.5	0.05	2.9	3.2	3.5	0.01	2.8	0.91

Sample ID	La (ppm)	LOI (%)	Lu (ppm)	MgO (%)	MnO (%)	Mo (ppm)	Na_2O (%)	Nb (ppm)	Nd (ppm)	Ni (ppm)	P_2O_5 (%)	Pb (ppm)	Pr (ppm)
HOR534	8.0	2.10	0.16	0.08	0.02	1.4	0.03	11.6	7.3	4.1	0.02	3.8	1.63
HOR535	7.2	1.97	0.09	0.07	<0.01	0.7	0.03	4.9	4.8	1.5	<0.01	2.1	1.26
HOR536	18.1	1.88	0.33	0.08	0.02	0.8	0.03	13.2	12.6	3.2	<0.01	3.4	3.80
HOR537	9.2	2.09	0.27	0.07	0.02	1.2	0.02	14.8	7.5	3.6	0.02	2.8	1.86
HOR538	7.6	2.14	0.09	0.08	<0.01	1.2	0.03	3.5	5.2	4.2	0.02	2.4	1.39
HOR539	7.6	1.21	0.14	0.06	0.02	1.0	0.04	15.7	5.0	1.5	<0.01	2.9	1.47
HOR540	4.7	0.64	0.07	0.02	<0.01	1.7	0.03	2.1	3.8	4.3	0.02	2.6	1.12
HOR541	5.2	0.77	0.07	0.03	<0.01	1.7	0.04	1.4	5.6	3.4	0.03	2.6	1.38
HOR542	7.5	0.96	0.08	0.04	<0.01	1.5	0.04	1.8	6.5	5.5	0.02	2.7	1.67
HOR543	5.9	0.83	0.07	0.03	<0.01	1.5	0.03	1.9	4.5	2.7	0.01	2.2	1.33
HOR544	5.9	0.67	0.06	0.04	<0.01	1.1	0.03	2.1	4.5	3.4	<0.01	2.2	1.24
HOR545	5.9	0.69	0.07	0.03	<0.01	1.6	0.03	2.2	4.8	2.4	0.01	2.2	1.35
HOR546	6.9	0.64	0.08	0.04	<0.01	1.6	0.04	3.3	5.5	4.5	0.01	2.2	1.46
HOR547	4.7	0.56	0.06	0.02	<0.01	1.8	0.04	1.6	3.4	1.7	0.02	2.0	1.11
HOR548	4.8	0.38	0.07	0.02	<0.01	1.7	0.03	1.7	4.6	3.7	<0.01	1.7	1.12
HOR549	5.4	0.36	0.04	0.02	<0.01	1.7	0.04	1.4	3.8	1.7	<0.01	1.6	1.07
HOR550	3.7	0.42	0.07	0.03	<0.01	2.3	0.05	1.2	4.1	4.3	<0.01	2.0	0.97
HOR551	3.9	0.25	0.05	<0.01	<0.01	1.7	0.02	0.9	3.7	1.9	<0.01	1.5	0.93
HOR552	5.3	0.46	0.08	0.02	<0.01	2.2	0.03	2.4	5.3	4.4	0.01	2.7	1.41
HOR553	76.6	1.27	1.33	0.08	0.03	1.6	0.07	12.4	78.8	5.8	0.05	10.2	19.75
HOR554	98.2	3.36	1.99	0.16	0.05	1.8	0.06	19.7	106.3	17.4	0.18	11.5	26.93
HOR505	11.4	13.04	0.24	0.50	<0.01	0.7	0.25	10.6	10.2	5.7	0.02	13.1	2.78
HOR506	12.8	11.64	0.26	0.29	<0.01	0.8	0.22	13.0	12.2	3.8	0.01	13.1	3.08
HOR526	6.6	1.80	0.10	0.08	0.02	1.1	0.04	4.3	5.2	4.4	0.02	4.6	1.41
HOR701	36.2	21.47	0.36	1.46	0.03	0.4	0.54	6.2	32.2	12.6	0.02	9.7	7.79
HOR702	23.6	8.65	0.31	0.98	0.04	0.6	0.71	8.3	24.8	19.0	0.02	15.9	6.56

Sample ID	La (ppm)	LOI (%)	Lu (ppm)	MgO (%)	MnO (%)	Mo (ppm)	Na_2O (%)	Nb (ppm)	Nd (ppm)	Ni (ppm)	P_2O_5 (%)	Pb (ppm)	Pr (ppm)
HOR703	22.8	7.51	0.34	0.79	0.04	0.9	0.59	7.6	22.8	17.0	0.02	17.5	5.81
HOR704	22.7	7.40	0.29	0.72	0.03	0.9	0.54	7.5	22.8	12.5	0.02	17.7	5.50
HOR705	19.6	6.73	0.22	0.65	0.02	0.7	0.50	6.5	18.6	9.7	0.01	10.3	4.44
HOR706	24.1	7.21	0.23	0.72	0.02	0.7	0.55	6.8	20.2	10.0	0.01	10.4	5.45
HOR707	24.7	7.35	0.26	0.73	0.02	0.4	0.57	6.6	20.2	8.9	<0.01	10.3	5.13
HOR708	33.3	10.19	0.34	0.96	0.02	0.5	0.73	8.9	36.3	10.6	<0.01	11.2	9.26
HOR709	23.1	8.95	0.38	0.87	0.02	0.6	0.67	8.2	27.0	9.5	0.01	10.2	7.16
HOR710	15.1	9.86	0.30	0.85	0.01	0.4	0.69	8.6	14.6	11.0	0.01	14.8	3.88
HOR711	10.8	9.26	0.19	0.75	0.01	0.7	0.64	7.2	9.1	10.0	0.02	8.4	2.36
HOR712	8.0	7.76	0.16	0.30	<0.01	1.1	0.32	8.8	4.3	3.3	0.01	3.4	1.44
HOR713	4.8	5.46	0.10	0.13	<0.01	0.8	0.18	6.6	2.0	3.0	<0.01	2.7	0.80
HOR714	3.3	3.72	0.08	0.08	<0.01	0.9	0.11	5.1	2.0	1.8	<0.01	1.6	0.58
HOR715	2.7	3.08	0.08	0.05	<0.01	1.5	0.09	4.6	1.9	3.5	<0.01	2.1	0.54
HOR716	2.9	2.70	0.07	0.06	<0.01	1.1	0.08	4.3	2.2	2.0	<0.01	1.9	0.50
HOR717	3.4	3.06	0.07	0.07	<0.01	1.2	0.13	4.6	2.4	2.8	<0.01	1.8	0.59
HOR718	3.7	2.71	0.05	0.06	<0.01	1.3	0.10	3.2	2.1	1.5	<0.01	1.7	0.74
HOR719	3.7	2.67	0.07	0.06	<0.01	1.3	0.11	3.0	2.1	3.3	<0.01	1.9	0.58
HOR720	3.3	3.14	0.06	0.07	<0.01	1.2	0.09	2.1	1.7	1.9	<0.01	2.1	0.57
HOR721	3.6	2.57	0.05	0.07	<0.01	1.4	0.09	3.2	2.0	3.3	<0.01	2.3	0.64
HOR722	4.1	2.64	0.06	0.08	0.01	1.5	0.10	3.3	2.5	2.0	0.01	2.4	0.73
HOR723	4.8	2.89	0.12	0.08	<0.01	1.2	0.10	4.1	3.2	3.0	<0.01	2.5	0.80
HOR724	4.1	2.83	0.06	0.08	<0.01	1.3	0.11	2.7	2.5	2.0	<0.01	2.4	0.68
HOR725	4.1	2.55	0.06	0.06	<0.01	1.6	0.09	3.1	1.9	3.7	<0.01	2.2	0.67
HOR726	3.8	2.15	0.05	0.06	<0.01	1.0	0.07	2.2	2.4	1.6	0.01	2.1	0.64
HOR727	4.3	2.58	0.06	0.08	<0.01	1.6	0.22	3.9	2.6	3.8	<0.01	2.1	0.75
HOR728	4.6	2.93	0.06	0.11	<0.01	1.0	0.24	3.6	2.5	1.4	0.01	2.1	0.74

Sample ID	La (ppm)	LOI (%)	Lu (ppm)	MgO (%)	MnO (%)	Mo (ppm)	Na_2O (%)	Nb (ppm)	Nd (ppm)	Ni (ppm)	P_2O_5 (%)	Pb (ppm)	Pr (ppm)
HOR729	6.8	2.43	0.08	0.09	<0.01	1.0	0.22	4.6	3.2	2.9	0.01	2.6	1.03
HOR730	6.6	2.20	0.09	0.08	<0.01	0.9	0.21	3.4	3.5	1.3	<0.01	2.1	1.03
HOR731	6.2	2.12	0.07	0.07	<0.01	1.1	0.22	3.8	3.4	2.9	<0.01	2.4	0.91
HOR732	6.5	1.76	0.07	0.07	<0.01	0.9	0.21	3.9	3.4	1.0	<0.01	2.7	1.01
HOR733	5.5	1.30	0.04	0.05	<0.01	1.2	0.19	2.1	2.6	2.9	<0.01	2.5	0.77
HOR734	6.7	1.60	0.06	0.06	<0.01	1.4	0.20	1.8	3.1	1.1	<0.01	2.3	0.87
HOR735	8.8	1.65	0.08	0.06	<0.01	1.4	0.20	3.2	4.3	3.5	<0.01	3.4	1.16
HOR736	10.2	1.85	0.06	0.07	<0.01	1.1	0.22	3.2	3.4	1.3	<0.01	2.9	1.33
HOR737	8.6	1.73	0.05	0.06	<0.01	1.5	0.20	2.1	3.6	3.5	<0.01	2.9	1.24
HOR738	7.4	1.28	0.06	0.04	<0.01	1.4	0.18	2.2	3.7	1.3	<0.01	2.4	1.30
HOR739	6.3	1.11	0.05	0.05	<0.01	1.8	0.19	2.2	3.4	3.0	<0.01	2.6	1.02
HOR740	10.4	1.35	0.06	0.04	<0.01	1.2	0.19	2.2	5.5	1.8	<0.01	2.7	1.66
HOR741	7.7	0.93	0.08	0.04	<0.01	1.4	0.19	2.5	5.1	2.7	<0.01	2.1	1.45
HOR742	11.7	1.05	0.05	0.05	<0.01	1.1	0.19	1.8	6.1	1.8	0.01	2.1	1.81
HOR743	13.1	1.17	0.12	0.06	<0.01	1.6	0.20	3.2	7.5	4.2	0.01	2.1	2.07
HOR744	8.9	1.07	0.04	0.06	<0.01	1.9	0.18	1.6	5.2	2.2	<0.01	2.2	1.43
HOR745	26.4	1.08	0.09	0.06	<0.01	1.8	0.19	3.2	8.7	4.5	0.02	11.2	2.93
HOR746	8.2	0.94	0.09	0.05	<0.01	1.1	0.17	2.8	4.2	1.3	<0.01	2.2	1.45
HOR747	11.3	1.20	0.10	0.05	<0.01	1.2	0.18	3.3	5.6	3.2	0.01	3.6	1.76
HOR748	6.2	0.85	0.05	0.05	<0.01	1.4	0.18	1.3	4.5	1.8	<0.01	1.4	1.17
HOR749	6.6	0.92	0.06	0.04	<0.01	1.0	0.17	1.5	4.1	3.0	<0.01	1.6	1.27
HOR750	6.6	1.20	0.07	0.06	<0.01	1.4	0.21	1.5	4.8	2.0	0.01	1.6	1.25
HOR751	7.1	1.03	0.06	0.05	<0.01	1.4	0.18	1.6	4.1	3.1	0.01	1.6	1.28
HOR752	33.5	7.35	0.32	0.74	0.04	1.3	0.61	8.0	30.0	15.9	0.02	24.4	7.63
HOR753	8.6	1.70	0.05	0.06	<0.01	1.3	0.08	3.2	3.6	3.2	<0.01	3.1	1.18
HOR754	11.6	1.19	0.09	0.06	<0.01	1.3	0.21	3.2	9.5	1.9	0.01	2.1	2.45

Sample ID	La (ppm)	LOI (%)	Lu (ppm)	MgO (%)	MnO (%)	Mo (ppm)	Na_2O (%)	Nb (ppm)	Nd (ppm)	Ni (ppm)	P_2O_5 (%)	Pb (ppm)	Pr (ppm)
HOR755	12.6	1.40	0.14	0.07	<0.01	0.9	0.22	3.8	11.2	2.7	0.01	2.7	2.83
HOR756	15.1	2.11	0.14	0.09	<0.01	0.5	0.25	4.5	14.9	2.3	0.02	2.7	3.87
HOR757	14.7	1.96	0.12	0.08	<0.01	1.0	0.27	6.5	14.9	5.1	0.02	3.4	4.12
HOR758	15.2	1.85	0.17	0.09	<0.01	0.6	0.29	10.2	15.9	2.3	0.02	4.0	3.95
HOR759	22.9	1.40	0.27	0.10	0.01	1.0	0.33	12.6	19.5	3.5	0.02	7.0	5.23
HOR760	18.2	1.33	0.17	0.08	<0.01	0.8	0.27	12.9	16.3	2.1	0.02	5.9	4.36
HOR761	15.2	1.24	0.11	0.08	<0.01	0.7	0.27	5.8	17.5	2.6	0.02	3.3	4.49
HOR762	13.9	1.13	0.14	0.08	<0.01	0.9	0.35	5.7	14.0	2.4	0.02	4.1	3.58
HOR763	22.6	1.30	0.31	0.09	<0.01	0.8	0.26	10.6	23.4	3.1	0.02	6.6	6.23
HOR764	27.7	1.31	0.47	0.09	0.01	0.7	0.30	14.4	30.1	2.0	0.02	6.1	7.44
HOR765	21.1	1.58	0.29	0.11	<0.01	1.6	0.32	12.6	33.4	5.2	0.03	7.8	7.45
HOR766	12.8	1.43	0.16	0.07	<0.01	1.2	0.30	4.2	15.7	3.1	0.02	4.5	3.91
HOR767	11.7	1.10	0.11	0.07	<0.01	1.2	0.30	3.9	13.2	4.3	0.02	3.7	3.30
HOR768	13.9	1.28	0.16	0.11	<0.01	1.4	0.35	4.6	15.5	2.9	0.02	4.7	3.78
HOR769	12.9	1.19	0.19	0.08	<0.01	1.7	0.33	5.3	15.2	5.4	0.02	5.0	3.40
HOR770	137.6	1.67	2.44	0.17	0.06	1.0	0.32	31.3	124.2	4.7	0.07	9.6	33.02
HOR771	131.9	2.70	1.53	0.15	0.08	1.3	0.30	20.0	189.9	146.6	0.13	7.9	46.91
HOR772	50.4	1.41	0.88	0.14	0.03	0.8	0.33	17.6	47.6	4.0	0.04	5.2	12.30
HOR773	77.7	1.72	1.33	0.17	0.03	1.5	0.35	22.9	75.1	13.0	0.05	5.5	19.00
HOR774	120.1	4.90	2.01	0.28	0.08	1.0	0.29	22.0	133.7	35.7	0.12	10.2	33.39
HOR775	14.6	2.15	0.21	0.18	0.01	1.7	0.31	6.1	12.2	5.2	0.02	4.8	3.45
HOR776	10.9	2.35	0.21	0.15	0.01	1.2	0.34	5.1	9.4	5.2	0.02	3.9	2.52
HOR777	11.8	1.74	0.16	0.17	<0.01	1.6	0.38	4.4	9.5	5.1	0.03	5.5	2.87
HOR778	8.4	1.59	0.13	0.14	0.01	1.2	0.41	3.8	8.2	6.0	0.03	3.8	2.23
HOR779	20.9	5.01	0.30	0.35	0.02	0.9	0.36	13.7	19.1	7.3	0.04	7.1	5.15
HOR780	76.4	5.58	1.38	0.43	0.06	0.9	0.33	25.9	70.5	9.7	0.13	12.6	18.57

Sample ID	La (ppm)	LOI (%)	Lu (ppm)	MgO (%)	MnO (%)	Mo (ppm)	Na_2O (%)	Nb (ppm)	Nd (ppm)	Ni (ppm)	P_2O_5 (%)	Pb (ppm)	Pr (ppm)
HOR781	47.3	19.28	0.49	2.55	0.23	0.9	0.37	10.4	58.8	36.3	0.15	18.1	14.00
WIL15	21.9	10.89	0.28	1.28	0.08	0.8	0.62	10.1	21.8	26.2	0.10	11.9	5.43
WIL16	24.0	11.52	0.33	1.34	0.07	0.7	0.80	11.9	24.2	29.2	0.11	14.3	6.17
WIL17	19.0	6.93	0.25	0.83	0.04	0.6	0.46	8.0	18.9	17.2	0.06	6.0	4.71
WIL18	24.7	12.03	0.35	1.39	0.29	0.5	0.76	11.3	25.6	28.8	0.11	10.6	6.31
WIL19	11.5	5.10	0.18	0.56	0.02	0.7	0.34	5.7	11.3	13.4	0.04	5.0	2.96
WIL20	7.6	3.35	0.12	0.37	0.02	0.8	0.17	3.7	7.4	9.5	0.03	2.8	1.91
WIL21	2.8	0.26	0.05	0.02	<0.01	1.4	<0.01	0.8	2.1	1.4	<0.01	1.2	0.57
WIL22	2.8	0.30	0.04	0.03	<0.01	1.4	<0.01	0.9	1.9	4.9	<0.01	6.6	0.50
WIL23	2.5	0.08	0.04	<0.01	<0.01	1.4	<0.01	0.8	2.2	2.1	<0.01	1.9	0.54
WIL24	2.4	0.12	0.04	<0.01	<0.01	1.7	<0.01	1.1	2.2	10.0	<0.01	1.6	0.54
WIL25	2.3	0.21	0.03	<0.01	<0.01	1.1	<0.01	1.0	2.1	6.3	<0.01	1.4	0.55
WIL26	3.1	0.46	0.06	0.02	0.02	1.4	0.02	1.3	2.7	7.8	<0.01	2.0	0.74
WIL27	3.3	0.85	0.05	0.06	0.01	1.3	0.05	1.2	3.4	5.8	0.01	1.9	0.88
WIL28	2.2	0.13	0.04	<0.01	<0.01	1.5	<0.01	0.7	2.0	6.0	<0.01	1.2	0.52
WIL29	3.2	0.73	0.06	0.05	<0.01	1.2	0.06	1.2	2.8	3.9	<0.01	1.8	0.75
WIL30	2.7	0.27	0.04	<0.01	<0.01	1.5	<0.01	0.7	2.3	5.8	<0.01	1.4	0.58
WIL31	2.4	0.50	0.05	<0.01	0.01	1.1	<0.01	0.6	2.2	4.0	<0.01	1.3	0.57
WIL32	2.9	0.61	0.03	0.01	<0.01	1.6	<0.01	0.6	2.5	5.2	<0.01	1.1	0.64
WIL33	2.2	0.40	0.04	<0.01	<0.01	2.6	<0.01	0.6	1.7	3.2	<0.01	2.8	0.48
WIL34	2.3	0.49	0.04	<0.01	<0.01	2.6	<0.01	0.7	1.9	7.3	<0.01	1.5	0.58
WIL35	2.4	0.90	0.05	0.01	<0.01	2.3	<0.01	0.9	1.9	3.5	<0.01	3.4	0.57
WIL36	4.3	1.08	0.07	0.04	0.02	2.4	0.03	1.6	3.8	9.4	0.01	2.9	1.00
WIL37	4.7	1.29	0.08	0.06	0.02	1.6	0.05	2.0	4.0	4.5	0.01	2.7	1.06
WIL38	5.3	4.98	0.12	0.14	0.03	2.1	0.15	3.7	5.0	15.4	0.02	6.5	1.26
PIA04	4.1	3.73	0.09	0.14	<0.01	1.6	<0.01	1.4	3.3	2.5	<0.01	2.0	0.90

Sample ID	La (ppm)	LOI (%)	Lu (ppm)	MgO (%)	MnO (%)	Mo (ppm)	Na_2O (%)	Nb (ppm)	Nd (ppm)	Ni (ppm)	P_2O_5 (%)	Pb (ppm)	Pr (ppm)
PIA05	5.9	2.04	0.07	0.05	<0.01	2.0	<0.01	1.2	3.5	5.5	<0.01	2.0	0.98
PIA06	5.1	2.41	0.08	0.05	<0.01	1.5	<0.01	1.6	4.3	1.8	<0.01	2.0	1.06
PIA07	6.8	1.96	0.14	0.02	<0.01	1.8	<0.01	2.2	6.0	6.3	0.01	2.1	1.58
PIA08	3.9	1.15	0.08	0.01	<0.01	1.9	<0.01	0.8	3.7	1.4	<0.01	1.9	0.97
PIA09	4.1	1.59	0.09	<0.01	<0.01	1.8	<0.01	0.6	4.5	5.3	<0.01	1.8	1.17
PIA10	4.4	1.12	0.11	<0.01	<0.01	2.6	<0.01	0.8	5.7	3.3	0.01	3.2	1.43
PIA11	6.0	3.22	0.13	0.04	<0.01	3.6	<0.01	1.6	6.9	8.4	0.02	3.0	1.77
PIA12	6.1	3.74	0.13	0.04	<0.01	2.7	<0.01	1.7	6.5	3.0	0.01	3.3	1.62
PIA13	6.1	4.95	0.18	0.04	<0.01	4.2	<0.01	1.8	6.5	7.6	0.03	3.5	1.65
PIA14	5.5	5.36	0.17	0.09	0.01	4.0	<0.01	2.7	6.8	12.6	0.03	3.4	1.63
PIA15	7.9	3.89	0.18	0.10	0.02	3.5	<0.01	3.9	7.8	7.7	0.02	3.1	2.03
KND01	7.7	10.39	0.04	0.09	<0.01	2.2	0.08	1.3	7.8	3.8	0.01	1.1	1.86
KND02	10.1	10.67	0.04	0.13	<0.01	2.2	0.15	1.4	7.5	1.5	0.02	1.6	2.03
KND03	10.3	5.90	0.06	0.13	<0.01	2.4	0.19	1.9	4.3	5.8	0.02	2.7	1.40
KND04	5.9	2.31	0.09	0.03	0.01	2.7	0.02	2.8	4.4	3.7	<0.01	3.8	1.24
KND05	4.1	1.25	0.06	0.02	<0.01	2.7	0.09	1.1	3.9	7.9	<0.01	2.7	1.04
KND06	3.0	0.76	0.05	<0.01	<0.01	2.1	0.01	0.7	2.6	3.2	<0.01	2.0	0.71
KND07	3.6	0.94	0.07	<0.01	<0.01	2.7	<0.01	1.2	3.3	7.7	<0.01	2.3	0.82
KND08	3.0	2.23	0.06	<0.01	<0.01	2.1	<0.01	0.5	3.0	3.5	<0.01	2.0	0.72
KND09	4.7	3.37	0.05	0.02	<0.01	2.3	0.01	0.5	3.4	7.8	<0.01	5.5	0.93
KND10	9.8	4.15	0.13	0.05	<0.01	2.0	0.05	3.5	8.2	3.7	<0.01	11.3	2.12
KND11	5.3	1.70	0.08	0.06	<0.01	2.3	0.03	2.2	4.3	11.1	<0.01	8.9	1.16
KND12	9.0	4.12	0.13	0.38	0.02	2.2	0.18	3.6	8.4	7.7	0.02	10.2	2.18
KND13	8.5	3.44	0.11	0.26	0.02	2.7	0.13	2.9	7.9	11.7	0.02	14.7	2.00
BER02	3.1	1.33	0.05	0.20	<0.01	1.5	<0.01	1.8	2.1	2.5	<0.01	1.6	0.59
BER03	10.7	7.36	0.14	2.12	0.01	1.0	0.09	3.7	8.8	7.0	<0.01	9.8	2.35

Sample ID	La (ppm)	LOI (%)	Lu (ppm)	MgO (%)	MnO (%)	Mo (ppm)	Na_2O (%)	Nb (ppm)	Nd (ppm)	Ni (ppm)	P_2O_5 (%)	Pb (ppm)	Pr (ppm)
BER04	7.3	5.36	0.10	1.56	0.01	1.1	0.06	2.8	6.3	4.0	<0.01	4.8	1.68
BER05	7.4	5.33	0.11	1.47	0.01	1.5	0.06	2.8	5.7	6.7	<0.01	4.4	1.67
BER06	3.7	0.95	0.04	0.18	0.01	2.7	0.02	1.0	2.6	1.8	<0.01	3.6	0.77
BER07	2.2	0.16	0.04	0.03	<0.01	2.3	0.01	0.4	1.6	1.5	<0.01	1.2	0.49
BER08	2.6	-0.15	0.08	<0.01	<0.01	3.2	<0.01	0.7	1.9	9.6	<0.01	1.1	0.59
BER09	1.6	-0.02	0.06	<0.01	<0.01	1.9	<0.01	0.5	1.5	1.5	<0.01	1.1	0.39
BER10	3.7	0.00	0.07	0.02	<0.01	3.0	<0.01	0.6	2.7	8.8	<0.01	1.2	0.69
MAN04	26.5	8.66	0.31	0.90	0.01	0.5	0.62	13.7	20.0	14.0	0.04	10.1	5.50
MAN05	4.3	0.55	0.07	0.05	0.02	3.3	0.03	1.7	3.1	3.7	<0.01	2.4	0.85
MAN06	11.1	2.16	0.16	0.26	0.02	2.9	0.20	5.0	8.5	8.1	0.02	3.6	2.31
MAN07	32.2	7.06	0.47	0.89	0.02	0.5	0.87	13.7	24.4	12.4	0.03	7.9	6.90
MAN08	40.5	4.23	0.57	0.63	0.02	1.2	0.82	14.3	33.6	12.7	0.05	7.2	9.04
MAN09	43.1	6.71	0.58	0.77	0.02	0.9	0.94	14.7	41.7	26.5	0.07	17.1	10.91
MAN10	36.3	5.33	0.48	0.65	0.02	1.2	0.80	14.6	30.4	15.0	0.05	10.0	8.25
MAN11	46.6	7.15	0.46	0.88	0.02	1.2	0.78	16.7	38.5	18.0	0.07	16.0	10.82
MAN12	38.1	7.82	0.46	0.89	0.01	0.6	0.85	16.6	31.8	13.6	0.06	12.4	8.66
MAN13	38.6	7.24	0.48	0.82	0.01	0.8	0.81	15.5	32.9	16.1	0.07	13.1	8.87
MAN14	41.0	7.56	0.54	0.94	0.08	1.1	0.81	15.9	37.6	25.7	0.07	18.1	9.92
MAN15	40.2	7.40	0.52	0.90	0.08	1.2	0.77	15.3	35.3	17.4	0.06	15.0	9.29
MAN16	45.8	6.76	0.81	0.85	0.06	1.0	0.90	18.0	38.1	16.9	0.06	18.0	9.79
MAN17	12.9	3.47	0.23	0.33	0.14	2.7	0.18	5.1	11.6	9.2	0.09	6.8	3.09
MAN18	5.9	2.15	0.11	0.14	0.14	2.6	0.10	2.6	5.5	20.3	0.07	8.4	1.41
MAN19	8.7	1.19	0.18	0.10	0.03	2.6	0.09	2.6	8.3	7.0	0.08	4.7	2.16
MAN20	4.6	0.73	0.10	0.03	0.03	2.4	0.04	1.6	4.9	10.1	0.07	3.7	1.15
MAN21	5.1	0.81	0.11	0.04	0.03	2.7	0.04	1.7	4.8	13.8	0.07	3.9	1.26
MAN22	4.4	1.09	0.11	0.03	0.03	2.6	0.03	1.2	4.2	7.5	0.07	4.2	1.14

Sample ID	La (ppm)	LOI (%)	Lu (ppm)	MgO (%)	MnO (%)	Mo (ppm)	Na_2O (%)	Nb (ppm)	Nd (ppm)	Ni (ppm)	P_2O_5 (%)	Pb (ppm)	Pr (ppm)
MAN23	9.1	0.94	0.19	0.08	0.03	2.7	0.10	3.8	7.7	10.5	0.04	3.6	2.10
MAN24	13.3	3.01	0.26	0.18	0.04	2.1	0.17	5.3	13.9	9.1	0.05	5.0	3.42
MAN25	5.2	0.51	0.11	0.03	0.02	2.2	0.04	1.7	5.4	8.7	0.02	2.4	1.25
MAN26	12.4	0.52	0.26	0.06	0.02	2.4	0.10	5.0	10.6	3.5	0.02	2.8	2.77
MAN27	13.9	0.55	0.31	0.06	0.02	2.2	0.09	5.5	11.3	7.0	0.02	2.6	2.94
WAL11	23.2	7.29	0.40	0.79	0.06	1.1	1.03	14.8	22.5	26.2	0.19	26.0	5.63
WAL12	20.5	5.97	0.34	0.64	0.12	1.5	0.86	13.5	18.7	27.7	0.12	22.4	4.94
WAL13	5.1	2.38	0.10	0.05	0.02	2.8	0.07	1.4	5.4	9.1	0.02	4.4	1.30
WAL14	2.9	0.48	0.06	0.02	0.02	2.3	<0.01	1.1	3.1	9.5	<0.01	1.5	0.82
WAL15	3.7	0.76	0.06	0.03	0.03	2.6	<0.01	1.0	3.1	6.5	0.01	2.3	0.81
WAL16	33.1	3.33	0.96	0.14	0.04	2.1	0.03	28.2	27.7	8.6	0.03	5.7	7.18
WAL17	10.0	1.76	0.15	0.12	0.03	2.2	0.09	5.1	8.0	7.2	0.03	15.7	1.90
WAL18	9.3	2.59	0.17	0.13	0.03	2.3	0.13	5.6	7.6	13.1	0.03	11.3	1.97
MOR04	13.3	12.27	0.18	4.08	0.06	4.9	0.27	4.2	11.8	13.3	0.06	98.1	3.14
MOR05	1.8	0.87	0.04	0.28	0.01	6.3	<0.01	1.0	1.4	7.9	<0.01	0.9	0.37
MOR06	3.3	0.06	0.03	0.05	<0.01	2.9	<0.01	0.6	1.4	1.8	<0.01	1.1	0.41
MOR07	2.0	0.03	0.03	0.03	<0.01	3.7	<0.01	0.7	1.5	7.8	<0.01	1.0	0.37
MOR08	3.2	0.95	0.04	0.27	0.02	3.4	0.02	1.2	2.0	2.8	<0.01	2.6	0.55
MOR09	2.4	0.09	0.03	<0.01	<0.01	3.2	<0.01	0.6	1.3	7.9	<0.01	1.7	0.39
MOR10	2.9	0.23	0.04	0.02	<0.01	2.5	<0.01	0.6	1.7	2.3	<0.01	0.8	0.51
MOR11	2.5	0.20	0.04	0.04	0.01	3.3	<0.01	0.8	1.7	6.6	<0.01	4.0	0.47
MOR12	2.3	0.23	0.04	0.02	<0.01	3.0	<0.01	0.4	1.9	2.2	<0.01	8.8	0.49
MOR13	2.6	0.36	0.04	0.02	<0.01	3.7	<0.01	1.1	1.6	7.6	<0.01	2.0	0.44
MOR14	2.8	0.45	0.04	0.08	<0.01	3.1	<0.01	0.7	2.0	1.9	<0.01	4.1	0.48
MOR15	2.7	0.07	0.06	0.02	0.01	3.7	<0.01	0.7	1.9	7.0	<0.01	27.8	0.47
MOR16	2.6	0.23	0.05	0.01	0.01	2.4	<0.01	0.3	1.9	2.3	<0.01	5.3	0.47

Sample ID	La (ppm)	LOI (%)	Lu (ppm)	MgO (%)	MnO (%)	Mo (ppm)	Na_2O (%)	Nb (ppm)	Nd (ppm)	Ni (ppm)	P_2O_5 (%)	Pb (ppm)	Pr (ppm)
MOR17	2.6	0.06	0.05	0.02	<0.01	3.6	<0.01	0.8	2.1	7.3	<0.01	3.4	0.53
MOR18	2.3	0.14	0.05	0.02	<0.01	3.1	<0.01	0.4	2.1	2.4	<0.01	7.2	0.48
MOR19	2.5	0.07	0.06	0.03	<0.01	3.5	<0.01	0.7	1.9	6.5	<0.01	0.8	0.53
MOR20	2.9	0.40	0.06	0.02	0.02	3.2	<0.01	1.9	2.5	3.1	<0.01	1.5	0.66
MOR21	3.2	0.46	0.07	0.03	0.02	3.8	<0.01	1.4	3.0	8.2	<0.01	3.0	0.75
MOR22	2.5	0.43	0.06	0.02	0.01	2.9	<0.01	1.2	2.2	2.6	<0.01	1.4	0.58
BT01	5.5	3.33	0.08	0.10	<0.01	1.2	0.11	5.3	3.6	4.0	0.01	3.3	1.09
BT02	3.9	3.17	0.07	0.08	<0.01	1.6	0.12	2.9	3.1	5.0	0.01	3.4	0.80
BT03	4.4	2.95	0.07	0.08	<0.01	1.3	0.11	2.9	3.5	4.9	0.01	3.7	0.97
BT04	4.6	3.03	0.08	0.09	<0.01	1.3	0.12	2.8	3.3	4.6	0.01	5.0	0.96
BT05	5.0	3.04	0.07	0.10	<0.01	0.7	0.12	3.0	3.5	3.5	0.01	4.0	1.00
BT06	4.8	2.99	0.07	0.09	<0.01	1.4	0.12	2.1	3.5	6.1	0.01	4.6	1.04
BT07	5.7	2.37	0.08	0.08	<0.01	0.9	0.11	3.4	4.4	4.1	<0.01	3.4	1.14
BT08	7.3	2.51	0.15	0.08	<0.01	1.6	0.12	1.9	7.7	6.4	0.02	6.5	2.10
BT09	8.2	2.15	0.10	0.08	<0.01	1.2	0.11	2.5	5.9	5.4	0.01	4.1	1.65
BT10	7.7	1.72	0.08	0.08	<0.01	1.5	0.09	3.7	5.3	6.1	0.01	4.3	1.48
BT11	6.2	1.50	0.06	0.06	<0.01	1.1	0.08	2.6	4.5	4.8	0.01	4.8	1.12
BT12	6.1	1.57	0.10	0.06	<0.01	1.5	0.09	1.5	4.8	5.4	0.01	5.1	1.29
BT13	3.9	1.61	0.07	0.06	<0.01	1.4	<0.01	2.4	3.1	4.8	<0.01	2.8	0.78
BT14	4.7	2.70	0.07	0.11	<0.01	1.2	0.02	2.6	3.9	4.4	<0.01	4.0	1.02
BT15	4.2	2.47	0.06	0.12	<0.01	1.0	0.03	2.1	3.0	4.1	0.01	3.7	0.86
BT16	4.1	2.59	0.07	0.12	<0.01	1.4	0.04	2.6	3.2	4.3	0.01	3.9	0.91
BT17	5.2	2.58	0.08	0.12	<0.01	1.1	0.05	2.8	4.2	3.5	<0.01	4.2	1.11
BT18	4.5	2.63	0.13	0.12	<0.01	1.4	0.05	3.1	3.7	4.6	<0.01	4.4	1.10
BT19	6.3	2.30	0.09	0.12	<0.01	1.1	0.05	3.1	4.8	6.1	0.02	5.1	1.32
BT20	8.0	2.66	0.11	0.14	<0.01	1.3	0.06	2.5	6.3	6.1	0.03	5.5	1.79

Sample ID	La (ppm)	LOI (%)	Lu (ppm)	MgO (%)	MnO (%)	Mo (ppm)	Na_2O (%)	Nb (ppm)	Nd (ppm)	Ni (ppm)	P_2O_5 (%)	Pb (ppm)	Pr (ppm)
BT21	7.0	2.36	0.11	0.13	<0.01	1.2	0.06	2.5	6.1	5.1	0.03	4.5	1.66
BT22	6.1	1.99	0.08	0.10	<0.01	1.4	0.05	2.1	5.6	6.2	0.02	3.9	1.48
BT23	15.0	2.07	0.12	0.11	<0.01	2.1	0.07	2.0	16.2	6.1	0.02	9.5	4.34
BT24	19.3	1.23	0.14	0.06	<0.01	1.5	0.05	1.6	21.3	7.5	0.02	4.7	5.70
BT25	18.9	1.05	0.11	0.06	<0.01	1.3	0.06	1.5	21.0	6.1	0.02	5.5	5.62
BT26	9.1	1.30	0.26	0.05	<0.01	2.5	0.04	0.9	14.3	11.7	0.03	9.7	3.33
BT27	37.3	1.31	0.41	0.06	<0.01	2.1	0.09	1.7	50.1	11.1	0.03	4.4	12.59
BT28	14.1	1.45	0.27	0.13	0.02	1.7	0.26	5.1	15.2	10.2	0.02	4.6	3.60
BT29	21.5	1.59	0.34	0.20	0.01	1.4	0.35	5.4	21.5	8.3	0.03	4.3	5.42
BT30	14.2	1.21	0.20	0.15	0.01	1.5	0.29	4.2	15.6	8.0	0.02	4.8	3.83
BT31	15.1	1.75	0.18	0.18	0.01	1.5	0.30	4.9	16.1	7.5	0.02	5.7	3.99
BT32	23.0	6.89	0.33	0.43	0.03	2.6	0.26	5.8	26.7	16.0	0.08	7.8	6.45
BT33	2.9	41.94	0.03	0.66	0.01	0.7	<0.01	0.8	2.7	<0.1	0.04	3.3	0.65
BT35	5.1	0.81	0.08	0.06	0.02	3.5	<0.01	3.6	4.1	13.5	<0.01	2.8	1.04
BT36	7.0	3.93	0.12	0.14	<0.01	1.9	0.03	7.5	4.6	3.9	0.02	6.2	1.35
BT37	5.7	5.84	0.10	0.14	<0.01	1.8	0.04	6.1	3.7	8.1	0.01	4.7	0.99
BT38	4.1	3.21	0.07	0.08	<0.01	1.3	<0.01	3.4	2.4	3.9	0.01	3.4	0.79
BT39	4.5	2.97	0.07	0.07	<0.01	1.3	0.03	3.5	3.0	4.4	0.01	3.5	0.81
BT40	4.0	2.21	0.07	0.06	<0.01	2.0	0.03	2.5	3.1	3.4	0.01	5.2	0.75
BT41	4.2	2.31	0.08	0.06	<0.01	1.7	0.04	2.8	3.6	3.2	<0.01	5.9	0.98
BT42	5.7	2.35	0.12	0.08	<0.01	1.5	0.04	2.8	8.1	4.1	<0.01	7.8	1.90
BT43	17.6	2.59	0.25	0.13	0.01	1.8	0.05	3.7	22.5	6.9	0.02	9.0	5.50
BT44	12.2	2.09	0.24	0.11	<0.01	1.6	0.06	3.5	17.0	5.7	0.01	5.9	4.20
BT45	22.5	2.03	0.23	0.09	<0.01	2.0	0.02	2.8	28.1	7.1	0.03	8.8	7.66
MBR06	9.4	7.66	0.14	0.64	0.01	0.9	0.29	5.7	6.6	4.3	0.01	4.7	1.79
MBR07	11.6	14.55	0.16	0.49	0.02	1.1	0.14	4.4	9.5	2.9	0.02	16.5	2.55

Sample ID	La (ppm)	LOI (%)	Lu (ppm)	MgO (%)	MnO (%)	Mo (ppm)	Na_2O (%)	Nb (ppm)	Nd (ppm)	Ni (ppm)	P_2O_5 (%)	Pb (ppm)	Pr (ppm)
MBR08	9.4	12.08	0.14	0.62	0.01	1.1	0.19	3.9	8.5	3.7	0.01	9.3	1.97
MBR09	10.2	11.21	0.14	0.50	0.01	1.1	0.14	3.8	9.2	2.6	0.02	4.1	2.34
MBR10	9.5	12.07	0.15	0.47	0.02	1.4	0.12	3.4	8.3	2.8	0.02	13.5	2.15
MBR11	11.7	21.67	0.14	0.98	0.02	0.8	0.18	3.7	9.5	5.0	0.03	6.7	2.61
MBR12	9.2	26.75	0.12	1.17	0.02	0.9	0.14	3.3	9.0	6.0	0.02	6.9	2.05
MBR13	7.0	30.09	0.10	1.06	0.01	0.9	0.12	2.4	6.9	4.4	0.02	3.5	1.67
MBR14	9.9	21.90	0.15	1.27	0.01	1.1	0.20	4.0	8.3	6.3	0.02	5.5	2.15
MBR15	7.9	27.98	0.10	0.87	0.01	1.1	0.12	2.6	7.2	4.9	0.02	6.1	1.85
MBR16	5.1	39.76	0.04	0.69	0.01	0.5	<0.01	0.7	4.2	1.1	0.05	2.9	1.05
FT04	9.4	5.53	0.12	1.06	0.01	2.5	0.40	4.7	7.0	6.6	0.01	5.1	1.81
FT05	3.6	1.77	0.07	0.18	0.01	3.3	0.14	2.7	2.7	8.3	<0.01	3.1	0.76
FT06	4.9	3.48	0.09	0.29	0.01	5.6	0.15	3.8	4.4	7.0	0.02	6.9	1.07
FT07	4.2	1.57	0.07	0.17	0.01	3.8	0.12	3.6	2.7	10.5	<0.01	4.4	0.70
FT08	3.9	1.26	0.07	0.12	0.02	5.8	0.11	3.5	2.6	5.8	<0.01	5.5	0.70
FT09	3.4	1.34	0.05	0.25	<0.01	4.5	0.08	1.9	2.4	8.9	<0.01	3.2	0.69
FT10	4.2	2.53	0.06	0.10	<0.01	6.7	0.09	2.1	4.9	7.3	0.03	21.2	1.29
FT11	6.4	1.99	0.06	0.21	<0.01	5.0	0.11	2.5	4.8	8.9	0.01	6.3	1.32
FT12	4.8	1.43	0.05	0.13	0.02	7.2	0.10	2.9	3.9	6.6	0.01	5.1	1.00
FT13	5.8	1.96	0.05	0.14	<0.01	6.3	0.10	2.1	5.4	9.2	0.03	15.5	1.33
FT14	53.0	5.20	0.15	0.97	<0.01	3.6	0.37	5.2	57.3	10.6	0.06	5.2	15.31
FT15	99.0	7.17	0.37	1.13	0.02	2.3	0.39	3.9	108.7	24.4	0.06	5.5	26.77
NGA01	14.5	6.23	0.24	0.71	<0.01	1.2	0.14	4.2	14.8	12.7	0.01	8.0	3.88
NGA02	21.0	6.60	0.22	1.00	0.04	1.0	0.41	5.9	17.5	12.4	0.01	10.6	4.38
NGA03	20.0	9.31	0.30	1.43	0.01	0.5	0.55	8.1	20.2	13.2	0.01	11.9	5.10
NGA04	19.0	10.68	0.29	1.58	0.01	0.6	0.61	10.4	15.9	11.3	0.02	13.0	4.29
NGA05	13.2	6.35	0.20	0.76	<0.01	1.0	0.30	7.6	11.0	9.5	0.01	6.9	2.86

Sample ID	La (ppm)	LOI (%)	Lu (ppm)	MgO (%)	MnO (%)	Mo (ppm)	Na_2O (%)	Nb (ppm)	Nd (ppm)	Ni (ppm)	P_2O_5 (%)	Pb (ppm)	Pr (ppm)
NGA06	8.2	3.95	0.10	0.30	<0.01	1.0	0.17	4.6	4.8	5.3	0.01	3.8	1.31
NGA07	9.5	4.86	0.13	0.51	<0.01	1.3	0.23	5.6	6.3	6.1	0.01	6.5	1.76
NGA08	8.1	4.30	0.11	0.40	<0.01	1.0	0.21	4.9	5.9	5.4	0.01	4.5	1.53
NGA09	8.7	4.51	0.11	0.44	<0.01	1.6	0.20	5.1	5.5	5.4	<0.01	7.2	1.53
NGA10	8.4	3.97	0.13	0.39	<0.01	1.3	0.18	4.3	5.9	7.3	<0.01	5.0	1.60
NGA11	10.4	5.06	0.17	0.61	0.01	1.5	0.28	5.2	8.3	6.4	0.01	6.9	2.29
NGA12	7.0	2.88	0.08	0.26	<0.01	1.3	0.16	3.7	4.8	4.0	<0.01	6.9	1.26
NGA13	6.7	3.03	0.10	0.26	<0.01	0.9	0.16	3.9	4.3	3.9	<0.01	6.4	1.22
NGA14	5.6	2.05	0.08	0.16	<0.01	1.2	0.08	2.4	3.3	4.5	<0.01	5.2	0.94
NGA15	6.0	2.95	0.09	0.29	<0.01	0.5	0.12	2.8	4.1	3.2	<0.01	4.5	1.14
NGA16	4.7	1.28	0.06	0.09	<0.01	0.8	0.05	1.6	2.7	2.9	<0.01	2.5	0.77
NGA17	4.3	1.07	0.09	0.07	<0.01	1.5	0.04	1.5	3.0	4.3	<0.01	3.2	0.84
NGA18	3.5	0.84	0.05	0.05	<0.01	0.9	0.02	1.2	2.6	2.5	<0.01	2.1	0.73
NGA19	3.5	0.41	0.07	0.03	<0.01	1.6	0.02	0.8	2.9	4.0	<0.01	3.6	0.74
NGA20	3.4	0.59	0.07	0.03	<0.01	1.3	0.03	0.9	2.9	3.8	<0.01	1.7	0.75
NGA21	4.0	0.16	0.08	<0.01	<0.01	1.7	<0.01	0.6	2.2	4.7	<0.01	2.1	0.66
NGA22	3.3	0.41	0.07	0.03	<0.01	1.6	<0.01	0.8	2.6	4.6	<0.01	1.9	0.69
NGA23	2.9	0.36	0.07	0.01	<0.01	1.6	<0.01	0.4	2.0	4.6	<0.01	1.8	0.57
NGA24	2.4	0.32	0.08	0.01	<0.01	1.5	<0.01	0.5	2.0	3.9	<0.01	2.5	0.60
NGA25	3.6	0.36	0.13	0.01	<0.01	1.5	<0.01	0.7	2.9	3.5	<0.01	1.8	0.75
NGA26	2.8	0.20	0.08	<0.01	<0.01	1.3	<0.01	0.5	1.9	4.1	<0.01	1.3	0.59
NGA27	2.9	0.33	0.06	0.02	<0.01	1.3	0.01	0.6	2.3	4.2	<0.01	2.1	0.64
NGA28	3.2	0.38	0.09	0.02	<0.01	1.5	<0.01	0.7	2.7	4.3	<0.01	2.5	0.71
NGA29	2.7	0.17	0.06	<0.01	<0.01	1.7	<0.01	0.3	2.0	4.6	<0.01	1.9	0.53
NGA30	2.6	0.15	0.06	<0.01	<0.01	3.1	<0.01	0.4	2.8	5.1	<0.01	1.4	0.65
NGA31	2.5	0.22	0.06	<0.01	<0.01	1.2	<0.01	0.3	1.8	3.9	<0.01	1.2	0.50

Sample ID	La (ppm)	LOI (%)	Lu (ppm)	MgO (%)	MnO (%)	Mo (ppm)	Na_2O (%)	Nb (ppm)	Nd (ppm)	Ni (ppm)	P_2O_5 (%)	Pb (ppm)	Pr (ppm)
NGA32	3.5	0.30	0.07	0.02	<0.01	1.3	<0.01	0.7	2.5	3.8	<0.01	1.5	0.71
NGA33	3.1	0.25	0.07	0.01	<0.01	1.5	<0.01	0.6	2.4	4.5	<0.01	1.6	0.62
NGA34	3.8	0.27	0.07	<0.01	<0.01	2.4	<0.01	0.8	3.2	7.2	<0.01	3.7	0.83
NGA35	4.2	0.44	0.07	0.02	<0.01	1.5	0.02	1.0	3.8	4.5	<0.01	3.2	0.96
NGA36	3.1	0.34	0.07	0.01	<0.01	1.7	<0.01	0.6	2.6	3.6	<0.01	2.0	0.66
NGA37	4.0	0.43	0.08	0.02	<0.01	1.6	0.02	1.0	3.3	4.5	<0.01	2.7	0.91
NGA38	17.8	4.77	0.28	0.17	0.06	1.0	0.05	3.5	19.1	52.8	0.02	5.3	4.51
NGA39	11.0	5.96	0.25	0.17	0.11	4.4	0.03	1.7	12.5	30.0	0.02	9.4	2.81
TEM03	7.0	2.21	0.05	0.23	<0.01	1.4	0.17	2.5	2.2	3.8	<0.01	3.0	0.72
TEM04	8.2	2.58	0.07	0.26	<0.01	1.0	0.19	2.1	2.2	3.1	<0.01	4.5	0.74
TEM05	5.5	2.13	0.07	0.20	<0.01	1.0	0.15	2.1	2.6	3.8	<0.01	2.3	0.74
TEM06	2.9	0.61	0.04	0.04	<0.01	2.1	0.04	1.1	1.9	4.0	<0.01	2.9	0.48
TEM07	2.9	0.29	0.05	0.02	<0.01	2.3	0.02	0.7	1.8	4.0	<0.01	2.9	0.50
TEM08	2.2	0.39	0.05	0.03	<0.01	16.4	0.02	0.9	1.5	4.7	<0.01	41.8	0.44
TEM09	2.7	0.25	0.05	0.03	<0.01	2.9	0.03	0.6	1.8	5.5	<0.01	4.5	0.47
TEM10	2.5	0.35	0.05	0.02	<0.01	3.0	0.03	1.0	1.9	4.8	<0.01	4.0	0.43
TEM11	2.7	0.31	0.04	0.03	<0.01	2.7	0.04	0.9	1.9	5.2	<0.01	3.0	0.51
TEM12	5.7	1.46	0.09	0.22	0.01	4.0	0.21	3.3	4.6	4.1	<0.01	17.3	1.16
TEM13	4.3	1.02	0.08	0.16	0.01	5.5	0.14	2.5	3.7	5.1	<0.01	14.4	0.96
TEM14	5.0	1.78	0.06	0.10	<0.01	2.3	0.14	2.2	3.8	8.8	<0.01	8.6	1.09
TEM15	14.2	6.28	0.17	0.23	<0.01	1.6	0.22	4.0	17.3	19.3	0.01	5.0	4.32
NDA01	2.9	1.73	0.05	0.57	<0.01	1.7	<0.01	0.7	2.4	5.8	<0.01	3.0	0.59
NDA02	2.3	1.68	0.04	0.53	<0.01	1.6	0.02	0.5	1.8	5.2	<0.01	27.0	0.47
NDA03	3.6	3.79	0.07	0.64	0.01	1.8	0.04	0.7	3.7	6.7	0.01	11.0	0.86
NDA04	2.7	0.19	0.04	0.04	<0.01	1.8	<0.01	0.5	2.1	4.7	<0.01	3.5	0.56
OAK03	3.7	1.24	0.14	0.28	<0.01	1.3	0.06	6.5	4.0	5.9	<0.01	6.4	1.08

Sample ID	La (ppm)	LOI (%)	Lu (ppm)	MgO (%)	MnO (%)	Mo (ppm)	Na2O (%)	Nb (ppm)	Nd (ppm)	Ni (ppm)	P_2O_5 (%)	Pb (ppm)	Pr (ppm)
OAK04	10.8	1.25	0.23	0.15	0.01	0.8	0.05	12.7	7.8	5.8	<0.01	6.6	2.24
OAK05	6.7	3.18	0.09	0.18	<0.01	0.9	0.05	4.8	4.4	3.2	<0.01	4.4	1.13
OAK06	12.9	1.95	0.07	0.09	<0.01	0.7	0.06	4.4	5.3	3.1	0.01	3.7	1.78
OAK07	9.4	1.02	0.07	0.05	<0.01	1.0	0.04	3.2	4.6	4.2	0.01	2.4	1.50
OAK08	10.3	4.13	0.10	0.66	<0.01	0.9	0.10	2.9	8.3	6.2	0.03	13.5	2.14
OAK09	7.7	1.78	0.08	0.26	0.01	1.3	0.07	2.4	6.4	5.3	<0.01	5.3	1.63
OAK10	4.5	0.46	0.05	0.04	<0.01	1.6	<0.01	1.1	3.1	4.8	0.01	2.1	0.82
OAK11	9.8	2.71	0.15	0.16	0.02	1.2	0.08	4.6	7.4	11.3	0.10	7.2	1.96
OAK12	23.9	8.00	0.33	0.44	0.01	0.5	0.38	21.2	16.6	6.4	0.04	3.9	4.66
OAK13	24.0	8.17	0.31	0.44	0.01	0.6	0.31	21.0	17.1	9.3	0.05	4.5	4.67
OAK14	35.2	9.60	0.37	0.62	<0.01	0.6	0.52	23.7	37.2	8.7	0.06	8.5	9.40
OAK15	33.0	10.79	0.34	0.70	<0.01	0.5	0.53	25.4	30.9	6.1	0.06	10.6	8.10
OAK16	35.2	10.22	0.33	0.67	<0.01	0.7	0.49	23.7	31.4	8.6	0.05	9.2	8.17
OAK17	31.5	9.20	0.33	0.58	<0.01	1.4	0.47	22.6	28.3	9.7	0.07	8.4	7.39
OAK18	28.7	9.83	0.32	0.63	<0.01	1.3	0.49	22.7	25.3	9.2	0.05	10.8	6.53
OAK19	26.3	7.65	0.27	0.49	<0.01	1.1	0.34	18.0	26.9	8.0	0.04	5.7	6.80
OAK20	29.7	9.32	0.29	0.58	<0.01	0.5	0.43	21.0	26.5	9.0	0.05	7.9	6.78
OAK21	13.4	3.30	0.18	0.22	<0.01	1.7	0.20	9.6	9.2	4.8	0.03	5.0	2.48
PIN04	3.1	0.25	0.05	0.03	<0.01	3.2	<0.01	1.8	2.1	9.0	<0.01	3.6	0.59
PIN05	4.6	0.49	0.06	0.03	0.01	4.5	0.02	2.5	3.4	5.0	<0.01	3.1	0.87
PIN06	6.8	0.00	0.21	0.01	0.01	3.0	<0.01	5.5	6.4	8.9	<0.01	3.2	1.62
PIN07	8.6	-0.03	0.28	<0.01	0.02	3.2	<0.01	6.9	7.7	4.2	<0.01	3.4	1.99
PIN08	11.1	0.00	0.35	0.02	0.02	2.9	<0.01	9.5	9.2	8.8	0.01	3.7	2.55
PIN09	7.0	0.06	0.23	0.02	0.02	4.1	<0.01	7.6	6.4	5.3	<0.01	4.2	1.65
PIN10	13.7	1.65	0.15	0.13	0.01	3.1	0.07	6.1	14.5	10.0	0.01	5.4	3.67
PV02	3.0	1.01	0.06	0.14	0.01	3.4	0.06	2.6	2.1	5.4	0.01	1.6	0.63

Sample ID	La (ppm)	LOI (%)	Lu (ppm)	MgO (%)	MnO (%)	Mo (ppm)	Na_2O (%)	Nb (ppm)	Nd (ppm)	Ni (ppm)	P_2O_5 (%)	Pb (ppm)	Pr (ppm)
PV03	4.9	0.97	0.06	0.15	<0.01	2.6	0.07	2.3	3.4	8.1	0.02	1.9	0.88
PV04	5.4	1.25	0.07	0.19	0.01	3.2	0.10	2.5	3.7	5.3	0.03	2.4	0.98
PV05	3.1	0.24	0.05	0.05	0.01	3.8	<0.01	1.2	2.3	9.6	0.05	4.7	0.57
PV06	2.8	-0.02	0.04	0.02	0.01	4.0	<0.01	1.7	2.2	4.2	0.01	2.2	0.62
PV07	3.6	0.15	0.06	0.03	<0.01	3.3	<0.01	1.6	3.0	9.5	0.01	7.5	0.81
PV08	2.7	0.16	0.04	0.02	0.02	3.3	<0.01	1.7	2.2	5.3	0.01	1.9	0.55
PV09	3.1	0.20	0.05	0.02	0.01	4.2	<0.01	1.3	2.3	9.4	0.01	2.3	0.64
RB02	5.0	2.82	0.12	0.03	0.01	7.2	<0.01	4.2	6.7	6.9	0.02	28.3	1.63
RB03	14.4	11.88	0.32	0.44	<0.01	4.6	0.10	9.7	12.3	23.9	0.02	18.5	3.26
RB04	22.6	14.31	0.33	0.61	0.01	1.9	0.12	8.5	20.7	22.6	0.02	18.4	5.36
RB05	80.5	27.57	0.54	0.97	0.02	0.6	0.13	5.8	65.6	13.9	0.02	15.0	16.60
KI1_01	31.6	8.37	0.45	1.04	0.02	1.1	0.29	9.0	30.4	18.9	0.02	13.2	8.19
KI1_02	12.8	5.53	0.21	0.54	0.01	1.2	0.16	6.1	11.0	8.6	0.01	7.2	2.96
KI1_03	18.8	6.99	0.29	0.77	0.02	1.1	0.20	7.3	17.5	14.6	0.01	9.4	4.54
KI1_04	15.7	7.33	0.20	0.57	0.02	0.6	0.15	7.1	12.1	8.4	0.01	7.5	3.15
KI1_05	27.9	8.55	0.30	0.72	0.02	1.4	0.18	6.7	23.5	10.6	0.02	10.9	5.93
KI1_06	30.1	10.95	0.35	0.79	0.01	1.8	0.23	8.7	26.8	8.9	0.02	17.5	6.67
KI1_07	20.9	7.43	0.27	0.58	0.01	1.4	0.19	7.6	19.8	10.5	0.02	11.7	4.85
KI1_08	12.9	4.24	0.23	0.33	<0.01	1.2	0.08	6.0	11.1	6.3	0.01	7.1	3.05
KI1_09	10.9	2.94	0.21	0.21	<0.01	2.2	0.05	7.3	8.9	6.1	<0.01	7.1	2.41
KI1_10	19.6	3.49	0.26	0.35	<0.01	1.4	0.12	7.0	16.9	7.0	0.01	9.6	4.55
KI1_11	21.2	8.07	0.21	0.47	<0.01	0.9	0.15	8.6	11.9	10.1	0.02	16.0	3.39
KI1_12	31.6	10.48	0.26	0.62	<0.01	0.3	0.19	10.4	16.7	10.3	0.02	16.2	4.93
KI1_13	263.9	15.69	0.94	0.96	0.02	0.6	0.22	11.5	229.4	37.1	0.10	20.6	58.25
KI10_01	43.2	14.13	0.58	0.59	0.01	1.0	0.08	8.0	44.4	23.5	0.03	12.6	11.11
KI10_02	36.1	7.89	0.71	0.47	0.02	1.3	0.06	5.4	48.6	17.0	0.02	10.2	11.89

KI10_03	243.5	14.14	1.52	1.70	<0.01	0.2	0.28	10.8	254.9	31.1	0.04	35.6	66.68
KI10_04	219.5	19.17	1.37	1.86	0.02	0.2	0.25	7.9	231.0	36.8	0.04	21.1	57.83
KI10_05	61.8	28.24	0.57	1.00	0.02	0.4	0.15	5.3	62.4	14.8	0.03	7.8	15.36
OLC01	0.8	7.82	0.03	0.12	0.02	0.5	0.13	0.1	0.7	2.5	0.03	0.9	0.19
OLC02	2.8	9.98	0.54	0.29	0.04	3.1	0.06	<0.1	7.3	4.4	0.27	1	1.17
OLC03	0.7	7.9	0.05	0.1	0.02	5.4	0.12	<0.1	1.5	3.7	0.06	0.4	0.27
OLC04	6.1	12.79	0.68	0.32	0.03	2	0.34	1.5	11.9	4.1	0.26	3.3	2.52
OLC05	5.1	5.93	0.1	0.41	<0.01	<0.1	1.35	6.1	3	1.3	<0.01	0.8	0.97
OLC06	5.7	11.21	0.13	1.8	0.02	4.6	1.56	3.2	5.7	5.1	0.03	4.3	1.29
OLC07	6.5	22.35	0.11	9.25	0.02	0.2	0.23	1.9	6.6	1.3	<0.01	2.3	1.57
OLC08	12.9	35.29	0.24	2.11	0.02	<0.1	0.19	1.7	13.3	4.9	0.04	2.8	3.2
OLC09	4	44.13	0.03	1.77	0.02	0.2	<0.01	0.7	3.1	<0.1	0.05	1.4	0.86
OLC10	10.9	13.33	1.28	0.16	0.04	3	0.05	0.4	22.6	1.6	0.92	3.3	4.39
OLC11	11.1	41.39	0.1	1.23	0.04	0.4	0.03	0.6	13.8	0.5	0.03	1.6	3.2
OLC12	22.8	38.21	0.42	1.22	0.06	2.3	0.08	3.8	25.5	13.4	0.02	3.4	6.05

Sample ID	Rb (ppm)	Sb (ppm)	Se (ppm)	SiO_2 (%)	Sm (ppm)	Sn (ppm)	Sr (ppm)	SUM (%)	Ta (ppm)	Tb (ppm)	Th (ppm)	TiO_2 (%)	Tl (ppm)
LYR01	27.5	<0.1	0.8	96.8	1.17	1	37.1	101.04	0.4	0.18	4.4	0.06	<0.1
LYR02	11.0	<0.1	<0.5	97.1	0.43	<1	12.5	100.27	0.1	0.07	1.8	0.06	<0.1
LYR03	8.1	0.3	13.4	88.5	0.53	1	9.9	100.83	0.1	0.08	1.9	0.05	<0.1
LYR04	13.3	0.1	<0.5	97.5	0.48	<1	24.9	100.57	0.1	0.10	3.5	0.12	<0.1
LYR05	9.4	0.2	0.5	93.4	0.40	<1	10.0	100.26	0.2	0.07	1.8	0.15	<0.1
LYR06	15.8	0.1	<0.5	94.8	0.47	<1	19.9	99.96	0.3	0.06	2.4	0.25	<0.1
LYR07	14.2	0.1	<0.5	94.7	0.53	<1	18.0	100.45	0.3	0.08	2.1	0.24	<0.1
LYR08	10.7	<0.1	<0.5	95.7	0.38	<1	16.0	100.13	0.2	0.06	2.2	0.11	<0.1
LYR09	9.8	0.2	0.9	85.9	0.63	<1	24.3	100.24	0.2	0.09	3.7	0.23	<0.1
LYR10	10.3	<0.1	<0.5	93.0	0.62	<1	20.5	100.37	0.2	0.07	3.1	0.19	<0.1
LYR11	13.3	<0.1	<0.5	88.1	4.73	<1	24.0	100.12	<0.1	1.14	4.3	0.12	<0.1
LYR12	22.2	<0.1	<0.5	92.4	0.78	<1	37.5	100.50	0.4	0.12	2.7	0.22	<0.1
LYR13	27.6	<0.1	<0.5	91.5	1.12	<1	36.3	99.99	0.4	0.17	4.0	0.27	<0.1
LYR14	11.8	<0.1	<0.5	79.5	0.92	<1	71.8	99.70	0.2	0.22	3.9	0.19	<0.1
LYR15	12.6	<0.1	<0.5	76.5	1.14	1	159.0	100.30	0.4	0.24	16.2	0.29	<0.1
LYR16	27.4	<0.1	<0.5	91.9	1.06	1	35.9	100.35	0.5	0.16	3.8	0.29	<0.1
LCP01	37.5	<0.1	<0.5	64.8	2.44	1	292.9	100.29	0.3	0.28	3.0	0.23	<0.1
LCP02	24.5	<0.1	<0.5	63.2	1.07	<1	194.8	100.23	0.2	0.15	1.7	0.15	<0.1
LCP03	22.8	<0.1	<0.5	65.3	1.88	<1	118.2	100.40	0.3	0.29	2.3	0.21	<0.1
LCP04	28.7	<0.1	<0.5	85.7	1.96	2	61.6	100.63	0.9	0.35	4.9	0.57	<0.1
LCP05	23.2	0.1	<0.5	88.7	2.20	2	26.6	99.74	1.6	0.48	7.0	1.11	<0.1
LCP06	15.7	<0.1	<0.5	97.0	0.99	<1	12.9	100.57	0.2	0.20	2.1	0.10	<0.1
LCP07	27.7	<0.1	<0.5	93.9	1.85	<1	29.0	99.91	0.2	0.18	2.9	0.19	<0.1
LCP08	25.4	<0.1	<0.5	93.8	1.25	<1	26.3	100.19	0.2	0.14	2.0	0.08	<0.1
LCP09	45.0	<0.1	<0.5	92.8	0.83	1	31.6	100.69	0.2	0.10	2.4	0.12	<0.1
LCP10	25.1	<0.1	<0.5	94.7	0.57	<1	28.3	100.29	0.1	0.08	1.9	0.05	<0.1

Sample ID	Rb (ppm)	Sb (ppm)	Se (ppm)	SiO_2 (%)	Sm (ppm)	Sn (ppm)	Sr (ppm)	SUM (%)	Ta (ppm)	Tb (ppm)	Th (ppm)	TiO_2 (%)	Tl (ppm)
LCP11	19.8	<0.1	<0.5	97.2	0.44	<1	18.4	100.50	<0.1	0.07	1.2	0.05	<0.1
LCP12	17.0	<0.1	<0.5	96.9	0.42	<1	17.0	100.18	<0.1	0.06	1.4	0.05	<0.1
LCP13	5.5	0.2	<0.5	96.0	0.70	<1	6.5	100.57	0.1	0.17	1.8	0.04	<0.1
LCP14	5.7	<0.1	<0.5	99.0	0.52	<1	6.0	100.71	0.1	0.11	1.7	0.03	<0.1
LCP15	6.5	0.7	3.1	84.8	1.75	<1	18.4	100.10	0.2	0.43	3.0	0.07	<0.1
LCP16	13.6	<0.1	<0.5	96.1	0.40	<1	9.2	101.02	0.2	0.10	2.1	0.08	<0.1
LCP17	14.8	<0.1	<0.5	96.8	0.47	<1	9.1	100.09	0.1	0.08	1.4	0.09	<0.1
LCP18	7.9	0.2	<0.5	95.5	0.40	<1	18.8	99.56	0.2	0.09	1.7	0.08	<0.1
LCP19	4.1	0.5	1.7	45.2	8.33	<1	664.5	100.39	<0.1	1.57	0.9	0.07	<0.1
LCP20	1.3	<0.1	<0.5	4.7	1.48	<1	1244.4	100.67	<0.1	0.33	0.4	0.02	<0.1
LCP21	40.7	<0.1	<0.5	78.7	1.27	1	68.4	99.82	0.4	0.20	5.6	0.35	<0.1
LCP22	35.6	0.1	<0.5	93.5	0.72	1	26.8	100.60	0.2	0.10	2.2	0.13	<0.1
LCP23	17.8	<0.1	0.5	96.7	0.52	<1	16.3	100.16	0.2	0.06	1.2	0.10	<0.1
RC01	2.3	<0.1	<0.5	90.9	0.28	1	6.8	100.57	0.3	0.07	2.5	0.24	<0.1
RC02	2.3	<0.1	<0.5	82.5	0.34	2	7.5	100.06	0.3	0.08	4.1	0.33	<0.1
RC03	0.3	<0.1	<0.5	96.7	0.31	1	5.8	100.19	1.0	0.13	6.3	0.76	<0.1
RC04	5.9	<0.1	<0.5	90.1	0.46	<1	14.6	100.34	0.4	0.11	4.9	0.40	<0.1
RC05	15.8	<0.1	<0.5	87.7	0.78	1	22.7	100.34	0.5	0.15	5.3	0.42	<0.1
RC06	20.1	<0.1	<0.5	86.6	0.88	1	23.0	99.82	0.4	0.15	4.8	0.39	<0.1
RC07	38.6	<0.1	<0.5	75.5	1.70	2	40.3	100.71	0.7	0.25	7.6	0.61	<0.1
RC08	35.5	<0.1	<0.5	77.1	1.62	2	42.0	100.19	0.6	0.24	7.0	0.63	<0.1
RC09	49.7	<0.1	<0.5	69.1	2.05	2	64.7	100.13	0.8	0.31	8.4	0.72	0.1
RC10	53.3	<0.1	<0.5	67.8	2.21	2	68.3	100.10	0.9	0.33	7.7	0.83	<0.1
RC11	51.9	<0.1	<0.5	70.5	8.10	2	309.0	99.91	0.8	0.61	7.8	0.74	0.1
RC12	8.2	<0.1	<0.5	94.5	0.42	<1	12.6	100.19	0.2	0.08	1.7	0.15	<0.1
RC13	26.6	0.1	3.5	65.4	2.09	2	46.2	100.63	0.6	0.38	17.5	0.49	<0.1

Sample ID	Rb (ppm)	Sb (ppm)	Se (ppm)	SiO_2 (%)	Sm (ppm)	Sn (ppm)	Sr (ppm)	SUM (%)	Ta (ppm)	Tb (ppm)	Th (ppm)	TiO_2 (%)	Tl (ppm)
RC14	5.0	<0.1	<0.5	81.8	0.62	<1	13.8	100.48	0.4	0.15	8.2	0.34	<0.1
RC15	37.0	<0.1	<0.5	75.2	1.54	2	37.4	99.83	0.6	0.24	7.2	0.59	<0.1
NY01	11.2	<0.1	<0.5	89.7	0.97	1	21.9	100.56	0.7	0.22	6.0	0.44	<0.1
NY02	12.6	<0.1	<0.5	87.4	0.93	2	36.9	100.19	0.5	0.21	6.0	0.48	<0.1
NY03	15.9	<0.1	<0.5	85.3	0.97	2	39.4	99.90	0.6	0.21	6.4	0.46	<0.1
NY04	13.2	<0.1	<0.5	88.1	0.95	6	30.7	99.81	0.6	0.20	6.3	0.48	<0.1
NY05	16.5	<0.1	1.5	86.5	1.10	1	37.5	100.80	0.7	0.29	6.4	0.55	<0.1
NY06	16.7	<0.1	<0.5	84.8	0.82	2	24.1	100.00	0.7	0.23	5.8	0.47	<0.1
NY07	9.7	<0.1	<0.5	88.9	0.72	2	22.3	100.16	0.8	0.20	6.4	0.50	<0.1
NY08	38.6	<0.1	1.4	80.2	1.23	2	70.7	100.01	0.6	0.22	6.0	0.54	<0.1
NY09	9.3	<0.1	<0.5	87.2	0.72	<1	19.0	99.57	0.6	0.17	5.6	0.42	<0.1
NY10	41.3	<0.1	0.9	80.1	1.41	2	76.1	100.88	0.7	0.24	6.5	0.55	<0.1
GRQ01	18.7	0.4	0.6	81.1	2.11	3	28.9	100.64	0.9	0.30	12.2	0.52	<0.1
GRQ02	25.0	0.1	<0.5	83.9	1.51	3	14.9	100.05	0.7	0.22	8.3	0.28	<0.1
GRQ03	25.7	<0.1	<0.5	86.7	1.32	2	15.5	100.69	0.7	0.24	6.1	0.38	0.1
GRQ04	17.1	<0.1	<0.5	87.8	2.15	2	11.7	99.86	0.5	0.35	9.1	0.35	<0.1
GRQ05	9.0	<0.1	<0.5	92.2	1.70	2	11.2	100.12	0.4	0.29	6.7	0.23	<0.1
GRQ06	7.6	<0.1	<0.5	92.7	1.31	2	12.8	99.85	0.3	0.20	4.8	0.20	<0.1
GRQ07	8.9	<0.1	<0.5	87.7	22.82	5	19.4	99.37	2.0	3.46	67.9	1.47	<0.1
GRQ08	18.8	<0.1	<0.5	88.6	1.43	2	22.6	99.73	0.5	0.23	6.0	0.30	<0.1
GRQ09	20.5	<0.1	<0.5	83.9	19.84	5	37.7	99.63	3.6	3.31	60.7	1.64	<0.1
GRQ10	15.5	<0.1	<0.5	83.3	2.28	3	36.8	100.20	1.4	0.45	21.9	0.93	<0.1
GRQ11	24.7	0.2	<0.5	82.5	1.31	3	14.4	100.11	0.5	0.21	8.5	0.29	<0.1
SRQ01	2.5	0.2	<0.5	1.6	0.34	<1	1762.8	100.65	<0.1	0.09	1.1	0.02	<0.1
SRQ02	4.2	0.1	<0.5	3.8	0.55	<1	1782.2	100.41	<0.1	0.16	1.3	0.02	<0.1
SRQ03	10.5	0.2	<0.5	8.3	2.64	<1	993.8	100.63	<0.1	0.82	2.4	0.05	<0.1

Sample ID	Rb (ppm)	Sb (ppm)	Se (ppm)	SiO_2 (%)	Sm (ppm)	Sn (ppm)	Sr (ppm)	SUM (%)	Ta (ppm)	Tb (ppm)	Th (ppm)	TiO_2 (%)	Tl (ppm)
SRQ04	87.7	<0.1	<0.5	61.2	3.84	2	77.1	100.75	0.6	0.58	13.1	0.56	<0.1
SRQ05	16.7	<0.1	<0.5	93.6	0.60	<1	20.3	99.96	0.1	0.12	1.7	0.12	<0.1
SRQ06	6.9	0.1	0.8	95.7	0.77	<1	13.5	100.35	0.3	0.17	1.8	0.11	<0.1
SRQ07	7.0	0.6	0.8	94.6	0.88	<1	14.9	100.38	0.6	0.21	3.2	0.43	<0.1
SRQ08	5.6	0.1	0.7	97.1	0.54	<1	8.5	100.21	0.1	0.13	1.6	0.09	<0.1
SRQ09	11.6	0.2	0.5	96.4	1.47	<1	19.7	99.85	0.1	0.20	2.5	0.07	<0.1
SRQ10	5.5	0.1	<0.5	97.6	0.56	<1	7.5	100.10	<0.1	0.12	1.7	0.10	<0.1
UQ01	2.6	0.1	0.7	90.5	1.68	<1	8.3	100.05	0.2	0.21	5.5	0.18	<0.1
UQ02	3.4	0.2	0.6	91.9	1.25	1	6.2	99.51	0.3	0.16	6.5	0.18	<0.1
UQ03	21.3	<0.1	<0.5	87.8	1.60	2	16.6	100.41	0.8	0.28	11.2	0.60	<0.1
UQ04	21.6	<0.1	<0.5	84.4	1.98	2	19.1	100.37	0.8	0.39	12.0	0.57	<0.1
UQ05	18.8	0.2	<0.5	80.4	3.67	2	24.0	100.01	1.4	0.68	20.7	0.55	<0.1
UQ06	20.6	<0.1	<0.5	88.9	1.27	2	13.5	100.04	0.6	0.21	8.8	0.44	<0.1
UQ07	13.3	<0.1	<0.5	87.5	1.07	2	19.9	100.32	0.5	0.20	6.0	0.32	<0.1
UQ08	11.1	<0.1	<0.5	89.4	1.43	2	44.4	100.10	1.3	0.49	5.3	0.76	<0.1
UQ09	8.3	<0.1	<0.5	84.6	1.75	2	31.4	99.79	1.1	0.52	13.1	0.70	<0.1
UQ10	7.9	<0.1	<0.5	87.5	1.09	2	27.7	100.13	0.9	0.30	8.0	0.55	<0.1
UQ11	11.8	<0.1	<0.5	85.6	0.98	9	37.5	100.23	0.9	0.30	7.2	0.59	<0.1
UQ12	50.3	<0.1	<0.5	64.1	3.35	3	105.7	100.10	0.8	0.59	9.1	0.66	0.2
UQ13	2.3	<0.1	<0.5	91.1	1.46	<1	8.2	100.71	0.2	0.17	4.4	0.22	<0.1
CCH01	10.3	<0.1	<0.5	94.1	0.82	<1	13.1	99.84	0.1	0.13	2.5	0.18	<0.1
CCH02	11.7	<0.1	<0.5	93.4	0.93	<1	20.9	100.06	0.1	0.11	2.4	0.16	<0.1
CCH03	33.1	<0.1	<0.5	84.9	1.22	<1	56.1	99.92	0.2	0.16	3.1	0.38	<0.1
CCH04	21.9	<0.1	<0.5	91.0	0.86	<1	36.0	99.84	0.3	0.13	2.8	0.28	<0.1
CCH05	23.9	<0.1	<0.5	87.7	1.45	1	42.3	100.15	0.2	0.17	3.0	0.28	<0.1
CCH06	29.3	<0.1	<0.5	88.0	1.19	1	37.4	99.67	0.5	0.19	4.9	0.50	<0.1
CCH07	26.7	<0.1	<0.5	89.7	1.76	<1	39.8	100.72	0.3	0.20	3.5	0.33	<0.1

Sample ID	Rb (ppm)	Sb (ppm)	Se (ppm)	SiO_2 (%)	Sm (ppm)	Sn (ppm)	Sr (ppm)	SUM (%)	Ta (ppm)	Tb (ppm)	Th (ppm)	TiO_2 (%)	Tl (ppm)
CCH08	12.2	<0.1	<0.5	91.1	0.50	<1	26.7	99.82	0.2	0.08	2.9	0.29	<0.1
CCH09	31.0	<0.1	<0.5	87.3	0.90	<1	46.2	99.94	0.3	0.14	2.8	0.34	<0.1
FE01	7.3	<0.1	<0.5	70.2	0.92	<1	42.0	100.56	0.4	0.19	1.8	0.23	<0.1
NHW01	8.0	<0.1	<0.5	89.7	2.26	3	11.3	99.34	1.1	0.35	9.7	0.46	<0.1
NHW02	8.7	<0.1	0.8	87.3	1.21	2	21.2	98.57	0.4	0.21	7.6	0.31	<0.1
NHW03	7.6	<0.1	0.9	90.1	1.37	<1	16.4	99.06	0.5	0.21	7.4	0.32	<0.1
BB01	97.3	0.1	<0.5	80.9	3.50	2	47.6	100.03	0.5	0.50	8.1	0.25	0.1
BB02	130.4	<0.1	<0.5	74.8	7.05	5	78.8	100.15	1.5	1.13	18.6	0.65	0.3
HC01	12.1	<0.1	<0.5	91.1	0.56	<1	21.6	99.69	0.2	0.10	3.3	0.22	<0.1
HC02	13.9	<0.1	<0.5	90.1	0.77	1	16.0	99.98	0.3	0.13	3.5	0.28	<0.1
HC03	13.4	<0.1	<0.5	90.3	0.94	1	16.8	100.03	0.5	0.20	5.6	0.39	<0.1
HC04	17.6	0.1	<0.5	77.1	1.57	2	33.7	99.86	0.8	0.33	18.6	0.59	<0.1
HC05	36.6	<0.1	<0.5	84.9	1.86	2	46.1	99.28	0.5	0.27	6.2	0.37	<0.1
GOR01	6.9	<0.1	<0.5	90.7	0.62	1	13.9	99.68	0.2	0.10	5.4	0.29	<0.1
GOR02	7.5	<0.1	<0.5	89.0	0.80	2	17.7	98.93	0.3	0.11	5.6	0.27	<0.1
GOR03	9.5	<0.1	<0.5	87.1	0.86	1	21.6	99.92	0.5	0.14	6.8	0.27	<0.1
GOR04	45.5	<0.1	1.7	51.7	1.88	3	49.2	100.16	1.2	0.31	18.6	0.97	0.1
DIA01	12.6	<0.1	<0.5	84.4	0.73	2	44.4	100.15	0.6	0.18	8.5	0.44	<0.1
DIA02	11.2	<0.1	<0.5	91.6	0.73	<1	16.9	100.28	0.6	0.12	5.2	0.36	<0.1
DIA03	12.9	<0.1	<0.5	87.9	0.96	2	14.3	99.92	0.8	0.20	7.4	0.52	<0.1
DIA04	11.7	<0.1	<0.5	90.8	0.47	<1	10.3	99.76	0.3	0.09	3.9	0.22	<0.1
DIA05	13.9	<0.1	<0.5	91.1	0.49	<1	10.4	99.83	0.3	0.08	4.1	0.23	<0.1
DIA06	11.7	<0.1	<0.5	91.4	0.54	<1	10.0	100.15	0.1	0.08	3.9	0.21	<0.1
WF01	10.1	<0.1	1.6	90.7	1.03	1	13.5	100.31	0.3	0.16	6.4	0.27	<0.1
WF02	10.3	<0.1	0.5	91.6	0.61	<1	14.0	100.08	0.2	0.10	4.3	0.16	<0.1
WF03	10.6	<0.1	0.7	90.4	0.61	<1	15.9	100.27	0.3	0.11	5.7	0.21	<0.1

Sample ID	Rb (ppm)	Sb (ppm)	Se (ppm)	SiO_2 (%)	Sm (ppm)	Sn (ppm)	Sr (ppm)	SUM (%)	Ta (ppm)	Tb (ppm)	Th (ppm)	TiO_2 (%)	Tl (ppm)
WF04	11.6	<0.1	2.0	87.0	0.79	1	16.0	99.81	0.4	0.13	7.6	0.29	<0.1
TDQ01	11.9	0.1	<0.5	91.2	0.56	<1	11.1	99.99	0.1	0.08	4.5	0.15	<0.1
TDQ02	10.0	<0.1	<0.5	91.1	0.45	<1	9.7	99.48	0.1	0.08	4.0	0.13	<0.1
TDQ03	10.3	0.1	<0.5	91.2	0.41	<1	11.7	100.01	0.2	0.08	4.1	0.14	<0.1
TDQ04	11.2	<0.1	<0.5	91.4	0.42	<1	12.6	100.28	0.1	0.08	4.9	0.18	<0.1
TDQ05	9.4	0.1	<0.5	89.7	0.43	<1	15.3	100.46	0.3	0.09	6.2	0.21	<0.1
WFN01	6.4	<0.1	<0.5	87.9	0.86	1	14.4	99.30	0.4	0.18	7.9	0.29	<0.1
WFN02	6.2	<0.1	<0.5	88.5	1.00	1	22.2	99.75	0.5	0.16	7.3	0.32	<0.1
WFN03	8.6	<0.1	<0.5	89.6	0.73	<1	17.2	99.92	0.2	0.13	6.9	0.28	<0.1
WFN04	9.1	<0.1	<0.5	89.2	0.72	<1	16.4	100.04	0.4	0.13	5.1	0.29	<0.1
GRQ04	19.8	0.2	<0.5	85.2	2.52	2	16.1	100.19	0.5	0.38	12.4	0.37	<0.1
CCH03	38.5	<0.1	<0.5	84.4	1.95	1	67.8	100.20	0.2	0.17	3.8	0.25	<0.1
SRQ09	10.7	<0.1	<0.5	96.2	1.56	<1	21.2	99.75	<0.1	0.21	3.7	0.07	<0.1
SP01	6.8	1.7	0.9	87.7	0.98	1	20.7	99.48	0.5	0.18	15.1	0.34	<0.1
SP02	9.8	<0.1	<0.5	86.0	0.93	1	28.8	100.03	0.4	0.14	5.5	0.35	<0.1
SP03	8.3	3.4	3.1	71.9	4.07	1	30.4	99.87	0.3	0.49	34.2	0.25	<0.1
SP04	9.5	<0.1	<0.5	88.5	0.87	1	35.6	100.35	0.4	0.16	5.6	0.35	<0.1
SP05	9.6	0.1	<0.5	82.7	1.34	<1	109.9	99.78	0.4	0.20	6.4	0.42	<0.1
SP06	9.7	<0.1	<0.5	82.0	1.75	1	65.8	99.80	0.5	0.29	6.4	0.36	<0.1
SP07	8.8	<0.1	<0.5	81.7	2.29	3	40.8	99.99	0.8	0.38	14.1	0.55	<0.1
SP08	6.7	<0.1	<0.5	82.0	2.71	2	63.8	99.87	0.9	0.39	10.9	0.56	<0.1
SP09	2.4	0.9	0.7	60.7	7.52	1	22.8	99.80	0.7	1.04	24.0	0.47	<0.1
SP10	5.2	0.4	0.5	63.7	3.38	2	24.0	100.33	1.0	0.62	19.8	0.73	<0.1
CW01	44.3	<0.1	<0.5	47.8	24.09	3	1342.8	100.51	5.5	2.48	9.3	3.67	<0.1
CW02	15.9	0.2	<0.5	81.4	11.65	4	77.9	100.42	2.0	1.72	38.2	1.39	<0.1
CW03	8.9	0.3	<0.5	66.6	7.97	3	23.5	100.32	0.9	1.21	20.2	0.73	<0.1

Sample ID	Rb (ppm)	Sb (ppm)	Se (ppm)	SiO_2 (%)	Sm (ppm)	Sn (ppm)	Sr (ppm)	SUM (%)	Ta (ppm)	Tb (ppm)	Th (ppm)	TiO_2 (%)	Tl (ppm)
CW04	10.0	0.4	0.8	73.8	4.83	2	15.8	100.10	0.9	0.84	19.4	0.64	<0.1
CW05	9.1	1.0	0.6	71.4	4.87	3	13.6	99.78	1.5	0.70	26.7	1.24	<0.1
CW06	9.6	0.8	0.6	75.9	3.75	2	10.8	99.86	1.1	0.67	28.2	0.91	<0.1
CW07	1.3	<0.1	<0.5	93.1	3.77	5	12.3	99.81	2.4	0.81	14.3	1.79	<0.1
CW08	1.2	0.1	<0.5	88.5	3.83	6	18.2	99.91	2.7	0.88	14.7	1.92	<0.1
CW09	4.4	0.1	0.8	88.4	0.51	<1	6.7	100.29	0.2	0.08	6.0	0.14	<0.1
CW10	9.8	0.5	1.2	64.6	2.64	3	20.6	100.24	1.3	0.48	30.5	1.07	<0.1
WA01	11.4	0.7	1.9	61.9	1.92	2	13.3	99.98	0.7	0.31	23.6	0.45	<0.1
WA02	5.4	1.4	3.5	62.1	1.36	1	6.7	100.24	0.5	0.23	24.8	0.37	<0.1
WA03	5.3	1.1	5.7	57.1	1.72	3	10.3	100.24	0.6	0.29	28.2	0.46	<0.1
WA04	4.2	1.3	4.8	54.6	1.58	<1	8.1	100.44	0.6	0.20	23.1	0.40	<0.1
WA05	1.9	0.2	2.1	58.0	1.79	7	2.2	100.70	1.5	0.65	38.1	0.23	<0.1
WA06	4.4	<0.1	<0.5	69.9	1.52	6	3.1	99.91	1.9	0.78	19.3	0.37	<0.1
WA07	6.6	2.8	1.1	53.6	4.17	2	6.7	100.10	0.5	0.58	17.6	0.29	<0.1
WA08	7.2	2.4	2.7	48.6	4.64	2	7.7	101.01	0.4	0.68	22.0	0.34	<0.1
WA09	116.0	<0.1	<0.5	76.8	10.49	5	22.5	100.61	1.3	1.52	17.9	0.16	<0.1
WA10	87.8	1.0	0.8	68.9	7.88	4	26.2	100.21	1.1	1.20	22.1	0.33	<0.1
WA11	3.7	1.5	4.2	58.5	1.61	4	5.1	99.97	0.4	0.21	21.1	0.34	<0.1
HP01	6.2	<0.1	<0.5	85.5	0.61	2	22.5	100.86	0.4	0.11	6.6	0.32	<0.1
HP02	4.4	0.1	<0.5	88.3	1.11	<1	18.1	100.70	0.4	0.17	11.1	0.24	<0.1
HP03	2.4	0.3	0.5	40.7	2.48	1	40.8	99.86	0.3	0.39	10.3	0.24	<0.1
GOR05	1.7	0.4	1.9	68.7	1.55	1	18.6	99.94	0.6	0.18	25.1	0.34	<0.1
GOR06	9.3	0.4	0.8	67.2	1.61	3	13.6	99.51	1.0	0.29	9.5	0.75	<0.1
GOR07	8.8	0.4	0.8	68.5	1.77	2	13.3	99.55	1.0	0.29	10.6	0.73	<0.1
GOR08	20.6	<0.1	1.6	73.1	1.32	3	26.0	98.94	0.8	0.23	6.7	0.71	<0.1
SH01	0.8	0.6	2.8	65.4	1.35	2	66.9	100.06	0.7	0.27	22.8	0.43	<0.1

Sample ID	Rb (ppm)	Sb (ppm)	Se (ppm)	SiO_2 (%)	Sm (ppm)	Sn (ppm)	Sr (ppm)	SUM (%)	Ta (ppm)	Tb (ppm)	Th (ppm)	TiO_2 (%)	Tl (ppm)
SH02	1.1	0.4	1.4	67.1	2.52	2	42.5	99.80	1.2	0.46	12.6	0.64	<0.1
SH03	4.2	<0.1	0.9	88.5	1.04	2	25.6	99.54	0.8	0.27	12.1	0.41	<0.1
MP01	6.3	0.3	0.6	81.0	1.32	2	25.8	99.10	0.9	0.23	17.8	0.46	<0.1
MP02	3.3	0.2	0.7	82.3	1.05	2	20.3	99.78	0.8	0.19	16.5	0.51	<0.1
GL01	21.8	<0.1	<0.5	84.5	1.95	3	23.2	99.55	0.7	0.31	10.5	0.42	<0.1
CW11	12.0	0.2	1.2	72.2	1.62	2	40.8	99.40	0.9	0.27	9.9	0.60	<0.1
HHQ01	2.7	<0.1	<0.5	89.3	0.69	2	17.9	100.30	0.5	0.16	9.8	0.30	<0.1
MR01	15.6	1.1	6.5	50.2	12.91	3	551.7	99.42	1.3	1.59	35.0	0.80	<0.1
MR02	17.7	<0.1	1.0	76.0	3.62	3	324.1	99.59	1.1	0.52	12.2	0.84	<0.1
WRC01	13.8	<0.1	<0.5	56.5	1.83	<1	405.1	100.13	0.2	0.25	2.8	0.16	<0.1
DIA10	5.9	0.4	2.6	65.1	1.24	2	34.0	99.21	0.7	0.22	20.5	0.52	<0.1
DIA11	7.4	0.8	0.5	54.6	2.84	3	17.2	99.84	0.9	0.44	17.2	0.66	<0.1
BAL01	66.9	<0.1	<0.5	63.60	4.23	2	479.2	99.37	1.0	0.54	8.0	0.55	0.1
BAL02	13.6	<0.1	<0.5	94.66	0.80	<1	26.3	99.39	0.2	0.16	2.1	0.14	<0.1
BAL03	13.7	0.1	<0.5	88.86	3.32	<1	79.2	99.42	0.1	0.40	3.9	0.14	<0.1
BAL04	15.1	0.3	<0.5	91.22	1.95	<1	27.1	100.03	0.5	0.30	4.7	0.36	<0.1
BAL05	12.3	1.3	6.7	84.92	1.83	1	49.8	99.10	0.3	0.27	6.7	0.26	<0.1
BAL06	9.5	1.2	5.9	85.93	1.00	2	43.2	99.34	0.3	0.22	7.8	0.24	<0.1
WEN01	38.8	<0.1	<0.5	76.17	3.35	1	121.8	99.36	0.7	0.49	5.5	0.49	<0.1
WEN02	34.3	<0.1	<0.5	79.46	4.17	3	79.4	99.66	1.5	0.59	8.0	1.11	<0.1
WEN03	34.2	<0.1	<0.5	81.11	3.38	2	85.8	99.57	1.0	0.52	7.6	0.89	<0.1
WEN04	44.7	<0.1	<0.5	79.00	4.10	2	104.2	99.80	0.8	0.61	8.1	0.94	<0.1
WEN05	18.8	<0.1	<0.5	84.49	2.88	3	59.5	99.39	1.0	0.45	7.8	0.99	<0.1
WEN06	30.8	<0.1	<0.5	82.65	3.20	2	76.7	99.57	0.9	0.54	8.4	0.94	<0.1
WEN07	8.7	<0.1	0.8	91.19	1.26	<1	25.6	99.66	0.3	0.22	2.9	0.21	<0.1
WEN08	20.9	<0.1	<0.5	86.57	2.36	<1	50.1	99.61	0.5	0.32	3.9	0.39	<0.1
WEN09	14.1	<0.1	<0.5	88.04	1.91	2	38.7	99.63	0.7	0.27	4.2	0.48	<0.1

Sample ID	Rb (ppm)	Sb (ppm)	Se (ppm)	SiO_2 (%)	Sm (ppm)	Sn (ppm)	Sr (ppm)	SUM (%)	Ta (ppm)	Tb (ppm)	Th (ppm)	TiO_2 (%)	Tl (ppm)
WEN10	11.1	<0.1	<0.5	90.34	2.09	6	32.0	100.16	0.6	0.29	7.6	0.51	<0.1
WEN11	3.4	<0.1	<0.5	94.40	0.41	<1	39.9	99.60	0.1	0.14	1.8	0.14	<0.1
WEN12	4.4	<0.1	<0.5	87.53	0.39	<1	22.8	99.35	<0.1	0.12	1.3	0.06	<0.1
WEN13	3.0	<0.1	0.8	92.11	0.39	<1	15.8	99.41	<0.1	0.10	0.7	0.04	<0.1
WEN14	2.2	<0.1	<0.5	95.83	0.40	<1	12.0	99.27	<0.1	0.12	1.6	0.09	<0.1
WEN15	4.4	0.1	0.8	91.82	1.09	<1	23.8	99.33	0.2	0.21	3.4	0.23	0.2
WEN16	2.9	0.1	<0.5	94.42	0.77	3	20.4	99.34	0.2	0.18	2.1	0.15	<0.1
WEN17	4.6	0.1	<0.5	92.61	0.99	9	21.7	99.34	0.2	0.17	2.8	0.23	<0.1
WEN18	11.3	0.2	0.6	83.29	2.76	<1	74.6	98.48	0.5	0.31	6.4	0.48	0.1
WEN19	10.1	0.2	<0.5	85.78	2.01	2	56.5	99.21	0.3	0.32	4.3	0.42	<0.1
BUN01	61.2	<0.1	<0.5	92.40	1.36	1	29.8	99.69	0.2	0.19	2.4	0.07	<0.1
BUN02	58.5	0.1	<0.5	92.20	1.42	2	24.4	99.64	0.2	0.26	4.1	0.11	<0.1
BUN03	53.1	0.2	<0.5	90.94	1.34	3	40.6	99.56	0.1	0.24	3.5	0.11	<0.1
BUN04	57.8	0.2	<0.5	89.97	1.00	6	28.9	99.70	0.2	0.27	4.3	0.12	<0.1
BUN05	86.1	0.1	<0.5	86.02	6.47	9	71.3	100.52	0.7	1.03	19.3	0.42	<0.1
BUN06	58.9	0.2	<0.5	84.34	2.70	6	57.2	99.33	0.5	0.41	10.7	0.15	<0.1
BUN07	72.5	0.1	<0.5	88.58	1.27	2	36.6	99.15	0.1	0.28	6.2	0.10	<0.1
BUN08	92.6	0.2	<0.5	83.21	3.41	5	66.7	99.45	0.7	0.61	12.7	0.33	<0.1
BUN09	68.1	0.3	<0.5	82.24	1.94	4	39.2	99.24	0.3	0.34	16.6	0.21	<0.1
BUN10	57.0	0.1	<0.5	86.64	3.71	3	31.5	99.81	0.4	0.55	10.4	0.22	<0.1
BUN11	50.4	<0.1	<0.5	88.92	2.90	3	27.7	99.52	0.2	0.45	5.8	0.17	<0.1
BUN12	41.1	<0.1	<0.5	89.18	2.25	3	26.4	99.46	0.2	0.34	5.8	0.14	<0.1
BUN13	43.9	<0.1	<0.5	90.27	2.07	2	25.3	99.42	0.3	0.33	5.0	0.13	<0.1
BUN14	29.3	<0.1	<0.5	94.29	1.09	4	14.0	99.68	0.3	0.18	2.8	0.09	<0.1
BUN15	25.0	<0.1	<0.5	94.77	1.01	7	13.3	99.58	0.1	0.16	2.7	0.08	<0.1
BUN16	20.4	<0.1	<0.5	96.89	0.99	1	11.8	100.85	0.1	0.17	1.8	0.07	<0.1
BUN17	22.9	<0.1	<0.5	95.54	1.03	3	11.8	99.69	0.2	0.17	1.9	0.08	<0.1

Sample ID	Rb (ppm)	Sb (ppm)	Se (ppm)	SiO_2 (%)	Sm (ppm)	Sn (ppm)	Sr (ppm)	SUM (%)	Ta (ppm)	Tb (ppm)	Th (ppm)	TiO_2 (%)	Tl (ppm)
BUN18	20.9	<0.1	<0.5	94.97	1.04	4	11.0	99.82	0.1	0.15	3.7	0.07	<0.1
BUN19	21.1	<0.1	<0.5	94.67	1.05	9	12.2	99.26	0.1	0.14	3.3	0.07	<0.1
BUN20	31.6	<0.1	<0.5	94.69	0.95	<1	14.3	99.52	0.1	0.17	2.8	0.07	<0.1
BUN21	7.3	<0.1	<0.5	82.38	0.85	15	56.5	98.71	0.1	0.15	1.7	0.08	0.1
BUN22	13.6	0.1	<0.5	81.62	1.21	39	40.6	99.09	0.3	0.20	2.9	0.11	<0.1
BUN23	7.7	<0.1	<0.5	96.78	0.49	5	8.3	99.48	<0.1	0.07	1.2	0.06	<0.1
BUN24	8.0	<0.1	<0.5	96.77	0.26	4	8.2	99.56	<0.1	0.07	0.9	0.06	0.1
BUN25	13.0	<0.1	<0.5	96.74	0.63	5	9.1	100.31	0.1	0.10	2.0	0.07	<0.1
BUN26	13.6	<0.1	<0.5	95.05	0.64	13	9.9	99.39	<0.1	0.10	1.6	0.07	<0.1
BUN27	16.0	<0.1	<0.5	91.79	1.19	10	20.4	99.37	0.1	0.19	3.6	0.11	<0.1
BUN28	11.7	<0.1	<0.5	93.66	0.69	4	14.7	99.46	0.1	0.13	1.9	0.07	<0.1
BUN29	9.0	0.1	<0.5	82.95	0.68	2	10.4	99.44	0.2	0.11	1.6	0.09	0.1
BUN30	12.3	0.3	<0.5	75.41	0.89	2	12.2	99.21	0.2	0.16	2.7	0.13	0.2
HOR101	25.1	<0.1	2.2	67.73	1.58	2	31.8	99.50	0.8	0.26	14.7	0.77	<0.1
HOR102	19.8	0.1	2.3	73.18	1.56	2	27.3	99.26	1.0	0.24	13.9	0.77	<0.1
HOR103	21.3	<0.1	1.3	76.37	1.23	1	23.0	99.49	0.6	0.21	9.0	0.63	<0.1
HOR104	28.7	<0.1	0.7	66.04	1.51	3	36.2	99.38	0.9	0.24	12.2	0.85	<0.1
HOR105	20.8	<0.1	0.7	71.22	1.30	2	30.8	99.31	0.8	0.22	10.0	0.75	<0.1
HOR106	14.9	<0.1	1.0	75.14	0.91	2	21.5	99.46	0.6	0.23	9.6	0.62	<0.1
HOR107	10.6	<0.1	0.9	79.88	0.88	2	16.8	99.62	0.6	0.18	10.5	0.51	<0.1
HOR108	9.7	<0.1	0.6	84.90	0.77	2	12.9	99.24	0.7	0.16	7.7	0.46	<0.1
HOR109	8.7	<0.1	0.7	87.49	0.59	1	10.2	99.58	0.5	0.13	4.6	0.38	<0.1
HOR110	8.6	<0.1	<0.5	89.85	0.76	<1	8.9	99.48	0.3	0.12	4.6	0.33	<0.1
HOR111	7.3	<0.1	<0.5	86.41	0.66	<1	10.2	100.41	0.3	0.13	6.0	0.37	<0.1
HOR112	9.1	<0.1	<0.5	88.77	0.47	<1	9.8	99.30	0.4	0.10	4.0	0.28	<0.1
HOR113	8.0	<0.1	<0.5	90.93	0.91	1	17.9	99.46	0.5	0.16	5.3	0.46	<0.1

Sample ID	Rb (ppm)	Sb (ppm)	Se (ppm)	SiO_2 (%)	Sm (ppm)	Sn (ppm)	Sr (ppm)	SUM (%)	Ta (ppm)	Tb (ppm)	Th (ppm)	TiO_2 (%)	Tl (ppm)
HOR114	4.7	<0.1	<0.5	90.38	0.53	<1	8.1	98.91	0.3	0.09	4.4	0.27	<0.1
HOR115	9.5	<0.1	<0.5	91.61	0.52	<1	8.7	100.81	0.4	0.11	2.8	0.27	<0.1
HOR116	6.2	<0.1	<0.5	91.67	0.37	<1	7.3	99.77	0.3	0.09	3.9	0.21	<0.1
HOR117	5.3	<0.1	<0.5	92.90	0.46	<1	5.7	99.89	0.3	0.09	3.1	0.18	<0.1
HOR118	4.7	<0.1	<0.5	91.41	0.57	<1	5.6	99.42	0.2	0.10	3.0	0.18	<0.1
HOR119	4.5	<0.1	<0.5	91.26	0.70	<1	5.3	99.87	0.2	0.10	3.2	0.16	<0.1
HOR120	3.8	<0.1	<0.5	89.73	0.92	<1	4.3	99.47	0.2	0.13	3.6	0.15	<0.1
HOR121	5.2	<0.1	<0.5	88.63	1.18	<1	6.8	99.68	0.2	0.17	4.1	0.20	<0.1
HOR122	7.7	<0.1	<0.5	91.86	0.67	<1	9.2	99.80	0.3	0.11	4.0	0.19	<0.1
HOR123	8.9	<0.1	<0.5	90.73	0.57	<1	10.0	100.16	0.3	0.11	4.5	0.19	<0.1
HOR124	7.1	<0.1	<0.5	92.25	0.53	<1	9.0	100.11	0.4	0.10	3.1	0.17	<0.1
HOR125	6.8	<0.1	<0.5	93.11	0.49	<1	7.9	99.90	0.2	0.08	2.4	0.13	<0.1
HOR126	7.8	<0.1	<0.5	92.57	0.50	<1	8.6	100.09	0.3	0.08	3.3	0.13	0.1
HOR127	8.2	<0.1	<0.5	91.55	0.46	<1	12.2	99.96	0.2	0.08	5.1	0.13	<0.1
HOR128	7.0	<0.1	<0.5	93.00	0.42	<1	11.8	100.33	0.2	0.08	4.9	0.13	<0.1
HOR129	8.7	<0.1	<0.5	90.39	0.58	<1	13.8	99.81	0.2	0.09	4.5	0.17	<0.1
HOR130	4.0	<0.1	<0.5	95.96	0.64	<1	30.5	99.92	0.1	0.10	2.1	0.05	<0.1
HOR131	44.5	<0.1	<0.5	91.87	1.34	2	26.4	100.05	0.3	0.19	3.0	0.17	<0.1
HOR132	11.8	0.1	0.6	93.88	2.15	<1	45.5	100.18	0.3	0.30	4.1	0.19	<0.1
HOR133	7.0	<0.1	<0.5	95.39	0.85	<1	39.3	99.82	0.2	0.11	2.6	0.12	<0.1
HOR134	11.2	<0.1	<0.5	95.24	0.96	<1	62.6	99.73	0.3	0.15	2.6	0.11	<0.1
HOR135	21.6	<0.1	<0.5	96.25	0.86	<1	30.1	99.71	0.2	0.14	1.9	0.06	<0.1
HOR136	50.2	0.9	<0.5	33.14	7.85	3	611.2	99.16	1.0	1.20	11.2	0.23	<0.1
HOR137	41.9	0.3	<0.5	73.66	9.66	4	68.1	99.28	1.1	1.43	22.7	0.85	<0.1
HOR501	12.2	<0.1	<0.5	92.15	0.66	<1	12.7	99.70	0.2	0.12	2.5	0.27	<0.1
HOR503	10.6	<0.1	0.8	88.47	1.43	<1	13.9	99.93	0.6	0.19	9.6	0.41	<0.1

Sample ID	Rb (ppm)	Sb (ppm)	Se (ppm)	SiO_2 (%)	Sm (ppm)	Sn (ppm)	Sr (ppm)	SUM (%)	Ta (ppm)	Tb (ppm)	Th (ppm)	TiO_2 (%)	Tl (ppm)
HOR504	23.3	0.1	2.6	60.87	2.34	3	23.8	100.38	0.8	0.30	14.4	0.73	<0.1
HOR507	20.7	<0.1	<0.5	66.93	1.62	2	29.8	99.29	0.7	0.27	13.5	0.70	<0.1
HOR508	20.8	<0.1	0.5	63.43	1.60	3	29.1	99.23	0.6	0.26	15.8	0.76	<0.1
HOR509	8.0	<0.1	<0.5	78.28	0.96	2	14.5	99.19	0.7	0.19	10.1	0.59	<0.1
HOR510	7.6	<0.1	<0.5	74.86	1.05	2	14.0	99.09	0.7	0.21	11.8	0.57	<0.1
HOR511	6.6	<0.1	<0.5	80.71	0.95	1	11.3	99.24	0.6	0.15	9.3	0.52	<0.1
HOR512	7.5	<0.1	<0.5	83.87	0.69	1	11.5	99.26	0.6	0.15	8.7	0.46	<0.1
HOR513	2.4	<0.1	<0.5	88.96	0.68	<1	6.5	99.46	0.6	0.13	5.9	0.38	<0.1
HOR514	5.1	<0.1	<0.5	86.73	0.96	<1	8.8	99.11	0.6	0.16	6.8	0.46	<0.1
HOR515	6.0	0.1	<0.5	89.00	0.73	2	9.4	99.53	0.4	0.15	6.2	0.36	<0.1
HOR516	6.6	<0.1	<0.5	92.10	0.66	<1	7.5	99.82	0.3	0.11	4.6	0.19	<0.1
HOR517	5.9	<0.1	<0.5	93.71	0.58	<1	6.6	100.75	0.2	0.09	3.5	0.14	<0.1
HOR518	6.6	<0.1	<0.5	93.64	0.71	<1	8.0	99.91	0.2	0.10	3.3	0.15	<0.1
HOR519	4.8	<0.1	<0.5	93.97	0.49	<1	7.8	99.74	0.1	0.08	2.9	0.14	<0.1
HOR520	3.9	<0.1	<0.5	94.91	0.58	<1	6.2	100.19	0.2	0.09	2.9	0.19	<0.1
HOR521	7.6	0.1	<0.5	92.95	0.80	1	9.7	99.99	0.4	0.10	3.4	0.21	<0.1
HOR522	6.3	<0.1	<0.5	91.89	1.23	<1	8.9	99.58	0.5	0.15	5.0	0.41	<0.1
HOR523	6.1	<0.1	<0.5	93.62	0.57	<1	5.9	99.96	0.2	0.09	2.9	0.18	<0.1
HOR524	7.3	<0.1	<0.5	93.05	0.70	<1	7.5	99.75	0.2	0.10	2.2	0.16	<0.1
HOR525	5.5	<0.1	<0.5	93.07	0.62	<1	6.8	99.77	0.2	0.08	2.2	0.11	<0.1
HOR527	6.3	<0.1	<0.5	92.69	0.91	<1	7.1	100.07	0.3	0.12	3.4	0.23	<0.1
HOR528	6.7	<0.1	<0.5	92.35	0.96	<1	7.2	99.93	0.3	0.12	3.8	0.23	<0.1
HOR529	6.8	<0.1	<0.5	92.37	1.03	<1	8.8	99.94	0.3	0.15	3.6	0.31	<0.1
HOR530	5.6	<0.1	<0.5	92.68	0.91	<1	7.1	99.62	0.4	0.10	2.6	0.27	<0.1
HOR531	6.4	<0.1	<0.5	91.12	1.22	2	8.3	99.57	0.5	0.17	3.9	0.40	<0.1
HOR532	5.8	<0.1	<0.5	93.00	0.97	1	8.5	100.76	0.5	0.13	3.5	0.30	<0.1

Sample ID	Rb (ppm)	Sb (ppm)	Se (ppm)	SiO_2 (%)	Sm (ppm)	Sn (ppm)	Sr (ppm)	SUM (%)	Ta (ppm)	Tb (ppm)	Th (ppm)	TiO_2 (%)	Tl (ppm)
HOR533	6.4	<0.1	<0.5	91.99	0.79	2	8.0	99.78	0.3	0.11	2.7	0.20	<0.1
HOR534	6.7	<0.1	<0.5	91.04	1.14	<1	8.8	99.93	0.8	0.20	4.6	0.66	<0.1
HOR535	7.4	<0.1	<0.5	92.91	0.80	<1	9.0	99.89	0.3	0.12	3.5	0.33	<0.1
HOR536	7.2	<0.1	<0.5	91.94	2.45	2	10.5	99.49	1.3	0.36	10.5	0.80	<0.1
HOR537	6.9	<0.1	<0.5	90.57	1.29	1	8.2	99.43	1.0	0.26	6.8	0.76	<0.1
HOR538	7.8	<0.1	<0.5	91.73	1.06	<1	8.4	99.57	0.2	0.12	3.6	0.20	<0.1
HOR539	4.3	<0.1	<0.5	94.26	1.01	1	8.7	99.91	1.3	0.16	3.1	0.83	<0.1
HOR540	2.1	0.1	0.6	96.57	0.91	<1	6.0	99.99	0.2	0.13	1.9	0.11	<0.1
HOR541	2.6	<0.1	0.7	95.92	0.99	<1	6.0	99.81	<0.1	0.13	1.6	0.09	<0.1
HOR542	3.4	0.1	<0.5	94.71	1.06	<1	6.9	99.43	0.2	0.14	2.2	0.08	<0.1
HOR543	2.8	<0.1	<0.5	95.79	0.89	<1	7.8	99.57	0.1	0.12	2.1	0.10	<0.1
HOR544	2.3	<0.1	<0.5	96.64	0.79	<1	8.2	99.79	0.2	0.11	1.9	0.11	<0.1
HOR545	2.4	<0.1	<0.5	96.56	0.83	<1	9.3	99.95	0.2	0.11	2.1	0.12	<0.1
HOR546	2.7	<0.1	<0.5	96.46	0.95	<1	10.4	99.84	0.2	0.11	2.6	0.15	<0.1
HOR547	1.9	<0.1	<0.5	97.19	0.67	<1	9.1	99.85	0.1	0.10	1.9	0.08	0.1
HOR548	1.6	<0.1	<0.5	97.32	0.69	<1	8.7	99.69	<0.1	0.09	2.2	0.07	<0.1
HOR549	1.7	<0.1	<0.5	97.59	0.57	<1	5.8	99.61	0.1	0.08	1.8	0.06	<0.1
HOR550	2.3	<0.1	<0.5	97.47	0.63	<1	8.1	99.92	<0.1	0.10	1.7	0.05	<0.1
HOR551	1.6	<0.1	<0.5	98.07	0.69	<1	5.2	99.81	<0.1	0.09	1.6	0.04	<0.1
HOR552	3.8	0.2	<0.5	96.87	1.07	<1	7.5	99.63	0.2	0.15	3.0	0.09	<0.1
HOR553	10.0	0.6	<0.5	91.67	14.79	2	16.2	99.04	0.9	1.90	37.7	0.76	0.1
HOR554	14.2	1.0	<0.5	78.86	23.03	3	19.1	99.29	1.3	3.08	52.2	1.16	<0.1
HOR505	41.2	<0.1	0.9	55.95	2.38	4	36.2	99.48	0.7	0.31	13.5	0.81	<0.1
HOR506	28.1	<0.1	2.4	55.97	2.70	3	37.8	99.37	0.8	0.36	18.5	0.91	<0.1
HOR526	6.7	<0.1	<0.5	92.10	1.05	2	7.9	99.58	0.5	0.15	4.0	0.30	<0.1
HOR701	38.6	<0.1	<0.5	45.34	6.47	2	284.1	98.99	0.5	0.83	7.4	0.43	0.1

Sample ID	Rb (ppm)	Sb (ppm)	Se (ppm)	Si_{O2} (%)	Sm (ppm)	Sn (ppm)	Sr (ppm)	SUM (%)	Ta (ppm)	Tb (ppm)	Th (ppm)	TiO_2 (%)	Tl (ppm)
HOR702	50.5	<0.1	<0.5	71.68	4.66	1	57.5	99.88	0.8	0.66	10.0	0.62	0.1
HOR703	39.6	<0.1	<0.5	73.74	4.64	2	54.7	99.30	0.5	0.60	10.0	0.54	<0.1
HOR704	36.8	<0.1	<0.5	73.64	4.30	2	68.2	98.84	0.5	0.55	8.9	0.52	0.1
HOR705	33.1	<0.1	<0.5	78.69	3.49	1	53.2	99.88	0.4	0.43	7.7	0.44	0.1
HOR706	37.6	<0.1	<0.5	77.22	4.12	1	47.3	99.73	0.6	0.52	7.7	0.47	0.1
HOR707	39.3	<0.1	<0.5	76.93	4.15	1	48.8	99.83	0.7	0.51	8.5	0.48	0.1
HOR708	53.6	<0.1	<0.5	68.42	6.03	3	58.7	99.60	0.7	0.76	9.7	0.62	0.1
HOR709	49.1	<0.1	<0.5	72.20	5.50	2	56.6	99.80	0.6	0.77	9.2	0.57	0.1
HOR710	50.2	<0.1	<0.5	70.67	3.85	1	55.1	100.70	0.7	0.49	10.0	0.61	0.1
HOR711	45.6	<0.1	<0.5	71.72	1.70	1	47.3	99.56	0.5	0.27	9.1	0.55	0.1
HOR712	20.4	<0.1	1.2	72.12	1.02	2	29.8	98.48	0.6	0.17	11.8	0.64	<0.1
HOR713	10.0	<0.1	1.1	80.03	0.58	2	17.1	99.28	0.4	0.11	10.2	0.47	<0.1
HOR714	7.3	<0.1	0.5	86.02	0.45	1	13.4	99.45	0.4	0.08	5.9	0.36	<0.1
HOR715	4.3	<0.1	0.7	87.16	0.37	<1	8.8	98.71	0.4	0.08	7.3	0.30	<0.1
HOR716	6.0	<0.1	<0.5	88.24	0.33	<1	9.5	98.16	0.3	0.07	5.3	0.28	<0.1
HOR717	7.5	<0.1	0.5	87.76	0.34	2	12.8	98.60	0.2	0.07	4.4	0.31	<0.1
HOR718	8.2	<0.1	<0.5	88.32	0.41	<1	10.9	98.14	0.3	0.08	3.8	0.22	<0.1
HOR719	7.5	<0.1	<0.5	89.21	0.40	1	8.6	98.85	0.1	0.06	4.0	0.18	<0.1
HOR720	7.7	<0.1	<0.5	89.39	0.40	<1	8.5	98.80	0.2	0.07	3.4	0.14	<0.1
HOR721	9.1	<0.1	0.6	89.59	0.50	<1	10.7	98.91	0.2	0.07	3.6	0.18	<0.1
HOR722	10.1	<0.1	<0.5	89.19	0.62	<1	11.4	98.68	0.2	0.08	4.1	0.21	<0.1
HOR723	12.0	<0.1	0.7	88.02	0.58	1	14.2	98.46	0.3	0.13	4.0	0.28	<0.1
HOR724	11.7	<0.1	<0.5	88.99	0.50	<1	13.2	98.88	0.1	0.06	3.3	0.18	<0.1
HOR725	10.5	<0.1	0.5	89.79	0.56	<1	12.4	98.96	0.1	0.07	3.7	0.18	<0.1
HOR726	9.3	<0.1	<0.5	90.18	0.48	1	9.7	98.18	0.2	0.06	3.8	0.15	<0.1
HOR727	11.3	0.1	<0.5	89.59	0.53	1	12.9	98.98	0.2	0.08	4.2	0.18	<0.1

Sample ID	Rb (ppm)	Sb (ppm)	Se (ppm)	SiO_2 (%)	Sm (ppm)	Sn (ppm)	Sr (ppm)	SUM (%)	Ta (ppm)	Tb (ppm)	Th (ppm)	TiO_2 (%)	Tl (ppm)
HOR728	13.8	<0.1	0.6	89.03	0.42	1	13.3	99.11	0.3	0.08	4.3	0.21	<0.1
HOR729	11.9	<0.1	<0.5	90.60	0.55	<1	17.4	99.32	0.3	0.10	3.9	0.27	<0.1
HOR730	11.3	<0.1	<0.5	91.11	0.67	<1	12.7	98.94	0.3	0.10	3.8	0.20	<0.1
HOR731	11.5	<0.1	<0.5	91.28	0.47	<1	12.5	98.91	0.3	0.09	3.6	0.21	<0.1
HOR732	10.2	<0.1	<0.5	92.53	0.46	<1	16.0	98.94	0.4	0.10	2.9	0.21	<0.1
HOR733	7.1	<0.1	<0.5	93.89	0.42	<1	11.0	98.82	0.1	0.06	2.5	0.11	<0.1
HOR734	8.8	<0.1	<0.5	93.10	0.44	<1	12.0	98.95	0.2	0.07	3.3	0.11	<0.1
HOR735	8.7	0.1	<0.5	92.94	0.62	1	14.9	99.12	0.2	0.08	3.4	0.16	<0.1
HOR736	9.4	<0.1	<0.5	92.40	0.63	1	16.7	99.06	0.3	0.10	3.6	0.16	<0.1
HOR737	10.0	<0.1	<0.5	92.70	0.63	<1	13.9	99.26	0.1	0.09	2.3	0.11	<0.1
HOR738	9.1	<0.1	<0.5	93.74	0.73	<1	15.7	98.79	0.3	0.09	2.2	0.11	<0.1
HOR739	9.2	<0.1	<0.5	94.04	0.50	<1	12.3	98.82	0.2	0.08	2.6	0.11	<0.1
HOR740	8.0	<0.1	<0.5	93.54	0.88	<1	12.6	98.93	0.2	0.11	3.3	0.11	<0.1
HOR741	7.6	<0.1	<0.5	96.11	0.88	<1	12.6	100.10	0.2	0.11	2.4	0.14	<0.1
HOR742	11.0	<0.1	<0.5	94.43	0.90	<1	18.9	99.00	0.1	0.10	3.1	0.10	<0.1
HOR743	10.3	<0.1	<0.5	94.52	1.28	<1	22.4	99.74	0.3	0.19	3.0	0.16	<0.1
HOR744	8.7	<0.1	<0.5	95.13	0.83	<1	17.3	100.23	0.2	0.09	2.6	0.09	<0.1
HOR745	6.4	<0.1	<0.5	94.30	1.03	<1	27.4	99.03	0.3	0.13	3.4	0.17	<0.1
HOR746	5.4	<0.1	<0.5	95.00	0.86	2	11.8	98.91	0.2	0.13	3.2	0.16	<0.1
HOR747	7.6	<0.1	<0.5	94.21	0.94	1	17.2	99.42	0.3	0.13	3.8	0.18	<0.1
HOR748	13.1	<0.1	<0.5	94.95	0.81	<1	15.6	99.24	0.2	0.11	2.0	0.05	<0.1
HOR749	14.4	<0.1	<0.5	94.55	0.82	<1	14.8	98.96	0.2	0.11	2.2	0.06	<0.1
HOR750	18.4	<0.1	<0.5	93.58	0.92	1	16.2	99.15	0.1	0.12	2.2	0.07	<0.1
HOR751	19.6	<0.1	<0.5	93.87	0.84	<1	16.8	99.13	0.2	0.12	2.0	0.06	<0.1
HOR752	38.2	0.2	<0.5	69.23	5.55	2	84.8	99.19	0.6	0.65	11.9	0.57	<0.1
HOR753	8.5	<0.1	<0.5	93.56	0.67	1	15.4	99.87	0.2	0.08	3.1	0.16	<0.1

Sample ID	Rb (ppm)	Sb (ppm)	Se (ppm)	SiO_2 (%)	Sm (ppm)	Sn (ppm)	Sr (ppm)	SUM (%)	Ta (ppm)	Tb (ppm)	Th (ppm)	TiO_2 (%)	Tl (ppm)
HOR754	17.0	0.2	<0.5	93.63	1.66	<1	17.7	99.13	0.2	0.18	5.2	0.18	<0.1
HOR755	24.1	0.1	<0.5	92.34	2.32	1	26.3	98.95	0.3	0.26	4.1	0.20	<0.1
HOR756	31.4	<0.1	<0.5	90.12	3.06	<1	36.1	99.59	0.4	0.31	4.6	0.24	<0.1
HOR757	30.0	0.1	<0.5	90.24	2.95	1	36.3	99.01	0.5	0.28	5.7	0.34	<0.1
HOR758	31.3	0.2	<0.5	90.19	3.06	2	37.0	98.94	0.7	0.30	10.1	0.56	<0.1
HOR759	29.2	0.2	<0.5	91.06	3.48	2	38.0	98.92	1.0	0.42	10.5	0.71	<0.1
HOR760	32.5	0.2	<0.5	90.99	2.87	1	39.4	98.82	0.9	0.34	9.1	0.72	<0.1
HOR761	37.6	0.1	<0.5	91.49	3.49	2	35.8	98.97	0.5	0.36	9.5	0.28	<0.1
HOR762	33.7	<0.1	<0.5	92.21	2.74	<1	35.1	99.36	0.4	0.30	5.5	0.31	<0.1
HOR763	37.7	0.2	<0.5	92.44	4.60	2	34.6	100.47	0.9	0.56	12.3	0.57	<0.1
HOR764	36.6	0.2	<0.5	91.02	5.60	2	38.4	98.98	1.2	0.78	13.0	0.80	<0.1
HOR765	45.2	1.1	<0.5	89.11	7.08	2	34.7	98.68	0.8	0.80	31.5	0.53	<0.1
HOR766	53.8	0.2	<0.5	89.74	3.22	1	36.8	99.02	0.4	0.41	7.1	0.18	<0.1
HOR767	44.0	0.4	<0.5	92.01	2.87	1	34.2	99.35	0.3	0.32	5.5	0.15	<0.1
HOR768	81.8	0.3	<0.5	88.95	3.45	3	42.7	99.07	0.3	0.41	5.0	0.17	0.2
HOR769	55.9	0.4	<0.5	90.30	2.96	2	37.8	99.05	0.3	0.39	9.5	0.21	<0.1
HOR770	49.1	0.4	<0.5	85.77	23.29	7	42.1	98.39	2.6	3.07	73.9	1.91	<0.1
HOR771	46.1	0.7	<0.5	80.51	39.52	5	35.3	98.41	1.5	4.09	37.0	1.08	<0.1
HOR772	48.0	0.2	<0.5	89.67	9.48	2	35.1	99.63	1.3	1.25	25.8	1.00	<0.1
HOR773	48.9	0.3	<0.5	86.66	14.30	5	38.4	98.82	1.6	1.90	39.4	1.28	<0.1
HOR774	53.9	0.9	0.7	71.09	26.80	4	35.4	98.41	1.7	4.12	45.6	1.23	<0.1
HOR775	54.5	0.2	<0.5	88.20	2.45	1	36.1	99.96	0.5	0.33	9.3	0.29	<0.1
HOR776	54.1	0.4	<0.5	84.43	2.14	<1	35.3	98.85	0.4	0.32	6.6	0.25	<0.1
HOR777	53.9	0.4	<0.5	88.46	2.22	1	37.5	99.04	0.4	0.28	7.7	0.19	<0.1
HOR778	56.2	0.4	<0.5	88.58	1.87	<1	37.4	99.26	0.3	0.24	5.9	0.20	<0.1
HOR779	58.0	0.2	0.9	76.39	3.95	2	43.0	99.02	1.0	0.49	14.5	0.72	<0.1
HOR780	54.0	0.3	1.3	71.58	14.31	6	45.1	98.30	2.1	1.98	35.3	1.43	<0.1

Sample ID	Rb (ppm)	Sb (ppm)	Se (ppm)	SiO_2 (%)	Sm (ppm)	Sn (ppm)	Sr (ppm)	SUM (%)	Ta (ppm)	Tb (ppm)	Th (ppm)	TiO_2 (%)	Tl (ppm)
HOR781	42.0	0.6	0.7	38.84	12.66	3	202.2	98.40	0.6	1.51	19.4	0.45	<0.1
WIL15	55.2	<0.1	<0.5	62.94	4.26	3	134.1	100.33	0.8	0.63	8.3	0.72	0.1
WIL16	61.8	<0.1	<0.5	58.79	4.87	3	127.2	100.00	0.8	0.71	8.8	0.85	0.1
WIL17	41.3	<0.1	<0.5	75.04	3.85	3	84.7	99.82	0.8	0.52	6.4	0.55	<0.1
WIL18	60.7	<0.1	<0.5	57.78	5.04	2	141.4	99.69	0.8	0.70	8.5	0.83	0.1
WIL19	29.7	<0.1	<0.5	81.75	2.21	2	54.8	100.10	0.4	0.34	4.3	0.40	<0.1
WIL20	18.8	<0.1	<0.5	88.06	1.67	<1	44.0	99.70	0.3	0.22	3.1	0.25	<0.1
WIL21	4.0	<0.1	<0.5	97.97	0.37	<1	8.8	100.06	<0.1	0.07	1.2	0.07	<0.1
WIL22	6.2	<0.1	<0.5	98.35	0.36	<1	10.9	100.80	<0.1	0.06	0.9	0.07	<0.1
WIL23	4.8	0.1	<0.5	98.50	0.38	<1	9.8	100.02	<0.1	0.06	1.2	0.03	<0.1
WIL24	5.6	0.1	<0.5	98.65	0.50	<1	10.2	100.33	0.1	0.06	0.8	0.06	<0.1
WIL25	4.9	<0.1	<0.5	98.38	0.41	<1	9.0	99.96	<0.1	0.07	0.8	0.06	<0.1
WIL26	6.8	0.1	<0.5	97.22	0.58	<1	12.4	100.02	<0.1	0.09	1.4	0.12	<0.1
WIL27	7.4	<0.1	<0.5	95.84	0.68	<1	13.7	99.64	<0.1	0.09	1.4	0.13	<0.1
WIL28	4.1	<0.1	<0.5	98.36	0.35	<1	7.9	99.87	<0.1	0.06	1.0	0.09	<0.1
WIL29	6.1	<0.1	<0.5	96.21	0.54	<1	13.9	99.40	<0.1	0.10	1.6	0.11	<0.1
WIL30	5.8	<0.1	<0.5	98.13	0.49	<1	12.1	100.20	<0.1	0.07	1.1	0.08	<0.1
WIL31	4.4	<0.1	<0.5	99.11	0.49	<1	10.1	101.33	<0.1	0.07	1.1	0.07	<0.1
WIL32	4.6	<0.1	<0.5	97.53	0.52	<1	12.9	99.86	<0.1	0.07	1.1	0.07	<0.1
WIL33	4.3	0.1	<0.5	97.47	0.41	<1	9.5	99.73	<0.1	0.07	0.9	0.07	<0.1
WIL34	4.5	<0.1	<0.5	97.97	0.38	<1	9.7	100.44	<0.1	0.06	1.1	0.04	<0.1
WIL35	5.2	<0.1	<0.5	97.07	0.47	<1	33.9	100.24	<0.1	0.08	1.1	0.06	<0.1
WIL36	7.7	0.1	<0.5	95.52	0.74	<1	19.0	100.19	0.1	0.10	1.8	0.16	<0.1
WIL37	8.6	0.1	<0.5	95.12	0.77	<1	22.7	100.31	<0.1	0.12	1.7	0.18	<0.1
WIL38	13.7	0.1	<0.5	86.79	0.94	<1	28.8	99.77	0.2	0.15	2.4	0.30	<0.1
PIA04	9.3	<0.1	<0.5	90.66	0.61	<1	904.5	99.88	0.2	0.13	2.3	0.11	<0.1

Sample ID	Rb (ppm)	Sb (ppm)	Se (ppm)	SiO_2 (%)	Sm (ppm)	Sn (ppm)	Sr (ppm)	SUM (%)	Ta (ppm)	Tb (ppm)	Th (ppm)	TiO_2 (%)	Tl (ppm)
PIA05	5.0	<0.1	<0.5	94.34	0.68	<1	183.7	99.82	<0.1	0.12	2.9	0.10	<0.1
PIA06	5.4	0.1	<0.5	92.77	0.80	<1	263.9	99.12	0.2	0.14	2.6	0.12	<0.1
PIA07	4.0	0.1	<0.5	93.48	1.11	<1	149.6	98.77	0.2	0.21	3.7	0.15	<0.1
PIA08	3.9	0.1	<0.5	95.79	0.80	<1	238.3	99.32	<0.1	0.11	2.2	0.08	<0.1
PIA09	3.6	0.2	0.5	95.31	1.07	<1	205.2	99.62	<0.1	0.15	2.1	0.06	<0.1
PIA10	10.4	0.3	0.8	95.75	1.22	<1	95.1	100.62	0.1	0.22	2.0	0.05	<0.1
PIA11	10.0	0.4	0.7	88.66	1.51	<1	243.4	99.39	0.2	0.29	3.1	0.10	<0.1
PIA12	11.1	0.2	0.7	88.33	1.38	1	354.1	98.47	0.2	0.23	2.3	0.09	<0.1
PIA13	8.4	0.6	1.4	82.60	1.64	<1	393.3	96.87	0.2	0.31	3.7	0.10	<0.1
PIA14	7.7	0.5	0.8	78.79	1.57	<1	635.1	94.56	0.2	0.29	3.5	0.07	<0.1
PIA15	10.9	0.4	<0.5	86.25	1.73	<1	1126.1	98.28	0.3	0.30	4.9	0.16	<0.1
KND01	6.9	<0.1	<0.5	58.18	1.37	<1	1595.8	83.36	<0.1	0.12	1.1	0.06	<0.1
KND02	8.3	<0.1	<0.5	58.63	1.45	<1	2059.0	84.43	0.1	0.14	1.2	0.08	<0.1
KND03	12.9	<0.1	<0.5	84.15	0.83	<1	2144.2	97.43	0.1	0.10	2.3	0.11	<0.1
KND04	8.0	<0.1	<0.5	93.42	0.81	<1	453.7	99.26	0.2	0.13	2.2	0.18	<0.1
KND05	8.5	0.1	<0.5	96.22	0.73	<1	77.1	100.06	<0.1	0.11	1.4	0.04	<0.1
KND06	6.9	<0.1	<0.5	97.97	0.57	<1	21.1	100.65	<0.1	0.08	1.0	0.01	<0.1
KND07	5.8	0.1	<0.5	96.54	0.60	<1	82.6	99.76	<0.1	0.09	1.3	0.05	<0.1
KND08	5.5	<0.1	<0.5	92.59	0.55	<1	288.4	98.22	<0.1	0.09	1.1	0.01	<0.1
KND09	6.2	0.1	<0.5	87.52	0.70	<1	716.6	96.01	<0.1	0.09	1.0	<0.01	<0.1
KND10	16.1	0.1	<0.5	84.83	1.52	1	1002.4	96.22	0.2	0.23	2.4	0.14	<0.1
KND11	16.6	0.3	<0.5	93.97	0.90	<1	171.9	99.85	0.2	0.13	1.8	0.07	<0.1
KND12	39.0	0.4	<0.5	85.00	1.60	2	205.3	99.08	0.3	0.24	3.6	0.13	<0.1
KND13	27.1	0.4	<0.5	88.47	1.42	2	167.8	99.47	0.3	0.23	3.4	0.10	<0.1
BER02	7.8	0.1	<0.5	94.96	0.38	<1	49.7	99.72	0.2	0.06	1.6	0.13	<0.1
BER03	25.7	<0.1	<0.5	79.58	1.73	1	344.9	99.36	0.4	0.26	4.3	0.27	<0.1

Sample ID	Rb (ppm)	Sb (ppm)	Se (ppm)	SiO_2 (%)	Sm (ppm)	Sn (ppm)	Sr (ppm)	SUM (%)	Ta (ppm)	Tb (ppm)	Th (ppm)	TiO_2 (%)	Tl (ppm)
BER04	18.4	<0.1	<0.5	85.50	1.20	<1	250.3	100.13	0.3	0.18	3.2	0.24	<0.1
BER05	19.5	<0.1	<0.5	84.91	1.20	<1	258.7	99.88	0.4	0.20	3.4	0.21	<0.1
BER06	13.1	0.1	<0.5	94.68	0.54	<1	38.6	99.51	0.2	0.09	1.3	0.05	<0.1
BER07	8.7	<0.1	<0.5	98.19	0.39	<1	14.5	100.42	<0.1	0.07	0.9	0.01	<0.1
MAN05	11.7	0.1	<0.5	96.48	0.60	<1	7.7	100.38	0.2	0.12	2.6	0.09	<0.1
MAN06	43.1	0.2	<0.5	88.52	1.69	1	27.8	99.72	0.5	0.26	5.9	0.28	<0.1
MAN07	124.8	<0.1	<0.5	68.90	5.12	5	53.4	99.85	1.4	0.72	16.6	0.77	0.2
MAN08	110.2	0.1	<0.5	75.79	6.13	4	51.2	99.38	1.3	0.89	18.1	0.77	0.2
MAN09	121.3	0.1	0.6	69.82	8.52	5	57.4	99.69	1.2	1.23	15.7	0.79	0.2
MAN10	111.4	0.2	0.5	73.10	5.92	4	52.9	99.77	1.2	0.86	17.1	0.75	0.2
MAN11	134.1	0.2	0.9	64.77	7.79	5	65.7	99.57	1.4	0.97	16.9	0.90	0.3
MAN12	127.8	<0.1	<0.5	65.35	6.20	5	63.4	100.32	1.3	0.89	17.2	0.92	0.3
MAN13	119.4	0.1	0.6	67.30	6.01	5	61.2	100.20	1.3	0.89	16.6	0.87	0.2
MAN14	127.6	0.2	<0.5	67.26	7.30	5	54.0	99.51	1.3	1.04	17.7	0.86	0.2
MAN15	128.8	0.1	<0.5	68.44	6.94	5	54.6	99.61	1.3	0.99	15.9	0.82	0.2
MAN16	132.4	0.2	<0.5	70.51	7.27	5	56.0	100.30	1.5	1.31	16.3	0.83	0.2
MAN17	42.9	0.2	<0.5	85.00	2.38	1	50.2	100.30	0.5	0.40	5.0	0.22	<0.1
MAN18	24.7	0.7	<0.5	89.94	1.16	1	29.0	100.55	0.2	0.20	2.3	0.10	<0.1
MAN19	23.5	0.2	0.7	91.82	1.88	1	15.6	100.29	0.2	0.32	4.5	0.13	<0.1
MAN20	15.4	0.1	<0.5	94.25	1.13	<1	10.7	100.35	0.1	0.16	2.0	0.06	<0.1
MAN21	17.9	0.2	<0.5	92.93	1.01	<1	10.9	99.60	0.1	0.18	2.2	0.08	<0.1
MAN22	14.6	0.2	<0.5	94.14	0.90	<1	10.5	100.61	0.1	0.17	1.8	0.06	<0.1
MAN23	24.8	0.2	<0.5	92.91	1.69	1	17.6	99.95	0.4	0.28	3.7	0.21	<0.1
MAN24	33.2	0.2	<0.5	88.57	2.79	1	37.9	100.58	0.6	0.44	6.2	0.28	<0.1
MAN25	11.8	0.1	<0.5	96.87	0.96	<1	9.9	100.79	0.1	0.17	2.4	0.09	<0.1
MAN26	24.6	0.1	<0.5	95.60	2.07	1	20.0	100.72	0.6	0.36	5.4	0.25	<0.1
MAN27	24.3	<0.1	<0.5	95.31	2.19	1	19.8	100.27	0.5	0.41	6.2	0.27	<0.1

Sample ID	Rb (ppm)	Sb (ppm)	Se (ppm)	SiO_2 (%)	Sm (ppm)	Sn (ppm)	Sr (ppm)	SUM (%)	Ta (ppm)	Tb (ppm)	Th (ppm)	TiO_2 (%)	Tl (ppm)
WAL11	53.6	<0.1	0.5	71.01	4.40	2	121.3	101.33	1.2	0.68	8.3	1.13	<0.1
WAL12	46.8	0.1	1.0	75.38	3.89	1	101.9	100.20	0.9	0.59	6.9	0.95	<0.1
WAL13	4.8	0.1	0.7	95.41	1.18	<1	25.1	100.70	<0.1	0.19	1.4	0.09	<0.1
WAL14	3.8	<0.1	<0.5	97.46	0.54	3	8.5	100.18	<0.1	0.11	1.1	0.05	<0.1
WAL15	3.0	0.2	<0.5	97.09	0.73	<1	20.3	100.63	0.1	0.11	1.3	0.06	<0.1
WAL16	19.6	0.2	<0.5	87.52	5.04	3	30.2	100.02	2.2	0.97	16.5	2.48	<0.1
WAL17	20.0	0.1	<0.5	92.36	1.38	1	33.6	100.23	0.5	0.22	3.4	0.34	<0.1
WAL18	20.5	0.2	<0.5	90.57	1.56	2	41.0	100.52	0.5	0.24	3.4	0.38	<0.1
MOR04	31.4	0.1	<0.5	67.36	2.35	2	852.4	100.25	0.9	0.36	4.7	0.31	<0.1
MOR05	2.5	<0.1	<0.5	96.93	0.28	<1	48.5	100.71	<0.1	0.06	0.9	0.04	<0.1
MOR06	0.9	<0.1	<0.5	99.13	0.30	<1	12.8	100.70	0.2	0.06	1.0	0.03	<0.1
MOR07	2.7	<0.1	<0.5	98.90	0.25	<1	12.4	100.62	<0.1	0.05	0.8	0.07	<0.1
MOR08	3.7	0.2	0.7	95.78	0.43	1	62.1	100.15	1.0	0.07	1.6	0.10	<0.1
MOR09	3.5	<0.1	0.5	98.52	0.31	2	9.6	100.33	0.6	0.06	0.9	0.05	<0.1
MOR10	3.9	<0.1	<0.5	98.92	0.33	<1	10.2	100.87	0.1	0.07	1.0	<0.01	<0.1
MOR11	4.5	<0.1	<0.5	98.21	0.34	<1	12.1	100.44	<0.1	0.06	1.0	0.02	<0.1
MOR12	5.2	0.1	<0.5	98.85	0.44	<1	11.1	100.96	<0.1	0.07	1.0	0.02	<0.1
MOR13	5.8	0.1	<0.5	98.08	0.32	<1	11.8	100.47	0.9	0.06	0.8	0.02	<0.1
MOR14	5.2	<0.1	0.7	98.54	0.37	<1	14.1	100.98	0.9	0.06	0.7	0.01	<0.1
MOR15	3.0	<0.1	<0.5	98.39	0.47	<1	7.1	100.10	0.1	0.08	1.3	0.04	<0.1
MOR16	7.6	<0.1	<0.5	98.50	0.39	<1	10.6	100.72	0.2	0.08	1.0	0.02	<0.1
MOR17	7.2	<0.1	<0.5	98.35	0.37	<1	8.6	100.37	0.3	0.07	1.3	0.04	<0.1
MOR18	6.8	0.1	0.8	98.02	0.35	<1	9.9	100.06	0.2	0.07	1.0	0.10	<0.1
MOR19	6.0	<0.1	<0.5	98.51	0.34	<1	11.8	100.48	0.1	0.08	1.2	0.03	<0.1
MOR20	7.3	0.1	<0.5	98.33	0.50	<1	7.8	101.16	<0.1	0.10	1.3	0.04	<0.1
MOR21	7.0	0.1	<0.5	97.17	0.58	<1	10.0	100.11	0.1	0.13	1.4	0.04	<0.1

Sample ID	Rb (ppm)	Sb (ppm)	Se (ppm)	SiO_2 (%)	Sm (ppm)	Sn (ppm)	Sr (ppm)	SUM (%)	Ta (ppm)	Tb (ppm)	Th (ppm)	TiO_2 (%)	Tl (ppm)
MOR22	5.0	0.1	<0.5	97.71	0.52	<1	6.9	100.21	<0.1	0.09	1.2	0.04	<0.1
BT01	12.5	0.2	<0.5	86.99	0.73	<1	20.4	99.68	0.5	0.13	7.0	0.34	<0.1
BT02	14.7	0.1	<0.5	87.70	0.59	<1	15.5	99.97	0.3	0.09	5.1	0.20	<0.1
BT03	16.0	0.1	<0.5	88.37	0.78	<1	14.8	99.66	0.3	0.10	5.4	0.25	<0.1
BT04	17.2	0.2	<0.5	88.13	0.58	<1	14.5	100.10	0.4	0.11	5.9	0.21	<0.1
BT05	18.8	<0.1	<0.5	87.59	0.76	<1	15.7	99.21	0.4	0.11	4.7	0.21	<0.1
BT06	17.3	0.2	<0.5	87.98	0.71	<1	13.7	99.85	0.2	0.11	4.6	0.16	<0.1
BT07	26.0	<0.1	<0.5	91.17	0.81	2	17.1	100.59	0.7	0.12	4.4	0.17	<0.1
BT08	24.9	0.2	<0.5	88.64	1.97	<1	15.4	100.45	0.3	0.30	5.0	0.14	<0.1
BT09	25.6	0.1	<0.5	90.03	1.17	4	15.9	99.47	0.4	0.19	3.7	0.16	<0.1
BT10	21.1	<0.1	<0.5	92.14	1.09	3	17.2	99.88	0.5	0.14	4.2	0.26	<0.1
BT11	25.7	0.1	<0.5	92.91	0.79	4	16.7	99.86	0.3	0.12	3.1	0.12	<0.1
BT12	25.9	0.1	<0.5	92.22	1.21	<1	15.0	100.08	0.3	0.17	3.3	0.08	<0.1
BT13	9.7	0.1	<0.5	93.06	0.55	<1	10.7	99.81	0.4	0.09	3.4	0.19	<0.1
BT14	13.8	0.1	<0.5	89.17	0.70	<1	13.7	99.40	0.3	0.11	4.6	0.20	<0.1
BT15	14.6	0.1	<0.5	90.15	0.64	<1	12.8	99.96	0.2	0.10	4.1	0.19	<0.1
BT16	15.3	0.1	<0.5	89.42	0.66	<1	12.9	99.61	0.3	0.10	4.7	0.20	<0.1
BT17	15.9	0.1	<0.5	90.00	0.82	<1	13.2	99.89	0.2	0.13	4.6	0.22	<0.1
BT18	16.3	<0.1	<0.5	89.18	0.88	<1	14.4	99.88	0.3	0.17	4.6	0.28	<0.1
BT19	17.4	0.2	<0.5	90.05	0.96	<1	14.1	99.99	1.0	0.15	4.3	0.24	<0.1
BT20	19.9	0.2	<0.5	88.46	1.33	<1	15.9	99.63	0.5	0.18	5.0	0.20	<0.1
BT21	20.8	0.1	<0.5	89.72	1.16	<1	15.3	99.72	0.2	0.17	4.0	0.18	<0.1
BT22	21.7	0.1	<0.5	91.09	1.00	<1	16.1	100.09	0.2	0.15	3.9	0.15	<0.1
BT23	26.5	15.0	<0.5	90.24	2.69	<1	16.4	99.85	0.2	0.27	4.5	0.16	<0.1
BT24	27.4	0.1	<0.5	92.84	3.55	<1	17.0	100.00	0.2	0.39	3.3	0.14	<0.1
BT25	24.8	0.2	<0.5	94.82	3.53	<1	15.8	101.24	0.1	0.34	3.4	0.16	<0.1

Sample ID	Rb (ppm)	Sb (ppm)	Se (ppm)	SiO_2 (%)	Sm (ppm)	Sn (ppm)	Sr (ppm)	SUM (%)	Ta (ppm)	Tb (ppm)	Th (ppm)	TiO_2 (%)	Tl (ppm)
BT26	21.4	0.2	1.0	91.77	3.63	<1	12.7	100.18	0.1	0.55	2.6	0.10	<0.1
BT27	29.5	0.2	<0.5	91.91	9.74	<1	19.8	100.17	0.1	1.10	3.3	0.13	<0.1
BT28	46.7	0.2	<0.5	89.72	3.38	3	34.0	99.95	0.5	0.58	4.7	0.33	0.1
BT29	65.9	0.2	<0.5	88.63	4.08	2	40.7	100.15	0.5	0.58	9.0	0.37	0.2
BT30	47.5	0.1	<0.5	91.05	2.95	2	37.5	100.45	0.6	0.38	5.1	0.29	0.1
BT37	16.2	0.2	<0.5	78.93	0.60	2	21.4	99.53	0.5	0.11	8.7	0.38	<0.1
BT38	12.4	0.2	<0.5	86.98	0.45	1	13.9	99.37	0.3	0.08	6.1	0.23	<0.1
BT39	14.4	0.2	<0.5	88.79	0.56	<1	15.0	100.40	0.3	0.08	5.2	0.23	<0.1
BT40	13.7	0.1	<0.5	90.56	0.65	<1	12.5	99.76	0.2	0.11	3.9	0.19	<0.1
BT41	13.9	0.1	<0.5	89.82	0.77	1	13.8	99.10	0.2	0.10	4.4	0.19	<0.1
BT42	14.6	0.2	<0.5	90.38	1.88	1	13.9	100.15	0.2	0.22	4.3	0.17	<0.1
BT43	18.9	0.3	<0.5	89.07	3.62	1	17.8	100.28	0.3	0.54	5.3	0.22	<0.1
BT44	20.3	0.2	<0.5	90.93	3.54	2	16.6	99.96	0.3	0.52	4.8	0.19	<0.1
BT45	30.3	0.2	<0.5	90.85	5.24	2	17.8	100.18	0.4	0.58	4.0	0.10	<0.1
MBR06	31.8	0.1	0.7	75.91	1.12	5	99.3	99.77	0.6	0.19	7.5	0.39	<0.1
MBR07	14.9	0.2	<0.5	63.70	1.84	3	272.3	100.17	1.7	0.29	4.5	0.22	<0.1
MBR08	22.8	0.1	<0.5	69.30	1.40	1	209.9	101.11	0.4	0.24	4.3	0.25	<0.1
MBR09	18.2	0.2	<0.5	70.39	1.79	<1	185.6	99.47	0.4	0.23	4.8	0.23	<0.1
MBR10	16.6	0.2	<0.5	69.74	1.54	<1	206.9	100.14	0.3	0.24	3.7	0.21	<0.1
MBR11	22.0	0.2	<0.5	47.22	1.91	<1	340.1	99.57	0.5	0.27	3.9	0.23	<0.1
MBR12	21.0	0.2	<0.5	36.65	1.53	1	450.1	99.72	0.6	0.22	3.4	0.19	<0.1
MBR13	14.7	0.2	<0.5	30.02	1.23	<1	648.5	99.94	0.2	0.19	2.5	0.14	<0.1
MBR14	27.3	0.1	0.9	45.69	1.63	1	348.9	99.80	0.4	0.24	5.7	0.28	<0.1
MBR15	15.8	0.2	<0.5	33.83	1.32	<1	379.9	99.51	0.2	0.20	2.9	0.16	<0.1
MBR16	3.5	0.2	0.6	4.55	0.74	<1	722.1	97.33	<0.1	0.11	1.3	0.02	<0.1
FT04	30.4	0.2	<0.5	80.33	1.21	1	91.9	99.40	0.3	0.17	5.8	0.29	<0.1
FT05	11.5	0.2	1.3	92.51	0.48	3	16.9	99.94	0.2	0.10	3.1	0.14	<0.1

Sample ID	Rb (ppm)	Sb (ppm)	Se (ppm)	SiO_2 (%)	Sm (ppm)	Sn (ppm)	Sr (ppm)	SUM (%)	Ta (ppm)	Tb (ppm)	Th (ppm)	TiO_2 (%)	Tl (ppm)
FT06	12.3	0.4	<0.5	82.90	0.81	2	36.3	99.89	0.4	0.14	8.6	0.18	<0.1
FT07	16.0	0.2	<0.5	92.01	0.51	2	16.7	99.98	0.4	0.09	3.2	0.15	<0.1
FT08	13.7	0.4	<0.5	92.46	0.51	2	13.1	100.20	0.3	0.08	4.2	0.13	<0.1
FT09	11.0	0.3	<0.5	94.61	0.45	1	44.6	101.24	0.2	0.08	3.5	0.08	<0.1
FT10	11.8	1.4	0.7	85.47	1.04	1	14.2	99.51	0.2	0.10	20.8	0.09	<0.1
FT11	16.9	0.6	1.6	90.18	0.88	1	22.6	100.06	0.2	0.11	7.3	0.11	<0.1
FT12	15.0	0.9	0.9	91.11	0.79	2	15.8	100.02	0.2	0.08	6.8	0.12	<0.1
FT13	17.0	0.9	1.2	88.07	0.92	<1	16.3	99.53	0.2	0.11	14.2	0.14	<0.1
FT14	63.1	0.4	3.2	74.14	10.19	1	38.8	99.44	0.5	0.78	7.4	0.24	<0.1
FT15	55.7	0.5	2.6	71.58	20.04	2	202.3	99.46	0.3	1.95	6.1	0.18	0.2
NGA01	48.0	<0.1	0.5	79.33	3.10	1	39.2	101.05	0.3	0.50	6.3	0.35	0.2
NGA02	46.0	<0.1	<0.5	75.91	3.06	2	86.7	99.14	0.6	0.46	7.4	0.44	0.1
NGA03	69.3	<0.1	<0.5	67.06	3.97	3	70.6	99.43	0.7	0.55	9.6	0.67	0.2
NGA04	79.4	<0.1	<0.5	63.50	3.18	3	84.7	100.32	0.8	0.48	10.5	0.72	0.2
NGA05	43.1	0.1	<0.5	77.77	2.15	2	44.0	100.53	0.4	0.32	8.0	0.50	<0.1
NGA06	25.2	<0.1	<0.5	86.15	0.83	2	26.5	100.71	0.4	0.13	6.7	0.31	<0.1
NGA07	32.3	<0.1	<0.5	82.96	1.23	2	34.6	100.28	0.4	0.20	5.9	0.38	0.1
NGA08	28.2	<0.1	0.7	84.85	0.93	1	34.1	100.39	0.2	0.15	6.1	0.34	<0.1
NGA09	29.3	<0.1	0.8	84.20	1.03	1	32.1	100.28	0.4	0.16	5.6	0.34	<0.1
NGA10	26.7	<0.1	<0.5	86.19	1.25	1	31.1	100.39	0.4	0.18	5.1	0.29	<0.1
NGA11	32.9	<0.1	<0.5	82.68	1.69	1	37.2	100.53	0.4	0.26	6.1	0.36	<0.1
NGA12	19.5	0.2	<0.5	89.43	0.74	1	26.2	100.39	0.4	0.13	4.5	0.24	<0.1
NGA13	20.4	<0.1	<0.5	89.48	0.92	1	26.4	100.88	0.3	0.13	5.0	0.24	<0.1
NGA14	13.9	0.1	<0.5	93.45	0.61	<1	17.3	101.47	0.2	0.10	3.6	0.18	<0.1
NGA15	20.7	<0.1	<0.5	89.44	0.80	<1	25.3	99.94	0.3	0.13	4.0	0.24	<0.1
NGA16	8.8	<0.1	<0.5	95.14	0.51	<1	14.7	100.21	0.2	0.08	2.9	0.13	<0.1

Sample ID	Rb (ppm)	Sb (ppm)	Se (ppm)	SiO_2 (%)	Sm (ppm)	Sn (ppm)	Sr (ppm)	SUM (%)	Ta (ppm)	Tb (ppm)	Th (ppm)	TiO_2 (%)	Tl (ppm)
NGA17	7.4	<0.1	<0.5	96.10	0.61	<1	13.5	100.59	0.1	0.10	2.2	0.10	<0.1
NGA18	5.8	0.1	<0.5	96.89	0.64	<1	12.7	100.44	<0.1	0.08	2.2	0.11	<0.1
NGA19	3.5	0.1	<0.5	98.93	0.61	<1	10.5	101.44	<0.1	0.11	2.1	0.05	<0.1
NGA20	3.8	0.1	<0.5	97.89	0.54	<1	9.9	100.51	0.1	0.11	1.9	0.08	<0.1
NGA21	1.8	0.2	<0.5	98.68	0.43	<1	9.2	100.15	<0.1	0.11	1.3	0.06	<0.1
NGA22	3.2	<0.1	<0.5	97.89	0.59	<1	9.3	100.27	0.1	0.10	1.8	0.08	<0.1
NGA23	2.8	0.1	<0.5	98.16	0.47	<1	9.0	100.17	<0.1	0.10	1.4	0.06	<0.1
NGA24	3.3	0.1	<0.5	98.56	0.51	<1	8.8	100.42	<0.1	0.11	1.7	0.06	<0.1
NGA25	3.5	0.1	<0.5	98.53	0.58	<1	11.0	100.56	0.1	0.15	2.0	0.05	<0.1
NGA26	2.9	0.1	<0.5	98.86	0.44	<1	7.8	100.42	<0.1	0.10	1.9	0.05	<0.1
NGA27	3.5	<0.1	<0.5	98.54	0.51	<1	8.9	100.57	0.1	0.10	1.8	0.07	<0.1
NGA28	3.8	0.1	<0.5	98.06	0.63	<1	9.2	100.28	0.1	0.12	2.2	0.08	<0.1
NGA29	2.2	0.1	<0.5	99.05	0.30	<1	7.1	100.55	<0.1	0.08	1.3	0.04	<0.1
NGA30	2.6	0.1	<0.5	99.25	0.59	<1	6.4	100.68	<0.1	0.09	1.7	0.05	<0.1
NGA31	2.5	<0.1	<0.5	99.19	0.46	<1	7.7	100.67	<0.1	0.09	1.3	0.04	<0.1
NGA32	3.6	<0.1	<0.5	97.87	0.58	<1	9.7	99.84	<0.1	0.10	2.2	0.05	<0.1
NGA33	3.4	0.1	<0.5	98.09	0.50	<1	9.2	99.88	<0.1	0.09	1.6	0.04	<0.1
NGA34	2.7	0.3	<0.5	98.18	0.59	<1	8.3	100.35	<0.1	0.11	2.7	0.05	<0.1
NGA35	6.0	0.2	<0.5	97.46	0.78	<1	9.5	100.08	<0.1	0.13	2.4	0.12	<0.1
NGA36	4.0	<0.1	<0.5	98.69	0.52	<1	9.7	100.67	<0.1	0.10	2.0	0.06	<0.1
NGA37	6.1	0.1	<0.5	97.57	0.58	<1	11.5	100.20	<0.1	0.11	1.9	0.06	<0.1
NGA38	22.5	0.8	0.5	81.38	3.72	1	19.6	99.96	0.2	0.60	4.9	0.18	0.4
NGA39	12.3	1.1	2.3	74.14	2.87	<1	16.1	99.92	0.2	0.50	3.2	0.10	<0.1
TEM03	11.7	<0.1	<0.5	91.87	0.47	1	17.2	100.26	0.2	0.07	3.2	0.15	<0.1
TEM04	12.6	<0.1	<0.5	90.81	0.38	<1	22.1	99.83	0.2	0.09	3.5	0.12	<0.1
TEM05	11.6	0.1	<0.5	92.04	0.55	<1	14.3	99.93	0.2	0.10	3.3	0.16	<0.1

Sample ID	Rb (ppm)	Sb (ppm)	Se (ppm)	SiO_2 (%)	Sm (ppm)	Sn (ppm)	Sr (ppm)	SUM (%)	Ta (ppm)	Tb (ppm)	Th (ppm)	TiO_2 (%)	Tl (ppm)
TEM06	2.8	0.1	<0.5	97.63	0.41	<1	8.7	100.79	0.2	0.07	2.2	0.06	<0.1
TEM07	2.3	0.1	0.8	98.60	0.37	<1	8.1	100.69	<0.1	0.08	1.7	0.08	<0.1
TEM08	2.1	0.1	<0.5	97.72	0.40	<1	6.8	99.98	<0.1	0.07	1.6	0.07	<0.1
TEM09	2.1	0.2	0.7	98.40	0.35	<1	7.2	100.47	0.1	0.07	1.6	0.04	<0.1
TEM10	2.4	0.1	<0.5	98.07	0.34	<1	7.7	100.37	<0.1	0.07	1.7	0.06	<0.1
TEM11	2.5	0.1	<0.5	97.90	0.40	<1	8.4	100.25	0.1	0.07	1.7	0.05	<0.1
TEM12	5.0	0.1	0.6	93.81	0.99	<1	29.9	100.00	0.3	0.17	4.3	0.09	<0.1
TEM13	3.9	0.1	<0.5	95.51	0.73	<1	27.7	100.21	0.3	0.13	3.1	0.05	<0.1
TEM14	7.1	0.2	1.2	93.24	0.91	<1	19.9	100.78	0.2	0.12	2.1	0.12	<0.1
TEM15	16.1	0.1	<0.5	84.54	3.78	<1	24.1	100.56	0.2	0.50	4.7	0.28	<0.1
NDA01	7.2	0.1	<0.5	94.48	0.48	<1	234.1	99.88	<0.1	0.08	1.2	0.05	<0.1
NDA02	7.0	0.2	<0.5	94.95	0.41	<1	247.2	100.19	<0.1	0.06	0.9	0.06	<0.1
NDA03	6.4	0.4	<0.5	88.92	0.72	1	262.9	99.38	0.1	0.13	1.4	0.07	<0.1
NDA04	8.8	0.3	<0.5	98.40	0.50	<1	24.2	100.54	0.1	0.08	0.9	0.04	<0.1
OAK03	13.5	<0.1	<0.5	94.24	0.86	<1	29.8	99.91	0.6	0.15	3.1	0.46	<0.1
OAK04	7.4	<0.1	<0.5	93.63	1.51	1	39.0	100.26	1.0	0.26	6.0	0.95	<0.1
OAK05	6.6	<0.1	<0.5	90.01	0.69	<1	51.8	99.99	0.4	0.12	2.5	0.38	<0.1
OAK06	7.3	<0.1	<0.5	92.05	0.63	<1	64.4	99.56	0.3	0.10	1.9	0.27	<0.1
OAK07	7.6	<0.1	<0.5	95.95	0.74	2	51.4	100.83	0.2	0.10	1.7	0.22	<0.1
OAK08	27.4	<0.1	<0.5	86.76	1.34	<1	54.2	100.22	0.2	0.17	4.3	0.21	<0.1
OAK09	13.0	<0.1	<0.5	92.98	1.16	<1	43.2	99.90	0.2	0.17	2.8	0.15	<0.1
OAK10	3.1	0.1	<0.5	97.58	0.60	<1	38.2	100.31	<0.1	0.07	1.0	0.10	<0.1
OAK11	10.0	0.2	<0.5	91.36	1.63	<1	52.9	100.73	0.3	0.23	3.2	0.35	<0.1
OAK12	37.4	<0.1	0.7	68.96	3.10	2	96.0	99.77	1.5	0.44	9.3	1.47	<0.1
OAK13	34.7	<0.1	0.7	68.78	3.10	2	92.2	99.94	1.4	0.46	8.5	1.40	<0.1
OAK14	43.4	<0.1	1.6	63.68	7.07	3	94.7	99.93	1.5	0.90	9.3	1.54	<0.1

Sample ID	Rb (ppm)	Sb (ppm)	Se (ppm)	SiO_2 (%)	Sm (ppm)	Sn (ppm)	Sr (ppm)	SUM (%)	Ta (ppm)	Tb (ppm)	Th (ppm)	TiO_2 (%)	Tl (ppm)
OAK15	45.4	0.1	1.3	60.42	6.07	3	98.9	99.66	1.9	0.79	10.0	1.52	<0.1
OAK16	40.7	0.1	1.5	62.18	6.05	3	89.6	99.42	1.7	0.75	11.6	1.33	<0.1
OAK17	39.7	0.2	2.5	63.98	5.53	4	92.5	99.78	2.0	0.72	11.1	1.39	<0.1
OAK18	41.0	0.2	3.9	62.15	4.88	3	91.2	99.51	2.1	0.66	10.4	1.38	<0.1
OAK19	32.9	0.1	0.9	71.00	5.13	2	76.3	99.57	1.3	0.61	8.3	1.03	<0.1
OAK20	39.5	<0.1	<0.5	66.05	4.86	3	87.0	99.60	1.4	0.64	9.6	1.26	<0.1
OAK21	16.8	0.1	<0.5	86.93	1.84	1	49.0	100.40	0.7	0.26	5.4	0.65	<0.1
PIN04	4.5	0.3	<0.5	97.80	0.44	2	7.1	100.34	0.1	0.06	1.7	0.03	<0.1
PIN05	11.9	0.3	<0.5	96.06	0.60	2	10.4	100.33	0.1	0.09	2.0	0.05	<0.1
PIN06	7.1	0.3	<0.5	97.39	1.43	2	8.4	100.05	0.5	0.26	3.7	0.31	<0.1
PIN07	6.6	0.3	<0.5	97.79	1.55	3	7.0	100.36	0.6	0.34	4.9	0.32	<0.1
PIN08	7.2	0.2	<0.5	97.56	1.89	2	8.9	100.59	0.8	0.41	5.6	0.51	<0.1
PIN09	7.3	0.3	<0.5	97.26	1.24	2	10.1	100.64	0.6	0.26	3.6	0.36	<0.1
PIN10	30.6	0.3	0.6	92.00	2.94	2	26.1	100.89	0.5	0.36	5.8	0.31	<0.1
PV02	6.7	0.2	<0.5	94.83	0.43	<1	13.4	100.07	0.2	0.07	1.9	0.12	<0.1
PV03	7.0	0.1	<0.5	95.92	0.59	<1	13.3	100.90	0.2	0.09	2.5	0.13	<0.1
PV04	8.9	0.2	<0.5	93.98	0.59	<1	15.2	100.11	0.2	0.10	2.3	0.16	<0.1
PV05	1.9	0.1	<0.5	97.83	0.41	<1	8.4	100.47	0.1	0.06	1.2	0.04	<0.1
PV06	1.4	0.2	<0.5	97.94	0.44	1	8.0	100.08	<0.1	0.07	1.1	0.04	<0.1
PV07	2.6	0.2	<0.5	99.03	0.58	<1	11.0	101.49	<0.1	0.09	1.3	0.07	<0.1
PV08	2.7	0.2	<0.5	98.04	0.33	<1	9.4	100.34	<0.1	0.06	1.1	0.04	<0.1
PV09	4.7	0.2	<0.5	97.90	0.47	<1	13.0	100.46	<0.1	0.07	1.1	0.05	<0.1
RB02	6.5	0.5	<0.5	78.37	1.41	<1	16.7	99.56	0.3	0.20	4.9	0.25	<0.1
RB03	60.1	0.1	2.4	56.32	2.80	3	63.7	100.37	0.8	0.45	16.7	0.82	<0.1
RB04	54.8	0.3	0.8	49.88	4.31	3	78.3	99.82	0.7	0.58	16.1	0.63	0.2
RB05	43.8	0.2	<0.5	25.40	11.63	2	209.0	100.17	0.3	1.35	13.5	0.45	0.1

Sample ID	Rb (ppm)	Sb (ppm)	Se (ppm)	SiO_2 (%)	Sm (ppm)	Sn (ppm)	Sr (ppm)	SUM (%)	Ta (ppm)	Tb (ppm)	Th (ppm)	TiO_2 (%)	Tl (ppm)
KI1_01	57.1	<0.1	<0.5	71.56	6.71	2	64.5	100.12	0.7	0.98	10.4	0.72	0.2
KI1_02	34.8	<0.1	<0.5	81.35	2.39	2	35.8	100.59	0.5	0.36	7.1	0.47	0.1
KI1_03	44.8	<0.1	<0.5	76.07	3.82	2	44.7	99.96	0.6	0.58	8.4	0.54	0.2
KI1_04	40.2	<0.1	<0.5	75.62	2.25	2	59.7	99.86	0.4	0.34	7.8	0.54	<0.1
KI1_05	34.2	<0.1	<0.5	73.34	4.34	2	97.7	100.30	0.5	0.68	7.1	0.52	<0.1
KI1_06	37.8	0.1	<0.5	64.09	5.13	2	122.9	99.85	0.7	0.75	9.6	0.69	<0.1
KI1_07	36.9	<0.1	<0.5	74.84	3.52	2	56.2	100.44	0.7	0.57	7.9	0.68	<0.1
KI1_08	17.0	<0.1	<0.5	85.44	2.41	1	64.1	99.69	0.6	0.38	5.1	0.48	<0.1
KI1_09	16.6	<0.1	<0.5	88.70	1.83	2	26.8	99.70	0.6	0.29	5.6	0.50	<0.1
KI1_10	22.3	0.1	<0.5	86.81	3.46	2	30.0	100.02	0.4	0.55	6.1	0.51	<0.1
KI1_11	52.2	0.1	<0.5	72.49	2.26	2	53.1	99.87	0.6	0.37	17.2	0.60	<0.1
KI1_12	66.1	<0.1	<0.5	63.83	3.24	3	70.2	99.24	0.8	0.51	21.7	0.79	0.1
KI1_13	86.8	0.2	1.0	45.16	38.42	4	104.9	99.47	0.9	3.94	21.4	0.86	0.1
KI10_01	43.4	0.2	1.5	58.45	9.10	2	89.8	99.79	0.6	1.29	12.5	0.58	0.1
KI10_02	27.2	0.2	1.0	76.10	11.15	1	51.9	99.66	0.4	1.85	9.0	0.39	0.1
KI10_03	87.8	0.2	1.7	55.29	43.55	3	81.4	99.40	0.8	4.77	23.9	0.72	0.2
KI10_04	74.5	0.3	1.3	47.35	39.71	2	121.4	100.74	0.6	4.30	20.8	0.51	0.2
KI10_05	30.3	0.3	<0.5	30.83	11.58	1	245.7	100.32	0.6	1.53	7.9	0.34	0.1
OLC01	2	<0.1	<0.5	88	0.19	<1	36.9	100.39	<0.1	0.04	1.2	<0.01	<0.1
OLC02	0.3	<0.1	<0.5	49.1	1.99	<1	66.6	100.59	<0.1	0.6	5.4	<0.01	<0.1
OLC03	<0.1	0.2	<0.5	75.9	0.31	<1	29	99.75	<0.1	0.07	1.9	<0.01	<0.1
OLC04	14.4	<0.1	<0.5	20.5	3.51	<1	124.8	100.62	<0.1	0.77	13.6	0.06	<0.1
OLC05	39.8	<0.1	<0.5	85.7	0.66	1	39.1	99.69	0.4	0.13	3.1	0.33	<0.1
OLC06	52.2	<0.1	2.1	62.2	1.02	<1	112.8	100	0.3	0.15	7	0.21	<0.1
OLC07	15.8	0.2	<0.5	49.6	1.32	<1	491	99.57	0.2	0.24	3	0.13	<0.1
OLC08	13.5	<0.1	<0.5	20.3	2.76	<1	1303.9	99.45	0.1	0.45	3.3	0.14	<0.1

OLC09	4.9	<0.1	<0.5	3.8	0.66	<1	902.2	99.94	<0.1	0.09	1.5	0.04	<0.1
OLC10	0.9	<0.1	<0.5	5.7	6.75	<1	35.2	100.72	<0.1	1.69	10.2	0.01	<0.1
OLC11	6.3	<0.1	<0.5	4.4	2.67	<1	1588	100.36	<0.1	0.37	3.7	0.04	<0.1
OLC12	13.3	0.2	<0.5	9.9	5.3	<1	1242	100.28	0.2	1.09	5.9	0.14	0.1

Sample ID	Tm (ppm)	TOT/C (%)	TOT/S (%)	U (ppm)	V (ppm)	W (ppm)	Y (ppm)	Yb (ppm)	Zn (ppm)	Zr (ppm)
LYR01	0.12	0.02	<0.02	8.2	51	16.0	6.4	0.77	3	128.6
LYR02	0.05	<0.02	<0.02	0.5	31	8.6	3.2	0.41	2	29.6
LYR03	0.06	0.05	<0.02	0.5	17	5.7	3.4	0.44	3	34.6
LYR04	0.06	<0.02	<0.02	0.7	146	3.7	2.4	0.32	2	40.3
LYR05	0.05	0.04	0.03	0.4	15	2.8	3.2	0.36	4	34.6
LYR06	0.04	0.03	<0.02	1.0	57	2.5	2.5	0.31	4	52.0
LYR07	0.06	0.03	0.03	0.9	39	2.2	3.3	0.46	3	74.0
LYR08	0.04	<0.02	<0.02	0.9	26	1.5	2.4	0.22	2	33.1
LYR09	0.05	0.06	0.03	1.8	171	1.5	3.1	0.42	8	69.5
LYR10	0.06	0.08	<0.02	0.8	40	1.3	3.2	0.41	3	87.6
LYR11	0.63	0.04	<0.02	2.5	74	1.0	37.6	3.88	25	38.1
LYR12	0.08	0.04	<0.02	1.8	51	1.4	5.0	0.63	11	75.6
LYR13	0.12	0.04	0.04	7.6	48	1.7	7.4	0.95	7	147.7
LYR14	0.12	0.04	0.02	3.8	56	0.9	7.2	0.82	2	62.7
LYR15	0.15	0.04	0.07	3.1	146	1.2	9.4	1.05	3	140.0
LYR16	0.11	0.04	0.03	7.1	49	1.4	6.1	0.69	7	128.9
LCP01	0.12	3.08	0.02	2.9	40	0.8	8.6	0.74	18	67.2
LCP02	0.07	3.85	<0.02	1.9	23	0.5	5.1	0.52	12	35.0
LCP03	0.15	3.59	<0.02	0.8	40	0.7	12.3	1.08	11	41.8
LCP04	0.19	0.56	<0.02	1.1	87	2.2	13.2	1.32	30	172.3
LCP05	0.45	0.02	0.03	2.7	116	2.7	25.5	3.19	31	786.6
LCP06	0.13	<0.02	<0.02	0.8	35	0.7	6.0	0.76	8	67.4
LCP07	0.09	<0.02	<0.02	0.8	29	<0.5	5.8	0.66	13	107.6
LCP08	0.06	<0.02	<0.02	1.0	39	<0.5	4.0	0.45	18	42.0
LCP09	0.05	0.03	<0.02	0.8	40	0.7	3.9	0.43	15	39.2
LCP10	0.04	<0.02	<0.02	0.8	34	<0.5	3.2	0.35	12	36.5

Sample ID	Tm (ppm)	TOT/C (%)	TOT/S (%)	U (ppm)	V (ppm)	W (ppm)	Y (ppm)	Yb (ppm)	Zn (ppm)	Zr (ppm)
LCP11	0.04	<0.02	<0.02	0.4	12	<0.5	2.5	0.28	5	24.6
LCP12	0.04	<0.02	<0.02	0.5	14	<0.5	2.6	0.31	5	35.5
LCP13	0.10	<0.02	<0.02	0.8	39	<0.5	6.7	0.71	15	35.6
LCP14	0.07	<0.02	<0.02	0.7	11	<0.5	4.9	0.66	3	35.8
LCP15	0.25	0.04	0.02	2.3	118	1.4	14.0	1.57	25	51.4
LCP16	0.07	<0.02	0.03	0.8	26	<0.5	4.2	0.49	2	40.4
LCP17	0.06	<0.02	<0.02	1.0	22	<0.5	3.6	0.40	<1	32.7
LCP18	0.06	<0.02	0.02	1.9	60	0.8	3.9	0.35	1	40.0
LCP19	0.76	6.85	0.03	4.0	75	<0.5	63.0	4.27	1	22.9
LCP20	0.16	12.32	<0.02	2.8	27	<0.5	20.0	0.94	1	8.8
LCP21	0.13	0.10	0.09	1.6	74	0.6	8.1	0.92	10	130.4
LCP22	0.05	0.02	<0.02	0.8	33	0.8	3.4	0.38	10	29.6
LCP23	0.05	<0.02	<0.02	0.4	15	<0.5	2.1	0.37	4	21.4
RC01	0.07	0.05	<0.02	0.4	15	<0.5	2.5	0.48	<1	67.1
RC02	0.07	0.07	0.04	0.7	27	<0.5	3.0	0.32	<1	90.1
RC03	0.12	<0.02	0.02	1.1	24	1.6	6.5	0.96	<1	163.7
RC04	0.09	0.04	0.07	0.7	37	0.9	5.3	0.55	1	126.5
RC05	0.11	0.10	0.07	1.0	44	1.1	6.2	0.84	5	137.2
RC06	0.12	0.06	0.09	0.9	42	0.6	6.5	0.78	8	169.5
RC07	0.18	0.11	0.22	1.5	82	0.9	10.2	1.28	20	184.6
RC08	0.17	0.06	0.31	1.6	80	1.1	9.7	1.22	18	210.9
RC09	0.19	0.09	0.22	1.7	108	1.2	12.3	1.39	27	199.2
RC10	0.21	0.07	0.15	1.9	84	1.4	12.1	1.42	29	206.1
RC11	0.23	0.12	0.08	2.3	104	1.3	12.5	1.54	29	211.8
RC12	0.06	0.04	<0.02	0.4	16	<0.5	3.6	0.34	6	39.6
RC13	0.26	0.12	0.13	2.0	187	0.6	17.3	1.70	24	197.1

Sample ID	Tm (ppm)	TOT/C (%)	TOT/S (%)	U (ppm)	V (ppm)	W (ppm)	Y (ppm)	Yb (ppm)	Zn (ppm)	Zr (ppm)
RC14	0.12	0.04	0.06	1.1	78	0.7	6.9	0.84	7	124.4
RC15	0.17	0.06	0.20	1.4	81	1.0	9.2	1.13	20	197.0
NY01	0.19	0.04	<0.02	1.2	38	1.3	9.8	1.12	2	259.6
NY02	0.18	0.05	0.05	1.2	44	1.1	9.7	1.21	2	245.5
NY03	0.16	0.07	<0.02	1.4	46	1.1	9.1	1.13	3	220.1
NY04	0.16	0.09	<0.02	1.3	45	0.9	9.0	1.09	2	280.3
NY05	0.27	0.08	<0.02	1.9	57	1.1	14.5	1.73	3	362.0
NY06	0.26	0.05	0.02	1.2	48	1.1	12.7	1.72	3	304.8
NY07	0.19	0.07	<0.02	1.6	71	1.3	10.0	1.20	3	307.8
NY08	0.17	0.20	0.04	4.3	75	1.1	9.5	1.09	16	241.2
NY09	0.16	0.05	<0.02	1.0	45	1.2	8.6	1.10	2	264.8
NY10	0.19	0.22	0.05	4.4	79	1.4	10.4	1.35	15	246.7
GRQ01	0.18	0.02	0.05	1.5	142	1.9	10.1	1.15	3	188.4
GRQ02	0.11	0.05	0.02	1.1	84	1.3	6.2	0.73	4	76.3
GRQ03	0.11	0.05	<0.02	1.1	52	1.8	7.3	0.81	3	91.3
GRQ04	0.20	0.04	<0.02	1.5	61	1.3	11.2	1.14	3	263.4
GRQ05	0.15	0.12	<0.02	1.1	34	1.2	9.6	0.93	2	224.5
GRQ06	0.11	0.05	<0.02	0.9	33	1.1	6.5	0.57	2	133.8
GRQ07	1.93	0.06	<0.02	11.0	56	3.9	115.0	12.72	3	4553.9
GRQ08	0.13	0.08	<0.02	1.0	32	1.5	7.0	0.83	2	120.3
GRQ09	2.34	0.05	<0.02	10.8	62	4.7	129.0	14.60	3	4363.8
GRQ10	0.33	0.05	<0.02	2.6	88	3.8	18.1	2.35	5	547.2
GRQ11	0.10	0.06	0.05	1.2	83	1.4	6.0	0.69	5	68.0
SRQ01	0.07	13.99	<0.02	3.5	149	1.5	3.4	0.45	5	15.4
SRQ02	0.15	13.65	<0.02	3.6	126	0.7	9.8	1.01	6	19.4
SRQ03	0.71	12.31	0.07	4.6	182	1.1	37.3	4.57	7	45.1

Sample ID	Tm (ppm)	TOT/C (%)	TOT/S (%)	U (ppm)	V (ppm)	W (ppm)	Y (ppm)	Yb (ppm)	Zn (ppm)	Zr (ppm)
SRQ04	0.23	0.31	0.08	3.8	282	2.1	13.9	1.38	27	253.3
SRQ05	0.07	0.03	0.06	1.0	48	0.5	3.8	0.47	4	46.4
SRQ06	0.10	0.03	<0.02	2.0	31	0.8	6.2	0.63	14	31.2
SRQ07	0.17	0.04	<0.02	2.6	44	1.0	9.1	1.07	8	346.3
SRQ08	0.08	<0.02	<0.02	0.7	12	<0.5	4.8	0.56	3	43.8
SRQ09	0.09	0.03	<0.02	1.1	14	<0.5	4.7	0.47	9	28.5
SRQ10	0.08	<0.02	<0.02	0.7	11	<0.5	4.1	0.40	3	56.4
UQ01	0.08	0.05	<0.02	1.2	185	<0.5	4.9	0.61	9	41.6
UQ02	0.07	<0.02	0.02	1.0	74	0.7	3.3	0.40	6	53.1
UQ03	0.17	0.03	<0.02	2.0	32	2.1	10.4	1.05	2	173.9
UQ04	0.24	0.04	<0.02	1.9	60	1.8	13.2	1.44	6	176.0
UQ05	0.35	0.05	<0.02	3.1	166	2.0	17.8	2.20	23	150.5
UQ06	0.12	0.03	<0.02	0.8	19	1.4	6.3	0.71	4	74.3
UQ07	0.13	0.06	<0.02	1.5	33	0.9	6.9	0.76	3	68.6
UQ08	0.43	0.03	0.04	1.7	28	2.3	23.8	2.66	1	305.5
UQ09	0.42	0.06	0.02	2.1	85	1.8	23.2	2.72	1	413.7
UQ10	0.25	0.04	<0.02	1.3	53	1.8	13.1	1.58	3	364.1
UQ11	0.26	0.06	<0.02	1.3	34	1.4	14.0	1.82	3	414.1
UQ12	0.34	0.78	0.06	1.1	65	1.7	19.6	2.12	18	290.9
UQ13	0.08	0.04	<0.02	1.0	154	<0.5	4.1	0.47	9	40.1
CCH01	0.07	0.04	<0.02	0.5	11	<0.5	3.4	0.44	2	52.8
CCH02	0.05	0.06	<0.02	0.7	10	<0.5	2.9	0.40	2	39.0
CCH03	0.09	0.05	0.03	0.8	34	0.6	5.0	0.64	6	71.3
CCH04	0.08	0.05	<0.02	0.6	22	<0.5	4.5	0.57	3	81.3
CCH05	0.08	0.06	0.02	0.6	29	<0.5	4.8	0.57	3	64.4
CCH06	0.12	0.05	<0.02	1.0	29	0.7	7.4	0.89	4	140.6

Sample ID	Tm (ppm)	TOT/C (%)	TOT/S (%)	U (ppm)	V (ppm)	W (ppm)	Y (ppm)	Yb (ppm)	Zn (ppm)	Zr (ppm)
CCH07	0.10	0.04	<0.02	0.8	25	0.6	5.7	0.69	4	90.1
CCH08	0.05	0.07	0.02	0.6	21	<0.5	2.5	0.36	4	80.9
CCH09	0.08	0.04	<0.02	0.7	29	<0.5	4.7	0.57	6	71.2
FE01	0.14	0.13	0.15	0.6	16	0.6	8.5	1.01	2	159.7
NHW01	0.22	0.08	<0.02	1.3	37	1.2	13.6	1.74	6	379.8
NHW02	0.14	0.12	<0.02	1.2	44	1.1	8.5	0.79	4	170.3
NHW03	0.13	0.09	<0.02	1.2	33	0.9	7.4	0.81	5	263.6
BB01	0.25	0.08	<0.02	3.8	35	1.7	15.2	1.81	26	155.3
BB02	0.57	0.07	<0.02	3.8	71	3.8	36.0	3.92	46	426.3
HC01	0.07	0.06	<0.02	1.0	23	0.6	4.0	0.42	<1	84.6
HC02	0.09	0.04	<0.02	0.9	26	<0.5	4.7	0.64	1	94.5
HC03	0.12	0.04	<0.02	0.9	39	0.9	6.6	1.10	<1	113.3
HC04	0.21	0.22	<0.02	2.0	166	1.7	11.1	1.49	3	192.0
HC05	0.15	0.10	<0.02	1.0	50	0.6	8.5	0.88	13	157.3
GOR01	0.08	0.04	<0.02	0.7	37	0.8	4.6	0.51	3	180.6
GOR02	0.07	0.06	<0.02	0.9	46	0.7	4.8	0.41	3	164.5
GOR03	0.09	0.05	<0.02	0.8	59	0.5	5.5	0.61	2	105.4
GOR04	0.27	0.43	<0.02	2.7	182	2.2	13.9	1.68	7	229.3
DIA01	0.17	0.05	<0.02	0.8	58	1.2	9.3	1.09	3	126.7
DIA02	0.10	0.04	<0.02	1.0	32	0.9	6.5	0.49	2	94.4
DIA03	0.20	0.04	0.03	1.3	46	1.5	12.1	0.99	4	336.4
DIA04	0.07	0.02	<0.02	0.7	34	0.7	4.6	0.51	3	68.2
DIA05	0.08	0.06	<0.02	0.8	27	0.7	3.6	0.37	4	73.2
DIA06	0.07	0.04	<0.02	0.5	26	<0.5	4.0	0.27	3	65.9
WF01	0.11	0.06	<0.02	1.1	37	<0.5	5.9	0.92	4	128.2
WF02	0.06	0.04	<0.02	0.9	29	<0.5	3.4	0.73	3	75.5

Sample ID	Tm (ppm)	TOT/C (%)	TOT/S (%)	U (ppm)	V (ppm)	W (ppm)	Y (ppm)	Yb (ppm)	Zn (ppm)	Zr (ppm)
WF03	0.10	0.04	<0.02	0.9	35	0.9	4.6	0.42	3	79.7
WF04	0.10	0.10	<0.02	1.3	53	1.1	5.1	0.52	4	74.1
TDQ01	0.06	0.04	0.02	0.8	38	<0.5	3.5	0.46	4	54.5
TDQ02	0.05	0.06	<0.02	0.5	27	0.8	3.1	0.29	3	48.0
TDQ03	0.06	0.04	<0.02	0.5	27	<0.5	3.3	0.32	4	52.2
TDQ04	0.06	0.05	<0.02	0.6	35	0.5	3.5	0.51	4	64.9
TDQ05	0.06	0.06	<0.02	0.7	52	1.0	4.4	0.53	3	82.7
WFN01	0.14	0.04	<0.02	1.2	43	1.3	6.8	0.89	1	233.2
WFN02	0.11	0.16	<0.02	1.1	40	1.5	6.2	0.90	1	214.1
WFN03	0.07	0.03	<0.02	0.7	40	1.0	4.7	0.77	2	94.3
WFN04	0.10	0.05	<0.02	0.8	36	0.7	5.6	0.80	2	122.7
GRQ04	0.26	0.03	<0.02	1.8	68	1.0	14.5	1.94	4	348.6
CCH03	0.10	0.04	<0.02	0.9	28	0.5	4.8	0.54	6	84.3
SRQ09	0.10	<0.02	<0.02	1.1	<8	<0.5	5.4	0.45	9	38.7
SP01	0.12	0.04	<0.02	0.9	216	4.0	7.1	0.82	2	124.4
SP02	0.10	0.03	0.04	0.8	38	1.7	5.9	0.72	2	90.4
SP03	0.22	0.04	0.04	2.0	1026	1.5	12.9	1.26	7	79.3
SP04	0.12	0.04	<0.02	0.8	33	1.5	6.6	0.88	3	91.5
SP05	0.15	0.06	0.12	1.0	43	1.7	6.9	0.92	1	87.6
SP06	0.19	0.05	0.13	1.0	57	1.1	8.7	1.27	<1	83.9
SP07	0.24	0.09	0.02	1.6	83	1.5	13.4	1.71	2	397.5
SP08	0.25	0.06	0.04	1.6	79	1.6	12.4	1.77	<1	286.5
SP09	0.45	0.10	0.03	6.6	1178	1.2	21.9	2.84	<1	214.8
SP10	0.39	0.08	0.03	5.9	361	1.9	20.5	2.79	<1	305.3
CW01	0.39	0.21	<0.02	2.1	170	1.2	39.2	1.94	49	416.6
CW02	1.26	0.14	<0.02	6.6	132	3.5	67.6	8.79	11	2555.9

Sample ID	Tm (ppm)	TOT/C (%)	TOT/S (%)	U (ppm)	V (ppm)	W (ppm)	Y (ppm)	Yb (ppm)	Zn (ppm)	Zr (ppm)
CW03	0.77	0.13	<0.02	4.2	72	2.4	36.8	5.68	18	1154.2
CW04	0.57	0.17	0.03	3.1	190	2.2	30.9	4.32	22	914.0
CW05	0.50	0.24	<0.02	4.2	362	3.8	27.0	3.95	8	1305.7
CW06	0.53	0.25	<0.02	3.5	409	2.6	28.7	3.82	5	960.8
CW07	0.74	0.09	<0.02	3.8	56	4.1	37.9	5.45	<1	1349.4
CW08	0.77	0.15	<0.02	4.8	108	4.0	40.8	5.80	<1	1413.2
CW09	0.05	0.20	<0.02	0.8	63	0.6	3.1	0.37	1	59.2
CW10	0.40	0.45	<0.02	3.7	605	3.8	20.6	3.29	2	720.5
WA01	0.23	0.20	<0.02	3.2	427	2.6	10.8	1.83	4	380.8
WA02	0.18	0.15	0.02	2.2	630	2.5	9.5	1.45	4	456.0
WA03	0.22	0.19	0.02	1.9	715	3.5	11.5	1.28	3	493.7
WA04	0.15	0.19	0.05	1.7	722	3.1	7.3	1.02	6	357.8
WA05	0.72	0.06	0.10	4.5	120	<0.5	32.9	5.16	25	603.6
WA06	0.88	0.05	0.04	4.5	11	1.2	40.7	6.35	4	693.1
WA07	0.28	0.09	0.12	2.7	633	2.7	17.9	1.99	33	282.6
WA08	0.34	0.12	0.13	1.7	746	3.5	13.2	2.27	29	274.1
WA09	0.75	0.02	<0.02	3.9	<8	0.7	44.7	5.18	42	430.7
WA10	0.65	0.24	<0.02	3.7	225	1.6	38.5	4.38	45	462.9
WA11	0.14	0.09	0.07	1.4	742	2.3	8.0	1.09	4	354.6
HP01	0.10	0.06	<0.02	0.9	57	1.0	5.5	0.75	<1	105.6
HP02	0.13	0.04	<0.02	1.1	238	0.8	7.4	0.76	<1	160.9
HP03	0.22	0.48	0.04	2.8	513	13.8	10.9	1.25	1	111.3
GOR05	0.10	0.25	0.04	1.8	270	1.4	5.9	0.85	2	275.1
GOR06	0.22	0.26	<0.02	1.5	414	2.4	12.8	1.56	2	438.5
GOR07	0.23	0.20	0.02	1.7	403	2.4	10.8	1.46	1	406.5
GOR08	0.18	0.32	<0.02	1.3	108	2.0	9.3	1.46	3	287.6

Sample ID	Tm (ppm)	TOT/C (%)	TOT/S (%)	U (ppm)	V (ppm)	W (ppm)	Y (ppm)	Yb (ppm)	Zn (ppm)	Zr (ppm)
SH01	0.23	0.35	0.04	11.3	499	2.1	9.9	1.56	2	418.6
SH02	0.31	0.30	0.03	7.6	590	1.7	19.9	2.26	2	466.3
SH03	0.28	0.05	<0.02	3.0	159	1.4	14.9	2.12	1	378.2
MP01	0.21	0.10	<0.02	2.5	600	1.9	9.8	1.83	3	333.8
MP02	0.17	0.08	0.02	3.4	222	1.3	8.0	1.01	2	243.6
GL01	0.22	0.18	<0.02	1.7	87	2.6	13.4	1.54	2	278.8
CW11	0.20	0.16	0.07	1.5	288	2.6	10.0	1.25	3	373.4
HHQ01	0.15	0.08	<0.02	3.5	88	1.3	8.0	1.06	2	299.6
MR01	0.62	0.35	0.04	4.3	756	2.6	40.6	5.04	16	414.9
MR02	0.30	0.17	<0.02	1.7	76	2.7	18.6	2.38	2	423.3
WRC01	0.13	4.98	0.04	0.5	24	0.6	10.8	1.13	5	97.4
DIA10	0.16	0.25	0.04	6.5	344	1.5	8.7	1.20	1	288.4
DIA11	0.26	0.10	<0.02	1.2	818	1.8	15.2	1.79	4	284.1
BAL01	0.40	1.87	0.03	1.7	78	4.2	25.9	2.81	19	270.5
BAL02	0.04	0.06	<0.02	0.4	13	0.8	3.6	0.49	4	46.2
BAL03	0.14	0.48	0.05	1.6	26	5.2	11.4	1.09	12	65.2
BAL04	0.17	0.10	0.04	6.6	51	1.5	11.2	1.42	26	331.2
BAL05	0.10	0.30	0.04	3.2	429	3.2	9.1	0.96	20	176.6
BAL06	0.07	0.16	0.06	1.6	538	1.2	7.0	1.04	16	101.7
WEN01	0.24	0.50	0.03	1.3	67	1.9	16.0	1.89	30	242.9
WEN02	0.34	0.07	0.02	2.0	74	3.4	19.8	2.60	30	454.3
WEN03	0.37	0.06	0.04	2.1	65	1.9	18.8	2.14	18	300.6
WEN04	0.40	0.04	0.03	1.8	76	1.7	19.5	2.80	26	337.2
WEN05	0.30	0.04	<0.02	1.8	64	3.6	16.6	2.14	19	312.9
WEN06	0.34	0.08	0.04	2.3	66	3.4	17.4	2.24	30	361.0
WEN07	0.09	0.05	0.15	1.1	18	1.5	5.4	0.66	14	117.0

Sample ID	Tm (ppm)	TOT/C (%)	TOT/S (%)	U (ppm)	V (ppm)	W (ppm)	Y (ppm)	Yb (ppm)	Zn (ppm)	Zr (ppm)
WEN08	0.15	0.07	0.10	1.6	33	2.1	11.6	1.24	33	166.7
WEN09	0.24	0.06	0.10	1.5	40	1.0	10.9	1.36	18	215.8
WEN10	0.12	0.08	0.10	2.1	31	5.2	9.0	1.51	18	554.3
WEN11	0.12	0.20	0.03	0.9	8	1.0	5.5	0.76	14	129.9
WEN12	0.07	1.04	<0.02	0.8	<8	<0.5	2.1	0.35	6	55.2
WEN13	0.06	0.49	0.05	0.6	<8	<0.5	1.6	0.36	5	39.8
WEN14	0.08	0.10	0.24	0.8	<8	<0.5	3.4	0.35	4	110.8
WEN15	0.12	0.22	1.02	1.7	14	<0.5	5.4	0.75	5	259.2
WEN16	0.20	0.11	0.76	0.9	<8	<0.5	6.5	1.27	5	180.1
WEN17	0.14	0.13	1.19	0.8	10	<0.5	6.4	0.56	6	209.7
WEN18	0.20	0.65	1.41	1.9	43	1.4	9.8	1.22	13	325.9
WEN19	0.15	0.67	0.89	1.5	34	1.5	8.7	1.39	21	224.7
BUN01	0.06	0.13	<0.02	0.7	10	<0.5	5.2	0.76	11	33.0
BUN02	0.24	0.03	<0.02	1.1	19	0.5	8.2	1.06	7	61.8
BUN03	0.13	0.12	<0.02	1.2	22	1.3	6.8	0.90	10	47.8
BUN04	0.13	0.07	<0.02	1.3	25	1.4	8.9	1.09	11	53.6
BUN05	0.60	0.07	<0.02	3.1	35	2.5	38.8	3.74	17	543.6
BUN06	0.28	0.15	0.03	2.6	31	1.2	12.3	1.23	34	89.7
BUN07	0.14	0.08	<0.02	1.1	36	1.5	7.5	0.85	26	53.9
BUN08	0.33	0.07	<0.02	2.7	56	1.3	19.9	1.96	42	249.9
BUN09	0.18	0.12	<0.02	1.9	125	1.7	10.3	1.22	23	91.3
BUN10	0.25	0.07	<0.02	1.6	77	1.5	15.7	1.77	27	182.2
BUN11	0.24	0.09	<0.02	1.0	38	1.3	13.3	1.62	27	123.5
BUN12	0.18	1.15	0.02	1.2	40	1.0	10.7	1.04	40	79.2
BUN13	0.17	0.18	<0.02	1.0	38	1.3	10.1	1.18	23	79.6
BUN14	0.10	0.04	<0.02	0.7	18	0.5	6.2	0.61	18	42.8

Sample ID	Tm (ppm)	TOT/C (%)	TOT/S (%)	U (ppm)	V (ppm)	W (ppm)	Y (ppm)	Yb (ppm)	Zn (ppm)	Zr (ppm)
BUN15	0.08	0.03	<0.02	0.6	17	0.6	5.6	0.56	11	32.7
BUN16	0.08	0.02	<0.02	0.4	14	<0.5	5.6	0.59	9	32.9
BUN17	0.07	<0.02	<0.02	0.4	10	<0.5	6.2	0.47	11	33.1
BUN18	0.06	0.04	<0.02	0.5	26	<0.5	5.0	0.47	9	33.5
BUN19	0.08	0.03	<0.02	0.3	20	0.5	5.3	0.48	8	33.6
BUN20	0.10	0.04	<0.02	0.6	19	0.6	5.2	0.61	11	36.5
BUN21	0.08	1.24	0.11	0.4	12	<0.5	6.4	0.76	8	39.7
BUN22	0.13	0.97	0.10	0.5	23	0.9	8.4	0.81	50	90.8
BUN23	0.04	0.05	0.21	0.3	<8	<0.5	2.9	0.26	15	31.8
BUN24	0.03	0.03	0.36	0.2	<8	2.8	2.4	0.29	89	29.5
BUN25	0.05	0.08	0.27	0.3	<8	<0.5	2.8	0.30	24	35.3
BUN26	0.06	0.18	0.51	0.3	10	<0.5	3.6	0.40	26	45.0
BUN27	0.13	1.67	0.50	0.8	36	<0.5	7.2	0.73	46	66.8
BUN28	0.07	0.60	0.69	0.4	16	0.5	4.3	0.49	102	43.8
BUN29	0.07	0.25	5.21	0.4	13	<0.5	4.7	0.43	85	56.1
BUN30	0.08	0.38	8.98	0.6	14	<0.5	5.4	0.57	112	82.4
HOR101	0.18	0.27	<0.02	1.7	147	2.2	10.4	1.30	4	232.6
HOR102	0.17	0.21	<0.02	1.6	121	2.1	10.0	1.09	4	193.6
HOR103	0.16	0.21	<0.02	1.1	79	1.5	7.8	1.08	5	168.8
HOR104	0.19	0.27	<0.02	1.7	97	1.8	9.7	1.39	3	199.9
HOR105	0.15	0.14	0.02	1.3	98	2.0	8.9	1.35	2	169.4
HOR106	0.14	0.14	<0.02	1.3	89	1.3	9.1	1.10	7	151.8
HOR107	0.16	0.13	0.02	1.0	85	1.9	7.9	1.20	2	183.0
HOR108	0.15	0.10	<0.02	0.9	65	3.8	7.7	1.01	13	171.0
HOR109	0.10	0.07	<0.02	0.8	55	1.5	6.2	0.83	4	167.8
HOR110	0.09	0.05	<0.02	0.5	31	1.1	5.0	0.61	3	147.5

Sample ID	Tm (ppm)	TOT/C (%)	TOT/S (%)	U (ppm)	V (ppm)	W (ppm)	Y (ppm)	Yb (ppm)	Zn (ppm)	Zr (ppm)
HOR111	0.10	0.05	<0.02	0.7	45	1.1	5.5	0.72	3	146.3
HOR112	0.11	0.05	<0.02	0.4	32	0.7	4.6	0.62	4	128.9
HOR113	0.12	0.03	<0.02	0.8	37	1.4	7.2	0.90	2	151.2
HOR114	0.09	0.03	<0.02	0.8	23	1.1	4.9	0.57	2	165.6
HOR115	0.10	0.03	<0.02	0.5	16	1.1	5.3	0.70	2	142.5
HOR116	0.07	0.04	<0.02	0.5	27	1.1	3.7	0.51	4	127.3
HOR117	0.08	0.07	<0.02	0.6	22	0.6	4.0	0.48	3	109.1
HOR118	0.07	0.04	<0.02	0.7	16	0.6	3.8	0.52	2	112.1
HOR119	0.07	0.04	<0.02	0.7	15	0.6	3.7	0.54	2	129.5
HOR120	0.09	0.05	<0.02	0.8	19	0.7	4.2	0.53	2	91.8
HOR121	0.11	0.08	<0.02	1.2	26	0.8	5.6	0.74	4	160.8
HOR122	0.10	0.02	<0.02	0.6	22	0.7	4.3	0.58	2	144.4
HOR123	0.08	0.04	<0.02	0.7	17	<0.5	4.7	0.59	2	95.0
HOR124	0.07	0.04	<0.02	0.9	11	0.8	3.8	0.56	3	88.5
HOR125	0.05	<0.02	<0.02	0.5	12	0.5	3.3	0.49	1	54.7
HOR126	0.05	0.02	<0.02	0.6	18	0.9	3.0	0.37	2	52.7
HOR127	0.05	<0.02	<0.02	0.7	23	0.6	3.4	0.40	2	56.4
HOR128	0.05	<0.02	<0.02	0.5	21	0.8	2.6	0.42	3	61.2
HOR129	0.06	0.03	<0.02	0.8	24	0.5	3.8	0.55	2	55.9
HOR130	0.05	0.05	0.03	0.4	9	0.8	3.5	0.44	6	48.1
HOR131	0.12	0.05	<0.02	0.6	13	1.0	6.2	0.68	2	70.3
HOR132	0.15	0.17	0.04	1.0	32	1.3	9.6	1.03	9	154.2
HOR133	0.08	0.11	0.04	0.6	9	1.0	4.1	0.56	8	84.5
HOR134	0.09	0.06	0.06	0.5	<8	1.2	5.3	0.67	10	75.9
HOR135	0.08	0.03	0.03	0.5	<8	0.6	4.9	0.53	4	57.0
HOR136	0.54	5.46	0.26	3.4	433	1.7	33.3	3.34	53	156.2

Sample ID	Tm (ppm)	TOT/C (%)	TOT/S (%)	U (ppm)	V (ppm)	W (ppm)	Y (ppm)	Yb (ppm)	Zn (ppm)	Zr (ppm)
HOR137	0.90	0.57	0.28	5.1	156	2.0	49.9	6.45	25	1173.0
HOR501	0.10	<0.02	<0.02	0.6	21	0.8	5.4	0.57	4	177.6
HOR503	0.13	0.08	<0.02	1.0	44	1.3	6.7	0.83	4	215.0
HOR504	0.18	0.20	0.07	1.8	277	1.8	9.2	1.31	4	231.4
HOR507	0.17	0.13	0.07	1.5	105	1.2	9.5	1.38	3	191.4
HOR508	0.16	0.11	0.07	1.3	114	1.5	9.0	1.41	3	194.0
HOR509	0.14	0.05	0.05	1.0	70	2.0	7.9	1.06	2	243.1
HOR510	0.17	0.05	0.06	0.9	107	1.5	9.2	1.31	1	175.5
HOR511	0.13	0.11	0.04	0.8	71	1.3	6.9	0.92	<1	230.5
HOR512	0.12	0.03	0.04	0.7	57	1.3	6.8	0.88	2	194.5
HOR513	0.11	0.02	0.03	0.7	42	1.2	5.5	0.74	<1	189.2
HOR514	0.13	0.05	0.03	1.0	51	1.4	6.9	0.77	1	260.2
HOR515	0.12	0.03	0.02	0.8	58	1.2	6.3	0.83	3	219.6
HOR516	0.07	0.03	0.02	0.6	35	0.7	4.0	0.62	2	133.4
HOR517	0.05	0.03	<0.02	0.5	31	0.7	4.0	0.42	2	64.4
HOR518	0.06	0.03	<0.02	0.6	30	0.7	3.6	0.43	4	91.5
HOR519	0.06	0.03	<0.02	0.4	23	0.9	3.5	0.49	4	68.5
HOR520	0.08	0.03	<0.02	0.5	23	1.0	3.8	0.49	5	113.5
HOR521	0.06	0.05	<0.02	0.8	35	2.3	3.7	0.53	8	155.8
HOR522	0.11	0.04	<0.02	1.1	36	1.8	6.6	0.80	8	323.9
HOR523	0.07	0.02	<0.02	0.7	24	0.7	3.2	0.46	7	87.6
HOR524	0.06	0.10	<0.02	0.5	28	0.9	3.3	0.47	7	79.0
HOR525	0.06	0.03	<0.02	0.5	22	0.6	3.1	0.39	7	37.4
HOR527	0.09	0.03	<0.02	0.8	31	0.7	4.0	0.52	6	160.2
HOR528	0.08	0.04	<0.02	0.8	28	0.6	4.0	0.59	6	149.9
HOR529	0.09	0.03	<0.02	0.8	32	1.3	5.3	0.77	7	235.8

Sample ID	Tm (ppm)	TOT/C (%)	TOT/S (%)	U (ppm)	V (ppm)	W (ppm)	Y (ppm)	Yb (ppm)	Zn (ppm)	Zr (ppm)
HOR530	0.08	0.02	<0.02	0.9	35	0.6	4.4	0.52	5	242.7
HOR531	0.13	0.04	<0.02	1.3	45	2.1	6.9	0.87	9	275.2
HOR532	0.10	0.03	<0.02	0.8	32	1.5	5.0	0.56	6	199.0
HOR533	0.06	0.03	<0.02	0.4	37	1.3	2.9	0.42	5	97.6
HOR534	0.15	0.03	<0.02	1.2	48	1.7	8.9	0.94	8	322.7
HOR535	0.08	0.02	<0.02	0.5	11	0.7	4.7	0.59	2	169.6
HOR536	0.30	<0.02	<0.02	1.5	28	2.0	15.2	1.99	2	967.3
HOR537	0.21	0.04	<0.02	1.4	79	2.3	10.6	1.56	6	815.9
HOR538	0.07	0.03	<0.02	0.6	40	1.8	3.8	0.49	6	61.4
HOR539	0.12	0.04	<0.02	0.7	25	3.8	6.5	0.81	2	281.6
HOR540	0.09	0.05	<0.02	0.3	17	0.9	4.7	0.60	5	65.4
HOR541	0.07	0.03	<0.02	0.3	15	1.3	5.2	0.43	6	47.9
HOR542	0.07	0.03	<0.02	0.4	21	1.0	5.0	0.59	11	48.5
HOR543	0.07	0.04	<0.02	0.4	12	1.1	5.0	0.57	6	79.2
HOR544	0.05	0.03	<0.02	0.4	10	0.8	4.1	0.53	6	72.3
HOR545	0.07	0.04	<0.02	0.5	12	1.0	3.9	0.55	5	75.4
HOR546	0.07	0.03	<0.02	0.6	11	1.4	4.0	0.60	4	147.0
HOR547	0.09	0.03	<0.02	0.4	9	0.8	3.8	0.45	5	87.4
HOR548	0.08	0.02	<0.02	0.4	10	0.9	3.5	0.54	3	81.1
HOR549	0.05	0.03	<0.02	0.2	10	1.4	3.7	0.32	3	57.6
HOR550	0.05	0.03	<0.02	0.3	<8	0.9	3.3	0.37	5	40.8
HOR551	0.07	<0.02	<0.02	0.4	<8	<0.5	3.9	0.36	3	34.6
HOR552	0.10	0.02	<0.02	0.6	13	0.9	4.9	0.71	5	105.7
HOR553	1.18	0.03	<0.02	5.6	137	3.0	72.2	8.21	13	2063.1
HOR554	1.81	0.04	<0.02	8.0	328	3.9	106.7	12.36	54	2967.9
HOR505	0.22	0.23	0.08	1.8	141	2.3	10.8	1.60	7	166.1

Sample ID	Tm (ppm)	TOT/C (%)	TOT/S (%)	U (ppm)	V (ppm)	W (ppm)	Y (ppm)	Yb (ppm)	Zn (ppm)	Zr (ppm)
HOR506	0.25	0.18	0.08	2.2	180	2.1	13.0	1.73	4	248.0
HOR526	0.10	0.03	<0.02	1.0	41	1.2	4.8	0.66	8	204.1
HOR701	0.40	4.43	0.11	1.2	49	1.0	42.3	2.51	13	171.3
HOR702	0.33	0.14	0.03	1.2	103	1.4	21.4	2.19	17	267.9
HOR703	0.27	0.22	0.03	1.3	114	2.5	19.1	2.01	16	283.4
HOR704	0.28	0.21	0.02	1.1	122	1.3	19.4	1.85	12	280.6
HOR705	0.22	0.15	0.03	1.0	71	0.9	15.1	1.65	11	218.5
HOR706	0.25	0.06	0.02	1.0	70	1.2	18.9	1.77	12	229.7
HOR707	0.22	0.05	<0.02	1.2	70	1.0	17.8	1.82	11	231.4
HOR708	0.38	0.05	0.09	1.5	94	1.9	33.8	2.15	15	228.9
HOR709	0.35	0.04	0.02	1.6	77	1.1	26.2	2.13	13	210.2
HOR710	0.27	0.04	0.03	1.7	93	1.3	15.7	1.88	21	219.6
HOR711	0.19	0.06	0.03	1.3	80	1.6	10.6	1.14	13	183.8
HOR712	0.13	0.13	0.04	1.6	91	1.3	8.5	1.02	7	153.7
HOR713	0.09	0.05	0.04	1.0	68	1.2	5.3	0.60	3	134.5
HOR714	0.07	0.03	0.03	0.6	48	1.0	4.1	0.55	2	99.6
HOR715	0.08	0.03	0.03	0.8	56	0.7	4.6	0.53	2	111.9
HOR716	0.07	0.02	0.03	0.6	43	0.6	3.8	0.46	2	100.2
HOR717	0.07	0.02	0.02	0.6	33	1.0	3.9	0.51	2	96.3
HOR718	0.05	0.02	0.02	0.6	33	<0.5	3.6	0.38	2	64.2
HOR719	0.05	0.03	0.03	0.6	29	0.9	3.0	0.34	2	63.8
HOR720	0.04	0.02	0.03	0.5	30	0.8	3.3	0.31	2	47.0
HOR721	0.04	0.03	0.03	0.6	29	1.6	3.7	0.31	3	69.8
HOR722	0.08	0.04	0.02	0.8	29	1.1	3.6	0.50	3	89.4
HOR723	0.16	0.03	0.02	1.0	28	1.0	9.5	0.92	3	76.7
HOR724	0.05	0.04	0.03	0.8	28	0.9	3.5	0.39	3	49.1
HOR725	0.06	0.04	<0.02	0.9	24	0.8	2.9	0.31	3	49.9

Sample ID	Tm (ppm)	TOT/C (%)	TOT/S (%)	U (ppm)	V (ppm)	W (ppm)	Y (ppm)	Yb (ppm)	Zn (ppm)	Zr (ppm)
HOR726	0.05	0.03	<0.02	0.8	22	0.7	2.6	0.25	2	43.9
HOR727	0.06	0.03	0.03	0.7	44	1.4	3.8	0.42	6	66.7
HOR728	0.06	0.04	0.03	1.0	44	1.0	3.3	0.36	2	62.2
HOR729	0.06	0.03	0.02	0.8	26	1.4	3.9	0.51	3	94.3
HOR730	0.06	0.02	0.02	0.8	25	<0.5	4.2	0.54	2	80.5
HOR731	0.05	0.03	<0.02	0.5	18	0.9	4.0	0.53	2	75.7
HOR732	0.06	<0.02	0.02	0.4	27	0.8	4.0	0.43	1	77.0
HOR733	0.04	<0.02	<0.02	0.2	21	<0.5	2.9	0.27	1	44.3
HOR734	0.04	<0.02	<0.02	0.2	21	1.1	3.1	0.29	2	47.4
HOR735	0.05	<0.02	0.02	0.3	26	3.6	3.8	0.44	2	61.0
HOR736	0.05	0.02	<0.02	0.4	21	7.7	3.8	0.41	4	52.6
HOR737	0.04	0.02	<0.02	0.4	22	2.2	2.8	0.40	3	43.8
HOR738	0.05	0.03	0.02	0.4	14	4.3	4.1	0.46	2	51.6
HOR739	0.04	0.03	<0.02	0.4	21	7.3	3.1	0.36	2	60.5
HOR740	0.06	0.03	<0.02	0.3	15	4.0	4.1	0.50	5	55.1
HOR741	0.06	<0.02	<0.02	0.5	20	4.6	3.8	0.45	3	122.0
HOR742	0.04	0.03	<0.02	0.4	16	4.7	4.3	0.38	5	60.0
HOR743	0.12	0.19	0.03	0.8	18	5.2	8.2	0.83	3	124.0
HOR744	0.05	0.03	<0.02	0.4	15	4.4	3.1	0.41	4	47.9
HOR745	0.08	0.03	0.03	0.6	24	4.5	6.2	0.63	5	131.9
HOR746	0.08	0.03	<0.02	0.5	15	2.1	5.6	0.56	5	111.4
HOR747	0.10	0.02	<0.02	0.4	17	3.7	6.5	0.64	4	118.5
HOR748	0.06	0.03	<0.02	0.4	11	2.4	4.1	0.46	4	41.4
HOR749	0.06	0.02	<0.02	0.4	15	4.2	4.1	0.50	5	38.5
HOR750	0.06	0.04	<0.02	0.6	24	2.7	4.1	0.55	4	39.8
HOR751	0.06	0.03	<0.02	0.6	28	3.1	4.2	0.38	4	48.8
HOR752	0.31	0.33	0.04	1.3	236	3.2	22.1	2.04	17	296.0

Sample ID	Tm (ppm)	TOT/C (%)	TOT/S (%)	U (ppm)	V (ppm)	W (ppm)	Y (ppm)	Yb (ppm)	Zn (ppm)	Zr (ppm)
HOR753	0.06	0.03	<0.02	0.4	19	2.8	3.5	0.48	4	58.2
HOR754	0.11	0.02	0.02	1.2	35	4.2	6.4	0.73	6	160.1
HOR755	0.15	0.03	<0.02	1.1	29	2.2	9.6	0.94	5	191.5
HOR756	0.14	0.03	0.03	1.0	38	2.8	8.6	0.87	5	66.7
HOR757	0.13	0.02	0.02	1.1	47	3.1	9.2	0.94	9	93.2
HOR758	0.15	<0.02	0.02	1.5	76	4.4	10.6	1.09	7	162.2
HOR759	0.31	0.03	0.02	2.2	74	3.5	18.5	1.87	4	480.2
HOR760	0.18	0.02	0.02	1.6	89	3.2	12.2	1.16	4	215.2
HOR761	0.13	0.02	<0.02	1.1	85	2.2	9.5	0.75	6	100.6
HOR762	0.16	<0.02	<0.02	0.9	91	1.6	8.9	0.90	9	123.1
HOR763	0.29	<0.02	<0.02	2.0	138	3.8	18.8	2.13	7	449.6
HOR764	0.47	<0.02	<0.02	2.2	124	3.0	28.5	3.25	6	727.5
HOR765	0.35	0.04	<0.02	3.1	270	6.3	20.1	2.39	17	352.8
HOR766	0.17	0.02	<0.02	1.0	134	1.8	11.3	1.18	12	81.9
HOR767	0.15	<0.02	<0.02	0.5	110	1.2	8.5	0.84	8	54.0
HOR768	0.17	0.02	<0.02	0.5	134	2.1	13.0	1.12	12	77.4
HOR769	0.19	0.03	<0.02	0.8	128	1.6	13.1	1.22	9	159.5
HOR770	2.13	0.03	<0.02	10.8	237	5.7	136.2	14.48	17	5074.3
HOR771	1.62	0.06	<0.02	6.1	373	4.3	86.6	10.34	318	1967.0
HOR772	0.84	0.02	<0.02	3.6	115	3.0	47.5	5.81	14	1429.5
HOR773	1.21	0.05	<0.02	5.3	189	4.2	71.1	8.25	32	2292.9
HOR774	2.16	0.06	<0.02	8.3	322	3.3	125.6	13.61	166	2267.7
HOR775	0.21	0.04	<0.02	1.0	126	2.9	14.6	1.39	17	279.3
HOR776	0.20	0.04	<0.02	0.8	93	2.3	14.0	1.33	42	125.9
HOR777	0.17	0.03	<0.02	0.7	137	2.9	9.3	1.04	19	70.7
HOR778	0.13	0.03	<0.02	0.7	123	2.4	8.8	0.94	34	75.3

Sample ID	Tm (ppm)	TOT/C (%)	TOT/S (%)	U (ppm)	V (ppm)	W (ppm)	Y (ppm)	Yb (ppm)	Zn (ppm)	Zr (ppm)
HOR779	0.28	0.12	<0.02	1.8	218	2.3	15.5	1.93	36	413.1
HOR780	1.27	0.05	<0.02	7.1	250	4.5	77.3	9.13	38	2215.8
HOR781	0.56	2.82	0.43	2.7	487	4.3	31.8	3.07	99	212.1
WIL15	0.30	1.18	0.09	1.5	105	1.0	18.6	1.87	43	125.3
WIL16	0.31	0.93	0.05	1.6	123	1.0	21.1	2.22	46	152.7
WIL17	0.25	0.47	0.02	1.2	69	2.9	17.1	1.66	28	143.6
WIL18	0.36	1.07	0.06	1.8	102	1.6	23.4	2.33	47	145.8
WIL19	0.17	0.27	0.02	0.8	46	0.8	11.5	1.20	25	83.7
WIL20	0.11	0.22	<0.02	0.5	28	0.5	7.1	0.82	14	70.1
WIL21	0.05	0.02	<0.02	0.2	<8	<0.5	2.7	0.33	6	24.5
WIL22	0.03	0.02	<0.02	0.2	<8	<0.5	2.2	0.25	5	26.6
WIL23	0.04	0.02	<0.02	0.2	<8	0.5	2.1	0.27	6	29.9
WIL24	0.03	0.02	0.06	0.3	<8	<0.5	2.1	0.24	9	34.0
WIL25	0.04	0.04	0.08	0.3	<8	<0.5	1.9	0.25	8	36.9
WIL26	0.06	0.07	0.13	0.5	<8	0.5	3.4	0.38	9	66.8
WIL27	0.05	0.06	0.20	0.5	<8	<0.5	2.9	0.34	9	48.0
WIL28	0.03	0.03	0.06	0.3	<8	<0.5	2.6	0.27	6	36.3
WIL29	0.06	0.08	0.06	0.4	<8	<0.5	3.1	0.33	8	37.2
WIL30	0.04	0.06	0.04	0.3	<8	<0.5	2.4	0.33	10	42.0
WIL31	0.05	0.10	0.09	0.6	<8	<0.5	2.5	0.32	15	35.5
WIL32	0.04	0.17	0.15	0.4	<8	<0.5	2.3	0.24	9	33.2
WIL33	0.04	0.07	0.14	0.3	<8	<0.5	2.3	0.26	11	36.8
WIL34	0.03	0.06	0.23	0.2	<8	<0.5	2.1	0.24	8	39.0
WIL35	0.05	0.16	0.28	0.6	<8	<0.5	3.2	0.30	12	43.6
WIL36	0.06	0.15	0.28	0.3	<8	<0.5	3.6	0.43	15	72.6
WIL37	0.07	0.16	0.32	0.4	9	<0.5	4.4	0.49	21	102.0

Sample ID	Tm (ppm)	TOT/C (%)	TOT/S (%)	U (ppm)	V (ppm)	W (ppm)	Y (ppm)	Yb (ppm)	Zn (ppm)	Zr (ppm)
WIL38	0.10	0.31	2.27	0.5	21	0.8	5.8	0.73	21	100.0
PIA04	0.08	0.04	0.89	0.7	8	<0.5	5.5	0.58	5	52.4
PIA05	0.07	0.05	0.46	0.6	<8	<0.5	4.8	0.47	3	52.2
PIA06	0.09	0.04	0.62	0.6	12	<0.5	5.5	0.63	4	60.0
PIA07	0.14	0.02	0.48	0.7	<8	0.7	8.5	0.87	3	127.3
PIA08	0.08	<0.02	0.33	0.7	<8	<0.5	3.8	0.46	3	48.8
PIA09	0.08	0.03	0.42	0.7	22	<0.5	4.1	0.53	9	43.2
PIA10	0.12	0.02	0.21	0.9	43	0.7	6.1	0.72	11	33.8
PIA11	0.15	0.05	0.92	1.1	53	0.9	11.3	0.89	21	61.2
PIA12	0.14	0.04	1.42	1.0	36	0.6	7.2	0.86	9	71.5
PIA13	0.20	0.06	1.93	1.6	72	0.9	10.5	1.21	28	91.4
PIA14	0.17	0.09	2.62	2.0	120	0.7	11.1	1.05	30	68.4
PIA15	0.19	0.12	1.23	2.3	88	2.1	11.0	1.21	23	130.2
KND01	0.04	0.04	6.91	0.3	26	<0.5	2.8	0.31	5	22.8
KND02	0.05	0.06	6.66	0.5	24	<0.5	2.7	0.28	5	33.1
KND03	0.06	0.07	1.88	0.9	28	<0.5	3.4	0.48	6	63.7
KND04	0.07	0.05	0.77	1.4	20	<0.5	4.3	0.50	4	136.9
KND05	0.05	0.05	0.27	0.6	15	<0.5	2.5	0.37	8	41.2
KND06	0.04	0.04	0.19	0.4	9	<0.5	2.4	0.34	6	24.9
KND07	0.06	0.04	0.36	0.6	11	<0.5	2.8	0.43	5	57.8
KND08	0.06	0.04	1.18	0.3	<8	<0.5	2.9	0.40	5	23.8
KND09	0.04	0.04	1.99	0.3	11	<0.5	2.9	0.29	6	26.2
KND10	0.14	0.06	2.50	0.9	24	0.5	8.7	0.91	10	140.5
KND11	0.08	0.09	0.70	0.6	21	0.9	4.9	0.61	10	64.3
KND12	0.12	0.81	0.91	0.9	48	0.8	8.2	0.76	27	81.9
KND13	0.12	0.54	0.95	1.0	34	0.6	7.9	0.73	20	84.1

Sample ID	Tm (ppm)	TOT/C (%)	TOT/S (%)	U (ppm)	V (ppm)	W (ppm)	Y (ppm)	Yb (ppm)	Zn (ppm)	Zr (ppm)
BER02	0.05	0.08	<0.02	0.3	20	0.6	2.4	0.37	3	59.1
BER03	0.14	1.19	0.02	0.6	56	2.0	8.3	0.89	15	94.5
BER04	0.11	0.84	<0.02	0.4	40	1.4	6.1	0.70	9	73.2
BER05	0.11	0.85	<0.02	0.5	41	1.5	5.9	0.68	16	71.9
BER06	0.05	0.11	<0.02	0.4	25	<0.5	2.8	0.35	4	37.1
BER07	0.05	0.03	<0.02	0.2	<8	<0.5	3.1	0.32	3	24.7
BER08	0.08	<0.02	<0.02	0.4	<8	<0.5	4.6	0.49	2	29.5
BER09	0.05	<0.02	<0.02	0.3	<8	<0.5	3.2	0.34	2	25.1
BER10	0.06	<0.02	<0.02	0.3	<8	<0.5	4.8	0.37	9	26.2
MAN04	0.29	0.29	0.02	2.3	118	2.5	16.3	2.11	31	212.8
MAN05	0.08	0.03	<0.02	0.6	17	<0.5	4.7	0.53	5	37.2
MAN06	0.16	0.09	<0.02	1.1	39	1.2	9.1	1.02	9	100.8
MAN07	0.49	0.26	0.02	2.8	79	2.6	27.5	3.11	27	325.1
MAN08	0.55	0.09	<0.02	3.3	71	3.3	32.3	3.74	25	463.7
MAN09	0.61	0.41	0.07	10.2	89	2.9	34.7	4.01	39	343.6
MAN10	0.45	0.15	<0.02	4.5	88	3.4	29.2	3.18	30	369.3
MAN11	0.47	0.22	0.04	3.6	97	3.4	28.8	3.13	45	235.5
MAN12	0.46	0.37	0.03	3.0	114	3.1	29.8	2.95	35	269.3
MAN13	0.48	0.26	0.02	4.1	110	2.8	30.9	3.26	35	299.6
MAN14	0.55	0.92	0.06	4.5	107	3.6	32.3	3.67	47	295.7
MAN15	0.53	0.86	0.08	3.8	91	3.0	31.8	3.44	40	293.4
MAN16	0.81	0.56	0.04	4.5	112	3.4	68.2	4.88	40	296.6
MAN17	0.25	0.63	0.02	1.4	62	0.9	13.8	1.47	17	104.6
MAN18	0.11	0.32	0.49	0.8	41	0.6	7.0	0.72	14	48.8
MAN19	0.19	0.08	<0.02	1.0	57	1.0	10.2	1.17	17	61.9
MAN20	0.11	0.06	0.05	0.7	42	<0.5	5.8	0.63	10	34.8

Sample ID	Tm (ppm)	TOT/C (%)	TOT/S (%)	U (ppm)	V (ppm)	W (ppm)	Y (ppm)	Yb (ppm)	Zn (ppm)	Zr (ppm)
MAN21	0.11	0.06	0.06	0.7	44	0.9	6.4	0.81	12	43.6
MAN22	0.10	0.06	0.04	0.7	36	0.7	6.2	0.70	12	42.5
MAN23	0.19	0.08	0.14	1.2	37	0.8	10.5	1.19	11	157.1
MAN24	0.25	0.37	0.22	1.9	63	1.3	14.0	1.51	24	189.1
MAN25	0.11	0.05	0.09	0.7	24	0.8	6.4	0.72	6	69.7
MAN26	0.24	0.05	0.08	1.4	21	1.1	14.4	1.54	10	254.8
MAN27	0.32	0.04	0.08	1.5	19	1.9	17.2	2.12	11	280.8
WAL11	0.40	0.32	0.06	1.9	113	1.7	24.0	2.48	34	307.3
WAL12	0.35	0.36	0.22	2.0	89	1.6	20.0	2.09	32	273.0
WAL13	0.09	0.97	0.19	0.6	26	<0.5	7.0	0.62	9	52.7
WAL14	0.06	0.11	0.15	0.4	10	<0.5	3.7	0.43	3	41.4
WAL15	0.06	0.07	0.37	0.4	13	<0.5	3.9	0.43	4	36.7
WAL16	0.81	0.87	0.25	5.8	106	3.7	39.8	5.69	19	1995.8
WAL17	0.13	0.14	0.44	0.9	32	1.3	7.7	0.90	13	149.6
WAL18	0.15	0.21	0.89	1.0	36	1.1	9.4	1.10	13	182.6
MOR04	0.18	2.50	0.09	5.4	56	0.6	11.0	1.10	22	86.5
MOR05	0.05	0.19	<0.02	0.6	10	<0.5	2.7	0.27	3	30.3
MOR06	0.03	0.04	<0.02	0.2	11	<0.5	2.1	0.18	2	25.6
MOR07	0.03	0.03	<0.02	0.3	<8	<0.5	1.9	0.22	1	24.1
MOR08	0.04	0.20	<0.02	0.7	<8	<0.5	2.6	0.31	3	31.8
MOR09	0.04	0.04	0.02	0.4	10	<0.5	2.1	0.23	2	22.1
MOR10	0.04	0.06	0.13	0.5	<8	<0.5	2.7	0.32	3	28.4
MOR11	0.04	0.07	0.09	0.5	<8	<0.5	2.1	0.27	5	24.6
MOR12	0.04	0.09	0.07	0.4	<8	<0.5	2.9	0.29	4	21.1
MOR13	0.04	0.13	0.07	0.6	<8	<0.5	2.5	0.31	4	23.5
MOR14	0.04	0.12	0.10	0.6	<8	<0.5	2.6	0.26	4	22.2

Sample ID	Tm (ppm)	TOT/C (%)	TOT/S (%)	U (ppm)	V (ppm)	W (ppm)	Y (ppm)	Yb (ppm)	Zn (ppm)	Zr (ppm)
MOR15	0.05	0.07	0.03	0.8	<8	<0.5	3.1	0.44	2	27.6
MOR16	0.05	0.12	0.06	0.5	<8	<0.5	3.2	0.32	3	24.9
MOR17	0.05	0.07	0.04	0.5	<8	<0.5	3.0	0.34	2	21.1
MOR18	0.05	0.09	0.05	0.6	<8	<0.5	2.6	0.30	2	21.2
MOR19	0.05	0.05	0.05	0.5	<8	<0.5	3.4	0.40	2	26.6
MOR20	0.06	0.09	0.10	0.6	30	1.9	3.9	0.46	4	26.5
MOR21	0.08	0.10	0.10	0.7	21	<0.5	5.1	0.57	4	26.1
MOR22	0.07	0.09	0.12	0.6	15	<0.5	3.7	0.43	3	26.2
BT01	0.08	0.05	0.03	0.7	72	0.9	5.0	0.60	4	81.1
BT02	0.06	0.05	0.03	0.7	54	0.8	3.8	0.43	5	53.5
BT03	0.07	0.05	0.02	0.7	53	0.7	3.5	0.43	4	60.8
BT04	0.08	0.05	0.03	0.7	67	0.7	3.6	0.48	4	67.2
BT05	0.07	0.04	0.03	0.8	53	0.8	3.8	0.49	5	57.1
BT06	0.06	0.10	0.04	0.7	49	0.7	4.1	0.44	5	49.9
BT07	0.08	0.05	<0.02	0.7	40	0.6	4.0	0.47	4	49.6
BT08	0.16	0.07	<0.02	1.2	83	0.7	6.7	1.00	8	53.2
BT09	0.10	0.06	<0.02	0.8	54	0.7	6.1	0.69	5	44.8
BT10	0.09	0.04	<0.02	0.7	33	1.2	4.6	0.54	11	70.0
BT11	0.07	0.04	<0.02	0.7	32	0.7	3.3	0.46	19	48.6
BT12	0.10	0.04	<0.02	0.9	26	0.9	5.3	0.68	14	42.4
BT13	0.06	0.10	<0.02	0.4	31	0.6	3.4	0.42	3	91.3
BT14	0.07	0.08	<0.02	0.5	48	0.6	3.7	0.48	7	55.4
BT15	0.07	0.09	<0.02	0.5	41	<0.5	3.2	0.42	5	45.9
BT16	0.07	0.06	<0.02	0.6	44	1.3	3.8	0.43	15	68.2
BT17	0.09	0.07	<0.02	0.7	41	0.6	4.3	0.56	7	77.9
BT18	0.13	0.07	<0.02	0.9	43	0.8	7.1	0.88	6	84.5

Sample ID	Tm (ppm)	TOT/C (%)	TOT/S (%)	U (ppm)	V (ppm)	W (ppm)	Y (ppm)	Yb (ppm)	Zn (ppm)	Zr (ppm)
BT19	0.10	0.06	<0.02	0.7	55	0.7	4.8	0.65	15	83.7
BT20	0.10	0.05	<0.02	0.8	70	0.7	5.5	0.74	13	57.6
BT21	0.10	0.05	<0.02	0.8	49	0.7	5.1	0.67	16	65.3
BT22	0.09	0.05	<0.02	0.6	39	0.6	4.2	0.61	11	62.0
BT23	0.12	0.05	<0.02	0.9	38	0.6	6.6	0.80	14	70.2
BT24	0.14	0.03	<0.02	0.5	37	<0.5	10.0	0.91	14	60.8
BT25	0.12	0.03	<0.02	0.7	44	<0.5	8.6	0.74	11	47.6
BT26	0.25	0.04	<0.02	1.0	62	0.8	11.7	1.78	28	34.3
BT27	0.43	0.04	<0.02	1.0	54	0.7	22.9	2.72	33	80.3
BT28	0.29	0.03	<0.02	1.1	56	1.2	27.8	1.75	22	166.8
BT29	0.35	0.04	<0.02	1.3	70	1.2	25.2	2.30	22	347.1
BT30	0.20	0.03	<0.02	0.8	57	0.9	13.8	1.34	27	180.3
BT31	0.20	0.04	<0.02	0.8	66	1.1	12.7	1.20	28	129.1
BT32	0.33	1.00	<0.02	1.3	137	1.2	24.5	2.16	54	234.1
BT33	0.04	11.56	<0.02	0.4	20	<0.5	4.3	0.24	17	14.0
BT35	0.09	0.06	<0.02	1.0	46	1.0	5.2	0.59	7	110.5
BT36	0.10	0.16	<0.02	2.2	181	1.2	5.8	0.69	7	113.8
BT37	0.09	0.15	0.03	1.0	101	1.2	5.5	0.65	8	101.0
BT38	0.07	0.07	0.02	0.6	69	1.0	3.0	0.42	8	73.8
BT39	0.07	0.05	0.02	0.7	58	1.1	3.3	0.49	7	67.5
BT40	0.07	0.04	0.03	0.6	45	0.7	4.0	0.49	11	50.8
BT41	0.08	0.03	<0.02	0.8	42	<0.5	3.3	0.48	12	61.8
BT42	0.12	0.03	<0.02	0.7	47	0.5	4.7	0.78	13	77.2
BT43	0.27	0.06	<0.02	1.4	63	1.0	15.2	1.54	18	170.6
BT44	0.26	0.06	<0.02	1.5	43	0.5	12.8	1.60	17	173.0
BT45	0.28	0.05	<0.02	1.4	42	0.7	9.7	1.70	16	50.9

Sample ID	Tm (ppm)	TOT/C (%)	TOT/S (%)	U (ppm)	V (ppm)	W (ppm)	Y (ppm)	Yb (ppm)	Zn (ppm)	Zr (ppm)
MBR06	0.13	0.86	<0.02	1.0	83	1.4	7.1	0.97	10	191.7
MBR07	0.15	3.55	0.02	0.8	49	1.0	10.1	0.99	7	253.1
MBR08	0.13	2.55	0.14	0.8	43	1.0	8.6	0.90	7	202.9
MBR09	0.14	2.55	0.02	0.8	47	0.8	8.6	0.90	8	245.3
MBR10	0.15	2.98	<0.02	0.7	38	1.0	9.8	0.91	6	221.9
MBR11	0.14	5.30	0.04	1.3	49	0.8	8.5	0.95	9	152.5
MBR12	0.12	6.87	0.03	1.4	39	0.7	7.4	0.76	8	125.0
MBR13	0.11	8.05	0.05	1.1	32	<0.5	6.8	0.71	7	109.4
MBR14	0.14	5.14	0.04	1.4	76	0.6	9.0	0.95	8	137.9
MBR15	0.11	7.32	0.14	1.0	29	<0.5	7.2	0.70	9	124.0
MBR16	0.05	10.69	1.43	2.3	24	<0.5	4.2	0.31	9	17.0
FT04	0.11	0.46	0.04	2.6	81	2.2	6.2	0.78	10	101.7
FT05	0.07	0.15	0.02	0.6	37	1.1	4.1	0.50	15	68.2
FT06	0.09	0.16	0.06	3.2	117	1.7	4.1	0.63	11	86.2
FT07	0.06	0.10	0.02	0.8	43	3.6	4.1	0.42	17	70.7
FT08	0.06	0.08	<0.02	0.7	48	1.6	3.3	0.44	20	60.3
FT09	0.05	0.17	<0.02	0.8	46	1.2	3.2	0.44	5	50.3
FT10	0.06	0.10	0.05	3.0	317	1.8	2.9	0.39	11	50.7
FT11	0.06	0.12	0.03	1.2	114	1.9	3.7	0.36	7	57.3
FT12	0.05	0.08	0.03	1.3	129	1.5	3.0	0.35	9	54.8
FT13	0.05	0.08	0.04	2.1	198	1.6	2.9	0.30	12	56.9
FT14	0.17	0.12	0.04	2.5	161	1.8	13.0	1.00	28	117.7
FT15	0.47	0.88	0.14	4.0	119	1.7	34.0	2.77	43	88.9
NGA01	0.25	0.16	<0.02	0.6	73	1.0	16.0	1.59	16	161.5
NGA02	0.23	0.24	0.03	1.0	80	3.3	15.8	1.62	18	168.0
NGA03	0.29	0.09	0.02	1.1	118	2.4	17.4	2.02	24	174.3

Sample ID	Tm (ppm)	TOT/C (%)	TOT/S (%)	U (ppm)	V (ppm)	W (ppm)	Y (ppm)	Yb (ppm)	Zn (ppm)	Zr (ppm)
NGA04	0.29	0.09	0.04	1.5	136	1.8	16.0	2.03	23	175.0
NGA05	0.21	0.07	0.02	1.1	100	2.4	11.0	1.31	14	169.5
NGA06	0.10	0.06	<0.02	1.0	59	2.0	4.7	0.53	6	90.5
NGA07	0.11	0.08	0.02	0.7	58	2.2	7.0	0.83	11	97.5
NGA08	0.11	0.07	<0.02	0.9	52	1.8	5.8	0.69	7	99.1
NGA09	0.09	0.07	<0.02	0.9	50	2.4	5.6	0.64	11	97.9
NGA10	0.12	0.06	<0.02	0.9	56	2.4	6.1	0.86	8	98.1
NGA11	0.16	0.09	<0.02	1.0	65	1.5	7.4	0.94	11	114.9
NGA12	0.08	0.07	<0.02	0.8	38	1.6	4.7	0.61	14	77.2
NGA13	0.08	0.06	<0.02	0.7	37	1.9	4.3	0.56	11	69.7
NGA14	0.07	0.05	<0.02	0.6	29	1.5	4.1	0.50	10	66.2
NGA15	0.09	0.04	<0.02	0.7	32	1.2	4.7	0.57	8	74.8
NGA16	0.05	0.03	<0.02	0.5	20	0.7	3.1	0.39	7	47.5
NGA17	0.08	0.04	<0.02	0.4	15	0.6	3.9	0.51	9	45.8
NGA18	0.05	0.03	<0.02	0.4	17	0.6	2.1	0.33	6	33.3
NGA19	0.07	0.03	<0.02	0.5	<8	0.6	4.2	0.53	13	42.5
NGA20	0.08	0.03	<0.02	0.4	<8	0.7	4.1	0.48	7	42.5
NGA21	0.08	<0.02	<0.02	0.4	<8	<0.5	4.1	0.51	11	30.5
NGA22	0.07	0.03	<0.02	0.4	<8	<0.5	3.6	0.48	6	33.0
NGA23	0.08	<0.02	<0.02	0.4	<8	<0.5	4.1	0.48	8	34.3
NGA24	0.09	0.02	<0.02	0.4	<8	<0.5	4.8	0.54	6	32.0
NGA25	0.12	0.03	<0.02	0.5	<8	<0.5	7.3	0.84	6	39.0
NGA26	0.07	<0.02	<0.02	0.5	<8	<0.5	4.2	0.50	5	27.5
NGA27	0.06	0.03	<0.02	0.3	<8	<0.5	3.6	0.43	8	35.8
NGA28	0.09	0.03	<0.02	0.5	<8	<0.5	4.9	0.60	6	36.9
NGA29	0.06	<0.02	<0.02	0.3	<8	<0.5	3.3	0.42	6	29.0

Sample ID	Tm (ppm)	TOT/C (%)	TOT/S (%)	U (ppm)	V (ppm)	W (ppm)	Y (ppm)	Yb (ppm)	Zn (ppm)	Zr (ppm)
NGA30	0.06	<0.02	<0.02	0.3	<8	<0.5	3.3	0.48	4	31.6
NGA31	0.05	0.02	<0.02	0.3	<8	<0.5	3.7	0.45	5	32.6
NGA32	0.07	0.03	<0.02	0.3	<8	<0.5	4.3	0.45	4	35.5
NGA33	0.06	<0.02	<0.02	0.2	<8	0.7	3.8	0.40	4	36.3
NGA34	0.08	0.02	<0.02	1.2	64	<0.5	4.3	0.51	9	41.7
NGA35	0.07	0.03	<0.02	0.9	40	<0.5	5.0	0.56	6	45.9
NGA36	0.07	0.03	<0.02	0.4	10	<0.5	3.7	0.41	5	31.4
NGA37	0.08	0.03	<0.02	0.5	14	<0.5	4.1	0.50	5	42.1
NGA38	0.31	1.02	0.14	1.6	77	0.9	18.1	1.95	79	116.8
NGA39	0.27	1.43	0.08	3.4	88	0.5	16.0	1.72	53	86.9
TEM03	0.05	0.04	<0.02	0.6	25	0.8	2.9	0.33	4	49.8
TEM04	0.06	0.05	<0.02	0.7	25	0.8	3.3	0.42	6	48.8
TEM05	0.06	0.04	<0.02	0.5	25	0.7	3.9	0.46	5	52.3
TEM06	0.05	0.04	<0.02	0.6	17	<0.5	2.8	0.28	10	36.6
TEM07	0.05	0.03	<0.02	0.3	<8	<0.5	2.9	0.34	7	30.4
TEM08	0.05	0.05	<0.02	0.4	<8	<0.5	3.1	0.37	48	36.1
TEM09	0.04	<0.02	<0.02	0.2	<8	<0.5	2.7	0.31	15	36.1
TEM10	0.05	0.03	<0.02	0.3	<8	<0.5	2.7	0.31	7	32.8
TEM11	0.04	<0.02	<0.02	0.3	<8	<0.5	2.6	0.27	7	39.2
TEM12	0.09	0.09	0.02	1.3	13	<0.5	5.9	0.57	17	43.9
TEM13	0.08	0.07	<0.02	1.3	<8	<0.5	5.2	0.52	21	35.8
TEM14	0.06	0.04	0.02	1.1	42	0.8	3.6	0.39	26	38.9
TEM15	0.18	0.41	0.75	6.6	101	0.8	8.3	1.14	36	66.5
NDA01	0.05	0.46	0.04	0.5	19	<0.5	2.6	0.28	8	23.7
NDA02	0.03	0.49	<0.02	0.2	<8	<0.5	2.4	0.26	17	25.6
NDA03	0.08	1.14	0.17	0.8	10	<0.5	5.0	0.52	73	27.7

Sample ID	Tm (ppm)	TOT/C (%)	TOT/S (%)	U (ppm)	V (ppm)	W (ppm)	Y (ppm)	Yb (ppm)	Zn (ppm)	Zr (ppm)
NDA04	0.05	0.07	0.07	0.2	<8	<0.5	3.3	0.27	11	23.6
OAK03	0.12	0.07	<0.02	0.8	31	1.0	5.9	0.79	7	276.4
OAK04	0.21	0.05	0.02	1.6	49	1.7	11.0	1.37	8	453.9
OAK05	0.08	0.52	<0.02	0.5	26	1.0	4.8	0.53	6	164.0
OAK06	0.06	0.04	<0.02	0.3	27	0.7	3.4	0.41	5	54.9
OAK07	0.07	0.03	<0.02	0.3	13	0.7	3.4	0.48	5	82.8
OAK08	0.10	0.46	0.03	1.0	26	0.5	5.4	0.62	22	83.5
OAK09	0.07	0.14	0.03	1.0	23	<0.5	4.6	0.52	8	61.7
OAK10	0.04	0.08	<0.02	0.3	<8	<0.5	2.7	0.31	7	48.9
OAK11	0.13	0.55	0.02	1.0	60	0.7	7.2	0.92	31	199.7
OAK12	0.31	0.09	0.04	4.8	106	1.2	15.3	2.04	33	385.1
OAK13	0.30	0.14	0.04	5.1	111	1.6	14.9	1.92	37	370.8
OAK14	0.39	0.15	0.04	8.3	139	1.6	24.1	2.49	24	283.8
OAK15	0.36	0.24	0.07	12.1	189	1.9	23.1	2.24	22	278.5
OAK16	0.34	0.19	0.04	12.7	173	1.3	21.1	2.36	40	317.6
OAK17	0.34	0.14	0.05	11.8	234	1.7	18.7	2.27	44	277.8
OAK18	0.32	0.23	0.04	15.3	298	1.2	17.4	2.15	37	257.4
OAK19	0.26	0.16	0.03	8.8	133	1.3	14.9	1.63	29	223.3
OAK20	0.30	0.18	0.04	11.0	137	1.5	17.6	1.84	28	235.2
OAK21	0.17	0.09	0.02	5.1	40	0.8	8.9	1.06	10	290.6
PIN04	0.05	0.05	<0.02	0.3	17	<0.5	2.4	0.25	9	30.5
PIN05	0.06	0.05	<0.02	0.5	17	0.5	2.9	0.38	8	34.8
PIN06	0.20	0.03	<0.02	0.9	40	1.1	12.1	1.41	12	230.9
PIN07	0.29	0.04	<0.02	1.2	20	1.1	15.4	1.88	11	411.3
PIN08	0.35	0.09	<0.02	1.4	22	1.9	20.0	2.28	9	599.6
PIN09	0.22	0.04	<0.02	0.9	26	1.4	12.3	1.46	14	268.0

Sample ID	Tm (ppm)	TOT/C (%)	TOT/S (%)	U (ppm)	V (ppm)	W (ppm)	Y (ppm)	Yb (ppm)	Zn (ppm)	Zr (ppm)
PIN10	0.16	0.10	<0.02	1.0	87	1.7	10.1	1.01	74	139.0
PV02	0.04	0.07	<0.02	0.5	17	<0.5	2.7	0.30	4	50.8
PV03	0.06	0.04	<0.02	0.5	24	0.9	3.3	0.40	5	56.8
PV04	0.07	0.06	<0.02	0.5	25	<0.5	4.0	0.44	6	61.0
PV05	0.05	0.08	<0.02	0.4	<8	<0.5	2.6	0.31	4	45.3
PV06	0.05	0.03	<0.02	0.4	<8	<0.5	2.1	0.28	4	36.6
PV07	0.05	0.05	<0.02	0.5	9	<0.5	3.7	0.35	8	47.9
PV08	0.04	0.04	0.06	1.3	<8	<0.5	2.3	0.24	6	34.0
PV09	0.05	0.03	0.05	1.3	<8	<0.5	2.8	0.29	5	36.3
RB02	0.13	0.25	<0.02	1.3	218	0.9	6.3	0.85	2	265.8
RB03	0.30	0.31	<0.02	2.9	155	1.7	13.0	2.10	10	246.6
RB04	0.34	1.14	<0.02	1.9	214	2.1	18.9	2.20	11	196.6
RB05	0.55	5.29	0.03	1.3	143	1.7	46.8	3.67	7	120.9
KI1_01	0.45	0.17	<0.02	1.3	77	2.2	27.5	2.86	33	280.7
KI1_02	0.21	0.09	<0.02	0.8	61	2.2	13.1	1.41	11	243.9
KI1_03	0.27	0.09	<0.02	1.1	68	2.4	17.0	1.84	20	240.8
KI1_04	0.20	0.32	<0.02	1.0	64	2.3	12.2	1.33	9	233.7
KI1_05	0.29	0.88	<0.02	1.1	72	2.0	21.7	1.89	27	217.7
KI1_06	0.33	1.23	<0.02	1.8	108	2.8	21.3	2.05	33	295.5
KI1_07	0.26	0.33	<0.02	1.3	73	1.9	16.3	1.74	28	272.6
KI1_08	0.20	0.36	<0.02	1.0	63	1.7	11.8	1.31	12	355.0
KI1_09	0.18	0.09	<0.02	1.0	52	1.6	10.0	1.21	11	349.0
KI1_10	0.25	0.10	<0.02	1.0	72	2.1	15.3	1.66	29	281.6
KI1_11	0.20	0.06	<0.02	0.9	151	1.9	11.1	1.25	13	151.2
KI1_12	0.27	0.07	<0.02	1.3	140	2.0	16.3	1.87	13	190.7
KI1_13	1.06	0.31	<0.02	1.7	253	2.9	88.9	6.50	21	185.8

Sample ID	Tm (ppm)	TOT/C (%)	TOT/S (%)	U (ppm)	V (ppm)	W (ppm)	Y (ppm)	Yb (ppm)	Zn (ppm)	Zr (ppm)
KI10_01	0.63	1.80	<0.02	1.2	144	1.9	40.3	3.78	10	275.9
KI10_02	0.80	0.74	<0.02	0.8	88	1.8	53.4	4.65	9	230.2
KI10_03	1.71	0.13	<0.02	1.2	294	2.6	143.0	10.60	29	235.0
KI10_04	1.55	2.50	<0.02	2.7	284	1.4	131.2	9.05	32	188.0
KI10_05	0.66	6.75	<0.02	2.4	114	0.7	62.1	3.82	11	143.3
OLC01	0.02	0.07	<0.02	3.1	86	<0.5	1.3	0.18	7	51.5
OLC02	0.49	0.3	<0.02	5.8	593	0.6	19.4	3.39	3	127.9
OLC03	0.06	0.08	<0.02	11.6	279	<0.5	1.9	0.47	2	28.1
OLC04	0.59	0.25	0.05	2.4	316	0.7	27.2	4.28	9	70.1
OLC05	0.09	0.07	0.06	0.9	71	1.1	4.5	0.75	4	147.5
OLC06	0.11	0.22	0.14	53.8	329	1.5	5.6	0.78	12	114.7
OLC07	0.11	5.13	<0.02	3.9	52	<0.5	8.2	0.72	2	94.2
OLC08	0.21	9.11	0.15	1.6	41	2.9	16	1.36	3	99
OLC09	0.04	11.04	0.03	2.3	24	<0.5	3.6	0.22	2	16
OLC10	1.16	0.43	0.14	1.9	601	<0.5	52.5	8.27	4	178.3
OLC11	0.14	11.55	0.04	1.6	32	<0.5	11.7	0.67	5	18.2
OLC12	0.53	9.96	0.03	7.9	61	<0.5	68.2	3.17	13	47.1

Appendix C – Results of 3D geological modelling of the Murray Basin

Deep Exploration Technologies Cooperative Research Centre

3D modelling of the Late Tertiary stratigraphy of the Murray Basin, SE Australia

Accompanying isopach maps

McLennan, S.M. (University of Adelaide) & van der Wielen, S.E. (University of Adelaide/DMITRE)

DEEP EXPLORATION TECHNOLOGIES CRC
Uncovering the future

ANGLO AMERICAN
BARRICK AUSTRALIA
bhpbilliton
BOART LONGYEAR
GOLD FIELDS
Newcrest Mining Limited
VALE
Government of South Australia
Primary Industries and Resources SA
An Australian Government Initiative
CRC
CSIRO
Curtin University
THE UNIVERSITY OF ADELAIDE AUSTRALIA
Australian Government
Geoscience Australia
THE UNIVERSITY OF WESTERN AUSTRALIA

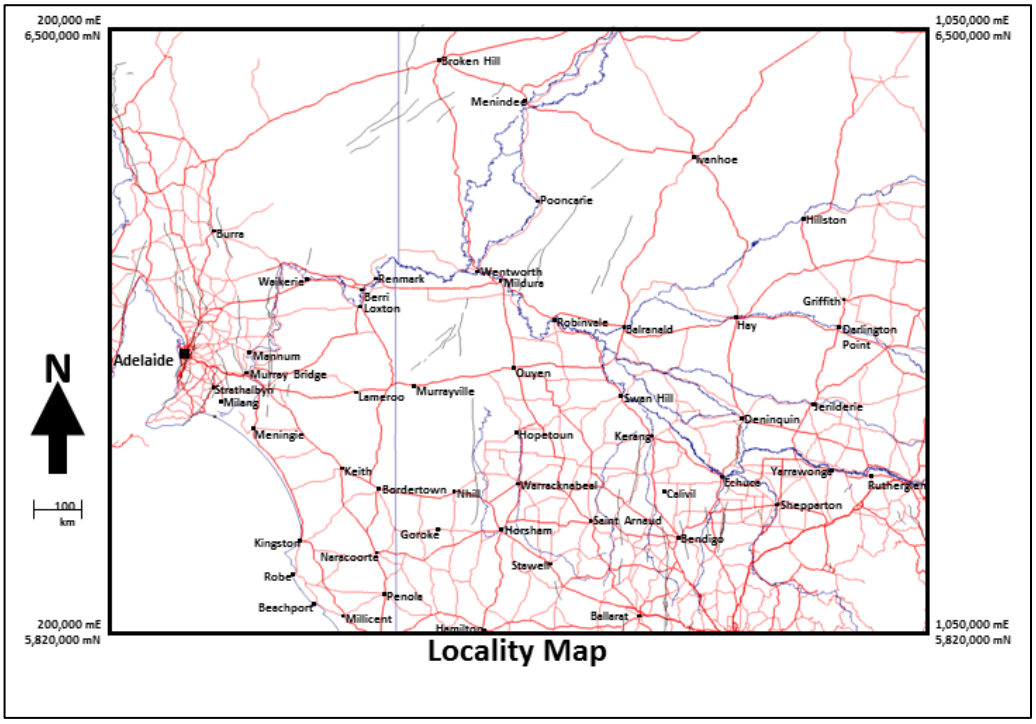

Locality Map

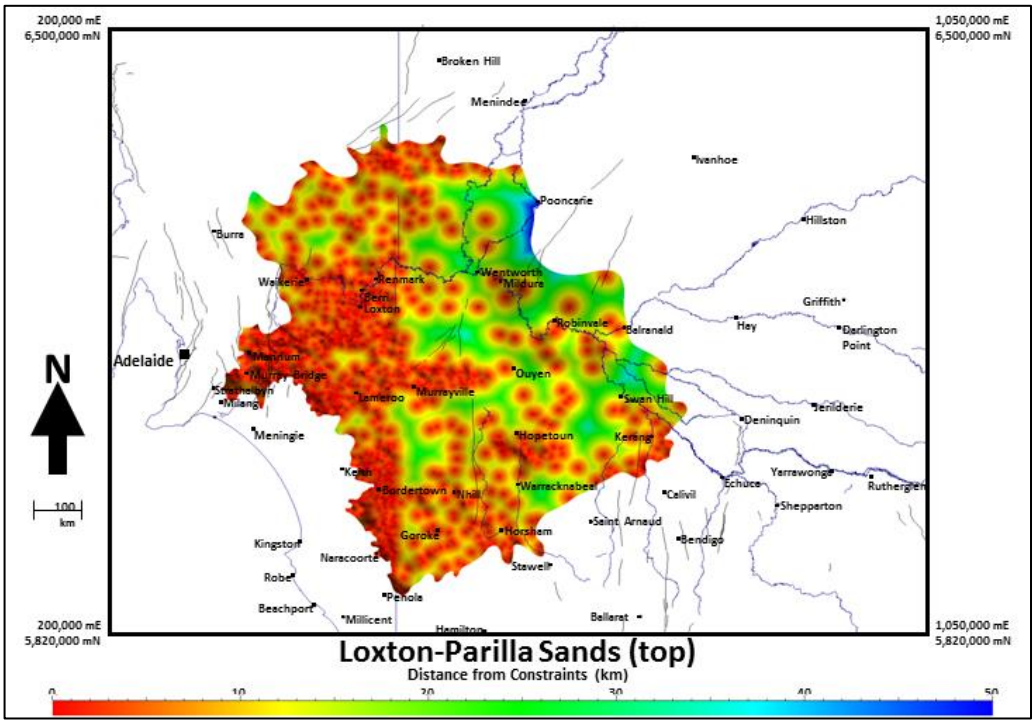

Loxton-Parilla Sands (top)

Distance from Constraints (km)

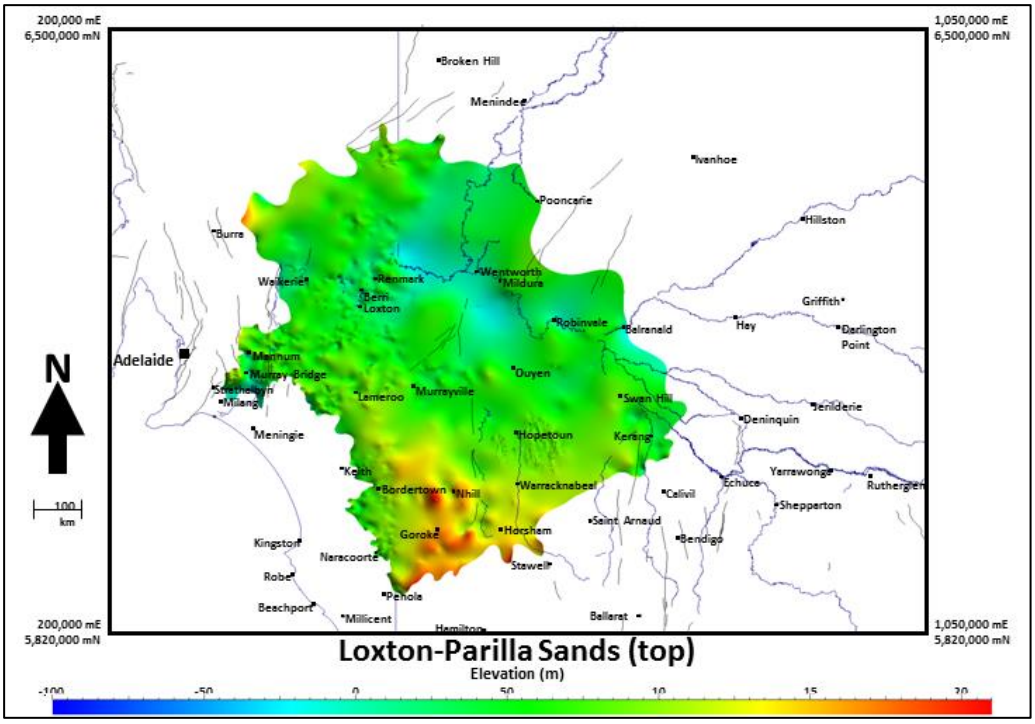
200,000 mE
6,500,000 mN
1,050,000 mE
6,500,000 mN
Broken Hill
Menindee
Ivanhoe
Pooncarie
Hillston
Burra
Wentworth
Mildura
Renmark
Waikerie
Berri
Loxton
Griffith
Robinvale
Hay
Darlington Point
Balranald
Adelaide
Mannum
Murray Bridge
Swan Hill
Deniliquin
Jerilderie
Lameroo
Murrayville
Duyen
Meningie
Hopetoun
Kerang
Keith
Bordertown
Nhill
Warracknabeal
Yarrawonga
Echuca
Rutherglen
Calivil
Shepparton
Saint Arnaud
Bendigo
Horsham
Goroke
Kingston
Naracoorte
Stawell
Robe
Penola
Beachport
Millicent
Hamilton
Ballarat
N
100 km
200,000 mE
5,820,000 mN
1,050,000 mE
5,820,000 mN
Loxton-Parilla Sands (top)
Elevation (m)
-100
-50
0
50
10
15
20

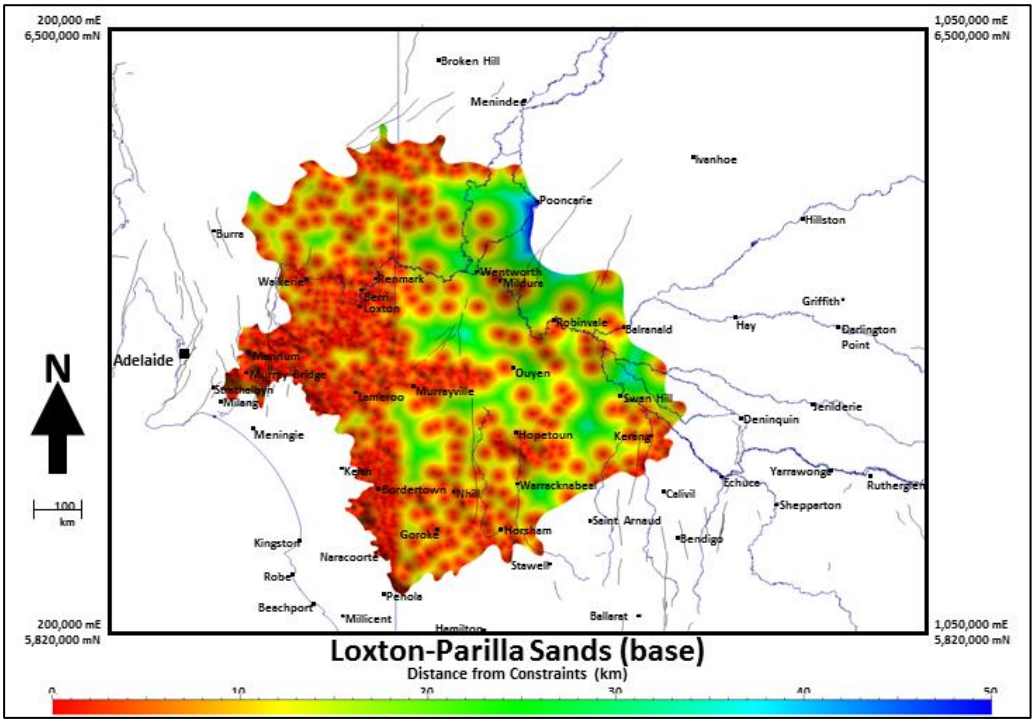
200,000 mE
6,500,000 mN
1,050,000 mE
6,500,000 mN
Broken Hill
Menindee
Ivanhoe
Pooncarie
Hillston
Burra
Wentworth
Mildura
Renmark
Waikerie
Berri
Loxton
Griffith
Robinvale
Hay
Darlington Point
Balranald
Adelaide
Mannum
Murray Bridge
Swan Hill
Deniliquin
Jerilderie
Lameroo
Murrayville
Duyen
Meningie
Hopetoun
Kerang
Keith
Bordertown
Nhill
Warracknabeal
Yarrawonga
Echuca
Rutherglen
Calivil
Shepparton
Saint Arnaud
Bendigo
Horsham
Goroke
Kingston
Naracoorte
Stawell
Robe
Penola
Beachport
Millicent
Hamilton
Ballarat
N
100 km
200,000 mE
5,820,000 mN
1,050,000 mE
5,820,000 mN
Loxton-Parilla Sands (base)
Distance from Constraints (km)
0
10
20
30
40
50

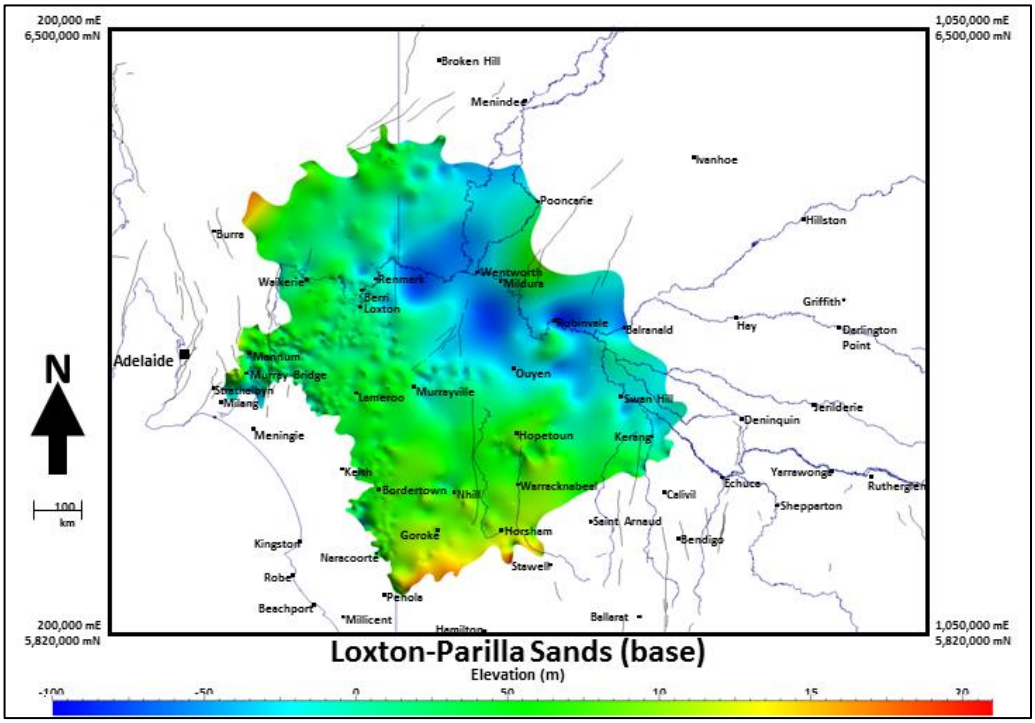
200,000 mE
6,500,000 mN
1,050,000 mE
6,500,000 mN
Broken Hill
Menindee
Ivanhoe
Pooncarie
Hillston
Burra
Wentworth
Mildura
Renmark
Berri
Loxton
Griffith
Robinvale
Balranald
Hay
Darlington Point
Adelaide
Murray Bridge
Ouyen
Swan Hill
Lameroo
Murrayville
Deniliquin
Meningie
Hopetoun
Kerang
Bordertown
Warracknabeal
Yarrawonga
Echuca
Rutherglen
Celivil
Shepparton
Saint Arnaud
Bendigo
Goroke
Horsham
Kingston
Naracoorte
Stawell
Robe
Penola
Beachport
Millicent
Ballarat
Hamilton
200,000 mE
5,820,000 mN
1,050,000 mE
5,820,000 mN
N
100 km
Loxton-Parilla Sands (base)
Elevation (m)
-100
-50
0
50
10
15
20

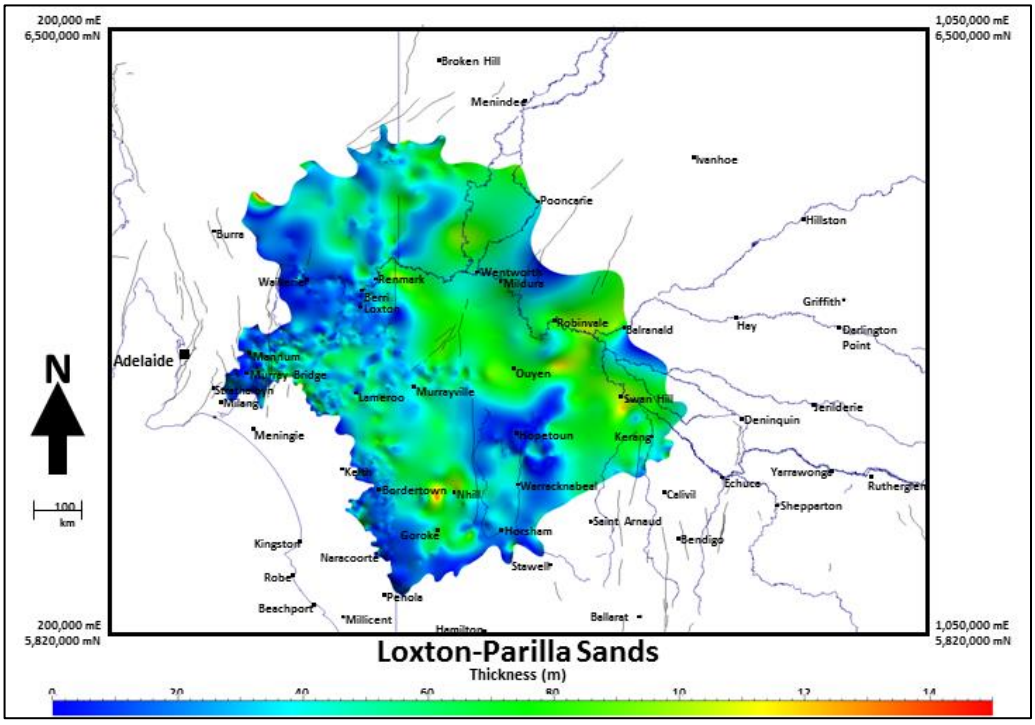
200,000 mE
6,500,000 mN
1,050,000 mE
6,500,000 mN
Broken Hill
Menindee
Ivanhoe
Pooncarie
Hillston
Burra
Wentworth
Mildura
Renmark
Berri
Loxton
Griffith
Robinvale
Balranald
Hay
Darlington Point
Adelaide
Murray Bridge
Ouyen
Swan Hill
Lameroo
Murrayville
Deniliquin
Meningie
Hopetoun
Kerang
Bordertown
Warracknabeal
Yarrawonga
Echuca
Rutherglen
Celivil
Shepparton
Saint Arnaud
Bendigo
Goroke
Horsham
Kingston
Naracoorte
Stawell
Robe
Penola
Beachport
Millicent
Ballarat
Hamilton
200,000 mE
5,820,000 mN
1,050,000 mE
5,820,000 mN
N
100 km
Loxton-Parilla Sands
Thickness (m)
0
20
40
60
80
10
12
14

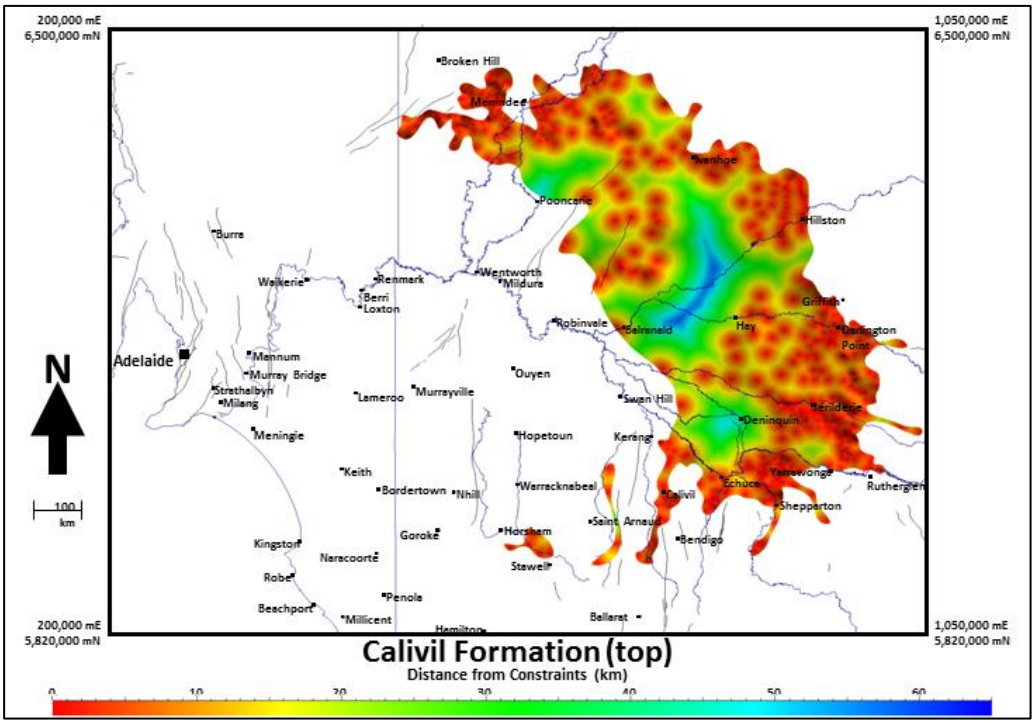
200,000 mE
6,500,000 mN
1,050,000 mE
6,500,000 mN
Broken Hill
Menindee
Wanaaring
Pooncarie
Hillston
Burra
Wentworth
Mildura
Renmark
Waikerie
Berri
Loxton
Griffith
Robinvale
Balranald
Hay
Darlington Point
Adelaide
Mannum
Murray Bridge
Strathalbyn
Milang
Lameroo
Murrayville
Ouyen
Swan Hill
Deniliquin
Jerilderie
Meningie
Hopetoun
Kerang
Keith
Bordertown
Nhill
Warracknabeal
Echuca
Yarrawonga
Rutherglen
Calivil
Shepparton
Saint Arnaud
Bendigo
Horsham
Goroke
Kingston
Naracoorte
Stawell
Robe
Penola
Beachport
Millicent
Hamilton
Ballarat
N
100 km
200,000 mE
5,820,000 mN
1,050,000 mE
5,820,000 mN
Calivil Formation (top)
Distance from Constraints (km)
0
10
20
30
40
50
60

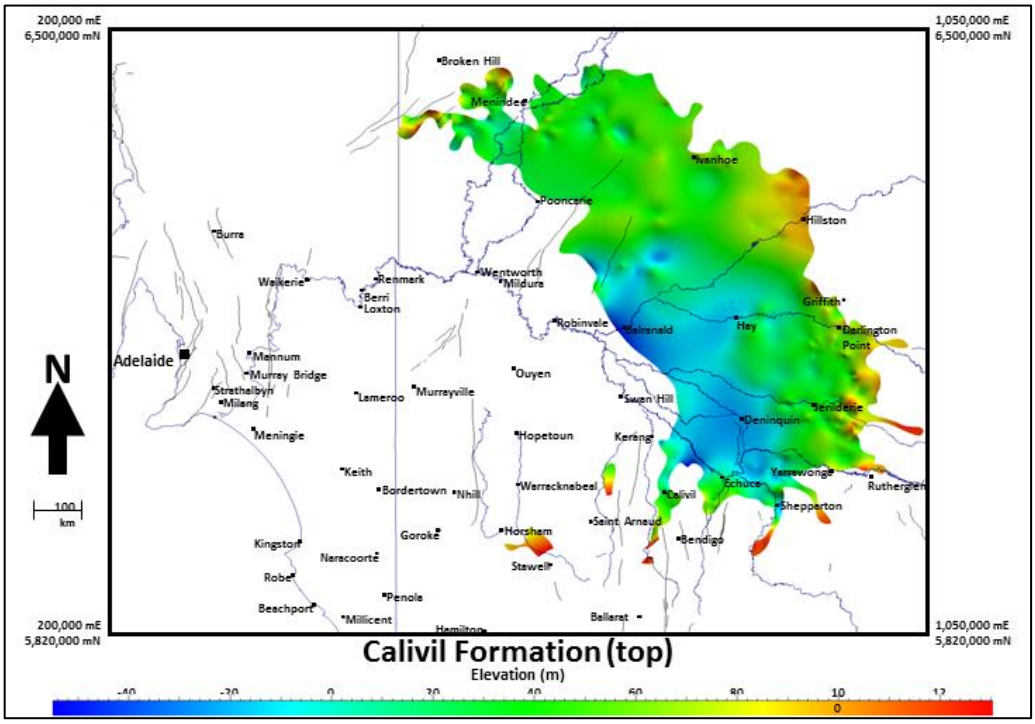
200,000 mE
6,500,000 mN
1,050,000 mE
6,500,000 mN
Broken Hill
Menindee
Wanaaring
Pooncarie
Hillston
Burra
Wentworth
Mildura
Renmark
Waikerie
Berri
Loxton
Griffith
Robinvale
Balranald
Hay
Darlington Point
Adelaide
Mannum
Murray Bridge
Strathalbyn
Milang
Lameroo
Murrayville
Ouyen
Swan Hill
Deniliquin
Jerilderie
Meningie
Hopetoun
Kerang
Keith
Bordertown
Nhill
Warracknabeal
Echuca
Yarrawonga
Rutherglen
Calivil
Shepparton
Saint Arnaud
Bendigo
Horsham
Goroke
Kingston
Naracoorte
Stawell
Robe
Penola
Beachport
Millicent
Hamilton
Ballarat
N
100 km
200,000 mE
5,820,000 mN
1,050,000 mE
5,820,000 mN
Calivil Formation (top)
Elevation (m)
-40
-20
0
20
40
60
80
100
120
0

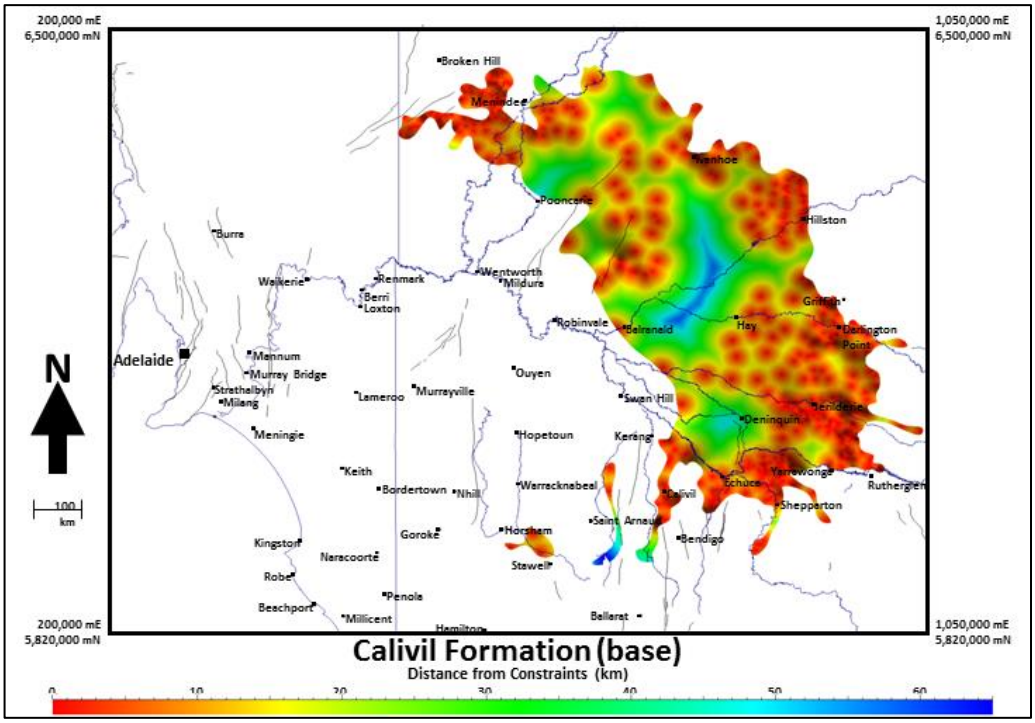
200,000 mE
6,500,000 mN
1,050,000 mE
6,500,000 mN
Broken Hill
Menindee
Ivanhoe
Pooncarie
Hillston
Burre
Wentworth
Renmark
Mildura
Wilkerie
Berri
Loxton
Griffith
Robinvale
Balranald
Hay
Darlington
Point
N
Adelaide
Mannum
Murray Bridge
Strathalbyn
Milang
Ouyen
Lameroo
Murrayville
Swan Hill
Deniliquin
Meningie
Hopetoun
Kerang
Keith
Bordertown
Nhill
Warracknabeal
Echuca
Yarrawonga
Ruthergien
Calivil
Shepparton
100
km
Saint Arnaud
Kingston
Goroke
Horsham
Bendigo
Naracoorte
Stawell
Robe
Penola
Beachport
Millicent
Hamilton
Ballarat
200,000 mE
5,820,000 mN
1,050,000 mE
5,820,000 mN
Calivil Formation (base)
Distance from Constraints (km)
0
10
20
30
40
50
60

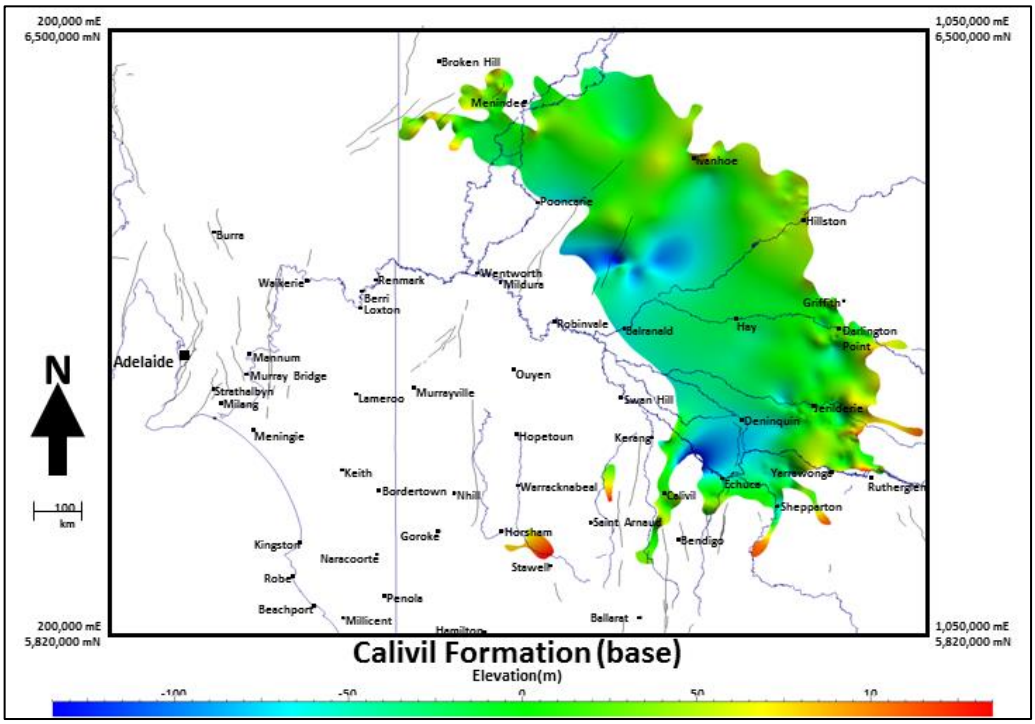
200,000 mE
6,500,000 mN
1,050,000 mE
6,500,000 mN
Broken Hill
Menindee
Ivanhoe
Pooncarie
Hillston
Burre
Wentworth
Renmark
Mildura
Wilkerie
Berri
Loxton
Griffith
Robinvale
Balranald
Hay
Darlington
Point
N
Adelaide
Mannum
Murray Bridge
Strathalbyn
Milang
Ouyen
Lameroo
Murrayville
Swan Hill
Deniliquin
Meningie
Hopetoun
Kerang
Keith
Bordertown
Nhill
Warracknabeal
Echuca
Yarrawonga
Ruthergien
Calivil
Shepparton
100
km
Saint Arnaud
Kingston
Goroke
Horsham
Bendigo
Naracoorte
Stawell
Robe
Penola
Beachport
Millicent
Hamilton
Ballarat
200,000 mE
5,820,000 mN
1,050,000 mE
5,820,000 mN
Calivil Formation (base)
Elevation(m)
-100
-50
0
50
10

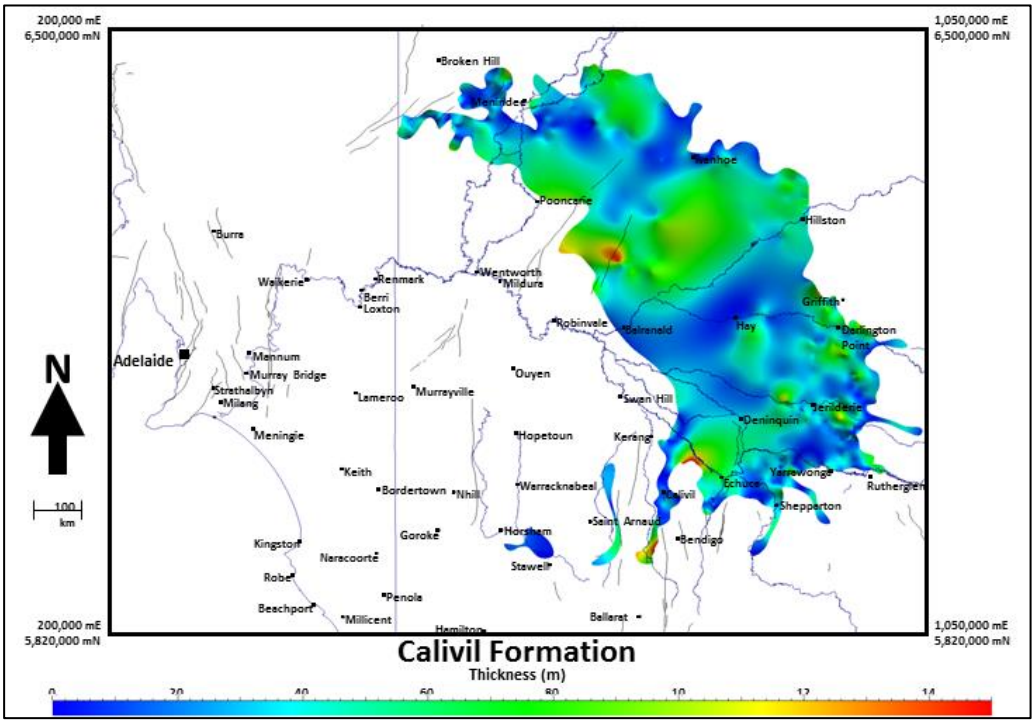
200,000 mE
6,500,000 mN
1,050,000 mE
6,500,000 mN
Broken Hill
Menindee
Ivanhoe
Pooncarie
Hillston
Burra
Wentworth
Renmark
Mildura
Waikerie
Berri
Loxton
Griffith
Robinvale
Balranald
Hay
Darlington Point
Adelaide
Mannum
Murray Bridge
Strathalbyn
Milang
Lameroo
Murrayville
Ouyen
Swan Hill
Jerilderie
Deniliquin
Meningie
Hopetoun
Kerang
Keith
Bordertown
Nhill
Warracknabeal
Calivil
Yarrawonga
Echuca
Rutherglen
Shepparton
Saint Arnaud
Bendigo
Kingston
Goroke
Horsham
Naracoorte
Stawell
Robe
Penola
Beachport
Millicent
Hamilton
Ballarat
200,000 mE
5,820,000 mN
1,050,000 mE
5,820,000 mN
N
100
km
Calivil Formation
Thickness (m)
0
20
40
60
80
10
12
14

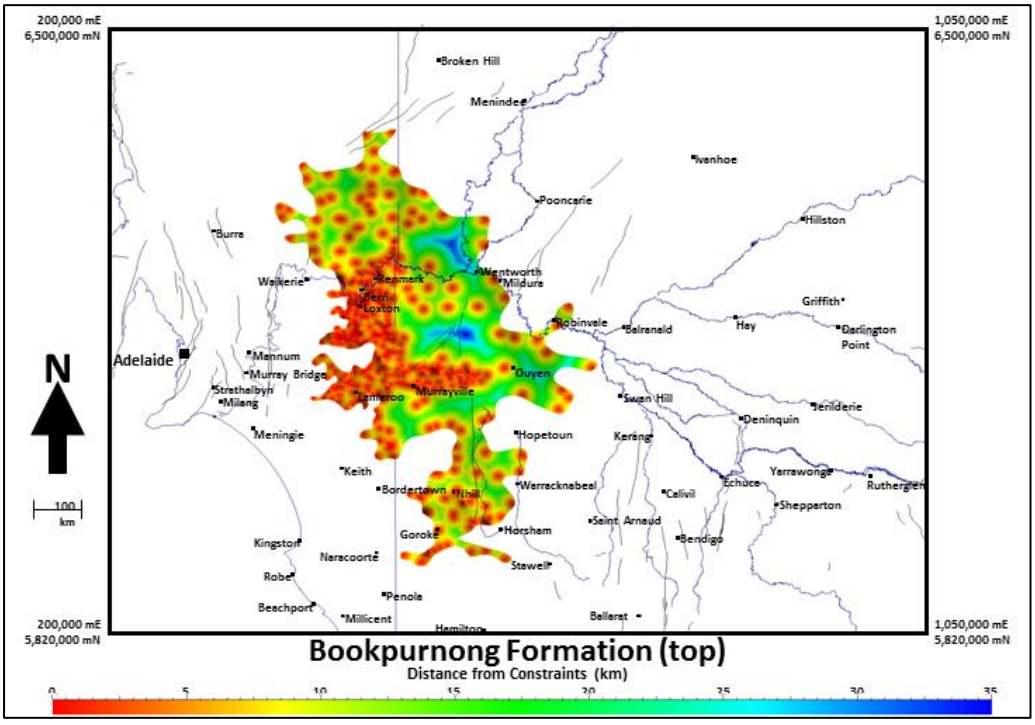
200,000 mE
6,500,000 mN
1,050,000 mE
6,500,000 mN
Broken Hill
Menindee
Ivanhoe
Pooncarie
Hillston
Burra
Wentworth
Renmark
Mildura
Waikerie
Berri
Loxton
Griffith
Robinvale
Balranald
Hay
Darlington Point
Adelaide
Mannum
Murray Bridge
Strathalbyn
Milang
Lameroo
Murrayville
Ouyen
Swan Hill
Jerilderie
Deniliquin
Meningie
Hopetoun
Kerang
Keith
Bordertown
Nhill
Warracknabeal
Calivil
Yarrawonga
Echuca
Rutherglen
Shepparton
Saint Arnaud
Bendigo
Kingston
Goroke
Horsham
Naracoorte
Stawell
Robe
Penola
Beachport
Millicent
Hamilton
Ballarat
200,000 mE
5,820,000 mN
1,050,000 mE
5,820,000 mN
N
100
km
Bookpurnong Formation (top)
Distance from Constraints (km)
0
5
10
15
20
25
30
35

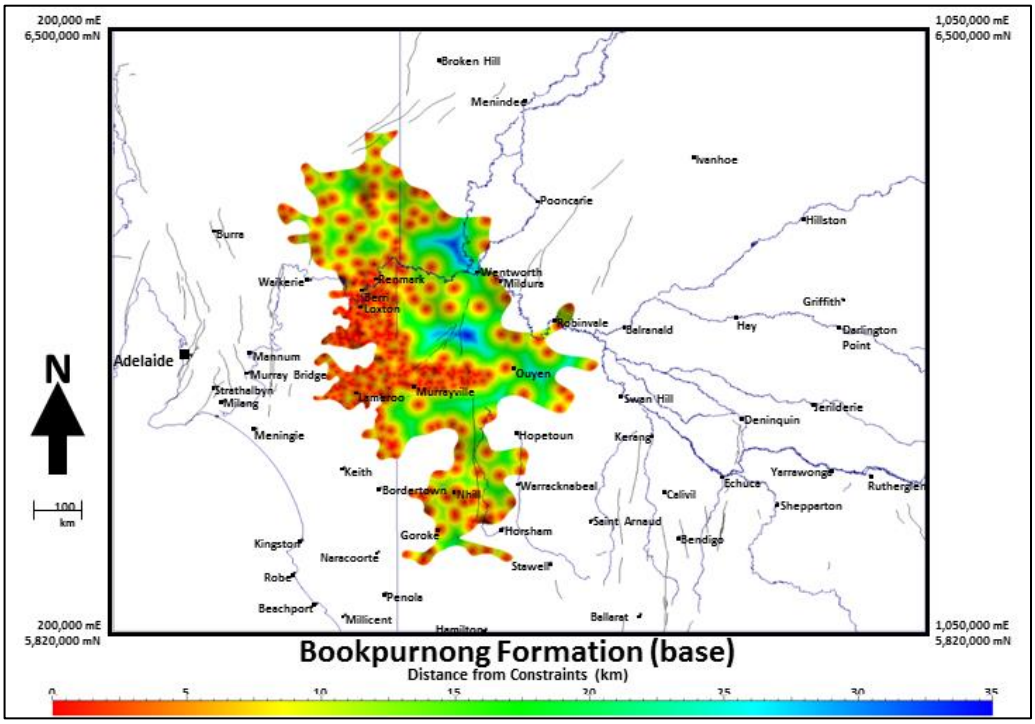
200,000 mE
6,500,000 mN
1,050,000 mE
6,500,000 mN
Broken Hill
Menindee
Ivanhoe
Pooncarie
Hillston
Burra
Wentworth
Mildura
Renmark
Waikerie
Berri
Loxton
Griffith
Robinvale
Balranald
Hay
Darlington Point
Adelaide
Mannum
Murray Bridge
Strathalbyn
Milang
Lameroo
Murrayville
Ouyen
Swan Hill
Jerilderie
Deniliquin
Meningie
Hopetoun
Kerang
Keith
Bordertown
Nhill
Warracknabeal
Echuca
Yarrawonga
Rutherglen
Celivil
Shepparton
Saint Arnaud
Horsham
Goroke
Bendigo
Kingston
Naracoorte
Stawell
Robe
Penola
Beachport
Millicent
Hamilton
Ballarat
200,000 mE
5,820,000 mN
1,050,000 mE
5,820,000 mN
N
100 km
Bookpurnong Formation (base)
Distance from Constraints (km)
0
5
10
15
20
25
30
35

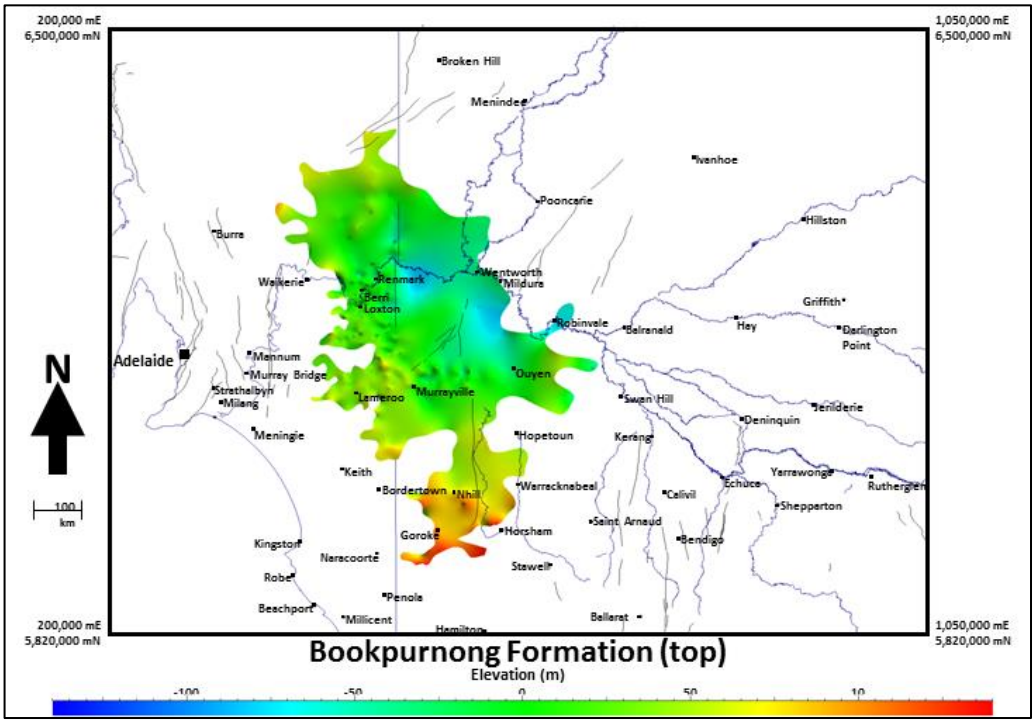
200,000 mE
6,500,000 mN
1,050,000 mE
6,500,000 mN
Broken Hill
Menindee
Ivanhoe
Pooncarie
Hillston
Burra
Wentworth
Mildura
Renmark
Waikerie
Berri
Loxton
Griffith
Robinvale
Balranald
Hay
Darlington Point
Adelaide
Mannum
Murray Bridge
Strathalbyn
Milang
Lameroo
Murrayville
Ouyen
Swan Hill
Jerilderie
Deniliquin
Meningie
Hopetoun
Kerang
Keith
Bordertown
Nhill
Warracknabeal
Echuca
Yarrawonga
Rutherglen
Celivil
Shepparton
Saint Arnaud
Horsham
Goroke
Bendigo
Kingston
Naracoorte
Stawell
Robe
Penola
Beachport
Millicent
Hamilton
Ballarat
200,000 mE
5,820,000 mN
1,050,000 mE
5,820,000 mN
N
100 km
Bookpurnong Formation (top)
Elevation (m)
-100
-50
0
50
100

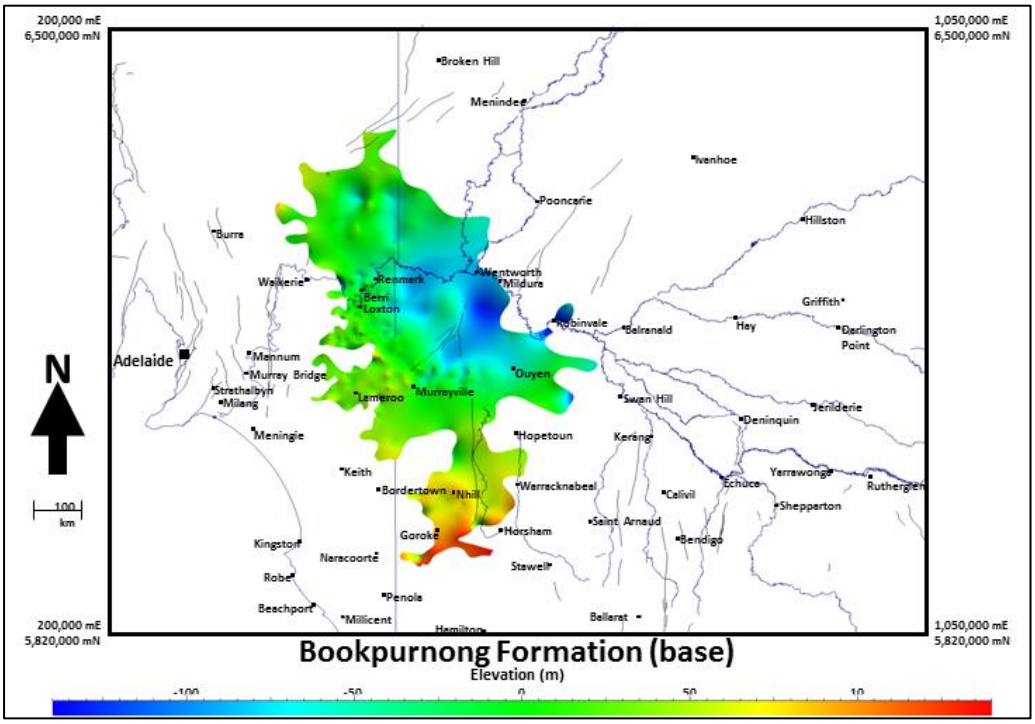
200,000 mE
6,500,000 mN
1,050,000 mE
6,500,000 mN
Broken Hill
Menindee
Ivenhoe
Pooncarie
Hillston
Burra
Wentworth
Mildura
Renmark
Berri
Loxton
Waikerie
Griffith
Robinvale
Balranald
Hay
Darlington Point
Adelaide
Mannum
Murray Bridge
Stathalbyn
Milang
Lameroo
Murrayville
Ouyen
Swan Hill
Deniliquin
Tenilderie
Meningie
Hopetoun
Kerang
Keith
Bordertown
Nhill
Warracknabeal
Echuca
Yarrawonga
Rutherglen
Calivil
Shepparton
Saint Arnaud
Bendigo
Horsham
Goroke
Kingston
Naracoorte
Stawell
Robe
Penola
Beachport
Millicent
Hamilton
Ballarat
N
100 km
200,000 mE
5,820,000 mN
1,050,000 mE
5,820,000 mN
Bookpurnong Formation (base)
Elevation (m)
-100
-50
0
50
100

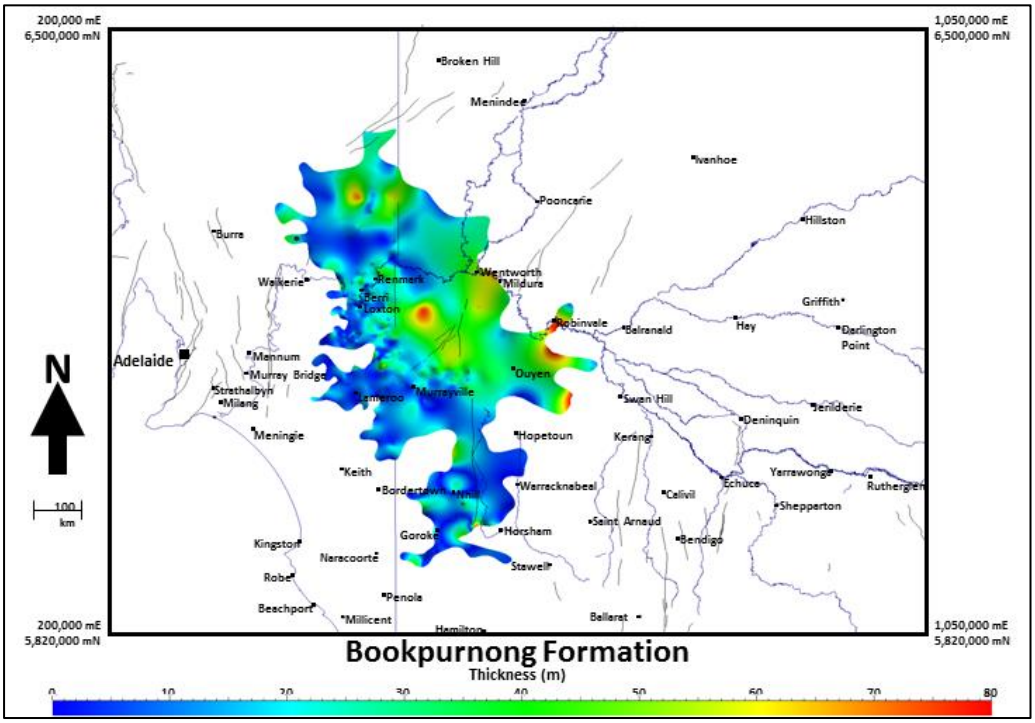
200,000 mE
6,500,000 mN
1,050,000 mE
6,500,000 mN
Broken Hill
Menindee
Ivenhoe
Pooncarie
Hillston
Burra
Wentworth
Mildura
Renmark
Berri
Loxton
Waikerie
Griffith
Robinvale
Balranald
Hay
Darlington Point
Adelaide
Mannum
Murray Bridge
Stathalbyn
Milang
Lameroo
Murrayville
Ouyen
Swan Hill
Deniliquin
Tenilderie
Meningie
Hopetoun
Kerang
Keith
Bordertown
Nhill
Warracknabeal
Echuca
Yarrawonga
Rutherglen
Calivil
Shepparton
Saint Arnaud
Bendigo
Horsham
Goroke
Kingston
Naracoorte
Stawell
Robe
Penola
Beachport
Millicent
Hamilton
Ballarat
N
100 km
200,000 mE
5,820,000 mN
1,050,000 mE
5,820,000 mN
Bookpurnong Formation
Thickness (m)
0
10
20
30
40
50
60
70
80

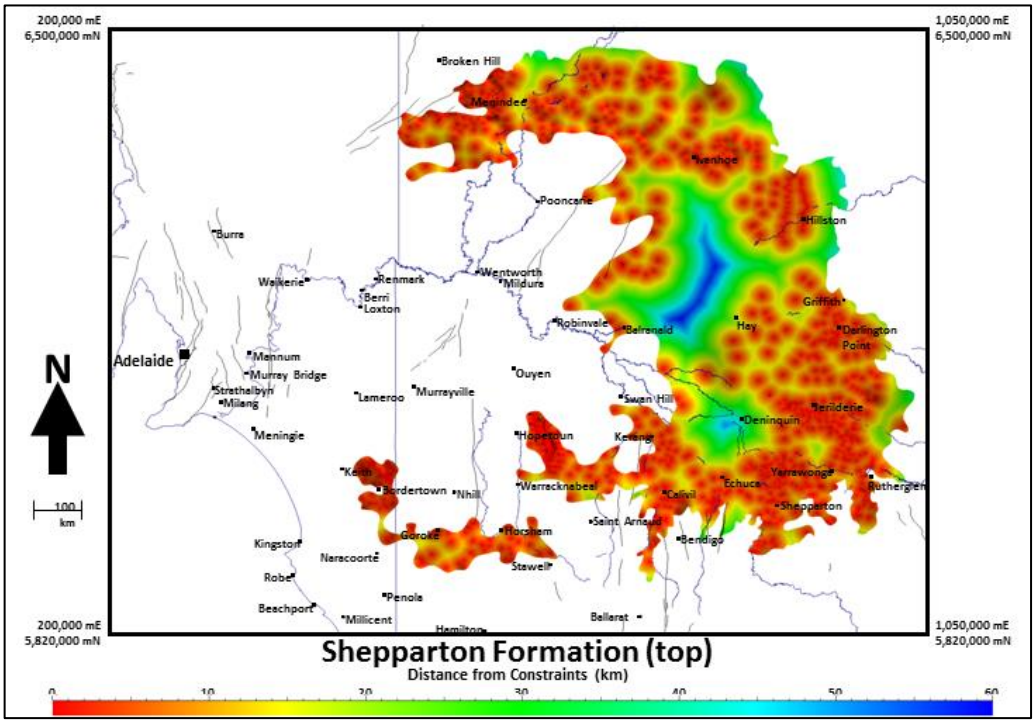
200,000 mE
6,500,000 mN
1,050,000 mE
6,500,000 mN
Broken Hill
Menindee
Ivanhoe
Pooncarie
Hillston
Burra
Wentworth
Mildura
Renmark
Berri
Loxton
Waikerie
Griffith
Robinvale
Hay
Darlington Point
Adelaide
Mannum
Murray Bridge
Strathalbyn
Milang
Lameroo
Murrayville
Ouyen
Swan Hill
Ierilderie
Deniliquin
Meningie
Hopetoun
Kerang
Keith
Bordertown
Nhill
Warracknabeal
Yarrawonga
Rutherglen
Echuca
Calivil
Shepparton
Saint Arnaud
Bendigo
Horsham
Goroke
Kingston
Naracoorte
Stawell
Robe
Penola
Beachport
Millicent
Hamilton
Ballarat
N
100
km
200,000 mE
5,820,000 mN
1,050,000 mE
5,820,000 mN
Shepparton Formation (top)
Distance from Constraints (km)
0
10
20
30
40
50
60

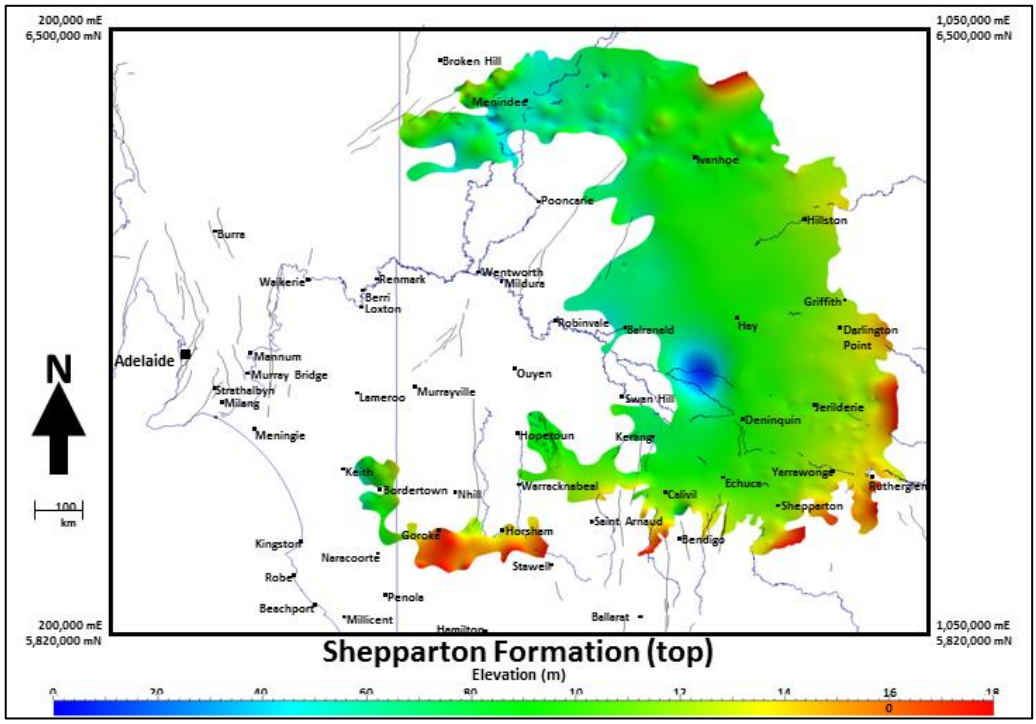
200,000 mE
6,500,000 mN
1,050,000 mE
6,500,000 mN
Broken Hill
Menindee
Ivanhoe
Pooncarie
Hillston
Burra
Wentworth
Mildura
Renmark
Berri
Loxton
Waikerie
Griffith
Robinvale
Hay
Darlington Point
Adelaide
Mannum
Murray Bridge
Strathalbyn
Milang
Lameroo
Murrayville
Ouyen
Swan Hill
Ierilderie
Deniliquin
Meningie
Hopetoun
Kerang
Keith
Bordertown
Nhill
Warracknabeal
Yarrawonga
Rutherglen
Echuca
Calivil
Shepparton
Saint Arnaud
Bendigo
Horsham
Goroke
Kingston
Naracoorte
Stawell
Robe
Penola
Beachport
Millicent
Hamilton
Ballarat
N
100
km
200,000 mE
5,820,000 mN
1,050,000 mE
5,820,000 mN
Shepparton Formation (top)
Elevation (m)
0
20
40
60
80
10
12
14
16
18
0

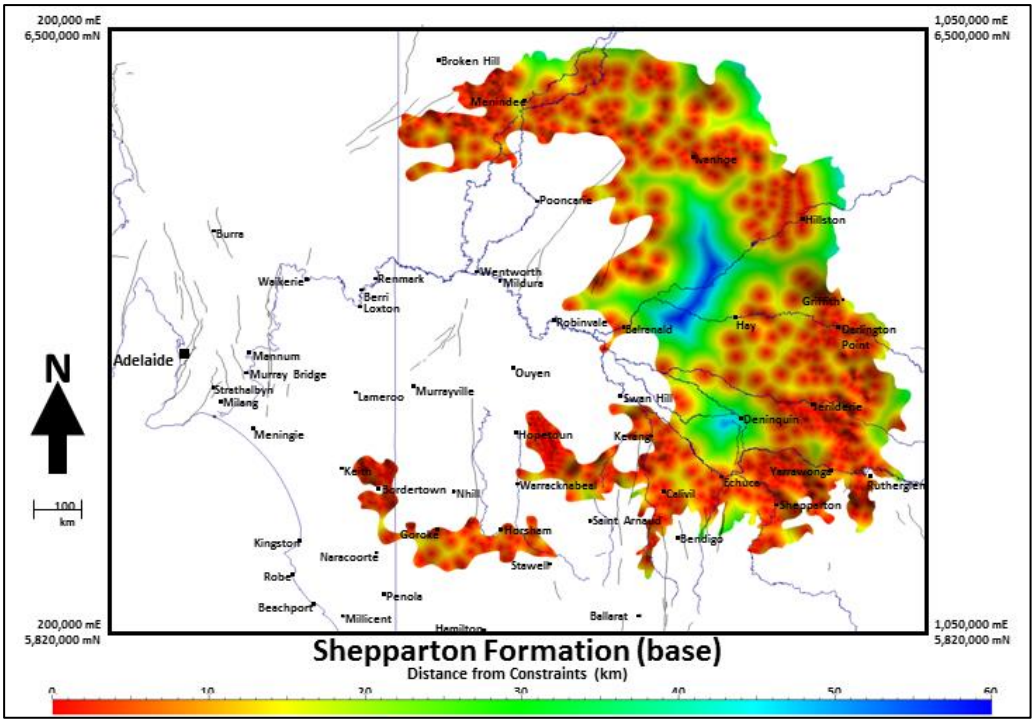
200,000 mE
6,500,000 mN
1,050,000 mE
6,500,000 mN
Broken Hill
Menindee
Ivanhoe
Pooncarie
Hillston
Burra
Wentworth
Renmark
Mildura
Waikerie
Berri
Loxton
Griffith
Robinvale
Hay
Darlington Point
Adelaide
Mannum
Murray Bridge
Strathalbyn
Milang
Lameroo
Murrayville
Ouyen
Swan Hill
Deniliquin
Meningie
Hopetoun
Kerang
Keith
Bordertown
Nhill
Warracknabeal
Echuca
Yarrawonga
Rutherglen
Calivil
Shepparton
Saint Arnaud
Horsham
Bendigo
Kingston
Naracoorte
Stawell
Robe
Penola
Beachport
Millicent
Hamilton
Ballarat
200,000 mE
5,820,000 mN
1,050,000 mE
5,820,000 mN
N
100 km
Shepparton Formation (base)
Distance from Constraints (km)
0
10
20
30
40
50
60

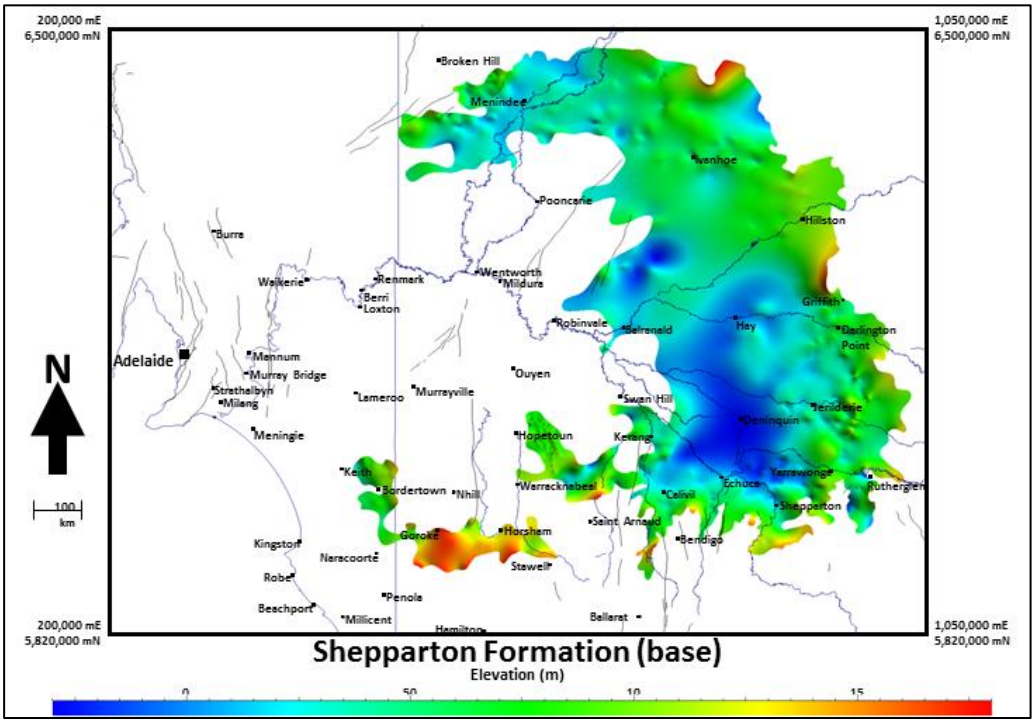
200,000 mE
6,500,000 mN
1,050,000 mE
6,500,000 mN
Broken Hill
Menindee
Ivanhoe
Pooncarie
Hillston
Burra
Wentworth
Renmark
Mildura
Waikerie
Berri
Loxton
Griffith
Robinvale
Hay
Darlington Point
Adelaide
Mannum
Murray Bridge
Strathalbyn
Milang
Lameroo
Murrayville
Ouyen
Swan Hill
Deniliquin
Meningie
Hopetoun
Kerang
Keith
Bordertown
Nhill
Warracknabeal
Echuca
Yarrawonga
Rutherglen
Calivil
Shepparton
Saint Arnaud
Horsham
Bendigo
Kingston
Naracoorte
Stawell
Robe
Penola
Beachport
Millicent
Hamilton
Ballarat
200,000 mE
5,820,000 mN
1,050,000 mE
5,820,000 mN
N
100 km
Shepparton Formation (base)
Elevation (m)
0
50
10
15

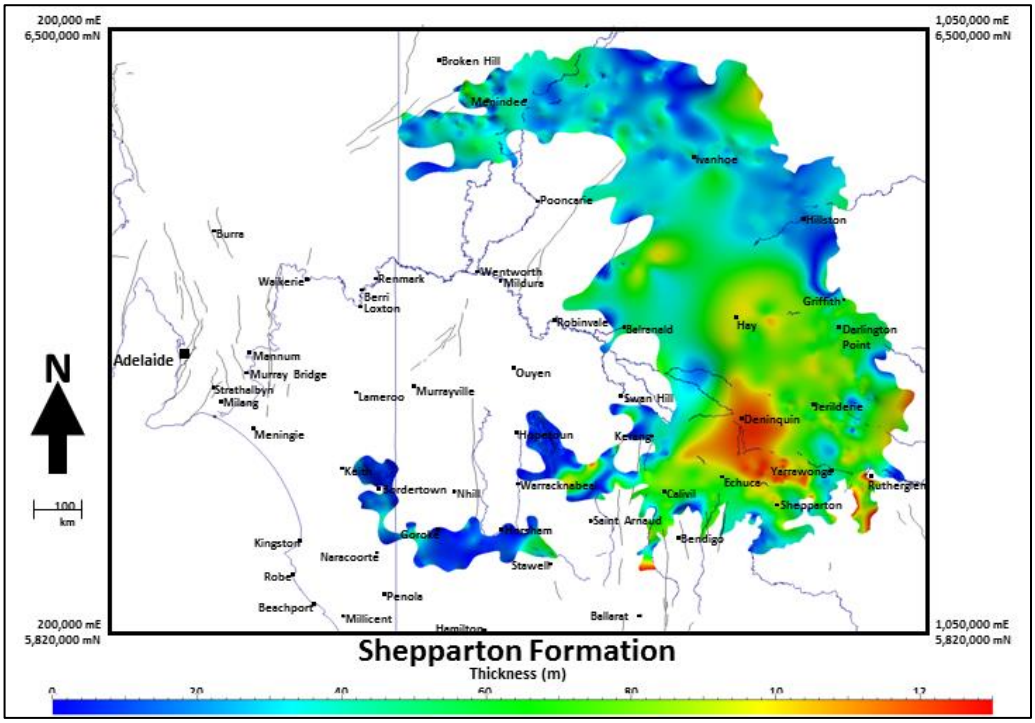
200,000 mE
6,500,000 mN
1,050,000 mE
6,500,000 mN
Broken Hill
Menindee
Ivanhoe
Pooncarie
Hillston
Burre
Wentworth
Mildura
Renmark
Berri
Loxton
Griffith
Robinvale
Hay
Darlington Point
Adelaide
Mannum
Murray Bridge
Strathalbyn
Milang
Lameroo
Murrayville
Ouyen
Swan Hill
Deniliquin
Tooleybuc
Meningie
Hopetoun
Kerang
Yarrawonga
Echuca
Rutherglen
Bordertown
Nhill
Warracknabeal
Calivil
Shepparton
Saint Arnaud
Bendigo
Kingston
Naracoorte
Stawell
Robe
Penola
Beachport
Millicent
Ballarat
Hamilton
N
100 km
200,000 mE
5,820,000 mN
1,050,000 mE
5,820,000 mN
Shepparton Formation
Thickness (m)
0
20
40
60
80
100
120

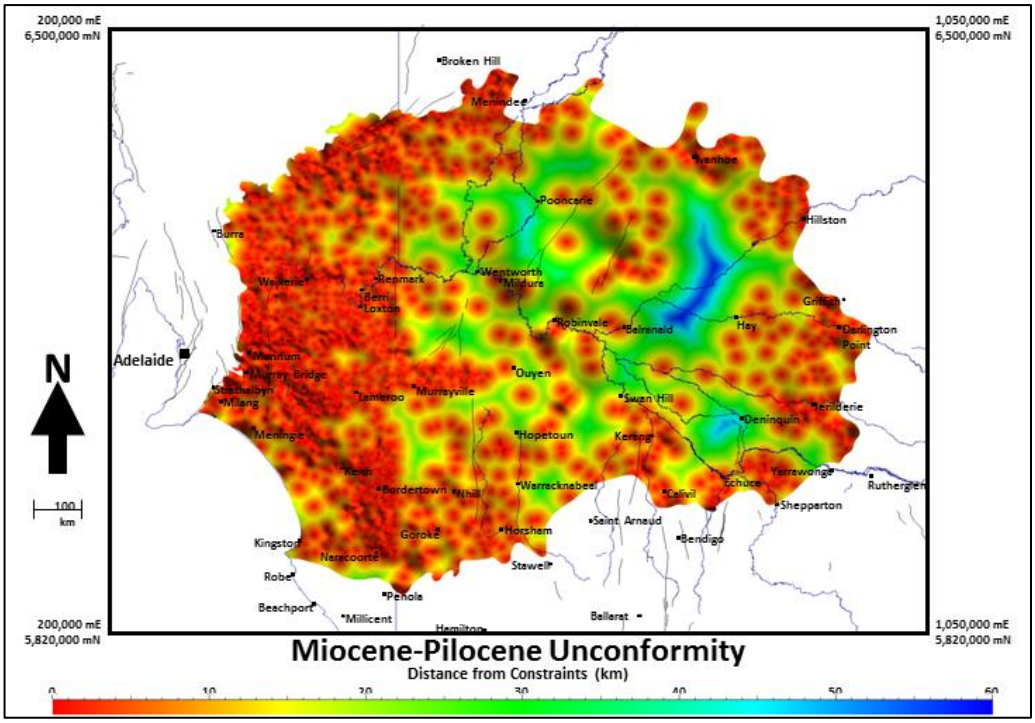
200,000 mE
6,500,000 mN
1,050,000 mE
6,500,000 mN
Broken Hill
Menindee
Ivanhoe
Pooncarie
Hillston
Burre
Wentworth
Mildura
Renmark
Berri
Loxton
Griffith
Robinvale
Hay
Darlington Point
Adelaide
Mannum
Murray Bridge
Strathalbyn
Milang
Lameroo
Murrayville
Ouyen
Swan Hill
Deniliquin
Tooleybuc
Meningie
Hopetoun
Kerang
Yarrawonga
Echuca
Rutherglen
Bordertown
Nhill
Warracknabeal
Calivil
Shepparton
Saint Arnaud
Bendigo
Kingston
Naracoorte
Stawell
Robe
Penola
Beachport
Millicent
Ballarat
Hamilton
N
100 km
200,000 mE
5,820,000 mN
1,050,000 mE
5,820,000 mN
Miocene-Pilocene Unconformity
Distance from Constraints (km)
0
10
20
30
40
50
60

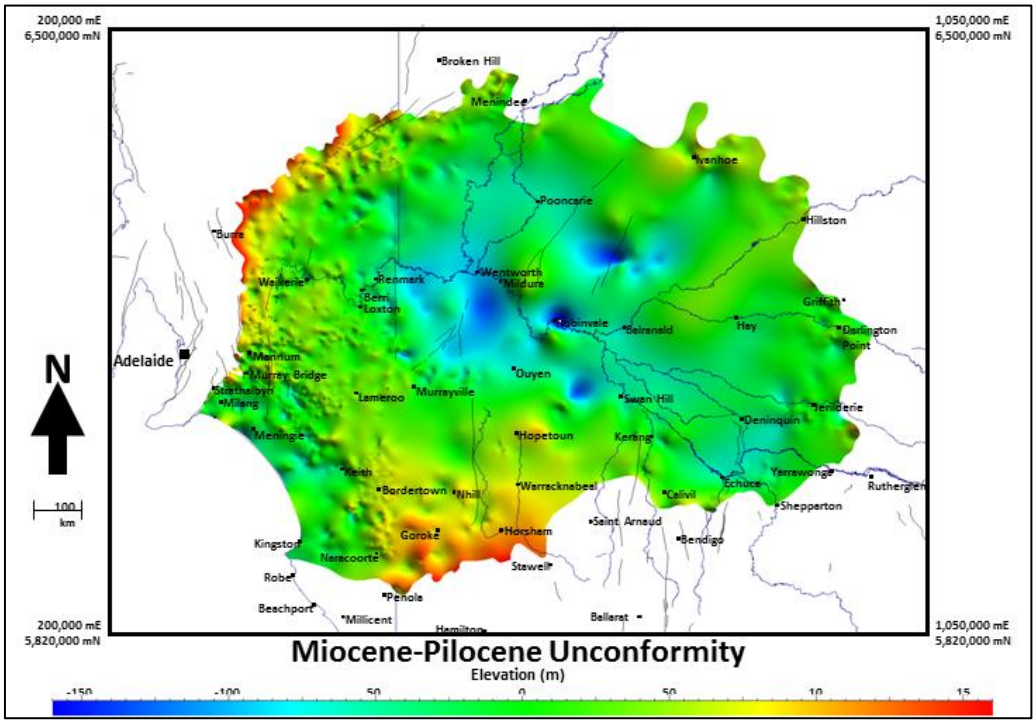

Acknowledgements

The work has been supported by the Deep Exploration Technologies CRC whose activities are funded by the Australian Government's CRC Programme.

This is DET CRC Presentation 2014/523

Appendix D – Petrographic thin sections

SMM01
Profile: Spicer's Pit
Sample: SP01
654135 mE 6006077 mN

SMM02
Profile: Spicer's Pit
Sample: SP03
654135 mE 6006077 mN

SMM03
Profile: Spicer's Pit
Sample: SP10
654135 mE 6006077 mN

SMM04
Profile: Overland Corner
Sample: OLC10
438788 mE 6221631 mN

SMM05
Profile: Wannon
Sample: WA07
584775 mE 5832102 mN

SMM06
Profile: Lyrup
Sample: LYR15
467260 mE 6211224 mN

SMM07
Profile: Hewitt Pit
Sample: HP03
641063 mE 5998612 mN

SMM09
Profile: Goroke
Sample: GOR06
546475 mE 5935480 mN

SMM10
Profile: Diapur
Sample: DIA10, DIA11
537057 mE 5979858 mN

SMM11
Profile: Ultima
Sample: UQ10
708327 mE 6075854 mN

SMM12
Profile: Ultima
Sample: UQ08
708327 mE 6075854 mN

Appendix E – Results of electron microprobe major element mapping

Section: SMM01

Map 1:

- 128 x 128 pixels
- 2 µm pixels
- 50 ms dwell time
- 16 minutes acquisition time

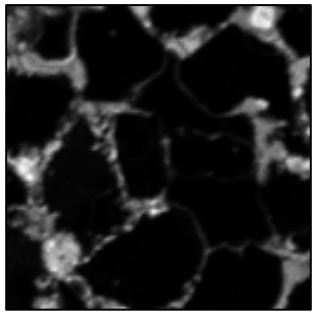

Al

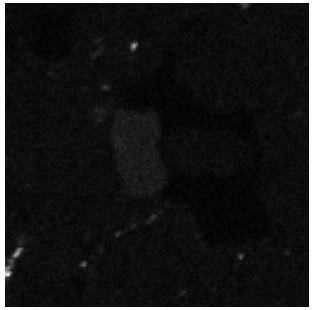

Ba

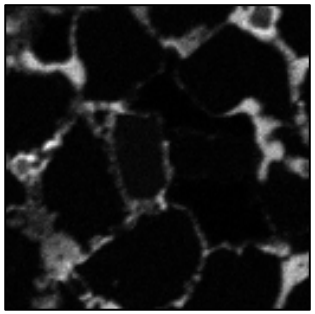

Fe

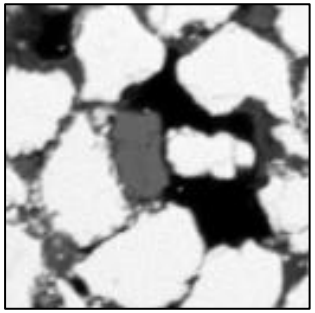

Si

Ti

Map 2:

- 512 x 512 pixels
- 2 µm pixels
- 50 ms dwell time
- 260 minutes acquisition time

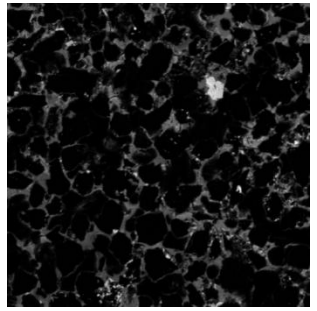

Al

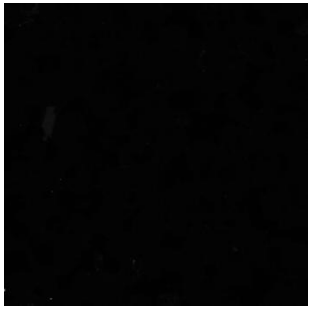

Ba

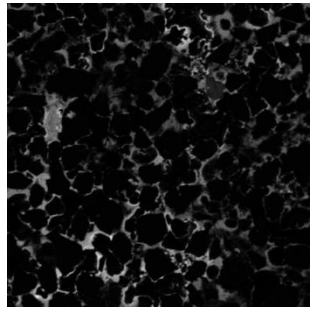

Fe

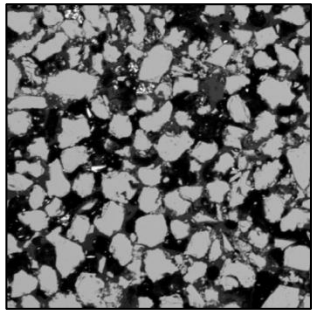

Si

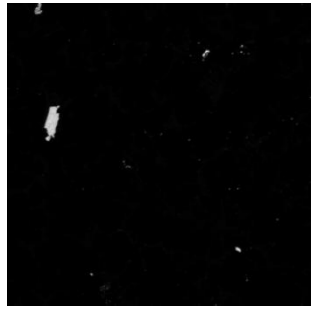

Ti

Section: SMM02

Map 1:

- 30 x 300 pixels
- 1 µm pixels
- 50 ms dwell time
- 90 minutes acquisition time

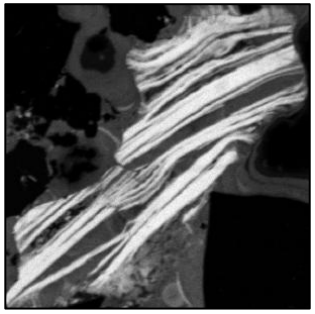

Al

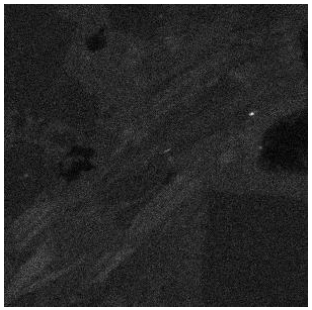

Ba

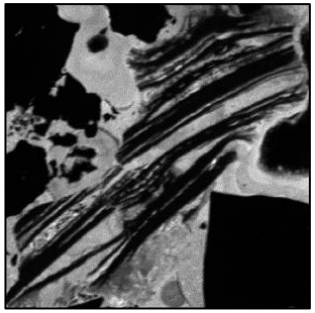

Fe

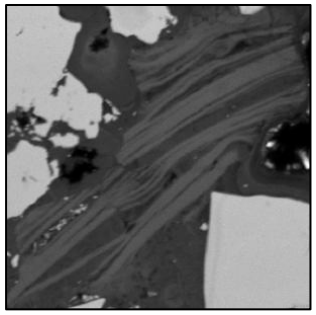

Si

Ti

Map 2:

- 90 x 90 pixels
- 1 µm pixels
- 50 ms dwell time
- 8 minutes acquisition time

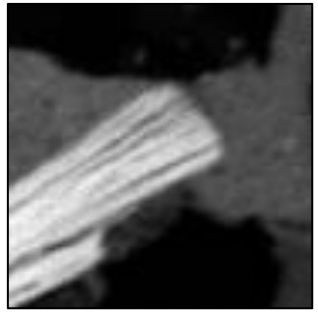

Al

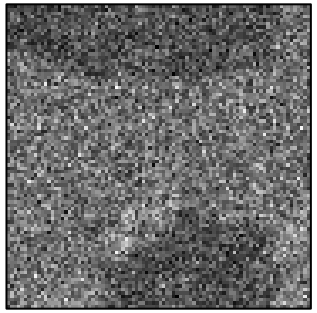

Ba

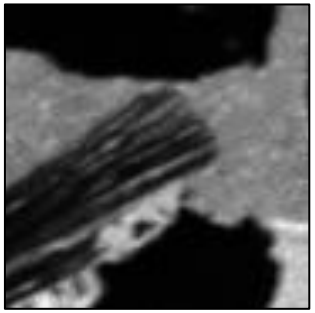

Fe

Si

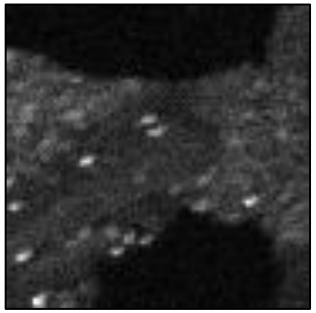

Ti

Section: SMM02 (continued)

Map 3:

- 350 x 600 pixels
- 3 µm pixels
- 50 ms dwell time
- 195 minutes acquisition time

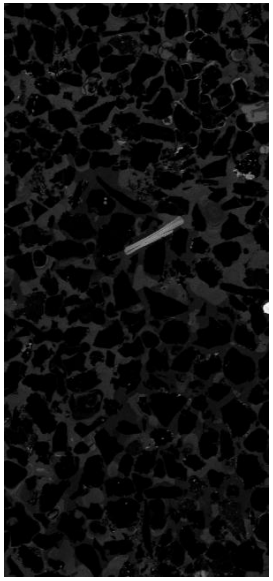

Al

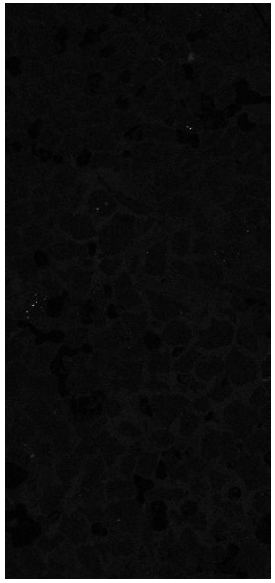

Ba

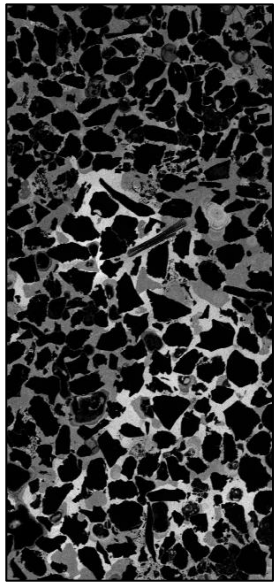

Fe

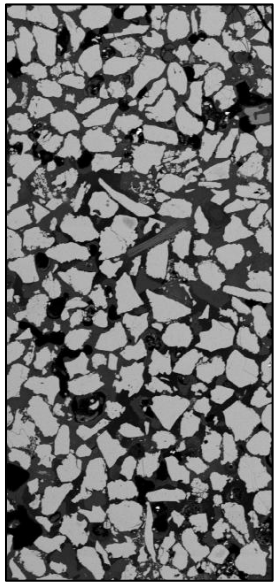

Si

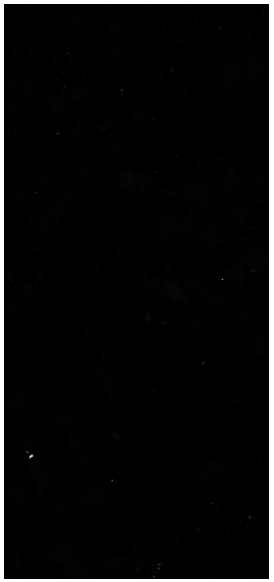

Ti

Section: SMM03

Map 1:

- 1024 x 1024 pixels
- 4 µm pixels
- 50 ms dwell time
- 1050 minutes acquisition time

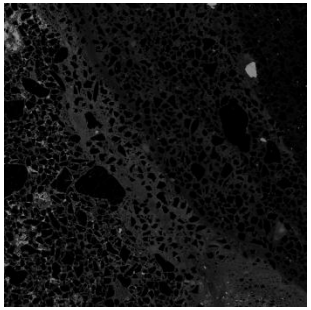

Al

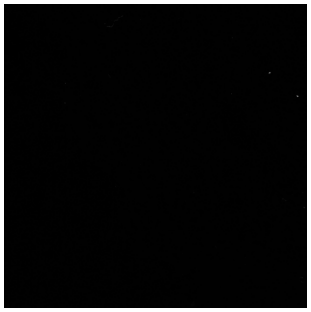

Ba

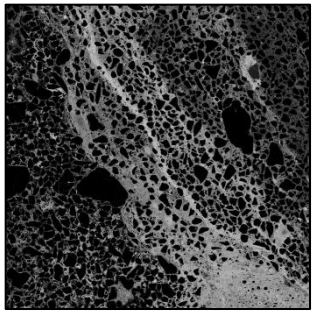

Fe

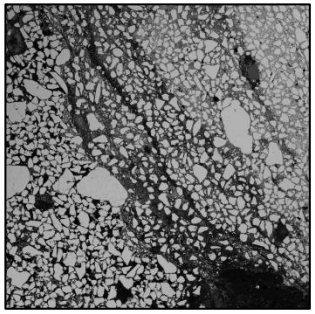

Si

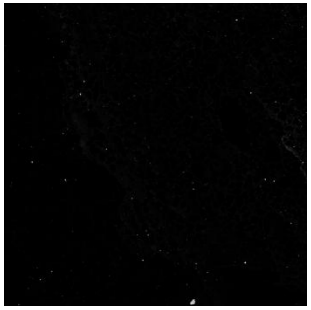

Ti

Map 2:

- 512 x 512 pixels
- 2 µm pixels
- 50 ms dwell time
- 270 minutes acquisition time

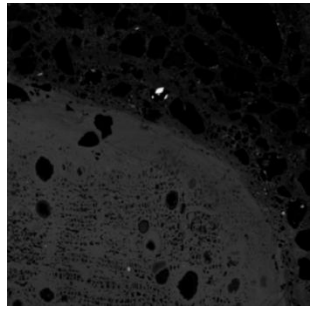

Al

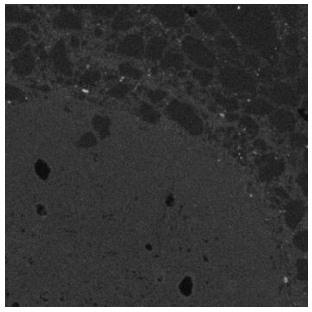

Ba

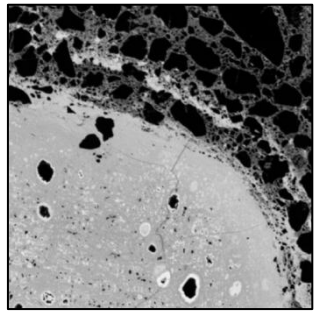

Fe

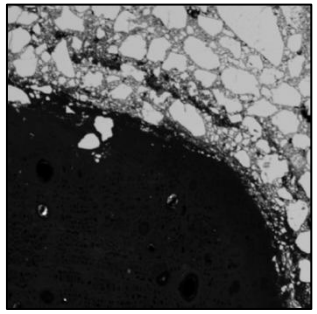

Si

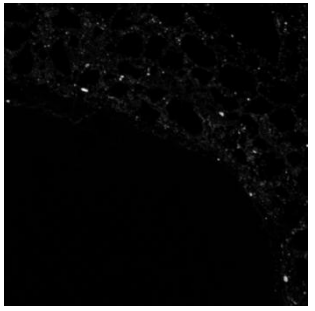

Ti

Section: SMM03 (continued)

Map 3:

- 900 x 900 pixels
- 4 µm pixels
- 50 ms dwell time
- 810 minutes acquisition time

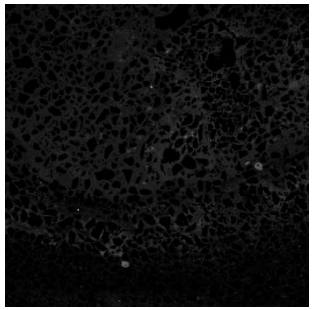

Al

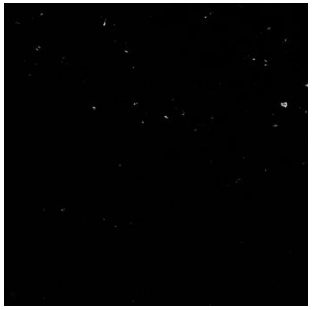

Ba

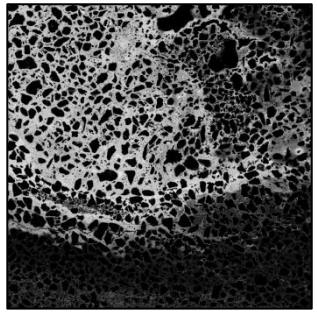

Fe

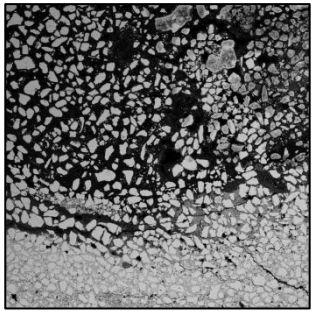

Si

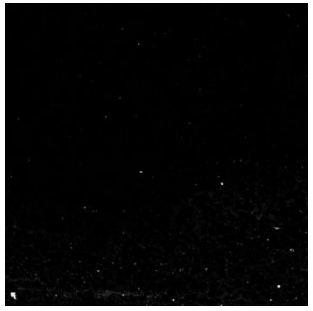

Ti

Map 4:

- 500 x 600 pixels
- 2 µm pixels
- 50 ms dwell time
- 300 minutes acquisition time

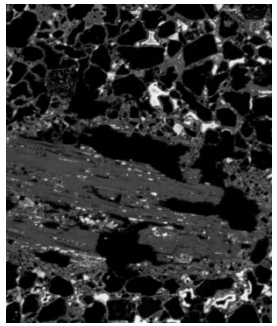

Al

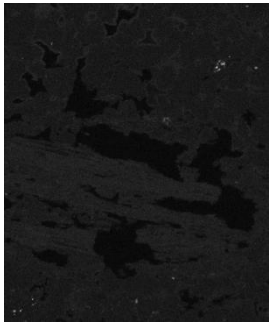

Ba

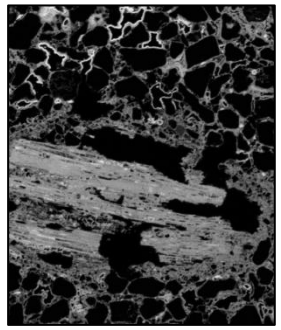

Fe

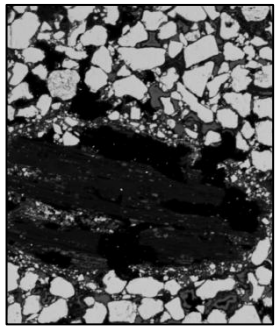

Si

Ti

Section: SMM03 (continued)

Map 5:

- 920 x 920 pixels
- 4 µm pixels
- 50 ms dwell time
- 840 minutes acquisition time

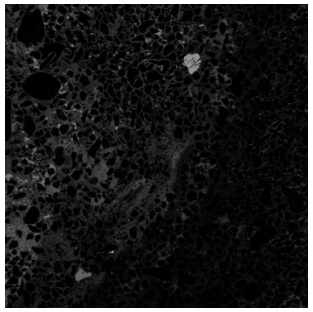

Al

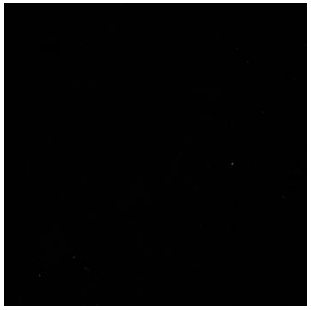

Ba

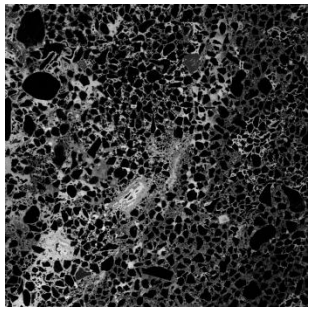

Fe

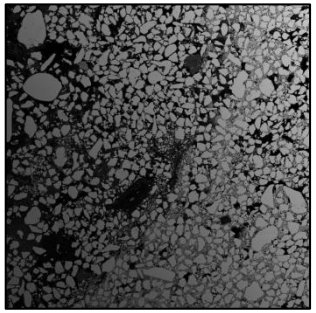

Si

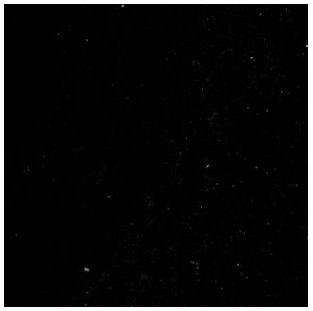

Ti

Section: SMM04

Map 1:

- 128 x 128 pixels
- 1 µm pixels
- 50 ms dwell time
- 20 minutes acquisition time

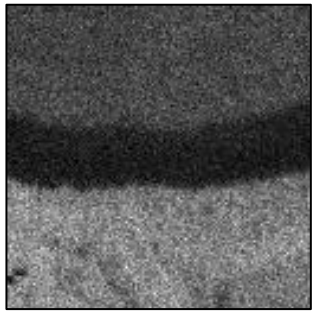

Al

Ba

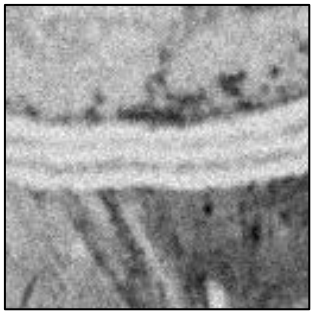

Fe

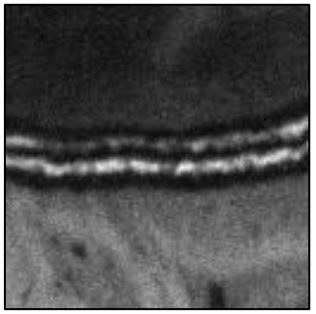

Si

Ti

Map 2:

- 450 x 450 pixels
- 1 µm pixels
- 80 ms dwell time
- 330 minutes acquisition time

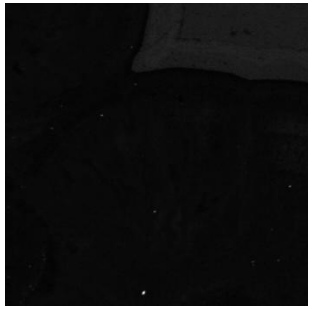

Al

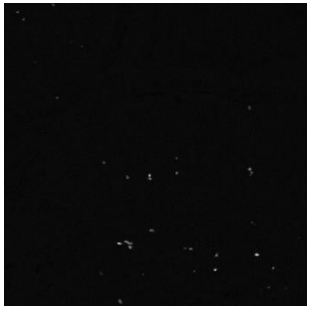

Ba

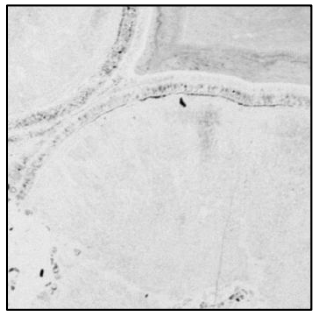

Fe

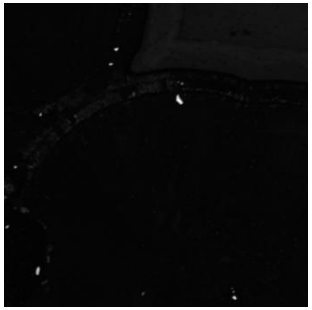

Si

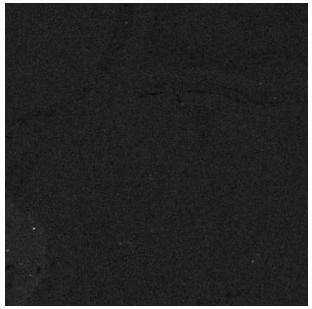

Ti

Section: SMM05

Map 1:

- 128 x 128 pixels
- 10 µm pixels
- 50 ms dwell time
- 16 minutes acquisition time

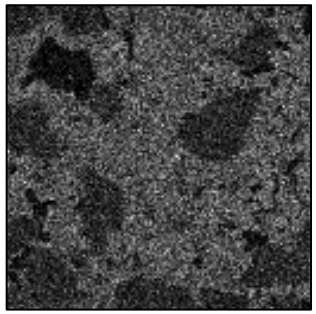

As

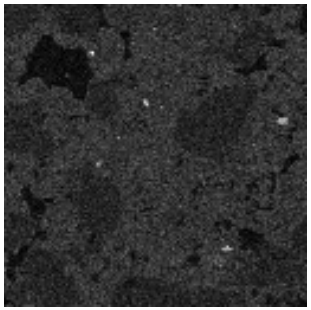

Ba

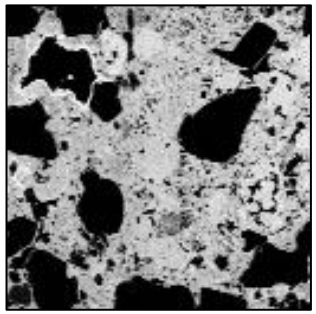

Fe

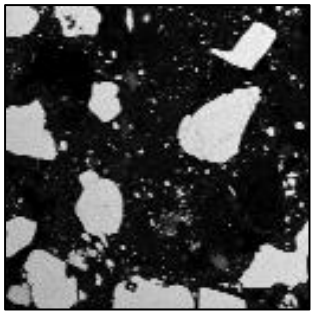

Si

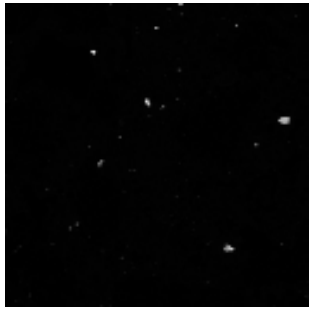

Ti

Map 2:

- 128 x 128 pixels
- 10 µm pixels
- 50 ms dwell time
- 16 minutes acquisition time

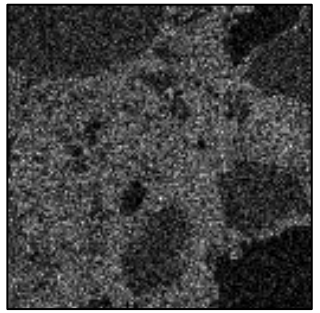

As

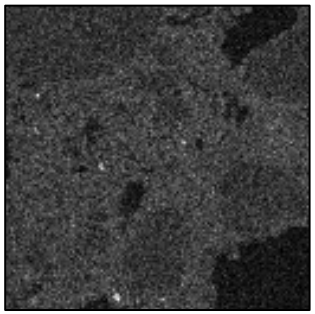

Ba

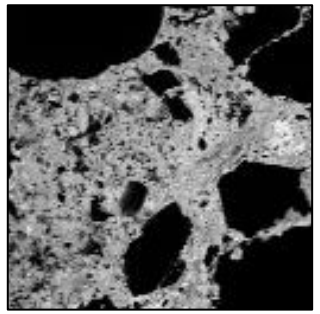

Fe

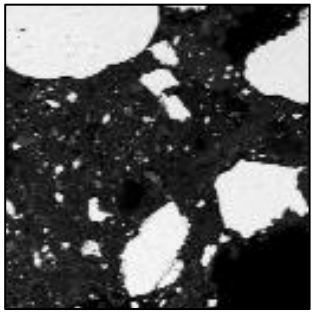

Si

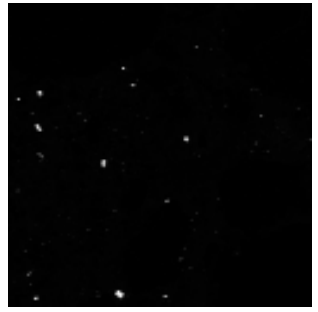

Ti

Section: SMM05 (continued)

Map 3:

- 400 x 400 pixels
- 4 µm pixels
- 80 ms dwell time
- 256 minutes acquisition time

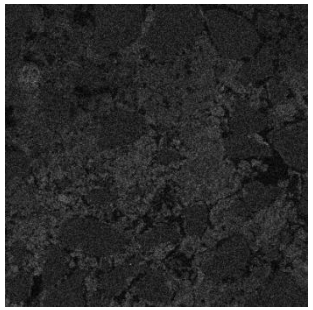

As

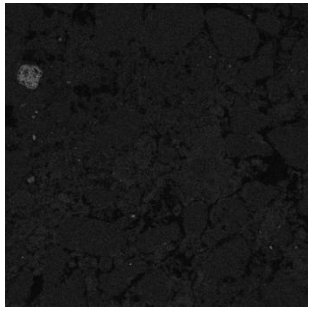

Ba

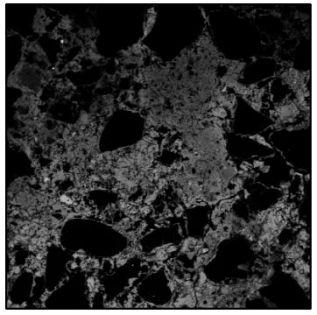

Fe

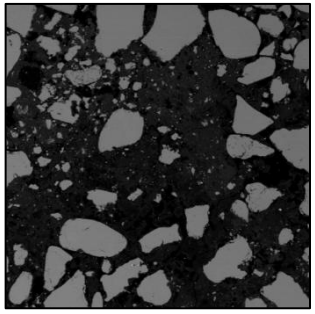

Si

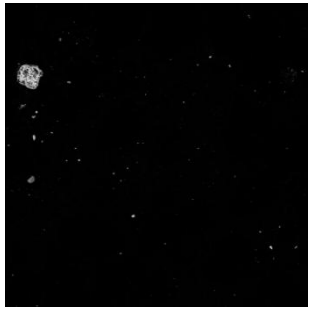

Ti

Map 4:

- 800 x 800 pixels
- 5 µm pixels
- 80 ms dwell time
- 1024 minutes acquisition time

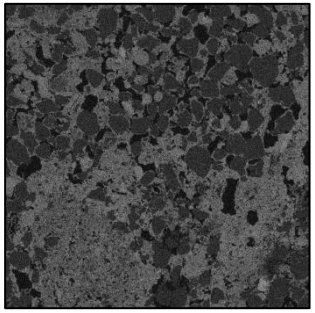

As

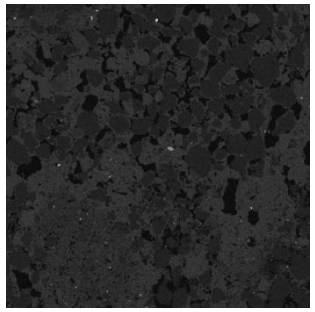

Ba

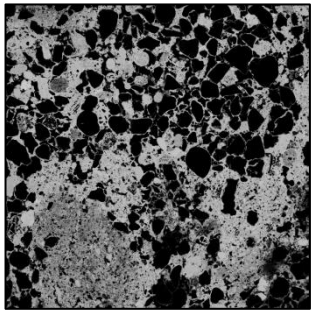

Fe

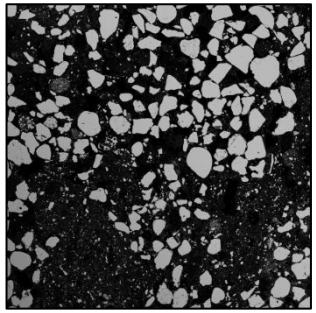

Si

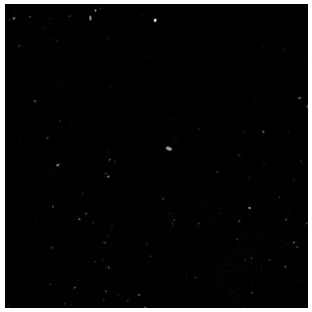

Ti

Section: SMM05 (continued)

Map 5:

- 450 x 1500 pixels
- 5 µm pixels
- 50 ms dwell time
- 690 minutes acquisition time

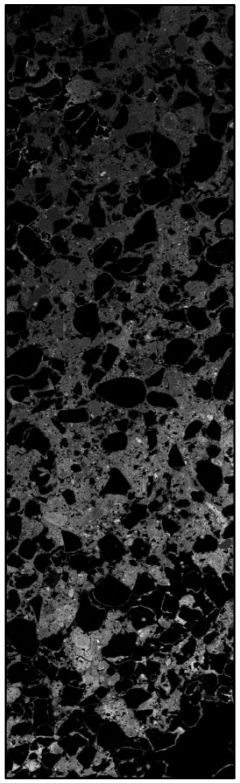

Al

Ba

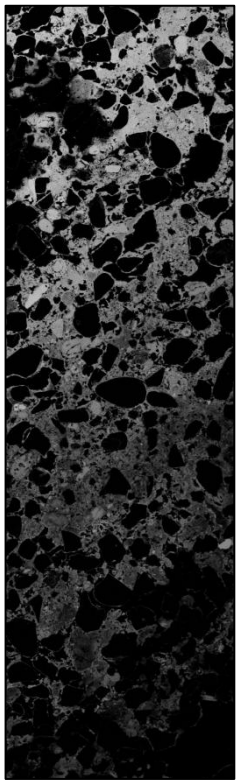

Fe

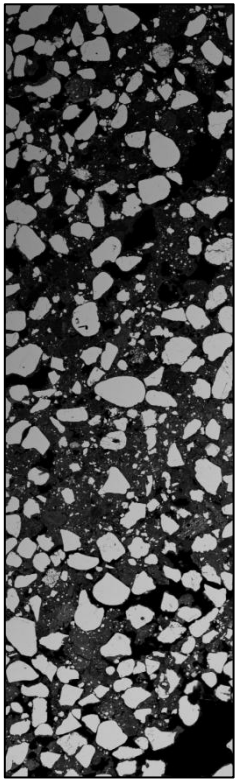

Si

Ti

Section: SMM06

Map 1:

- 1024 x 1024 pixels
- 4 µm pixels
- 50 ms dwell time
- 1050 minutes acquisition time

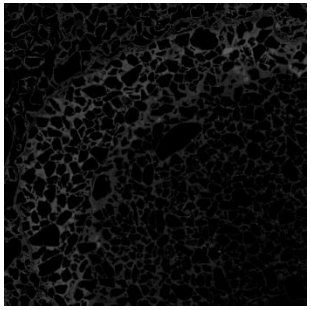

Al

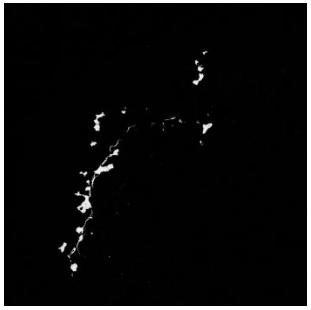

Ba

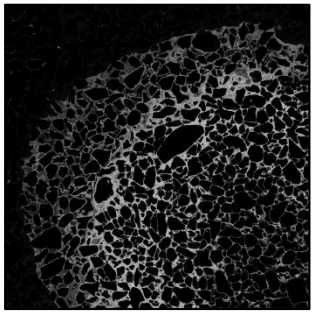

Fe

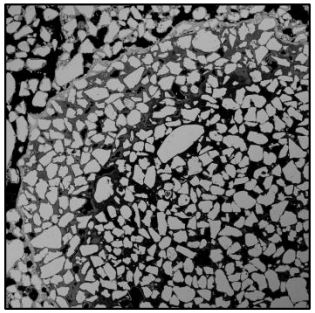

Si

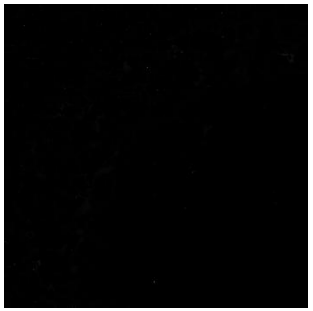

Ti

Map 2:

- 150 x 150 pixels
- 2 µm pixels
- 50 ms dwell time
- 22 minutes acquisition time

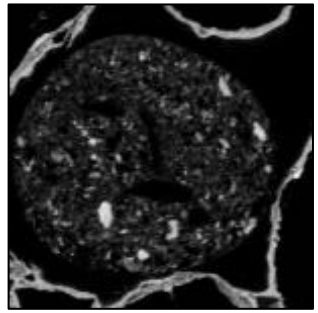

Al

Ba

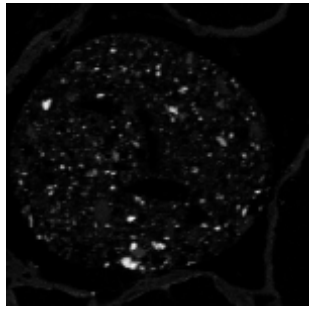

Fe

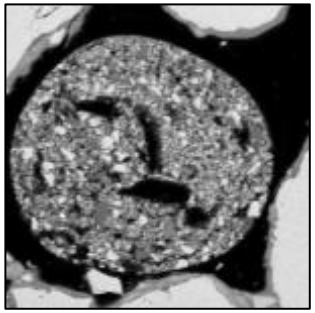

Si

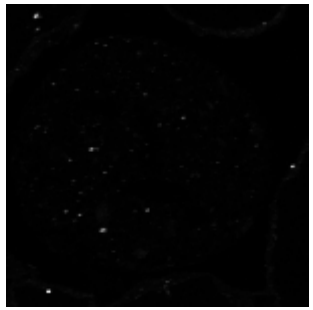

Ti

Section: SMM06 (continued)

Map 3:

- 1024 x 1024 pixels
- 4 µm pixels
- 50 ms dwell time
- 1050 minutes acquisition time

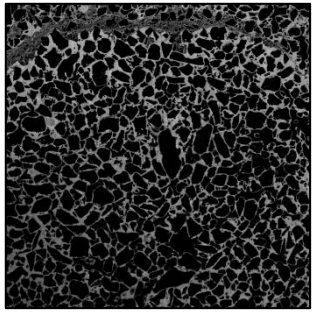

Al

Ba

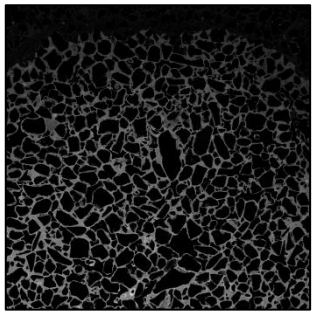

Fe

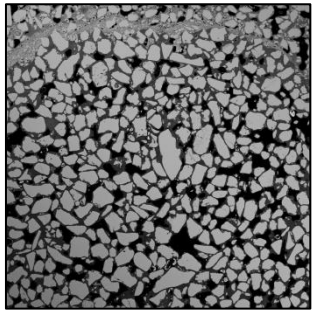

Si

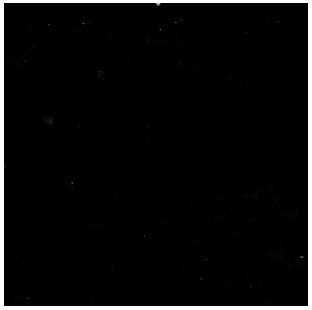

Ti

Map 4:

- 128 x 128 pixels
- 3µm pixels
- 50 ms dwell time
-
- 16 minutes acquisition time

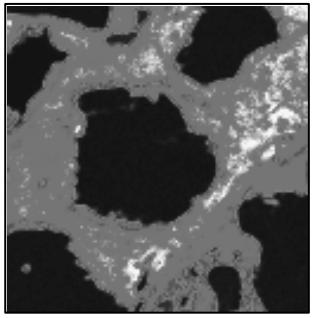

Al

Ba

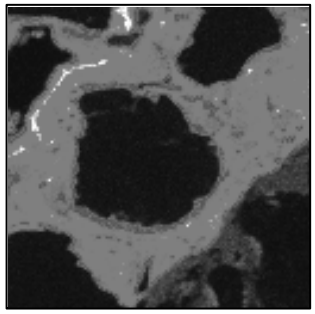

Fe

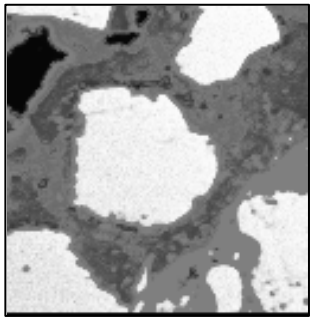

Si

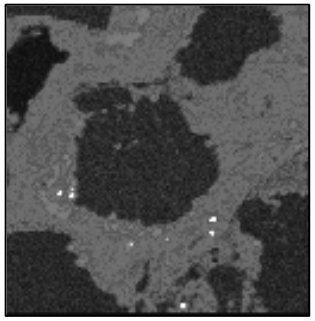

Ti

Section: SMM06 (continued)

Map 5:

- 850 x 850 pixels
- 4 µm pixels
- 50 ms dwell time
- 720 minutes acquisition time

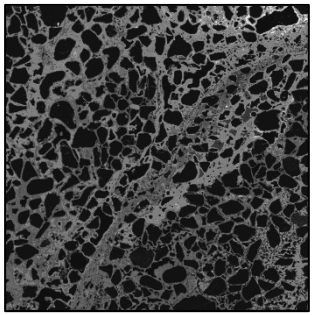

Al

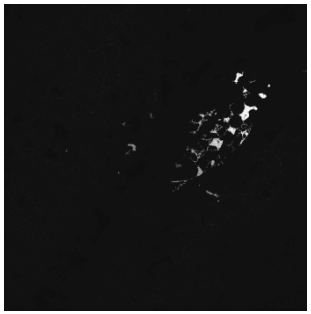

Ba

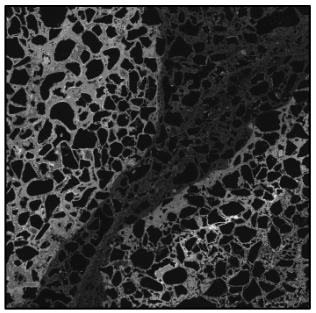

Fe

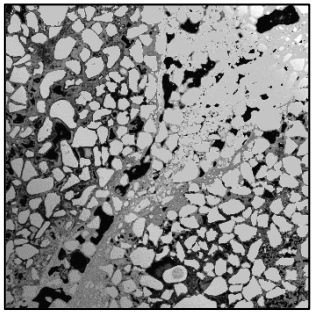

Si

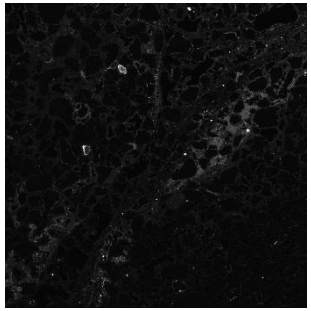

Ti

Map 6:

- 1000 x 400 pixels
- 4 µm pixels
- 50 ms dwell time
- 390 minutes acquisition time

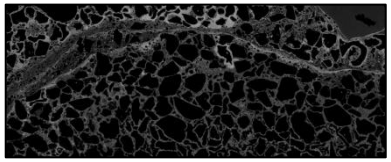

Al

Ba

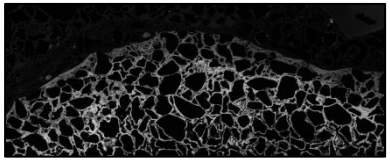

Fe

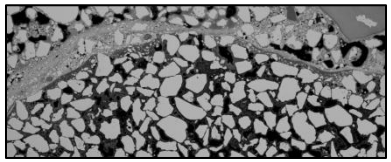

Si

Ti

Section: SMM07

Map 1:

- 512 x 512 pixels
- 3 µm pixels
- 50 ms dwell time
- 262 minutes acquisition time

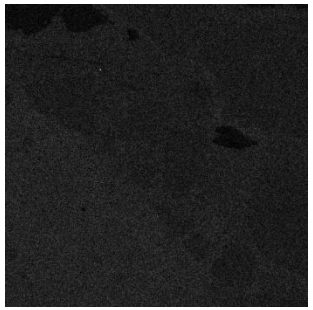

Al

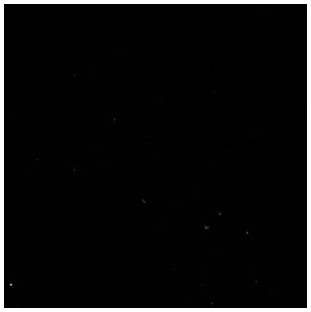

Ba

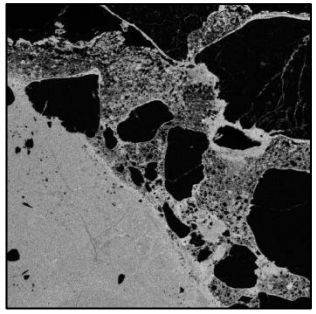

Fe

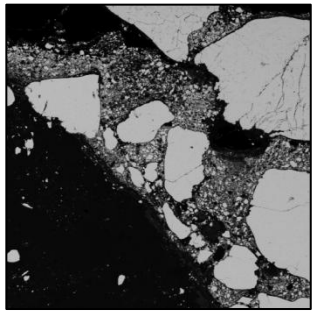

Si

Ti

Map 2:

- 950 x 950 pixels
- 3 µm pixels
- 50 ms dwell time
- 900 minutes acquisition time

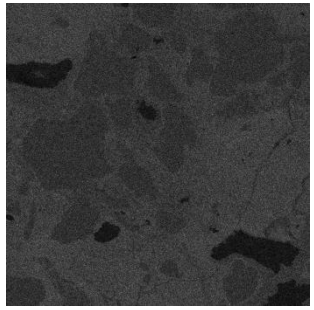

Al

Ba

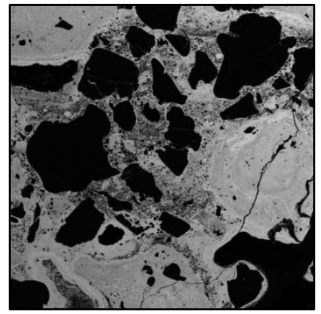

Fe

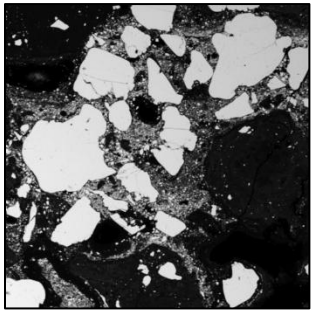

Si

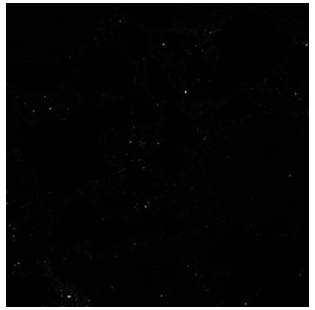

Ti

Section: SMM09

Map 1:

- 600 x 300 pixels
- 4 µm pixels
- 50 ms dwell time
- 180 minutes acquisition time

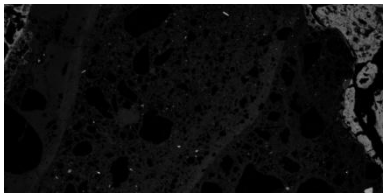

Al

Ba

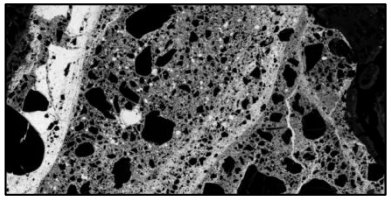

Fe

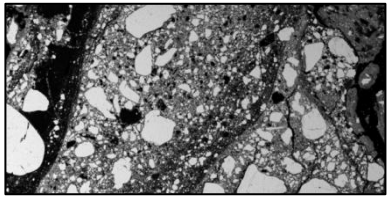

Si

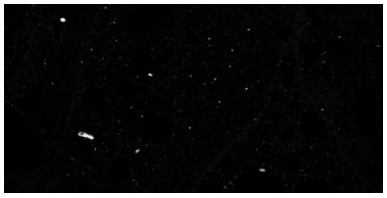

Ti

Map 2:

- 300 x 300 pixels
- 4 µm pixels
- 50 ms dwell time
- 90 minutes acquisition time

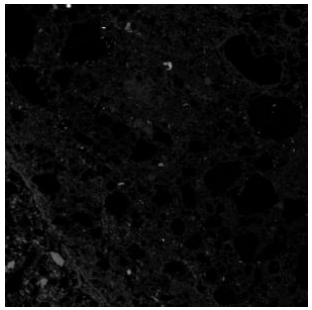

Al

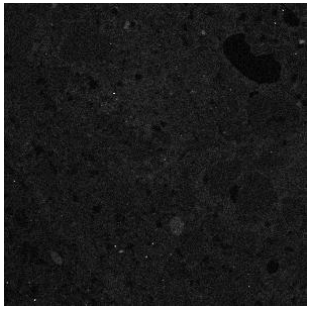

Ba

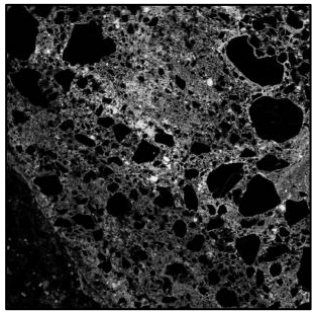

Fe

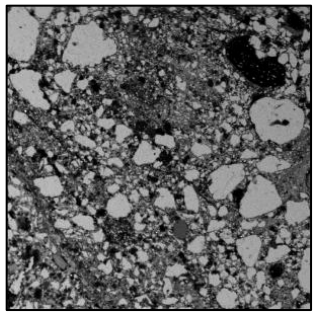

Si

Ti

Section: SMM09 (continued)

Map 3:

- 300 x 300 pixels
- 4 µm pixels
- 50 ms dwell time
- 90 minutes acquisition time

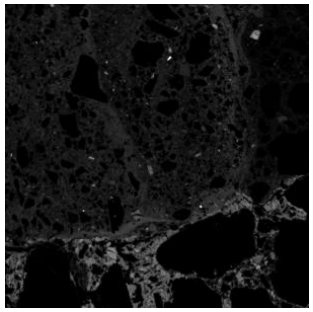

Al

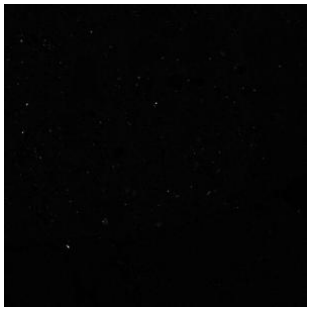

Ba

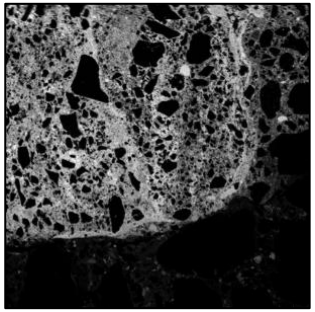

Fe

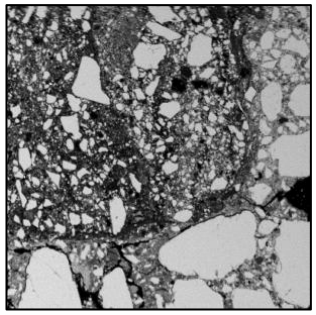

Si

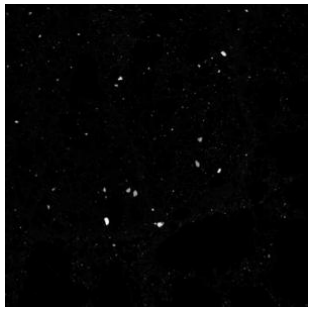

Ti

Map 4:

- 512 x 512 pixels
- 4 µm pixels
- 50 ms dwell time
- 242 minutes acquisition time

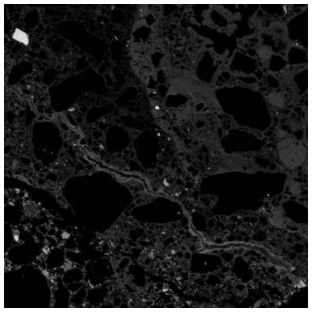

Al

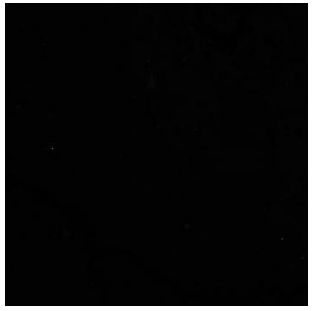

Ba

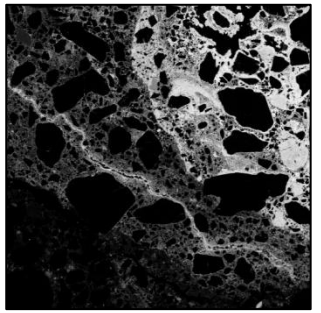

Fe

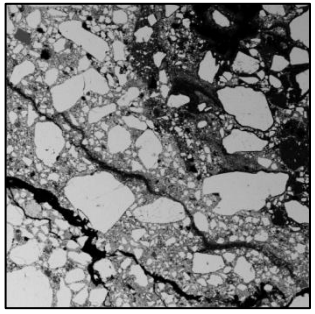

Si

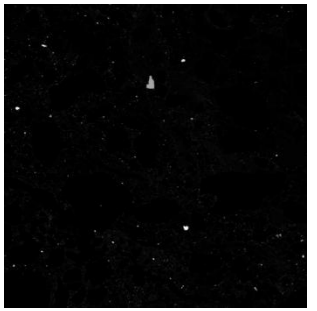

Ti

Section: SMM09 (continued)

Map 5:

- 600 x 600 pixels
- 4 µm pixels
- 50 ms dwell time
- 360 minutes acquisition time

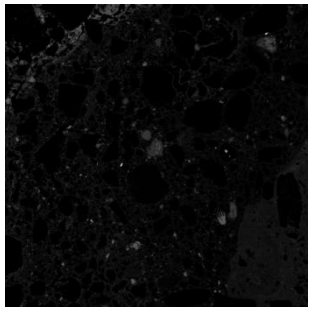

Al

Ba

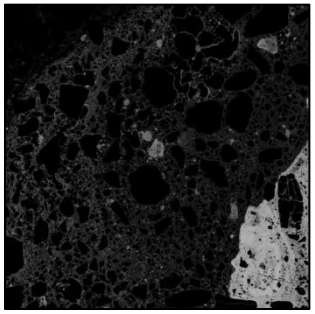

Fe

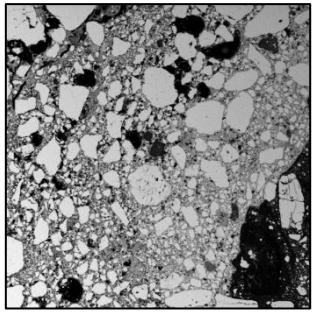

Si

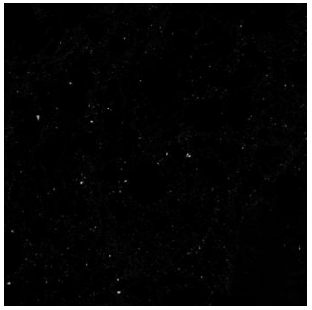

Ti

Map 6:

- 450 x 450 pixels
- 4 µm pixels
- 50 ms dwell time
- 202 minutes acquisition time

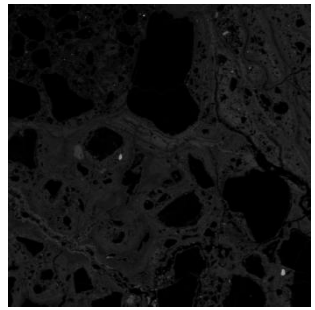

Al

Ba

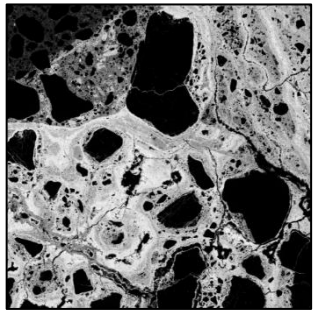

Fe

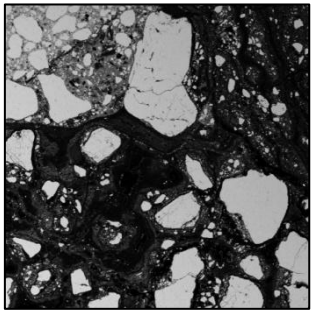

Si

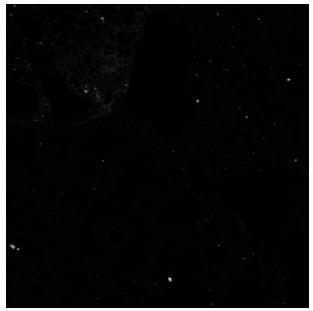

Ti

Section: SMM09 (continued)

Map 7:

- 400 x 400 pixels
- 3 µm pixels
- 50 ms dwell time
- 160 minutes acquisition time

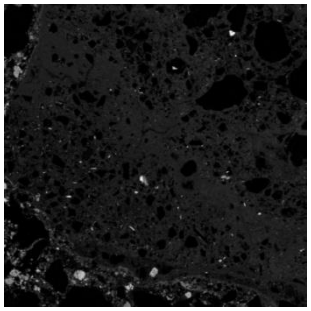

Al

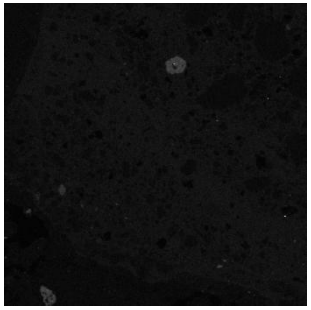

Ba

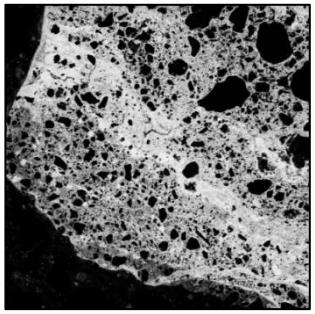

Fe

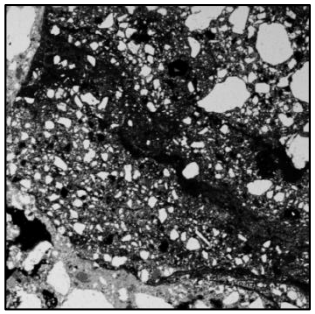

Si

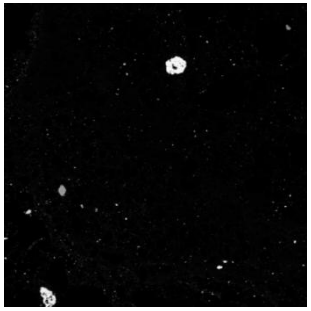

Ti

Section: SMM10

Map 1:

- 64 x 64 pixels
- 10 µm pixels
- 50 ms dwell time
- 4 minutes acquisition time

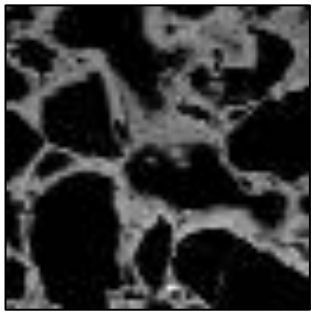

Al

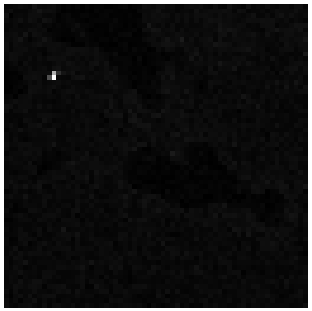

Ba

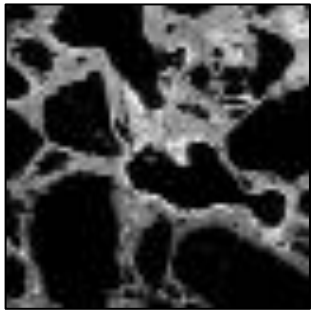

Fe

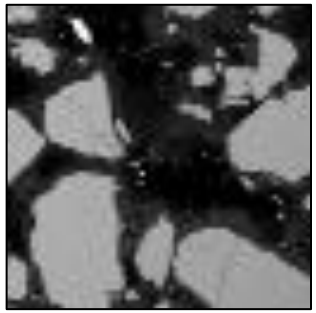

Si

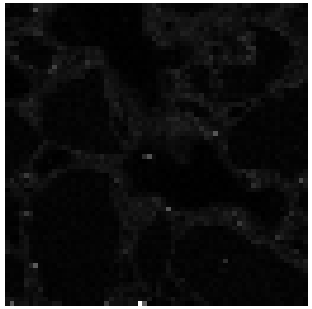

Ti

Map 2:

- 700 x 300 pixels
- 4 µm pixels
- 50 ms dwell time
- 210 minutes acquisition time

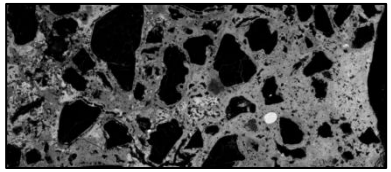

Al

Ba

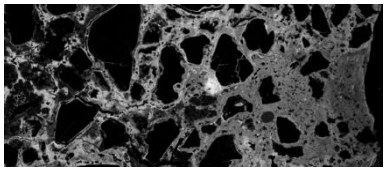

Fe

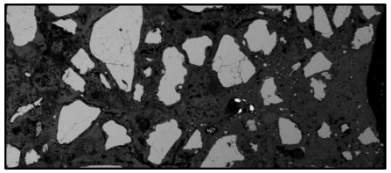

Si

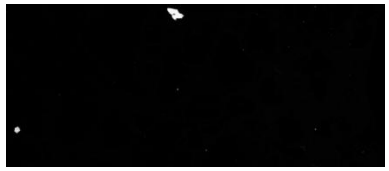

Ti

Section: SMM10 (continued)

Map 3:

- 256 x 256 pixels
- 2 µm pixels
- 50 ms dwell time
- 65 minutes acquisition time

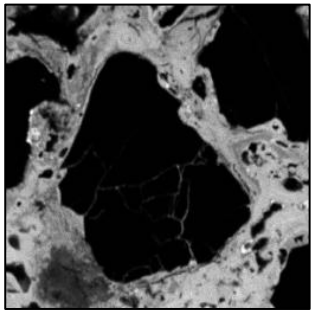

Al

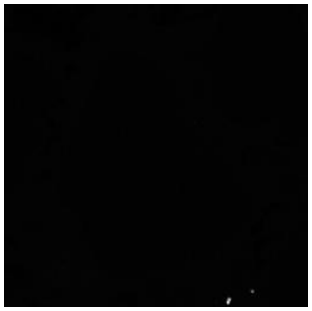

Ba

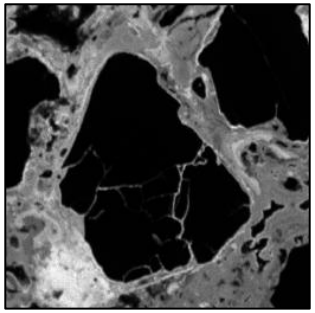

Fe

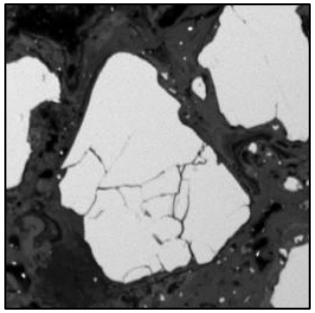

Si

Ti

Map 4:

- 200 x 128 pixels
- 1 µm pixels
- 50 ms dwell time
- 25 minutes acquisition time

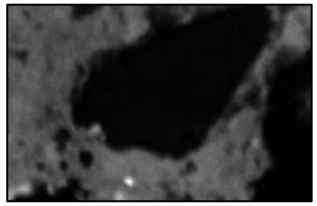

Al

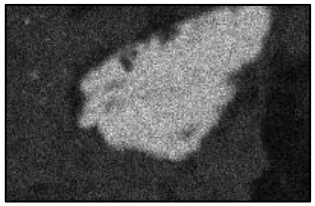

Ba

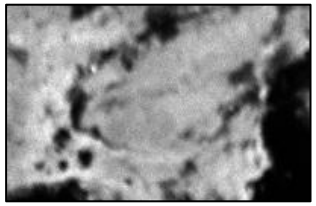

Fe

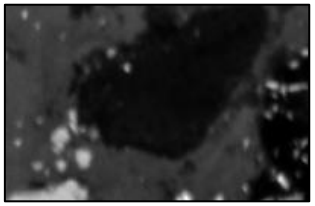

Si

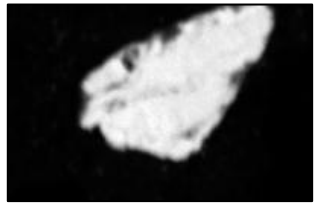

Ti

Section: SMM10 (continued)

Map 5:

- 200 x 200 pixels
- 1 µm pixels
- 50 ms dwell time
- 40 minutes acquisition time

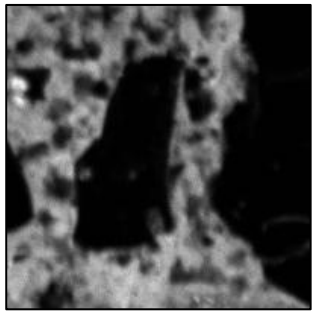

Al

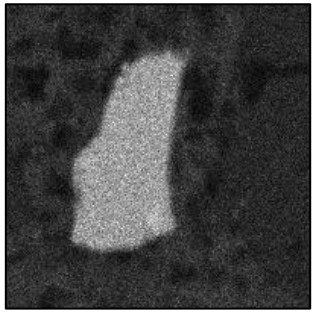

Ba

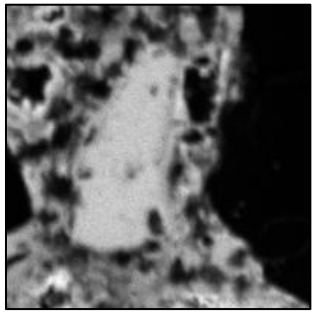

Fe

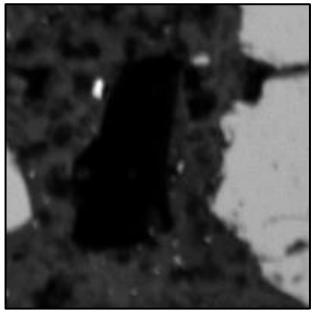

Si

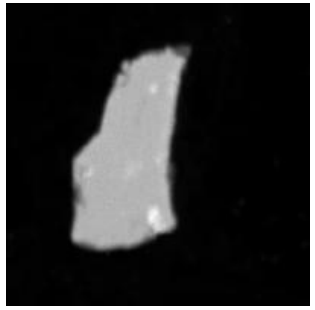

Ti

Map 6:

- 200 x 200 pixels
- 1 µm pixels
- 50 ms dwell time
- 40 minutes acquisition time

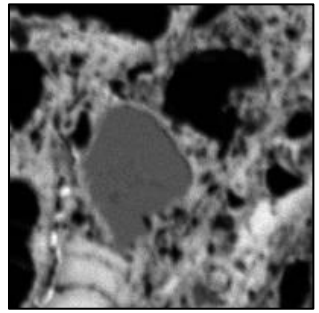

Al

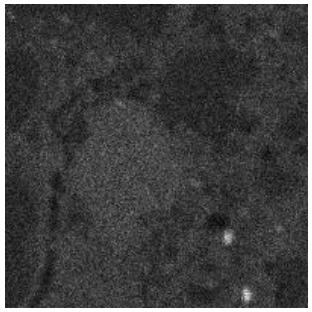

Ba

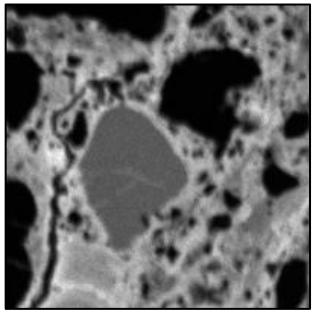

Fe

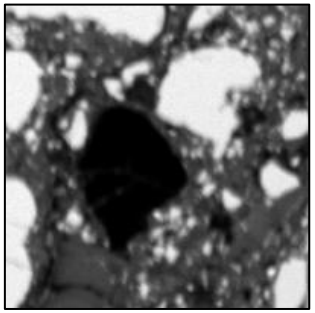

Si

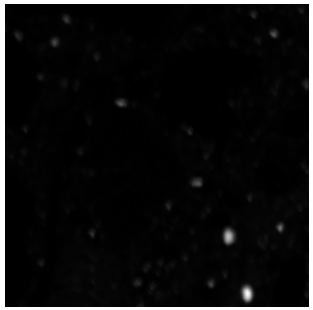

Ti

Section: SMM10 (continued)

Map 7:

- 512 x 800 pixels
- 4 µm pixels
- 50 ms dwell time
- 410 minutes acquisition time

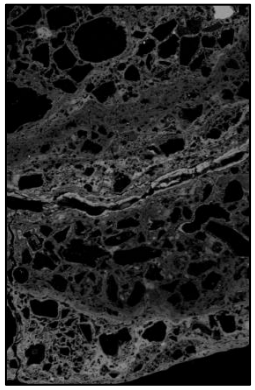

Al

Ba

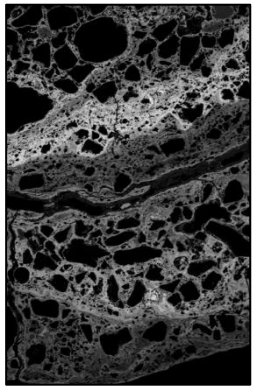

Fe

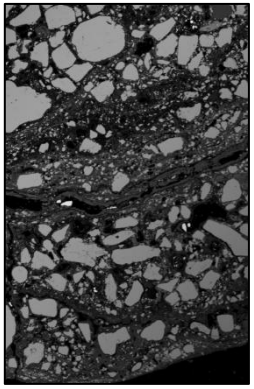

Si

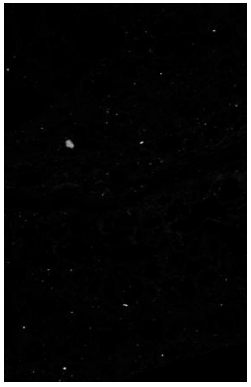

Ti

=**Section: SMM10 (continued)**

Map 8:

- 256 x 256 pixels
- 2 µm pixels
- 50 ms dwell time
- 65 minutes acquisition time

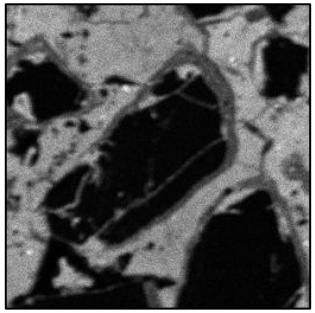

Al

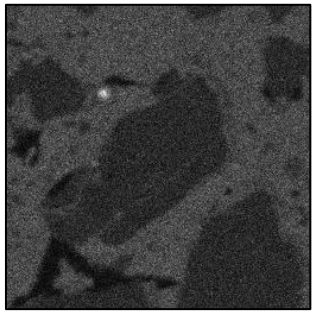

Ba

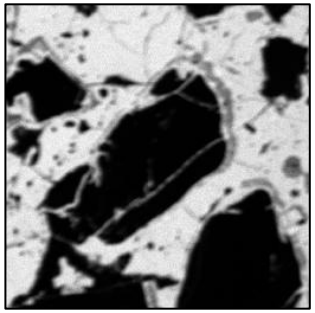

Fe

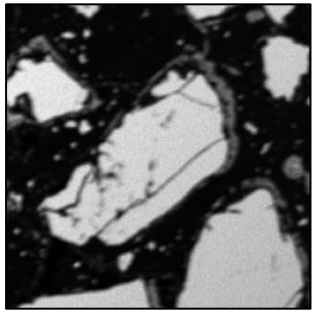

Si

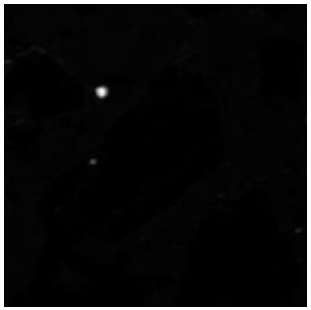

Ti

Section: SMM10 (continued)

Map 9:

- 512 x 512 pixels
- 2 µm pixels
- 50 ms dwell time
- 262 minutes acquisition time

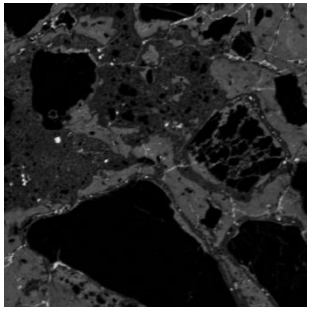

Al

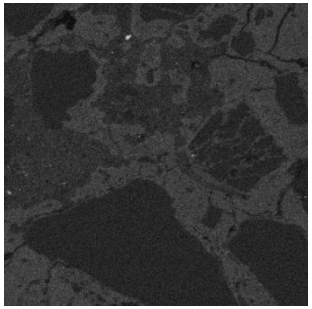

Ba

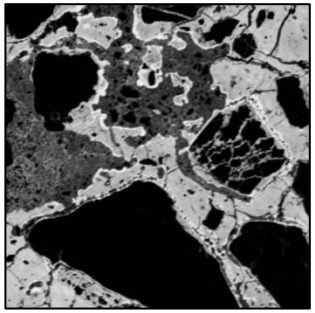

Fe

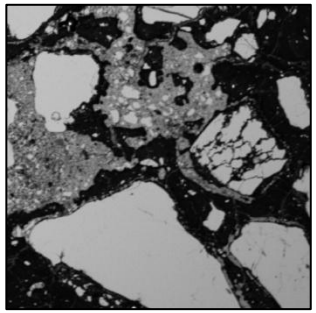

Si

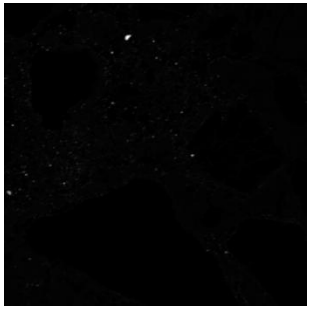

Ti

Map 10:

- 200 x 350 pixels
- 3 µm pixels
- 50 ms dwell time
- 70 minutes acquisition time

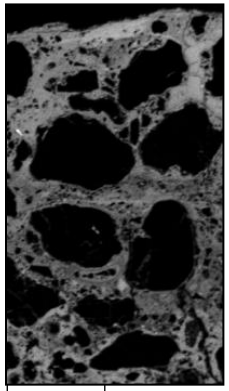

Al

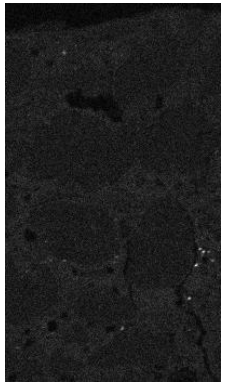

Ba

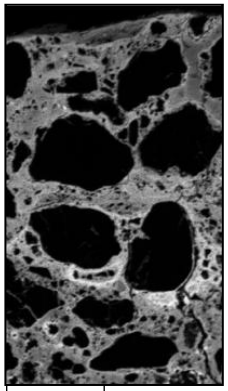

Fe

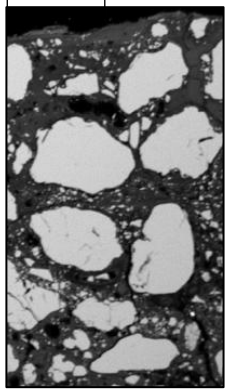

Si

Ti

Section: SMM10 (continued)

Map 11:

- 600 x 200 pixels
- 4 µm pixels
- 50 ms dwell time
- 120 minutes acquisition time

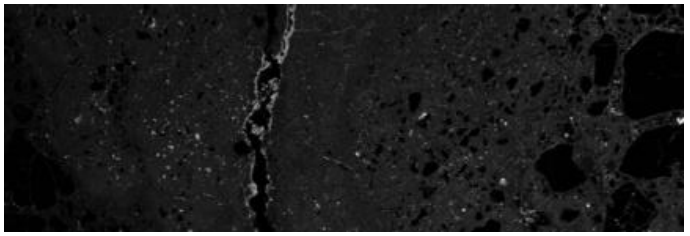

Al

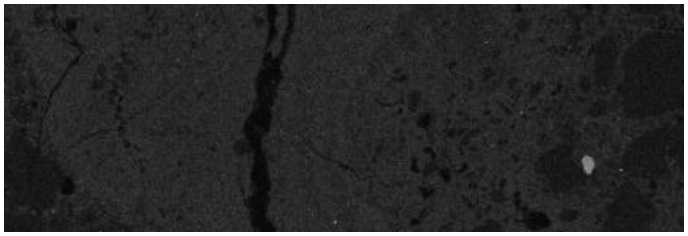

Ba

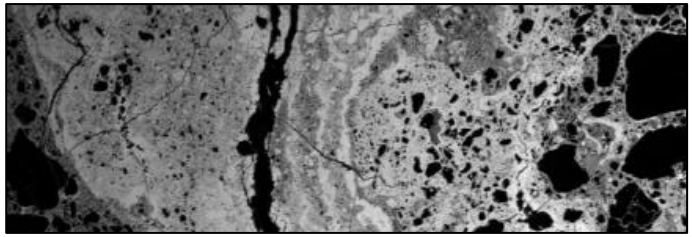

Fe

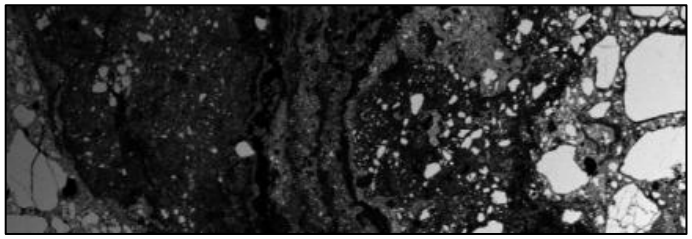

Si

Ti

Section: SMM10 (continued)

Map 12:

- 300 x 600 pixels
- 2 µm pixels
- 50 ms dwell time
- 180 minutes acquisition time

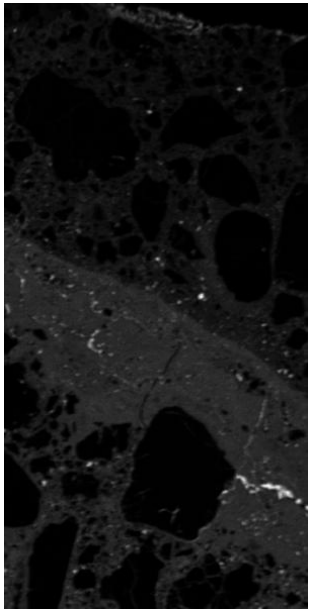

Al

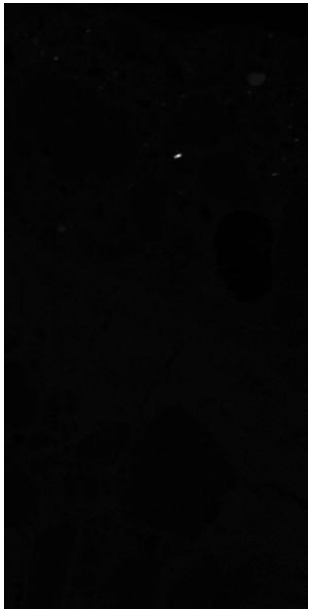

Ba

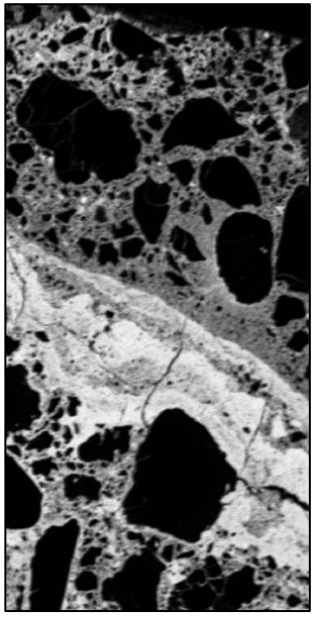

Fe

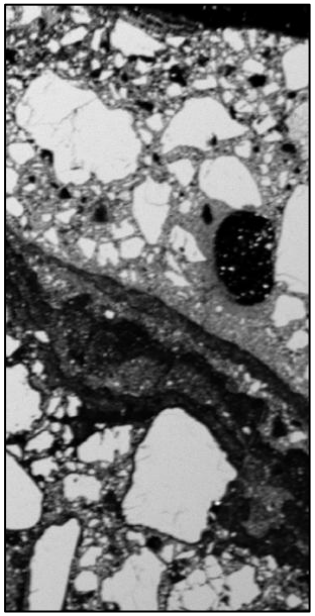

Si

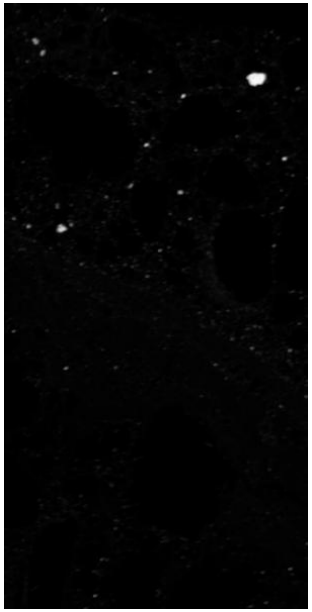

Ti

Section: SMM10 (continued)

Map 13:

- 256 x 256 pixels
- 4 µm pixels
- 50 ms dwell time
- 65 minutes acquisition time

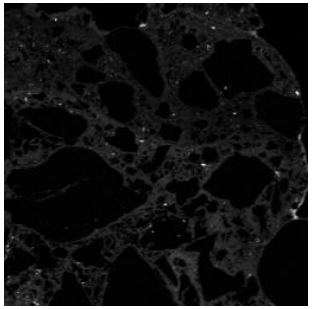

Al

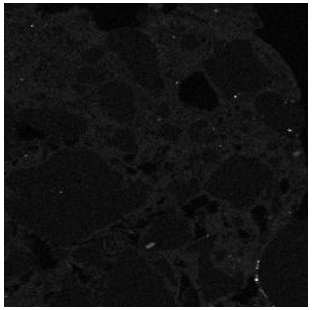

Ba

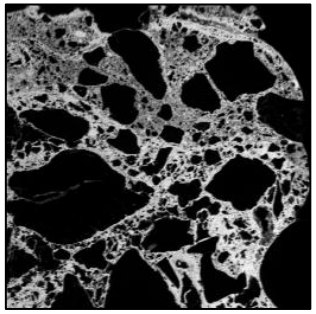

Fe

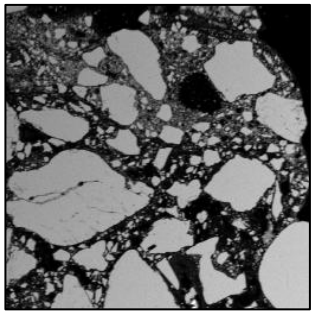

Si

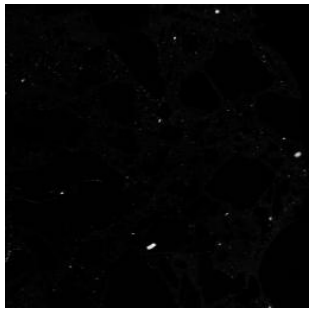

Ti

Map 14:

- 600 x 800 pixels
- 4 µm pixels
- 50 ms dwell time
- 480 minutes acquisition time

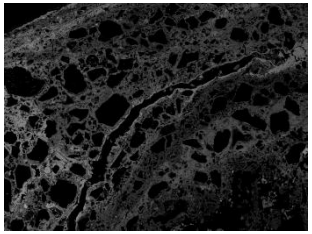

Al

Ba

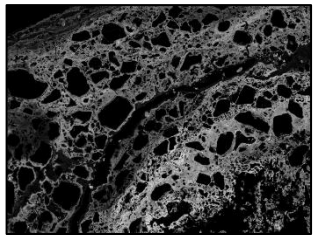

Fe

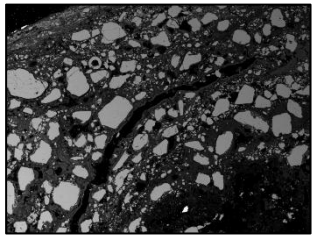

Si

Ti

Section: SMM10 (continued)

Map 15:

- 800 x 600 pixels
- 4 µm pixels
- 50 ms dwell time
- 480 minutes acquisition time

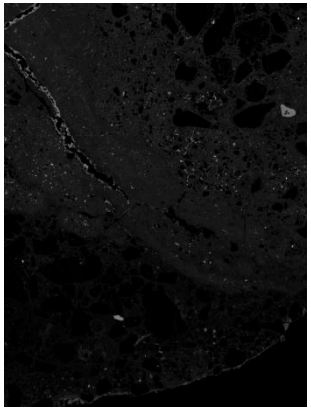

Al

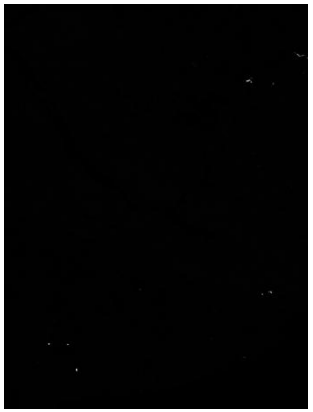

Ba

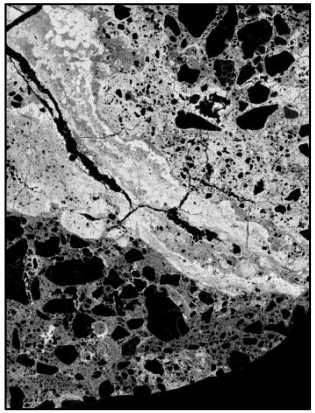

Fe

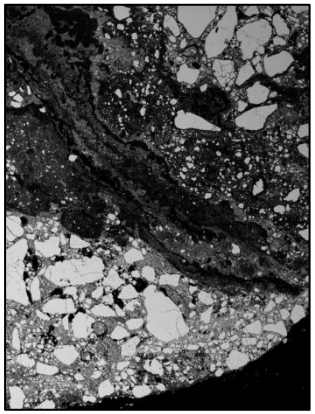

Si

Ti

Section: SMM11

Map 1:

- 512 x 512 pixels
- 4 µm pixels
- 50 ms dwell time
- 462 minutes acquisition time

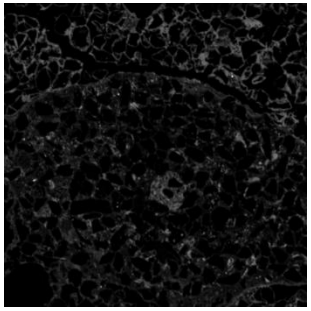

Al

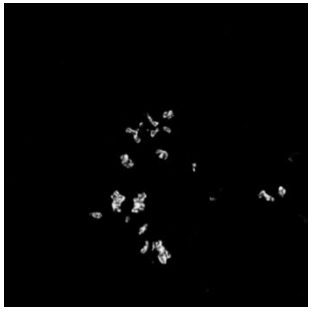

Ba

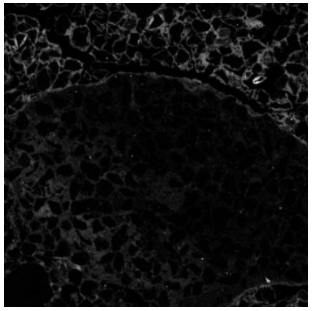

Fe

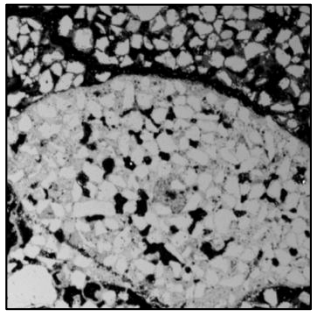

Si

Ti

Map 2:

- 256 x 256 pixels
- 4 µm pixels
- 50 ms dwell time
- 65 minutes acquisition time

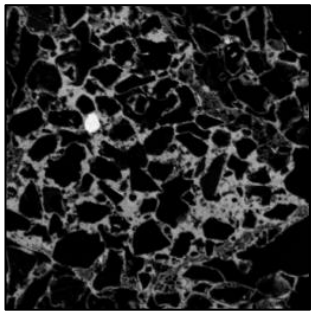

Al

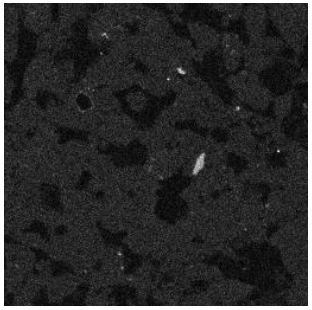

Ba

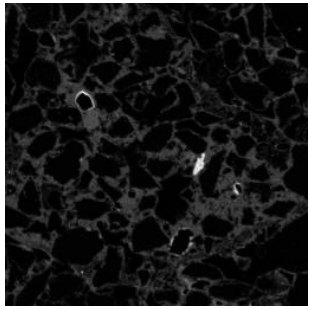

Fe

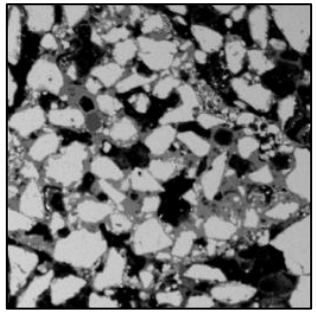

Si

Ti

Section: SMM11 (continued)

Map 3:

- 200 x 200 pixels
- 4 µm pixels
- 50 ms dwell time
- 40 minutes acquisition time

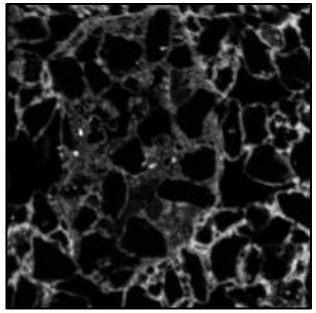

Al

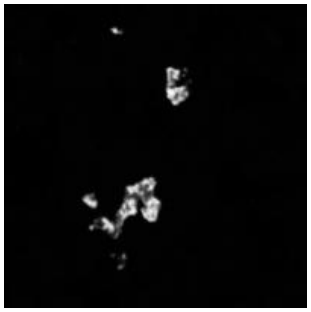

Ba

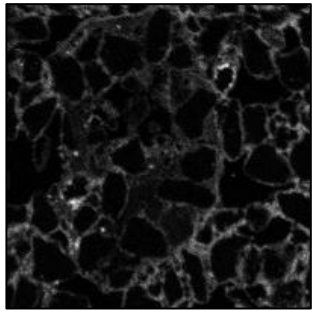

Fe

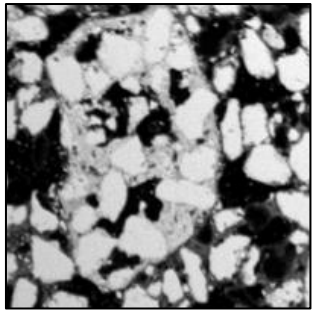

Si

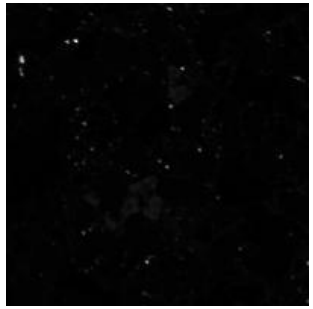

Ti

Section: SMM12

Map 1:

- 128 x 128 pixels
- 5 µm pixels
- 50 ms dwell time
- 16 minutes acquisition time

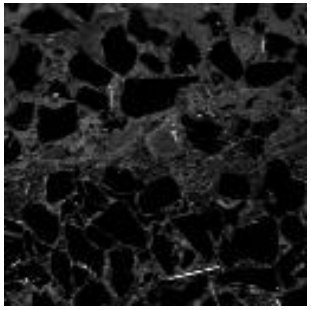

Al

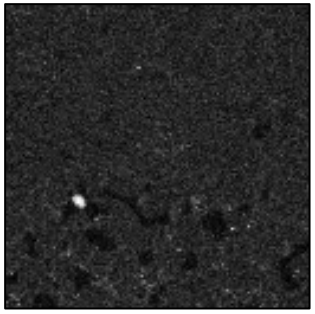

Ba

Fe

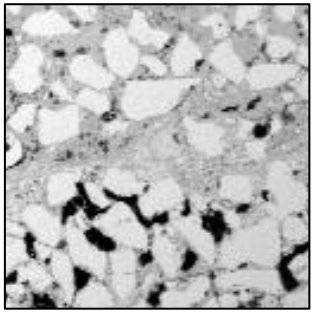

Si

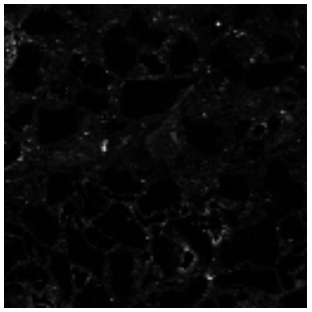

Ti

Appendix F – Results of laser ablation trace element mapping

Thin section: SMM02

Map 1:

- 95 rasters @ 924 µm path length
- Spot size: 17 µm
- Path separation: 17 µm
- 21 µm/s scan rate
- 210 minutes acquisition time

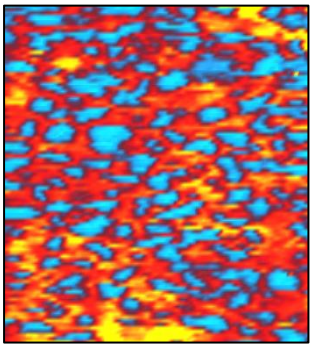

^{75}As

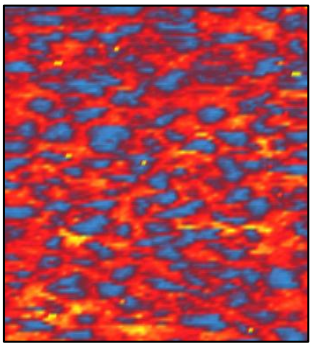

^{59}Co

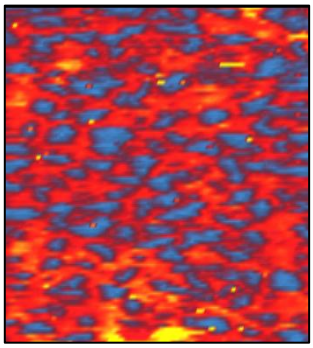

^{52}Cr

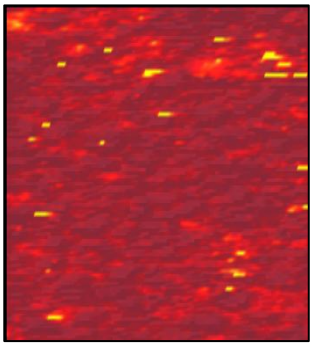

^{65}Cu

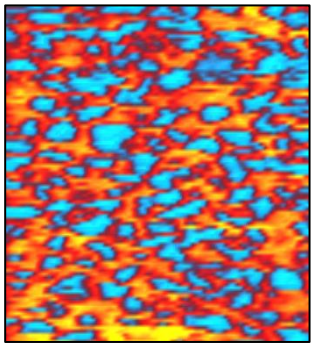

^{57}Fe

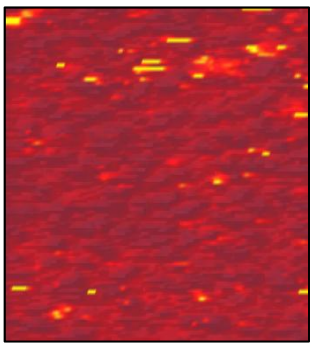

^{55}Mn

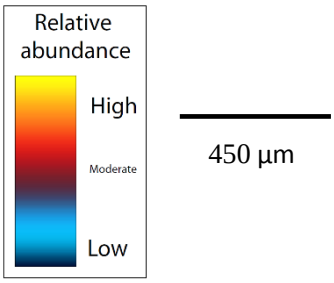

SMM02 (continued)

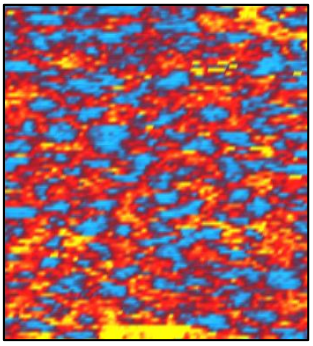

^{95}Mo

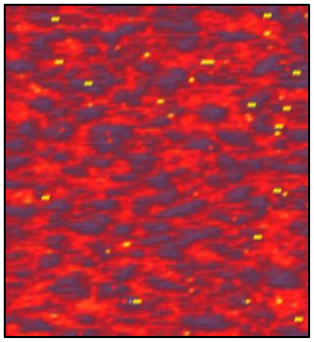

^{60}Ni

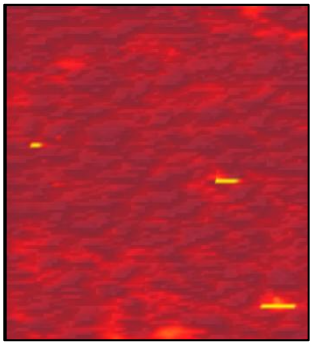

^{208}Pb

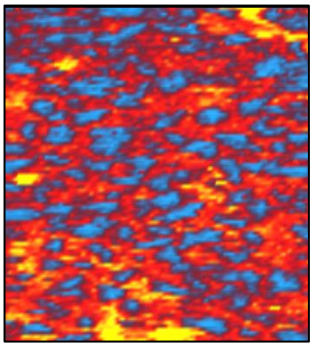

^{121}Sb

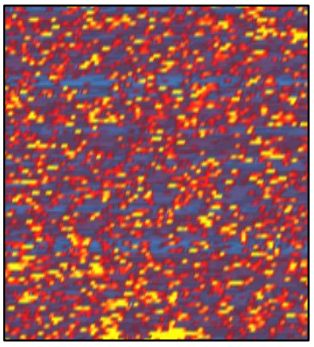

^{77}Se

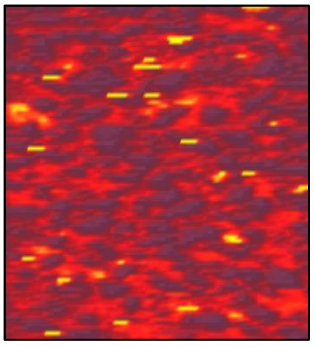

^{49}Ti

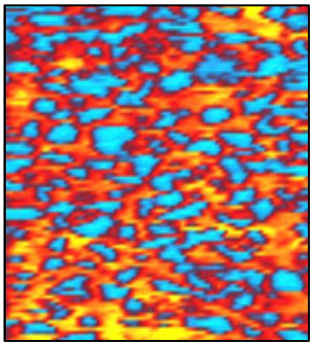

^{51}V

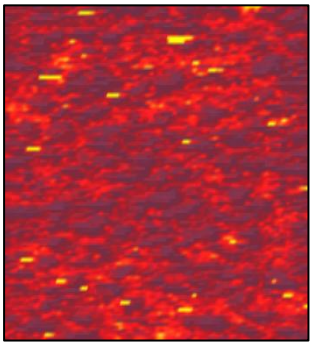

^{182}W

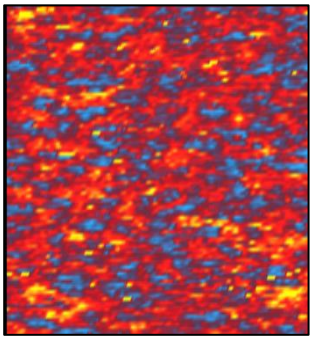

^{66}Zn

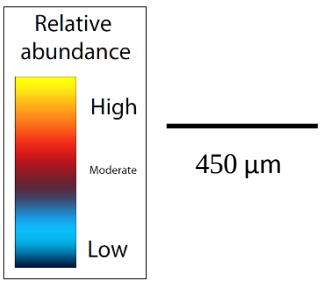

450 µm

Thin section: SMM03

Map 1:

- 105 rasters @ 1959 µm path length
- Spot size: 26 µm
- Path separation: 26 µm
- 28 µm/s scan rate
- 300 minutes acquisition time

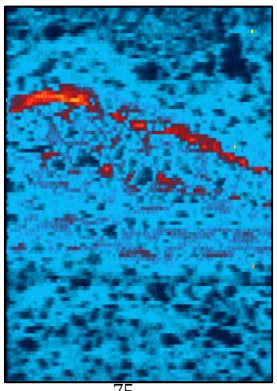

^{75}As

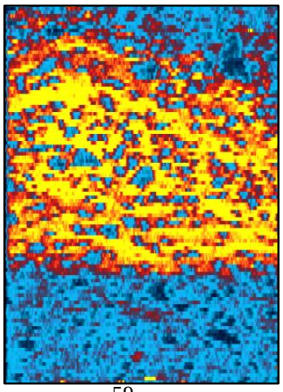

^{59}Co

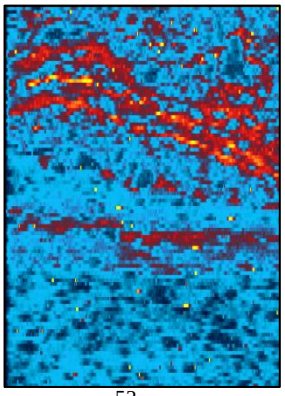

^{52}Cr

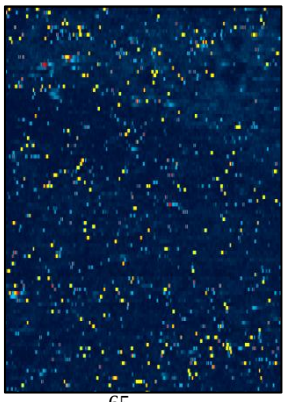

^{65} Cu

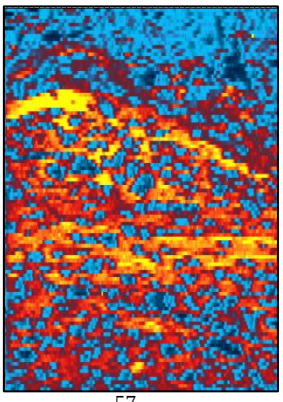

^{57}Fe

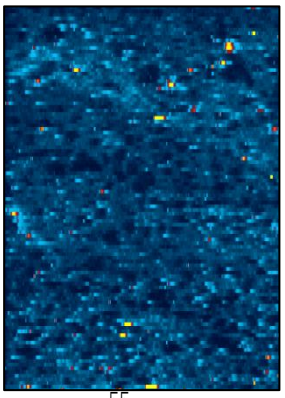

^{55}Mn

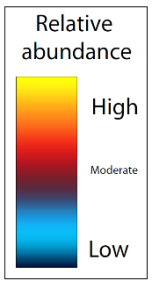

Map 1 (continued):

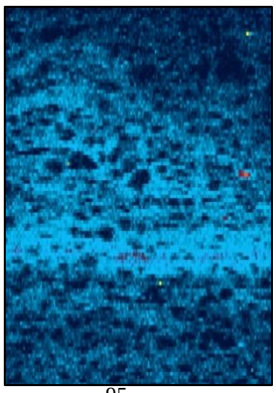

^{95}Mo

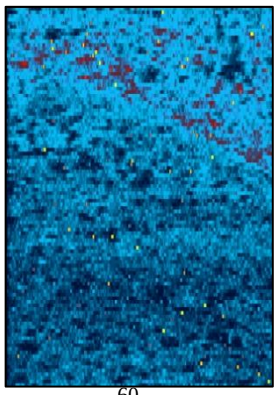

^{60}Ni

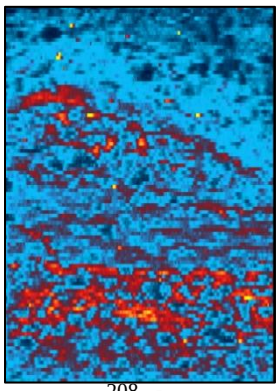

^{208}Pb

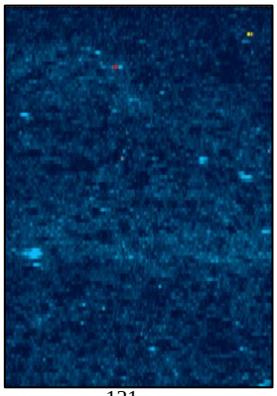

^{121}Sb

^{77}Se

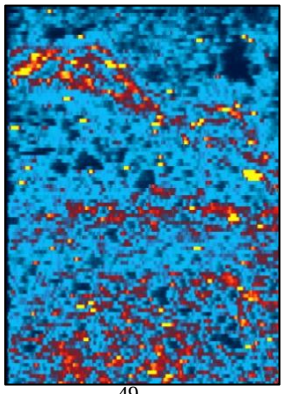

^{49}Ti

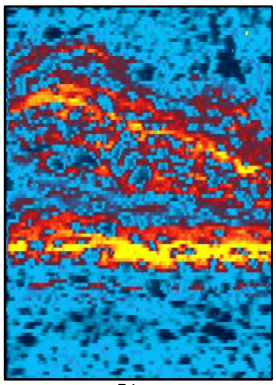

^{51}V

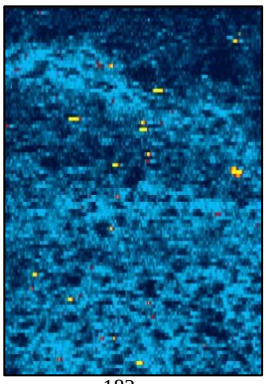

^{182}W

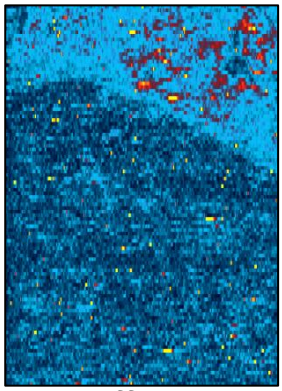

^{66}Zn

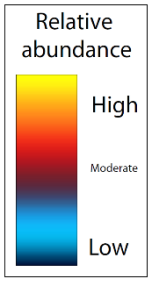

1000 µm

Thin section: SMM03

Map 2:

- 111 rasters @ 2019 µm path length
- Spot size: 19 µm
- Path separation: 19 µm
- 21 µm/s scan rate
- 233 minutes acquisition time

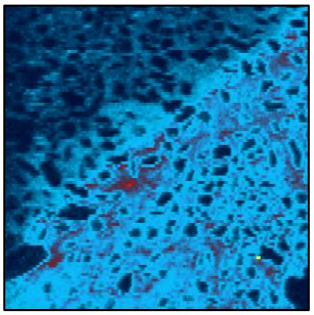

^{75}As

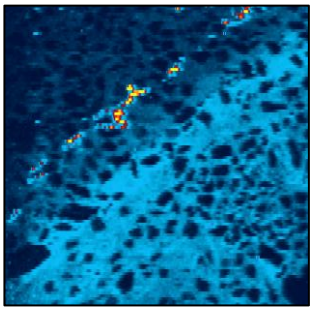

^{59}Co

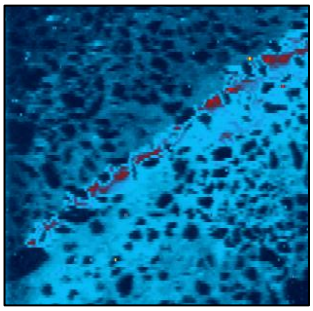

^{52}Cr

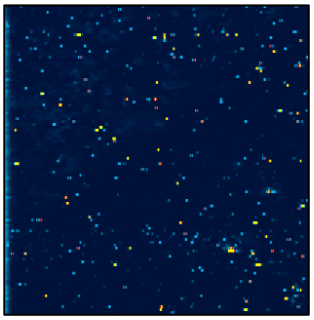

^{65}Cu

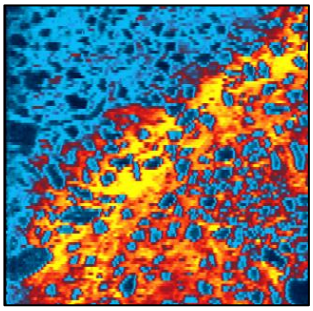

^{57}Fe

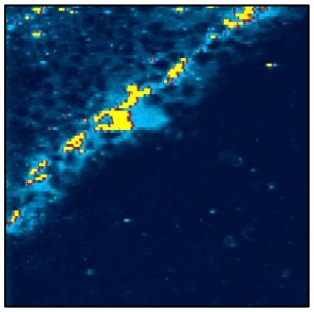

^{55}Mn

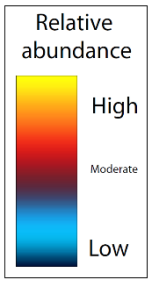

1000 µm

Map 2 (continued):

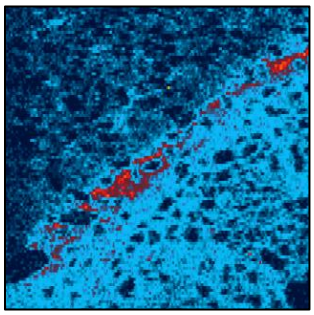

^{95}Mo

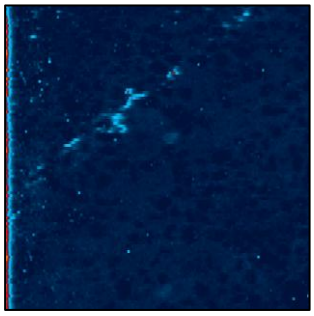

^{60}Ni

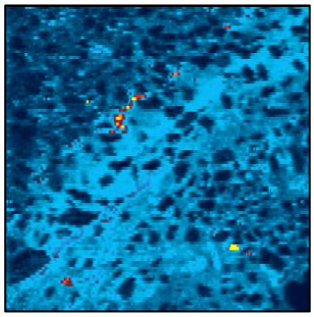

^{208}Pb

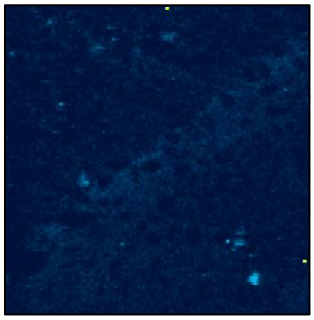

^{121}Sb

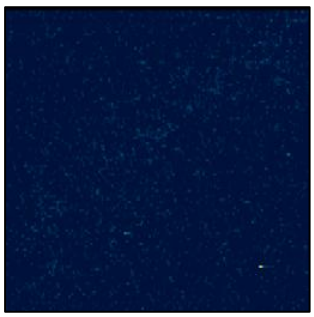

^{77}Se

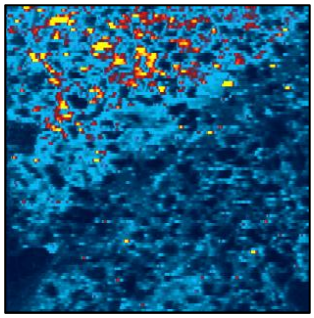

^{49}Ti

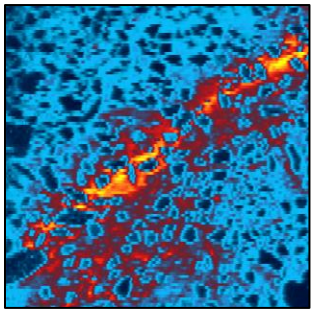

^{51}V

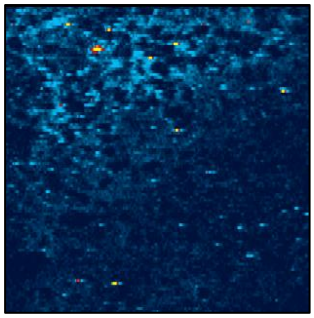

^{182}W

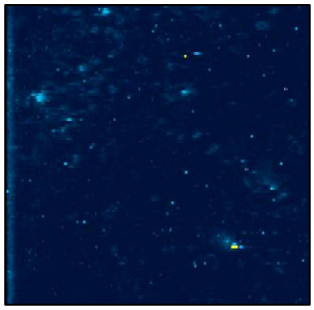

^{66}Zn

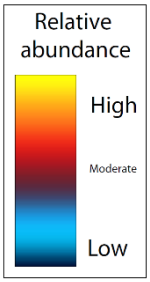

Thin section: SMM03

Map 3:

- 95 rasters @ 1218 µm path length
- Spot size: 21 µm
- Path separation: 21 µm
- 23 µm/s scan rate
- 250 minutes acquisition time

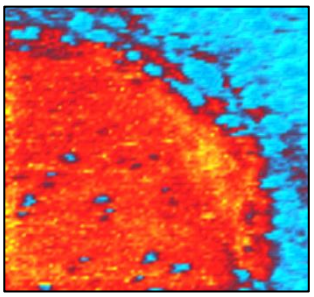

^{75}As

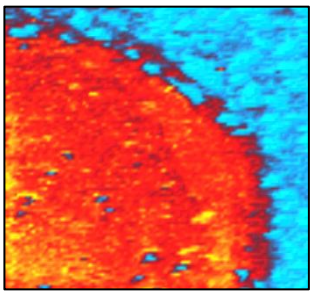

^{59}Co

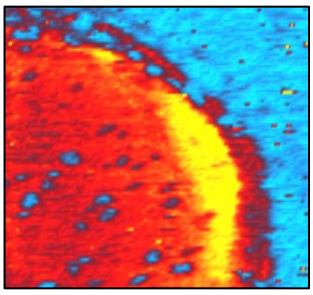

^{52}Cr

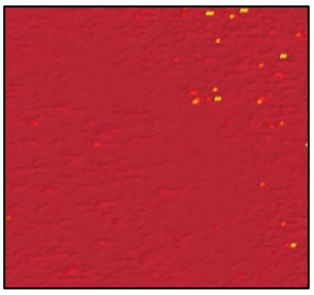

^{65}Cu

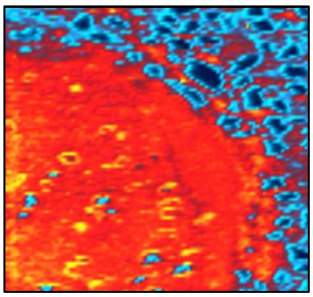

^{57}Fe

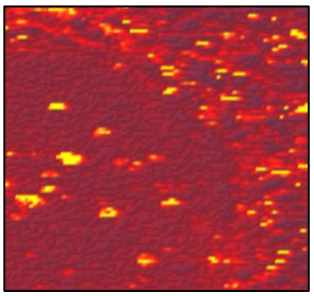

^{55}Mn

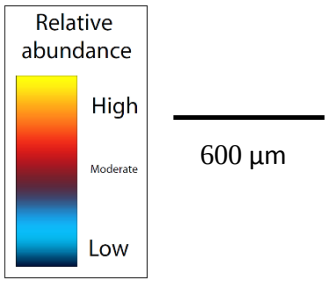

Map 3 (continued):

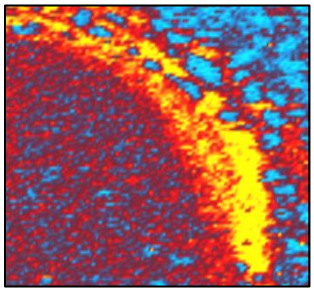

^{95}Mo

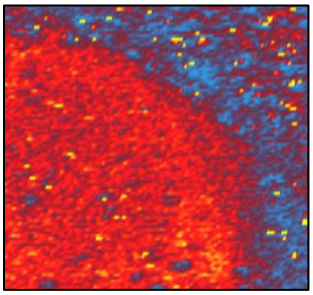

^{60}Ni

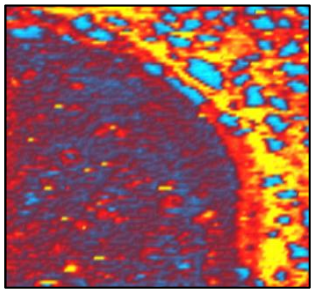

^{208}Pb

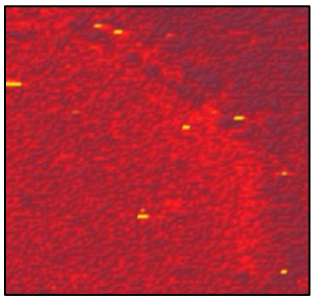

^{121}Sb

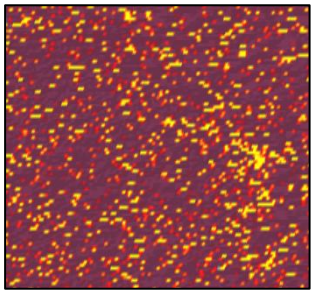

^{77}Se

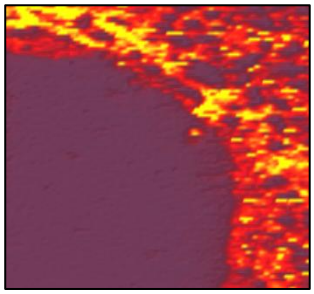

^{49}Ti

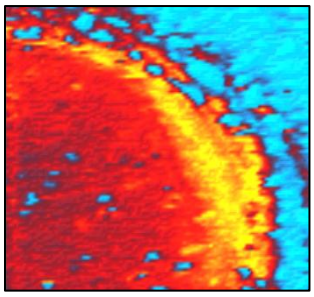

^{51}V

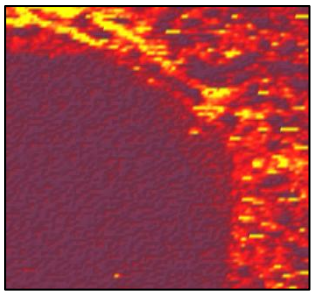

^{182}W

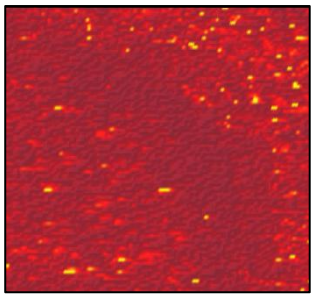

^{66}Zn

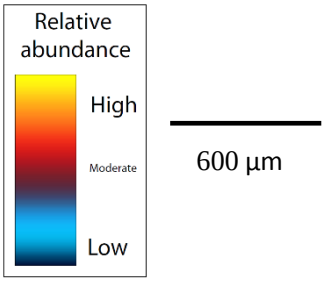

Thin section: SMM03

Map 4:

- 181 rasters @ 2919 µm path length
- Spot size: 21 µm
- Path separation: 21 µm
- 23 µm/s scan rate
- 690 minutes acquisition time

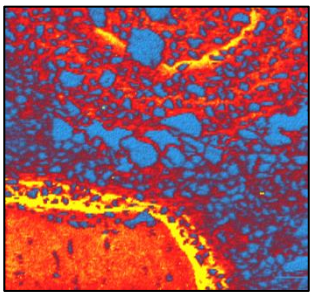

^{75}As

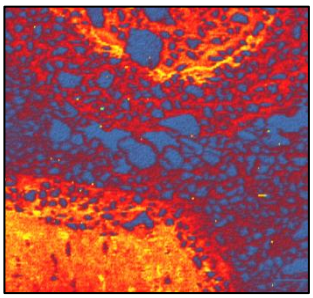

^{59}Co

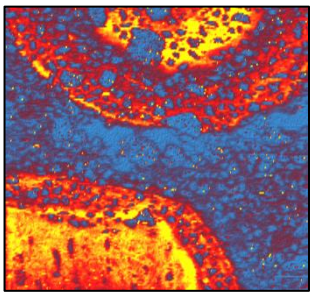

^{52}Cr

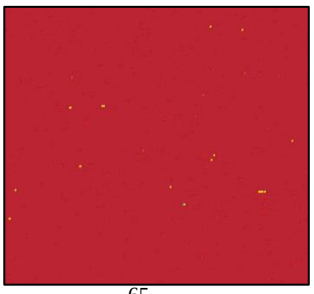

^{65}Cu

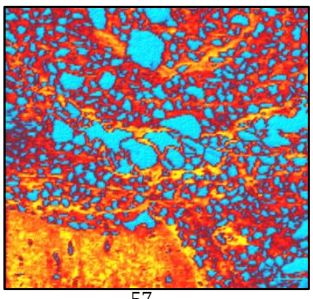

^{57}Fe

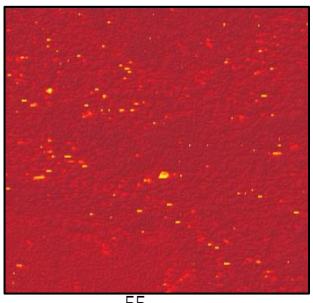

^{55}Mn

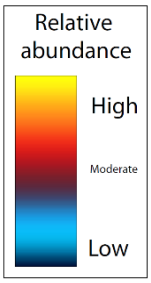

1500 µm

Map 4 (continued):

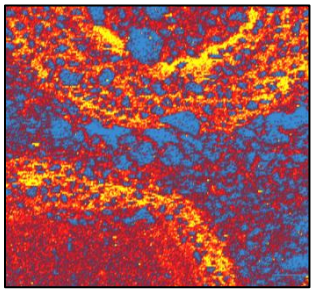

^{95}Mo

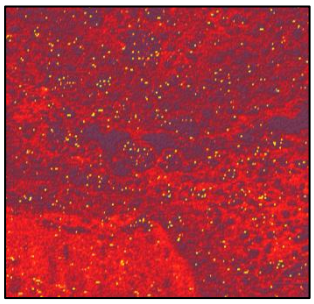

^{60}Ni

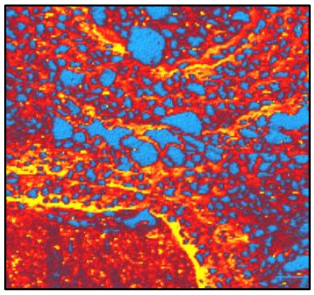

^{208}Pb

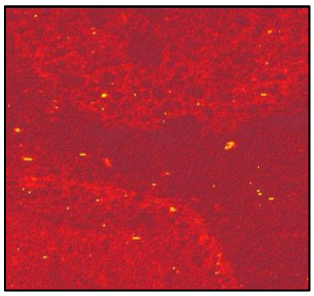

^{121}Sb

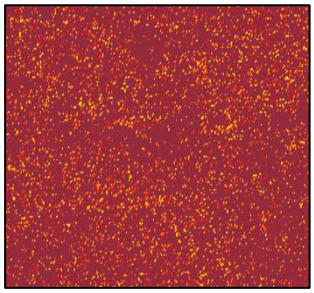

^{77}Se

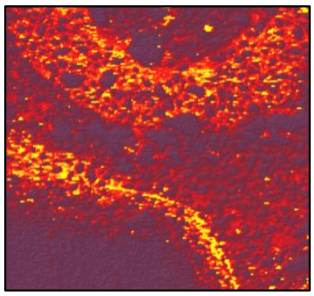

^{49}Ti

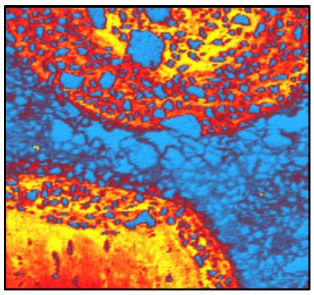

^{51}V

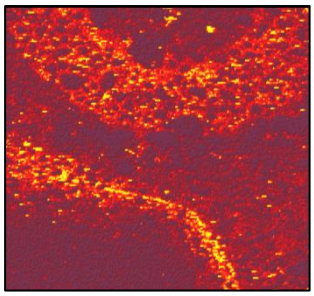

^{182}W

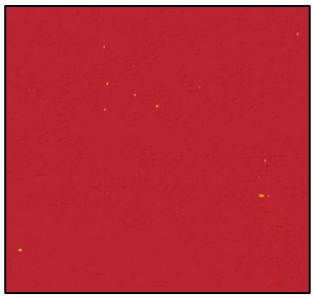

^{66}Zn

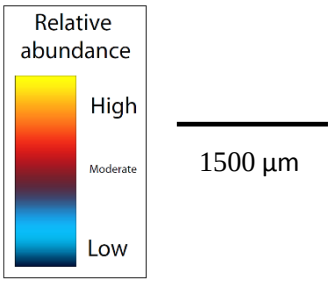

Thin section: SMM04

Map 1:

- 59 rasters @ 1142 µm path length
- Spot size: 21 µm
- Path separation: 21 µm
- 23 µm/s scan rate
- 150 minutes acquisition time

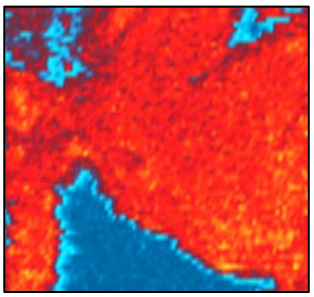

^{75}As

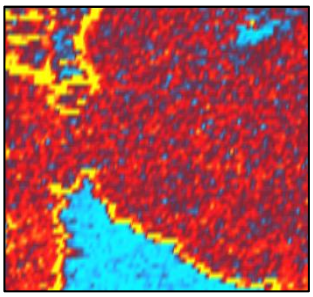

^{59}Co

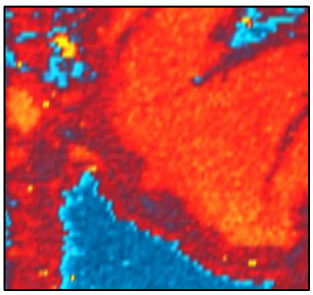

^{52}Cr

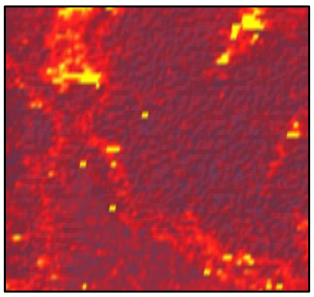

^{65}Cu

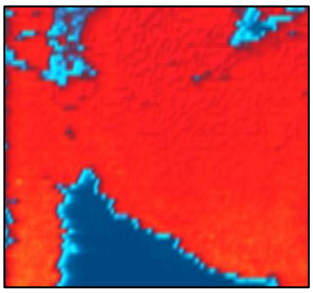

^{57}Fe

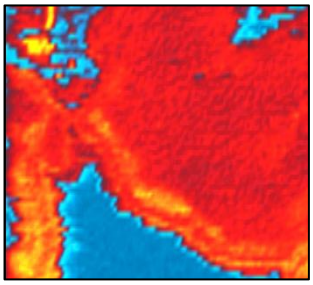

^{55}Mn

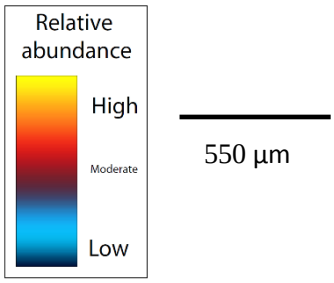

Map 1 (continued):

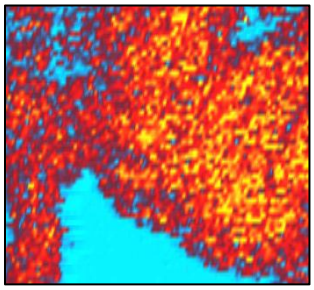

^{95}Mo

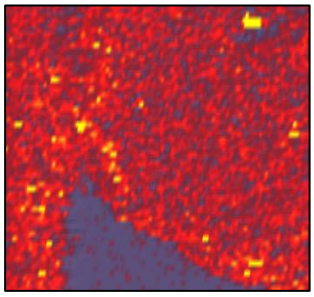

^{60}Ni

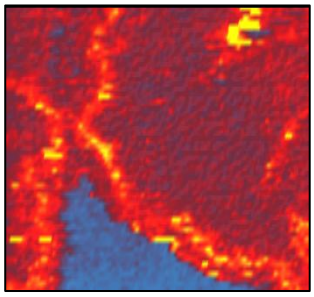

^{208}Pb

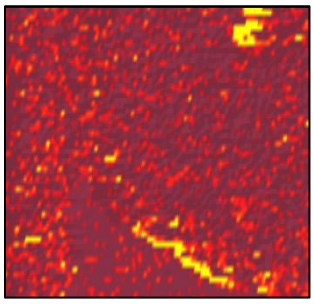

^{121}Sb

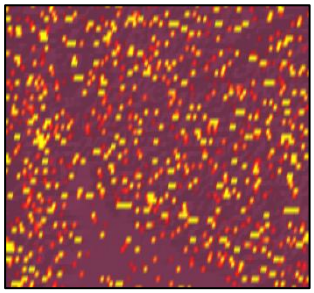

^{77}Se

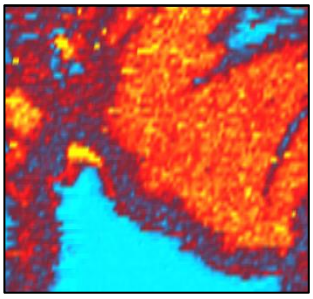

^{49}Ti

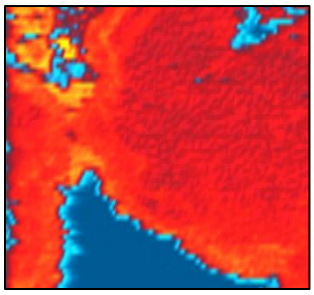

^{51}V

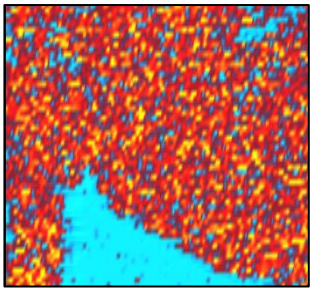

^{182}W

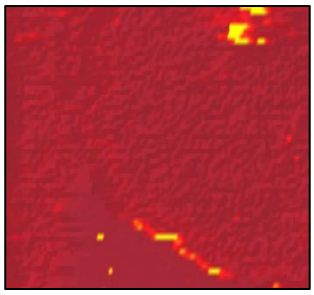

^{66}Zn

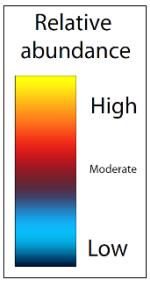

550 µm

Thin section: SMM05

Map 1:

- 54 rasters @ 1727 µm path length
- Spot size: 26 µm
- Path separation: 26 µm
- 30 µm/s scan rate
- 85 minutes acquisition time

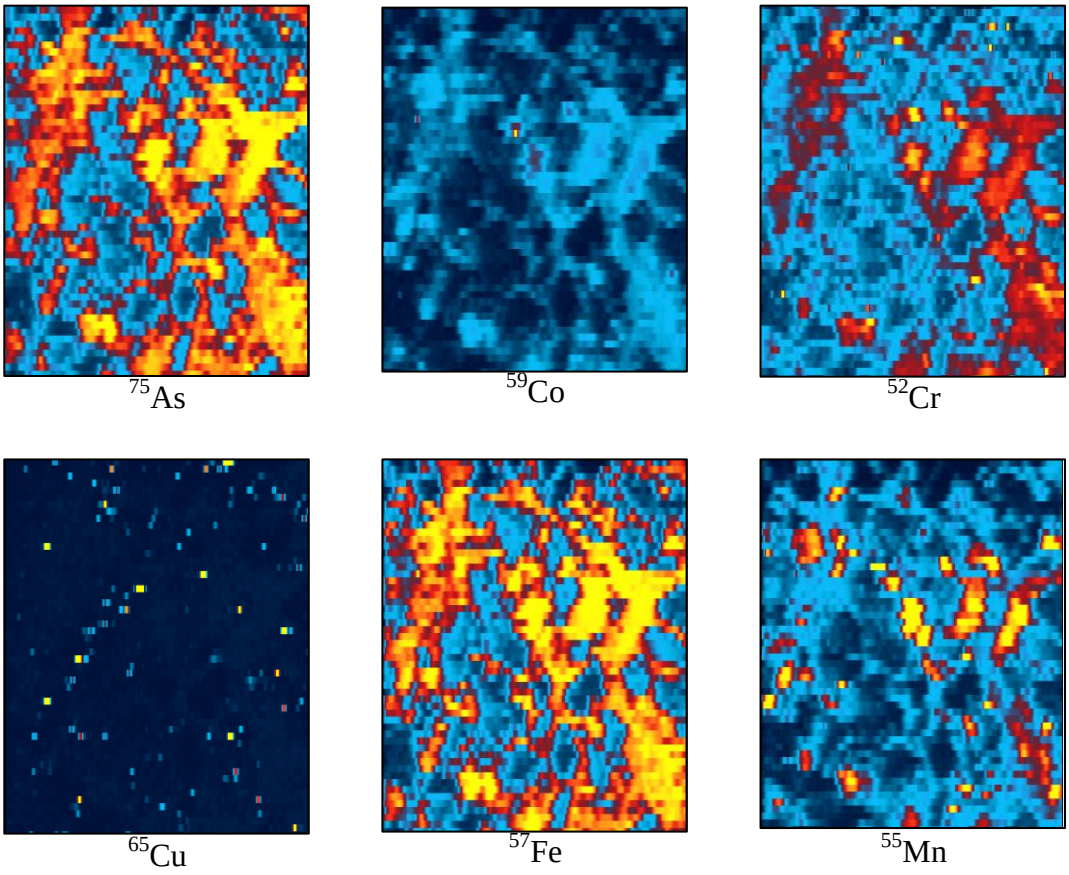

Map 1 (continued):

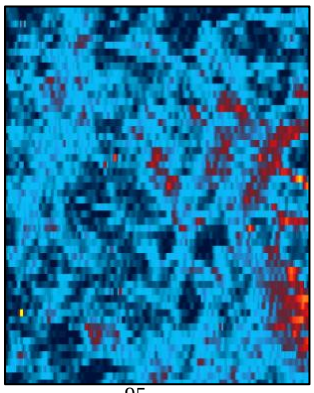

^{95}Mo

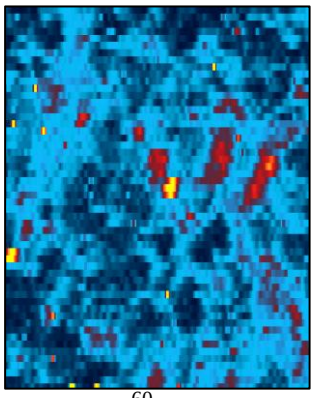

^{60}Ni

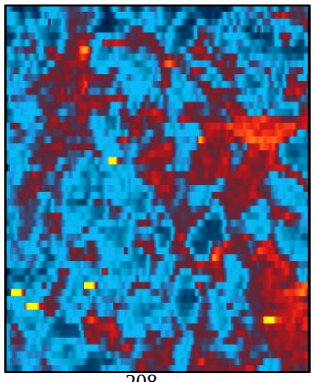

^{208}Pb

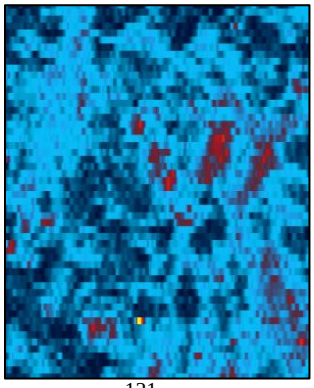

^{121}Sb

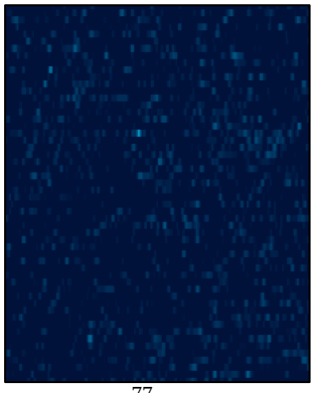

^{77}Se

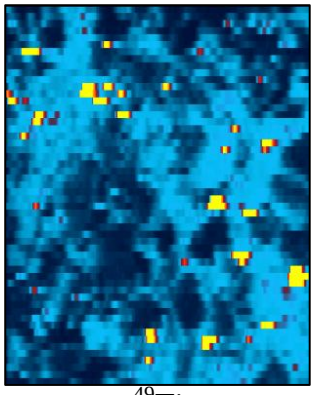

^{49}Ti

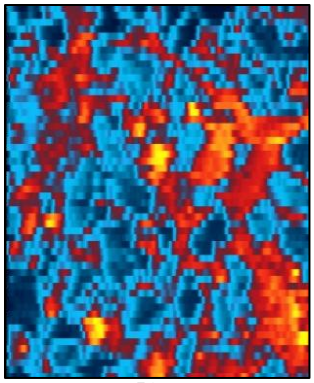

^{51}V

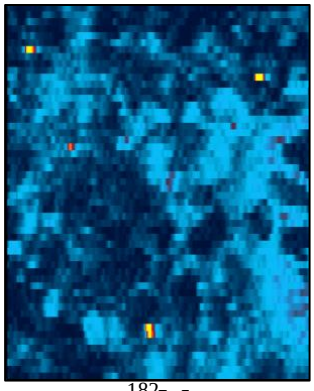

^{182}W

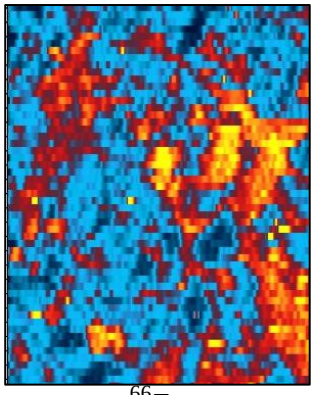

^{66}Zn

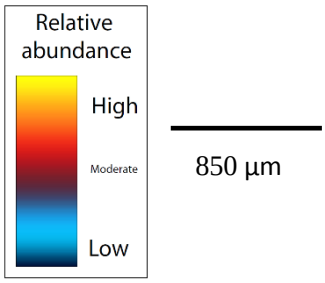

850 µm

Thin section: SMM05

Map 2:

- 119 rasters @ 2119.8 µm path length
- Spot size: 17 µm
- Path separation: 17 µm
- 20 µm/s scan rate
- 390 minutes acquisition time

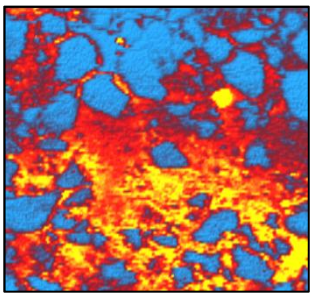

^{75}As

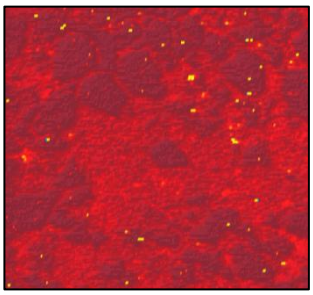

^{59}Co

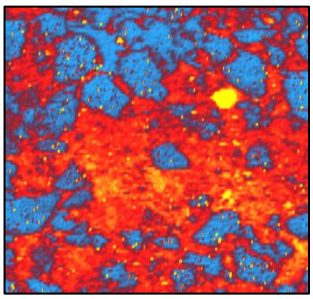

^{52}Cr

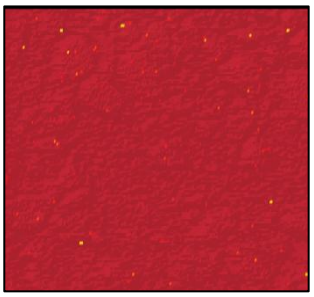

^{65}Cu

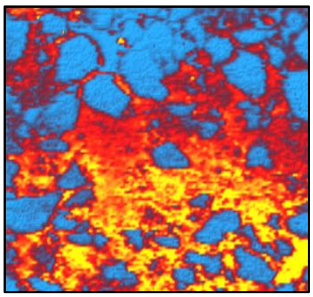

^{57}Fe

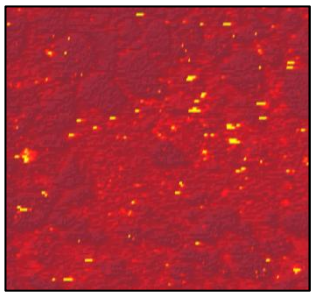

^{55}Mn

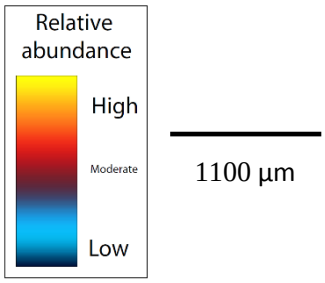

Map 2 (continued):

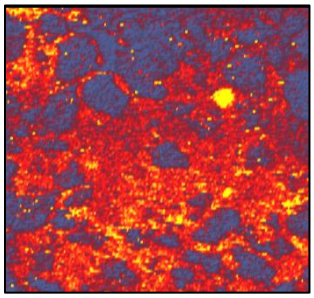

^{95}Mo

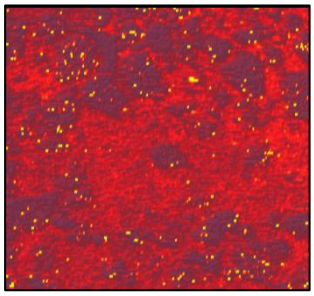

^{60}Ni

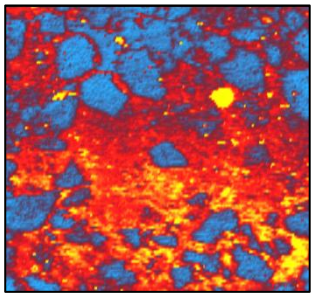

^{208}Pb

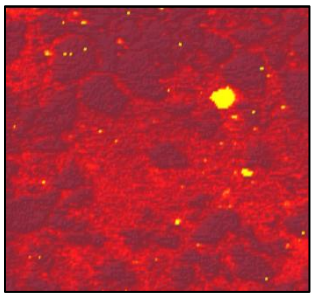

^{121}Sb

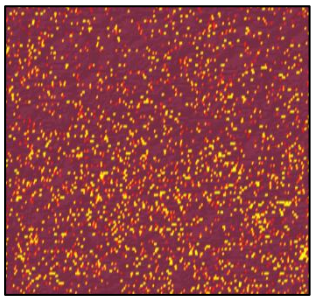

^{77}Se

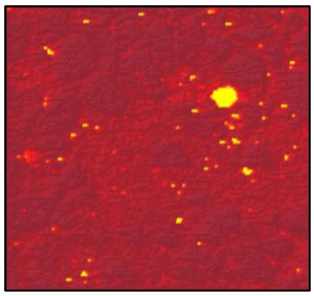

^{49}Ti

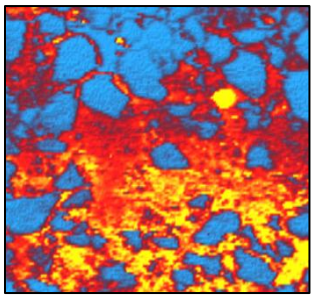

^{51}V

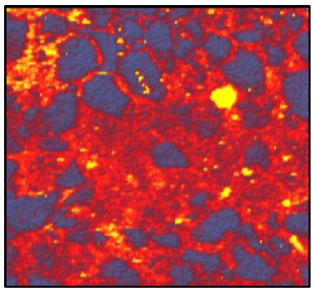

^{182}W

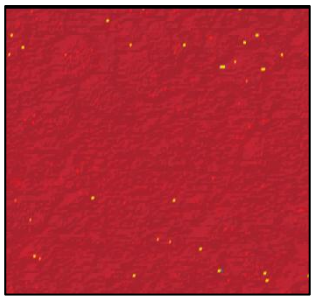

^{66}Zn

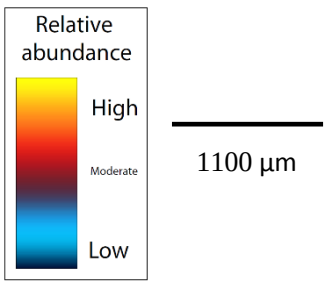

1100 µm

Thin section: SMM05

Map 3:

- 211 rasters @ 2514 µm path length
- Spot size: 17 µm
- Path separation: 17 µm
- 20 µm/s scan rate
- 600 minutes acquisition time

NB: The He tank ran empty during this acquisition – the transfer of ablated material to the ICP-MS and therefore the data acquisition was delayed and not optimised.

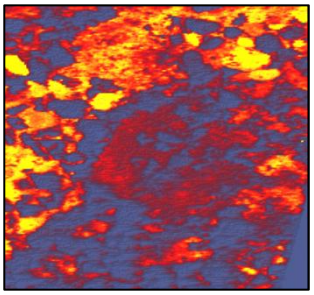

^{75}As

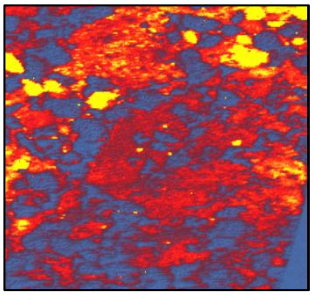

^{59}Co

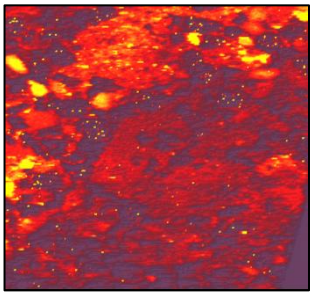

^{52}Cr

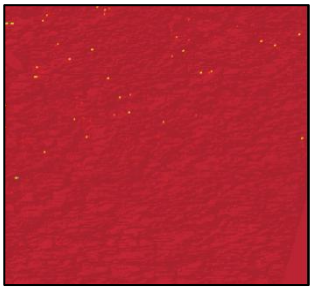

^{65}Cu

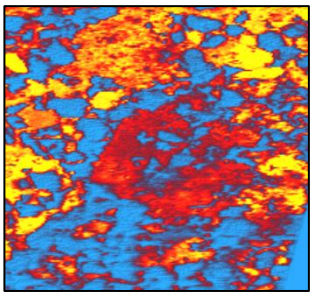

^{57}Fe

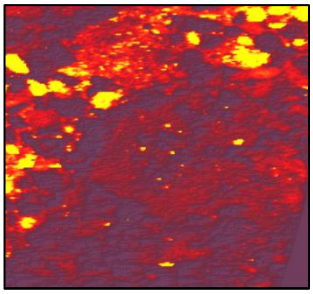

^{55}Mn

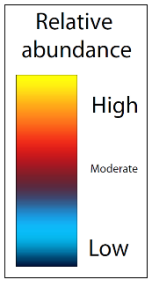

1250 µm

Map 3 (continued):

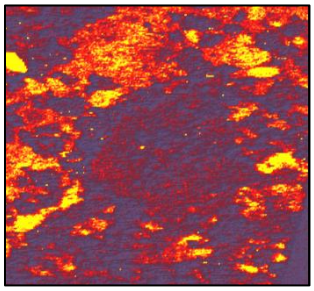

^{95}Mo

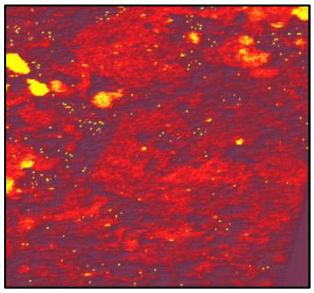

^{60}Ni

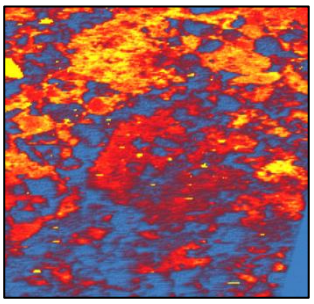

^{208}Pb

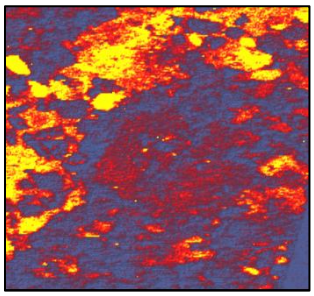

^{121}Sb

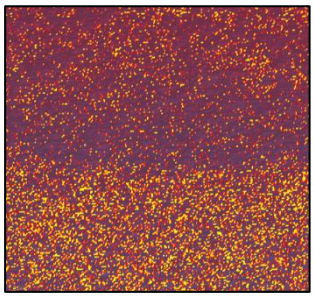

^{77}Se

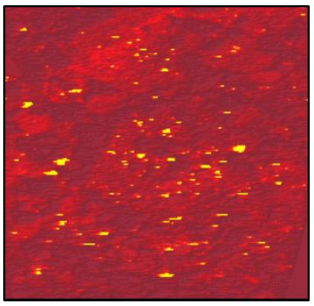

^{49}Ti

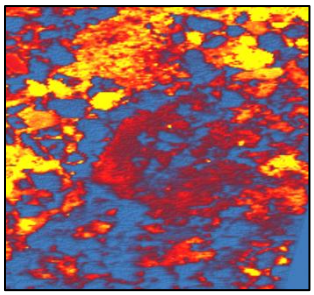

^{51}V

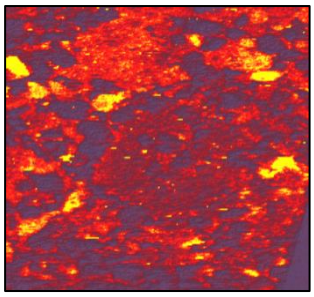

^{182}W

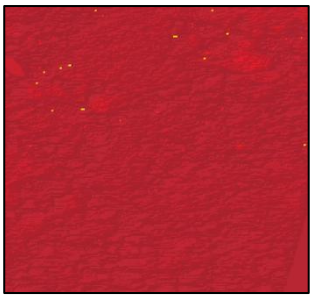

^{66}Zn

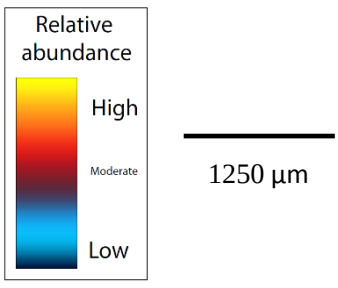

1250 µm

Thin section: SMM06

Map 1:

- 109 rasters @ 2261 µm path length
- Spot size: 17 µm
- Path separation: 17 µm
- 20 µm/s scan rate
- 360 minutes acquisition time

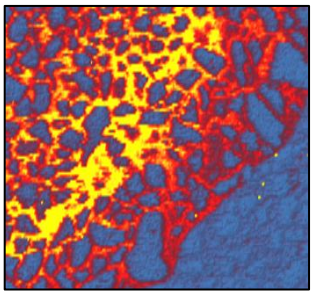

^{75}As

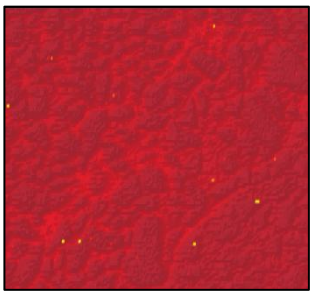

^{59}Co

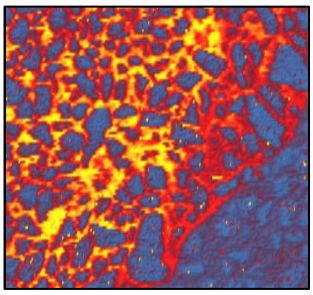

^{52}Cr

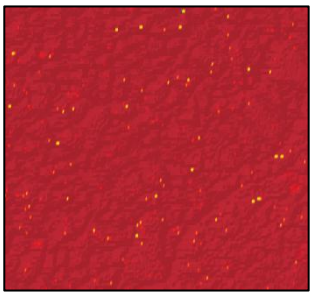

^{65}Cu

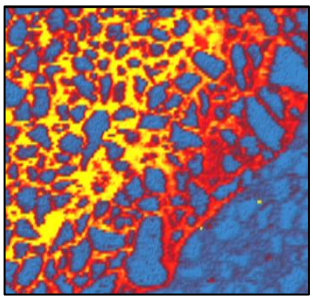

^{57}Fe

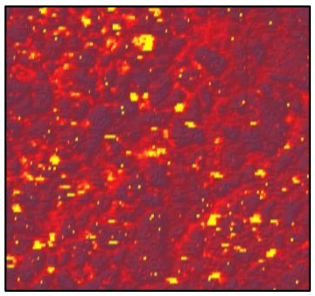

^{55}Mn

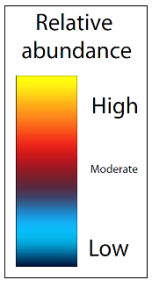

1100 µm

Map 1 (continued):

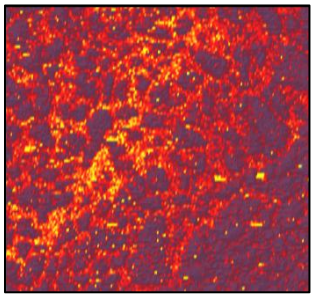

^{95}Mo

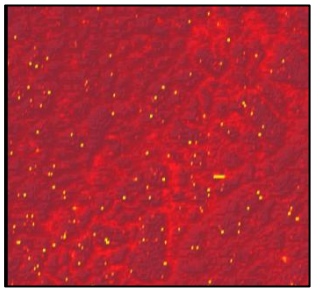

^{60}Ni

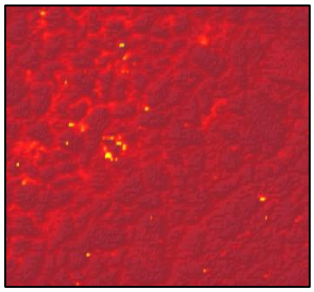

^{208}Pb

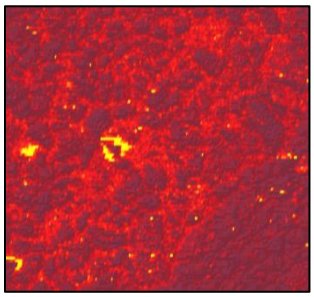

^{121}Sb

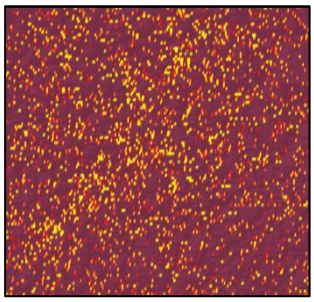

^{77}Se

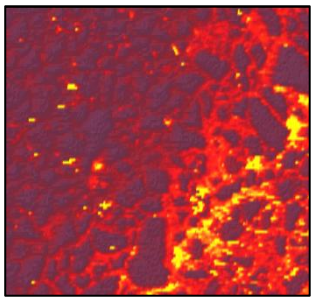

^{49}Ti

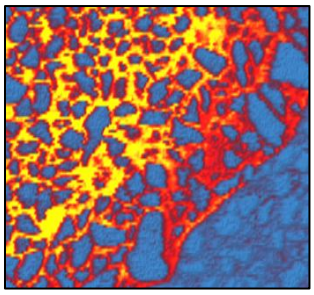

^{51}V

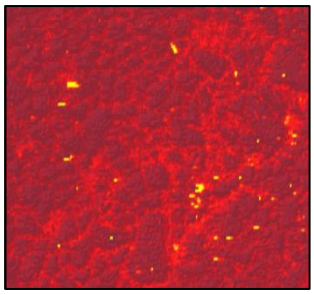

^{182}W

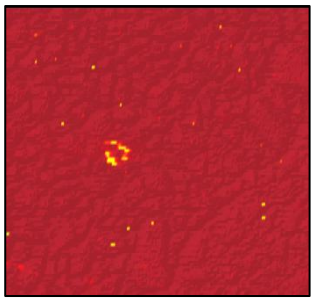

^{66}Zn

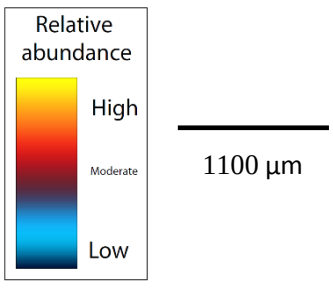

1100 µm

Thin section: SMM06

Map 2:

- 167 rasters @ 3260 µm path length
- Spot size: 17 µm
- Path separation: 17 µm
- 20 µm/s scan rate
- 690 minutes acquisition time

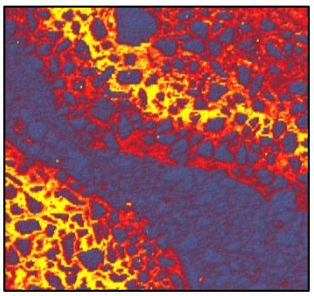

^{75}As

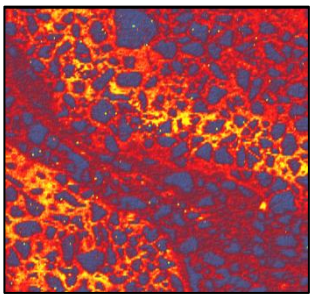

^{59}Co

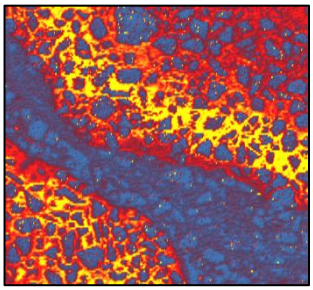

^{52}Cr

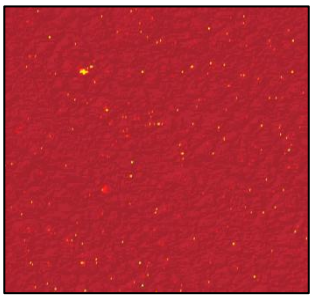

^{65}Cu

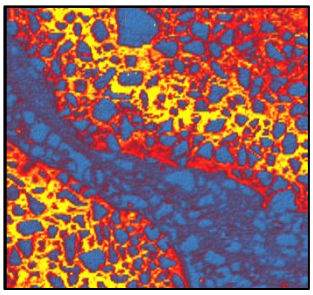

^{57}Fe

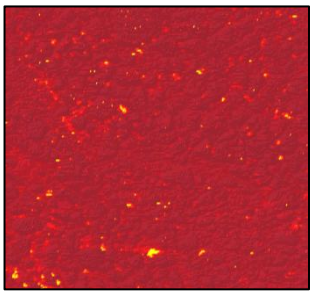

^{55}Mn

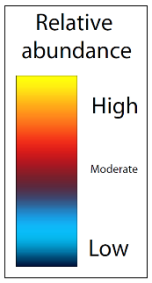

Map 2 (continued):

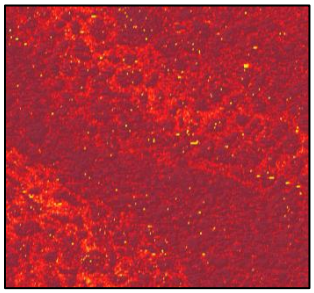

^{95}Mo

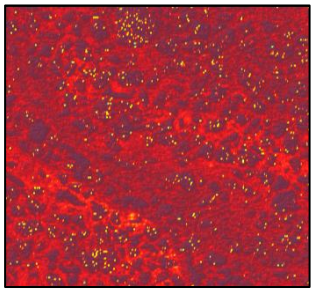

^{60}Ni

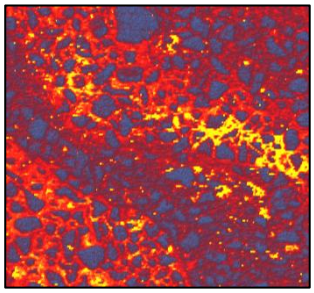

^{208}Pb

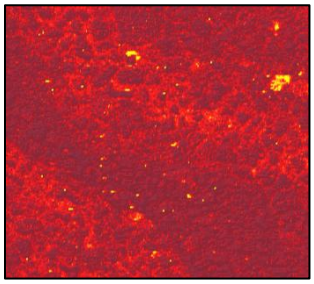

^{121}Sb

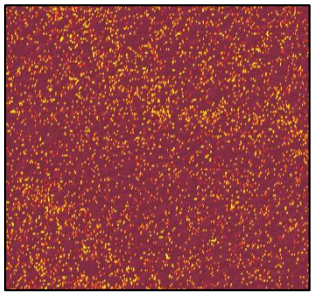

^{77}Se

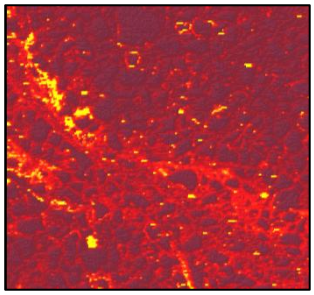

^{49}Ti

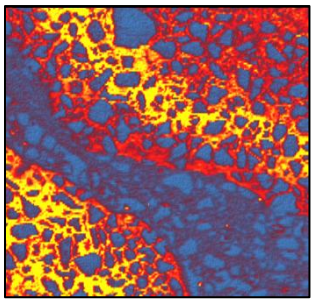

^{51}V

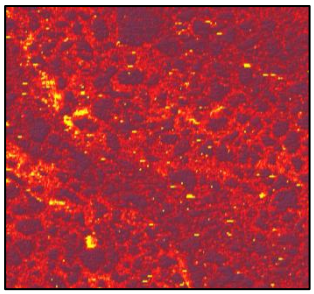

^{182}W

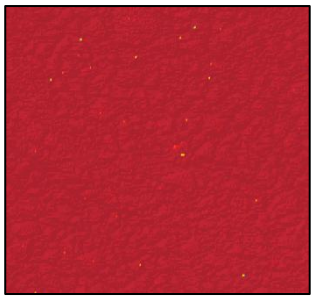

^{66}Zn

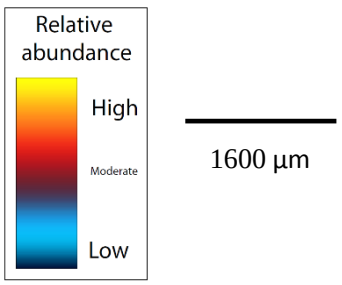

1600 µm

Section: SMM07

Map 1:

- 55 rasters @ 1797 µm path length
- Spot size: 17 µm
- Path separation: 17 µm
- 20 µm/s scan rate
- 330 minutes acquisition time

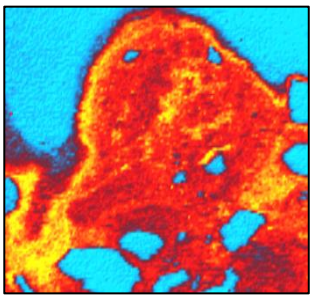

^{75}As

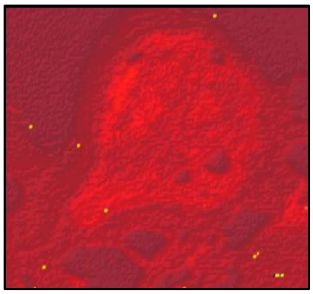

^{59}Co

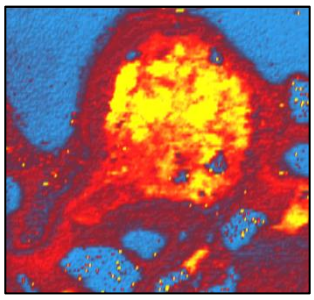

^{52}Cr

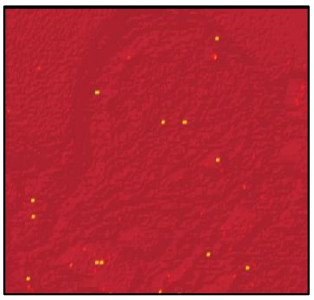

^{65}Cu

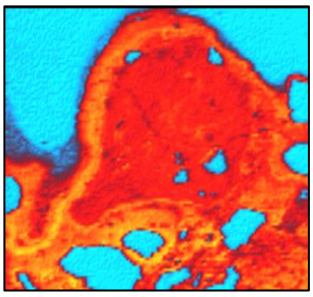

^{57}Fe

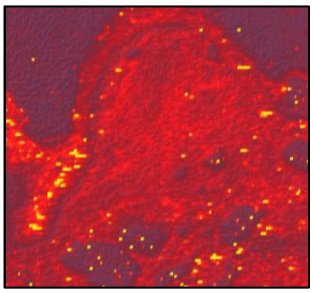

^{55}Mn

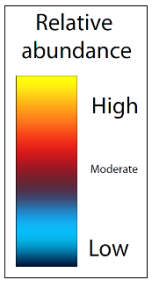

900 µm

Map 1 (continued):

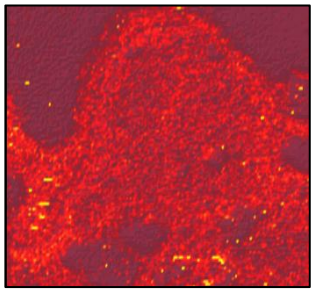

^{95}Mo

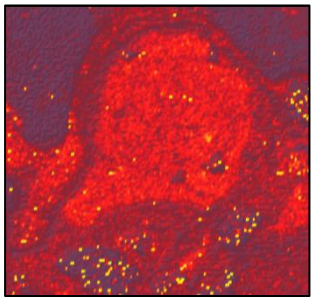

^{60}Ni

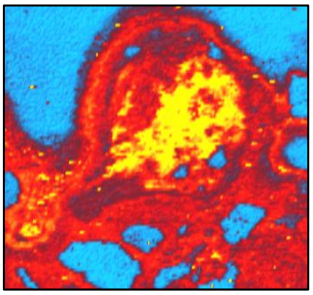

^{208}Pb

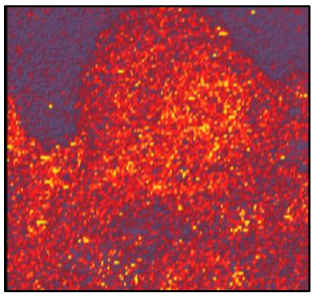

^{121}Sb

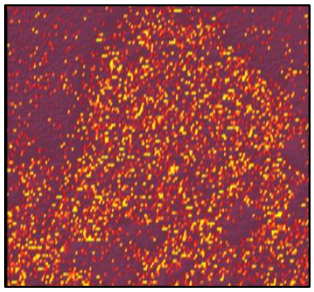

^{77}Se

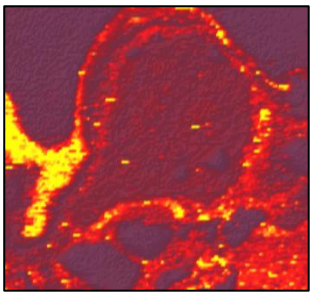

^{49}Ti

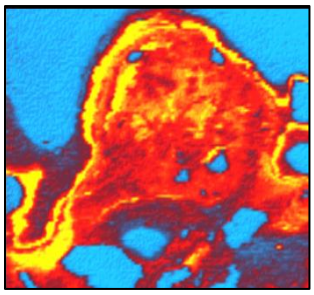

^{51}V

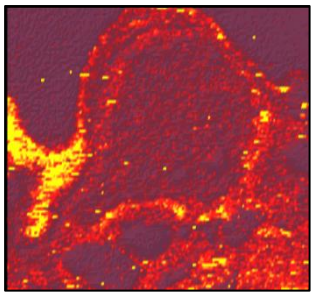

^{182}W

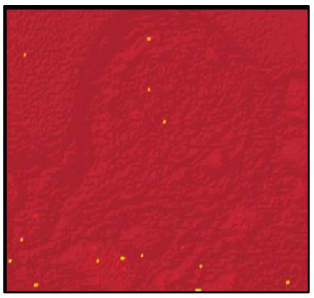

^{66}Zn

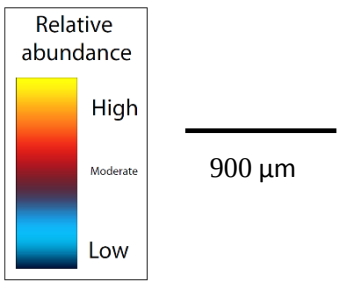

Section: SMM07

Map 2:

- 91 rasters @ 1453 µm path length
- Spot size: 17 µm
- Path separation: 17 µm
- 20 µm/s scan rate
- 240 minutes acquisition time

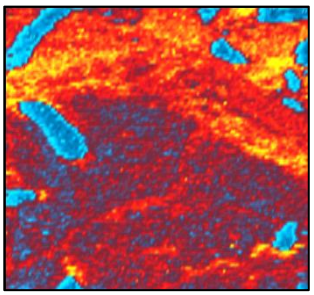

^{75}As

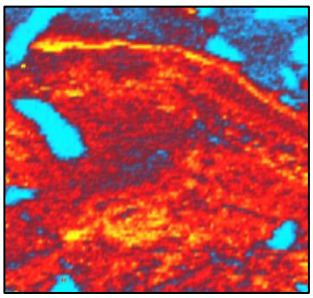

^{59}Co

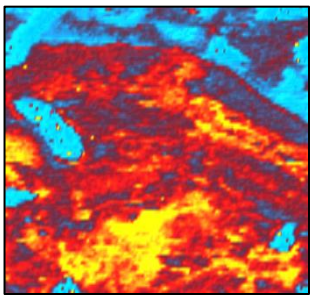

^{52}Cr

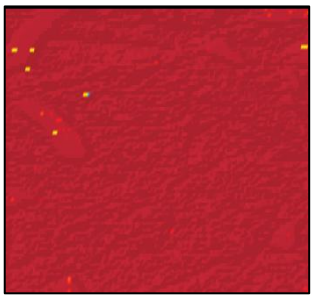

^{65}Cu

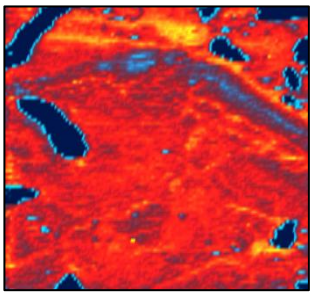

^{57}Fe

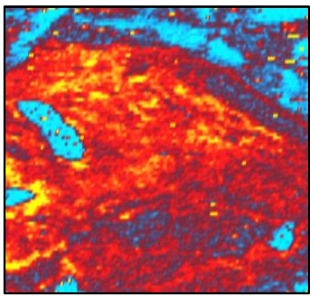

^{55}Mn

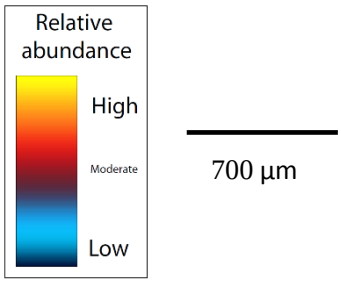

Map 2 (continued):

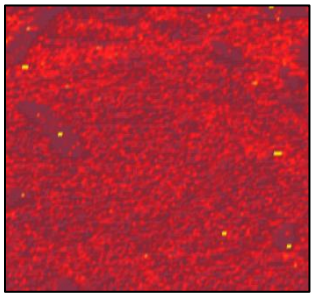

^{95}Mo

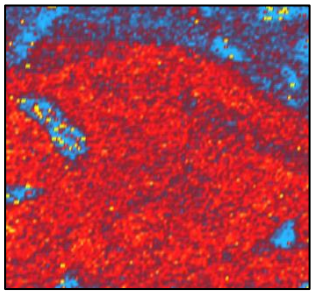

^{60}Ni

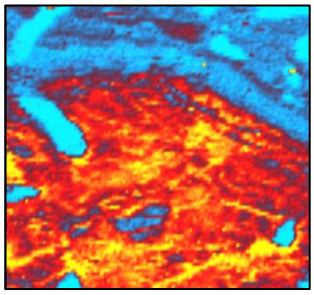

^{208}Pb

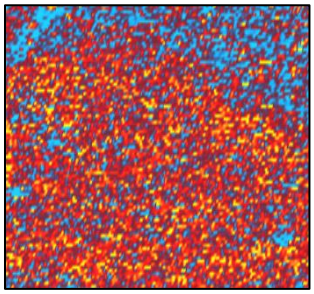

^{121}Sb

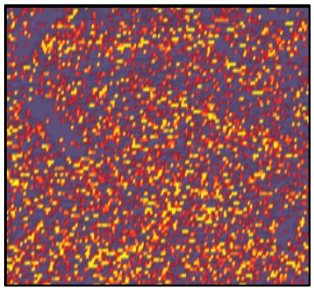

^{77}Se

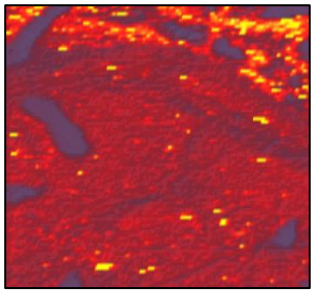

^{49}Ti

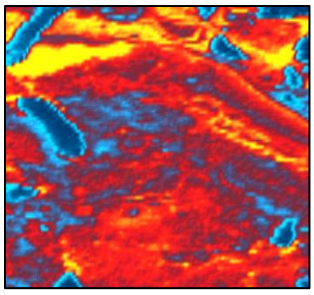

^{51}V

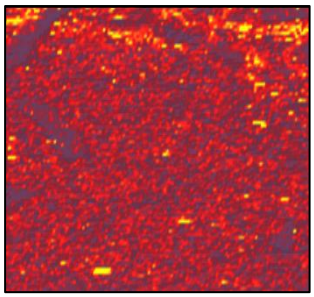

^{182}W

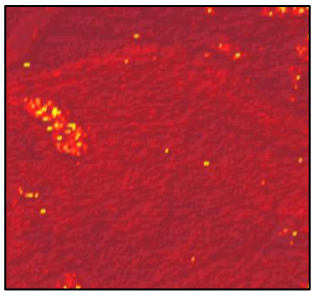

^{66}Zn

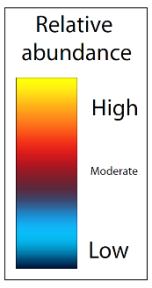

700 µm

Section: SMM09

Map 1:

- 95 rasters @ 1169 µm path length
- Spot size: 17 µm
- Path separation: 17 µm
- 20 µm/s scan rate
- 200 minutes acquisition time

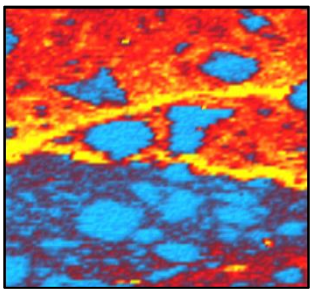

^{75}As

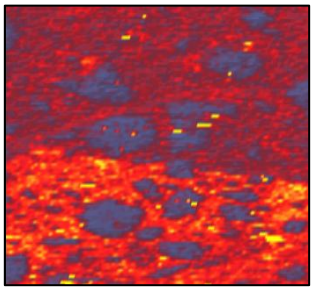

^{59}Co

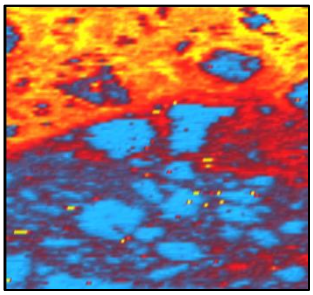

^{52}Cr

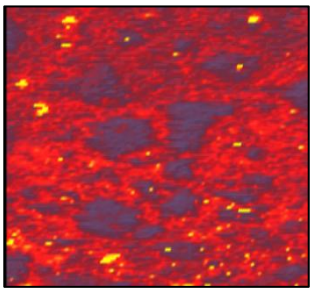

^{65}Cu

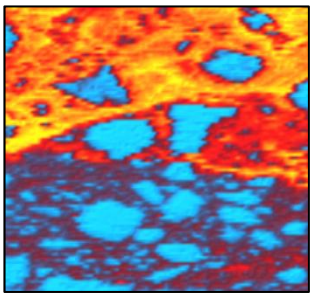

^{57}Fe

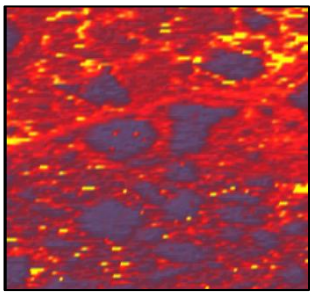

^{55}Mn

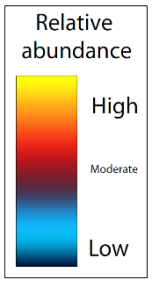

600 µm

Map 1 (continued):

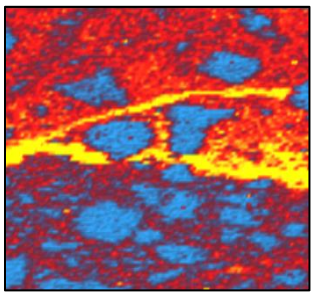

^{95}Mo

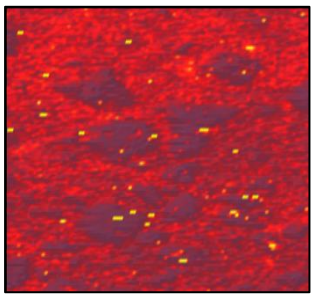

^{60}Ni

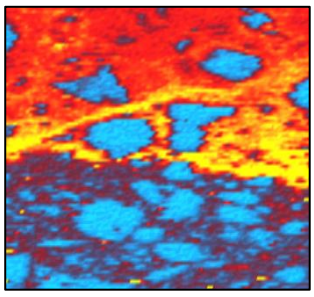

^{208}Pb

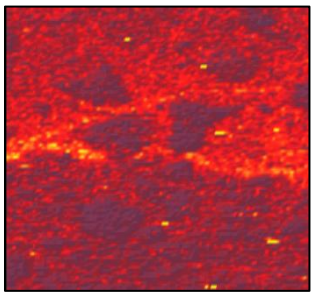

^{121}Sb

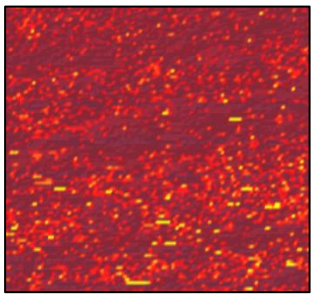

^{77}Se

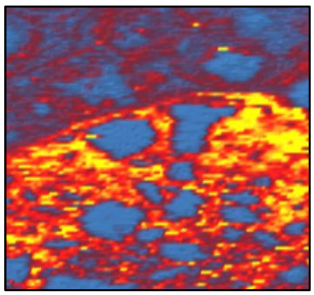

^{49}Ti

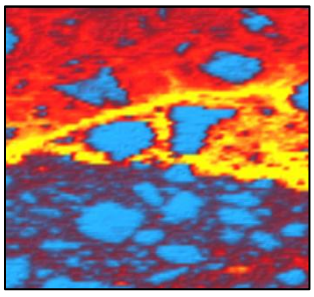

^{51}V

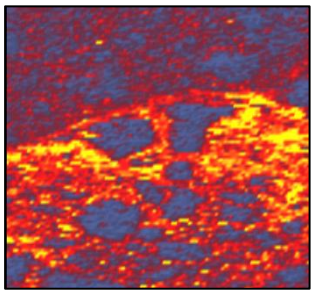

^{182}W

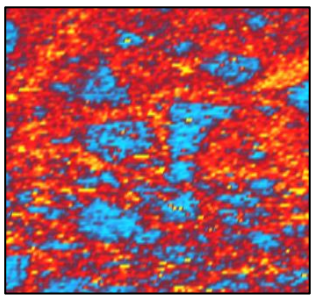

^{66}Zn

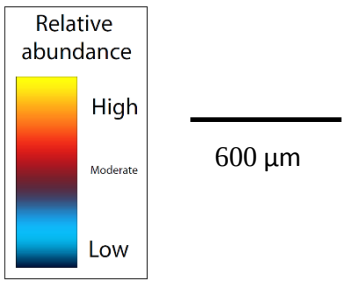

Section: SMM09

Map 2:

- 185 rasters @ 1946 µm path length
- Spot size: 17 µm
- Path separation: 17 µm
- 20 µm/s scan rate
- 540 minutes acquisition time

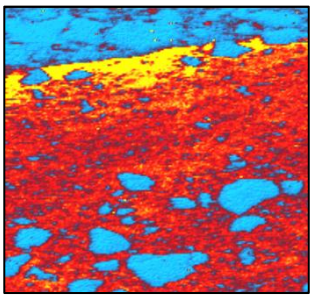

^{75}As

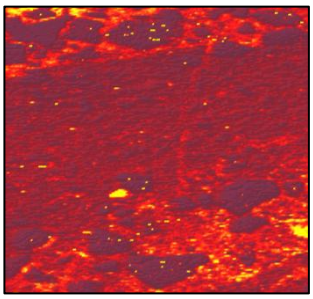

^{59}Co

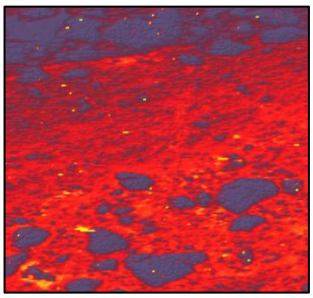

^{52}Cr

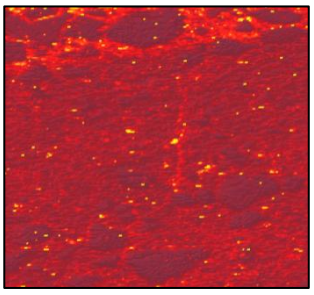

^{65}Cu

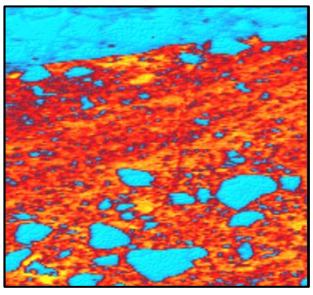

^{57}Fe

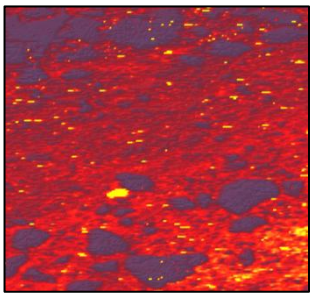

^{55}Mn

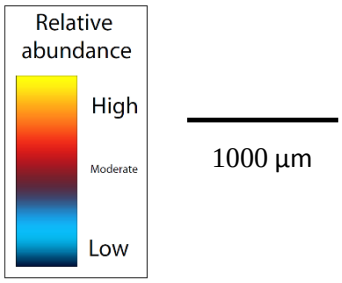

Map 2 (continued):

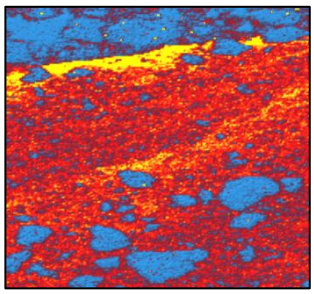

^{95}Mo

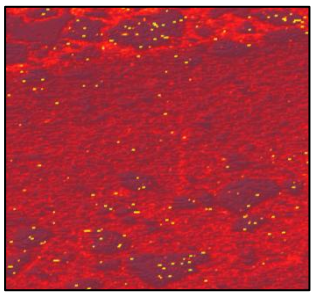

^{60}Ni

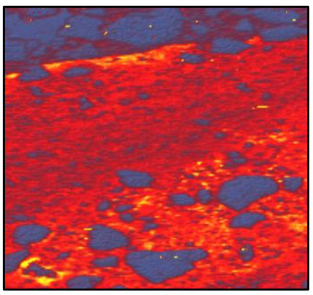

^{208}Pb

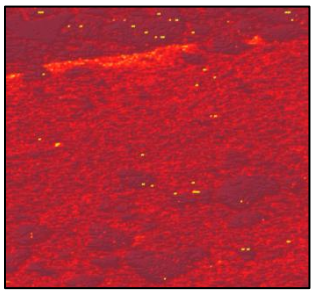

^{121}Sb

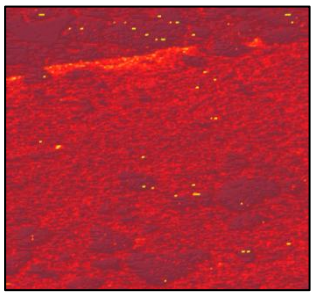

^{77}Se

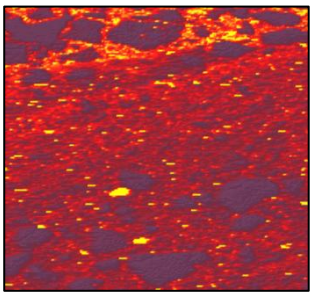

^{49}Ti

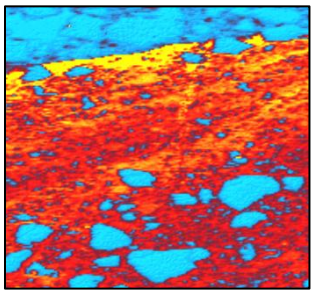

^{51}V

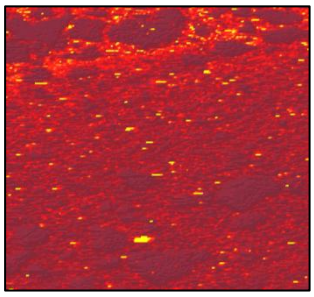

^{182}W

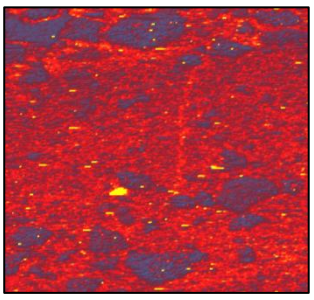

^{66}Zn

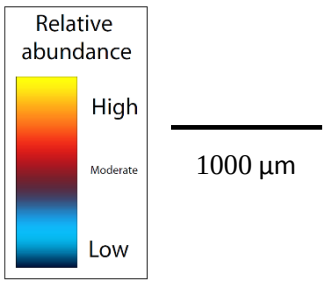

1000 µm

Section: SMM10

Map 1:

- 105 rasters @ 1385 µm path length
- Spot size: 17 µm
- Path separation: 17 µm
- 20 µm/s scan rate
- 260 minutes acquisition time

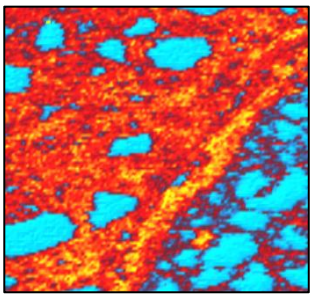

^{75}As

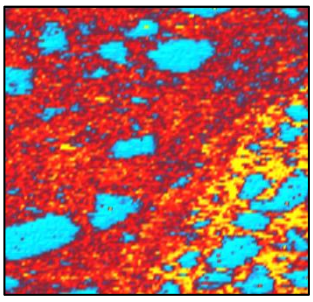

^{59}Co

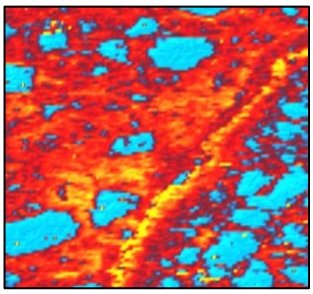

^{52}Cr

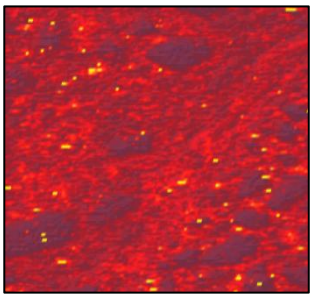

^{65}Cu

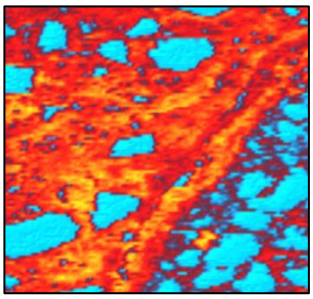

^{57}Fe

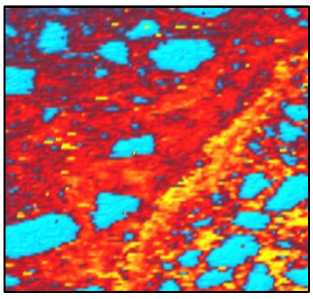

^{55}Mn

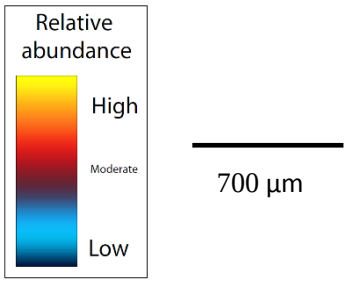

Map 1 (continued):

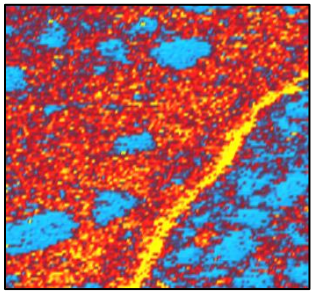

^{95}Mo

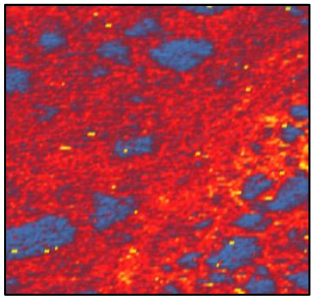

^{60}Ni

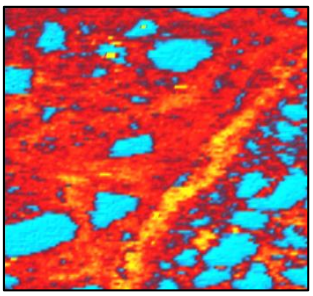

^{208}Pb

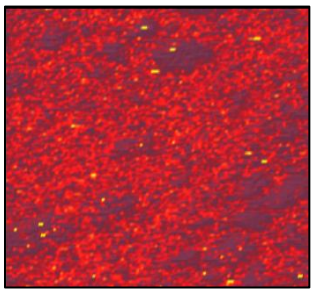

^{121}Sb

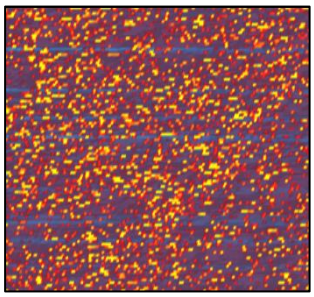

^{77}Se

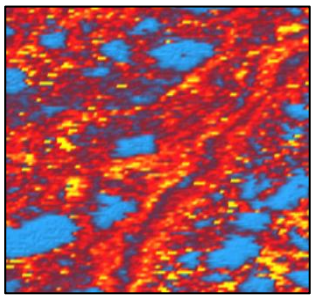

^{49}Ti

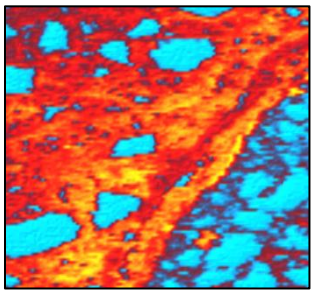

^{51}V

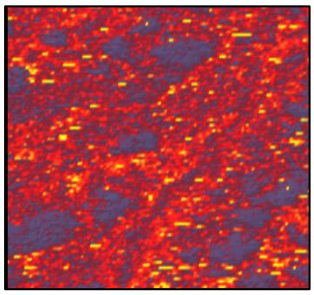

^{182}W

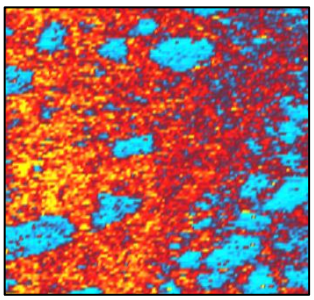

^{66}Zn

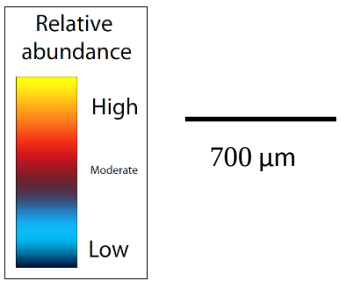

Section: SMM10

Map 2:

- 187 rasters @ 2088 µm path length
- Spot size: 17 µm
- Path separation: 17 µm
- 20 µm/s scan rate
- 500 minutes acquisition time

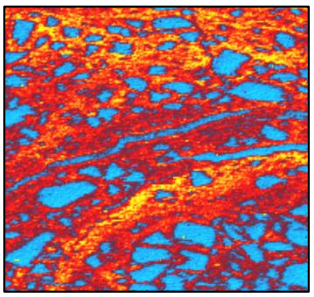

^{75}As

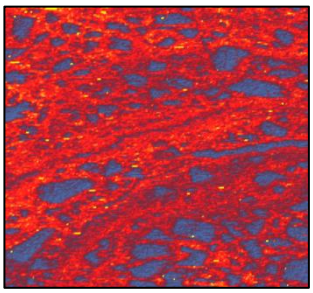

^{59}Co

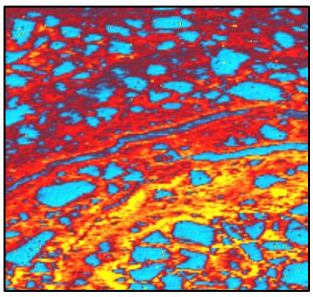

^{52}Cr

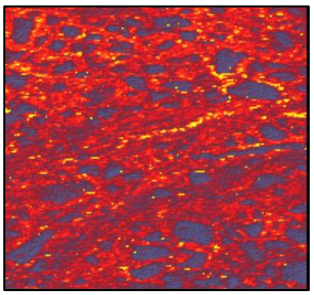

^{65}Cu

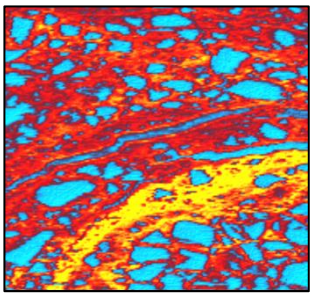

^{57}Fe

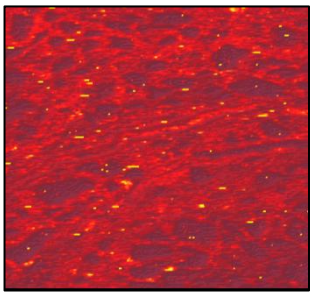

^{55}Mn

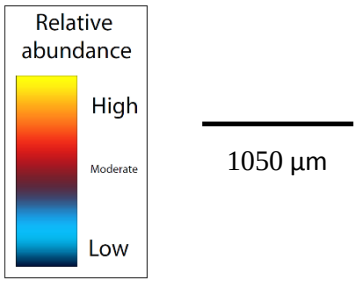

Map 2 (continued):

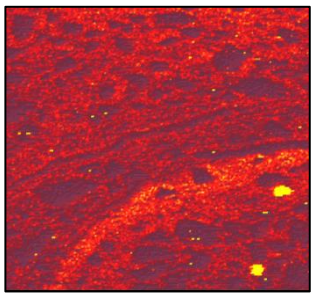

^{95}Mo

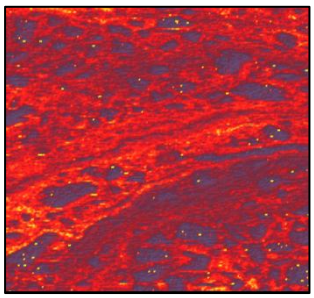

^{60}Ni

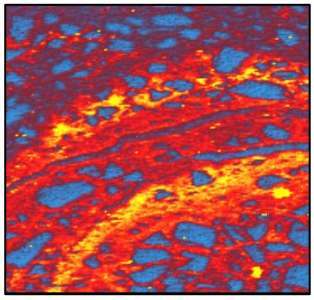

^{208}Pb

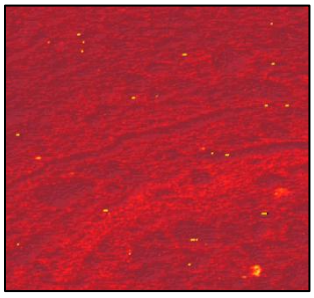

^{121}Sb

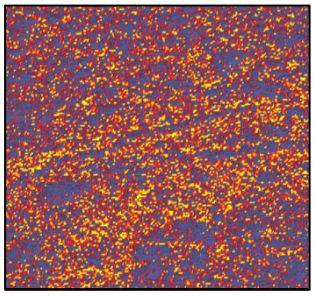

^{77}Se

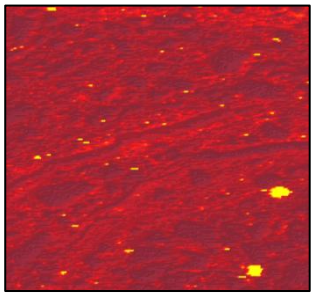

^{49}Ti

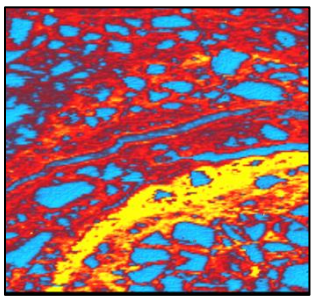

^{51}V

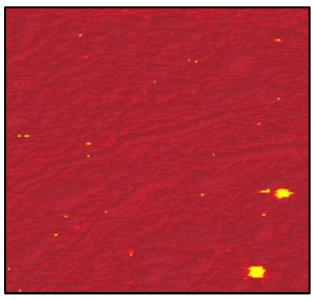

^{182}W

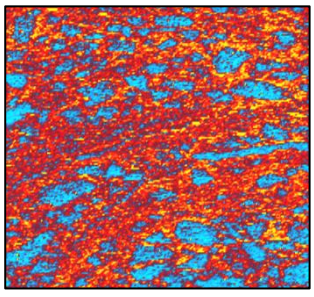

^{66}Zn

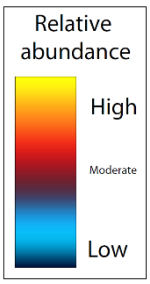

1050 µm